Evidence-Based Complementary and Alternative Medicine

Traditional Medicine in Liver Disease and Inflammation

Lead Guest Editor: Yunxia Li
Guest Editors: Hongwei Zhang and Jianbo Wan

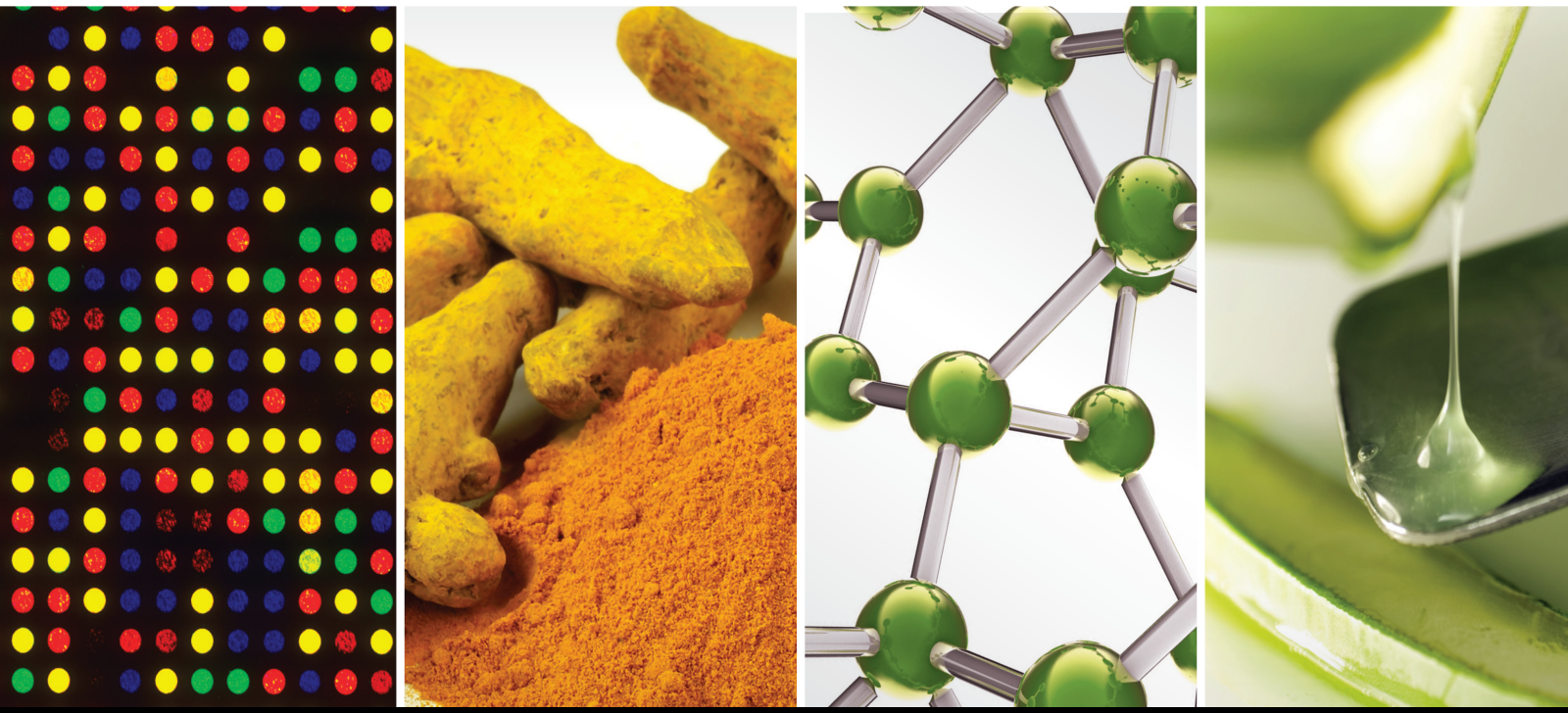

Traditional Medicine in Liver Disease and Inflammation

Evidence-Based Complementary and Alternative Medicine

Traditional Medicine in Liver Disease and Inflammation

Lead Guest Editor: Yunxia Li
Guest Editors: Hongwei Zhang and Jianbo Wan

Chief Editor

Associate Editors

Academic Editors

Contents

Hindawi
Evidence-Based Complementary and Alternative Medicine
Volume 2021, Article ID 9863714, 16 pages
https://doi.org/10.1155/2021/9863714

Research Article

Based on Network Pharmacology and RNA Sequencing Techniques to Explore the Molecular Mechanism of Huatan Jiangzhuo Decoction for Treating Hyperlipidemia

Xiaowen Zhou,[1] **Zhenqian Yan**,[1] **Yaxin Wang**,[1] **Qi Ren**,[1] **Xiaoqi Liu**,[2] **Ge Fang**,[3] **Bin Wang**,[4] **and Xiantao Li**[1]

[1]*Laboratory of TCM Syndrome Essence and Objectification, School of Basic Medical Sciences, Guangzhou University of Chinese Medicine, Guangzhou 510006, China*
[2]*Guangzhou Sagene Tech Co., Ltd., Guangzhou 510006, China*
[3]*College of Traditional Chinese Medicine, Hunan University of Chinese Medicine, Changsha 410208, China*
[4]*Shenzhen Traditional Chinese Medicine Hospital, Shenzhen 518000, China*

Correspondence should be addressed to Xiantao Li; lxt150@126.com

Received 22 May 2020; Revised 12 March 2021; Accepted 18 March 2021; Published 12 April 2021

Academic Editor: Jianbo Wan

Background. Hyperlipidemia, due to the practice of unhealthy lifestyles of modern people, has been a disturbance to a large portion of population worldwide. Recently, several scholars have turned their attention to Chinese medicine (CM) to seek out a lipid-lowering approach with high efficiency and low toxicity. This study aimed to explore the mechanism of Huatan Jiangzhuo decoction (HTJZD, a prescription of CM) in the treatment of hyperlipidemia and to determine the major regulation pathways and potential key targets involved in the treatment process. *Methods*. Data on the compounds of HTJZD, compound-related targets (C-T), and known disease-related targets (D-T) were collected from databases. The intersection targets (I-T) between C-T and D-T were filtered again to acquire the selected targets (S-T) according to the specific index. Gene ontology (GO) and Kyoto Encyclopedia of Genes and Genomes (KEGG) pathway enrichment, as well as network construction, were applied to predict the putative mechanisms of HTJZD in treating hyperlipidemia. Thereafter, an animal experiment was conducted to validate the therapeutic effect of HTJZD. In addition, regulated differentially expressed genes (DEGs) were processed from the RNA sequencing analysis results. Common genes found between regulated DEGs and S-T were analyzed by KEGG pathway enrichment to select the key targets. Lastly, key targets were validated by real-time quantitative reverse transcription PCR (qRT-PCR) analysis. *Results*. A total of 210 S-T were filtered out for enrichment analysis and network construction. The enrichment results showed that HTJZD may exert an effect on hyperlipidemia through the regulation of lipid metabolism and insulin resistance. The networks predict that the therapeutic effect of HTJZD may be based on the composite pharmacological action of these active compounds. The animal experiment results verify that HTJZD can inhibit dyslipidemia in rats with hyperlipidemia, suppress lipid accumulation in the liver, and reverse the expression of 202 DEGs, which presented an opposite trend in the model and HTJZD groups. Six targets were selected from the common targets between 210 S-T and 202 regulated DEGs, and the qRT-PCR results showed that HTJZD could effectively reverse Srebp-1c, Cyp3a9, and Insr mRNA expression ($P < 0.01$). *Conclusion*. In brief, network pharmacology predicted that HTJZD exerts a therapeutic effect on hyperlipidemia. The animal experimental results confirmed that HTJZD suppressed the pathological process induced by hyperlipidemia by regulating the expression of targets involved in lipid metabolism and insulin resistance.

1. Introduction

Hyperlipidemia is a condition wherein lipid-glucose metabolic disruption occurs, and it is mainly characterized by the derangements of lipoproteins circulating in the blood, such as high levels of total cholesterol (TC), triglyceride (TG) and/or low-density lipoprotein cholesterol (LDL-c), or aberrant declined level of low-density lipoprotein cholesterol (HDL-c) [1, 2]. Growing evidence has proven that hyperlipidemia could hardly avoid developing cardiovascular disease,

nephropathy, type 2 diabetes mellitus, and nonalcoholic fatty liver disease and would even elevate the cerebellar toxicity especially for the cholesterol overload [3–5]. Hyperlipidemia is an epidemic disease worldwide, with the number of expected cases reaching 78 million by 2022 in major countries, playing an important role in high morbidity and mortality of cardiovascular diseases [6]. Lifestyle improvements and drug interventions should be under discussion to limit the progress of hyperlipidemia.

Currently, statins, the first-line recommended therapy for lowering lipid, are the widely used drugs for hyperlipidemia [7]. Nevertheless, accompanying the favorable effects of reducing cholesterol biosynthesis, statins cause adverse effects, such as myalgia, hepatic and renal toxicity, and cognitive disorder [8]. It seems that the Pcsk9 inhibitor, a new agent, is beneficial as it lowers the LDL levels [9]. However, the high cost and the side effects of the Pcsk9 inhibitor cannot be ignored [10, 11]. Accordingly, several researchers have made efforts to seek help from CM, which is a healthcare-focused medicine system with abundant practice experience. In the CM theory, lipid deposition is a pathological phenomenon of phlegm and blood blocking of the veins, which results from the dysfunction of the liver, incapability of transportation and transformation of the spleen, and irregularity of fluid metabolism [12–14]. Contemporary experts have found that treating hyperlipidemia based on the guidance of the CM theory could be possible. Peng et al. [15] discovered that decoctions, characterized by tonifying spleen and resolving phlegm, exerted a curative effect on turbid phlegm syndrome of hyperlipidemia. Wang et al. [13] stated that decoctions that clear the liver and eliminate dampness could increase bile secretion and reduce cholesterol absorption.

Huatan Jiangzhuo decoction (HTJZD) was termed based on the therapeutic method of resolving phlegm and reducing turbidity of the CM theory. It includes the following nine herbs: Poria, Alismatis Rhizoma, Atractylodis Macrocephalae Rhizoma, Atractylodis Rhizoma, Pinelliae Rhizoma Praeparatum, Citri Reticulatae Pericarpium, Glycyrrhizae Radix et Rhizoma, Ginseng Radix et Rhizoma, and Citri Reticulatae Pericarpium Viride. It has been reported that hypolipidemic efficacy is found in a portion of ingredients in these herbs. For example, *Alisma orientale* could increase the HDL-c/LDL-c ratio and regulate abnormal cholesterol-related markers in high-fat diet (HFD)-fed rats [16]. *Poria cocos* attenuates the perturbations of bile acid biosynthesis [17]. Moreover, immature *Citrus reticulata* extract could ameliorate HFD-induced obesity by initiating browning of beige adipocytes [18]. In addition, our previous studies [19, 20] have suggested that HTJZD could suppress the pathological process of hyperlipidemia, but the underlying mechanism has not been fully explained.

This study resorted to network pharmacology combined with RNA sequencing techniques to promote our understanding concerning the molecular mechanism of HTJZD in treating hyperlipidemia. Network pharmacology is a novel bioinformatic technology that is applied to elucidate the occurrence and development of diseases based on system biology and biological network equilibrium. It is also generally used to guide the discovery of new drugs and clarify the mechanism of CM [21]. The RNA sequencing technology is a dynamic connection between the species' genome and its external physiological status, indicating the quality and quantity of gene expression in the specific organ at a specific physiological stage [22]. Combining these techniques to conduct bioinformatic research provides more possibility of exploring the therapeutic mechanism of HTJZD.

2. Materials and Methods

2.1. Prediction of Putative Targets of Compounds in HTJZD. The compounds of each herb in HTJZD were collected from TCMSP (https://tcmspw.com/tcmsp.php). TCMSP is a composite website that contains information about active compounds, potential targets, related diseases, and pharmacodynamics data of CM. ADME parameters were used to evaluate the compounds, of which are oral bioavailability (OB) $\geq 30\%$ and drug likeness (DL) of ≥ 0.18 were the inclusion criteria used to select the active compounds of HTJZD in this study. Subsequently, the related targets of selected compounds were obtained from TCMSP, ETCM (http://www.tcmip.cn/ETCM/index.php/Home/Index/), and Swiss Target Prediction (http://www.swisstargetprediction.ch/). Candidate target genes from ETCM should meet the prediction confidence index of ≥ 0.80. Targets of compounds predicted by Swiss Target Prediction should attain the canonical SMILEs or InChI from PubChem (https://pubchem.ncbi.nlm.nih.gov/) first and then be pasted in the website to acquire ones with the probability of ≥ 0.

2.2. Collecting Known Hyperlipidemia-Related Targets. Hyperlipidemia targets were collected from DisGeNET (https://www.disgenet.org/) and GeneCards (https://www.genecards.org/) with "hyperlipidemia" as the keyword. DisGeNET contains a large number of genes and variants related to human diseases and serves as a multifunctional platform to meet diverse research purposes. GeneCards is a composite database that provides known and predicted genes of *Homo sapiens* regarding multiple omics and functional information.

2.3. Network Construction and Analysis. Compound-related targets (C-T) and disease-related targets (D-T) were standardized in UniProtKB (https://www.uniprot.org/) based on *H. sapiens* genes to delete duplicate values. Then, the intersection targets (I-T) of C-T and D-T were searched and used to explore the correlation among I-T on STRING (https://www.string-db.org/). The minimum required interaction score was set as "highest confidence (0.900)" on STRING, and the simple tabular text output was downloaded from it. Lastly, the node (selected targets, S-T) interaction meeting the criteria of "a combined score of ≥ 0.95" was screened out to construct the herb-compound-S-T network and S-T-pathway network in Cytoscape 3.7.2 for visualizing the results.

2.4. GO Functional Annotation and KEGG Pathway Enrichment Analysis. S-T were input to g:Profiler (https://biit.cs.ut.ee/gprofiler/gost) for KEGG signaling pathway enrichment analysis and GO functional annotation including biological process (BP), cellular component (CC), and molecular function (MF). The website, g:Profiler, updated in a timely manner, serves as a collection of functional enrichment analysis (g:Gost), gene ID conversion (g:Convert), and SNP id to gene name (g:SNPense). The GO results were depicted by GraphPad Prism 8, and the KEGG pathway results were painted by ggplot2 packages in R Studio (version 4.0.2).

Animal experiments were conducted to evaluate the therapeutic effects of HTJZD for treating hyperlipidemia and validate the potential key targets for efficacy.

2.5. Chemicals and Reagents. The detection kits for TC, TG, LDL-c, and HDL-c were purchased from the Nanjing Jiancheng Bioengineering Institute (Nanjing, China). HE staining and Oil Red O staining associated reagents were purchased from Sinopharm Chemical Reagent Co., Ltd (Shanghai, China) and Wuhan Servicebio Technology Co., Ltd (Wuhan, China), respectively. Bestar qPCR RT kit (batch number: 2220) and SYBR Green qPCR Master Mix kit (batch number: 2043) were produced by DBI Bioscience Co., Ltd. (batch number: H97451, specification: 20 mg/tablet). Atorvastatin was diluted to 0.72 mg/mL in distilled water and preserved at 4°C.

2.6. Preparation of HTJZD Extraction. HTJZD is composed of Alismatis Rhizoma (10 g), Poria (15 g), Atractylodis Macrocephalae Rhizoma (15 g), Atractylodis Rhizoma (10 g), Pinelliae Rhizoma Praeparatum (10 g), Citri Reticulatae Pericarpium (10 g), Glycyrrhizae Radix et Rhizoma (10 g), Ginseng Radix et Rhizoma (10 g), and Citri Reticulatae Pericarpium Viride (10 g). All medicines were the herbal decoction pieces (Figure 1(a)) purchased from Zisun Chinese Pharmaceutical Co., Ltd. (Guangzhou, China) and Yulin Chinaherborn Pharmaceutical Co., Ltd. (Guangxi, China). The mixture was soaked with pure water 10 times for 20 minutes, followed by boiling for 1 h and then adding pure water five times for 30-minute boiling. The medical herbal extraction was evaporated, concentrated to 2.52 g/mL, and then stored at 4°C prior to use.

2.7. Animals and Experimental Design. Forty male Sprague-Dawley (SD) rats (6-week-old, weight: 190 g ± 10 g) were purchased from Guangzhou Southern Medical University Laboratory Animal Science and Technology Development Co., Ltd., China (Certificate No. 44002100009585). All the animals were housed in the Laboratory Animal Center of Guangzhou University of Chinese Medicine (Guangzhou, China) under the standard and controlled conditions, 21–25°C temperature, 50–70% humidity, and 12-h light-dark cycle. HFD was obtained from Guangdong Medical Laboratory Animal Center, China. HFD recipe consists of 52.2% maintenance feed, 0.4% premix feed, 20% sucrose, 15% lard, 1.2% cholesterol, 0.2% sodium cholate, 10% casein, 0.6% calcium hydrophosphate, and 0.4% mountain flour.

This research design is based on a previous exploratory experimental model [23, 24]. After 1-week acclimatization, the 40 animals were randomly divided into the normal group (N, fed with chow diet, n= 10) and the HFD group (n = 30). The hyperlipidemia model establishment in way of feeding with HFD lasted for 30 days. Before collecting the blood samples, all the rats had to be fasted for 12 h. Serum lipids were measured using the kits to evaluate the establishment of hyperlipidemia model. In the intervention phase, the HFD group was continuously supplied with HFD but regrouped into three groups: model group (M, n = 10) administered saline, atorvastatin group (A, n = 10) administered 1.8 mg/kg per day of atorvastatin, and HTJZD group (H, n = 10) administered 12.6 g/kg per day of HTJZD. Each rat was given an intragastric dose of 1 mL/100g.

After 4 weeks of intervention, all animals were sacrificed for blood sample and liver sample collection. The blood samples were centrifuged at 3,500 rpm for 10 minutes to obtain the isolated serum and stored at −20°C immediately for subsequent biochemical testing. The liver tissues were stored at −80°C. The protocol was approved by the Animal Experimental Ethics Committee of Guangzhou University of Chinese Medicine.

2.8. Biochemical Analysis. After 30 days of feeding, blood samples were collected from the rats' posterior ocular venous plexus to judge the development of hyperlipidemia. Moreover, after 4 weeks of intervention, the animals were sacrificed for blood collection from abdominal aorta. Serum TC, TG, LDL-c, and HDL-c levels of each group were measured by detection kits (enzyme-labeling assay) according to the manufacture's operating instructions.

2.9. Evaluation Standard of HLP Model Establishment and Treatment. According to *The Evaluation Method of Auxiliary Hypolipidemic Function* [25] issued by Chinese State Food and Drug Administration, the mixed hyperlipidemia model establishment has to meet these requirements of lipid indexes: compared with those in the control group, serum TG, TC, or LDL-c levels have to be elevated significantly ($P < 0.05$) in the model group. As for the identification of treatment efficiency in the mixed hyperlipidemia model, conditions of the effective intervention wherein serum TC or LDL-c levels were significantly reduced ($P < 0.05$) were not accompanied by a significant increase in the HDL-c level or a decrease in the TG level in the intervention group when compared with the control group.

2.10. Histological Examinations. After dissection, liver specimens were fixed in 4% (w/v) paraformaldehyde for 24 h, followed by flushing with running water overnight. Moreover, tissues were dehydrated with graded ethanol and embedded in paraffin blocks. Thereafter, paraffin blocks were sectioned to 4 μm slices spread on the glass slides, which were then rehydrated and stained with HE. In

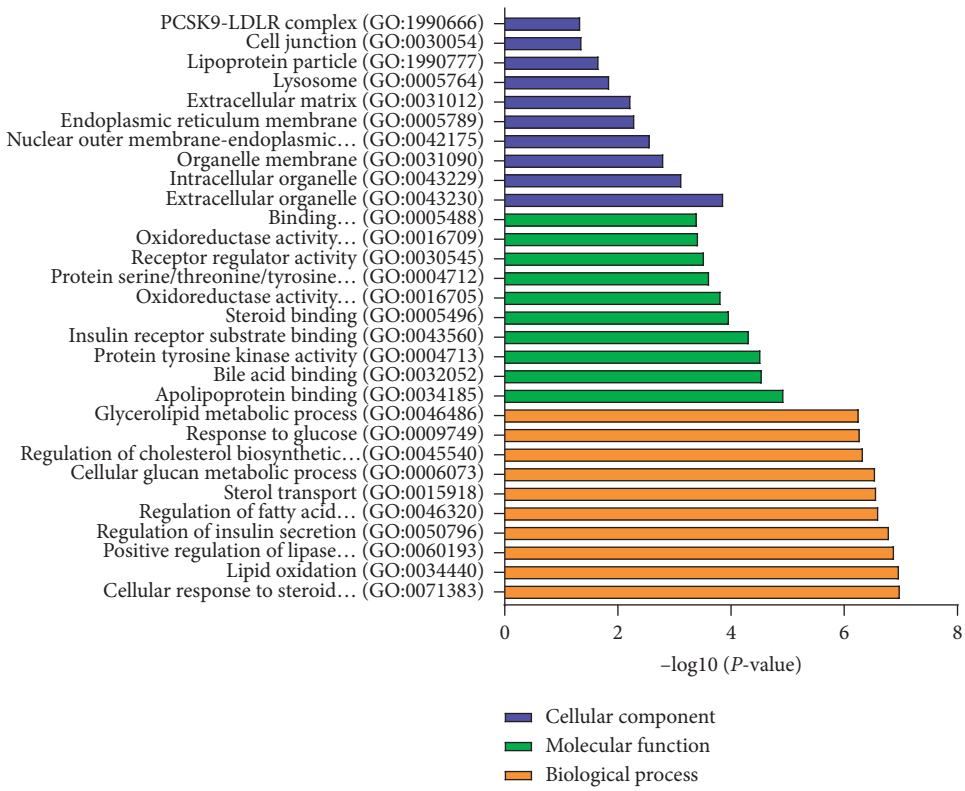

Figure 1: The GO functional analysis was processed by g:Profiler. 210 S-T were enriched in GO functional annotations ($P < 0.05$). Biological process (BP), molecular function (MF), and cellular components (CC) indicated the potential mechanism of treating hyperlipidemia with HTJZD.

addition, liver tissues were made into frozen samples. Fresh tissues were preserved in fixer for over 24 h, dehydrated with sucrose solution at 4°C, subsequently embedded on a molder with optimal cutting temperature freezing compound, and sectioned into 8 μm slices for Oil Red O staining. All sections were observed by an upright optical microscope (Nikon Eclipse E100, Japan) and an image collection system (Nikon DS-US, Japan) at 200× magnification.

2.11. RNA Sequencing Analysis. Total RNA was extracted from liver tissue samples of three groups (N group, M group, and H group) by using TRIzol reagent. Moreover, agar gel electrophoresis and NanoDrop were applied to test the purity and qualify the concentration of RNA. Agilent 2100 Bioanalyzer was facilitated to examine RNA quality. The transcriptomic library of cDNA was constructed and verified by Qubit 3.0 and Agilent 2100. After the library was purified, the sequencer HiSeq 2500 (Illumina, USA) was used on all samples for paired-end sequencing. Clean reads were obtained according to the following filter criteria-eliminating low quality reads and reads that comprise adapters. Consequently, TopHat2 was applied in setting genome (Rnor_6.0) as sequencing alignment reference to clean reads used to attain the information from and beyond the referenced genome. Each gene expression was assessed by fragments per kilobase of transcript per million fragments mapped (FPKM). The computational method of FPKM is below:

$$\text{FPKM} = \frac{\text{cDNA Fragments}}{\text{Mapped Fragments (Millions)} \times \text{Transcript Length (kb)}}. \quad (1)$$

DESeq was chosen for analyzing differential expression of genes in three groups. Screening criteria concerning a false discovery rate (FDR) of < 0.05 and fold change (FC) of > 1.5 or < 0.7 were used to identify significant DEGs. Venn diagram was painted by Draw.io, and the heatmap was processed by pheatmap package of R Studio (version 4.0.2).

2.12. Screening Out the Common Genes between Regulated DEGs and S-T. Given that DEGs acquired from RNA-seq were based on *Rattus norvegicus* genomes, S-T from *H. Sapiens* have to be mapped to the orthology of rat in the HUGO Gene Nomenclature Committee (HGNC, https://www.genenames.org/) in order to search out the common genes between regulated DEGs and S-T.

2.13. Key Targets Validation by qRT-PCR Analysis. Total RNA was reversed to cDNA by Bestar qPCR RT kit (DBI Biosciences, Germany). Subsequently, each cDNA sample was used to quantify the expression of respective gene by SYBR Green qPCR Master Mix kit (DBI Biosciences, Germany). The 20 μL reaction system containing cDNA, SYBR Green qPCR Master Mix, forward and reverse primers, and RNase-free ddH2O was placed into fluorescent qPCR

analyzer Mx3000P (Agilent, USA), through a procedure of 40 cycles at 94°C for 2 min predegeneration, 94°C for 20 s degeneration, 58°C for 20 s renaturation, and 72°C for 20 s extension. Each sample was performed in triplicate with glyceraldehyde-3-phosphate dehydrogenase (GAPDH) as the reference. Gene primer sequences of Srebp-1c, Pcsk9, Insr, Gck, Cyp7a1, and Cyp3a9 used for reverse transcription polymerase chain reaction (PCR) are listed in Table 1. The data of qRT-PCR were analyzed by the $2^{-\Delta\Delta Ct}$ method to qualify the relative expression levels of candidate genes.

2.14. Statistical Analysis. All the data had passed the normal distribution test. Moreover, one-way analysis of variance was used to test if data met variance homogeneity. If so, the LSD test was used for multiple comparisons; if not, Welch's analysis of variance combined with the Games–Howell test was applied. All results are expressed as mean ± SD. P-values of < 0.05 were considered statistically significant. All the steps were performed by using SPSS (IBM, USA, version 20.0).

3. Results

3.1. Identification of Compounds, C-T, D-T, I-T, and S-T. Based on the inclusive criteria of OB $\geq 30\%$ and DL ≥ 0.18, a total of 120 active compounds (Supplemental Table 1) were picked up from TCMSP. 1001 C-T (Supplemental Table 2) were collected from three databases (TCMSP, ETCM, Swiss Target Prediction) and standardized by UniProtKB. Additionally, 1297 D-T (Supplemental Table 2) were searched out from DisGeNET and GeneCards, with the name normalized. Furthermore, 282 I-T (Supplemental Table 2) were found in C-T and D-T after the intersection performed. Then, 282 I-T were put into STRING to determine the interaction relationship among the targets, and lastly 210 S-T (Supplemental Table 2) were identified according to the criteria of combined score of ≥0.95 in the node interaction index. Totally, 103 components (Supplemental Table 1) containing 210 S-T were left to construct the network.

3.2. GO Annotations and KEGG Pathway Enrichment Analysis of 210 S-T. A total of 210 S-T, with strong connection among them, may play a key role for HTJZD in the treatment of hyperlipidemia. From BP annotations in the GO functional enrichment analysis (Figure 1) results ($P < 0.05$), the targets are mainly grouped into cellular response to steroid hormone stimulus, lipid oxidation, regulation of insulin secretion, regulation of fatty acid oxidation, and others. These targets were associated with apolipoprotein binding, bile acid binding, insulin receptor substrate binding, and others in MF annotation. In addition, it is predicted that HTJZD exerts a regulation effect on hyperlipidemia through the alteration of CC such as cellular organelle, organelle membrane, and lipoprotein particles. KEGG pathway enrichment analysis ($P < 0.05$) was performed as shown in Figure 2. The size and color of the bubble were determined by gene number and –log10(P-value), respectively. A total of 210 S-T were mainly enriched in the insulin resistance pathway, nonalcoholic fatty liver disease pathway, HIF-1 signaling pathway, PI3K-Akt signaling pathway, insulin signaling pathway, AMPK signaling pathway, etc.

We found that GO annotations and KEGG pathway enrichments showed a better view of the connections between targets and the underlying therapeutic mechanisms of HTJZD. From the enrichment results, lipid metabolism and insulin resistance processes presented a strong connection with the potential regulation effect of HTJZD in treating hyperlipidemia, which may shed light on the exploration of the efficacy of HTJZD.

3.3. Network Construction. The interaction network of herb-compound-S-T (Figure 3) was composed of 322 nodes and 2,207 edges. It is evident that herbs and compounds were strongly associated with the common targets between compounds and disease. In other words, HTJZD had an effect on hyperlipidemia through the regulation of these targets by major active ingredients. MOL000173 (wogonin), MOL004328 (naringenin), MOL000358 (beta-sitosterol), MOL0002714 (baicalein), and MOL000422 (kaempferol) are the top five nodes with high degree among the compounds in the network. Most of them have been identified as the effective ingredients to modulate the glucolipid metabolism.

The KEGG pathway enrichment results and interaction relation among 210 S-T from STRING provided original data to construct the S-T-pathway network (Figure 4). The network consisted of 230 nodes and 1,057 edges, in which color depth was determined by the degree of S-T nodes and edge was determined by the combined score. It is predicted that HTJZD acts on these potential targets on the pathways to be involved in the treatment of the disease. The insulin resistance pathway, PI3K-Akt signaling pathway, and nonalcoholic fatty liver disease are characterized by relatively high –log10(P-value) in Figure 2 and also by the relative high degree in the network, which may provide more possibility for the search of potential targets within the pathway.

3.4. Effect of HTJZD Treatment on Serum Lipid Levels, Body Weight, and Liver Index in HFD-Fed Rats. As shown in Figure 5, we observed the significant accumulation of serum TC and TG as well as the decrease in the HDL-c level in HFD-fed rats after 30 days, which indicated the development of hyperlipidemia in the HFD group (Figure 5(a)), according to *The Evaluation Method of Auxiliary Hypolipidemic Function* [25]. After 4 weeks of treatment, compared with the M group, the A and H groups remarkably reversed the growth of TC level (Figure 5(b), $P < 0.05$). Compared with atorvastatin, HTJZD was more advantageous in lowering TG and increasing HDL-c levels (Figures 5(c) and 5(e)). However, neither of two measures was statistically effective in LDL reduction, even if there exists a downward trend (Figure 5(d)). Therefore, HTJZD was determined as the medicine that positively reduces serum cholesterol. In addition, the liver index in the H group was significantly lower than that in the M and A groups (Figure 5(g)), which

Table 1: Primer sequences used for qRT-PCR.

Gene name	Forward primer (5′-3′)	Reverse primer (5′- 3′)
GAPDH	CCTCGTCTCATAGACAAGATGGT	GGGTAGAGTCATACTGGAACATG
Srebp-1c	GCAAGTACACAGGAGGCCAT	AGATCTCTGCCAGTGTTGCC
Cyp7a1	GGAAGACTCTTTGCCGTCCA	CAAAATTCCCAAGCCTGCCC
Cyp3a9	AGAATTCGAGCCCTGCTGTC	CCGATCCCTGCCTCATGTTT
Pcsk9	CAAGGACTGGGGTAGTGCTG	CTCCGATGATGTCCTTCCCG
Insr	GCTACCTGGCCACTATCGAC	AACTGCCCATTGATGACGGT
Gck	CTGCTTAAGCTGGTGGACGA	GAAGCCCCAGAGTGCTTAGG

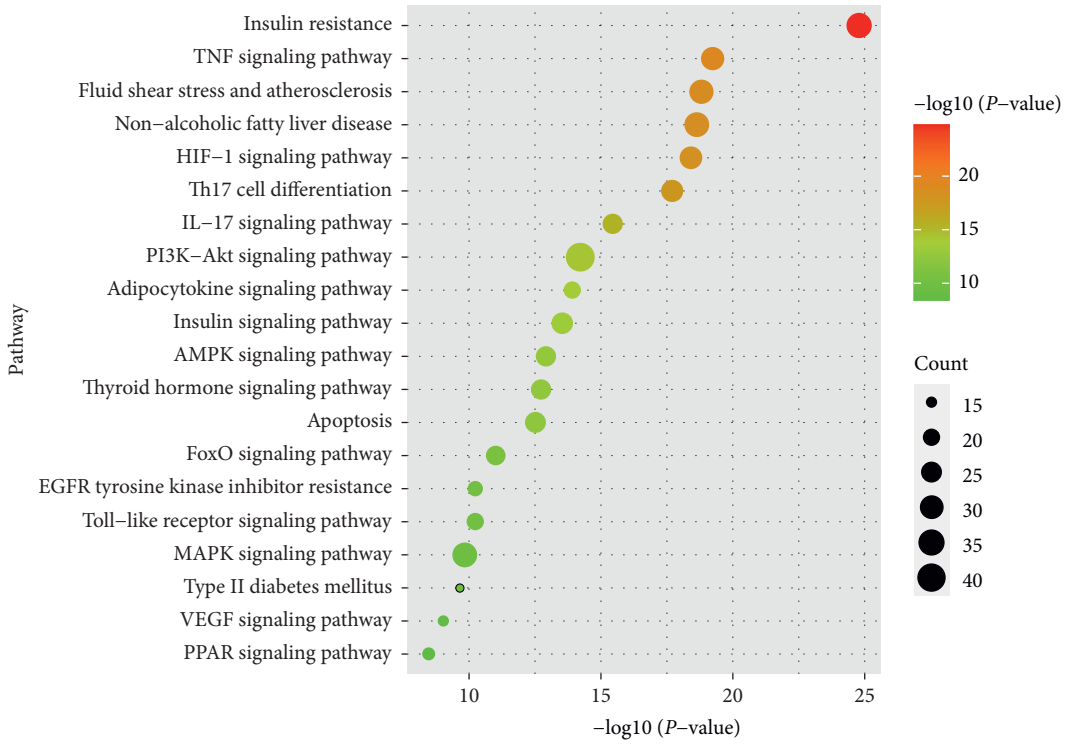

Figure 2: The KEGG pathway enrichment was processed by g:Profiler. 210 S-T were applied for KEGG pathway analysis ($P < 0.01$) to predict the critical pathways involved in the treatment of hyperlipidemia with HTJZD.

indicated the improvement of liver morphology and was later verified in pathological morphology examinations (Figures 6(a) and 6(b)). However, two treatments were not sensitive to reduce body weight and Lee's index (Figures 5(f) and 5(h)).

3.5. Effects of HTJZD Treatment on Hyperlipidemia-Related Pathological Process of Histology. The results of Oil Red O staining showed that lipid droplets were augmentative in the M group while a portion disappeared after atorvastatin and HTJZD intervention (Figure 6(a)). In addition, HE staining analysis showed that liver structure changed after HFD was supplemented in rats. Numerous lipid deposits in the normal liver cells induce the degeneration of liver and inflammatory cell infiltration in the portal area (Figure 6(b)). However, atorvastatin and HTJZD could obviously alleviate the damaged liver tissue and recover liver structure (Figure 6(b)). From the aforementioned results, HTJZD exerted lipid-lowering and liver protection effects similar to those of atorvastatin.

3.6. DEGs Regulated by HTJZD. This transcriptome study aimed to search out the potential targets, which were altered by hyperlipidemia and can be reversely regulated via the intervention of HTJZD, as the regulated DEGs. Based on the cutoff of FDR of < 0.05 and FC > 1.5 or < 0.7, a total of 2,502 DEGs (1,704 upregulated; 798 downregulated) were screened out from M versus N, and 1,936 (848 upregulated; 1,088 downregulated) from M versus H. In addition, compared with the upregulation and downregulation parts, respectively, 202 (124 upregulated and 78 downregulated) were the regulated DEGs (Figure 7). Furthermore, the chosen 202 regulated DEGs are listed in Supplemental Table 3 and visualized as a heatmap in Figure 8. All the regulated DEGs were grouped by hierarchical clustering based on FPKM of each gene in each sample. We observed that the

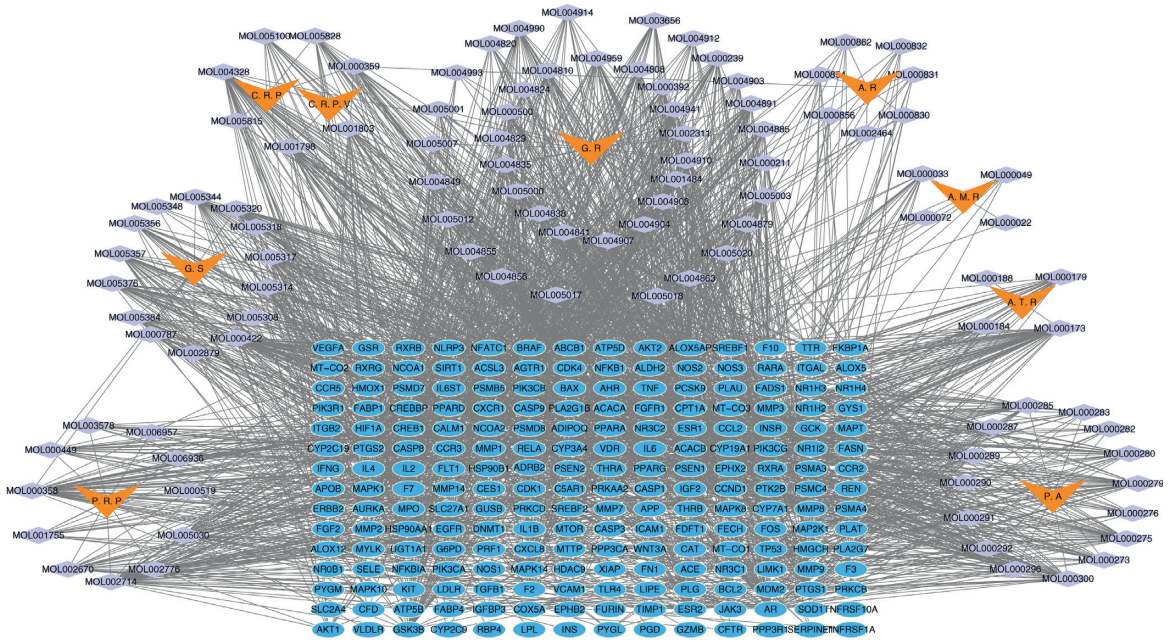

Figure 3: Herb-compound-S-T network was constructed to reveal the "multicompound, multitarget" mechanism of HTJZD. The network was composed of 9 herbs, 103 compounds, and 210 S-T. Orange nodes: herbs; purple nodes: compounds; blue nodes: S-T; P. A: Poria; A. R: Alismatis Rhizoma; A. M. R: Atractylodis Macrocephala Rhizoma; A. T. R: Atractylodis Rhizoma; P. R. P: Pinelliae Rhizoma Praeparatum; C. R. P: Citri Reticulatae Pericarpium; C. R. P. V: Citri Reticulatae Pericarpium Viride; G. S: Ginseng Radix et Rhizoma; G. R: Glycyrrhizae Radix et Rhizoma. For molecule names of compounds, refer to Supplemental Table 1 or look up the information on TCMSP.

expression of these genes was significantly altered in the model group when compared to control group. Nevertheless, after the administration of HTJZD, the expression of these genes was recovered to normal level. Therefore, it can be seen that the therapeutic effect of HTJZD on HLP may be due to the regulation of these genes.

3.7. Common Genes between Regulated DEGs and S-T. A total of 210 S-T were mapped to 301 targets (Supplemental Table 4) of *R. norvegicus* genomes in the HGNC. Furthermore, 10 common targets (Figure 9), namely, Prf1, Cyp3a62, Srebf1, Pcsk9, Cyp7a1, Aldh1b1, Mmp2, Insr, Cyp3a9, and Gck, were found between 301 targets and 202 regulated DEGs. It is clear that 10 common targets (Table 2) presented an opposite trend in the model group and HTJZD group in RNA sequencing analysis, which may be attributed to validity and feasibility. Therefore, these common targets were put into the g:Profiler website for KEGG pathway enrichment. The result (Table 3) showed four key pathways ($P < 0.05$), namely, steroid hormone biosynthesis pathway, insulin signaling pathway, cholesterol metabolism pathway, and linoleic acid metabolism pathway, involved in HTJZD in treating rats with hyperlipidemia. Moreover, six key targets, namely, Srebf1, Cyp7a1, Cyp3a9, Pcsk9, Insr, and Gck, were selected from the results for further validation.

3.8. Validation of the Hypolipidemic Effects of HTJZD by qRT-PCR Analysis. Six genes of Srebp-1c, Cyp7a1, Cyp3a9, Pcsk9, Insr, and Gck, closely associated with lipid metabolism and insulin signaling pathway, were selected for qRT-PCR analysis (Figure 10). Srebp-1c and Pcsk9 mRNA levels increased ($P < 0.01$) significantly in the M group compared with the N group, while the Cyp7a1, Cyp3a9, Insr, and Gck levels declined ($P < 0.05$), which indicated that HFD leads to the lipid–glucose metabolism disorders in SD rats. However, the mRNA expression in rats administered HTJZD showed a different picture. The expressions of Srebp-1c, Cyp3a9, and Insr mRNA were turning to a significant reversal ($P < 0.01$) in the H group when compared with the M group, which is consistent with the transcriptomic results, while Cyp7a1, Pcsk9, and Gck mRNA expression had no significant difference compared with rats with hyperlipidemia.

4. Discussion

Hyperlipidemia is a chronic disorder generally caused by a long-term unbalanced diet, which is manifested pathologically with aberrant lipid accumulation and energy metabolism disruption [26–28]. In addition, it is considered that lipid accumulation, especially ectopic fat deposition, leads to insulin resistance, impairing the lipolytic function of insulin, generating an amount of free fatty acids, and eventually accelerating the occurrence of metabolic diseases [29–31]. Therefore, attenuating hyperlipidemia via regulating lipid metabolism and insulin resistance could be effective solutions to reduce the biosynthesis of lipid and boost lipid consumption.

The results of active compounds collected from TCMSP indicated that HTJZD serves as a multicomponent prescription and especially contains the ingredients with lipid-lowering, glucose-reducing, and antioxidative effects. In the

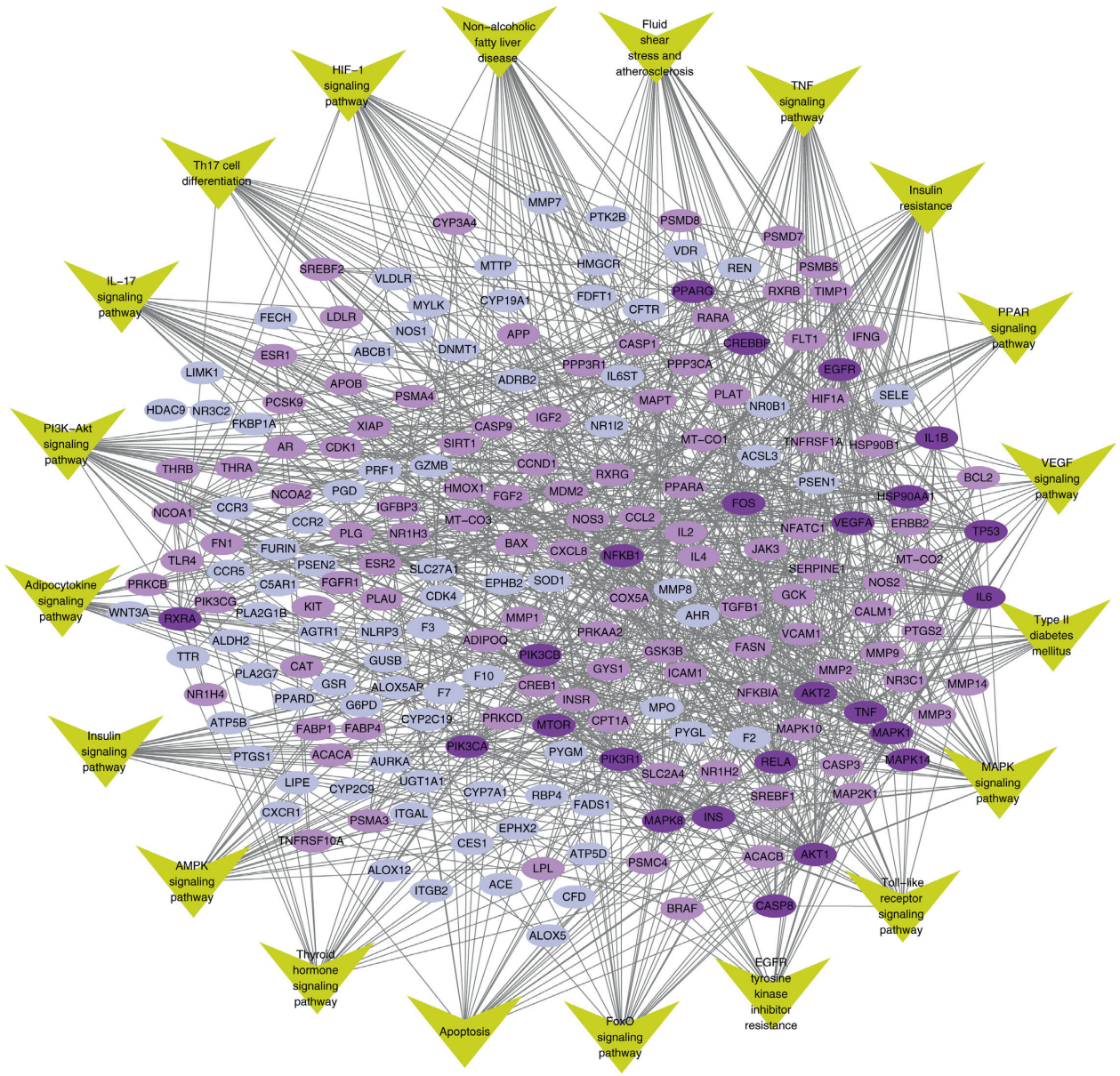

Figure 4: S-T–pathway network was constructed to present the "multipathway, multitarget" mechanism of HTJZD. It reveals the intersection of S-T and the relation between S-T and KEGG pathways. Green nodes represent the pathways, and nodes with gradient purple color are S-T. Depth of purple was determined by the degree value of nodes. The edge between the nodes was determined by the combined score analyzed by STRING.

herb–compound–S-T network, wogonin, naringenin, beta-sitosterol, baicalein, and kaempferol are the potential compounds that may play a significant role in suppressing the progression of hyperlipidemia. Wogonin, screened out from the compounds of Atractylodis Rhizoma, has been reported to have an antioxidative effect and protect HFD-fed rats from developing nonalcoholic fatty liver disease [32]. Naringenin, found in three compounds (Citri Reticulatae Pericarpium, Glycyrrhizae Radix et Rhizoma, and Citri Reticulatae Pericarpium Viride) of HTJZD, inhibits the expression of lipogenic genes and improves hepatic steatosis in middle-aged Apoe $^{-/-}$ mice [33]. Kaempferol also could effectively reduce the lipid accumulation in mice and alleviate the insulin resistance in diabetic rats [34, 35].

The animal experimental results showed that HTJZD could reverse ($P < 0.05$) TC level (Figure 5(b)) and Liver index (Figure 5(g)) in HFD-fed rat model. In addition, HTJZD showed advantages over atorvastatin in TG reduction (Figure 5(c)) and HDL-c elevation (Figure 5(e)), but these were not statistically significant. We speculate that if the administration time is extended, the advantages of this decoction for restoring the normal serum lipids will be more prominent. To further disclose the roles of HTJZD in hyperlipidemia treatment, RNA sequencing technique was performed to investigate the changes of RNA sequence in rat

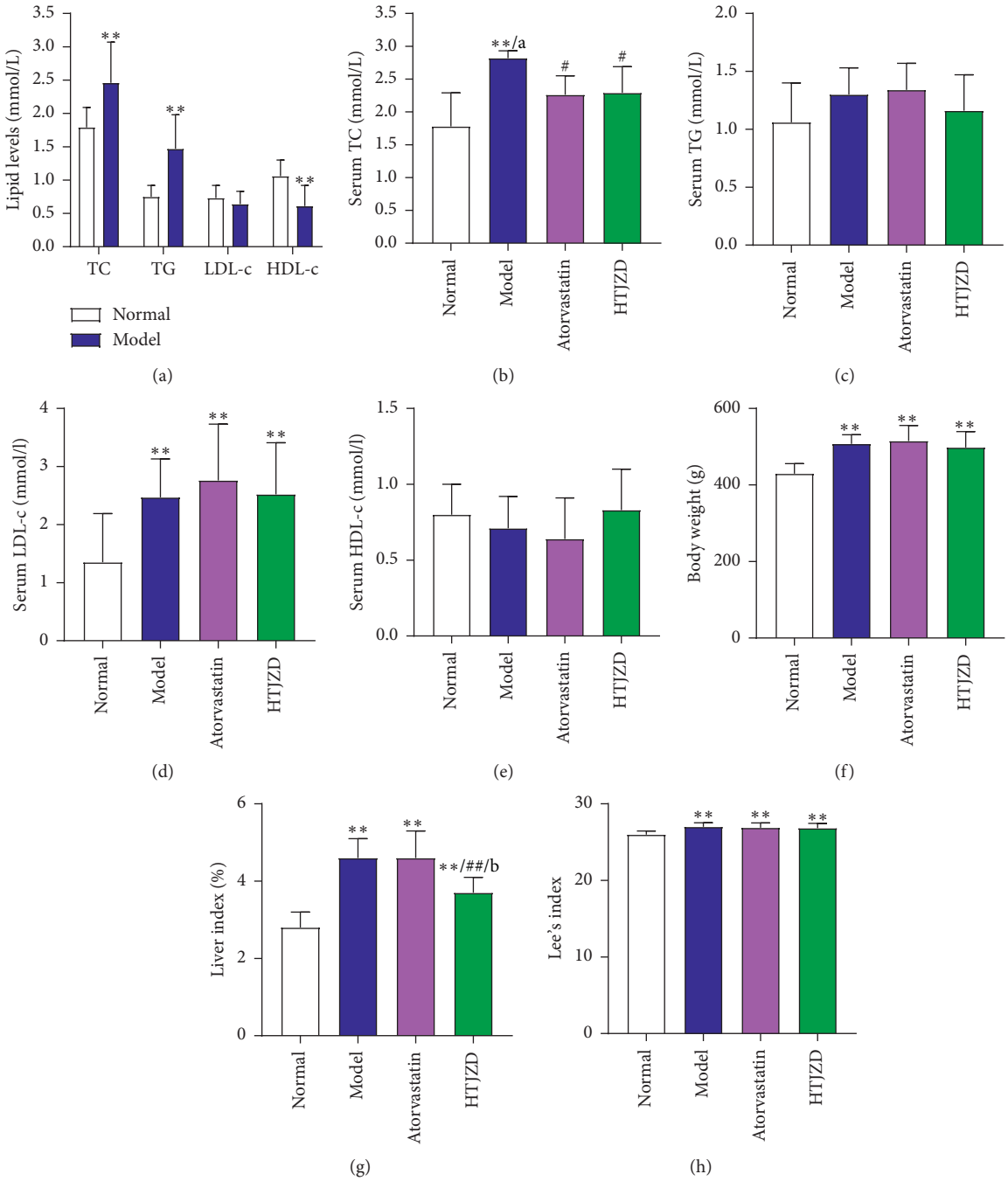

FIGURE 5: The rat model with hyperlipidemia was established by feeding HFD in male Sprague–Dawley rats after 30 days. (a) The lipid levels in rats after modeling time. After 4-week intervention, (b) serum TC, (c) serum TG, (d) serum LDL-c, (e) serum HDL-c level, (f) body weight, (g) liver index, and (h) Lee's index were analyzed to evaluate the hypolipidemic effect of HTJZD. Data were represented as the mean ± SD. $^{*}P < 0.05$, $^{**}P < 0.01$, compared with the normal group; $^{\#}P < 0.05$, $^{\#\#}P < 0.01$, compared with the model group; a: $P < 0.05$, b: $P < 0.01$, compared with the atorvastatin group.

liver. This study found that the expressions of 202 genes were conversely altered after the intervention of HTJZD, which showed that the intervention strategy had an impact on the disease.

Furthermore, the GO and KEGG analysis of S-T, S-T–pathway network, and KEGG pathway enrichment of 10 common genes between regulated DEGs and S-T all indicated that HTJZD exerted therapeutic action on hyperlipidemia by modulating lipid metabolism and insulin resistance. Lipid metabolism regulation should be considered as the pivotal function of HTJZD. With the transcript variants of Srebp-1a and Srebp-1c, Srebp1 (also known as Srebf1) is significant transcription factor involved in regulating liposomal homeostasis.

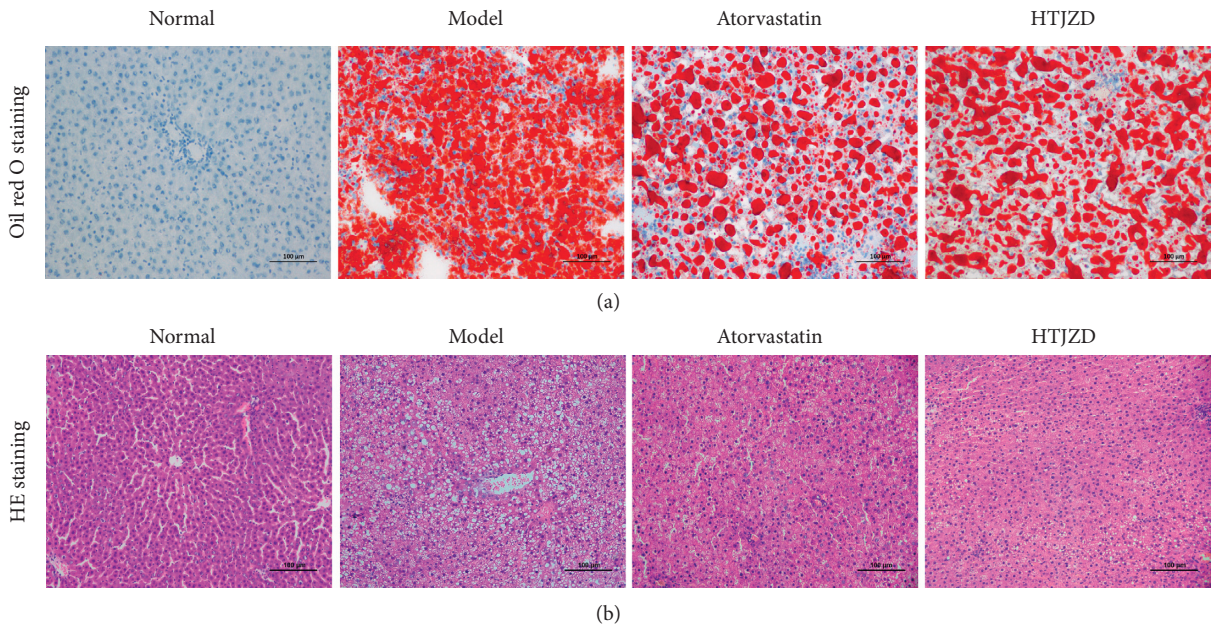

Figure 6: Liver samples were used for staining methods after 4-week intervention. (a) Oil Red O staining of liver tissue in each group (magnification, 200×). (b) HE staining of liver tissue in each group (magnification, 200×).

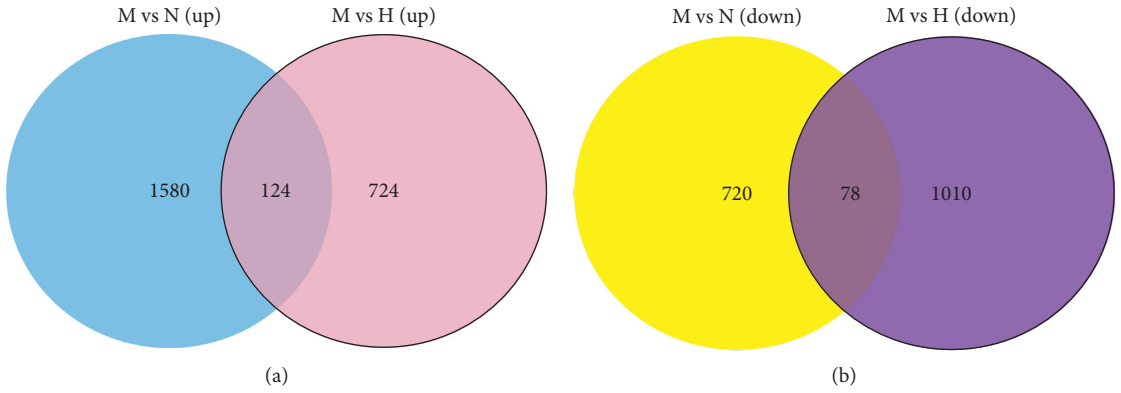

Figure 7: 202 regulated DEGs. A Venn diagram showing the distribution of overlapped DEGs of model group when compared with normal group and HTJZD group, respectively. 124 were the common genes upregulated both in model vs normal (blue part) and model vs HTJZD (pink part) groups. 78 were the shared genes downregulated both in model vs normal (yellow part) and model vs HTJZD (purple part) groups.

It transcriptionally regulates the expression of its downstream lipogenic genes involving in the synthesis of fatty acid and triglyceride [36, 37]. It is noted that the activation of AMPK could inhibit the activation of Srebp1 and acetyl-CoA carboxylase 1 (Acc1), leading to the reduction of lipid biosynthesis [38]. Cytochrome P450, family three, subfamily A (Cyp3a), is involved in the biological transformation of endogenous substrates and mainly mediates drug metabolism [39]. Moreover, when liver damage by HFD occurs, the expression and bioactivity of Cyp3a are impaired [40]. HTJZD could recover the expression of cytochrome P450, family three, subfamily A, polypeptide 9 (Cyp3a9), which is decreased by HFD and functions in two significant signaling pathways, that is, steroid hormone biosynthesis and linoleic acid metabolism, when HTJZD treats hyperlipidemia. In addition, proprotein convertase subtilisin/kexin type 9 (Pcsk9) and cholesterol 7α-hydroxylase (Cyp7a1) were the key genes both enriched in the cholesterol metabolism pathways in hyperlipidemia rats treated with HTJZD. Evidence from genetic studies supports the role of Pcsk9, a serine protease, in the regulation of hepatic apolipoprotein B uptake and degradation of low-density lipoprotein receptor (LDLR) [41–43]. Moreover, Pcsk9 is another downstream gene of Srebp-1c and is regulated by it, serving as a significant gene to promote cholesterol synthesis. Cyp7a1 is the rate-limiting enzyme, which is pivotal in the process of de novo bile acid synthesis [44, 45]. In addition, the activation of Cyp7a1 could inhibit

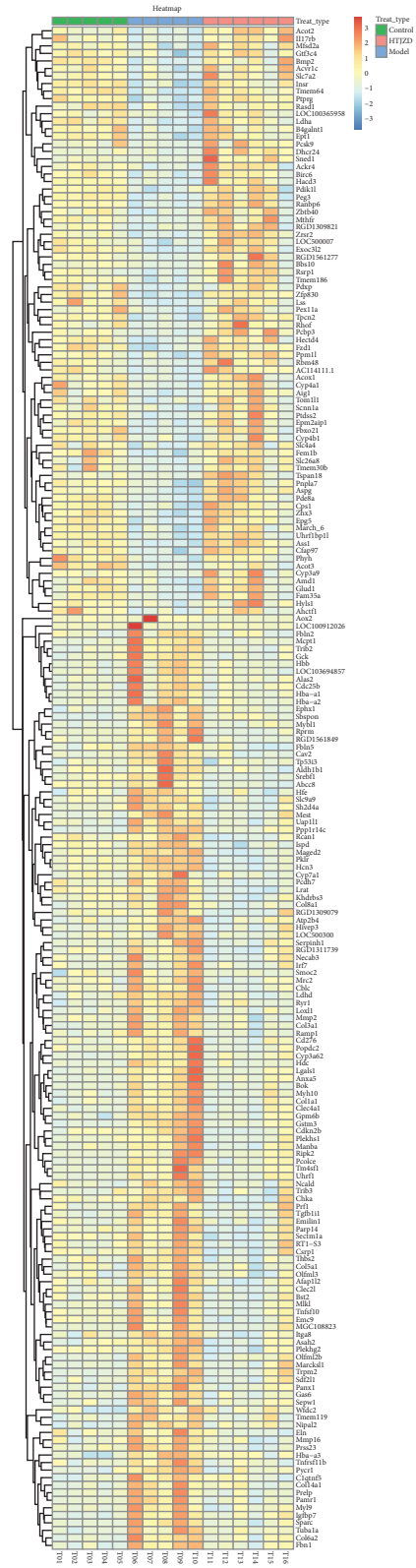

Figure 8: Hierarchical clustering heatmap of 202 regulated DEGs presenting different expression in liver samples of control group, model group, and HTZJD group, respectively. Samples are grouped by three modules on columns: T01-T05 within green module is control group; T06-T10 of blue module belongs to model group; T11-T16 clustered to pink module is HTJZD group. Expression of genes is represented on rows as a color lump in gradient color, transformed by FPKM and processed by pheatmap package in R Studio. Color scale is used to explain the variant expression of genes, with darker blue for lower values and brighter red for higher value.

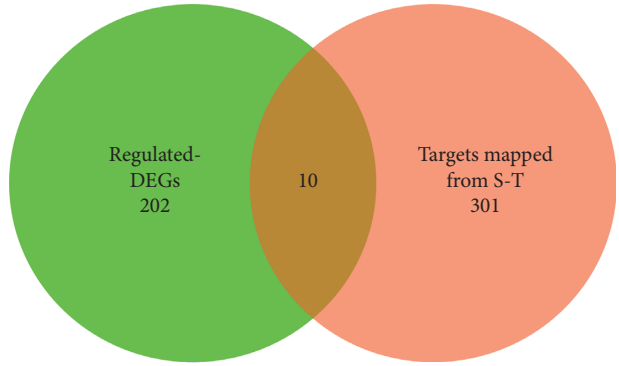

Figure 9: A Veen diagram showing 10 common targets between 202 regulated DEGs and 301 targets, mapped from the orthology of S-T in *Homo sapiens*.

Table 2: 10 common genes between regulated DEGs (HTJZD versus model) and S-T in RNA sequencing analysis.

Gene symbol	Fold change HTJZD vs model	FDR HTJZD vs model
Upregulated		
Pcsk9	3.606	0
Cyp3a9	2.935	0.007
Insr	1.682	0.012
Downregulated		
Srebp-1c	0.248	0
Gck	0.257	0
Cyp7a1	0.312	0.003
Aldh1b1	0.319	0.002
Prf1	0.488	0.04
Cyp3a62	0.497	0.014
Mmp2	0.519	0.008

Table 3: KEGG signaling pathways enrichment ($P < 0.05$) of 10 common genes.

Pathway ID	Pathway	Gene	*P*-value
KEGG:00140	Steroid hormone biosynthesis	Cyp3a62, Cyp7a1, Cyp3a9	0.001511
KEGG:04910	Insulin signaling pathway	Srebf1, Insr, Gck	0.017021
KEGG:04979	Cholesterol metabolism	Pcsk9, Cyp7a1	0.019844
KEGG:00591	Linoleic acid metabolism	Cyp3a62, Cyp3a9	0.030053

the function of Srebp-1c so as to inhibit the lipid accumulation [46, 47]. However, our transcriptomic results of this study about the expressions of Cyp7a1 and Pcsk9 were not in accordance with the reported ones. Nevertheless, some pertinent literature reported that the activation of Farnesoid X receptor (FXR, bile acid receptor) could induce the SHP so as to inhibit the expression of Cyp7a1 in the transcriptomic level [48, 49]. We speculated that HFD-fed rats had developed the symptoms of fatty liver and disorder of bile acid and consequently HTJZD could regulate bile acid metabolism by activating FXR.

Insulin resistance, regarded as another representative pathological feature of metabolic disorders, aggravating on account of the inhibition of the insulin receptor substrates (Irs) pathway, could also be regulated by AMPK signaling pathway [50]. Additionally, the initiation of insulin resistance could decrease AMPK phosphorylation, further increase the expression of Srebp-1c, and eventually suppress the Irs-1-related insulin signaling pathway [51]. The transcriptomic results showed the upregulation of Insr and downregulation of Srebp-1c in HTJZD-fed rats, indicating that HTJZD can activate the insulin signaling pathway while suppressing the insulin resistance pathway. Glucokinase (Gck) is a key enzyme in the regulation of glucose metabolism and insulin secretion. It is also the first rate-limiting enzyme in the glycolysis pathway. It catalyzes glucose phosphorylation and is a prerequisite for liver glycogen synthesis. Gck translocation mainly mediated whole-body glucose homeostasis, even the insulin-stimulated hepatic glycogen synthesis, which means that the activation of Gck could accelerate the synthesis process of hepatic glycogen and alleviate dysglycemia and dyslipidemia in liver [52]. However, our RNA sequencing results showed that Gck had not been improved by HTJZD, which indicated that HTJZD

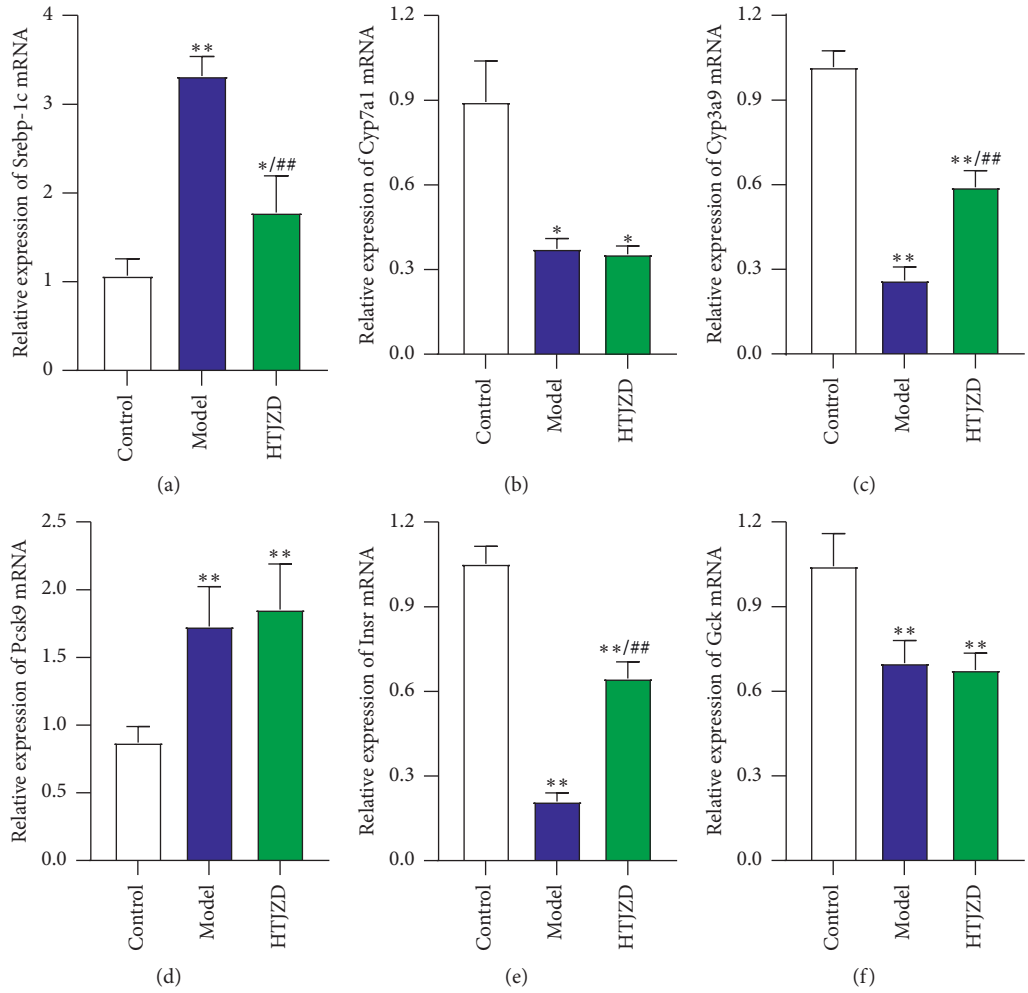

Figure 10: Validation of Srebp-1c (a), Cyp7a1 (b), Cyp3a9 (c), Pcsk9 (d), Insr (e), and Gck (f) mRNA expression levels in the liver tissues of rats by qRT-PCR analysis Data were expressed as mean ± SD. All the results were normalized to GAPDH mRNA expression. $^{*}P < 0.05$, $^{**}P < 0.01$, compared with the normal group; $^{\#}P < 0.05$, $^{\#\#}P < 0.01$, compared with the model group.

affects glucose metabolism in rats not through Gck associated pathways but mainly through Srebp-1c/Insr pathway.

Taken together, HTJZD acted as a hypolipidemic agent potentially via modulation of lipid metabolism and insulin resistance. An increasing number of studies report that the lipid metabolism-related signaling pathway and insulin signaling pathway could be regulated by natural compounds, which indicates that traditional herbal medicines are potential alternatives or supplements to treat metabolic diseases [53–55]. In addition, KEGG pathway enrichment results of 210 S-T also predict that HTJZD not only can treat hyperlipidemia, but also has the potential to cure other relevant diseases, such as type 2 II diabetes, nonalcoholic fatty liver disease, and obesity. Therefore, this study demonstrated the rationality of the principle of CM—treating different diseases with the same method—at the molecular mechanism level. It also reveals that invigorating the spleen and regulating qi, as well as reducing phlegm and removing turbidity, may be the scientific method of treating metabolic diseases in modern times.

5. Conclusion

Network pharmacology predicted that HTJZD may exert therapeutic effects on HLP. Moreover, the animal experiments verified that HTJZD effectively suppressed the pathological process of rat model fed with HFD. It is capable of regulating serum lipids of rats, reducing lipid deposition in rat's liver, and reversing the expression of genes which related to lipid metabolism and insulin resistence. Among six candidate targets (Srebp-1c, Cyp7a1, Cyp3a9, Pcsk9, Insr, and Gck), Srebp-1c and Insr may play central role in the treatment of hyperlipidemia.

5.1. Limitations. There are several limitations to the present study. Repeated experiments and prolonged intervention duration are needed in future studies. What has to be focused is whether the compensation mechanism, leading to the opposite expression of genes contrary to what was expected, exists in the liver sites with more severe lipid lesion. Furthermore, a blood glucose level test should be performed

to further support the intervention effect on insulin resistance of HTJZD. We will pursue a more systematic comprehensive analysis of HTJZD intervening hyperlipidemia and relevant metabolic disorders in future study.

Data Availability

The data used to support the results of this study are included within the article and the supplementary materials.

Ethical Approval

This study was approved by the Animal Experimental Ethics Committee of Guangzhou University of Chinese Medicine. We conformed to the provisions of the Helsinki Declaration as revised in 2013.

Disclosure

The authors are accountable for all aspects of the work in ensuring that questions related to the accuracy or integrity of any part of the work are appropriately investigated and resolved. Xiaowen Zhou and Zhenqian Yan are co-first authors.

Conflicts of Interest

The authors have no conflicts of interest to declare.

Authors' Contributions

Xiaowen Zhou and Xiaoqi Liu designed the protocol of study and drafted the manuscript. Xiaowen Zhou and Qi Ren participated in data collection and data analysis. Zhenqian Yan and Yaxin Wang participated in manuscript revision and polishing. Ge Fang and Bin Wang conducted the animal experiments. Xiantao Li guided this study and provided the administrative and laboratory equipment support. All the authors revised the manuscript critically and reached an agreement on the final version of the manuscript. Xiaowen Zhou and Zhenqian Yan contributed equally to this work.

Acknowledgments

This study was supported by the Natural Science Foundation of Guangdong Province (No. 2020A1515010725) and Key Areas of Research and Development Plan of Guangdong Province (No. 2020B1111100001). In addition, the authors thank the Research Center for Integrative Medicine of Guangzhou University of Chinese Medicine (Key Laboratory of Chinese Medicine Pathogenesis and Therapy Research) for experimental support. English editing services in terms of language and grammar revisions were provided by editors from http://www.enago.cn.

Supplementary Materials

Supplemental Table 1: 120 compounds of herbs in HTJZD meeting the criteria of OB ≥ 30% and DL ≥ 0.18 were picked up from TCMSP. Supplemental Table 2: 1001 compound-related targets (C-T) screened out from TCMSP, ETCM, and Swiss Target Prediction and 1297 disease-related targets (D-T) collected from DisGeNET and GeneCards. Supplemental Table 3: 202 regulated differentially expressed genes from RNA-seq analysis results. Supplemental Table 4: 301 targets of rat genomes mapped from the orthology of selected-targets (S-T) in human sapiens were obtained from HGNC. The supplemental materials are accessible to the interested readers on the website of Evidence-Based Complementary and Alternative Medicine. (*Supplementary Materials*)

References

[1] Y. Ling, Z. Shi, X. Yang et al., "Hypolipidemic effect of pure total flavonoids from peel of Citrus (ptfc) on hamsters of hyperlipidemia and its potential mechanism," *Experimental Gerontology*, vol. 130, Article ID 110786, 2020.

[2] Z. Xian, Y. Liu, W. Xu, F. Duan, Z. Guo, and H. Xiao, "The anti-hyperlipidemia effects of raw polygonum multiflorum extract in vivo," *Biological & Pharmaceutical Bulletin*, vol. 40, no. 11, pp. 1839–1845, 2017.

[3] X. Chen, W. Yu, W. Li et al., "An anti-inflammatory chalcone derivative prevents heart and kidney from hyperlipidemia-induced injuries by attenuating inflammation," *Toxicology and Applied Pharmacology*, vol. 338, pp. 43–53, 2018.

[4] H. Zhong, K. Chen, M. Feng et al., "Genipin alleviates high-fat diet-induced hyperlipidemia and hepatic lipid accumulation in mice via miR-142a-5p/SREBP -1c axis," *The FEBS Journal*, vol. 285, no. 3, pp. 501–517, 2018.

[5] H. I. H. El-Sayyad, "Cholesterol overload impairing cerebellar function: the promise of natural products," *Nutrition*, vol. 31, no. 5, pp. 6210–6230, 2015.

[6] W. Q. Ni, X. L. Liu, Z. P. Zhuo et al., "Serum lipids and associated factors of dyslipidemia in the adult population in shenzhen," *Lipids in Health and Disease*, vol. 14, p. 71, 2015.

[7] B. Ibanez, S. James, S. Agewall et al., "Esc guidelines for the management of acute myocardial infarction in patients presenting with st-segment elevation: the task force for the management of acute myocardial infarction in patients presenting with st-segment elevation of the European society of cardiology (esc)," *European Heart Journal*, vol. 39, no. 2, pp. 119–177, 2017.

[8] D. Thakker, S. Nair, A. Pagada, V. Jamdade, and A. Malik, "Statin use and the risk of developing diabetes: a network meta-analysis," *Pharmacoepidemiology and Drug Safety*, vol. 25, no. 10, pp. 1131–1149, 2016.

[9] Ž. Reiner, "Pcsk9 inhibitors in clinical practice: expectations and reality," *Atherosclerosis*, vol. 270, pp. 187-188, Mar 2018.

[10] F. J. Raal, E. A. Stein, R. Dufour et al., "Pcsk9 inhibition with evolocumab (amg 145) in heterozygous familial hypercholesterolaemia (Rutherford-2): a randomised, double-blind, placebo-controlled trial," *The Lancet*, vol. 385, no. 9965, pp. 331–340, 2015.

[11] S. Kang, H. Jeong, J. H. Baek et al., "Pib-pet imaging-based serum proteome profiles predict mild cognitive impairment and alzheimer's disease," *Journal of Alzheimer's Disease*, vol. 53, no. 4, pp. 1563–1576, 2016.

[12] J. Zhou, J. Chen, and S. S. Wei, "Traditional Chinese medicine based on spleen for treating hyperlipidemia," *Journal of*

Changchun University of Chinese Medicine, vol. 32, no. 2, pp. 309–312, 2016.

[13] J. P. Wang, J. M. Feng, L. F. Li, and C. Y. Zhang, "Treatment of hyperlipidemia from liver," *Jilin Journal of Traditional Chinese Medicine*, vol. 35, no. 11, pp. 1092–1094, 2015.

[14] T. Li and Y. Q. Zhao, "Discussion on hyperlipidemia based on the perspective of kidney blood," *Clinical Journal of Chinese Medicine*, vol. 5, no. 16, pp. 58-59, 2013.

[15] D. H. Peng, Y. P. Wang, X. Q. Liu, R. Xie, and X. T. Li, "Meta-analysis of curative effect of invigorating spleen to resolving phlegm on turbid phlegm syndrome of hyperlipidemia," *Tianjin Journal of Tranditional Chinese Medicine*, vol. 34, no. 11, pp. 733–737, 2017.

[16] E. Choi, E. Jang, and J. H. Lee, "Pharmacological activities of Alisma orientale against nonalcoholic fatty liver disease and metabolic syndrome: literature review," *Evidence-Based Complementary and Alternative Medicine*, vol. 2019, Article ID 2943162, 15 pages, 2019.

[17] H. Miao, Y. H. Zhao, N. D. Vaziri et al., "Lipidomics biomarkers of diet-induced hyperlipidemia and its treatment with Poria cocos," *Journal of Agricultural and Food Chemistry*, vol. 64, no. 4, pp. 969–979, 2016.

[18] Y. C. Chou, C. T. Ho, and M. H. Pan, "Immature Citrus reticulata extract promotes browning of beige adipocytes in high-fat diet-induced C57bl/6 mice," *J Agric Food Chemistry*, vol. 66, no. 37, pp. 9697–9703, 2018.

[19] D. H. Peng, *Study on the Effect and Mechanisms of Huatan Jiangzhuo Decoction Regulating Lipid Metabolism in Apoe-/- Mice With Phlegm Turbidity Syndrome of Hyperlipidemia*, Guangzhou University of Chinese Medicine, Guangzhou, China, 2017.

[20] Y. P. Wang, *The Study of Mechanisms of Huatan Jiangzhuo Decoction Regulating Lipid Metabolism in Apoe-/- Mice of Hyperlipidemia*, Guangzhou University of Chinese Medicine, Guangzhou, China, 2017.

[21] T.-t. Luo, Y. Lu, S.-k. Yan, X. Xiao, X.-l. Rong, and J. Guo, "Network pharmacology in research of Chinese medicine formula: methodology, application and prospective," *Chinese Journal of Integrative Medicine*, vol. 26, no. 1, pp. 72–80, 2020.

[22] X. Cai, X. Su, R. Wu, and S. B. Su, "Encountering strangers," *Chinese Urbanism*, vol. 13, p. 65, 2018.

[23] Y. P. Wang, D. H. Peng, X. Q. Liu, R. Xie, and X. T. Li, "Validation research and regulation exploration of highfat-introduced hyperlipidemia model in rat," *Chinese Journal of Comparative Medicine*, vol. 27, no. 1, pp. 5–10, 2017.

[24] D. H. Peng, Y. P. Wang, X. Q. Liu, and X. T. Li, "Experimental study on animal model of phlegm syndrome of hyperlipidemia and further thinking," *Chinese Archives of Traditional Chinese Medicine*, vol. 35, no. 9, pp. 2338–2341, 2017.

[25] "The evaluation method of auxiliary hypolipidemic function," *State Food and Drug Adiministration*, vol. 107, pp. 60–67, 2012.

[26] J. Dai, K. Liang, S. Zhao et al., "Chemoproteomics reveals baicalin activates hepatic Cpt1 to ameliorate diet-induced obesity and hepatic steatosis," *Proceedings of the National Academy of Sciences of the United States of America*, vol. 115, no. 26, pp. E5896–e905, 2018.

[27] A. A. van der Klaauw and I. S. Farooqi, "The hunger genes: pathways to obesity," *Cell*, vol. 161, no. 1, pp. 119–132, 2015.

[28] F. Wei, Y. Liu, C. Bi, and B. Zhang, "Nostoc sphaeroids kutz powder ameliorates diet-induced hyperlipidemia in C57bl/6j mice," *Food & Nutrition Research*, vol. 63, 2019.

[29] A. Tchernof and J. P. Després, "Pathophysiology of human visceral obesity: an update," *Physiological Reviews*, vol. 93, no. 1, pp. 359–404, 2013.

[30] E. N. Kuipers, N. M. Held, W. In et al., "A single day of high-fat diet feeding induces lipid accumulation and insulin resistance in Brown adipose tissue in mice," *American Journal of Physiology-Endocrinology and Metabolism*, vol. 317, no. 5, pp. E820–e30, 2019.

[31] N. Zhang, N. Zhang, L. Song et al., "Adipokines and free fatty acids regulate insulin sensitivity by increasing microrna-21 expression in human mature adipocytes," *Molecular Medicine Reports*, vol. 16, no. 2, pp. 2254–2258, 2017.

[32] B. Zhang, M. Li, Y. Zou et al., "Nfκb/Orai1 facilitates endoplasmic reticulum stress by oxidative stress in the Pathogenesis of non-alcoholic fatty liver disease," *Frontiers in Cell and Developmental Biology*, vol. 7, p. 202, 2019.

[33] Y. Q. Hua, Y. Zeng, J. Xu, and X. L. Xu, "Naringenin alleviates nonalcoholic steatohepatitis in middle-aged Apoe(-/-)Mice: role of Sirt1," *Phytomedicine*, vol. 81, Article ID 153412, 2021.

[34] Y. Lu, M. Shao, H. Xiang, P. Zheng, T. Wu, and G. Ji, "Integrative transcriptomics and metabolomics explore the mechanism of kaempferol on improving nonalcoholic steatohepatitis," *Food & Function*, vol. 11, no. 11, pp. 10058–10069, 2020.

[35] A. S. Alshehri, "Kaempferol attenuates diabetic nephropathy in streptozotocin-induced diabetic rats by a hypoglycaemic effect and concomitant activation of the Nrf-2/Ho-1/anti-oxidants axis," *Archives of Physiology and Biochemistry*, pp. 1–14, 2021.

[36] R. Bertolio, F. Napoletano, M. Mano et al., "Sterol regulatory element binding protein 1 couples mechanical cues and lipid metabolism," *Nature Communications*, vol. 10, no. 1, p. 1326, 2019.

[37] H. J. An, J. Y. Kim, M. G. Gwon et al., "Beneficial effects of Srebp decoy oligodeoxynucleotide in an animal model of hyperlipidemia," *International Journal of Molecular Sciences*, vol. 21, no. 2, p. 552, 2020.

[38] C. Moffat and M. Ellen Harper, "Metabolic functions of ampk: aspects of structure and of natural mutations in the regulatory gamma subunits," *IUBMB Life*, vol. 62, no. 10, pp. 739–745, 2010.

[39] F. Xie, X. Ding, and Q.-Y. Zhang, "An update on the role of intestinal cytochrome P450 enzymes in drug disposition," *Acta Pharmaceutica Sinica B*, vol. 6, no. 5, pp. 374–383, 2016.

[40] M. Li, B. Wang, B. Zhang, and X. Q. Liu, "Study on bioactivity change of Cyp3a in Chinese medicine," *Pharmacology and Clinics of Chinese Materia Medica*, vol. 26, no. 5, pp. 175–179, 2010.

[41] B. Di Bartolo, D. J. Scherer, A. Brown, P. J. Psaltis, and S. J. Nicholls, "Pcsk9 inhibitors in hyperlipidemia: current status and clinical outlook," *BioDrugs*, vol. 31, no. 3, pp. 167–174, 2017.

[42] M. C. McNutt, T. A. Lagace, and J. D. Horton, "Catalytic activity is not required for secreted Pcsk9 to reduce low density lipoprotein receptors in Hepg2 cells," *Journal of Biological Chemistry*, vol. 282, no. 29, pp. 20799–20803, 2007.

[43] C. Wu, C. Xi, J. Tong et al., "Design, synthesis, and biological evaluation of novel tetrahydroprotoberberine derivatives (thpbs) as proprotein convertase subtilisin/kexin type 9 (Pcsk9) modulators for the treatment of hyperlipidemia," *Acta Pharmaceutica Sinica B*, vol. 9, no. 6, pp. 1216–1230, 2019.

[44] D. Yang, C. Hu, X. Deng et al., "Therapeutic effect of chitooligosaccharide tablets on lipids in high-fat diets induced hyperlipidemic rats," *Molecules*, vol. 24, no. 3, 2019.
[45] Q. Wang, Y. Jiang, X. Luo et al., "Chitooligosaccharides modulate glucose-lipid metabolism by suppressing Smyd3 pathways and regulating gut microflora," *Marine Drugs*, vol. 18, no. 1, 2020.
[46] J. Yin, J. Wang, F. Li et al., "The fucoidan from the Brown seaweed ascophyllum nodosum ameliorates atherosclerosis in apolipoprotein E-deficient mice," *Food & Function*, vol. 10, no. 8, pp. 5124–5139, 2019.
[47] P. Costet, B. Cariou, G. Lambert et al., "Hepatic Pcsk9 expression is regulated by nutritional status via insulin and sterol regulatory element-binding protein 1c," *Journal of Biological Chemistry*, vol. 281, no. 10, pp. 6211–6218, 2006.
[48] A. H. Ali, E. J. Carey, and K. D. Lindor, "Recent advances in the development of farnesoid X receptor agonists," *Annals of Translational Medicine*, vol. 3, no. 1, p. 5, 2015.
[49] C. Zhang, Y. Gan, J. W. Lv et al., "The protective effect of obeticholic acid on lipopolysaccharide-induced disorder of maternal bile acid metabolism in pregnant mice," *International Immunopharmacology*, vol. 83, Article ID 106442, 2020.
[50] J. Naowaboot, S. Wannasiri, and P. Pannangpetch, "Morin attenuates hepatic insulin resistance in high-fat-diet-induced obese mice," *Journal of Physiology and Biochemistry*, vol. 72, no. 2, pp. 269–280, 2016.
[51] M. S. Seo, S. W. Hong, S. H. Yeon et al., "Magnolia officinalis attenuates free fatty acid-induced lipogenesis via ampk phosphorylation in hepatocytes," *J Ethnopharmacol*, vol. 157, pp. 140–148, 2014.
[52] Y. Nozaki, M. C. Petersen, D. Zhang et al., "Metabolic control analysis of hepatic glycogen synthesis in vivo," *Proceedings of the National Academy of Sciences of the United States of America*, vol. 117, no. 14, pp. 8166–8176, 2020.
[53] H. J. Han, X. Song, D. Yadav et al., "Ulmus macrocarpa hance modulates lipid metabolism in hyperlipidemia via activation of ampk pathway," *PLoS One*, vol. 14, no. 5, Article ID e0217112, 2019.
[54] C. Liu, J. Ma, J. Sun et al., "Flavonoid-rich extract of paulownia fortunei flowers attenuates diet-induced hyperlipidemia, hepatic steatosis and insulin resistance in obesity mice by ampk pathway," *Nutrients*, vol. 9, no. 9, 2017.
[55] J. T. Hwang, D. Y. Kwon, and S. H. Yoon, "Amp-activated protein kinase: a potential target for the diseases prevention by natural occurring polyphenols," *New Biotechnology*, vol. 26, no. 1-2, pp. 17–22, 2009.

Hindawi
Evidence-Based Complementary and Alternative Medicine
Volume 2021, Article ID 8856319, 15 pages
https://doi.org/10.1155/2021/8856319

Research Article

Kushenin Combined with Adefovir Dipivoxil or Entecavir for Chronic Hepatitis B: A Systematic Review and Meta-Analysis

Qingying Liao,[1] **Jianxia Wen**,[1,2] **Kunxiu Jiang**,[3] **Yanling Zhao**,[2] **and Xiao Ma**[1]

[1]*State Key Laboratory of Southwestern Chinese Medicine Resources, School of Pharmacy, Chengdu University of Traditional Chinese Medicine, Chengdu 611137, China*
[2]*Department of Pharmacy, The Fifth Medical Center of PLA General Hospital, Beijing 100039, China*
[3]*School of Pharmacy, Beijing University of Traditional Chinese Medicine, Beijing 102488, China*

Correspondence should be addressed to Xiao Ma; tobymaxiao@126.com

Received 16 September 2020; Revised 9 October 2020; Accepted 13 February 2021; Published 25 February 2021

Academic Editor: Hajime Nakae

Kushenin (KS) has become a traditional Chinese medicine preparation that plays an important role in treating chronic hepatitis B (CHB). Many clinical studies have discussed its curative effect and safety in combination with adefovir dipivoxil (ADV) or entecavir (ETV) for treating CHB, but there is still a lack of a systematic analysis. Therefore, this study evaluated the efficacy and safety of KS through a meta-analysis to better guide clinical treatment. Seven databases were searched to identify randomized controlled trials (RCTs) concerning KS combined with ADV or ETV for treating CHB. The primary outcomes included serum viral indices and adverse events, and the secondary outcomes were liver function indices. The risk of bias of the included RCTs was appraised by Cochrane software. STATA 15.1 and Review Manager 5.3 software were used for the meta-analysis. Thirty-two RCTs recruiting 3343 patients with CHB were collected for this meta-analysis. KS combined with ETV or ADV led to an amelioration of the CHB index to various degrees. In short, the meta-analysis indicated that the combination group, compared to the single group, showed great improvement in HBeAg seroconversion, frequency of undetectable HBV-DNA levels, loss of serum HBeAg, and loss of serum HBsAg. The combination treatment also decreased serum HBV-DNA levels when compared to the levels after the single treatment. However, KS combined with ADV or ETV displayed no remarkable difference in the incidence of adverse events or in serum ALT levels. Current evidence showed that, compared with the use of either drug alone, KS combined with ADV or ETV can improve the clinical efficacy of CHB treatment.

1. Introduction

Chronic hepatitis B (CHB), which is one of the most significant global health issues, seriously endangers the lives of humans worldwide. The number of people in the world who are chronically infected with hepatitis B virus exceeds 350 million, accounting for approximately 5% of the world's population [1]. Hepatitis B virus, which is a deoxyribonucleic acid virus of the hepadnaviridae family, only replicates in human hepatocytes and causes serious damage to human hepatocytes [2]. When human beings are infected with hepatitis B virus, if they do not receive effective treatment, the disease may slowly develop into liver fibrosis, cirrhosis and even hepatocellular carcinoma [3]. Therefore, it is very important to seek effective treatment for CHB to ensure a healthy life.

At present, there are mainly two methods used to treat CHB. One method is to take antiviral drugs, such as nucleoside analogues, which can prevent the release of infectious viruses; the other method is to use conventional or pegylated IFN-α to stimulate the patient's antiviral immune response [2]. However, antiviral therapy, which is the use of antiviral drugs such as nucleoside/nucleotide analogues to treat patients with CHB, not only has a high relapse rate after drug withdrawal but also promotes the development of drug resistance in the virus, thus accelerating the deterioration caused by the disease. In addition, immunomodulators such as conventional or polyethylene glycol interferon have very limited curative effects, and some side effects, such as flu-like symptoms, may occur during the treatment process [2, 4]. Consequently, we still need to find a safer and more effective therapy for CHB.

China is a region with a high incidence of CHB and has a long history using traditional Chinese medicine (TCM) to treat CHB, leading to increasingly improved treatment concepts and clinical experience [5]. Currently, TCM is still widely used to help patients with CHB in China and other countries. For example, some clinical studies show that more than 80% of the natural products considered helpful for liver diseases are Chinese herbal medicines or their extracts [6].

Consequently, therapy in which TCM is integrated with modern medicine has gradually become an important way to treat CHB. For example, Kushenin (KS) combined with adefovir dipivoxil (ADV) or entecavir (ETV) for CHB patients has an obvious curative effect, as confirmed in many clinical studies. However, an analysis of its curative effect and application characteristics from the perspective of evidence-based pharmacy is still lacking. To provide possibly better alternative therapies for global application, this study presented a meta-analysis of KS combined with ADV or ETV for patients with CHB and evaluated its efficacy through indicators such as serum liver fibrosis, serum viral indices, liver function index, and adverse events.

2. Materials and Methods

2.1. Research Registration. This research programme has been registered in PROSPERO, and the PROSPERO registration number is CRD42019138487.

2.2. Ethical Approval and Consent to Participate. As the current study does not involve animal experiments and patient consent, the ethics approval and consent to participate are not applicable.

2.3. Database and Search Strategy. The following English and Chinese databases were comprehensively searched by two researchers: China National Knowledge Infrastructure (CNKI), PubMed, Chinese Biomedical Database, Wanfang, Embase, Cochrane Library, and VIP medicine information system. The dates ranged from the inception of the databases to Sep 2020. The search strategy included only terminologies related to the intervention. Search terms included "Kushenin," "chronic hepatitis B," "adefovir dipivoxil," and "entecavir," and the search strategies were adjusted in different databases.

2.4. Inclusion Criteria. Four main inclusion criteria are listed as follows. (1) The studies were randomized controlled trials (RCTs) that were published in Chinese or English. (2) The diagnostic criteria of the patients with CHB conformed to those outlined in the "Viral Hepatitis Prevention Plan" or the "Guidelines for the Prevention and Treatment of Chronic Hepatitis B," and the hepatitis B e antigen (HBeAg) test was positive. (3) Subjects in the control group take only ADV or ETV. Patients in the experimental group take KS combined with ADV or ETV, and the administration route must be oral. The treatment course of the experimental group must be the same as that of the control group. (4) Studies with sufficient objective results were selected for this analysis. The primary outcomes of this review were serum viral indices and adverse events, and the secondary outcomes of this review included the liver function indices. The measured results in the current study were all based on reference to a certain period after the end of treatment. The included trials should report at least one of the aforementioned outcomes.

2.5. Exclusion Criteria. Studies meeting any of the following criteria were excluded from the analysis: (1) studies in which the subjects presented with severe symptoms, such as liver failure and liver cirrhosis or complications with other viral hepatitis diseases, autoimmune hepatitis, drug-induced hepatitis, hereditary liver disease, and so on, (2) non-RCTs such as literature reviews, comments, and animal experiments, (3) nonoriginal research or duplicate publications, (4) studies with missing data or incorrect data, and (5) literature with poor research quality or insufficient evaluation of outcomes.

2.6. Data Extraction. Two researchers searched the aforementioned Chinese and English databases, according to the retrieval strategy to obtain studies that may meet the inclusion criteria. Then, they read the full text of these articles and decided on the final studies to be included according to the inclusion and exclusion criteria. Data extraction was executed independently by two other researchers. Extracted information included baseline information of patients, intervention and control measures, outcome data, and other information, and these detailed data were imported into Cochrane Review Manager 5.3 to be prepared for further analysis. Missing data were requested from the corresponding authors.

2.7. Risk of Bias Assessment. A quality assessment of the included RCTs was carried out independently by two researchers with the use of the Cochrane risk of bias tool, which is a common tool for evaluating methodological quality. This tool has seven aspects, including blinding of participants and personnel (performance bias), random sequence generation (selection bias), blinding of outcome data (attrition bias), allocation concealment (selection bias), selective reporting (reporting bias), incomplete outcome data (attrition bias), and other sources of bias. Finally, three evaluation outcomes were noted for each aspect: high risk, low risk, and unclear risk. Studies that satisfied all criteria were classified as low risk. Trials that did not meet any criteria were classified as high risk. Studies were classified as unclear risk of bias if there was not enough information to make a judgment. Any differences arising in the process of study retrieval, data extraction, and quality assessment were settled through discussion and negotiation with another researcher.

2.8. Data Analysis. All data analyses were carried out by using STATA 15.1 and Cochrane Review Manager 5.3. Relative risk (RR) was used for binary variables, and

standardized mean difference (SMD) was used for continuous variables. Heterogeneity between the studies in effect measures was assessed using both the P test and the I^2 statistic. In detail, the I^2 value greater than 50% and the P value less than 0.01 were considered indicative of substantial heterogeneity, at which point the random effect model was used; otherwise, the fixed effect model was adopted.

Publication bias was evaluated by funnel plot analysis. If scatter points were symmetrically distributed on both sides of the funnel, the possibility of publication bias was small; otherwise, the possibility of publication bias was large. If the necessary data were available, subgroup analyses were carried out according to different treatment period.

3. Results

3.1. Characteristics of Included Trials. In total, 629 related studies were retrieved through the database search. Following the removal of 386 duplicated citations, 243 potentially relevant records were reserved. Next, 54 studies with comments and irrelevant to the study were further removed. Full-text articles of 189 publications were evaluated for further assessment. Among them, trials with insufficient evaluation of outcomes, animal studies, and trials not meeting evaluation and intervention criteria were excluded. Finally, a total of 32 trials recruiting 3343 patients were included for subsequent meta-analysis after reading the full-text [7–38] (Figure 1). Of these 32 articles, 18 articles included subjects treated with KS and ADV [7–24], and 14 articles included subjects treated with KS and ETV [25–38]. The control group was treated with ADV (10 mg/d, po, qd) or ETV (0.5 mg/d, po, qd) alone. Most of the experiment group was given KS (0.2 g/time, po, tid) [7–9, 11–14, 16, 18–21, 23–38] on the basis of the control group, and several studies used different doses of KS, 0.15 g/time, po, tid [17], 0.3 g/time, po, tid [10, 15], and 0.4 g/time, po, tid [22]. All drugs were administered orally. No significant differences appeared in the age, course of disease, or sex between the two groups, and fourteen studies reported slight adverse events (Table 1).

3.2. Methodological Quality of Included Trials. The methodological quality of the 32 included RCTs was evaluated and is presented in Figure 2. All trials were described as RCTs, of which five trials described the randomization method in detail [8, 17, 30, 31, 35]. Four trials [17, 31, 37, 38] adopted the random number table method and were considered to be of low risk of selection bias as the patients were randomly divided into two groups. All RCTs had complete data. However, the allocation concealment, blinding of participants and personnel, other bias reports, and blinding of outcome assessments were unclear in all trials. At the same time, the selective reporting of most studies was unclear, with only 10 studies considered to be of low risk with respect to reporting bias [8–11, 15, 16, 19, 25, 26, 31] (Figure 2).

3.3. Outcome Measures

3.3.1. Undetectable Serum HBV-DNA Rate. Thirty-two studies reported the undetectable serum HBV-DNA rate [7–38], 18 of which were in the KS + ADV group and the other 14 were in the KS + ETV group. Meta-analysis results showed that, compared with the ADV group, the KS + ADV group presented a significant improvement in the undetectable serum HBV-DNA rate (RR = 1.29, 95% CI (1.21, 1.39), $P < 0.00001$) ($I^2 = 13.0\%$, $P = 0.30$). Compared with the ETV group, the KS + ETV group also showed a significant improvement in the undetectable serum HBV-DNA rate [RR = 1.27, 95% CI (1.20, 1.34), $P < 0.00001$] ($I^2 = 59\%$, $P = 0.003$) (Figure 3).

3.3.2. Loss of Serum HBeAg Rate. Twenty-three studies [7–12, 14, 16, 19, 20, 23–35] reported the loss of serum HBeAg rate, 12 of which were in the KS + ADV group and the other 11 were in the KS + ETV group. Meta-analysis results showed that, compared with the ADV group, the KS + ADV group presented a significant improvement in the rate of loss of serum HBeAg [RR = 1.75, 95% CI (1.50, 2.03), $P < 0.00001$] ($I^2 = 0.0\%$, $P = 0.98$). Compared with the ETV group, the KS + ETV group also showed a significant improvement in the loss of serum HBeAg rate [RR = 1.59, 95% CI (1.41, 1.79), $P < 0.00001$] ($I^2 = 0.0\%$, $P = 0.66$) (Figure 4).

3.3.3. HBeAg Seroconversion Rate. Twenty-five studies reported the HBeAg seroconversion rate [8, 9, 11–15, 17–19, 21–26, 29, 30, 32–38], 14 of which belong to the KS + ADV group and the other 11 belong to the KS + ETV group. The meta-analysis results showed that, compared with the ADV group, the KS + ADV group had a significant improvement in the HBeAg seroconversion rate [RR = 1.90, 95% CI (1.61, 2.23), $P < 0.00001$] ($I^2 = 0.0\%$, $P = 0.99$). Compared with the ETV group, the KS + ETV group also showed a significant improvement in the HBeAg seroconversion rate [RR = 1.94, 95% CI (1.64, 2.28), $P < 0.00001$] ($I^2 = 11\%$, $P = 0.34$) (Figure 5).

3.3.4. Loss of Serum HBsAg Rate. Six studies reported the loss of serum HBsAg rate [9, 10, 12, 24, 31, 38], four of which were in the KS + ADV group and the other two were in the KS + ETV group. The meta-analysis results show that, compared with the ADV group, the KS + ADV group presented a significant improvement in the loss of serum HBsAg rate [RR = 3.01, 95% CI (1.32, 6.88), $P = 0.009$] ($I^2 = 0.0\%$, $P = 0.84$). Compared with the ETV group, the KS + ETV group also showed a significant improvement in the loss of serum HBsAg rate [RR = 1.67, 95% CI (1.34, 2.09), $P < 0.00001$] ($I^2 = 0.0\%$, $P = 0.75$) (Figure 6).

3.3.5. ALT Normalization Rate and Serum ALT Levels. Twenty-six studies reported the ALT normalization rate [7–16, 19–30, 33–36], 16 of which were in the KS + ADV group and the other 10 were in the KS + ETV group. The meta-analysis results show that, compared with the ADV

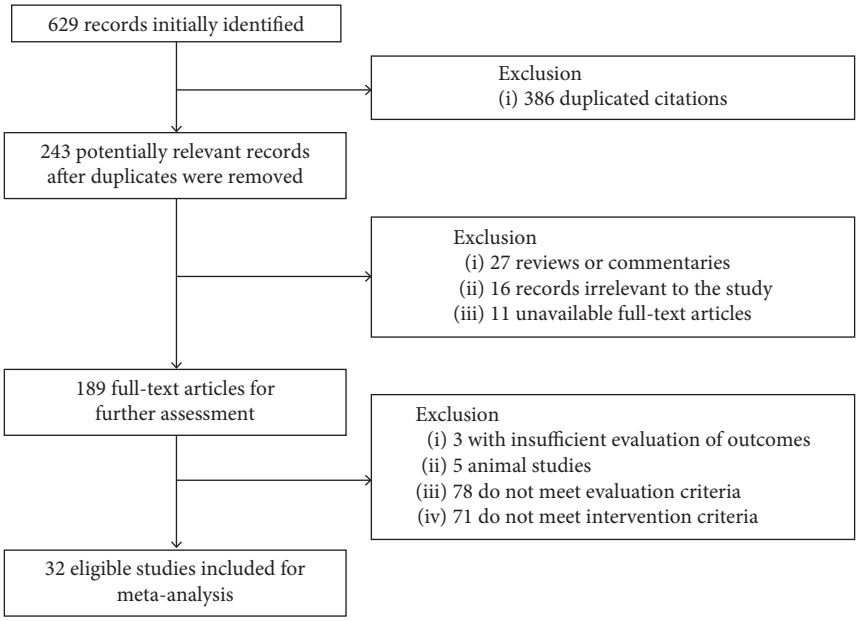

Figure 1: Flowchart of research selection.

Table 1: Characteristics of included studies on KS combined with ADV or ETV for the treatment of CHB.

Author, year	Cases C/T	Age (years) range, mean	Gender: male/female	Interventions C/T	Dosage and route of administration	Course of treatment	Adverse events	Outcome measures
Li et al., 2020	90/90	22–42, 32.3 ± 8.7	127/53	C: ETV T: ETV + KS	ETV: 0.5 mg/d, po, qd KS: 0.2 g/time, po, tid	6 months	NR	①③④
Xia et al., 2020	51/51	C: 18–63, 48 ± 9 T: 20–65, 48 ± 9	C: 29/22 T: 27/24	C: ETV T: ETV + KS	ETV: 0.5 mg/d, po, qd KS: 0.2 g/time, po, tid	1 year	√	①④⑦
Zhao and Li, 2019	62/62	C: 19–57, 32.56 ± 7.38 T: 21–58, 31.43 ± 6.79	C: 44/18 T: 45/17	C: ETV T: ETV + KS	ETV: 0.5 mg/d, po, qd KS: 0.2 g/time, po, tid	48 weeks	√	①④⑤⑥⑦
Wang et al., 2017	50/50	32.34 ± 7.44	C: 30/20 T: 32/18	C: ETV T: ETV + KS	ETV: 0.5 mg/d, po, qd KS: 0.2 g/time, po, tid	48 weeks	NR	①②⑤⑥⑦
Kang, 2016	40/40	47.5 ± 4.7	43/37	C: ETV T: ETV + KS	ETV: 0.5 mg/d, po, qd KS: 0.2 g/time, po, tid	48 weeks	0	①②③
Zhang et al., 2016	104/112	C: 21–57 T: 22–58	C: 57/47 T: 63/49	C: ETV T: ETV + KS	ETV: 0.5 mg/d, po, qd KS: 0.2 g/time, po, tid	48 weeks	NR	①②③④⑤⑦
Sun, 2016	53/53	39.5 ± 4.7	79/27	C: ETV T: ETV + KS	ETV: 0.5 mg/d, po, qd KS: 0.2 g/time, po, tid	12 months	√	①②③④⑤⑦
Fang et al., 2014	30/60	16–65	NR	C: ADV T: ADV + KS	ADV: 10 mg/d, po, qd KS: 0.2 g/time, po, tid	24 months	√	①②③

Table 1: Continued.

Author, year	Cases C/T	Age (years) range, mean	Gender: male/female	Interventions C/T	Dosage and route of administration	Course of treatment	Adverse events	Outcome measures
Qian and Hu, 2014	48/44	C: 35.13 ± 7.45 T: 34.27 ± 6.23	C: 41/7 T: 35/9	C: ADV T: ADV + KS	ADV: 10 mg/d, po, qd KS: 0.2 g/time, po, tid	1 year	√	①②③④⑤⑦
Ren et al., 2014	48/52	47.5 ± 4.8	53/47	C: ETV T: ETV + KS	ETV: 0.5 mg/d, po, qd KS: 0.2 g/time, po, tid	48 weeks	√	①②③
Wu, 2013	42/40	C: 36.6 ± 8.6 T: 36.9 ± 6.9	C: 24/18 T: 23/17	C: ADV T: ADV + KS	ADV: 10 mg/d, po, qd KS: 0.3 g/time, po, tid	12 months	0	①③④
Xu and Liang, 2013	40/40	16–65	NR	C: ADV T: ADV + KS	ADV: 10 mg/d, po, qd KS: 0.2 g/time, po, tid	48 weeks	√	①②③
Zhang, 2013	38/38	46.8 ± 3.9	39/37	C: ADV T: ADV + KS	ADV: 10 mg/d, po, qd KS: 0.2 g/time, po, tid	48 weeks	√	①③④
Gong and Sheng, 2013	50/52	C: 35.1 ± 4.5 T: 32.2 ± 5.6	C: 41/9 T: 42/10	C: ETV T: ETV + KS	ETV: 0.5 mg/d, po, qd KS: 0.2 g/time, po, tid	1 year	√	①②③④⑤⑦
Zhang et al., 2013	50/59	C: 31.5 (26, 37) T: 33.0 (28, 44)	C: 29/21 T: 38/21	C: ETV T: ETV + KS	ETV: 0.5 mg/d, po, qd KS: 0.4 g/time, po, tid	48 weeks	√	①②③④
Shen, 2013	36/34	16–48	42/28	C: ADV T: ADV + KS	ADV: 10 mg/d, po, qd KS: 0.2 g/time, po, tid	48 weeks	NR	①③④
Zhao, 2013	104/104	C: 32.8 ± 4.7 T: 31.3 ± 4.6	C: 68/36 T: 72/32	C: ETV T: ETV + KS	ETV: 0.5 mg/d, po, qd KS: 0.2 g/time, po, tid	1 year	NR	①②③④
Yin, 2013	50/50	C: 42.8 ± 8.1 T: 44.1 ± 9.2	C: 30/20 T: 29/21	C: ADV T: ADV + KS	ADV: 10 mg/d, po, qd KS: 0.2 g/time, po, tid	12 months	√	①②③④⑤⑦
Hu and Sun, 2012	52/54	C: 30.63 ± 10.53 T: 29.48 ± 8.27	C: 34/18 T: 38/16	C: ADV T: ADV + KS	ADV: 10 mg/d, po, qd KS: 0.2 g/time, po, tid	52 weeks	√	①②③④⑤
Lv et al., 2011	50/54	C: 33.5 T: 32.5	C: 39/11 T: 42/12	C: ADV T: ADV + KS	ADV: 10 mg/d, po, qd KS: 0.3 g/time, po, tid	9 months	0	①②③⑥
Yan et al., 2011	62/70	C: 32 ± 6 T: 32 ± 6	C: 49/13 T: 52/18	C: ADV T: ADV + KS	ADV: 10 mg/d, po, qd KS: 0.15 g/time, po, tid	52 weeks	√	①④
Yang et al., 2011	40/40	22–48 (37)	48/32	C: ADV T: ADV + KS	ADV: 10 mg/d, po, qd KS: 0.2 g/time, po, tid	12 months	√	①④⑦

Table 1: Continued.

Author, year	Cases C/T	Age (years) range, mean	Gender: male/female	Interventions C/T	Dosage and route of administration	Course of treatment	Adverse events	Outcome measures
Zhang, 2011	34/30	C: 35 T: 33	C: 23/11 T: 18/12	C: ADV T: ADV + KS	ADV: 10 mg/d, po, qd KS: 0.2 g/time, po, tid	3 years	√	①②③④
Cheng 2011	44/48	34 ± 5.8	63/29	C: ETV T: ETV + KS	ETV: 0.5 mg/d, po, qd KS: 0.2 g/time, po, tid	48 weeks	NR	①②③④
Yin and Ni, 2011	30/30	NR	NR	C: ETV T: ETV + KS	ETV: 0.5 mg/d, po, qd KS: 0.2 g/time, po, tid	48 weeks	NR	①②④
Shen, 2010	34/38	16–65	42/30	C: ADV T: ADV + KS	ADV: 10 mg/d, po, qd KS: 0.2 g/time, po, tid	12 months	NR	①②③④⑥
Zhang and Hu, 2010	32/46	C: 31.3 ± 7.9 T: 32.5 ± 8.3	C: 22/10 T : 32/14	C: ADV T: ADV + KS	ADV: 10 mg/d, po, qd KS: 0.2 g/time, po, tid	12 months	√	①③④
Zhou, 2010	115/115	42.5 ± 4.8	168/62	C: ADV T: ADV + KS	ADV: 10 mg/d, po, qd KS: 0.3 g/time, po, tid	48 weeks	√	①②③④⑥
Shao and Zhang, 2010	44/48	34 ± 5.8	63/29	C: ETV T: ETV + KS	ETV: 0.5 mg/d, po, qd KS: 0.2 g/time, po, tid	48 weeks	NR	①②③④
Zhang, 2009	40/40	18–55 (38)	60/20	C: ADV T: ADV + KS	ADV: 10 mg/d, po, qd KS: 0.2 g/time, po, tid	1 year	NR	①②③
Wei et al., 2008	39/33	15–65	43/29	C: ADV T: ADV + KS	ADV: 10 mg/d, po, qd KS: 0.2 g/time, po, tid	48 weeks	NR	①②③④
Liu et al., 2007	30/34	16–65	NR	C: ADV T: ADV + KS	ADV: 10 mg/d, po, qd KS: 0.2 g/time, po, tid	12 months	0	①②③④⑥

① Undetectable serum HBV-DNA rate, ② loss of serum HBeAg rate, ③ ALT normalization rate, ④ HBeAg seroconversion rate, ⑤ serum HBV-DNA level, ⑥ loss of serum HBsAg rate, and ⑦ serum ALT levels. 0, reported with no cases. Kushenin: KS; ADV: adefovir dipivoxil; ETV: entecavir; CHB: chronic hepatitis B; NR: not reported; C: control groups; T: trial groups; HBeAg: hepatitis B e antigen; HBsAg: hepatitis B surface antigen; ALT: alanine aminotransferase.

group, the KS + ADV group had a significant improvement in the ALT normalization rate [RR = 1.17, 95% CI (1.08, 1.26), $P = 0.0001$] ($I^2 = 60\%$, $P = 0.001$) (Figure 7(a)). Compared with the ETV group, the KS + ETV group also showed a significant improvement in the ALT normalization rate [RR = 1.08, 95% CI (1.03, 1.14), $P = 0.003$] ($I^2 = 0.0\%$, $P = 0.57$) (Figure 7(a)).

Nine studies reported serum ALT levels [11, 17, 19, 26, 30, 31, 34, 37, 38], three of which were in the KS + ADV group and the other six were in the KS + ETV group. The meta-analysis results indicate that, compared with ADV, KS + ADV did not show a significant effect on the serum ALT levels [SMD = −0.16, 95% CI (−0.50, 0.19), $P = 0.37$] ($I^2 = 57\%$, $P = 0.10$). Compared with ETV, KS + ETV also showed no significant effect on the serum ALT levels [SMD = −1.09, 95% CI (−2.17, 0.00), $P = 0.05$] ($I^2 = 97\%$, $p < 0.00001$) (Figure 7(b)).

3.3.6. Serum HBV-DNA Levels. Eight studies reported serum HBV-DNA levels [8, 11, 19, 26, 30, 31, 34, 38], three of which were in the KS + ADV group and the other five were in the KS + ETV group. The meta-analysis results show that, compared with the ADV group, the KS + ADV group

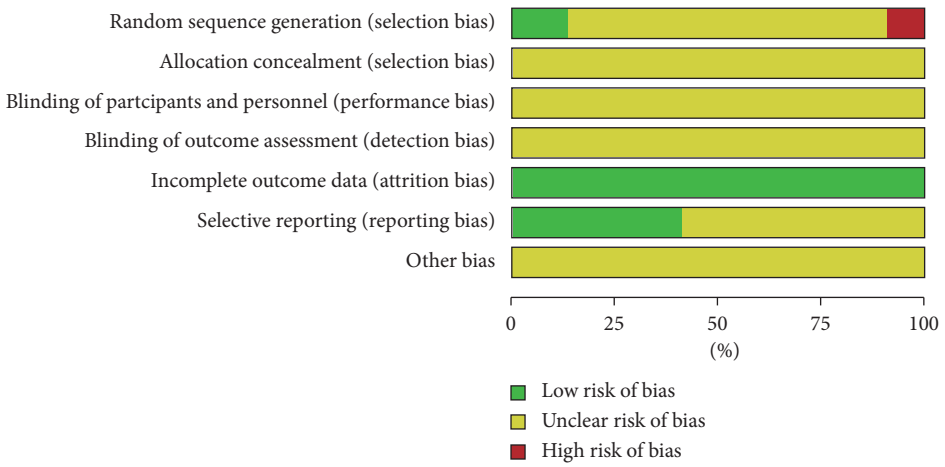

Figure 2: Methodological quality assessment of the included studies. Red square indicates a high risk of bias, green square indicates low risk of bias, and blank square indicates unclear risk of bias.

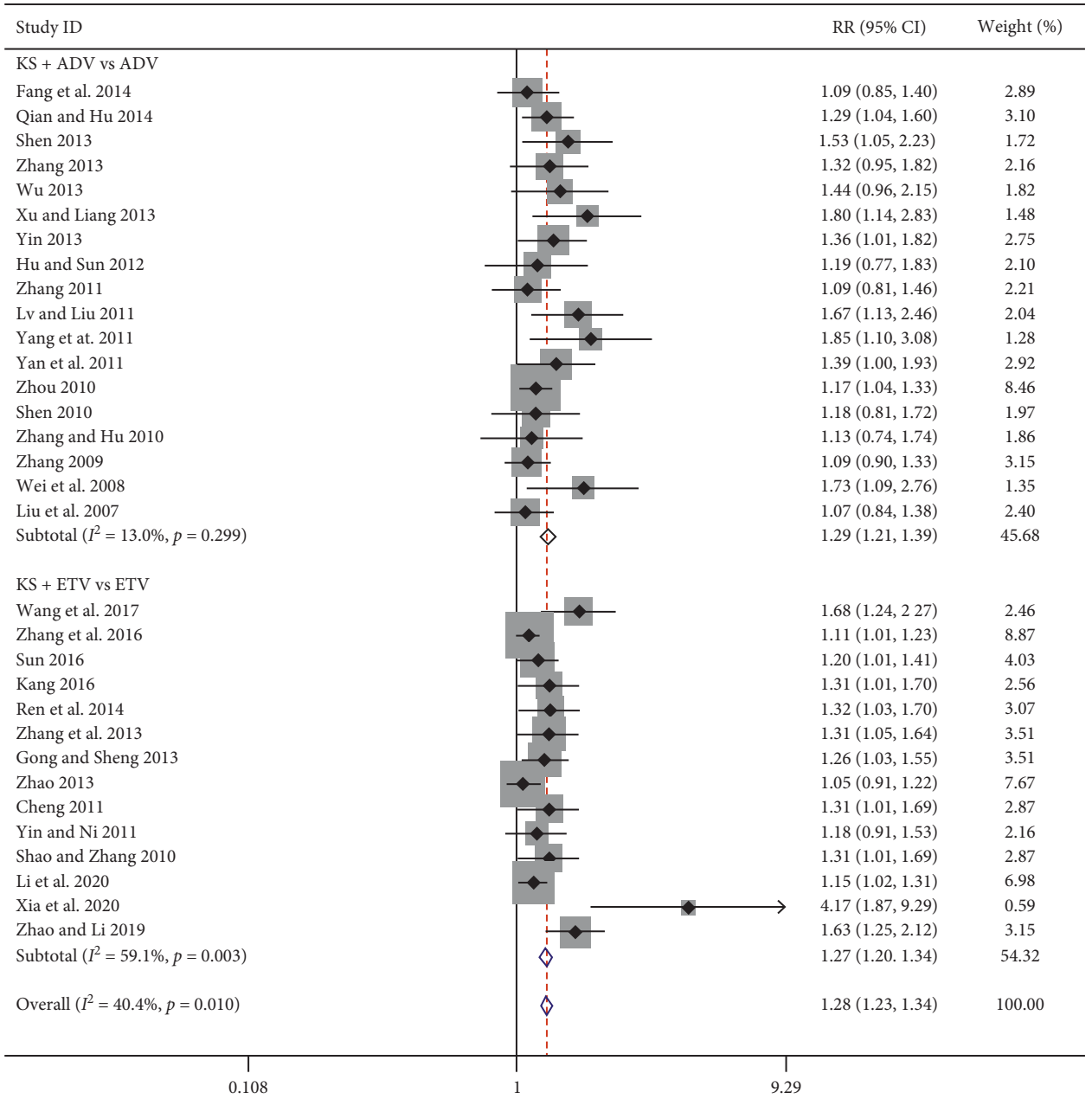

Figure 3: Forest plot of undetectable serum HBV-DNA rate in CHB patients treated with KS combined with ADV or ETV.

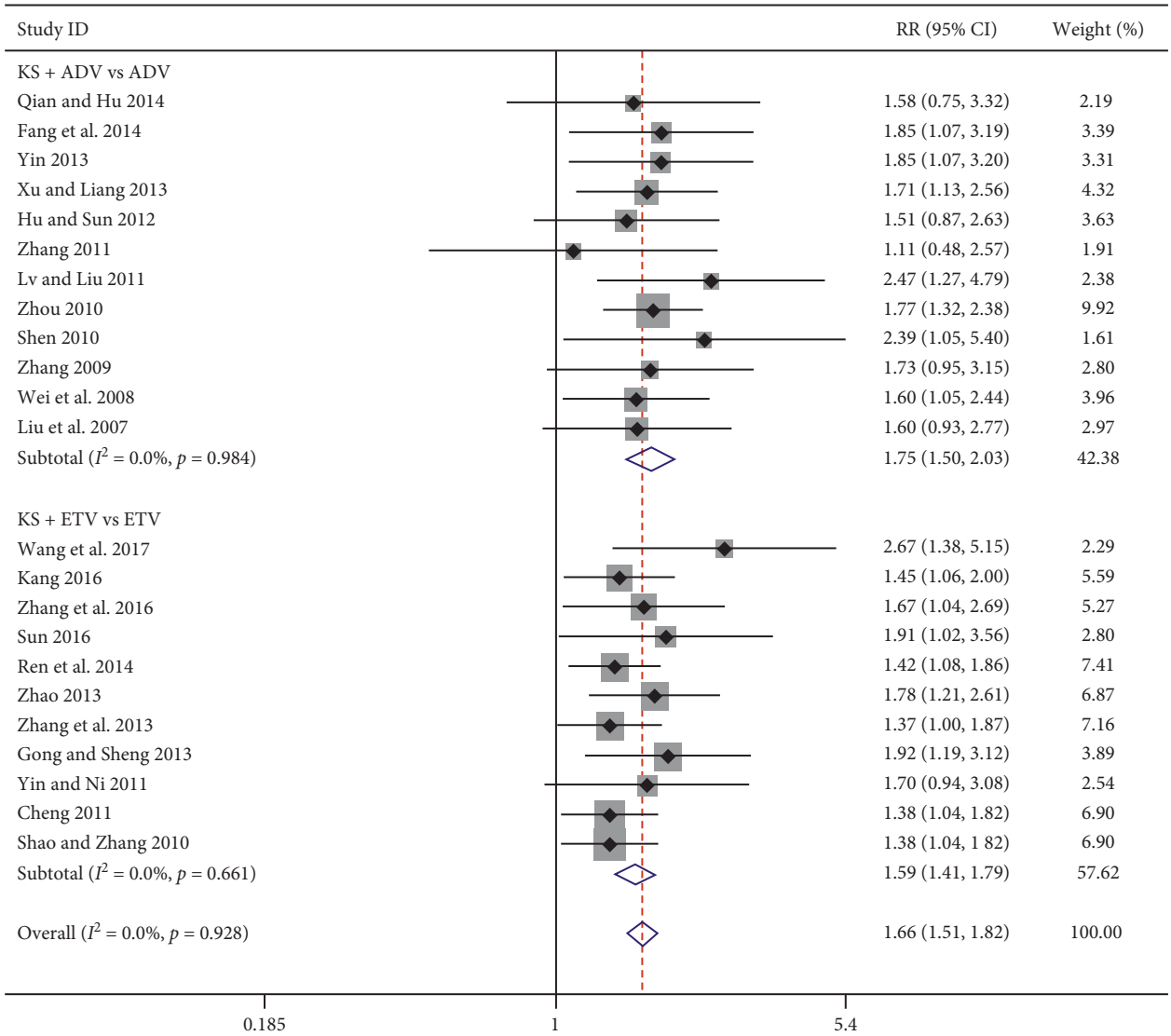

Figure 4: Forest plot of KS combined with ADV or ETV on loss of serum HBeAg rate.

experienced a significant reduction in serum HBV-DNA levels (SMD = −0.38, 95% CI (−0.62, −0.15), $P = 0.001$) ($I^2 = 2\%$, $P = 0.36$) (Figure 8(a)). Compared with the ETV group, the KS + ETV group also showed a significant reduction in serum HBV-DNA levels [SMD = −2.69, 95% CI (−4.12, −1.27), $P = 0.0002$] ($I^2 = 97\%$, $p < 0.00001$) (Figure 8(b)).

3.4. Adverse Events. Twenty-one studies reported on adverse reactions [7–11, 15–19, 21–24, 26–28, 30, 33, 37, 38], of which four mentioned that there were no obvious adverse reactions in either the single drug group or the combined drug group [9, 10, 15, 27]. The other 17 studies mentioned that patients experienced mild adverse reactions, mainly including nausea, vomiting, anorexia, acid regurgitation, abdominal discomfort, diarrhoea, dizziness, headache, fever, fatigue, chest tightness, skin pruritus, rash, creatinine elevation, proteinuria, and transient decrease in cholinesterase. All adverse reactions were mild, could be tolerated by patients, and gradually disappeared after symptomatic treatment or no treatment. Although there was no significant difference in the incidence of adverse reactions between the trial group and the control group, further investigation is still needed to carry out a systematic safety evaluation of the combination of KS and ETV or ADV (Supplemental Digital Content).

3.5. Subgroup Analysis on Different Courses of Treatment. Considering that different courses of treatment may affect the magnitude of the drug treatment effect, this study carried out a subgroup analysis according to the courses of treatment to more comprehensively appraise the curative effect of KS combined with ADV or ETV. As shown in Table 2, undetectable serum HBV-DNA rate, loss of serum HBeAg rate, HBeAg seroconversion rate, and ALT normalization rate less than one year and one year or more were analyzed in the forms of subgroup. The results indicated that, compared with the single drug group, KS combined with ADV or ETV

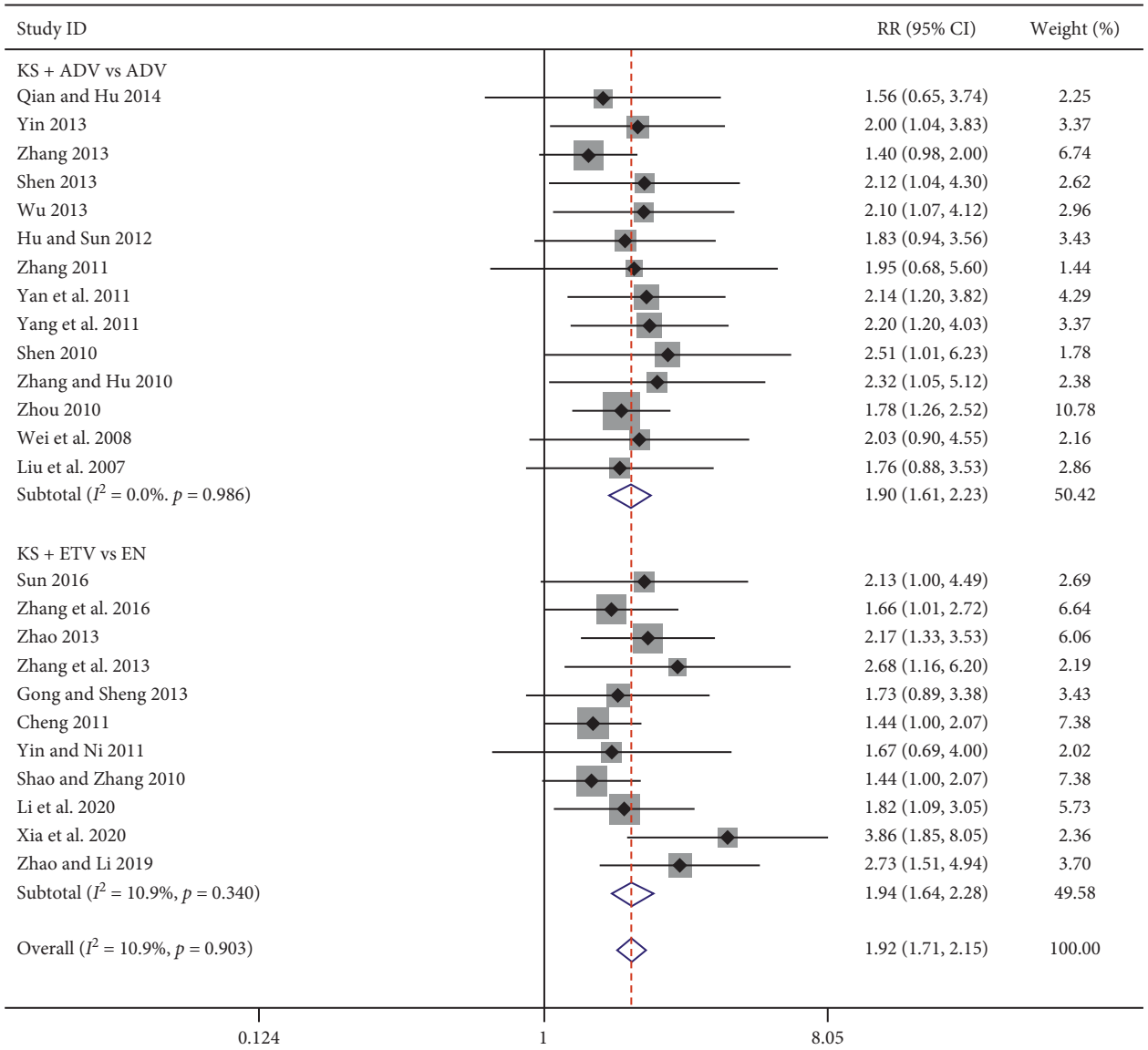

Figure 5: Forest plot of HBeAg seroconversion rate in patients treated with KS combined with ADV or ETV.

was more effective in terms of loss of serum HBeAg rate, HBeAg seroconversion rate, and ALT normalization rate while the treatment period was greater than or equal to one year. However, in less than one year, the undetectable serum HBV-DNA rate improved significantly. These results indicated that the potential publication bias still existed.

4. Discussion

In China, TCM treatment has always been an important method to prevent and treat CHB. For example, KS is a representative antiviral TCM preparation and has a potential antivirus effect. Modern pharmacological studies show that KS has certain antiviral, anti-inflammatory and antitumour effects, and it has attracted much attention in the treatment of CHB [39]. KS is a pure natural alkaloid drug separated from the root of *Sophora alopecuroides* and *Sophora flavescens* in Leguminosae. It is a mixed alkali of oxymatrine and a very small amount of oxysophocarpine, of which oxymatrine accounts for more than 98% and is the main component of KS [40]. The mechanism of action of KS is to inhibit the damage to hepatocytes caused by the hepatitis virus by promoting the expression of microRNA-122 and interferon-α in hepatocytes. Moreover, the anti-HBV effect of KS is produced by blocking the adsorption of hepatitis virus and entry into cells, inhibiting the expression of hepatocytes and secreting HBsAg, HBeAg, and HBV-DNA [41]. Our previous study [42] had assessed the clinical efficacy as well as the safety of KS combined with nucleoside analogues (NAs), including lamivudine (LAM), ADV, ETV, and telbivudine (TLV) for the treatment of CHB. The results indicated that the combination of KS and NAs improves the clinical efficacy of NAs in CHB with no obvious adverse effect. In this study, the literatures were updated, and a more detailed analysis of KS combined with ADV or ETV for the treatment of CHB was performed.

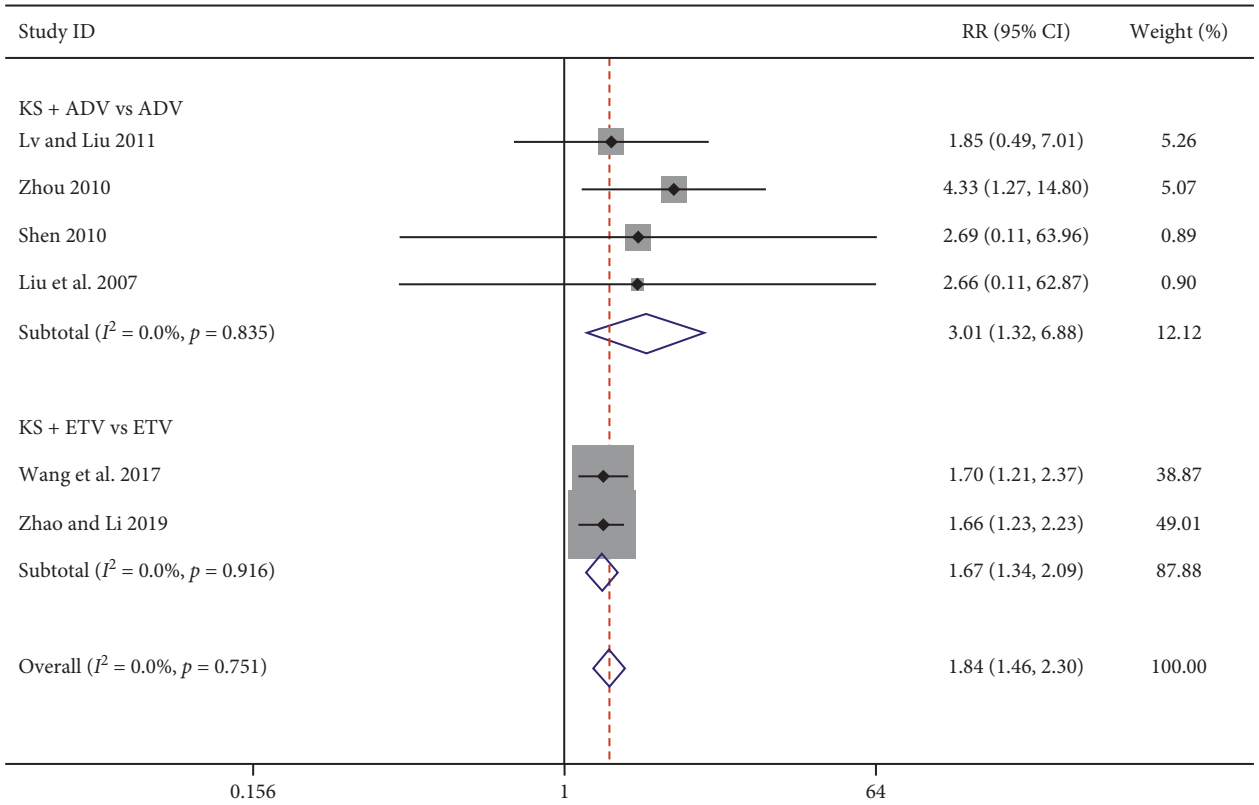

Figure 6: Forest plot of KS combined with ADV or ETV on loss of serum HBsAg rate.

Simultaneously, the loss of serum HBsAg rate and serum HBV-DNA levels of KS combined with ADV or ETV for CHB was analyzed, and a subgroup analysis of different courses of treatment was performed. However, due to the methodological quality of the included studies, more rigorous, large sample and well-designed RCTs are needed to confirm these findings.

This study had further confirmed the clinical efficacy of KS combined with ADV or ETV in the treatment of CHB from the perspective of evidence-based pharmacy through a meta-analysis. Thirty-two RCTs involving 3343 people with CHB were ultimately included. This meta-analysis showed that KS combined with ADV or ETV was effective in treating CHB, and this efficacy was manifested by different changes in various indicators of CHB. Compared with the single agents, the KS combined with ADV or ETV groups not only improved ALT normalization, loss of serum HBeAg, loss of serum HBsAg, HBeAg seroconversion, and undetectable serum HBV-DNA rates but also reduced serum HBV-DNA levels to a certain extent. These findings indicated that patients are transitioning to a much lower HBV replication state and degree of liver injury. No serious adverse reactions occurred in any of the included studies. Even though minor adverse reactions occurred, they were tolerated by patients and gradually disappeared, which showed that KS combined with ADV or ETV was very safe. Notably, there were no significant differences in side effects or serum ALT levels between the combined drug group and the single drug group, which may be related to an insufficient sample size. These results are consistent with a previous study [39]. At the same time, the results of the subgroup analysis according to course of treatment showed that, regardless of how the treatment process and dosage form change, the combined drug group showed significant improvement in the ALT normalization rate, undetectable serum HBV-DNA rate, HBeAg seroconversion rate, and loss of serum HBeAg rate, compared with the rates observed in the single drug group.

However, there were still some limitations to this analysis. The thirty-two trials included had shortcomings in methodology, and their quality evaluations indicated potential bias. For example, most of the included studies did not provide detailed explanations regarding the blinding of outcome assessment, allocation concealment, blinding of participants and personnel, and other bias reports, which directly affected the strength of evidence and reduced the quality and reliability of the included literature. Subgroup analysis showed that the significant improvement of undetectable serum HBV-DNA rate in KS combined with ADV or ETV group was seen in less than one year. Potential publication bias still existed. Furthermore, most of the studies were performed in the Chinese subcontinent, and the influence of geographical and genetic factors could not be ruled out in this systematic review. Therefore, improvements in the methodological quality of clinical research on CHB are still needed in the future. We still need to strictly design more reasonable, high-quality, large-scale and multicentre RCTs to further verify the curative effect and safety of KS

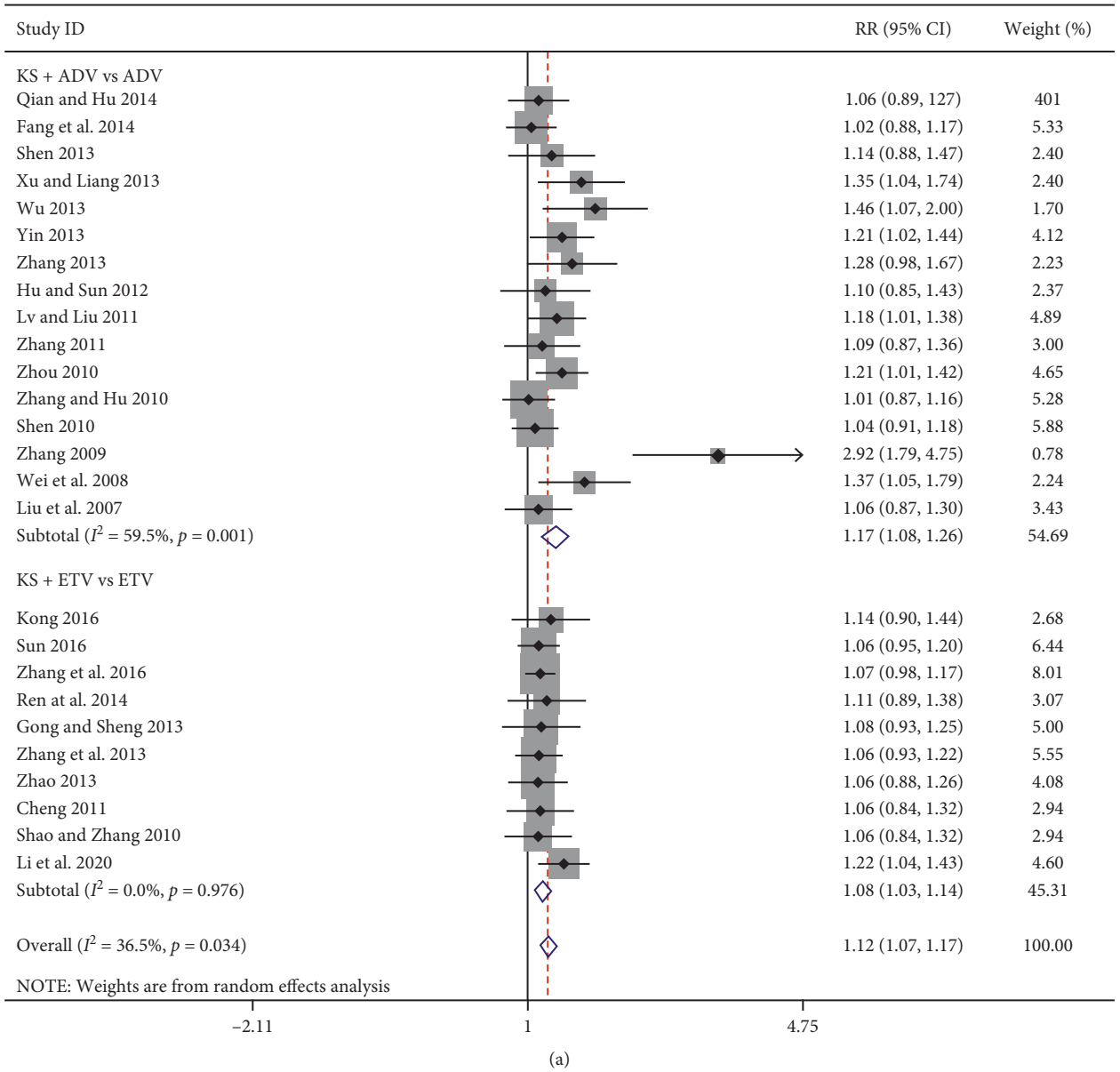

(a)

Figure 7: Continued.

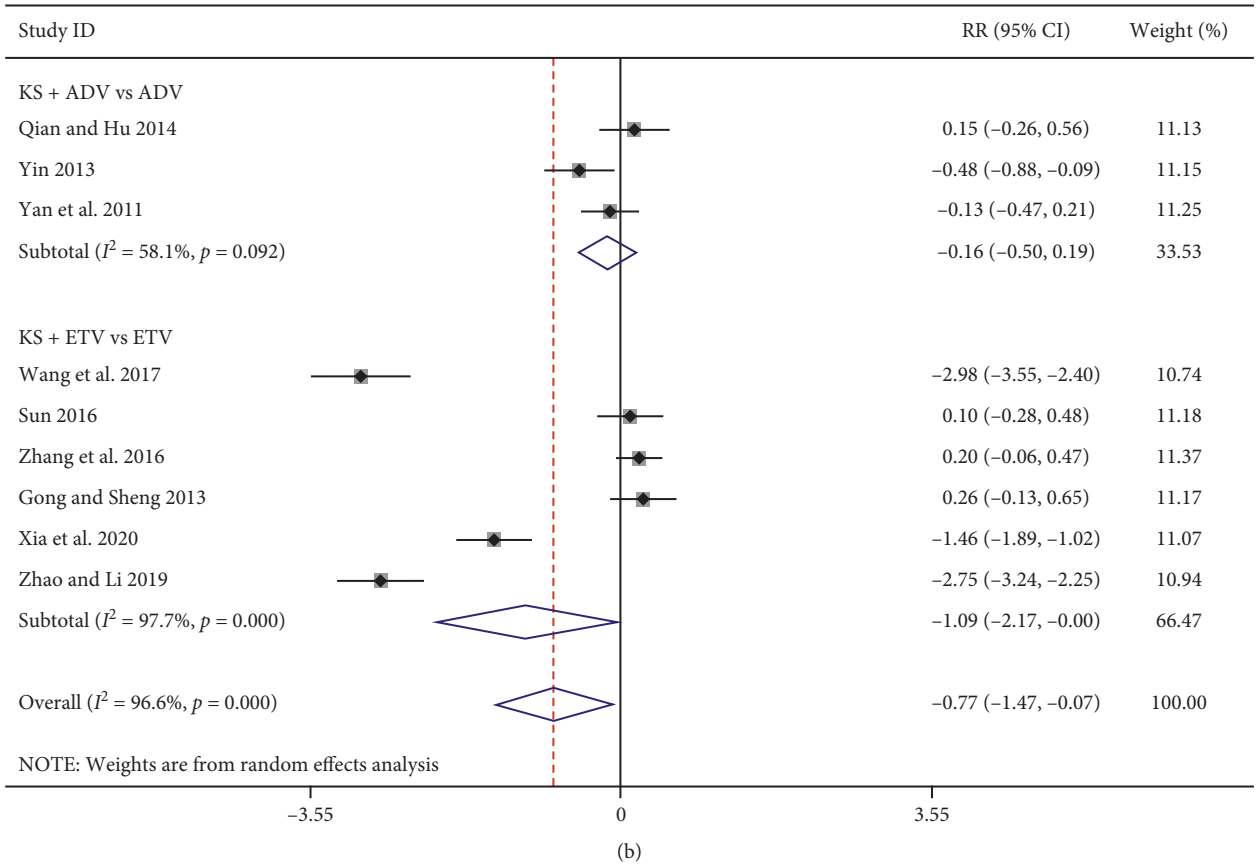

(b)

Figure 7: Forest plot of ALT normalization rate and serum ALT levels in CHB patients treated with KS combined with ADV or ETV. (a) ALT normalization rate. (b) Serum ALT levels.

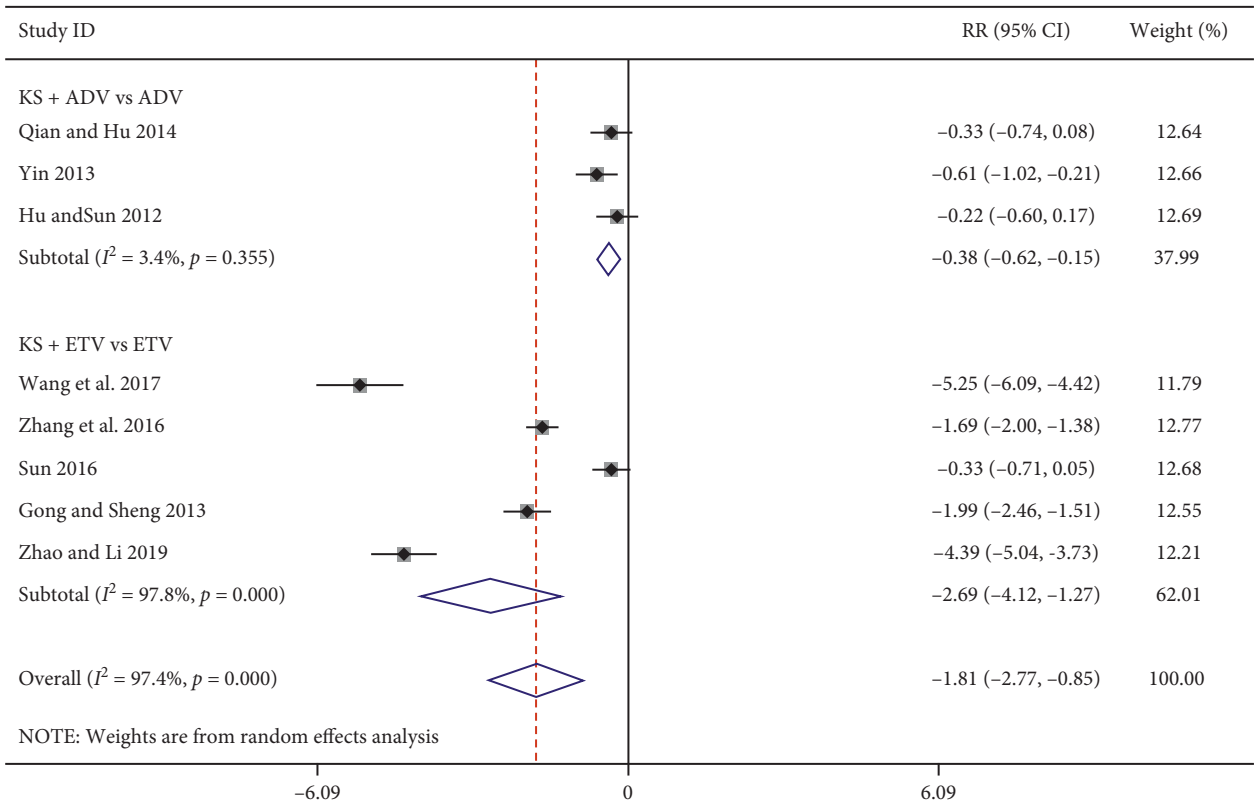

Figure 8: Forest plot of serum HBV-DNA levels in CHB patients treated with KS combined with ADV or ETV.

Table 2: Subgroup analysis on treatment period in patients with CHB treated with KS combined with ADV or ETV.

Outcomes	Trials	Participants	Treatment period	Control group	Trials group	Heterogeneity		RR (95% CI)	*P*-value
						P	I^2 (%)		
Undetectable serum HBV-DNA rate	16	1751	Less than one year	548/848	751/903	0.06	38	1.28 (1.21, 1.36)	<0.00001
	16	1592	One year or more	448/784	588/808	0.02	46	1.28 (1.19, 1.37)	<0.00001
Loss of serum HBeAg rate	13	1425	Less than one year	259/684	454/741	0.66	0	1.62 (1.45, 1.80)	<0.00001
	10	986	One year or more	124/487	222/499	0.98	0	1.74 (1.45, 2.08)	<0.00001
HBeAg seroconversion rate	10	1197	Less than one year	157/590	273/607	0.88	0	1.69 (1.45, 1.97)	<0.00001
	15	1504	One year or more	135/736	308/768	0.99	0	2.18 (1.83, 2.60)	<0.00001
ALT normalization rate	13	1411	Less than one year	509/678	632/733	0.51	0	1.11 (1.06, 1.17)	<0.00001
	13	1334	One year or more	475/659	574/675	0.0006	65	1.14 (1.05, 1.24)	<0.00001

KS: Kushenin; ADV: adefovir dipivoxil; ETV: entecavir; CHB: chronic hepatitis B; HBeAg: hepatitis B e antigen; HBsAg: hepatitis B surface antigen; ALT: alanine aminotransferase.

combined with ADV or ETV in the treatment of CHB to guide the clinical prescription of medications more reliably and accurately.

5. Conclusions

This systematic review and meta-analysis indicated that, on the basis of the RCTs currently available, compared with the use of a single drug, the combinations of KS with ADV or ETV not only improved the rates of ALT normalization, loss of serum HBeAg, undetectable serum HBV-DNA, HBeAg seroconversion, and loss of serum HBsAg but also decreased serum HBV-DNA levels to some extent. In addition, no serious adverse reactions occurred in any of the included studies. Furthermore, the combination drug group and single drug group did not show a significant difference in the incidence of side effects or ALT normalization. In summary, KS combined with ADV or ETV could be a safe and beneficial treatment for humans that could improve the efficacy of CHB treatment. However, we still need to carry out more high-quality, large-scale, multicentre RCTs worldwide to verify the efficacy of this treatment and guide the clinical prescription of medications more reasonably.

Abbreviations

CHB: Chronic hepatitis B
TCM: Traditional Chinese medicine
KS: Kushenin
ADV: Adefovir dipivoxil
ETV: Entecavir
CNKI: China National Knowledge Infrastructure
RCTs: Randomized controlled trials
HBeAg: Hepatitis B e antigen
SMD: Standardized mean difference
HBsAg: Hepatitis B surface antigen
ALT: Alanine aminotransferase.

Data Availability

The data used to support the findings of this study are available from the corresponding author upon reasonable request.

Conflicts of Interest

The authors declare no conflicts of interest.

Authors' Contributions

Qingying Liao and Jianxia Wen contributed equally to this study. QY L and JX W provided the manuscript. KX J and YL Z revised the drafts, retrieved data, and provided some important information to complete the work. X M conceived the idea and provided important information to complete the work.

Acknowledgments

This work was supported by the Sichuan Science and Technology Program (2019YJ0492), China Postdoctoral Science Found (2017M622987), Chengdu University of TCM Found (QNXZ2018025), Beijing Medical and Health Foundation (YWJKJJHKYJJ-B20645FN), and National Natural Science Foundation of China (81874365).

Supplementary Materials

Supplementary Table 1: adverse events of each study in detail. (*Supplementary Materials*)

References

[1] H. B. El-Serag, "Epidemiology of viral hepatitis and hepatocellular carcinoma," *Gastroenterology*, vol. 142, no. 6, pp. 1264–1273, 2012.

[2] N. Yang and A. Bertoletti, "Advances in therapeutics for chronic hepatitis B," *Hepatology International*, vol. 10, no. 2, pp. 277–285, 2016.
[3] R. G. Gish, B. D. Given, C. L. Lai et al., "Chronic hepatitis B: virology, natural history, current management and a glimpse at future opportunities," *Antiviral Research*, vol. 121, pp. 47–58, 2015.
[4] C.-K. Hui, N. Leung, S.-T. Yuen et al., "Natural history and disease progression in Chinese chronic hepatitis B patients in immune-tolerant phase," *Hepatology*, vol. 46, no. 2, pp. 395–401, 2007.
[5] H. P. Xie, Z. P. Liu, J. S. Zhang et al., "Traditional Chinese medicine syndrome patterns and their association with hepatitis B surface antigen levels during the natural history of chronic hepatitis B virus infection," *Evidence-Based Complementary and Alternative Medicine*, vol. 2018, Article ID 7482593, 9 pages, 2018.
[6] G. Wang, L. Zhang, and H. L. Bonkovsky, "Chinese medicine for treatment of chronic hepatitis B," *Chinese Journal of Integrative Medicine*, vol. 18, no. 4, pp. 253–255, 2012.
[7] C. Y. Fang, J. Y. Zhao, J. J. Shen et al., "Clinical study on 90 cases of chronic hepatitis B treated by marine dispersible tablets combined with Adefovir Dipivoxil," *Chinese Journal of Trauma and Disability Medicine*, vol. 22, p. 139, 2014.
[8] M. Hu and K. W. Sun, "Clinical study on Adefovir Dipivoxil combined with Oxymatrine in treating patients with HBeAg positive chronic hepatitis B," *Chinese Journal of Integrated Traditional and Western Medicine on Digestion*, vol. 20, pp. 170–173, 2012.
[9] X. F. Liu, X. Y. Tan, X. Y. Ning et al., "Clinical evaluation on marine capsules combined with the Adefovir Dipirovoxil for chronic hepatitis B," *Hebei Medicine*, vol. 3, pp. 256–258, 2007.
[10] M. L. Lv, Q. Liu, and Q. L. Jia, "Therapeutic effect of HBeAg positive chronic hepatitis B treated by kurorinone capsule combined with Adefovir dipivoxil capsule," *China Medical Herald*, vol. 8, pp. 62–64, 2011.
[11] X. M. Qian and J. H. Hu, "Clinical observation of Adefovir Dipivoxil combined with Oxymatrine in treating HBeAg positive chronic hepatitis B," *Modern Journal of Integrated Traditional Chinese and Western Medicine*, vol. 23, pp. 2368–2370, 2014.
[12] G. Q. Shen, "Clinical observation of Oxymatrine capsule combined with Adefovir Dipivoxil in treating chronic hepatitis B," *Chinese Journal of Primary Medicine and Pharmacy*, vol. 17, pp. 807-808, 2010.
[13] S. H. Shen, "Clinical observation on Adefovir Dipivoxil combined with oxymatrine in treating chronic hepatitis B," *China Practical Medicine*, vol. 8, pp. 141-142, 2013.
[14] J. S. Wei, L. Zhang, T. H. Deng et al., "Adefovir Dipivoxil combined with Oxymatrine in treating 33 cases of chronic hepatitis B," *Journal of Practical Traditional Chinese Internal Medicine*, vol. 3, p. 38, 2008.
[15] J. T. Wu, "Clinical observation of Oxymatrine combined with Adefovir Dipivoxil in treating HBeAg positive chronic hepatitis B patients," *Journal of Hubei University of Chinese Medicine*, vol. 15, pp. 56-57, 2013.
[16] Z. G. Xu and Y. Liang, "Clinical study on Adefovir Dipivoxil combined with Oxymatrine in treating chronic hepatitis B patients," *Chinese and Foreign Medical Research*, vol. 3, pp. 22-23, 2013.
[17] Z. W. Yan, S. H. Li, J. H. Chen et al., "Adefovir Dipivoxil and Oxymatrine combination therapy in treatment of patients with HBeAg-positive chronic hepatitis B," *Chinese Journal of Practical Medicine*, vol. 38, pp. 31–33, 2011.
[18] Q. Yang, J. S. Zhao, and K. Yang, "Adefovir Aipivoxil combined with Oxymatrine in treatment of chronic hepatitis B," *Clinical Medicine*, vol. 31, pp. 48-49, 2011.
[19] A. H. Yin, "Clinical observation on Adefovir Dipivoxil combined with Oxymatrine in treating 50 cases of chronic hepatitis B," *Hunan Journal of Traditional Chinese Medicine*, vol. 29, pp. 48-49, 2013.
[20] D. P. Zhang, "Adefovir Dipivoxil combined with Oxymatrine in treating 40 cases of chronic hepatitis B," *Herald of Medicine*, vol. 28, p. 9, 2009.
[21] J. C. Zhang and J. Hu, "Clinical study on Adefovir Dipivoxil combined with Oxymatrine capsule in treating chronic hepatitis B," *Chinese Hepatology*, vol. 15, pp. 34-35, 2010.
[22] L. C. Zhang, "Clinical value analysis of Adefovir Dipivoxil and Oxymatrine in treating chronic hepatitis B," *China Health Industry*, vol. 10, p. 82, 2013.
[23] R. L. Zhang, "Adefovir Dipivoxil combined with Oxymatrine in treatment of HBeAg positive chronic hepatitis B," *Clinical Medicine*, vol. 31, pp. 107-108, 2011.
[24] X. Q. Zhou, "Clinical observation on Adefovir Dipivoxil combined with Oxymatrine in treating chronic hepatitis B," *Chinese Journal of General Practice*, vol. 8, p. 202, 2010.
[25] D. Cheng, "Efficacy of entecavir combined with oxymatrine in the treatment of HBeAg-positive chronic hepatitis B//Hubei institute of traditional Chinese medicine for liver disease," *Proceedings of the Second Academic Conference of the Hepatology Committee of Hubei Institute of Traditional Chinese Medicine*, vol. 1, pp. 126–129, 2011.
[26] Y. Q. Gong and G. G. Sheng, "Clinical observation of Entecavir combined with Oxymatrine tablets in treating 52 cases of HBeAg positive chronic hepatitis B," *Chinese Journal of Integrated Traditional and Western Medicine on Liver Diseases*, vol. 23, pp. 25-26, 2013.
[27] H. H. Kang, "Clinical observation of Oxymatrine combined with Entecavir in treating 80 cases of chronic hepatitis B," *Guide of China Medicine*, vol. 14, pp. 218-219, 2016.
[28] W. X. Ren, M. Liu, and J. Jiao, "Entecavir and matrine in the treatment of patients with chronic hepatitis B," *Journal of Practical Hepatology*, vol. 17, pp. 184-185, 2014.
[29] Z. L. Shao and B. H. Zhang, "Clinical effect of Entecavir combined with Oxymatrine onpatients with HBeAg positive chronic hepatitis B," *Chinese Journal of Integrated Traditional and Western Medicine on Digestion*, vol. 18, pp. 92–94, 2010.
[30] Y. F. Sun, "Therapeutic effect of Oxymatrine combined with Entecavir on HBeAg positive chronic hepatitis B," *Clinical Medicine*, vol. 36, pp. 120-121, 2016.
[31] X. Q. Wang, B. Han, X. Y. Yuan et al., "Curative effect of entecavir combined with oxymatrine in the treatment of chronic hepatitis B," *Chinese Journal of Nosocomiology*, vol. 27, pp. 1494–1496, 2017.
[32] W. H. Yin and H. H. Ni, "Efficacy of Entecavir combined with Oxymatrine in the treatment of HBeAg-positive chronic hepatitis B," *Clinical Rational Drug Use*, vol. 4, pp. 60-61, 2011.
[33] C. Zhang, A. Shenand, and Z. J. Wu, "Efficacy of Entecavir combined with matrine in treatment of HBeAg-positiverelated chronic hepatitis B," *Journal of Chongqing Medical University*, vol. 38, pp. 294–296, 2013.
[34] Y. Zhang, Y. S. Yu, Z. H. Tang et al., "Entecavir combined with Kushenin in the treatment of patients with HBeAg-positive chronic hepatitis B," *China Tropical Medicine*, vol. 16, pp. 1208–1211, 2016.

[35] Y. Zhao, "Efficacy evaluation of Entecavir combined with Oxymatrine in treating chronic hepatitis B patients with positive E antigen," *Journal of Henan Medical College for Staff and Workers*, vol. 25, pp. 409–411, 2013.

[36] Y. H. Li, Y. F. Sun, J. J. Wang et al., "Efficacy of entecavir and matrine combination therapy in patients with chronic hepatitis B," *Journal of Practical Hepatology*, vol. 23, pp. 22–25, 2020.

[37] P. H. Xia, L. F. Liu, and J. B. Yu, "Effect of oxymatrine combined with antiviral therapy on chronic hepatitis B cirrhosis," *Chinese Remedies & Clinics*, vol. 20, pp. 762–764, 2020.

[38] Y. Zhao and Q. Q. Li, "Effect of oxymatrine combined with entecavir on liver fibrosis in patients with chronic hepatitis B," *Laboratory Medicine and Clinic*, vol. 16, pp. 3058–3060, 2019.

[39] F. L. Xiang and Z. S. Huang, "Study on the anti-hepatoma effect of oxymatrine," *Medical Recapitulate*, vol. 17, pp. 2992–2995, 2011.

[40] Y. Cai, "Research progress on pharmacological effects of oxymatrine," *Journal of Practical Traditional Chinese Medicine*, vol. 32, pp. 387–389, 2016.

[41] M. F. Zhang and Y. Q. Shen, "Research progress in clinical pharmacological effects of matrine alkaloids on hepatitis B virus," *Anti-Infection Pharmacy*, vol. 15, pp. 1–6, 2018.

[42] Z. Chen, X. Ma, Y. Zhao et al., "Kushenin combined with nucleos (t) ide analogues for chronic hepatitis B: a systematic review and meta-analysis," *Evidence-Based Complementary and Alternative Medicine*, vol. 2015, Article ID 529636, 12 pages, 2015.

Hindawi
Evidence-Based Complementary and Alternative Medicine
Volume 2021, Article ID 6291428, 8 pages
https://doi.org/10.1155/2021/6291428

Research Article

Study on the Expression Differences and the Correlation with H2BE Gene of Th Related Cytokines in SSDHS and LDSDS TCM-Syndromes of CHB Patients

Chao Liu, Yanfeng Zheng, Xia Li, Baixue Li, Li Wen, Dong Wang, Quansheng Feng, and Cen Jiang

College of Basic Medical Sciences, Chengdu University of Traditional Chinese Medicine, Chengdu 610075, China

Correspondence should be addressed to Quansheng Feng; fengqscdutcm@126.com and Cen Jiang; jiangcencdutcm@126.com

Received 24 July 2020; Revised 9 October 2020; Accepted 28 January 2021; Published 22 February 2021

Academic Editor: Weicheng Hu

Although our previous studies revealed that H2BE exhibited significantly differential expression between two CHB TCM-syndromes: Spleen-stomach dampness-heat syndrome, SSDHS and liver-depression spleen-deficiency syndrome, LDSDS, the underlying mechanisms remain largely unknown. Recent studies showed that dynamic expression fluctuation of Th related cytokines in CHB TCM-syndromes, and furthermore, their expression levels were largely regulated by H2BE. This study aims to detect the expression level differences of Th related cytokines between these two TCM-syndromes and further investigate the underlying regulatory mechanisms. The expression levels of the four Th related cytokines and H2BE were analyzed and the protein-protein interaction networks between H2BE and the four cytokines were constructed. Our results suggested that almost all the cytokines were significantly upregulated compared with the healthy group ($P < 0.05$). Interestingly, among the four cytokines, only IL-4 and INF-γ showed statistical significance between these two syndromes. The protein-protein interaction networks demonstrated that H2BE was indirectly associated with IL-4 and IL-10, and H2BE may regulate the expression levels of cytokines through GATA3. Taken together, our results indicated that IL-4 and INF-γ are two representative cytokines that may serve as two potential biochemical indicators of SSDHS and LDSDS in CHB patients; except what has been reported, our study found that one possible way for H2BE to regulate the expression of cytokines is to interact with GATA3 directly or indirectly.

1. Introduction

Chronic hepatitis B (CHB) is a serious worldwide health problem that is often tightly associated with serious liver diseases, such as liver cirrhosis and even hepatocellular carcinoma (HCC) [1]. It was reported that nearly 20–30% of chronic hepatitis patients could further lead to cirrhosis or HCC due to the failure of virus clearance, and 15–40% of chronic patients will progress to cirrhosis and even HCC without any treatments [2, 3]. Globally, around 257 million people are suffering HBV, and sexual, blood and perinatal are the three major modes of HBV transmission [4, 5]. It is worth noting that among the three transmission modes, vertically from mother to child is the major cause for chronic HBV infection which account for 80–90% of cases of chronic HBV infection, and nearly 5–10% cases were infected during adolescence and adulthood [1, 6]. Therefore, CHB has become a serious disease affecting human health.

For CHB treatment, the goal is to improve the life quality and prevent the formation of cirrhosis and HCC, and unfortunately, there is still no specific medicine that could cure it completely in western medicine. Chinese Traditional Medicine (TCM), as complementary and alternative medicine, is becoming more and more popular in treating complex diseases [7]. In addition, TCM treatments for some chronic diseases, such as cancer and CHB, especially when combined with western medicine, could produce incredible effects [8, 9]. TCM-syndrome, which is also called "ZHENG" in Mandarin Chinese, is the basic unit and the main perspective in TCM, which could help us understand the body

homeostasis and provide guidance for the treatment of diseases [10, 11]. In some Asian countries, TCM based on syndrome has been used to diagnose and guide the treatment of CHB for many years [12]. Patients who suffer from an identical disease would be treated with different methods based on the TCM-syndromes and vice versa. Different TCM-syndromes that received the same therapy could exhibit various responses [13]. Furthermore, utilizing TCM without taking syndrome classification into account could generate serious side effects [14]. On the other hand, until now, TCM-syndromes justification still mainly relies on experienced practitioners, which may lead to ambiguity and subjectivity for one syndrome by different doctors [12]. However, in reality, modern medicine has been closely combined with TCM, such as the biochemical indicators from modern clinical examination have been widely used in TCM diagnosis, and that is why patients often receive a biochemical indicator inspection report in a TCM clinic. These biochemical indicators could reflect the physical state more objectively than TCM-syndrome diagnosed by experienced practitioners. Therefore, establishing the relationship between these biochemical indicators with TCM-syndromes will make great significance for the development of TCM. Fortunately, considerable achievements have been made in this field [15].

Spleen-stomach dampness-heat syndrome (SSDHS) and liver-depression spleen-deficiency syndrome (LDSDS) are two common TCM-syndromes for CHB. A large sample investigation conducted by our team found that among 1260 CHB patients, 16.7% were SSDHS and 8.8% were LDSDS [16]. Thus, looking for effective biochemical indicators to differentiate SSDHS and LDSDS could be quite helpful for clinical considerations. In addition, the previous mRNA screening for the CHB two TCM-syndromes (SSDHS and LDSDS) in our laboratory found that there were 9 differentially expressed genes between the two syndromes. Among them, the expression of HIST2H2BE (H2BE) was the most significant one [17]. Studies found that the expression levels of histone could participate in many cellular processes, such as DNA replication, repair, recombination, transcriptional regulation, etc. [18, 19]. Further studies confirmed that histone fragments encoded by H2BE could act on the immune dominant epitopes in Th cells and then further stimulate the proliferation, differentiation, and IL-2 release of Th cells [20]. Under the stimulation of hepatitis B antigen, Th cells then mainly differentiate into two subgroups, Th1 and Th2. Th1 mainly participates in the cellular immune response by secreting interleukin-2 (IL-2) and INF-γ, and Th2 is mainly involved in the humoral immune response by secreting interleukin-4 (IL-4), interleukin-10 (IL-10) [21]. Thus, the equilibrium state of Th1/Th2 is considered as an important effective factor of hepatitis B chronicity [22].

Collectively, we suggested that the differential expression of H2BE in SSDHS and LDSDS could further lead to the ratio of Th1/Th2 change and then making SSDHS and LDSDS possess the different levels of cytokines. In order to investigate whether there is any relationship between CHB TCM-syndromes and cytokines, in this paper, we chose IL-2, IL-4, IL-10, and INF-γ as the research objects and examined the expression level of H2BE, IL-2, IL-4, IL-10, and INF-γ. Furthermore, the correlation between TCM-syndromes and the specific cytokines was analyzed. Our results could provide more details for the causes of the same disease with different TCM-syndromes and a reference for the further development of biochemical indicators of SSDHS and LDSDS syndromes.

2. Materials and Methods

2.1. Participants. A total of 31 CHB patients were enrolled from August 2018 to February 2019 in the Outpatient Department of Hepatology, General Hospital of Chengdu Military Region. Among the 31 CHB patients, there were 11 SSDHS CHB patients, 11 LDSDS, and 9 healthy volunteers (control group, CG). All the enrolled CHB patients underwent rigorous screening according to the selection criteria. The inclusion criteria were as follows:

(1) CHB patients' TCM-syndrome was differentiated by Chinese physicians with the title of associate professor or above

(2) The age of these cases who met the selection criteria in this study was between 18 and 65, male or female

(3) In addition, according to the diagnostic criteria in the 2015 guidelines for the prevention and treatment of chronic hepatitis B in China, CHB patients in this study were HBsAg or HBV-DNA positive for at least six months

The details of the samples are listed in Table 1. The TCM-syndrome types were identified according to the TCM-syndrome standards of chronic hepatitis B established by the Chinese Society of Traditional Chinese Medicine, 2017 [23]. This study was approved by the Medical Ethics Committee of Affiliated Hospital of Chengdu University of Traditional Chinese Medicine, China.

2.2. RNA Isolation and qRT-PCR Analysis. All the blood samples were collected from the participants' peripheral venous blood, and the samples were frozen in liquid nitrogen immediately and then stored at −80°C. Total RNAs were extracted by using TRIzol® Reagent (Life Technologies, USA) according to the manufacturer's protocol. The primers used for qRT-PCR analyses are listed in Table 2. CDNAs were synthesized by using the SuperScript™ III First-Strand Synthesis System (Life Technologies, USA). SYBR-based qRT-PCR (SYBR® Green Master Mix, Life Technologies, USA) were performed on a step-one real-time system (ABI company) by using the following reaction conditions: predenaturation at 95°C for 2 min, followed by 40 cycles of 95°C for 10 s and 60°C for 10 s, 40 cycles. Each sample was performed in three technical triplicates.

2.3. Serum Cytokine Measurements. Serum samples from 11 SSDHS, 11 LDSDS, and 9 healthy volunteers were collected by centrifuging at 3500 r/min, 4°C for 10 min, and stored at

Table 1: Baseline comparison of the clinical characteristics among the groups.

Group	Number of cases	Gender[a]		Age[b] ($\overline{x} \pm s$)
		Male	Female	
LDSDS	11	5 (45.5%)	6 (54.5%)	39.27 ± 8.661[c]
SSDHS	11	7 (63.6%)	4 (36.4%)	36.00 ± 12.578[c]
CG[d]	9	4 (44.4%)	5 (55.6%)	33.56 ± 8.00[c]
Total	31	16 (57.69%)	15 (42.31%)	—

[a]There was no significant difference in gender composition among the three groups by the chi-square test ($P > 0.05$). [b]There was no significant difference in age composition among the three groups by one-way analysis of variance ($P > 0.05$). [c]mean ± standard deviation. [d]Healthy group (control group).

Table 2: The primer pairs for qRT-PCR validation.

Primers	Sequence (5'-3')
H2BE-F	agtggctgagttcggctgtc
H2BE-R	gctgccaagcgtcagtcata
U6b-F	ggcagtcgaccgacgaata
U6b-R	cgtgaaagaccgcagcaa

−80°C. Four Th related cytokines (IL-2, IL-4, IL-10, INF-γ) were detected using human cytokines ELISA kits (Life Technologies, USA) based on the manufacturer's protocol. The optical density values of the four cytokines were determined by using a Labsystems Multiskan MS Reader. The concentration of each cytokine was calculated using a standard curve.

2.4. The Protein-Protein Interaction Networks Construction. The protein-protein interaction networks between H2BE and the four cytokines were constructed by using the GeneMANIA database (http://genemania.org/). Briefly, input the gene name of HIST2H2BE, IL-2, IL-4, and IL-10, respectively, and then click the search button to construct the networks.

2.5. Statistical Analysis. Data of qRT-PCR were processed using Microsoft 2010 based on the $2^{-\Delta\Delta Ct}$ method and the CG group was set as the control. The significance between the experimental groups (LDSDS, SSDHS) and control group (CG) was detected by using the one-way ANOVA method via the SPSS 24.0. In addition, the expression levels of the four cytokines were also analyzed using SPSS 24.0. The standards for the potential marker selection are that the potential marker which could not only distinguish the two syndromes but also could distinguish the syndromes from the healthy group (the significance condition is at least P value <0.05).

3. Results

3.1. Patient Characteristics. A total of 31 participants were enrolled in this study, including 11 LDSDS, 11 SSDHS, and 9 healthy subjects. Among the 11 LDSDS, 5 were males and 6 were females; among the 11 SSDHS, 7 were males and 4 were females; among the 9 healthy participants, there were 4 males and 5 females (Table 1). There was no significant difference in age at baseline (Table 1).

3.2. Cytokines Expression Level Analysis. To ascertain the expression levels of cytokines between CHB patients and healthy subjects, and also to identify the differently expressed cytokines between the LDSDS and SSDHS, the expression levels of the four cytokines were detected by ELISA. The results showed that the expression levels of IL-2 were significantly increased ($P < 0.01$) in LDSDS and SSDHS compared with the healthy group; however, there is no significant difference observed ($P > 0.05$) between LDSDS and SSDHS (Table 3). For IL-4, both LDSDS and SSDHS exhibited increased levels ($P < 0.05$) compared with the healthy group (Table 3). Significant increase of IL-10 was observed only in LDSDS, but not in SSDHS ($P < 0.01$) when compared with the healthy group, and there is a statistical difference ($P < 0.05$) between LDSDS and SSDHS. Finally, the expression levels of INF-γ in different groups were analyzed. Results showed that the expression levels of INF-γ in LDSDS and SSDHS showed a dramatic increase ($P < 0.05$) compared with the healthy group. Notably, the expression level of INF-γ in LDSDS was even increased compared with SSDHS ($P < 0.01$) (Table 3). Collectively, what attracts us most is that among the four cytokines, only IL-4 and INF-γ showed statistical differences not only between these two syndromes but also between the syndromes and healthy group, suggesting that these two cytokines may serve as the potential biochemical indicators of the TCM-syndromes of CHB, but these need to be further studied.

3.3. Analysis of H2BE Gene Expression Level. In order to illuminate the expression levels of H2BE in LDSDS, SSDHS, and the healthy group, we performed the qRT-PCR. QRT-PCR results showed that LDSDS-10 exhibited the highest expression level in the LDSDS group, while the lowest expression level was LDSDS-6. In the SSDHS group, SSDHS-10 showed the highest expression level and SSDHS-3 exhibited the lowest. Interestingly, the expression levels of H2BE in LDSDS were generally higher than that in SSDHS, which was consistent with the cytokines results (Figure 1). Moreover, when compared with the CG group, the expression levels of the H2BE in most of the CHB patients showed a trend of increase, suggesting that the expression level of H2BE may be related to the formation of TCM-syndromes to some extent, but this needs to be further studied in the following research.

3.4. Correlation Analysis between H2BE and the Cytokines. In order to further elucidate how H2BE works on the cytokines and also mine the latent genes which participate in

Table 3: Expression levels of the four cytokines detected with ELISA.

Cytokines	LDSDS	SSDHS	CG
IL-2	$133.451 \pm 20.078^{※※}$	$121.870 \pm 21.934^{※※}$	76.308 ± 14.061^{a}
IL-4	$68.194 \pm 10.387^{※※\#\#}$	$50.432 \pm 7.936^{※}$	39.618 ± 7.953^{a}
IL-10	$123.728 \pm 26.204^{※※\#}$	93.452 ± 13.689	81.416 ± 10.387^{a}
INF-ɣ	$159.037 \pm 33.737^{※※\#\#}$	$106.233 \pm 23.602^{※}$	80.097 ± 16.610^{a}

[a]mean ± standard deviation. ※The difference was statistically significant compared with the healthy group (P value <0.05). ※※The difference was statistically significant compared with the healthy group (P value <0.01). #The difference was statistically significant compared with the SSDHS group (P value <0.05). ##The difference was statistically significant compared with the SSDHS group (P value <0.01).

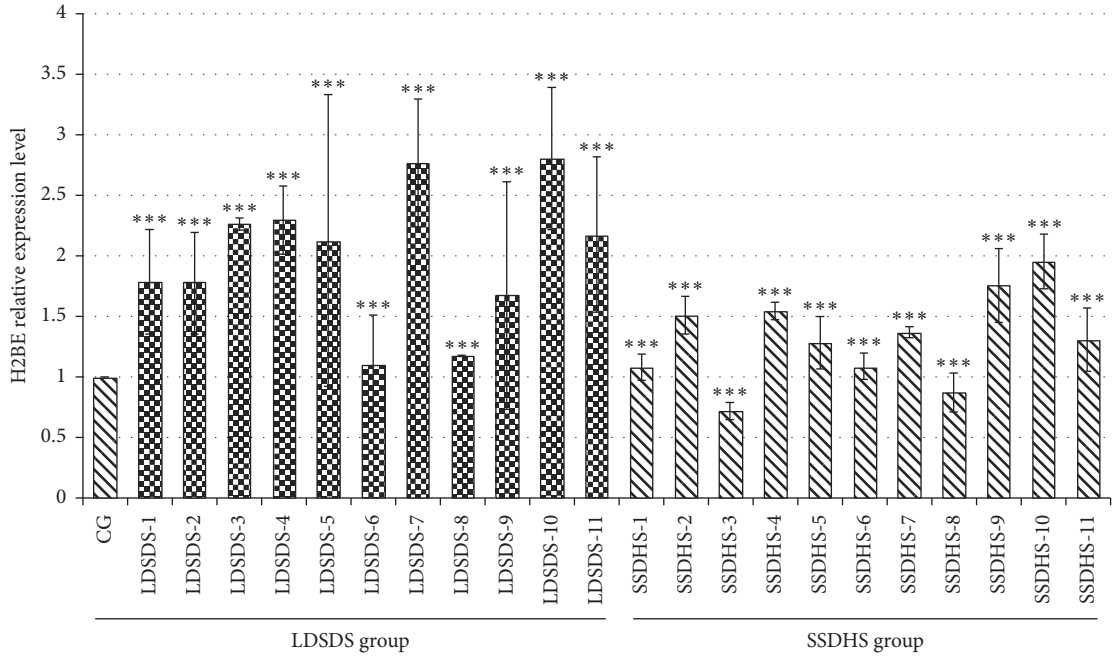

Figure 1: qRT-PCR validation of the H2BE gene in the three groups (LDSDS, SSDHS, and healthy group). The X-axis represents the samples studied in this study; the Y-axis represents the relative expression levels of genes. U6b gene was selected by our laboratory previously, which was used as a control. CG represents the healthy group. All data are from three technical repeats ($n = 3$). *** represents the significance level of the one-way ANOVA test, $P = 0.001$. Error bars denote |S|D.

the expression regulation of H2BE on the cytokines, the protein-protein interaction networks between H2BE and the four cytokines were constructed. The results demonstrated that H2BE, IL-2, IL-4, IL-10, and some other related molecules were correlated mainly through physical interaction (67.64%), coexpression (13.5%), and signaling pathway (4.35%) (Figure 2). Furthermore, after analyzing the major relationships in the network, we found that H2BE was indirectly associated with IL-4 and IL-10, and H2BE regulated the expression level of cytokines mainly through GATA3 (Figure 3). That is, the GATA3 gene acts as a bridge between H2BE and cytokines and also showed a coexpression pattern with H2BE, IL-4, and IL-10. These remind us that GATA3 may play an important role in the regulation of H2BE on cytokines expression, but this needs to be further researched.

4. Discussion

Hepatitis B is a hidden killer. People infected with a virus for decades may show only mild symptoms, which could be easily ignored and may ultimately develop into liver cirrhosis or even liver cancer [24]. So far, the direct-acting antiviral agents (DAAs) of western medicine still could not eliminate the virus completely [25]. Therefore, pretreatment is of great value in the treatment of CHB and liver cirrhosis. TCM has been widely used in CHB pretreatment since its unique advantages, such as low toxicity side effect, good curative effect, etc. [26]. TCM syndrome plays an important role in TCM treatment, and the same disease with different TCM syndromes in western medicine could receive different treatments in TCM [11]. However, due to the fact that TCM-syndrome is overrelying on experience, this greatly limits its application worldwide. Thus, excavating available biomarkers for TCM-syndrome diagnosis and elucidating the underline mechanisms of TCM-syndrome could greatly help the application of TCM all over the world.

Previous studies found that the imbalances of Th1/Th2 cells and their cytokines are important causes of CHB [27]. However, Th1 and Th2 levels are strongly associated with the cytokine levels elaborated above [21]. For different CHB TCM-syndromes, as the TCM-syndrome changes, the immune responses may also be changed due to the ratios of

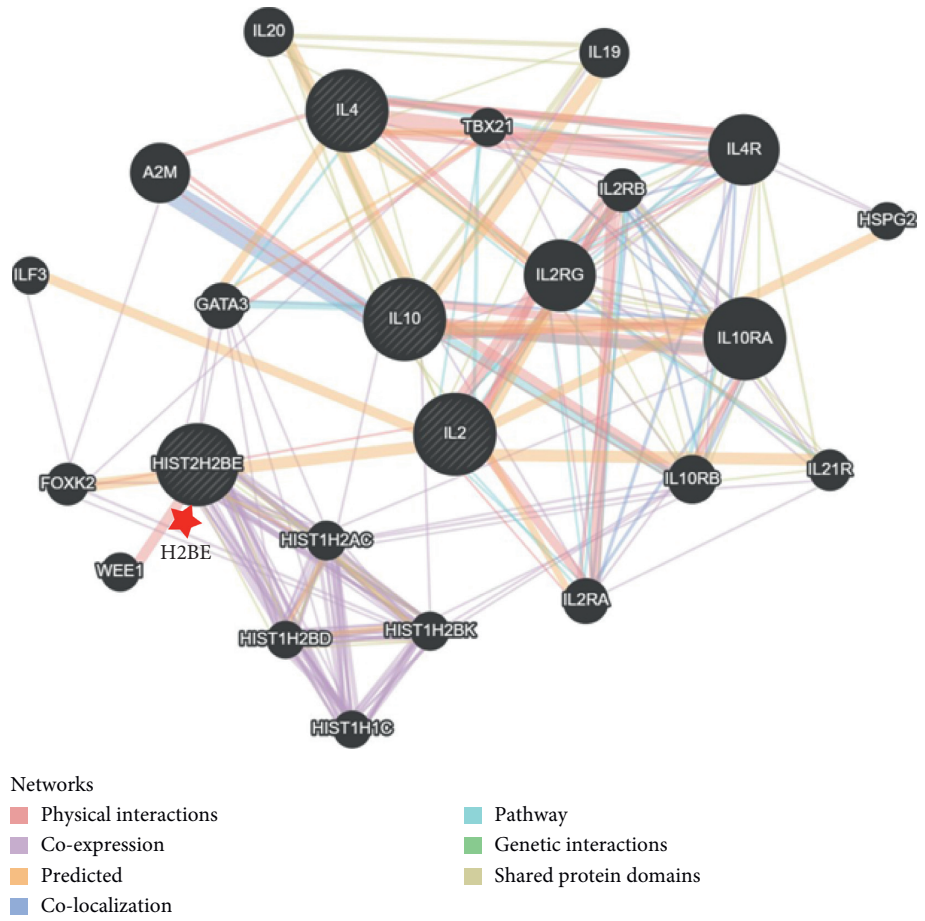

Figure 2: The protein-protein interaction networks between H2BE and the four cytokines. The networks between H2BE and the four cytokines were constructed by using the GeneMANIA database.

different cytokines are also changed. In this study, we found that the expression levels of almost all the examined cytokines were upregulated compared with the healthy group. Among the four cytokines, IL-4 and INF-γ showed statistical significance not only between the syndromes but also among the syndromes and healthy group, and these two cytokines may have potential as the biochemical indicators of the two TCM-syndromes. In addition, the results also demonstrated that almost all the cytokines were expressed much higher in LDSDS than in SSDHS, and this suggested that the immune response may be more intense in LDSDS than in SSDHS, and this result was also consistent with Lu et al. (2019) [11].

Histone is involved in many cellular processes such as transcriptional regulation, DNA replication, RNA splicing, etc., since the DNA is wrapped and interacts directly with histone proteins [28]. However, at present, a myriad of studies on histone mainly focus on histone modification, such as methylation, acetylation, phosphorylation, etc., rather than the effects generated by expression level changes [18, 29]. In yeast cells, researchers found that overexpression histone H4 could suppress SIR2-induced inviability, while overexpression H3 did not [30]. Singh et al. [19] found that overexpression histone H2A resulted in a significant decrease in susceptibility towards drugs currently in use in Leishmania parasites, and thus pointing to its role in drug resistance. For H2BE, a study on breast cancer found that overexpression or downregulation of H2BE could both lead to the decreased proliferation in breast cancer cell lines [31]. Furthermore, the expression level of H2BE was also associated with the cell function. That is, different cell types exhibit different expression levels of H2BE [32]. These indicated that H2BE might play an important role in regulating the physiological function of cells. Interestingly, in this study, we found that the expression levels of H2BE in LDSDS were basically higher than that in SSDHS and showed an increasing tendency in CHB patients compared with the healthy group.

In the nucleosome, H2BE is mostly exposed to the surface of the nucleosome compared with other nucleosome proteins [33, 34]. Hao [20] found that the subunit from 14th-28th amino acid of H2B was the dominant epitope that could interact with Th cells and stimulate more cytokines secreted. In this study, we have also investigated the protein-protein interaction networks between H2BE and the four cytokines, and the results displayed that GATA3 protein acts as a bridge between H2BE and cytokines and also showed a coexpression pattern with H2BE, IL-4, and IL-10. A myriad of studies reported that GATA3 could be expressed in large quantities in immune cells, such as T lymphocytes, NK cells, NKT cells, etc. [35–37]. Chen et al. [38] found that

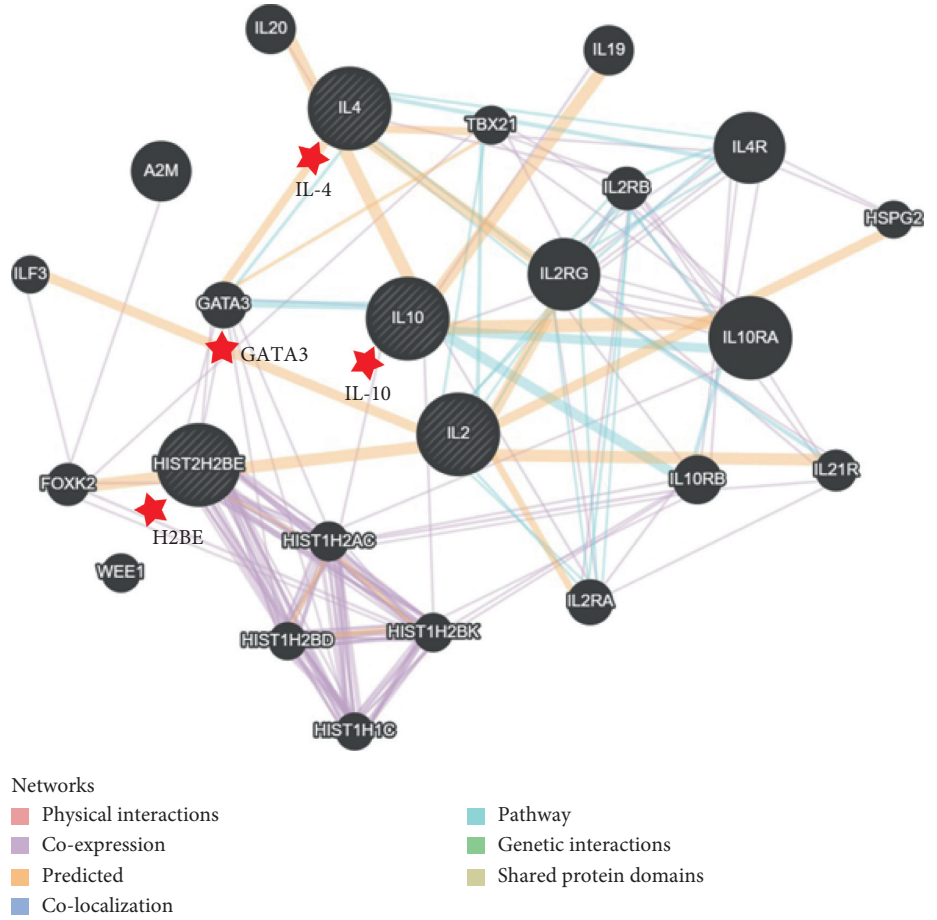

Figure 3: The major relationships with H2BE gene in the cytokines expression regulation. The networks between H2BE and the four cytokines were constructed by using the GeneMANIA database.

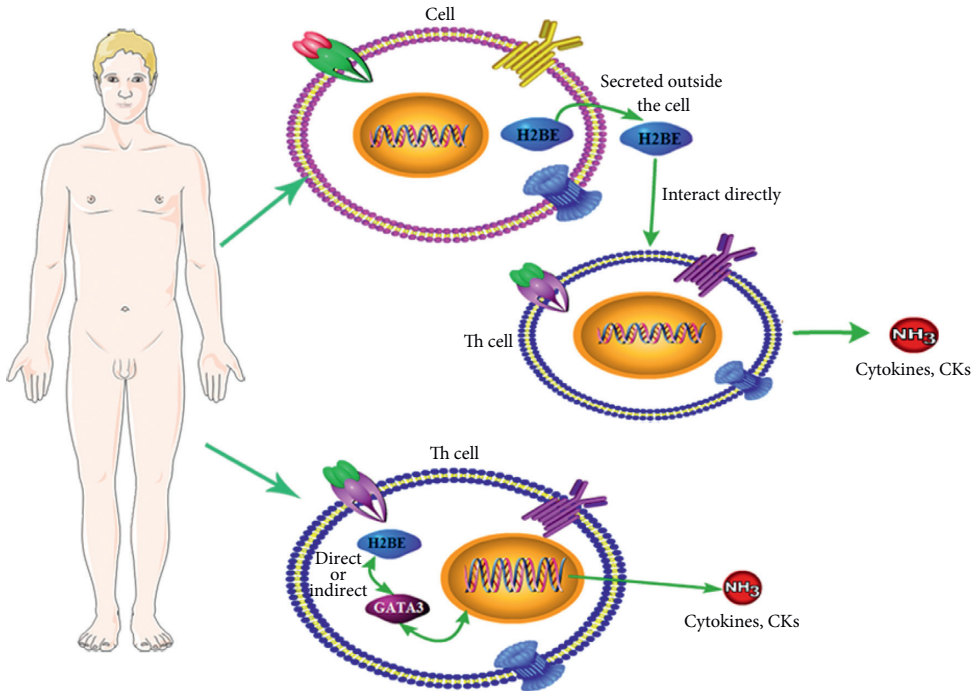

Figure 4: The possible regulatory pathways of H2BE involved in the secretions of cytokines.

overexpression GATA3 could affect cytokine secretions of Th1 and Th2. Thus, we suggested that one other possible way for the expression regulation of Th related cytokines by H2BE is through the direct or indirect interaction between H2BE and GATA3, among which GATA3 may be the intermediate node, with coexpression and other related pathways.

In summary, we believe that H2BE regulates cytokine secretions via the following two ways, (1) H2BE could interact with Th cells directly through a dominant epitope way, and (2) the other way is by regulating the GATA3 gene directly or indirectly and then further regulating the cytokine secretions (Figure 4). However, further studies are needed to clarify the relative regulation mechanisms of H2BE.

Data Availability

The datasets used and/or analyzed during the present study are available from the corresponding author upon reasonable request.

Ethical Approval

The protocol has been approved by the Medical Ethics Committee of Affiliated Hospital of Chengdu University of Traditional Chinese Medicine, China. All study participants will sign two informed consent forms, one kept by the patients and the other kept by the researcher.

Conflicts of Interest

The authors declare no conflicts of interest.

Authors' Contributions

CL and YZ were the principal actors in this research, including sample collection and manuscript preparation. XL, BL, LW, and DW were mainly responsible for assisting in sample collection. QF and CJ provided fund support and scientific research guidance.

Acknowledgments

The authors are grateful to Shanhong Tang in the General Hospital of Chengdu Military Region for sample collection. This work was supported by the National Natural Science Foundation of China (81803976) and "Xinglin Scholar" Scientific Research Promotion Program for Academic Talents of Chengdu University of TCM (BSH2019018).

References

[1] Y. Jin, N. Geng, L. Zhao et al., "The prevalence of HBV infection: a retrospective study of 13-years in a public hospital of northeast China," *Viral Immunology*, vol. 33, no. 2, pp. 99–104, 2019.

[2] M. F. Yuen, D. S. Chen, G. M. Dusheiko et al., "Hepatitis B virus infection," *Nature Reviews Disease Primers*, vol. 4, p. 18035, 2018.

[3] L. S. Y. Tang, E. Covert, E. Wilson, and S. Kottilil, "Chronic hepatitis B infection," *JAMA*, vol. 319, no. 17, pp. 1802–1813, 2018.

[4] S. Lanini, A. Ustianowski, R. Pisapia, A. Zumla, and G. Ippolito, "Viral hepatitis: etiology, epidemiology, transmission, diagnostics, treatment, and prevention," *Infectious Disease Clinics of North America*, vol. 33, no. 4, pp. 1045–1062, 2019.

[5] WHO Guidelines Approved by the Guidelines Review Committee, *Guidelines for the Prevention, Care and Treatment of Persons with Chronic Hepatitis B Infection*, World Health Organization, Geneva, Switzerland, 2015.

[6] Y.-F. Liaw, "Natural history of chronic hepatitis B virus infection and long-term outcome under treatment," *Liver International*, vol. 29, pp. 100–107, 2009.

[7] P. Hao, F. Jiang, J. Cheng, L. Ma, Y. Zhang, and Y. Zhao, "Traditional Chinese medicine for cardiovascular disease," *Journal of the American College of Cardiology*, vol. 69, no. 24, pp. 2952–2966, 2017.

[8] Y.-H. Liao, C.-I. Li, C.-C. Lin, J.-G. Lin, J.-H. Chiang, and T.-C. Li, "Traditional Chinese medicine as adjunctive therapy improves the long-term survival of lung cancer patients," *Journal of Cancer Research and Clinical Oncology*, vol. 143, no. 12, pp. 2425–2435, 2017.

[9] J. Li, "Clinical research progress in integrated traditional Chinese and Western medicine therapy for HBV-related liver failure," *Journal of Clinical Hepatology*, vol. 31, no. 1, pp. 42–47, 2015.

[10] A. Lu, M. Jiang, C. Zhang, and K. Chan, "An integrative approach of linking Traditional Chinese Medicine pattern classification and biomedicine diagnosis," *Journal of Ethnopharmacology*, vol. 141, no. 2, pp. 549–556, 2012.

[11] Y. Lu, Z. Fang, T. Zeng et al., "Chronic hepatitis B: dynamic change in Traditional Chinese medicine syndrome by dynamic network biomarkers," *Chinese Medicine*, vol. 14, p. 52, 2019.

[12] H. Kang, Y. Zhao, C. Li et al., "Integrating clinical indexes into four-diagnostic information contributes to the Traditional Chinese Medicine (TCM) syndrome diagnosis of chronic hepatitis B," *Scientific Reports*, vol. 5, p. 9395, 2015.

[13] S. Sun, J. Dai, W. Wang et al., "Metabonomic evaluation of ZHENG differentiation and treatment by Fuzhenghuayu tablet in hepatitis-B-caused cirrhosis," *Evidence-Based Complementary and Alternative Medicine*, vol. 2012, Article ID 453503, 8 pages, 2012.

[14] A. Yukiharu, "The truth of the accident-some patients died from side efects of Xiao Chai Hu Tang," *Journal of Tianjin University of Traditional Chinese Medicine*, vol. 21, no. 1, pp. 47-48, 2002.

[15] M. Jiang, C. Lu, C. Zhang et al., "Syndrome differentiation in modern research of traditional Chinese medicine," *Journal of Ethnopharmacology*, vol. 140, no. 3, pp. 634–642, 2012.

[16] W. Zheng, *Research on Correlations Among TCM Common Type of Syndromes and Laboratory Index in 1260 Patients with CHB*, Chengdu University of Traditional Chinese Medicine, Chengdu, China, 2011.

[17] C. J. Yang, H. W. Liu, and L. C. Wang, "Study on the differential gene expressions of chronic hepatitis B patients of gan depression pi deficiency syndrome and pi-wei damp-heat syndrome," *Chinese Journal of Integrated Traditional and Western Medicine*, vol. 32, pp. 1032–1037, 2012.

[18] P. B. Talbert and S. Henikoff, "Histone variants-ancient wrap artists of the epigenome," *Nature Reviews Molecular Cell Biology*, vol. 11, no. 4, pp. 264–275, 2010.

[19] R. Singh, D. Kumar, R. C. Duncan, H. L. Nakhasi, and P. Salotra, "Overexpression of histone H2A modulates drug susceptibility in Leishmania parasites," *International Journal of Antimicrobial Agents*, vol. 36, no. 1, pp. 50–57, 2010.

[20] F. Hao, *The Role of Nucleosome in the Pathogenesis of SLE and its H2B Peptide-Induced Immune Tolerance Therapies*, Third Military Medical University, Chongqing, China, 2003.

[21] T. Chen, Y. Chen, W. Bao, and W. Lu, "T-lymphocyte subsets and Th1/Th2 cytokines in convalescent patients with Epstein-Barr virus-associated aplastic anemia," *Hematology*, vol. 25, no. 1, pp. 11–16, 2020.

[22] A. Jafarzadeh and F. Shokri, "TH1 and TH2 responses are influenced by HLA antigens in healthy neonates vaccinated with recombinant hepatitis B vaccine," *Iranian Journal of Allergy, Asthma and Immunology*, vol. 11, no. 4, pp. 308–315, 2012.

[23] Hepatobiliary Branch of Chinese Society of Traditional Chinese Medicine, "Standard of TCM syndrome differentiation for viral hepatitis (2017 version)," *Chinese Journal of Integrated Traditional and Western Medicine on Liver Diseases*, 2017.

[24] T. Tu, S. Bühler, and R. Bartenschlager, "Chronic viral hepatitis and its association with liver cancer," *Biological Chemistry*, vol. 398, no. 8, pp. 817–837, 2017.

[25] Q. J. Wu, W. L. Lv, J. M. Li et al., "Efficacy and safety of YinQiSanHuang antiviral decoction in chronic hepatitis B: study protocol for a randomized, placebo controlled, double-blinded trial," *Trials*, vol. 21, no. 1, p. 482, 2020.

[26] Y. Y. Lu, Q. L. Chen, Y. Guan et al., "Study of ZHENG differentiation in hepatitis B-caused cirrhosis: a transcriptional profling analysis," *BMC Complementary and Alternative Medicine*, vol. 14, p. 371, 2014.

[27] M. Lee, M. A. Lee, S. K. Lee et al., "Expression of Th1 and Th2 type cytokines responding to HBsAg and HBxAg in chronic hepatitis B patients," *Journal of Korean Medical Science*, vol. 14, no. 2, pp. 175–181, 1999.

[28] C. Law, P. Cheung, and K. Adhvaryu, "Chemical "diversity" of chromatin through histone variants and histone modifications," *Current Molecular Biology Reports*, vol. 1, no. 1, pp. 39–59, 2015.

[29] T. C. Voss and G. L. Hager, "Dynamic regulation of transcriptional states by chromatin and transcription factors," *Nature Reviews Genetics*, vol. 15, no. 2, pp. 69–81, 2014.

[30] M. Matecic, S. Stuart, and S. G. Holmes, "SIR2-induced inviability is suppressed by histone H4 overexpression," *Genetics*, vol. 162, no. 2, pp. 973–976, 2002.

[31] S. R. Nayak, E. Harrington, D. Boone et al., "A role for histone H2B variants in endocrine-resistant breast cancer," *Hormones and Cancer*, vol. 6, no. 5-6, pp. 214–224, 2015.

[32] R. C. Molden, N. V. Bhanu, G. LeRoy et al., "Multi-faceted quantitative proteomics analysis of histone H2B isoforms and their modifications," *Epigenetics & Chromatin*, vol. 8, p. 15, 2015.

[33] J. P. Portanova, J. C. Cheronis, J. K. Blodgett, and B. L. Kotzin, "Histone autoantigens in murine lupus. Definition of a major epitope within an accessible region of chromatin," *Journal of Immunology (Baltimore, Md.: 1950)*, vol. 144, no. 12, pp. 4633–4640, 1990.

[34] C. Stemmer, J.-P. Briand, and S. Muller, "Mapping of linear histone regions exposed at the surface of the nucleosome in solution," *Journal of Molecular Biology*, vol. 273, no. 1, pp. 52–60, 1997.

[35] I.-C. Ho, T.-S. Tai, and S.-Y. Pai, "GATA3 and the T-cell lineage: essential functions before and after T-helper-2-cell differentiation," *Nature Reviews Immunology*, vol. 9, no. 2, pp. 125–135, 2009.

[36] T. Wang, A. L. Feldman, D. A. Wada et al., "GATA-3 expression identifies a high-risk subset of PTCL, NOS with distinct molecular and clinical features," *Blood*, vol. 123, no. 19, pp. 3007–3015, 2014.

[37] M. Anusree and B. Shashi, "Lower expression of GATA3 and T-bet correlates with down-regulated IL-10 in severe falciparum malaria," *Clinical & Translational Immunology*, vol. 4, no. 11, p. 49, 2015.

[38] S. Chen, L. Wu, L. Peng, X. Wang, and N. Tang, "Hepatitis B virus X protein (HBx) promotes ST2 expression by GATA2 in liver cells," *Molecular Immunology*, vol. 123, pp. 32–39, 2020.

Hindawi
Evidence-Based Complementary and Alternative Medicine
Volume 2021, Article ID 9415819, 10 pages
https://doi.org/10.1155/2021/9415819

Research Article

ChaiQi Decoction Alleviates Vascular Endothelial Injury by Downregulating the Inflammatory Response in ApoE-Model Mice

Bingran Wang,[1,2] **Jiayan Zhang**,[2] **Yuhong Lu**,[1] **Long Peng**,[1,2] **Wenling Yuan**,[1,2] **Yuqing Zhao**,[1,2] **and Liping Zhang**[1]

[1]*Graduate School, Beijing University of Chinese Medicine, Beijing, China*
[2]*Department of Gastroenterology, Dongfang Hospital, Beijing University of Chinese Medicine, Beijing, China*

Correspondence should be addressed to Liping Zhang; lpzhang2005@126.com

Received 19 July 2020; Revised 29 December 2020; Accepted 9 January 2021; Published 10 February 2021

Academic Editor: Jianbo Wan

Metabolic syndrome (MetS) is a pathological state of metabolic disorders that primarily occur in human proteins, fats, and carbohydrates. It is a complex cluster of core metabolic disorder syndromes including obesity, hyperglycemia, dyslipidemia, and hypertension, and vascular endothelial injury, occurring over time. The currently available treatment options cannot effectively manage MetS. In our previous research, we revealed ChaiQi decoction (CQD) as an effective prescription for improving MetS; however, the specific mechanism remains unclear. Herein, we assessed the efficacy and mechanism of CQD in ApoE gene knockout (ApoE-) mice. Mice were administered with CQD daily for 12 weeks, and the measurement of their body weight was taken monthly. To evaluate the metabolic levels of mice, we determined the fasting blood glucose (FBG), fasting serum insulin (FINS), insulin resistance index (IRI), triglyceride (TG), total cholesterol (TC), high-density lipoprotein cholesterol (HDL-C), and low-density lipoprotein cholesterol (LDL-C) levels. Furthermore, immunohistochemical analysis was adopted to determine the expression of ICAM-1 and VCAM-1 in vascular endothelium, while an optical microscope was adopted to observe the pathological morphology of abdominal aorta in mice. Tumor necrosis factor-α (TNF-α), interleukin-6 (IL-6), intercellular cell adhesion molecule-1 (ICAM-1), and vascular cell adhesion molecule-1 (VCAM-1) levels were determined using the ELISA method, whereas Western blotting was used to determine nuclear factor- (NF-) κB p65. Of note, intragastric CQD administration ameliorated ApoE-model mice, as evidenced by reduced levels of FBG, FINS, IRI, TG, TC, and LDL-C. Furthermore, CQD alleviated vascular endothelial injury and regularized the structure of the abdominal aorta by downregulating the expressions of proinflammatory cytokines TNF-α, IL-6, ICAM-1, VCAM-1, and NF-κB p65. Overall, these findings advocated that CQD ameliorates metabolic levels and vascular endothelial injury in mice by downregulating the inflammatory response and thus may be utilized as a novel MetS therapy.

1. Introduction

Metabolic syndrome (MetS) is a cluster of metabolic diseases that transpire together. With the changing lifestyle and westernized diet in recent years, people are increasingly consuming red meat, processed food, refined grain, sugar, and saturated fatty acids. This elevates the incidence of MetS which is estimated to be 25% in the United States, 23% in Europe, and 20–25% in South Asia [1]. Research showed that the risk of cardiovascular disease potentially is advanced by the symptoms of MetS and could become severe when several abnormalities occur concomitantly; this causes major adverse cardiac events (MACE) [2]. Moreover, the probability of cardiovascular diseases and stroke in MetS patients was previously reported to be 2-3 times higher than in non-MetS patients [3]. A prospective analysis conducted to determine the atherosclerosis risk in a community study indicated an 18% greater risk of incident MetS for individuals with the highest western dietary pattern score [4]. MetS symptoms, such as central obesity, dyslipidemia, insulin resistance (IR), and hypertension, are closely associated with vascular endothelial injury, increased intercellular cell adhesion molecule-1(ICAM-1), and vascular cell adhesion molecule-1 (VCAM-1); this promotes inflammation.

According to some investigations, reducing inflammation can prevent injury to vascular endothelium [5].

Research on the risk factors associated with metabolic syndrome is constantly on the rise. Several studies have revealed that inflammation is critically important in the occurrence and development of MetS. A study by Hotamisligil first proposed the new medical concept of metabolic inflammation, emphasizing that this low-grade, chronic systemic inflammation mainly arises due to excess nutrients and metabolites. Metabolic inflammation may have similar signaling pathways with typical inflammation [6]. Under normal circumstances, the body is at a steady-state level, and a dynamic balance is maintained between inflammation and metabolism. However, in case of a metabolic disorder, an imbalance occurs in the immune system, activating inflammatory signaling pathways, and prompts the body to release inflammatory factors or amplify an inflammatory response; this causes IR and eventually results in the occurrence of MetS.

Tumor necrosis factor-α (TNF-α) plays a vital role in the formation of IR [7]. A specific correlation between TNF-α level and hypertension exists. Furthermore, interleukin-6 (IL-6) both participates in inflammation and greatly influences the blood vessels; some findings suggest an important role for IL-6 in limiting endothelial dysfunction in response to angiotensin II [8]. Previous studies have reported that IL-6 is associated with obesity-related IR, which alters the formation of normal subcutaneous adipose tissue and interferes with lipid metabolism [9, 10]. Excess IL-6 levels can affect insulin receptor signal transduction and further induce IR. Besides, nuclear factor- (NF-) κB can mediate inflammation and participate in immune regulation and is also related to IR, central obesity, hypertension, lipid metabolism disorders, glucose metabolism disorders, and vascular remodeling. Increased levels and activation of the above inflammatory factors promote the occurrence of MetS.

At present, no effective treatment for MetS is clinically available, and the existing treatment options eliminate various metabolic abnormalities. Commonly used drugs include insulin sensitizers, lipid-lowering drugs, hypoglycemic drugs, and antihypertensive drugs which purposely control obesity and IR and reduce the occurrence of MACE and diabetes [11]. However, these treatments may cause adverse reactions, among them, cough, elevated serum creatinine, headache, gastrointestinal symptoms, and rashes. Notably, there is a lack of treatment for overall metabolic abnormalities; therefore, novel and effective drugs for MetS treatment should urgently be developed [12, 13].

ChaiQi decoction (CQD) is a new and effective traditional Chinese medicine prescription formulated by Zhang, a professor at the Beijing University of Chinese Medicine. In our previous study, we revealed that CQD relieved IR in mice models of MetS induced by an improper diet [14]. Besides, the diet-induced MetS mice model is unstable, the ApoE-mice are more stable and can highly simulate systemic metabolic and functional abnormality, though the actual mechanism of action is yet to be elucidated. Therefore, the present study sought to comprehensively explore the underlying molecular mechanism by which CQD exerts protective effects in ApoE-mice models.

2. Materials and Methods

2.1. Preparing CQD and LC-MS Analysis of Identified Compounds. CQD granules were purchased from the Pharmacy Department of Dongfang Hospital, Beijing University of Chinese Medicine (Beijing, China). The CQD granules contained ChaiQi ingredients in equal amounts as follows: Chaihu (radix bupleuri), 10 g; Huangqi (radix astragali), 30 g; Baizhu (rhizoma atractylodis macrocephalae), 10 g; Zhishi (fructus aurantii immaturus), 10 g and Sanqi (pseudoginseng), 3 g. CQD was decocted with boiling water at 100°C for 30 min and was prepared into a solution of 100 mg/ml concentration. Liquid chromatography-mass spectrometry (LC-MS) was used to identify the main components of CQD. Chromatographic separation was carried on a Symmety C18 column and the column temperature was maintained at 25°C. The mobile phase was composed of 0.1% formic acid (A) and acetonitrile (B) with gradient elution system (0–30 min, 90%A; 30–60 min, 90%⟶70%A; 60–100 min, 70%⟶40%A; 100–120 min, 40%⟶10%A) at a flow rate of 0.2 mL/min, and the injection volume was 10 μL. The electrospray ion source (ESI) was used for full scan in both positive and negative modes, 50 psi of nebulizer pressure, 10 L/min of spray gas flow, 350°C of spray gas temperature, 1.00 V of crushing voltage, and 50–1000 m/z of scanning range.

2.2. Experimental Animals. All the experimental procedures were approved by the Animal Ethics Committee of Beijing University of Chinese Medicine, following guidelines issued by Regulations of Beijing Laboratory Animal Management. In total, 8 male ApoE-mice as the model group and 8 male ApoE-mice as the CQD group, and 8 male C57BL/6J mice as the blank control group (all mice weighing 20–30 g and 6-week-old; Vital River Laboratory Animal Technology, Beijing, China) were housed in a specific pathogen-free room with a temperature range between 20 and 24oC, 50–60% humidity, light-controlled environment (12/12 h light/dark cycle), and free access to food and sterile tap water. All animals were allowed to adapt to the living conditions for 7 days before commencing the experiments.

2.3. Model Assessment and Experimental Procedure. The MetS model is spontaneously constructed using ApoE-mice. The successful development of the model is judged by detecting the degree of insulin resistance and blood lipid metabolism. CQD and distilled water were administered once daily. The mice in the CQD (8.19 g/kg/day, p.o., $n = 8$) group were administered with CQD for 12 weeks, whereas for the control ($n = 8$) group and model ($n = 8$) group, mice received only distilled water. All mice were sacrificed through cervical dislocation and blood samples collected from the Infraorbital venous plexus. The abdominal aorta was removed and cut into 2 sections. One section was fixed in 4% polyformaldehyde for histological analysis, while the

section was stored in the freezer at −80oC for further analysis.

2.4. Analysis of Blood Glucose and Insulin. A measure of the bodyweight of all mice was taken at the same time every month. Using the collected blood samples, fasting blood glucose (FBG) serum levels were assessed using mice ELISA kits (KH Bio-engineering, Shanghai, China), whereas fasting serum insulin (FINS) levels were assessed using mice radioimmunoassay kits (North Institute of Biotechnology, Beijing, China). The insulin resistance index (IRI) was calculated using the homeostasis model HOMA with the formula, IRI = (FBG × FINS)/22.5.

2.5. Assay for Serum Lipid Levels. Using the collected blood samples, triglyceride (TG), total cholesterol (TC), high-density lipoprotein cholesterol (HDL-C), and low-density lipoprotein cholesterol (LDL-C) levels were determined using mice ELISA kits (KH Bio-engineering, Shanghai, China).

2.6. Histological Analysis. After tissues were fixed in 4% polyformaldehyde for 24 h, they were taken out from polyformaldehyde and washed with running water. Then, tissues were dehydrated using a gradient-force dehydrator, embedded in paraffin blocks, and sectioned to 4 μm a thickness. Thereafter, the sections were stained with hematoxylin and eosin (HE). An optical microscope was used to observe the pathological changes in the aortas.

2.7. Immunohistochemical Analysis to Detect ICAM-1 and VCAM-1 Expression in Abdominal Aortic Endothelium. Vessel tissue sections were stained using labeled streptavidin-biotin technique and developed with diaminobenzidine to evaluate the expression levels of ICAM-1 and VCAM-1. Observing the stained area, the brownish-yellow particles in the nucleus or cytoplasm were positive expressions that were darker than the background. We observed 15 different fields of view under each specimen at high magnification and analyzed the data after image acquisition.

2.8. Detecting Related Inflammatory Factor. TNF-α, IL-6, ICAM-1, and VCAM-1 levels were assessed using mice ELISA kits (R&D Systems, USA), whereas Western blot was used to determine the expression of NF-κB p65, with the protocol as previously described [15]. The concentrations of proteins isolated from aorta abdominal tissues were determined using bicinchoninic acid (BCA) assay (CW-Biotech, Beijing, China). Then, the proteins were separated in 10% SDS-PAGE for 1.5 h before they were transferred to polyvinylidene fluoride (PVDF) membranes. The membranes were probed with NF-κB p65 (1 : 500) and β-actin (1 : 1000) antibodies (TDY-Biotech, Beijing, China) and incubated with goat polyclonal secondary antibody to rabbit antibodies (ZSGB-Biotech, Beijing, China). Eventually, densitometry was executed to quantify protein band intensities using the Image-pro analyzer.

2.9. Statistical Analysis. All data were expressed as mean-± standard deviation (SD) values. SPSS v22.0 (IBM Corp., Armonk, NY, USA) was used for statistical analyses. A comparison of data between groups was performed using one-way analysis of variance (ANOVA) and nonparametric test. $P < 0.05$ was considered statistically significant.

3. Results

3.1. Effect of CQD on Body Weight in Mice. All mice's initial weight was 20–30 g, and there was no statistically significant difference in body weight between the groups; all mice adapted effectively to entire experimental conditions, and no deaths occurred. By the end of the 12th week, the weight of mice in each group was higher compared to the initial weight, showing a statistically significant difference, $P < 0.05$. The weight change in the model group was significantly higher compared to the blank control group (1.21 ± 0.061 versus 1.057 ± 0.072, $P < 0.05$). Moreover, the weight change in the CQD group was visibly lower compared to the model group (1.14 ± 0.115 versus 1.21 ± 0.061, $P < 0.05$) (Figure 1).

3.2. Identification of Eight Compounds in CQD by LC-MS Analysis. By contrasting the different chromatographic peaks of CQD and Chinese herbal medicine monomers, we identified 8 compounds from 27 (Figure 2). Eight drug prototype compounds are as shown in Table 1.

3.3. Regulatory Effect of CQD on Blood Glucose and Insulin in Mice. The FBG level in the model group was significantly higher compared to the blank control group ($P < 0.05$), whereas the level in the CQD group was remarkably lower than that in the model group ($P < 0.05$) (Figure 3(a)). Besides, the FINS level in the model group was higher compared to that in the blank control group ($P < 0.05$), whereas the level in the CQD group was significantly lower than in the model group ($P < 0.05$) (Figure 3(b)). Furthermore, the IRI level in the model group was higher compared to the blank control group ($P < 0.05$), while the level in CQD group was notably lower compared to that in the model group ($P < 0.05$) (Figure 3(c)).

3.4. Effect of CQD on Serum Lipid in Mice. Here, the TG level in the model group was significantly higher compared to that in the blank control group ($P < 0.05$), while the level in the CQD group was remarkably lower than that in the model group ($P < 0.05$) (Figure 4(a)). Moreover, the TC level in the model group was higher compared to that in the blank control group ($P < 0.05$), whereas the level in the CQD group was significantly lower than that in the model group ($P < 0.05$) (Figure 4(b)). The LDL-C level in the model group was significantly higher compared to that in the blank control group ($P < 0.05$), whereas the level in the CQD group was remarkably lower than that in the model group

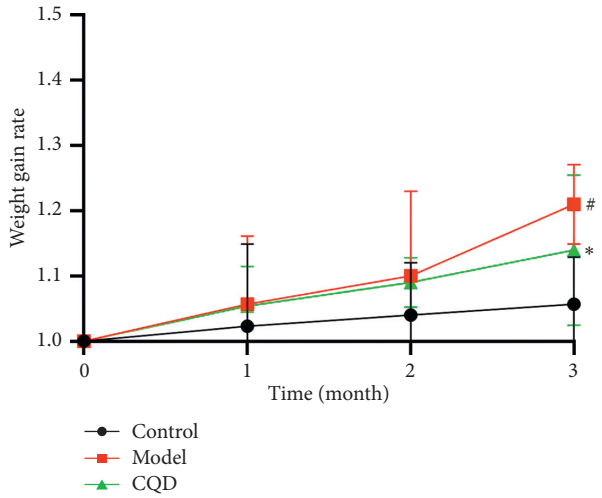

Figure 1: Changes in body weight of mice in each group. Weight gain rate = weight measured in each month/initial weight. Control: blank control group; model: model group; CQD: ChaiQi decoction group. Data are presented as the mean ± SD. $^{\#}P < 0.05$ versus the control group; $^{*}P < 0.05$ versus the model group ($n = 8$ mice per group).

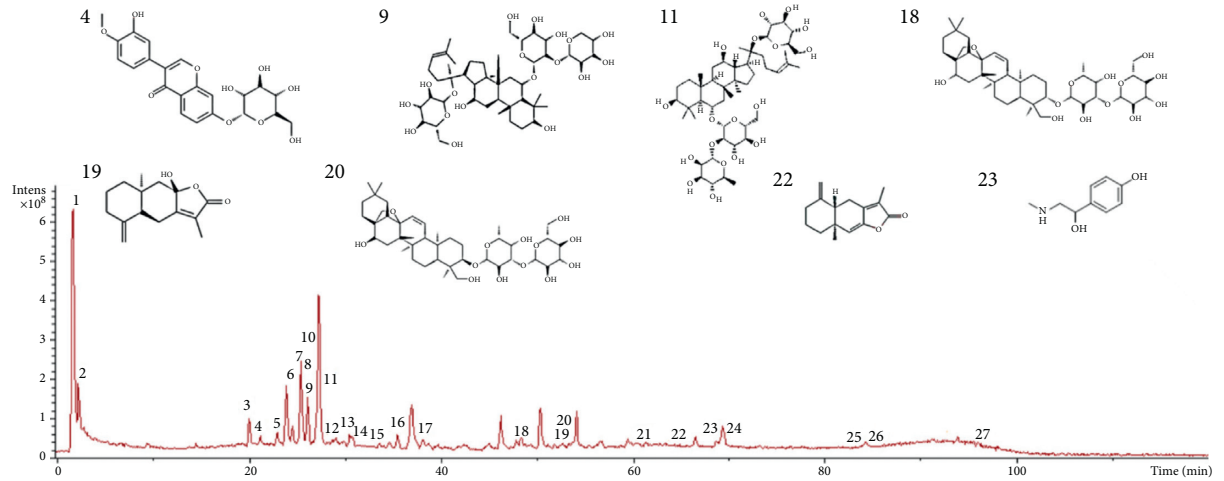

Figure 2: The HPLC fingerprints of BSHXDS components: (4) calycosin-7-glucoside; (9) notoginsenoside R1; (11) ginsenoside Re; (18) saikosaponin A; (19) atractylenolide III; (20) saikosaponin D; (22) atractylenolide I; (23) synephrine.

Table 1: Eight compounds identified in CQD.

No.	Compound	Retention time (min)	Source
4	Calycosin-7-glucoside	20.1	Huangqi (radix astragali)
9	Notoginsenoside R1	26.2	Sanqi (pseudoginseng)
11	Ginsenoside Re	27.3	Sanqi (pseudoginseng)
18	Saikosaponin A	48.3	Chaihu (radix bupleuri)
19	Atractylenolide III	52.6	Baizhu (rhizoma atractylodis macrocephalae)
20	Saikosaponin D	53.4	Chaihu (radix bupleuri)
22	Atractylenolide I	64.8	Baizhu (rhizoma atractylodis macrocephalae)
23	Synephrine	69.4	Zhishi (fructus aurantii immaturus)

($P < 0.05$) (Figure 4(c)). Additionally, the HDL-C level in the model group was higher than that in the blank control and CQD groups ($P < 0.05$) (Figure 4(d)); notably, the increase of HDL-C could be attributed to inflammation.

3.5. CQD Improved Histopathology in Mice. Compared with the blank control group (Figure 5(a)), the model group showed a damaged structure of the three abdominal aortic walls. The tunica intima was rough and became thick and

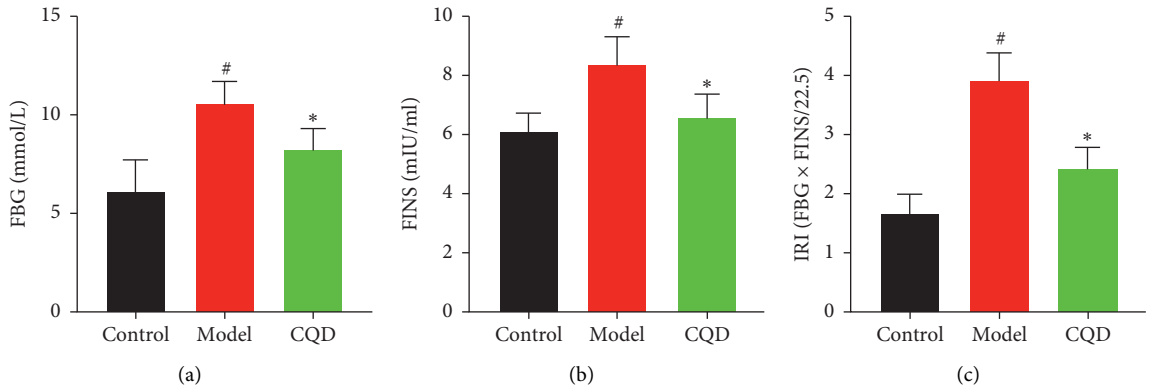

Figure 3: Regulatory effect of CQD on blood sugar and insulin. (a) FBG level; (b) FINS level; (c) IRI level; control: blank control group; model: model group; CQD: ChaiQi decoction group. $^{\#}P < 0.05$ versus the control group; $^{*}P < 0.05$ versus the model group ($n = 8$ mice per group).

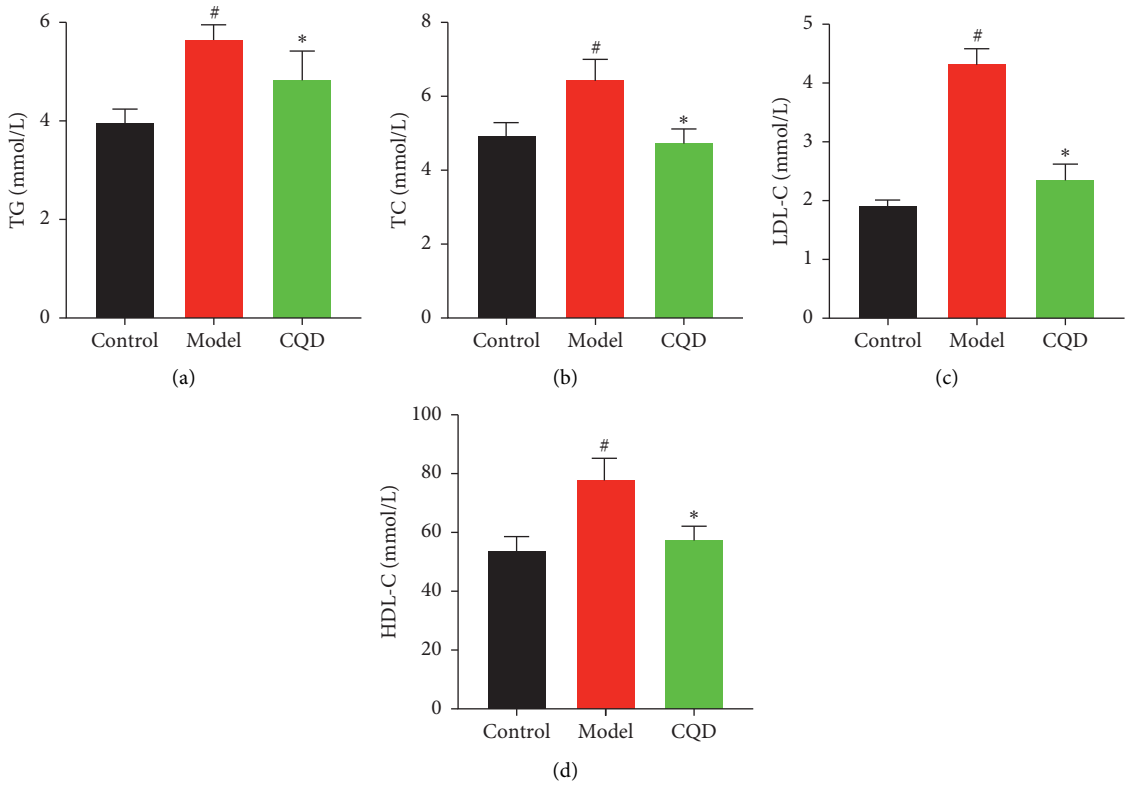

Figure 4: Effect of CQD on serum lipid in mice. (a) TG level; (b) TC level; (c) LDL-C level; (d) HDL-C level. Control: blank control group; model: model group; CQD: ChaiQi decoction group. $^{\#}P < 0.05$ versus the control group; $^{*}P < 0.05$ versus the model group ($n = 8$ mice per group).

protruded, and a few endothelial cells were damaged. The smooth muscles of tunica media were uneven showing disordered cells (Figure 5(b)). The manifestation of the CQD group was better than that of the model group (Figure 5(c)): less endothelial cells were damaged. The texture and thickening of the tunica intima, as well as the unevenness of the tunica media, were improved. Also, the smooth muscle cells exhibited a more regular arrangement.

3.6. CQD Lowered ICAM-1 and VCAM-1 Expression in Abdominal Aortic Endothelium. Through immunohistochemistry analysis, the brownish-yellow showed positive expression. The expression of ICAM-1 in the blank control group (Figure 6(a)) was extremely low, while, in the model group (Figure 6(b)), brown-yellow particles were highly deposited in the inner membrane, and some were fused into pieces but were significantly more than that in the blank

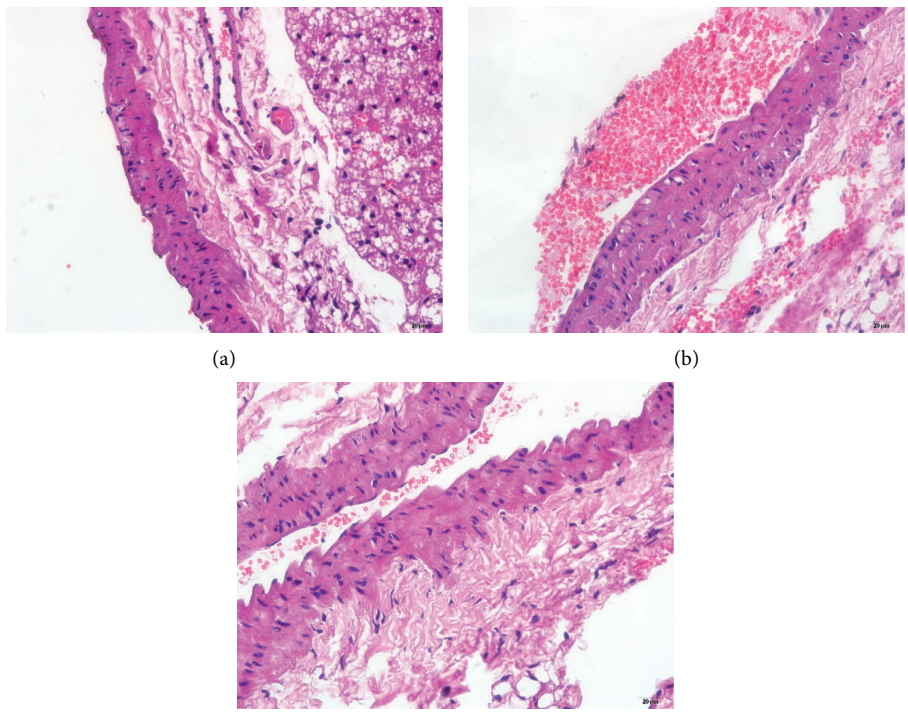

(a) (b) (c)

Figure 5: CQD improved histopathology in mice (×400). (a) Blank control group; (b) model group; (c) ChaiQi decoction group.

control group. Although the CQD group (Figure 6(c)) showed brown-yellow particles in the inner membrane, the expression level was significantly lower than that in the model group. Similarly, for ICAM-1, the expression of VCAM-1 in the blank control group (Figure 6(d)) was extremely low, whereas it was highly expressed in the inner membrane in the model group (Figure 6(e)); this was significantly higher compared to that in the blank control group. Meanwhile, in the CQD group, the expression of VCAM-1 in the inner membrane was lower compared to the model group (Figure 6(f)).

3.7. CQD Inhibited the Expression of TNF-α, IL-6, ICAM-1, and VCAM-1 in the Serum of Mice. The serum TNF-α, IL-6, ICAM-1, and VCAM-1 levels in the model group were significantly higher compared to that in the blank control group ($P < 0.05$). At the same time, TNF-α, IL-6, ICAM-1, and VCAM-1 levels in the CQD group were remarkably lower than in the model group ($P < 0.05$) (Figure 7(a)–7(d)).

3.8. CQD Lowered the Expression of NF-κB p65 in Mice. The expression of NF-κB p65 in the model group was significantly higher compared to that in the blank control group ($P < 0.05$), whereas NF-κB p65 expression in the CQD group was significantly lower than that in the model group ($P < 0.05$) (Figure 8(a)–8(c)).

4. Discussion

Based on the current understanding, MetS is a cluster of metabolic disorders, including central obesity, insulin resistance, diabetes, dyslipidemia, and hypertension. Notably, IR is the core in the progress of MetS and IR can change the metabolism of blood glucose and blood lipids, increase the level of free fatty acids, promote inflammation, accelerate oxidative stress, and alter the spectrum of adipocytokines [16, 17]. Insulin functions promote a reduction in glucose utilization; this elevates blood glucose levels and impairs glucose tolerance. Besides, IR is highly prevalent in MetS patients with vascular endothelial injuries. It can retard endothelium-dependent vasodilation thereby affecting the stability of blood vessels and mediate the formation of atherosclerosis [18]. Similarly, IR is, in most cases, accompanied by hyperinsulinemia. Normal insulin levels are crucial in maintaining vascular endothelial function. However, hyperinsulinemia has been revealed to potentially result in vascular endothelial dysfunction [19]. Normal endothelial cells regulate vascular smooth muscle cells by releasing endothelium-derived factors to maintain vascular tension. Further, it secretes numerous vasoactive substances including nitric oxide (NO) and endothelial contractile factor (ET) which finetune normal vessel integrity and tension stimulated by physiological doses of insulin [20]. Besides, NO is regarded as one of the important indicators of endothelial relaxation function. When Mets develops, the endothelial cells are damaged and NO synthesis is reduced, resulting in reduced endothelium-dependent vasodilation induced by vasodilators such as reactive hyperemia and acetylcholine and high ET secretion [21]. These events cause vasodilation disorders and endothelial dysfunction.

Herein, to reveal the effect of CQD on vascular endothelial injury caused by MetS, we selected ApoE-mice as the

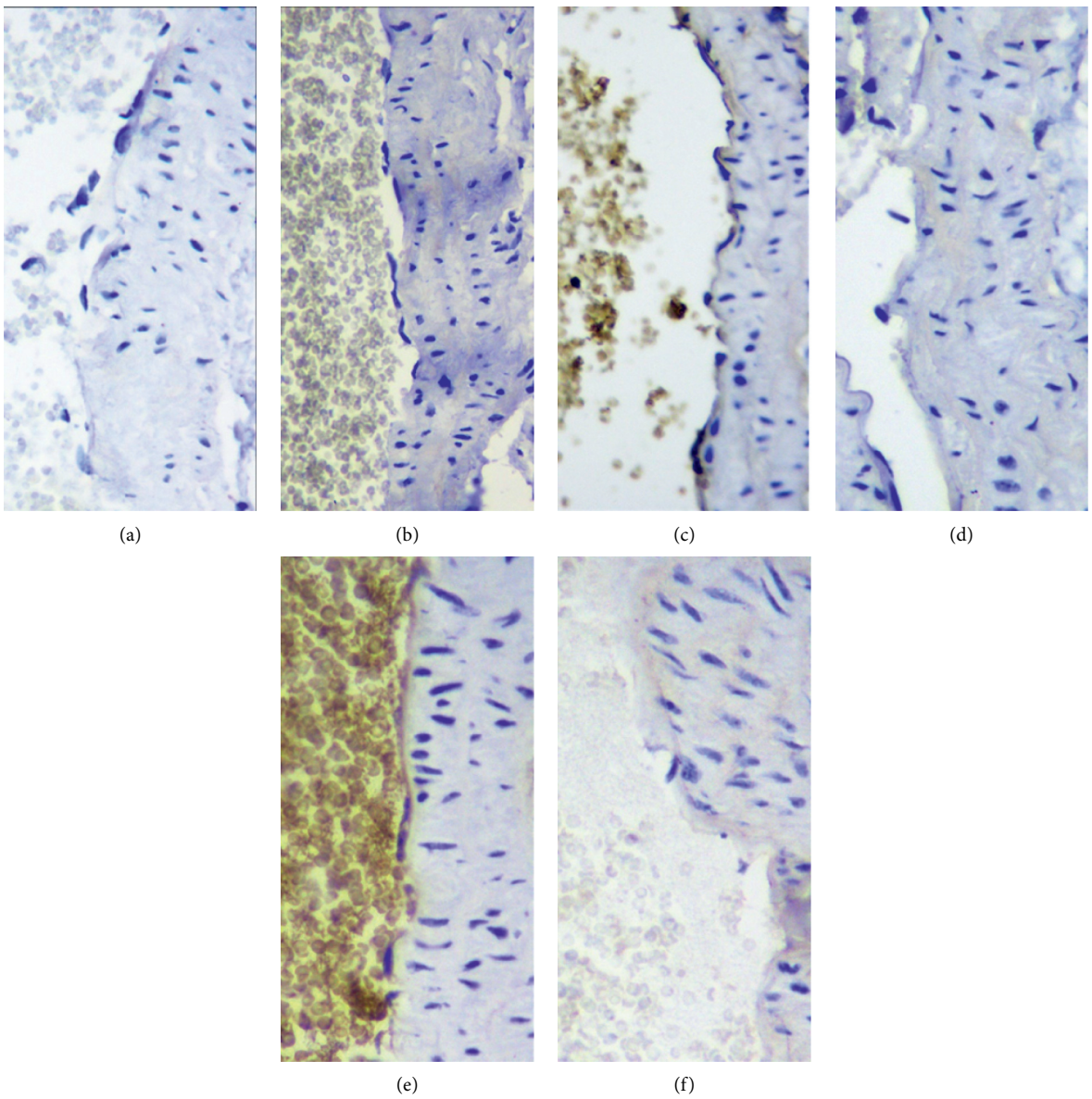

Figure 6: CQD lowered ICAM-1 and VCAM-1 expression in abdominal aortic endothelium. (a) ICAM-1 expression in the blank control group; (b) ICAM-1 expression in the model group; (c) ICAM-1 expression in the ChaiQi decoction group; (d) VCAM-1 expression in the blank control group; (e) VCAM-1 expression in the model group; (f) VCAM-1 expression in ChaiQi decoction group.

model for spontaneous Mets formation. Based on the previous findings, IR is considered to be a key factor in the occurrence and progression of MetS [22]. Therefore, we assessed the formation of MetS by determining the IRI of mice. In our study, the weight of mice increased as the experiment progressed, the disorders of blood glucose and lipid metabolism and IR occurred, indicating that we successfully established the MetS model. Accordingly, in the histological analysis, the abdominal aorta endothelium of the model group was severely damaged, and adhesion molecules were highly accumulated. On the other hand, the IRI and lipid metabolism in mice from the CQD group were lower, suggesting that the CQD had prominent therapeutic effects on ApoE-mice which resulted in MetS and vascular endothelial injury.

Studies have described MetS as a state of systemic low inflammation, and this low-level inflammatory reaction may bridge the components of metabolic syndrome, manifested as an abnormal production of inflammatory factors and activation of inflammatory signaling pathways [23–26]. When IR occurs, TNF-α is overexpressed in blood and adipose tissue and is negatively correlated with insulin sensitivity [27]. Many literature reports have confirmed that the high expression of IL-6 during IR is related to the activation of the NF-κB signaling pathway, and after the regulation of body mass index and fat content, the plasma IL-6 level is still associated with insulin sensitivity [28–31]. Moreover, when endothelial dysfunction occurs in the IR state, the expression of ICAM-1 and VCAM-1 is promoted; thus monocytes adhere to endothelial cells in circulation. Then, monocytes and lymphocytes gather

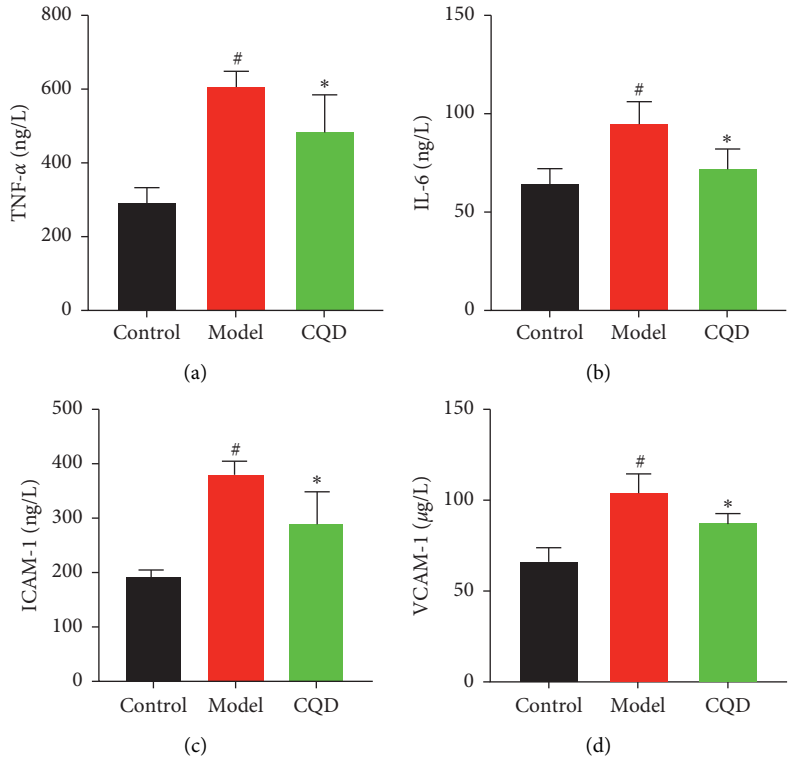

Figure 7: CQD inhibited the expression of TNF-α, IL-6, ICAM-1, and VCAM-1 in the serum of mice. Control: blank control group; model: model group; CQD: ChaiQi decoction group. $^{\#}P < 0.05$ versus the control group; $^{*}P < 0.05$ versus the model group ($n = 8$ mice per group).

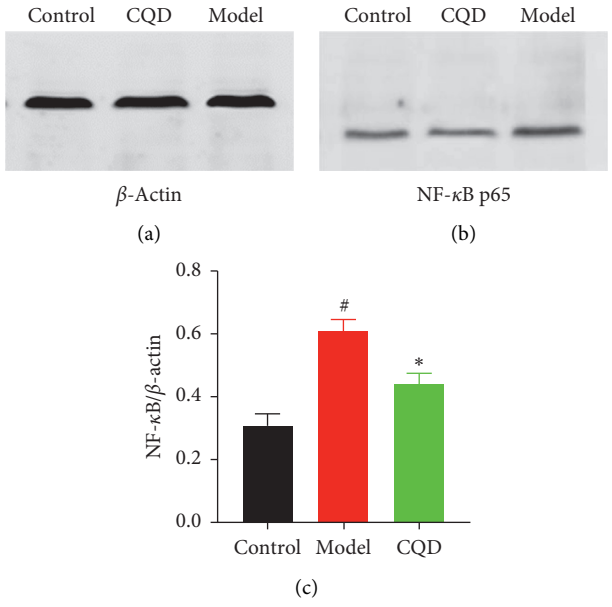

Figure 8: CQD lowered the expression of NF-κB p65 in mice. Control: blank control group; model: model group; CQD: ChaiQi decoction group. $^{\#}P < 0.05$ versus the control group; $^{*}P < 0.05$ versus the model group ($n = 8$ mice per group).

under the intima, triggering a series of inflammatory and immune reactions. Other assessments have shown that the NF-κB signaling pathway can be activated in different cells during the IR process. Activation of the NF-κB signaling pathway has been revealed to be closely associated with the occurrence of IR [32].

Vascular injury is a pathological process accompanied by a chronic inflammatory reaction. Inflammatory mediators have been reported to play an important role in the formation and development of vascular injury [33, 34]. When an inflammatory reaction occurs in blood vessels, B lymphocytes, T lymphocytes, and monocyte macrophages

are activated, producing numerous inflammatory factors such as IL-6 and TNF-α. In our study, under physiological conditions, ICAM-1 and VCAM-1 showed low expression or no expression. Notably, when the blood vessels were injured, they could induce the release of TNF-α, rapidly upregulate ICAM-1 and VCAM-1, and enhance the adhesion between leukocytes and vascular endothelial cells, thus activating endothelial cells. Moreover, ICAM-1 and VCAM-1 can promote aggregation of inflammatory cells and release of inflammatory mediators, damage the barrier function of the endothelium, and increase the permeability of vascular wall, thus causing endothelial injury and vascular dysfunction [35]. NF-κB, a ubiquitous factor in tissues and cells, can induce nuclear transcription activation, participate in immune regulation, and mediate an inflammatory response. NF-κB signaling pathway can activate a variety of immune and inflammatory cytokines, for example, TNF-α, IL-1, IL-6, ICAM-1, and VCAM-1. The proinflammatory pathway regulated by NF-κB is closely linked to metabolic vascular diseases. Some scholars believe that NF-κB is one of the initiating factors for atherosclerosis [36].

In this study, after observing a definite effect of CQD in ApoE-mice with MetS, we further explored the therapeutic mechanism. We assessed the serum levels of TNF-α, IL-1, IL-6, ICAM-1, and VCAM-1 to explore the role of inflammatory factors in the development of MetS and IR and then determined the content of NF-κB using Western blotting. Of note, we revealed that CQD could improve the level of MetS and reduce the injury of vascular endothelium in ApoE-model mice by reducing inflammatory factors and inhibiting the expression of NF-κB related pathway.

In the present study, using ApoE-mice model with vascular endothelial injury, we uncovered that CQD significantly improved the body weight, IRI, and serum lipid level as well as TNF-α, IL-6, ICAM-1, VCAM-1, and NF-κB content. The protective effects of CQD may be attributed to its significant regulation of inflammatory response and the NF-κB signaling pathway. Consequently, this reduces the generation and recruitment of inflammatory cytokines and promotes repair of the injured endothelium.

5. Conclusion

In this work, we identified eight compounds in CQD by liquid chromatography-mass spectrometry analysis and demonstrated that intragastric administration of CQD has a therapeutic effect on Mets, with IR and serum lipid levels as the main monitoring indicators. Notably, CQD can alleviate MetS and the resulting vascular endothelial injury, and the mechanism may be attributed to a significant downregulation of the inflammatory factors and NF-κB related signaling pathway. These findings suggest that CQD may be utilized as a novel therapeutic option for MetS and the resulting vascular endothelial injury.

Data Availability

All data are available upon reasonable request from Bingran Wang, bingranwang93@bucm.edu.cn.

Ethical Approval

Ethical approval for animal studies was provided by the Animal Experimentation Ethics Committee of Dongfang Hospital, Beijing University of Chinese Medicine.

Conflicts of Interest

The authors declare that they have no conflicts of interest.

Authors' Contributions

Wang BR, Chen X, Lu YH, and Zhang LP participated in designing the experiment and manuscript writing. Peng L, Zhao YQ, Yuan WL, and Zhang LP conducted the actual experiments. All authors read and approved the final manuscript.

Acknowledgments

This study was supported by the National Science Foundation of China (Grant no. 81273695).

References

[1] A. Sawant, R. Mankeshwar, S. Shah et al., "Prevalence of metabolic syndrome in urban India," *Cholesterol*, vol. 2011, Article ID 920983, 7 pages, 2011.

[2] L. E. Eberly, R. Prineas, J. D. Cohen et al., "Metabolic syndrome: risk factor distribution and 18-year mortality in the multiple risk factor intervention trial," *Diabetes Care*, vol. 29, no. 1, pp. 123–130, 2006.

[3] R. Gupta, "Metabolic syndrome as a marker of risk in type 2 diabetes," *The Indian Journal of Medical Research*, vol. 129, no. 5, pp. 481–484, 2009.

[4] P. L. Lutsey, L. M. Steffen, and J. Stevens, "Dietary intake and the development of the metabolic syndrome," *Circulation*, vol. 117, no. 6, pp. 754–761, 2008.

[5] I. A. Van den Oever, H. G. Raterman, M. T. Nurmohamed, and S. Simsek, "Endothelial dysfunction, inflammation, and apoptosis in diabetes mellitus," *Mediators Inflamm*, vol. 2010, Article ID 792393, 15 pages, 2010.

[6] G. S. Hotamisligil, "Inflammation and metabolic disorders," *Nature*, vol. 444, no. 7121, pp. 860–867, 2006.

[7] J. Swaroop, J. Naidu, and D. Rajarajeswari, "Association of TNF-α with insulin resistance in type 2 diabetes mellitus," *The Indian Journal of Medical Research*, vol. 135, no. 1, pp. 127–130, 2012.

[8] L. I. Schrader, D. A. Kinzenbaw, A. W. Johnson, F. M. Faraci, and S. P. Didion, "IL-6 deficiency protects against angiotensin II-induced endothelial dysfunction and hypertrophy," *Arteriosclerosis, Thrombosis, and Vascular Biology*, vol. 27, no. 12, pp. 2576–2581, 2007.

[9] T. Tchkonia, T. Thomou, Y. Zhu et al., "Mechanisms and metabolic implications of regional differences among fat depots," *Cell Metabolism*, vol. 17, no. 5, pp. 644–656, 2013.

[10] S. Almuraikhy, W. Kafienah, M. Bashah et al., "Interleukin-6 induces impairment in human subcutaneous adipogenesis in obesity-associated insulin resistance," *Diabetologia*, vol. 59, no. 11, pp. 2406–2416, 2016.

[11] S. Jang, B. H. Jang, Y. Ko et al., "Herbal medicines for treating metabolic syndrome:A systematic review of randomized controlled trials," *Evidence Based Complementary and*

Alternative Medicine, vol. 2016, Article ID 5936402, 17 pages, 2016.

[12] J. Q. Luo, F. Z. He, Z. M. Wang et al., "SLCO1B1 variants and angiotensin converting enzyme inhibitor (Enalapril)-induced cough: apharmacogenetic study[J]," *Scientific Reports*, vol. 5, p. 17253, 2015.

[13] Y. Zhang, Y. J. Liu, J. Zhang et al., "Effects of Pinggan Jiangya pill on blood pressure and body mass index for metabolic syndrome," *Journal of Emergency in Traditional Chinese Medicine*, vol. 19, no. 7, pp. 1128-1129, 2010.

[14] L. P. Zhang, J. Liu, Y. Wang et al., *Discussion on the Timing of Prevention and Treatment of Metabolic Syndrome by Strengthening Spleen and Liver*, Beijing University of Chinese Medicine, Beijing, China, (Chinese), 2011.

[15] F. Huang, C.-Y. Kao, S. Wachi, P. Thai, J. Ryu, and R. Wu, "Requirement for both JAK-mediated PI3K signaling and ACT1/TRAF6/TAK1-dependent NF-κB activation by IL-17a in enhancing cytokine expression in human airway epithelial cells," *The Journal of Immunology*, vol. 179, no. 10, pp. 6504–6513, 2007.

[16] R. Kumari, S. Kumar, and R. Kant, "An update on metabolic syndrome: metabolic risk markers and adipokines in the development of metabolic syndrome," *Diabetes & Metabolic Syndrome: Clinical Research & Reviews*, vol. 13, no. 4, pp. 2409–2417, 2019.

[17] S. Guo, "Insulin signaling, resistance, and metabolic syndrome: insights from mouse models into disease mechanisms," *Journal of Endocrinology*, vol. 220, no. 2, pp. T1–T23, 2014.

[18] S. Muntoni and S. Muntoni, "Insulin resistance: pathophysiology and rationale for treatment," *Annals of Nutrition and Metabolism*, vol. 58, no. 1, pp. 25–36, 2011.

[19] A. A. Lteif, K. Han, and K. J. Mather, "Obesity, insulin resistance, and the metabolic syndrome," *Circulation*, vol. 112, no. 1, pp. 32–38, 2005.

[20] S. Baratchi, K. Khoshmanesh, O. L. Woodman, S. Potocnik, K. Peter, and P. McIntyre, "Molecular sensors of blood flow in endothelial cells," *Trends in Molecular Medicine*, vol. 23, no. 9, p. 850, 2017.

[21] J. E. Barbato, B. S. Zuckerbraun, M. Overhaus, K. G. Raman, and E. Tzeng, "Nitric oxide modulates vascular inflammation and intimal hyperplasia in insulin resistance and the metabolic syndrome," *American Journal of Physiology-Heart and Circulatory Physiology*, vol. 289, no. 1, pp. H228–H236, 2005.

[22] Z. Gluvic, B. Zaric, I. Resanovic et al., "Link between metabolic syndrome and insulin resistance," *Current Vascular Pharmacology*, vol. 15, no. 1, pp. 30–39, 2017.

[23] I. J. Tsai, L. J. Beilin, I. B. Puddey, K. D. Croft, and A. Barden, "Impaired ex vivo leukotriene B4 production characterizes the metabolic syndrome and is improved after weight reduction," *The Journal of Clinical Endocrinology & Metabolism*, vol. 92, no. 12, pp. 4747–4752, 2007.

[24] J. I. León-Pedroza, L. A. González-Tapia, E. del Olmo-Gil, D. Castellanos-Rodríguez, G. Escobedo, and A. González-Chávez, "Low-grade systemic inflammation and the development of metabolic diseases: from the molecular evidence to the clinical practice," *Cirugía Y Cirujanos (English Edition)*, vol. 83, no. 6, pp. 543–551, 2015.

[25] C. J. Andersen, K. E. Murphy, and M. L. Fernandez, "Impact of obesity and metabolic syndrome on immunity," *Advances in Nutrition*, vol. 7, no. 1, pp. 66–75, 2016.

[26] N. Esser, S. Legrand-Poels, J. Piette, A. J. Scheen, and N. Paquot, "Inflammation as a link between obesity, metabolic syndrome and type 2 diabetes," *Diabetes Research and Clinical Practice*, vol. 105, no. 2, pp. 141–150, 2014.

[27] P. L. Ge, D. W. Han, and Z. H. Yan, "Effect of JiangZhiYin on fat factor in insulin resistance rats II," *Acta Chinese Medicine and Pharmacology*, vol. 28, no. 6, pp. 104-105, 2011.

[28] K. Ohashi, A. Kanazawa, S. Tsukada, and S. Maeda, "PKCε induces interleukin-6 expression through the MAPK pathway in 3T3-L1 adipocytes," *Biochemical and Biophysical Research Communications*, vol. 327, no. 3, pp. 707–712, 2005.

[29] S. Devaraj, S. K. Venugopal, U. Singh, and I. Jialal, "Hyperglycemia induces monocytic release of interleukin-6 via induction of protein kinase C- and -," *Diabetes*, vol. 54, no. 1, pp. 85–91, 2005.

[30] M. Jové, A. Planavila, J. C. Laguna, and M. Vázquez-Carrera, "Palmitate-induced interleukin 6 production is mediated by protein kinase C and nuclear-factor kappaB activation and leads to glucose transporter 4 down-regulation in skeletal muscle cells," *Endocrinology*, vol. 146, no. 7, pp. 3087–3095, 2005.

[31] J. M. Fernández-Real, M. Broch, J. Vendrell et al., "Interleukin-6 gene polymorphism and insulin sensitivity," *Diabetes*, vol. 49, no. 3, pp. 517–520, 2000.

[32] R. G. Baker, M. S. Hayden, and S. Ghosh, "NF-κB, inflammation, and metabolic disease," *Cell Metabolism*, vol. 13, no. 1, pp. 11–22, 2011.

[33] M. G. Ugur, R. Kutlu, and I. Kilinc, "The effects of smoking on vascular endothelial growth factor and inflammation markers: a case-control study," *The Clinical Respiratory Journal*, vol. 12, no. 5, pp. 1912–1918, 2018.

[34] T. Chen, J. Xing, and Y. Liu, "Effects of telmisartan on vascular endothelial function, inflammation and insulin resistance in patients with coronary heart disease and diabetes mellitus," *Experimental and Therapeutic Medicine*, vol. 15, no. 1, pp. 909–913, 2018.

[35] D. M. Moreira, R. L. da Silva, J. L. Vieira, T. Fattah, M. E. Lueneberg, and C. A. M. Gottschall, "Role of vascular inflammation in coronary artery disease: potential of anti-inflammatory drugs in the prevention of atherothrombosis," *American Journal of Cardiovascular Drugs*, vol. 15, no. 1, pp. 1–11, 2015.

[36] T. Collins, "Endothelial nuclear factor-kappa B and the initiation of the atherosclerotic lesion," *Laboratory Investigation; a Journal of Technical Methods and Pathology*, vol. 68, no. 5, pp. 499–508, 1993.

Hindawi
Evidence-Based Complementary and Alternative Medicine
Volume 2021, Article ID 1248920, 11 pages
https://doi.org/10.1155/2021/1248920

Research Article

System Pharmacology-Based Strategy to Decode the Synergistic Mechanism of GanDouLing for Wilson's Disease

Juan Zhang,[1] **Hong Chen**,[2] **Yuancheng Bao**,[1] **Daojun Xie**,[1] **Wenming Yang**,[1] **Huaizhou Jiang**,[3] **Ting Dong**,[1] **and Hui Han**[1]

[1]*Encephalopathy Center, The First Affiliated Hospital of Anhui University of Chinese Medicine, 117 Meishan Road, Shushan District, Hefei 230031, China*
[2]*Graduate School, Anhui University of Chinese Medicine, 103 Meishan Road, Shushan District, Hefei 230038, China*
[3]*Basic Department of Traditional Chinese Medicine, Anhui University of Chinese Medicine, 103 Meishan Road, Shushan District, Hefei 230038, China*

Correspondence should be addressed to Juan Zhang; zhangdoumi2019@163.com

Juan Zhang and Hong Chen contributed equally to this work.

Received 22 June 2020; Revised 12 December 2020; Accepted 13 January 2021; Published 29 January 2021

Academic Editor: Yunxia Li

Ethnopharmacological Relevance. GanDouLing (GDL) is a Chinese medicinal herb produced by the preparation center of Anhui Hospital of TCM for preventing and treating Wilson's disease (WD), an ATP7B mutation-inherited disease that affects copper transport and is characterized by liver and nervous system manifestations with variable and often unpredictable manifestations. However, the "multicomponent" and "multitarget" characteristics of TCM make it challenging to clarify the potential therapeutic mechanisms of GDL for WD. *Aim of the Study*. This study aimed at the systematic encoding of WD potential target for GDL and experimental verification for the relevant core targets, providing a deeper insight into the understanding of the mechanisms of GDL protection underlying WD with liver injury. *Material and Methods*. Following the strategy of the network pharmacology, we, firstly, predicted the active components of GDL and putative targets for WD. By employing clusterProfiler, the enrichment of functional and pathway terms was analyzed. Further, the protein-protein-interaction network was analyzed by STRING. Lastly, after establishing the toxic-milk mouse (TX) model with GDL treating, Hematoxylin and Eosin stain (HE) and western blotting (WB) for apoptosis biomarker were experimented. *Results*. Firstly, 324 active compounds have been identified in the GDL formula. Meanwhile, we identified 1496 human genes which are related to WD or liver cirrhosis. Functional and pathway enrichment analysis indicated that NOD-like receptor signaling pathway, bile secretion, calcium signaling pathway, steroid hormone biosynthesis, T cell receptor signaling pathway, apoptosis, MAPK signaling pathway, and so forth can be obviously regulated by GDL. Further, in a mouse model of WD, in vivo experiments showed that GDL treatment can not only reduce the pathological symptoms of the liver but also reduce the apoptosis of hepatocytes. *Conclusions*. In this study, systemic pharmacological methods were proposed and the mechanism of GDL combined therapy for WD was explored. This method can be used as a reference for the study of other mechanisms of traditional Chinese medicine.

1. Introduction

Wilson's disease (WD) is a hereditary disease which was first proposed by Kinnear Wilson in 1912 and caused by mutations in the ATP7B copper transporter gene that causes copper to accumulate in the liver and brain [1]. The phenotypic manifestations of WD are often highly variable, involving varying degrees of liver and/or neurological symptoms [2–4]. There is increasing evidence showing that the clinical manifestations of WD are affected by genetic and epigenetic factors [5–7], which may be responsible for the high phenotypic variability of WD. WD's liver damage ranges from mildly symptomatic to steatosis, cirrhosis, or acute liver failure. The involvement of the nervous system is

characterized by dyskinesia, manifested as Huntington's disease-like tonic and tremor.

According to its pathogenesis, WD is treated by blocking intestinal copper uptake by chelating agents, such as triene amine, tetrathiomolybdate, or zinc salts. However, their high cost or side effects may hinder clinical use [8]. At present, penicillamine (d-penicillamine) is widely used, because of its low cost and remarkable curative effect [9, 10]. But, with many adverse reactions, such as fever, rash, gastrointestinal reaction, leukopenia, systemic lupus erythematosus, and nephritis, which limit its clinical application [11], a large number of studies have shown that *Penicillium* has therapeutic effects on liver diseases [12, 13], especially WD [9, 13]. A large number of clinical practice and theoretical studies have proved that traditional Chinese medicine is an effective drug for the treatment of WD. Traditional Chinese medicine can eliminate the abnormal deposition of copper ions in the liver, brain, and other tissues through not only kidney metabolic pathway but also bile secretion, so as to improve the curative effect and reduce side effects. More importantly, the combination of traditional Chinese and Western medicine can reduce side effects. GanDouLing is a TCM, and as an in-hospital preparation, it was prepared by the First Affiliated Hospital of Anhui University of Traditional Chinese Medicine [14, 15], which has proved that there can be effective improvement of liver and neuropathy in clinical, animal, and cell models [16–19]. Specifically, it can effectively play an important role in removing blood stasis from the liver and gallbladder, promoting blood circulation and removing copper. GanDouLing is mainly composed of *Gynochthodes officinalis* (F.C.How) Razafim. & B.Bremer (Bajitian, BJT), *Schisandra chinensis* (Turcz.) Baill (Beiwuweizi, BWWZ), *Rheum officinale* Baill (Dahuang, DH), *Curcuma zedoaria* (Christm.) Roscoe (Ezhu, EZ), *Coptis chinensis* Franch (Huanglian, HL), *Curcuma longa* L. (Jianghuang, JH), *Lysimachia christinae* Hance (Jinqiancao, JQC), and *Rehmannia glutinosa* (Gaertn.) DC. (Shudihuang, SDH) [20, 21].

Network pharmacology is an emerging discipline, which is based on the characteristics of biomolecules and a number of authoritative databases showing us a preliminary understanding of mechanisms of medicine and disease. The previous research study used the method of network pharmacology to provide a promising method for understanding the pharmacological mechanism of TCM. In the article, we developed a network pharmacology analysis to determine the anti-WD mechanism of GDL and the experiments in vitro were then performed given the results of network pharmacology analysis.

2. Methods

2.1. Chemical Components Database, ADME Screening, and Targets Identification. GanDouLing is a TCM, and as an in-hospital preparation, it was prepared by the First Affiliated Hospital of Anhui University of Traditional Chinese Medicine and the quality control of chemical fingerprint has been performed [14, 15], which is mainly composed of BJT, BWWZ, DH, EZ, HL, JH, JQC, and SDH [20, 21]. Following with a strategy of system pharmacology, the pharmacology mechanisms of WD by GDL were encoded. Firstly, all compounds of GDL containing eight herbs were gathered from the TCMSP database (http://lsp.nwu.edu.cn/index.php) [22] with the parameter of oral bioavailability (OB) [23], drug-likeness (DL) [24], and so forth. Next, the active components were filtered out by the ADME method. Targets of the active components in GDL were predicted by BATMAN-TCM [25]; next, the intersection genes of GDL targets and WD-related genes including liver cirrhosis collected from the Comparative Toxicogenomics Database (CTD) [26] and DisGeNET [24, 27] were identified. Then, GO [28] and KEGG [29] pathway analysis was performed by clusterProfiler [30]. Last, the PPI network was constructed by STRING [31] and visualized by Cytoscape [32], and the modules of PPI were identified by MCODE [33].

2.2. Establishment of Animal Models. Twenty female TX mice (20 ± 2 g) and ten female DL mice were at the ages of 8–10 weeks [34]. Original mice were obtained from the Jackson laboratory with the help of Beijing Vital River Laboratory Animal Technology, Ltd. This study was carried out in strict accordance with the "National Institutes of Health Guidelines for the Care and Use of Experimental Animals." It was approved by the Institutional Animal Care and Use Committee of the Anhui Hospital of TCM.

The twenty female TX mice were divided into two groups, 10 mice in each group: the Wilson group and GanDouLing group (0.486 g/kg/day, GanDouLing was produced by the Anhui Hospital of TCM: the active ingredients of each herb were extracted with 65% ethanol and then combined with extracted filtrate; the filtrate combinations were baked into dry paste at the right temperature and starch was added and packed into GanDouLing troche) [16]. The ten female DL mice (20 ± 2 g) were treated as the control group. The mice in the GanDouLing groups were treated by intragastric administration with GanDouLing for 8 weeks. The Wilson group and control group were treated by intragastric administration with an equivalent volume of 0.9% saline every day. All the mice were housed in a controlled humidity (50–70%) and room temperature (18–22°C), fed in the isolation cages with independent air supply, and were given free access to food and water ad libitum in an alternating 12 h light/dark cycle over a period of 8 weeks.

2.3. Hematoxylin and Eosin Stain. The mice liver isolated tissues were fixed with 4% paraformaldehyde for 3 h and then dehydrated with ethanol and xylene. According to the previous literature, staining was carried out for liver samples [16]. The result of staining was that the cell nucleus was dyed blue by Hematoxylin and the cytoplasm was dyed red by Eosin.

2.4. Western Blot. According to the previous literature, HE staining was carried out for liver samples [16]. The details of antibodies are as follows: rabbit anti-B-cell lymphoma 2 (BCL-2) at 1 : 1000 (ab32124; Abcam, Cambridge, UK), rabbit anti-Bcl-2-associated X (BAX) at 1 : 1000 (ab32503;

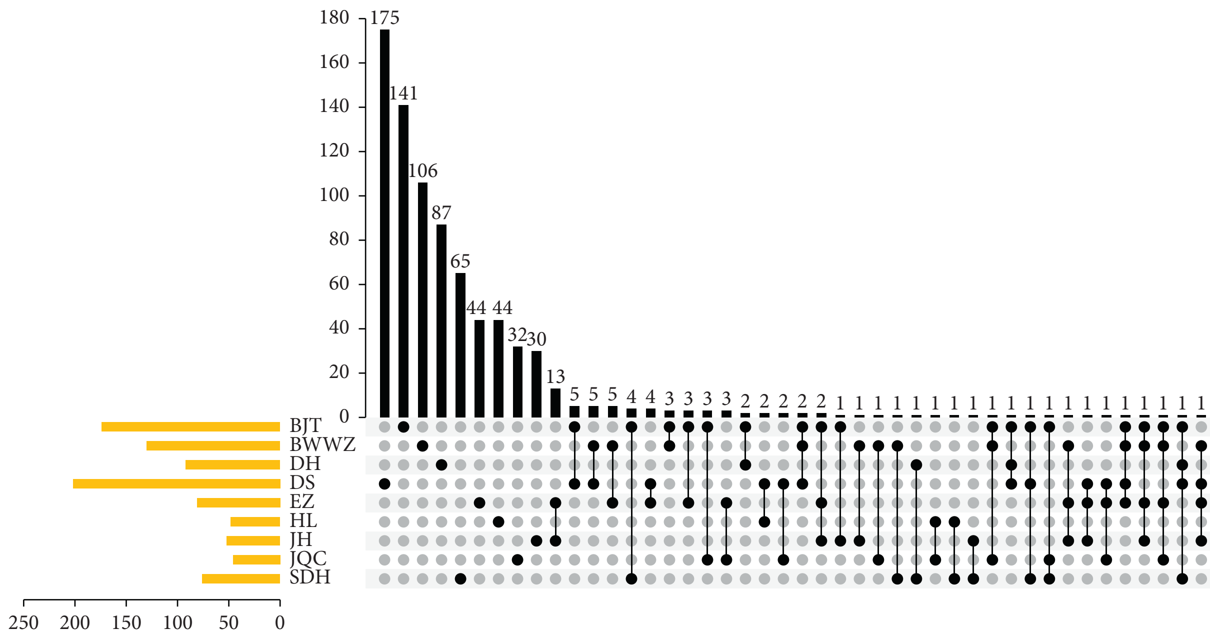

Figure 1: Upset chart showing the overlapping ingredients in each herb with GanDouLing.

Abcam, Cambridge, UK), and mouse anti-GAPDH at 1 : 2000 (sc-32233; Santa Cruz, Santa Cruz, CA, USA), goat anti-mouse IgG H&L at 1 : 2000 (sc-2005; Santa Cruz, Santa Cruz, CA, USA), or goat anti-rabbit IgG H&L at 1 : 5000 (ab6721; Abcam, Cambridge, UK).

2.5. Assay of Caspase-3 Activity. Caspase-3 activity assay kit (BB-4106; BestBio, Shanghai, China) and Caspase-8 activity assay kit (BB-4107; BestBio, Shanghai, China) were used to detect the activity of caspase-3 and caspase-8 in three groups, according to the manufacturer's protocol.

2.6. Statistical Analysis. GraphPad Prism 7 was employed for comparing the expression of Bcl-2 and Bax and the activity of caspase-3 and caspase-8. And the method of Student's *t*-test was used for analyzing the comparison. When $P < 0.05$, it was considered statistically significant.

3. Results

Following a system pharmacology model, the pharmacology mechanisms of WD by GDL were encoded. Firstly, all compounds of GDL were gathered from a database. Next, the active components were filtered out by the ADME method. Then, the targets, pathway, and PPI network were identified from integrated predictive models. Finally, we employed the TX-j mouse model for proving that GDL could improve WD liver injury by regulating apoptosis.

3.1. Active Components Target for Anti-WD in GDL. In total, 802 compounds were obtained for GDL, including 174 compounds for Bajitian, 130 compounds for Beiwuweizi, 92 compounds for Dahuang, 202 compounds for Danshen, 81 compounds for Ezhu, 48 compounds for Huanglian, 52 compounds for Jianghuang, 61 compounds for Jinqiancao, and 76 compounds for Shudihuang (Figure 1). Up to 65 compounds are contributed to more than one herb. By contrast, the other compounds belong to only one of the nine herbs. And then, two ADME properties of these components including OB and DL were focused to further state the components of GDL. Generally speaking, any TCM formulation consists of many components, but most of the components do not possess satisfactory properties of pharmacodynamic and pharmacokinetic. In the present study, OB and DL were adopted to filter for active components. After screening, 324 active components were screened out of the 802 components of GDL. And the targets for active components were predicted by BATMAN-TCM. In total, 1,496 genes were identified which are related to WD and liver cirrhosis, and 287 genes could be a target with 151 active components. And the components-target network was performed by Cytoscape (Figure 2).

3.2. GO and Pathway Analysis to Encode the Pharmacological Mechanisms of GDL. To explain the molecular biology of the therapy mechanism of GDL for WD, all target proteins were used to perform the enrichment of GO and KEGG pathways by clusterProfiler.

Enrichment analysis showed that a total of 2216 GO-terms with $P < 0.05$ were significantly enriched with 287 targets, 1915 of which were BP, 108 of which were CC, and 192 of which were MF. The top 10 enriched GO biological processes were response to organic cyclic compound (GO: 0014070), response to hormone (GO:0009725), response to organic substance (GO:0010033), response to lipid (GO: 0033993), response to organonitrogen compound (GO: 0010243), regulation of cell proliferation (GO:0042127), response to steroid hormone (GO:0048545), response to

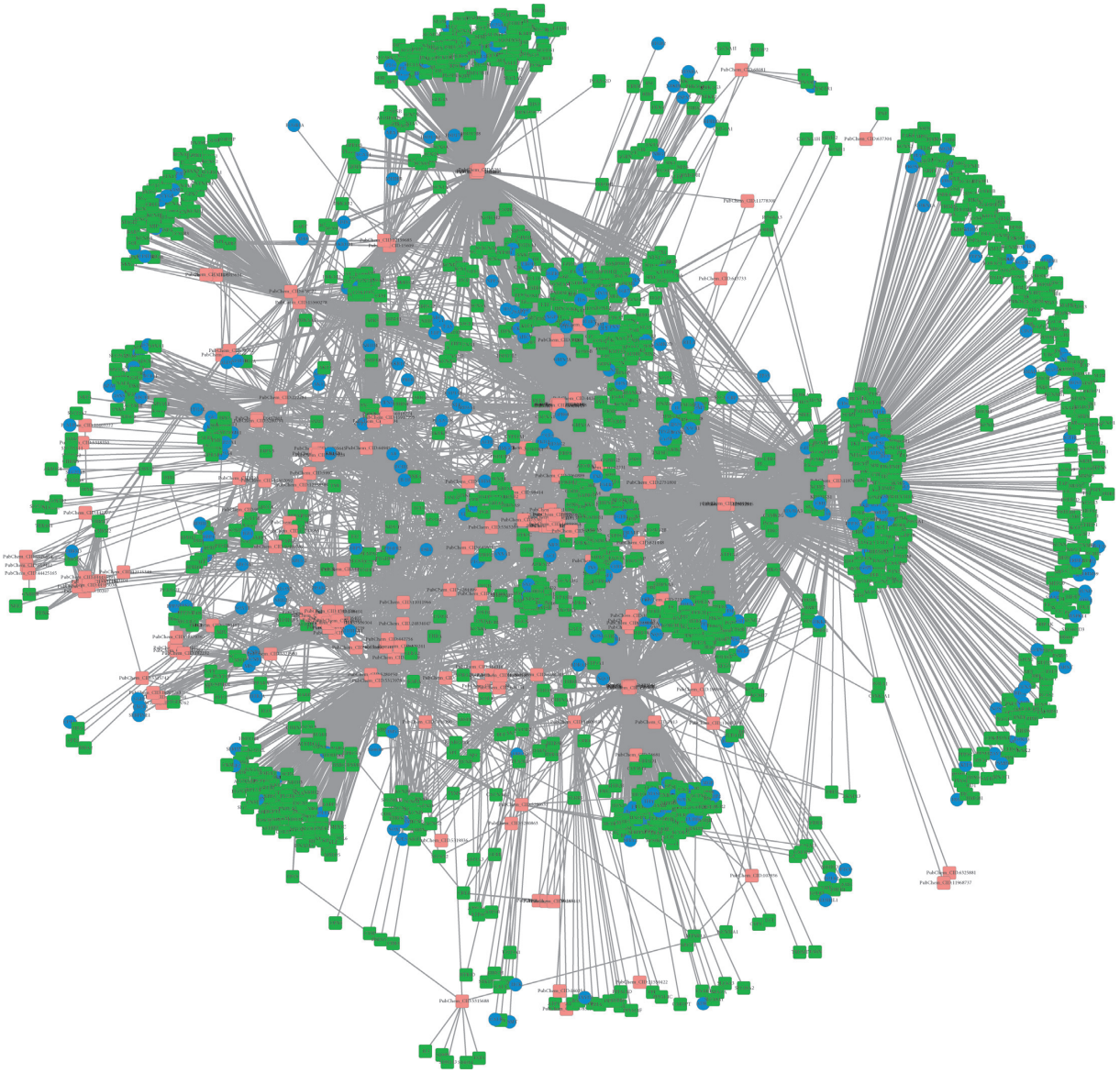

Figure 2: Ingredient-target network. Pink square represents active compounds in GanDouLing, green and blue nodes represent the target genes of active compounds, blue square represents common targets, and blue circles represent WD targets.

drug (GO:0042493), cell proliferation (GO:0008283), and cellular response to organic substance (GO:0071310). In particular, the results show that targets are involved in the regulation of cell death (GO:0010941, 93 targets), apoptotic process (GO:0006915, 97 targets), inflammatory response (GO:0006954, 58 targets), and so forth. Extracellular space (GO:0005615), cell surface (GO:0009986), vesicle (GO:0031982), membrane-bounded vesicle (GO:0031988), extracellular region (GO:0005576), cytoplasmic vesicle (GO:0031410), cytoplasmic membrane-bounded vesicle (GO:0016023), secretory granule (GO:0030141), cytoplasmic membrane-bounded vesicle lumen (GO:0060205), and cytosol (GO:0005829) were the top 10 enriched cellular components. The enriched GO molecular functions were receptor binding (GO:0005102), oxidoreductase activity (GO:0016491), identical protein binding (GO:0042802), enzyme binding (GO:0019899), steroid binding (GO:0005496), transcription factor binding (GO:0008134), carboxylic acid binding (GO:0031406), organic acid binding (GO:0043177), antioxidant activity (GO:0016209), and iron ion binding (GO:0005506). The top 30 GO-terms with the highest enrichment factor are shown in Figure 3(a).

For 287 targets, a total of 176 pathway terms were enriched by KEGG enrichment analysis, and 43 KEGG pathway terms were significant with $P < 0.05$. The top 10 enriched pathways were Chagas disease (American trypanosomiasis) (hsa05142), prostate cancer (hsa05215), leishmaniasis (hsa05140), osteoclast differentiation (hsa04380), malaria (hsa05144), African trypanosomiasis (hsa05143), pathways in cancer (hsa05200), adipocytokine signaling pathway (hsa04920), rheumatoid arthritis (hsa05323), and NOD-like receptor signaling pathway (hsa04621). In particular, we found that targets are involved in the bile secretion (hsa04976, 12 targets), calcium signaling pathway (hsa04020, 18 targets), T cell receptor signaling

FIGURE 3: GO and pathway analysis of the targets of WD targets. (a) The top 30 significant GO terms. (b) The top 30 signaling pathways. The different colors from green to red represent the *P* value. The different sizes of the shapes represent the gene count number. The larger the proportion is, the larger the dot; the redder the dot color, the more significant the *P* value will be.

pathway (hsa04660, 13 targets), fatty acid degradation (hsa00071, 7 targets), apoptosis (hsa04210, 10 targets), MAPK signaling pathway (hsa04010, 21 targets), cytokine-cytokine receptor interaction (hsa04060, 20 targets), PPAR signaling pathway (hsa03320, 8 targets), Toll-like receptor signaling pathway (hsa04620, 10 targets), ErbB signaling pathway (hsa04012, 9 targets), B cell receptor signaling pathway (hsa04662, 8 targets), Jak-STAT signaling pathway (hsa04630, 13 targets), and so forth. The top 30 pathway terms with the highest enrichment factors are shown in Figure 3(b).

3.3. PPI Network. The PPI network for the target genes was constructed based on the STRING database. As shown in Figure 4, the PPI network consists of 283 target genes and 4,332 edges, which means some target genes could interact with numerous genes. In fact, we found that dozens of target genes exhibited high degree characteristics, such as INS (insulin, degree = 160), ALB (albumin, degree = 152), AKT1 (AKT serine/threonine kinase 1, degree = 152), IL6 (interleukin 6, degree = 150), TP53 (tumor protein p53, degree = 128), TNF (tumor necrosis factor, degree = 125), and EGFR (epidermal growth factor receptor, degree = 111). High connectivity nodes with degree ≥70 are listed in Table 1.

The plug-in of MCODE was used to identify the modules with the PPI, and a total of 13 modules were gained. By sorting with MCODE score, two modules with MCODE score ≥3 and nodes ≥10 were screened out and named module 1 and module 2. And then, the subnetwork visualization was performed for module 1 and module 2 (Figure 5).

3.4. Effects of GDL on the Mouse Model of WD. In order to observe the protection effects of GDL with WD, TX mice were treated by intragastric administration with GanDouLing in 0.486 g/kg every day for 8 weeks. The results indicated that WD induced liver injury in the mouse model. HE staining results shown in Figure 6 suggested that the control group presented healthy tissues, whereas the WD models presented a diffuse lesion in the liver. A large number of hepatic parenchymal cells were observed to be necrotic in TX compared with the control. And GDL could effectively improve these lesions.

Collagen was stained blue in liver sections with Masson staining. The TX mice showed obvious collagen accumulation compared with the control group (Figure 6(b)), and administration GanDouLing can reverse.

3.5. Effects of GDL on Protein Expressions and Caspase Activity Associated with Apoptosis. In the analysis of network pharmacology, we found that there are more than 102 targets for anti-WD with GDL enriched to cell death, and up to 10 targets for anti-WD with GDL were enriched to the apoptosis signaling pathway, including NFKB1, PPP3CA, APAF1, RELA, AKT1, PPP3CB, IL1B, NFKBIA, TNF, and BCL2.

In order to explore the possible mechanism for WD, effects of the GDL formula on apoptosis relative proteins including Bcl-2 and Bax were observed using the western blotting method. In comparison with the control group, Bax was obviously overexpressed and Bcl-2 was suppressed in

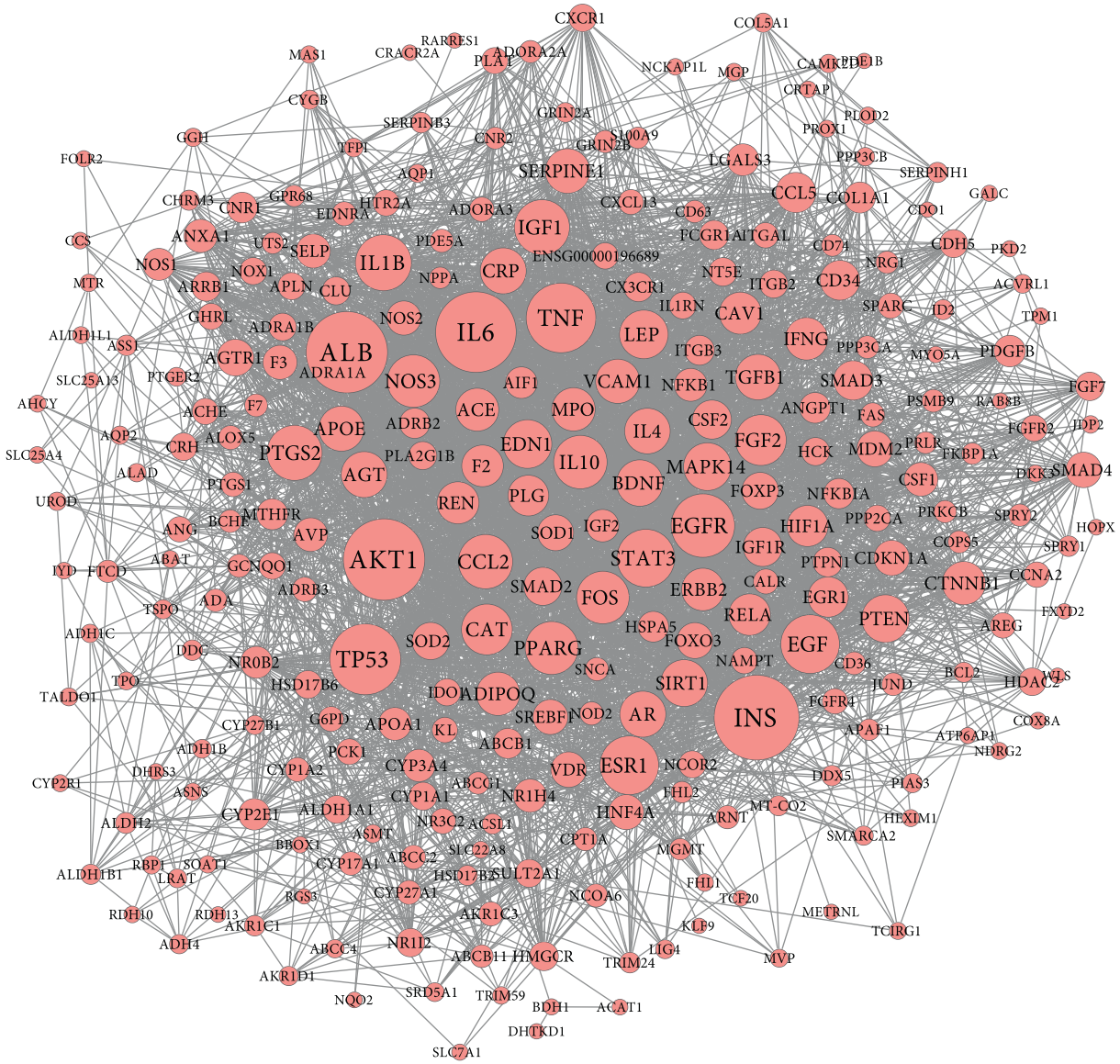

Figure 4: PPI network of WD targets. Red circles represent WD targets between ingredient targets from GanDouLing and WD significant targets.

the Wilson group, and GanDouLing could reverse the expression of Bax and Bcl-2 (Figures 7(a) and 7(b)). As shown in Figure 7(c), the TX group led to a 2.8-fold increase in caspase-3 and 1.9-fold increase in caspase-8 expression levels compared with controls. The above results indicated that GanDouLing can inhibit apoptosis of liver cells.

4. Discussion

At present, systemic pharmacology provides a powerful tool for encoding the compatibility and mechanism of traditional Chinese medicine [35–37]; there are many studies focusing on liver disease or injury based on the theory of systems pharmacology. On the basis of network pharmacology, the antioxidative effect of Zhizi Dahuang Decoction on alcoholic liver disease was expounded [38]. Wei et al. successfully revealed that 16 targets related to 11 compounds of SCG are closely related to the treatment of liver fibrosis, and TGF-β 1/Smad signal pathway is relatively important. They also demonstrated through animal experiments that SCG can significantly improve liver fibrosis by inhibiting TGF-β 1/Smad pathway [39]. In order to explain the pharmacological mechanism of Yinchenhao decoction (YCHD) which is a classical TCM formula that has been widely used in the treatment of liver fibrosis caused by chronic hepatitis B and jaundice for more than 1800 years, Cai et al. have employed the methods of network pharmacology and transcriptomic analysis to systematically describe the pharmacological mechanism [40]. At the same time, a large number of studies on the treatment of hepatocellular carcinoma with TCM have been carried out [41–43].

In this study, we performed the system pharmacology to construct a strategy for decoding the TCM pharmacologic molecular mechanism of GanDouLing which has proved

Table 1: The details of genes wih the node degree > 70.

Gene name	Node degree	Gene description
INS	160	Insulin
ALB	152	Albumin
AKT1	152	AKT serine/threonine kinase 1
IL6	150	Interleukin 6
TP53	128	Tumor protein p53
TNF	125	Tumor necrosis factor
EGFR	111	Epidermal growth factor receptor
EGF	100	Epidermal growth factor
ESR1	100	Estrogen receptor 1
STAT3	98	Signal transducer and activator of transcription 3
IL1B	94	Interleukin 1 beta
IGF1	92	Insulin-like growth factor 1
PTGS2	92	Prostaglandin-endoperoxide synthase 2
CCL2	90	C–C motif chemokine ligand 2
IL10	88	Interleukin 10
PPARG	87	Peroxisome proliferator-activated receptor gamma
NOS3	86	Nitric oxide synthase 3
FOS	86	Fos proto-oncogene, AP-1 transcription factor subunit
CAT	82	Catalase
FGF2	82	Fibroblast growth factor 2
LEP	77	Leptin
EDN1	77	Endothelin 1
MAPK14	75	Mitogen-activated protein kinase 14
PTEN	75	Phosphatase and tensin homolog
SIRT1	73	Sirtuin 1
BDNF	72	Brain derived neurotrophic factor
AGT	71	Angiotensinogen
CRP	71	C-reactive protein
AR	71	Androgen receptor

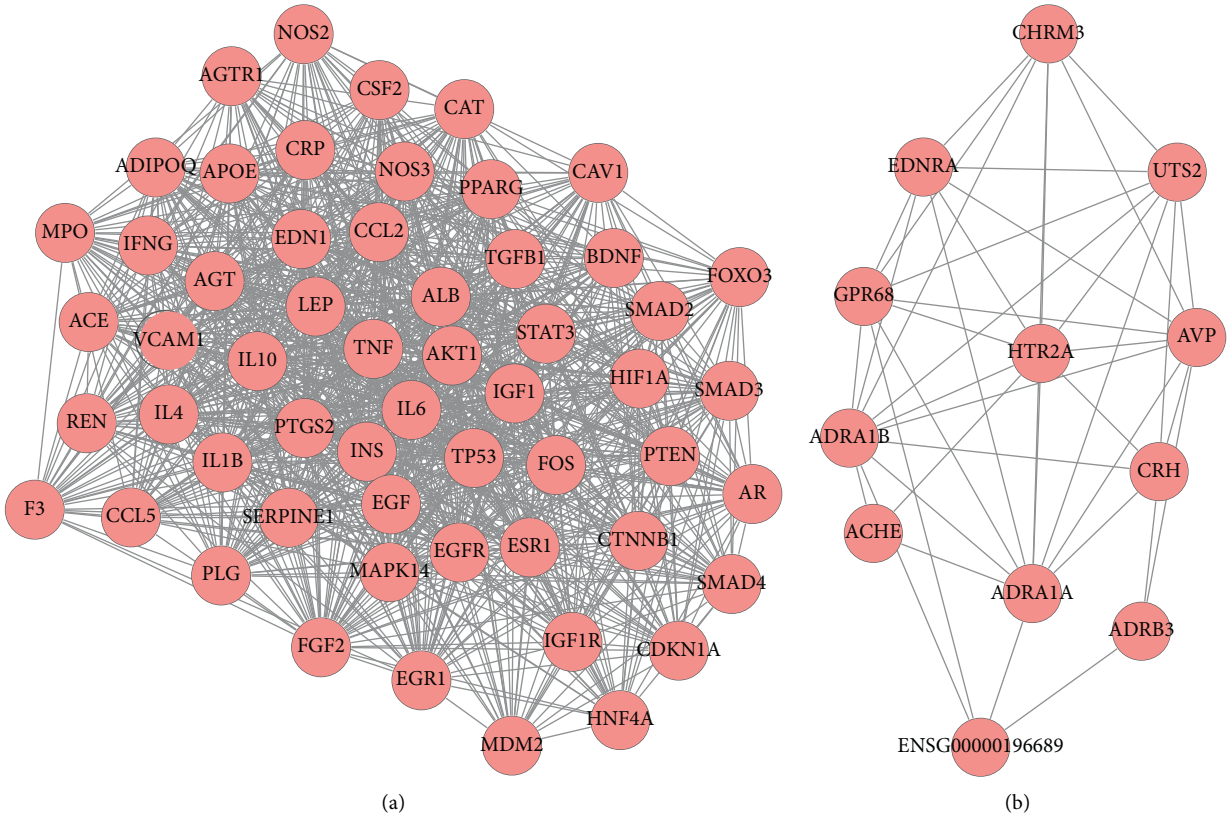

Figure 5: Two key modules network (a)-(b) of PPI network for GanDouLing target with WD.

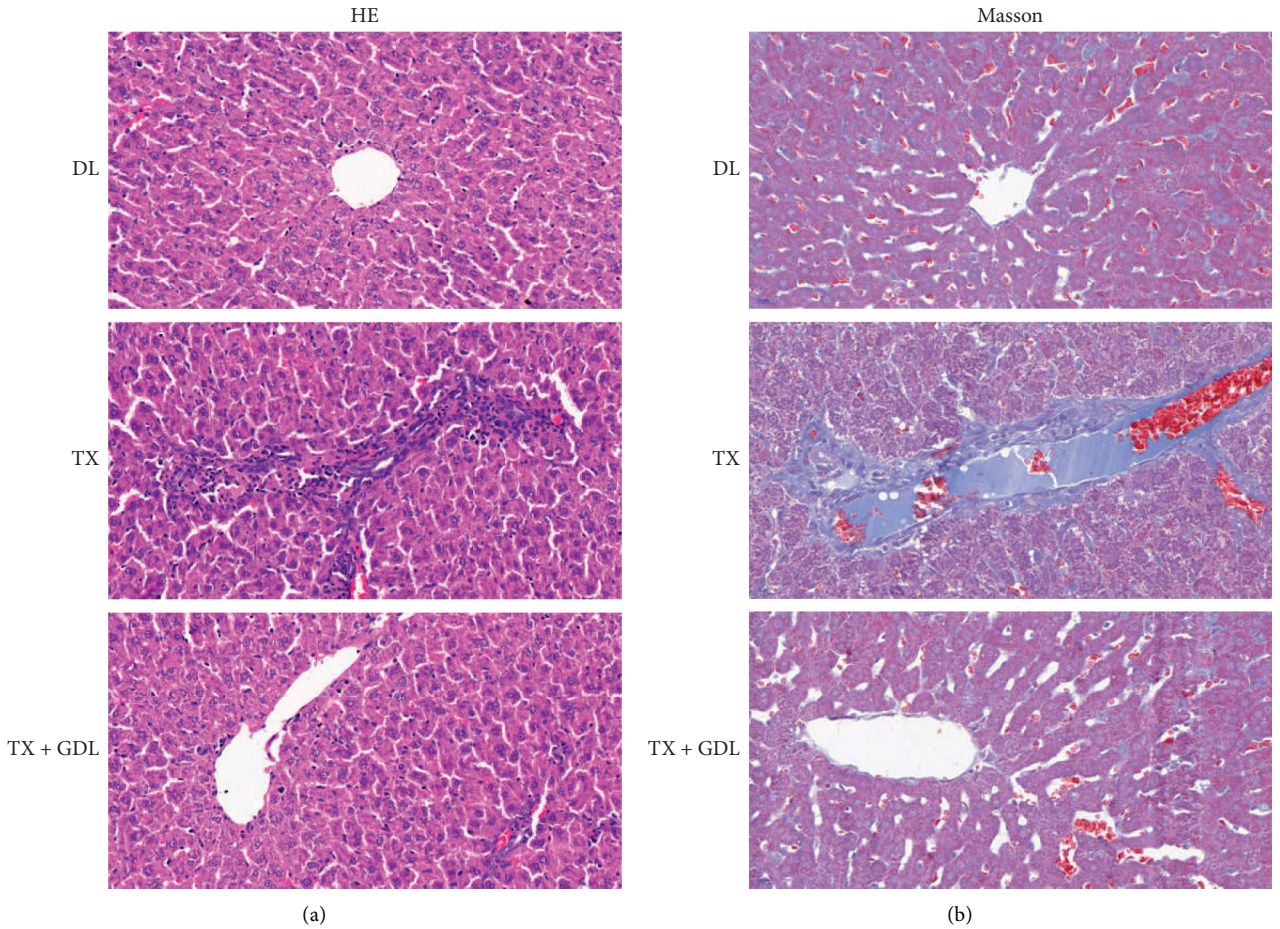

Figure 6: The liver injury induced by WD by HE (a) and Masson staining (b) in control (DL), WD (TX), and GanDouLing (TX + GDL) groups.

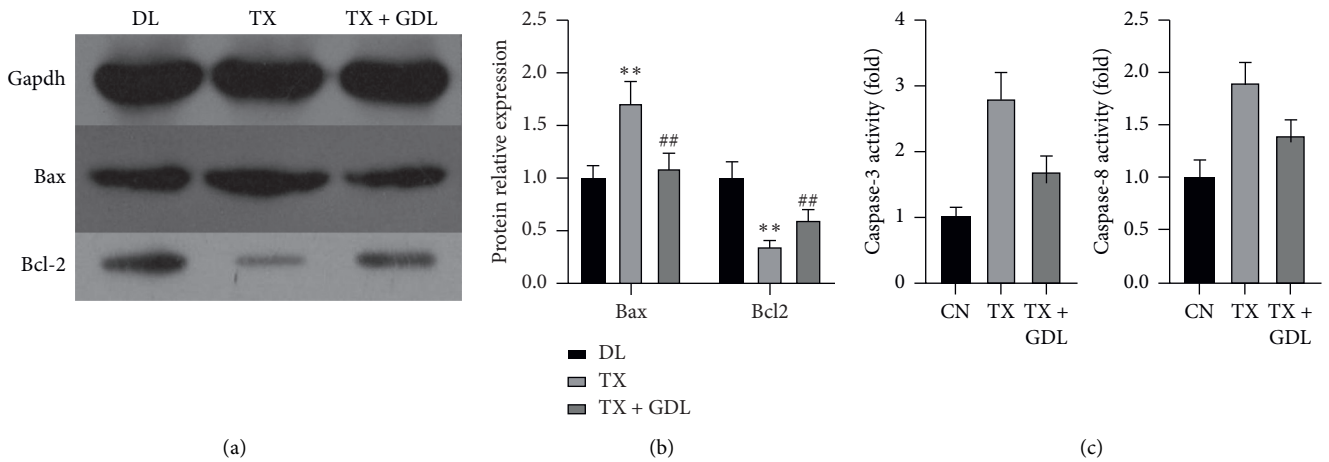

Figure 7: Effects of GanDouLing on protein expressions and caspase activity associated with apoptosis. (a)-(b) Western blotting result of Bcl-2 and Bax in the liver tissue. (c) The activity of Caspase-3 and Caspase-8 in the liver tissue.

that it can be an effective improvement of liver and neuropathy in clinical, animal, and cell models [16–19] With the integrated application of physical and chemical properties, network topological features, functional analysis, and path analysis provide a reference for the new method. However, its discovery mainly depends on theoretical analysis, so more experiments are needed to verify our findings and potential clinical significance. We find that some recent studies have introduced experiments such as transcriptome, proteomics, qPCR, and WB. [39, 40, 44]. In our study, with regular system pharmacology, we found that hundreds of GO-terms could be affected by GDL, such as cell proliferation, cell

death [45], inflammatory response [46], response to oxidative stress [47], and response to lipid [48]. Meanwhile, dozens of pathways could be affected by GDL including adipocytokine signaling pathway, NOD-like receptor signaling pathway, bile secretion, retinol metabolism, calcium signaling pathway, steroid hormone biosynthesis, T cell receptor signaling pathway, apoptosis [45], MAPK signaling pathway, cytokine-cytokine receptor interaction, PPAR signaling pathway, Toll-like receptor signaling pathway, B cell receptor signaling pathway, Jak-STAT signaling pathway, and focal adhesion.

The TX-j mouse model was employed for proving that GDL could improve WD liver injury, by regulating apoptosis. Firstly, HE and Masson staining showed that GanDouLing could improve the necrosis and fibrosis of the TX-j liver tissue. Furthermore, targeting the apoptosis signaling pathway identified by network pharmacology, we found that GanDouLing significantly inhibited the expression of proapoptosis Bax protein and promoted the expression of antiapoptosis BCL2. In addition, the activity of caspase-3 and caspase-8 was tested and found to be significantly increased in TX-j mice, which was consistent with the previous research results: the activity of caspase-3 increased in WD patients or copper-induced hepatocytes [49, 50]. Meanwhile, GanDouLing can reduce its activity to a certain extent.

5. Conclusion

In conclusion, the mechanism of GDL in the treatment of WD involves a variety of active components, targets, and pathways. In this study, 151 active components, 287 potential targets, and 43 related signaling pathways were predicted. Animal validation tests showed that GDL could effectively improve WD liver lesions, especially by inhibiting the apoptosis of liver tissues.

Data Availability

The datasets generated and/or analyzed during the current study are available from the corresponding author on reasonable request.

Conflicts of Interest

The authors declare no conflicts of interest.

Authors' Contributions

Juan Zhang, Daojun Xie, and Wenming Yang conceived and designed the study. Juan Zhang and Hong Chen performed the system pharmacology analysis. Juan Zhang and Hong Chen performed the animal experiments, HE analysis, and WB. Yuancheng Bao, Jingjing Xu, Huaizhou Jiang, Ting Dong, and Hui Han analyzed the data and previewed the manuscript. All authors read and approved the final manuscript. Juan Zhang and Hong Chen contributed equally to this work.

Acknowledgments

This study was supported by the National Natural Science Foundation of China (Grant no. 81774299) and Anhui Provincial Natural Science Foundation of China (Grant no. 170805MH199). The authors also thank the assistance in data analysis from Mr. Qiang Fan (Ao-Ji Bio-Tech Co., Ltd., Shanghai, China).

References

[1] C. Alastair, "Progressive lenticular degeneration: a familial nervous disease associated with cirrhosis of the liver, by S. A. Kinnier Wilson, (from the National Hospital, and the Laboratory of the National Hospital, Queen Square, London) Brain 1912: 34; 295–509," *Brain*, vol. 132, no. 8, pp. 1997–2001, 2009.

[2] D. Betel, M. Wilson, A. Gabow, D. S. Marks, and C. Sander, "The microRNA.org resource: targets and expression," *Nucleic acids research*, vol. 36, pp. D149–D153, 2008.

[3] S. Lutsenko, "Modifying factors and phenotypic diversity in Wilson's disease," *Annals of the New York Academy of Sciences*, vol. 1315, no. 1, pp. 56–63, 2014.

[4] S. M. Riordan and R. Williams, "The Wilson's disease gene and phenotypic diversity," *Journal of Hepatology*, vol. 34, no. 1, pp. 165–171, 2001.

[5] H. Dominik, K. Angelika, B. Ashima et al., "Diverse functional properties of Wilson disease ATP7B variants," *Gastroenterology*, vol. 142, no. 4, pp. 947–956.e945, 2012.

[6] M. Valentina, N. M. Shibata, K. K. Kharbanda et al., "Maternal choline modifies fetal liver copper, gene expression, DNA methylation, and neonatal growth in the tx-j mouse model of Wilson disease," *Epigenetics*, vol. 9, no. 2, pp. 286–296, 2014.

[7] M. Valentina, N. M. Shibata, K. K. Kharbanda et al., "Wilson's disease: changes in methionine metabolism and inflammation affect global DNA methylation in early liver disease," *Hepatology*, vol. 57, no. 2, pp. 555–565, 2013.

[8] K. I. Rodriguez-Castro, F. J. Hevia-Urrutia, and G. C. Sturniolo, "Wilson's disease: a review of what we have learned," *World Journal of Hepatology*, vol. 7, no. 29, pp. 2859–2870, 2015.

[9] K. F. Lowette, K. Desmet, P. Witters et al., "Wilson's disease: long-term follow-up of a cohort of 24 patients treated with D-penicillamine," *European Journal of Gastroenterology & Hepatology*, vol. 22, no. 5, pp. 564–571, 2010.

[10] M. Wiggelinkhuizen, M. E. C. Tilanus, C. W. Bollen, and R. H. J. Houwen, "Systematic review: clinical efficacy of chelator agents and zinc in the initial treatment of Wilson disease," *Alimentary Pharmacology & Therapeutics*, vol. 29, no. 9, pp. 947–958, 2010.

[11] U. Merle, M. Schaefer, P. Ferenci, and W. Stremmel, "Clinical presentation, diagnosis and long-term outcome of Wilson's disease: a cohort study," *Gut*, vol. 56, no. 1, pp. 115–120, 2007.

[12] A. Czlonkowska, J. Gajda, and M. Rodo, "Effects of long-term treatment in Wilson's disease with D-penicillamine and zinc sulphate," *Journal of Neurology*, vol. 243, no. 3, pp. 269–273, 1996.

[13] K. Kazemi, B. Geramizadeh, S. Nikeghbalian et al., "Effect of D-penicillamine on liver fibrosis and inflammation in Wilson disease," *Experimental and Clinical Transplantation: Official Journal of the Middle East Society for Organ Transplantation*, vol. 6, no. 4, pp. 261–263, 2008.

[14] M. B. Xu, P. Q. Rong, T. Y. Jin, P. P. Zhang, H. Y. Liang, and G. Q. Zheng, "Chinese herbal medicine for Wilson's disease: a

systematic review and meta-analysis," *Frontiers in Pharmacology*, vol. 10, p. 277, 2019.

[15] B. Zhang, T. Z. Jiang, and X. Y. Wang, "Study of gandouling tablet and glutathione on hepatolenticular degeneration," *Journal of Emergency Traditional Chinese Medicine*, vol. 5, 2010.

[16] Y. Chen, B. Zhang, S. Cao, W. Huang, and W. Yang, "Gandouling combined with penicillamine improves cerebrovascular injury via PERK/eIF2α/CHOP endoplasmic reticulum stress pathway in the mouse model of Wilson's disease," *Bioscience Reports*, vol. 38, no. 5, Article ID BSR20180800, 2018.

[17] T. Dong, W. M. Yang, W. U. Ming-Cai et al., "Effects of gandouling on ROS and Nrf2 of neural stem cells of mice cultured in high concentration copper," *Chinese Journal of Information on Traditional Chinese Medicine*, vol. 7, 2018.

[18] Z. Jing, X. Daojun, G. Yanbing et al., "Evaluation of efficacy and safety of gandouling plus sodium dimercaptosulphonate in treatment of patients with neurological Wilson's disease from China," *Journal of Traditional Chinese Medicine*, vol. 38, no. 5, pp. 781–786, 2018.

[19] Z. Jing, L. Li, H. Chen, and W. Yang, "Clinical efficacy and safety of gandouling plus low-dose D-penicillamine for treatment of Wilson's disease with neurological symptoms," *Journal of Traditional Chinese Medicine*, vol. 38, no. 1, pp. 89–94, 2018.

[20] C. Li, W. Sheng, Q. Xiu-Juan, and M. Mei, "Qualitative and quantitative analysis of active components of copditis rhizoma in gandouling pills by HPLC," *Chinese Journal of Information on Traditional Chinese Medicine*, vol. 25, no. 6, pp. 87–89, 2018.

[21] T. Wang and Y. C. Bao, "Application of cluster analysis in study of herbal compound," *Journal of Chengdu University of Traditional Chinese Medicine*, vol. 2, 2013.

[22] J. Ru, P. Li, J. Wang et al., "TCMSP: a database of systems pharmacology for drug discovery from herbal medicines," *Journal of Cheminformatics*, vol. 6, p. 13, 2014.

[23] X. Xu, W. Zhang, C. Huang et al., "A novel chemometric method for the prediction of human oral bioavailability," *International Journal of Molecular Sciences*, vol. 13, no. 6, pp. 6964–6982, 2012.

[24] J. Piñero, N. Queralt-Rosinach, A. Bravo et al., "DisGeNET: a discovery platform for the dynamical exploration of human diseases and their genes," *Database-Oxford*, vol. 2015, Article ID bav028, 2015.

[25] Z. Liu, F. Guo, Y. Wang et al., "BATMAN-TCM: a bioinformatics analysis tool for molecular mechANism of traditional Chinese medicine," *Scientific Reports*, vol. 6, no. 1, Article ID 21146, 2016.

[26] A. P. Davis, C. J. Grondin, R. J. Johnson et al., "The comparative toxicogenomics database: update 2019," *Nucleic Acids Research*, vol. 47, no. D1, pp. D948–D954, 2019.

[27] J. Piñero, À. Bravo, N. Queralt-Rosinach et al., "DisGeNET: a comprehensive platform integrating information on human disease-associated genes and variants," *Nucleic Acids Research*, vol. 45, no. D1, pp. D833–D839, 2017.

[28] Gene Ontology Consortium, J. A. Blake, M. Dolan et al., "Gene ontology annotations and resources," *Nucleic Acids Research*, vol. 41, pp. D530–D535, 2013.

[29] M. Kanehisa and S. Goto, "KEGG: kyoto encyclopedia of genes and genomes," *Nucleic Acids Research*, vol. 28, no. 1, pp. 27–30, 2000.

[30] G. Yu, L.-G. Wang, Y. Han, and Q.-Y. He, "clusterProfiler: an R package for comparing biological themes among gene clusters," *OMICS: A Journal of Integrative Biology*, vol. 16, no. 5, pp. 284–287, 2012.

[31] D. Szklarczyk, J. H. Morris, H. Cook et al., "The STRING database in 2017: quality-controlled protein-protein association networks, made broadly accessible," *Nucleic Acids Research*, vol. 45, no. D1, pp. D362–D368, 2016.

[32] P. Shannon, A. Markiel, O. Ozier et al., "Cytoscape: a software environment for integrated models of biomolecular interaction networks," *Genome Research*, vol. 13, no. 11, pp. 2498–2504, 2003.

[33] G. D. Bader and C. W. Hogue, "An automated method for finding molecular complexes in large protein interaction networks," *BMC Bioinformatics*, vol. 4, no. 1, p. 2, 2003.

[34] V. Medici and D. Huster, "Animal models of Wilson disease," *Handbook of Clinical Neurology*, vol. 142, pp. 57–70, 2017.

[35] D. C. Hao and P. G. Xiao, "Network pharmacology: a Rosetta stone for traditional Chinese medicine," *Drug Development Research*, vol. 75, no. 5, pp. 299–312, 2014.

[36] S. Li and B. Zhang, "Traditional Chinese medicine network pharmacology: theory, methodology and application," *Chinese Journal of Natural Medicines*, vol. 11, no. 2, pp. 110–120, 2013.

[37] W. Zhang, Y. Huai, Z. Miao, A. Qian, and Y. Wang, "Systems pharmacology for investigation of the mechanisms of action of traditional Chinese medicine in drug discovery," *Frontiers in Pharmacology*, vol. 10, p. 743, 2019.

[38] L. An and F. Feng, "Network pharmacology-based antioxidant effect study of Zhi-Zi-Da-Huang decoction for alcoholic liver disease," *Evidence-Based Complementary and Alternative Medicine*, vol. 2015, Article ID 492470, 6 pages, 2015.

[39] S. Wei, M. Niu, J. Wang et al., "A network pharmacology approach to discover active compounds and action mechanisms of San-Cao granule for treatment of liver fibrosis," *Drug Design, Development and Therapy*, vol. 10, pp. 733–743, 2016.

[40] F.-F. Cai, Y.-Q. Bian, R. Wu et al., "Yinchenhao decoction suppresses rat liver fibrosis involved in an apoptosis regulation mechanism based on network pharmacology and transcriptomic analysis," *Biomedicine & Pharmacotherapy*, vol. 114, Article ID 108863, 2019.

[41] L. Gao, K. X. Wang, Y. Z. Zhou, J. S. Fang, X. M. Qin, and G. H. Du, "Uncovering the anticancer mechanism of compound Kushen Injection against HCC by integrating quantitative analysis, network analysis and experimental validation," *Scientific Reports*, vol. 8, no. 1, p. 624, 2018.

[42] B. Gong, Y. Kao, C. Zhang, F. Sun, and H. Zhao, "Systematic investigation of scutellariae barbatae herba for treating hepatocellular carcinoma based on network pharmacology," *Evidence-Based Complementary and Alternative Medicine*, vol. 2018, Article ID 4365739, 12 pages, 2018.

[43] W. Zang, H. Bian, X. Huang et al., "Traditional Chinese medicine (TCM) *Astragalus membranaceus* and *Curcuma wenyujin* promote vascular normalization in tumor-derived endothelial cells of human hepatocellular carcinoma," *Anticancer Research*, vol. 39, no. 6, pp. 2739–2747, 2019.

[44] X. Zhang, D. Wang, X. Ren, A. G. Atanasov, R. Zeng, and L. Huang, "System bioinformatic approach through molecular docking, network pharmacology and microarray data analysis to determine the molecular mechanism underlying the effects of rehmanniae radix praeparata on cardiovascular diseases," *Current Protein & Peptide Science*, vol. 20, no. 10, pp. 964–975, 2019.

[45] D. Klein, J. Lichtmannegger, M. Finckh, and K. H. Summer, "Gene expression in the liver of Long-Evans cinnamon rats

during the development of hepatitis," *Archives of Toxicology*, vol. 77, no. 10, pp. 568–575, 2003.

[46] G. J. Brewer, "Tetrathiomolybdate anticopper therapy for Wilson's disease inhibits angiogenesis, fibrosis and inflammation," *Journal of Cellular and Molecular Medicine*, vol. 7, no. 1, pp. 11–20, 2010.

[47] A. Samuele, A. Mangiagalli, M.-T. Armentero et al., "Oxidative stress and pro-apoptotic conditions in a rodent model of Wilson's disease," *Biochimica et Biophysica Acta (BBA)-Molecular Basis of Disease*, vol. 1741, no. 3, pp. 325–330, 2005.

[48] B. H. Lee, J. H. Kim, J.-M. Kim et al., "The early molecular processes underlying the neurological manifestations of an animal model of Wilson's disease," *Metallomics*, vol. 5, no. 5, pp. 532–540, 2013.

[49] S. Strand, W. J. Hofmann, A. Grambihler et al., "Hepatic failure and liver cell damage in acute Wilson's disease involve CD95 (APO-1/Fas) mediated apoptosis," *Nature Medicine*, vol. 4, no. 5, pp. 588–593, 1998.

[50] J. Kalita, V. Kumar, and U. K. Misra, "A study on apoptosis and anti-apoptotic status in Wilson disease," *Molecular Neurobiology*, vol. 53, no. 10, pp. 6659–6667, 2015.

Hindawi
Evidence-Based Complementary and Alternative Medicine
Volume 2021, Article ID 8819245, 14 pages
https://doi.org/10.1155/2021/8819245

Research Article

A Study on the Therapeutic Efficacy of San Zi Yang Qin Decoction for Non-Alcoholic Fatty Liver Disease and the Underlying Mechanism Based on Network Pharmacology

Yiping Li,[1] **Yang Liu**,[1] **Ming Yang**,[2] **Qianlei Wang**,[1] **Yu Zheng**,[3] **Jiaoya Xu**,[1] **Peiyong Zheng**,[1] **and Haiyan Song**[1]

[1]*Institute of Digestive Diseases, Longhua Hospital, Shanghai University of Traditional Chinese Medicine, 725 Wanping Road, Shanghai 200032, China*
[2]*Office of National Drug Clinical Trial, Longhua Hospital, Shanghai University of Traditional Chinese Medicine, Shanghai 200032, China*
[3]*Department II of Digestive Diseases, Longhua Hospital, Shanghai University of Traditional Chinese Medicine, Shanghai 200120, China*

Correspondence should be addressed to Peiyong Zheng; zpychina@sina.com and Haiyan Song; songhy@126.com

Received 19 September 2020; Revised 16 December 2020; Accepted 22 December 2020; Published 8 January 2021

Academic Editor: Jianbo Wan

Objective. This study aims to explore the therapeutic efficacy of San Zi Yang Qin Decoction (SZ) and its potential mechanism in the treatment of non-alcoholic fatty liver disease (NAFLD) based on network pharmacology and *in vivo* experiments. *Methods*. Effective chemicals and targets of SZ were searched in online databases, according to the drug-likeness of compounds and the binomial distribution of targets. A disease-target-chemical network was established using NAFLD-associated genes screened through GeneCards database, Gene Ontology (GO) terms, and Kyoto Encyclopedia of Genes and Genomes (KEGG) pathways. Furthermore, animal experiments were conducted to verify the efficacy and mechanism of SZ predicted by network pharmacology. The NAFLD mouse model was established with C57BL/6J mice fed with a high-fat diet for 22 weeks. The mice in the control group were fed with a chow diet. From the 23rd week, the NAFLD mice were treated with intragastric SZ or normal saline for 8 weeks. After the glucose tolerance was measured, the mice were sacrificed, followed by the collection of serum and liver tissues. Pathological changes in liver tissues were examined by H&E staining. Additionally, alanine aminotransferase (ALT), aspartate aminotransferase (AST), serum fast blood glucose, and insulin levels were detected. Expression levels of TNF-α of serum and liver tissues were determined by ELISA and qRT-PCR, respectively. Western blot was used to detect the activation of AKT in liver tissues. *Results*. A total of 27 effective compounds and 20 targets of SZ were screened. GO analysis uncovered a significant correlation between the targets of SZ and those of NAFLD. KEGG analysis presented the signaling pathways enriched in SZ and NAFLD, including NAFLD, TNF-α, and apoptosis pathways. The area under the curve of major GO and KEGG pathways indicated the potential role of SZ in improving NAFLD. *In vivo* experiments demonstrated that SZ significantly alleviated hepatosteatosis and inflammatory cell infiltration in liver tissues, reduced serum transaminases, and improved insulin resistance and glucose tolerance of NAFLD mice. The protein level of phospho-AKT was upregulated by SZ. Additionally, SZ treatment obviously impaired the TNF-α level in the serum and liver tissue of NAFLD mice. *Conclusions*. According to the network pharmacology analysis and *in vivo* experiments, SZ could have therapeutic efficacy for NALFD. The mechanism mainly involves pathways relative to insulin resistance, TNF-α, and apoptosis. Our results provide a scientific basis for SZ in the clinical treatment of NAFLD.

1. Introduction

Non-alcoholic fatty liver disease (NAFLD) is a syndrome of hepatic excessive fat deposition that does not arise from alcohol abuse or other definite factors [1]. The spectrum of NAFLD includes non-alcoholic fatty liver (NAFL), non-alcoholic steatohepatitis (NASH), liver cirrhosis, and hepatocellular carcinoma. NAFLD is the most common liver disorder, with an incidence of about 20–33% in adults worldwide and up to 75% in the obese [2]. About 20% of NAFLD cases progress to NASH with liver inflammation and fibrosis, and even refractory liver diseases like cirrhosis and liver cancer [3]. It is believed that NAFLD develops through a multi-hit process. At first, excessive deposition of fatty acids leads to hepatosteatosis. As systematic insulin sensitivity decreases, lipolysis initiates in adipose tissues and de novo fatty acid increases in the liver, further aggravating hepatic lipid accumulation. With the aggravation of NAFLD, lipotoxicity gradually induces endoplasmic reticulum stress, oxidative stress, mitochondrial dysfunction, and endotoxin-induced release of inflammatory cytokines, etc. Eventually, the multi-hit process causes hepatocyte apoptosis, liver inflammation, and fibrosis [4].

Due to its complex pathogenesis, NAFLD still lacks effective treatments. In recent years, TCM has been widely applied in the treatment of NAFLD in China, with a definite efficacy featuring holistic treatment and multi-target regulation [5]. From the perspective of TCM theory, NAFLD is defined as a disease of "obesity, phlegm-fluid retention, and accumulation," according to its clinical symptoms and signs [6]. In NAFLD, the dysfunction of the liver in regulating Qi flow and the spleen in transforming and transporting food essence contribute to the pathological accumulation of phlegm, dampness, and stagnation of Qi.

San Zi Yang Qin Decoction (SZ), initially reported in Han Shi Yi Tong, is composed of Raphani semen (Laifuzi in China), Perilla fructus (Zisuzi in China), and Sinapis semen (Baijiezi in China). Raphani semen can reduce food stagnation and monitor Qi to eliminate phlegm. Perilla fructus can descend Qi to carry away phlegm, smooth the bowel, and relieve cough and asthma [7]. Sinapis semen is acrid and warm, facilitates Qi, dissipates gatherings, and resolves phlegm. Their combination can treat diseases resulting from abnormal Qi flow and phlegm stasis, like cough, short breath, excessive phlegm, chest impediment, and lack of appetite. SZ is particularly effective for pulmonary diseases, such as intractable cough, chronic obstructive pneumonia disease (COPD), and chronic bronchitis [8, 9]. According to the TCM theory of "treatment based on syndrome differentiation," and "homotherapy for heteropathy" during which the same therapy is administered for different diseases sharing the same pathogenesis, SZ has been recently applied in the treatment of diseases resulting from the stagnation of phlegm, dampness, and Qi, like NAFLD, hyperlipidemia, type 2 diabetes mellitus (T2DM), and breast hyperplasia [10–15]. However, *in vitro* and *in vivo* experiments and evidence-based analyses have not been carried out to validate the efficacy and interpret the related biological mechanisms of SZ [16, 17].

Network pharmacology is a novel research model based on systems biology and bioinformatics theories. It seeks to understand how drugs work from the system perspective and on the molecular level [18, 19]. Diverse active ingredients in TCM, especially TCM formulae, demonstrate complicated interactions, thus posing a great challenge to the research on TCM pharmacology. Accumulating evidence can reveal the efficacy and the underlying mechanism of a single active ingredient extracted from Chinese herbal medicine but is far from enough to explain those of the formulae, and the interactions between ingredients [20]. Network pharmacology has revolutionized TCM research from "one ingredient and one target" to "a complex of ingredients and a network of targets." Network pharmacology intends to illustrate the mechanism of a formula based on a systemic analysis [21, 22] and assess its possible efficacy according to the correlation between one chemical and its targets [23].

Using the approach of network pharmacology, the present study aimed to screen out the effective chemicals in SZ, define their targets associated with NAFLD, and describe the underlying mechanisms using online databases. Furthermore, we established an *in vivo* NAFLD mouse model to validate our results from database analyses.

2. Materials and Methods

2.1. Isolation of Main Chemicals in SZ. SZ is composed of Raphani semen, Perilla fructus, and Sinapis semen. The main chemicals in SZ were searched using the Traditional Chinese Medicine Systems Pharmacology Database and Analysis Platform (TCMSP, Version2.3) [24], Herb Ingredients' Targets (HIT) [25], Traditional Chinese Medicines Integrated Database (TCMID, Version2.0) [26], and Search Tool for Interactions of Chemical (STITCH, Version5.0) [27]. To estimate their drug-likeness, the physicochemical characteristics of collected chemicals were compared with those of known drugs, according to their AMDE (absorption, metabolism, distribution, excretion). In 2012, Liang et al. proposed that quantitative estimate of drug-likeness (QED) [28,29], an evaluation index of drug-likeness, could effectively estimate the AMDE of chemicals. QED was calculated using the following equation:

$$\mathrm{QED} = \exp\left(\frac{1}{n}\sum_{i=1}^{n}\ln d_i\right). \quad (1)$$

In this equation, d_i denotes the desirability function of 8 major molecular descriptors, including the relative molecular weight of the compound, oil/water partition coefficient, the number of hydrogen bond receptors, the number of hydrogen bond donors, polar surface area, the number of rotatable bonds in the compound, the number of aromatic rings in the compound, and the number of non-pharmaceutical substructures [30]. During the initial screening of chemicals, a threshold of 0.2 was set according to the QED of 1,805 drugs released by Food and Drug Administration (FDA) in the DrugBank [31].

2.2. Screening of Main Targets of Chemicals in SZ. Potential targets of the above-screened chemicals were searched from HIT, TCMID, STITCH, and TCMSP, and their names were normalized with the National Center for Biotechnology Information (NCBI) database. Enrichment score or gene score (GS) was calculated based on the binomial distribution $[p(X \geq k)]$ to screen out the targets:

$$p(X \geq k) = \sum_{m=k}^{k} C_n^m \left(\frac{g}{n}\right)^m \left(1 - \frac{g}{n}\right)^{n-m}, \quad (2)$$

$$\mathrm{GS} = \left\{ \begin{array}{ll} \dfrac{-\log(p(X \geq k))}{\mathrm{Rank}(p(X \geq k))}, & \text{if } p(X \geq k) \leq 0.05, \\ 0, & \text{otherwise,} \end{array} \right\}, \quad (3)$$

k is the number of chemicals with function on the studied targets, n is the total number of chemicals, and g is the average number of chemicals functioning on each target. After adjustment of the false discovery rate (FDR), the possibility of interaction among more than k chemicals in the total chemicals (n) of the targets was randomly calculated by equation (2). Equations (2) and (3) were used to assess the likelihood of random results. $p < 0.05$ suggested that the number of interactive chemicals was significantly larger than the expected and could be considered as the target goal. The database of SZ targets was established with an associated threshold of 400 and a significant threshold of 0.05.

2.3. Screening of Targets Associated with NAFLD. The relevant targets of NAFLD were searched from GeneCards [32] and funneled into a database.

2.4. Enrichment Analyses of GO and KEGG Pathways. Targets of SZ and NAFLD were subjected to enrichment analyses of Gene Ontology (GO) terms (including molecular functions, biological processes, and cellular components) and Kyoto Encyclopedia of Genes and Genomes (KEGG) pathways. A significant correlation ($p < 0.01$) between a gene set and GO terms and KEGG pathways was estimated by a hypergeometric distribution model as follows [23]:

$$p = 1 - \sum_{i=0}^{k-1} \frac{\binom{M}{i}\binom{N-M}{n-i}}{\binom{N}{n}}, \quad (4)$$

where N is the total number of genes, M is the number of KEGG pathways or annotated GO terms, n is the number of genes in the gene set to be analyzed, and k is the number of shared genes. p value after adjustment of FDR [33] was used to reflect the association strength between the target and enriched pathways or GO terms. $p < 0.01$ was considered statistically significant.

2.5. Establishment of NAFLD Mouse Model and Drug Intervention. A total of 18 five-week-old male C57BL/6J mice (Shanghai SLAC Laboratory Animal Co., Ltd.) were housed in the SPF-level animal center of Longhua Hospital, Shanghai University of Traditional Chinese Medicine. The mice were randomly divided into the control group ($n = 6$) and NAFLD group ($n = 12$) and fed with a normal diet and a high-fat diet, respectively. From the 23rd week, the mice in NAFLD group were randomly subgrouped into model group ($n = 6$) and SZ group ($n = 6$). The mice in SZ group were intervened by intragastric administration of SZ for eight weeks, while the remaining with normal saline. At the end of the experiment, all animals were fasted overnight and anesthetized through intraperitoneal injection of 30 mg/kg pentobarbital sodium. Blood samples were collected and serum was separated through centrifugation. The livers were collected and weighed and then frozen or fixed in 10% formalin for further investigation.

SZ, provided by the Pharmacy Department of Longhua Hospital, Shanghai University of Traditional Chinese Medicine, was composed of Raphani semen (9 g), Perilla fructus (9 g), and Sinapis semen (9 g). According to the guideline proposed by the Methodology of Pharmacology of Traditional Chinese Medicine, the dosage of SZ for each mouse was calculated to be equal to the clinical dose of a 70 kg adult (3.51 g crude drug/kg/d). These three herbs were mixed at a mass ratio of 1 : 1 : 1 and grinded and then extracted by boiling water twice (30 min each time). Afterwards, the total extract was concentrated to 3.51 g crude drug/mL and stored at 4°C. When used, each mouse was given 0.2 mL SZ at the corresponding concentration adjusted with 0.9% saline by gavage. The experimental protocols were approved by the Institutional Animal Care and Use Committee of Shanghai University of TCM (IACUC No.: LHERAW-19052).

2.6. Pathological Examination of Mouse Liver Tissues. After sacrifice, mouse liver tissues were fixed in 4% neutral paraformaldehyde solution for 24 h and then dehydrated and paraffin-embedded, until they were sliced into 5 μm sections for H&E staining and observation.

2.7. Serum Biochemistry. Serum samples collected from mice were examined in the Laboratory of the Longhua Hospital, Shanghai University of Traditional Chinese Medicine. In brief, relative levels of alanine aminotransferase (ALT), aspartate aminotransferase (AST), and fasting blood glucose (FBG) were detected using an automatic biochemical analyzer with commercial reagents (Roche).

2.8. Intraperitoneal-Injected Glucose Tolerance Test (IPGTT). IPGTT in the mice was conducted at the 8th week of intragastric administration. After fasting for 12 h, the blood glucose (BG) level was first measured as a baseline. Subsequently, the mice were intraperitoneally administrated with 1 g/kg glucose, followed by determination of tail vein blood glucose at 15, 30, 60, and 90 min with an automated

glucometer (Johnson, Shanghai, China). The area under the curve (AUC) was calculated for the results of IPGTT.

2.9. Western Blotting Analysis. The protein was extracted from liver tissues. BCA protein assay kit (CoWin Bioscience, Beijing, China) was applied to determine protein concentration. The protein (100 μg for each sample) was separated with 10% sodium dodecyl sulfate-polyacrylamide gel electrophoresis (SDS-PAGE) and then transferred to a PVDF membrane (Millipore, Billerica, MA, USA). After blockade with 5% skim milk, the membrane was incubated with targeted primary antibodies overnight at 4°C and then with secondary antibody at room temperature for 1 h. The Phospho-AKT and β-actin antibodies and secondary antibodies were purchased from Cell Signaling Technology (Danvers, MA, USA). Finally, the signals were detected by enhanced chemiluminescence (ECL) Detection Kit (Millipore, Billerica, MA, USA) and captured by G: BOX Chemi XT4 System (Syngene, Cambridge, UK). GeneTools software (Syngene) was used for quantification. The relative protein expression was normalized to β-actin.

2.10. ELISA of Serum TNF-α and Insulin. Serum levels of TNF-α and fast insulin (FIN) of mice were detected using ELISA (enzyme-linked immunosorbent assay) according to the manufacturer's protocols labeled on commercial kits (Shanghai WestTang Bio-tech Co., Ltd.).

2.11. Calculation of HOMA-IR. The homeostasis model assessment of insulin resistance (HOMA-IR) is an index that quantifies insulin resistance. Mouse HOMA-IR was calculated as follows: HOMA-IR = FBG (mmol/L) × FINS (μU/mL)/22.5. The unit conversion for FIN is as follows: 1 μg/L = 1000/45.4 μU/mL.

2.12. Quantitative RT-PCR. Primer sequences used in RT-PCR were verified using the Basic Local Alignment Search Tool (BLAST) and synthesized by Shanghai Shinegene Biotech Co., Ltd. (Table 1). RNA was isolated from mouse liver tissues using TRIzol method and reversely transcribed into cDNAs using the ABI reverse transcription kit. Later, cDNA was amplified by the StepOnePlus™ qRT-PCR system, with β-actin as the internal reference. Relative levels were calculated by $2^{-\Delta\Delta CT}$method.

2.13. Statistical Analyses. Statistical analyses and figure formatting were conducted by using SPSS 24.0 and Graphpad Prism 7.0, respectively. Data were expressed as mean ± SD. Normally distributed data with equal variance were compared by one-way ANOVA, followed by LSD t-test. $p < 0.05$ was considered statistically significant.

3. Results

3.1. Effective Chemicals in SZ and Their Targets. According to the searching results from TCMSP, HIT, and TCMID, 52 types of chemicals were found in Raphani semen, 128 in Perilla fructus, and 51 in Sinapis semen. After calculation with equation (1) and QED threshold 0.2, 27 effective chemicals in SZ were obtained, mainly including β-sitosterol, luteolin, stigmasterol, and mustard oil, etc. (Table 2). A database of chemicals within SZ was then established.

Table 1: The primer sequences for quantitative RT-PCR.

Gene	Primer sequence (5′-3′)
mβ-Actin	Forward: GAGACCTTCAACACCCCAGC Reverse: ATGTCACGCACGATTTCCC
mTNF-α	Forward: CCCTCCAGAAAAGACACCATG Reverse: CACCCCGAAGTTCAGTAGACAG

3.2. Targets of Effective Chemicals in SZ. Potential targets of the above-screened chemicals were searched in HIT, TCMID, STITCH, and TCMSP and normalized using NCBI database. After the calculation of GS using equations (2) and (3), 20 targets were selected, mainly including protein kinase B1 (AKT1), tumor necrosis factor (TNF), and caspase-3 (CASP3) (Table 3). A database was then established based on these targets.

3.3. Screening Targets of NAFLD. By searching the keyword "non-alcoholic fatty liver disease" in GeneCards, 75 genes associated with human NAFLD and a correlation score >30 were selected (Table 4). A database about the target genes of NAFLD was then established.

3.4. GO Enrichment Analysis on Targets of SZ and NAFLD. A total of 20 main targets of SZ and 75 targets of NAFLD were subjected to GO enrichment analysis of molecular functions, biological processes, and cellular components. As shown in Figure 1 and Figures S1 and S2, targets of SZ and NAFLD were correlated with each other and mainly enriched in oxidative stress, lipopolysaccharide (LPS) response, and fatty acid metabolism. In addition, it is considered that the cumulative distribution percentages of common enriched targets or pathways can be used to reflect the correlation between the medicine and the disease. A disease that is more closely associated with a medicine shares more common targets or pathways in the top k enriched targets [23]. In the present study, the cumulative distribution of enriched GO targets was 38.93%, and the area under the curve (AUC) of the top 30 enriched GO targets was up to 23.388, suggesting a close correlation between targets of SZ and NAFLD (Figure 2).

3.5. KEGG Enrichment Analysis. Potential pathways enriched in the targets of SZ and NAFLD were explored by KEGG enrichment analysis. A total of 126 pathways were enriched in SZ targets, 46 in NAFLD targets, and 34 in both. A total of 18 top pathways are depicted in Figure 3, including NAFLD, TNF-α, apoptosis, T2DM, lifespan regulation, adipokines, insulin resistance pathway, etc. The pathways shared by SZ and NAFLD showed a similarity of up to

Table 2: Active compounds of SZ.

Pubchem CID	Compound	QED
6431151	(-)-cis-Beta-Elemene beta-sitosterol	0.2169
222284	Stigmasterol	0.2418
5280794	Eugenol	0.2243
3314	Phenethyl isothiocyanate	0.5907
16741	Allyl isothiocyanate	0.4236
5971	Vitamin E	0.3523
14985	Luteolin	0.2430
5280445	Apigenin	0.4015
5280443	Phenylacetaldehyde	0.4928
998	Diisobutyl phthalate	0.4882
6782	Ethylparaben	0.4696
8434	Hexanal	0.6242
6184	Cholesterol	0.3489
5997	Dibutyl phthalate	0.2663
3026	Riboflavin	0.3671
493570	Benzyl isothiocyanate	0.2302
2346	Benzaldehyde	0.4282
240	Toluene	0.4731
1140	Ethylbenzene	0.3119
7500	2,2,2-	0.3400
8259	Trichloroethanol	0.3704
16666	l-Menthol	0.4438
5283335	2-Nonenal	0.2376
2724159	(-)-Perillaldehyde	0.3818
7362	Furfural	0.5598
7127	Methyleugenol	0.5328
253	Bioepiderm	0.3858

Table 3: The target genes of active compounds of SZ.

Gene ID	Gene symbol
836	CASP3
7124	TNF
207	AKT1
2936	GSR
3725	JUN
8856	NR1I2
9407	TMPRSS11D
1543	CYP1A1
218	ALDH3A1
224	ALDH3A2
2353	FOS
2950	GSTP1
4129	MAOB
4318	MMP9
5594	MAPK1
5595	MAPK3
7157	TP53
842	CASP9
847	CAT
8989	TRPA1

73.91%. In addition, the area under the curve of the top 30 overlapped pathways between SZ and NAFLD was 16.00 (Figure 4). These results showed multiple pathways were enriched in the targets of both SZ and NAFLD, suggesting a strong potential therapeutic efficacy of SZ on NAFLD.

In Figure 5, the network of NAFLD pathways enriched in both SZ and NAFLD targets was depicted. The major molecular targets regulated by SZ were labeled with the red star, including TNF-α, AKT, activator protein 1 (AP-1), and caspase-3. They could promote the development and aggravation of NAFLD from the initial phase (excessive lipid accumulation) to NASH, through regulating insulin resistance, endoplasmic reticulum stress, oxidative stress, inflammatory response, fibrosis, and cell apoptosis. Taken together, SZ might counter NAFLD by regulating the above-searched pathways.

3.6. SZ Alleviated Liver Histopathological Changes and Improved Liver Function. H&E staining of liver tissues showed a normal structure of the hepatic lobules in control mice. NAFLD mice showed diffusely distributed macrovesicular and vesicular steatosis in the hepatic lobule, local infiltration of inflammatory cells, and ballooning degeneration of hepatocytes. In comparison to the model mice, the liver pathology was significantly alleviated after SZ treatment, as manifested by reduced area and severity of steatosis. Notably, local infiltration of inflammatory cells and ballooning degeneration were absent in SZ group (Figure 6). In addition, serum ALT and AST were significantly higher in the model group than in the control group ($p < 0.01$) and were remarkably reduced by SZ treatment ($p < 0.01$).

3.7. SZ Improved Glucose Tolerance and Insulin Resistance. Compared with the mice in the control group, NAFLD mice showed significantly higher FBG ($p < 0.01$), which was reduced following SZ intervention ($p < 0.01$). IPGTT results and AUC values demonstrated that the ability of mice to regulate blood glucose was attenuated in the model group but obviously reversed by SZ treatment. HOMA-IR remained higher ($p < 0.01$) and phosphor-AKT was lower ($p < 0.05$) in NAFLD mice than in controls, indicating that insulin resistance existed in the model mice. SZ treatment significantly downregulated the HOMA-IR ($p < 0.01$) and activated hepatic AKT ($p < 0.05$) (Figure 7).

3.8. SZ Downregulated TNF-α Level of NAFLD Mice. ELISA data revealed a higher serum TNF-α in the model group than in the control group ($p < 0.05$). After intervention with SZ, serum TNF-α in NAFLD mice was remarkably reduced ($p < 0.05$). Consistently, SZ significantly downregulated the mRNA level of TNF-α in the liver tissues of NAFLD mice ($p < 0.01$) (Figure 8).

4. Discussion

In this study, effective chemicals in SZ, their targets, and pathways enriched in NAFLD were searched through online databases. Meanwhile, the efficacy of SZ in the treatment of NAFLD was estimated by the approach of network pharmacology. A total of 27 effective chemicals of SZ were obtained, including β-sitosterol, luteolin, stigmasterol, mustard oil, etc. Some of them, such as β-sitosterol and

Table 4: The target genes of NAFLD.

Gene ID	Gene symbol
5465	PPARA
4481	MSR1
1376	CPT2
3953	LEPR
1401	CRP
5468	PPARG
7099	TLR4
2678	GGT1
5728	PTEN
3586	IL10
7040	TGFB1
1499	CTNNB1
207	AKT1
836	CASP3
338	APOB
335	APOA1
406913	MIR126
348	APOE
406906	MIR122
3458	IFNG
3553	IL1B
5265	SERPINA1
847	CAT
355	FAS
3643	INSR
406986	MIR203A
7157	TP53
51085	MLXIPL
1571	CYP2E1
3667	IRS1
406901	MIR107
80339	PNPLA3
1649	DDIT3
406919	MIR130A
56729	RETN
407035	MIR31
407015	MIR26A1
3172	HNF4Amir
407040	34A
2147	F2
7422	VEGFA
5599	MAPK8
6347	CCL2
7124	TNF
406983	MIR200Amir
406984	200B
3077	HFE
3576	CXCL8
407018	MIR27A
19	ABCA1
406991	MIR21
3030	HADHA
407004	MIR22
1636	ACE
213	ALB
3630	INS
407029	MIR30A
9971	NR1H4
10062	NR1H3
406932	MIR140
6720	SREBF1
4023	LPL
3569	IL6
406952	MIR17
3479	IGF1
100380876	NAFLD1
9370	ADIPOQ
4547	MTTP
406921	MIR132
3952	LEP
174	AFP
26503	SLC17A5
5444	PON1
2168	FABP1
2875	GPT

luteolin, had been isolated and identified before [34, 35]. Then, 20 main targets highly correlated with NAFLD were screened out from the online database, including TNF, AKT, caspase-3, etc. Furthermore, GO and KEGG analyses showed that SZ was capable of regulating multiple biological processes and pathways enriched in NAFLD, TNF-α, apoptosis, T2DM, lifespan regulation, adipokines, insulin resistance pathway, etc. In another network pharmacology analysis of SZ in the treatment of asthma, 22 effective chemicals were extracted, which were similar to our study. In addition, enrichment analysis suggested that the therapeutic mechanism of SZ in treating asthma might involve signaling pathways of PI3K-Akt, TNF, and hypoxia inducible factor-1 [36]. This suggests that the traditional formula exerts similar effects on the regulation of molecular signaling pathways, even for different diseases. According to the method of Yang M. et al., a disease that is more closely associated with a medicine shares more terms in the top k enriched GO terms or KEGG pathways [23]. In the present study, the relative larger area under the curve of the top 30 GO terms and KEGG pathways was obtained, suggesting a close correlation and a stronger effect of SZ on NAFLD.

The approach of network pharmacology is just based on in silico analysis. Therefore, to validate the results from network pharmacology analysis, an *in vivo* NAFLD model was established with mice fed on a high-fat diet with or without SZ treatment. Diets rich in fat, like 30%–75% of total calories derived from saturated fatty acids (±unsaturated fatty acids), have been proved useful to induce metabolic alterations and NAFLD. This model can be used to mimic the pathological and molecular alterations in humans with NAFLD [37]. In this study, the mice fed with 30-week HFD displayed hepatosteatosis with inflammatory infiltration and ballooning hepatocytes in liver tissues, elevated serum ALT and AST, and decreased glucose tolerance, indicating the presence of NAFLD. SZ treatment significantly ameliorated histopathological changes (e.g., steatosis and inflammatory infiltration), downregulated serum transaminases, and improved glucose tolerance. These results confirmed the strong association between SZ and NAFLD predicted by network pharmacology analysis but also verified the effect of SZ on NAFLD predicted according to TCM theory.

It has been reported that modified San Zi Yang Qin Decoction (SZ plus dodder and glossy privet) could reduce the levels of FBG and 2 h postprandial blood glucose and increase the glucose tolerance in type 2 diabetes model rats induced by high-fat diet and multiple low-dose streptozotocin injections [15], which is consistent with our results. In addition, natural compounds in SZ, such as luteolin, β-sitosterol, and stigmasterol, can counter NAFLD or NASH in rodents. Luteolin alleviates NASH through repressing inflammatory pathways and oxidative stress [38]. β-Sitosterol prevents macrovesicular steatosis induced by a high-fructose diet and the progression of NAFLD to steatohepatitis [39]. After a 17-week treatment with 0.4% stigmasterol and β-sitosterol, NAFLD was significantly alleviated in mice fed with a high-fat western-style diet (HFWD) [40]. These natural compounds might be the effective ingredients of SZ;

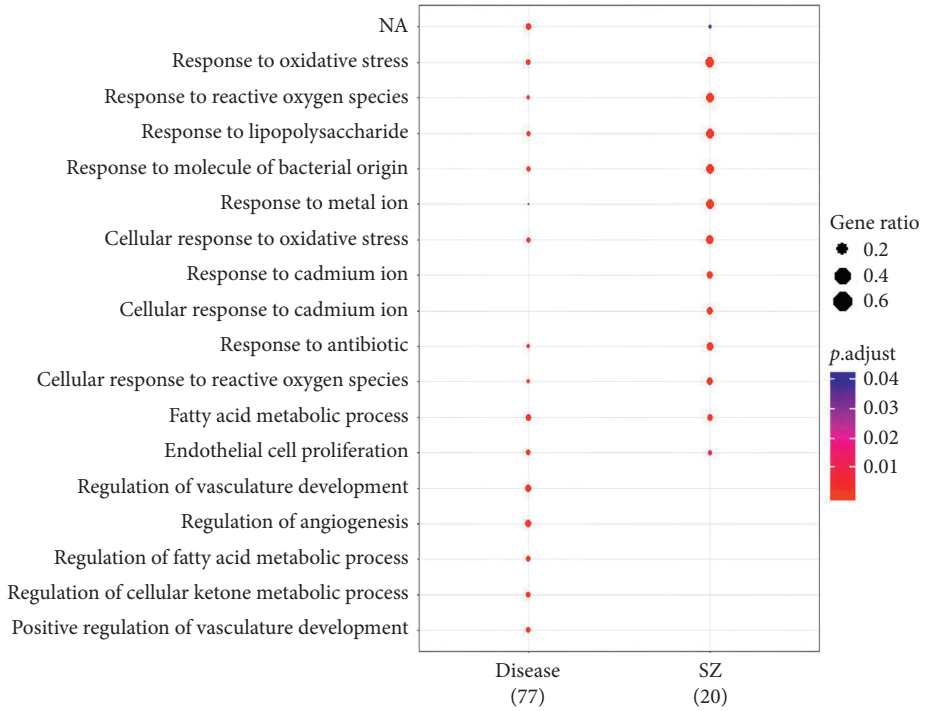

Figure 1: GO enrichment analysis of biological processes of SZ and NAFLD.

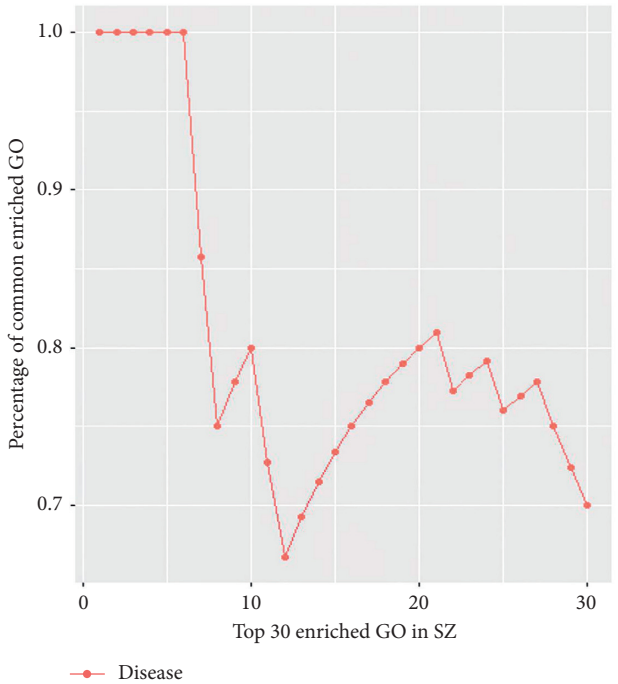

Figure 2: The cumulative distribution of percentages of common terms from the top 30 enriched GO terms in SZ for NAFLD.

therefore, these experimental data also support our findings of the therapeutic efficacy of SZ for NAFLD.

The pathogenesis of NAFLD is a parallel multi-hit process, including insulin sensitivity, oxidative stress, mitochondrial dysfunction, the release of inflammatory cytokines, etc. [4]. According to our network pharmacology analysis, SZ may function on NAFLD through regulating pathways associated with insulin resistance (IR), TNF-α, endoplasmic reticulum stress, oxidative stress, and hepatocyte apoptosis. Through these regulations, SZ rebalances lipid metabolism and protects against liver injury in NAFLD.

IR is a key step during the development of NAFLD. The inactivation of AKT signaling pathway is the key factor of IR [41, 42]. The liver is an important target organ of insulin.

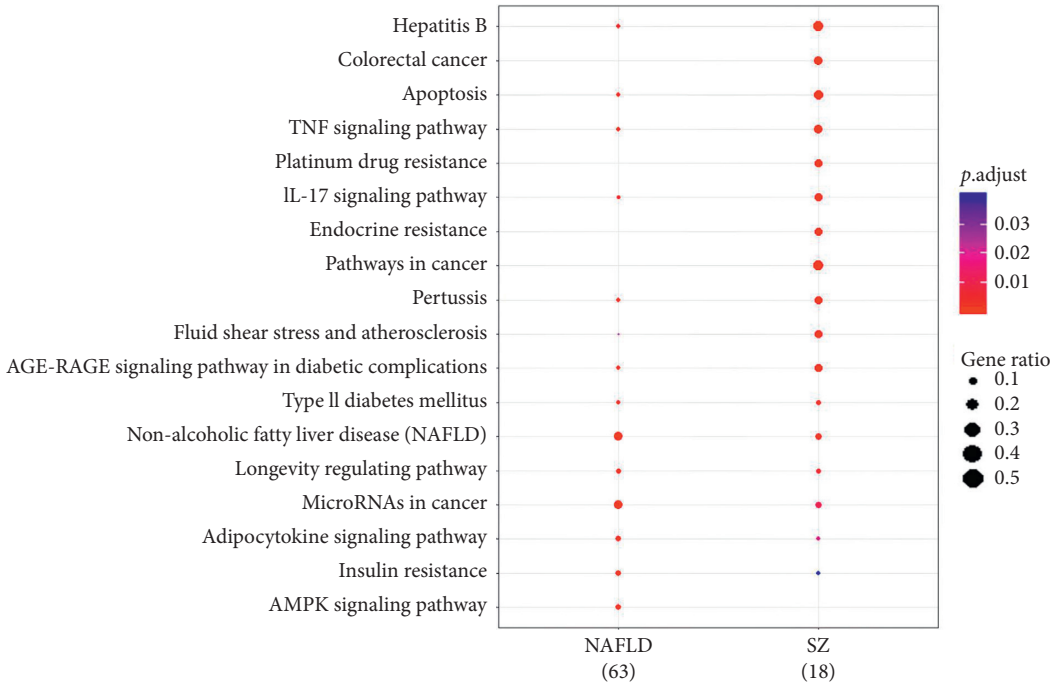

Figure 3: KEGG pathways enriched of SZ and NAFLD.

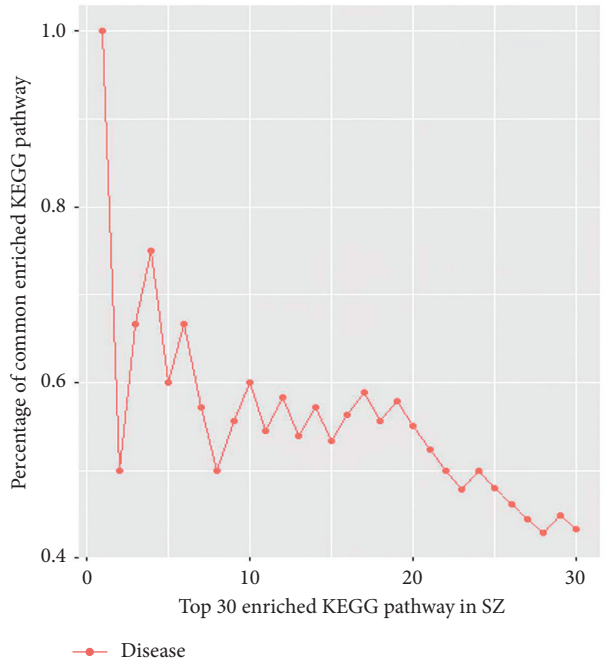

Figure 4: The cumulative distribution of percentages of common terms from the top 30 enriched KEGG terms in SZ for NAFLD.

Under physiological conditions, insulin can stimulate glycogen synthesis, repress the activities of gluconeogenesis enzymes, reduce blood glucose, and promote adipogenesis by activating AKT signaling pathway in hepatocytes [43]. Once insulin resistance occurs, an abnormally activated PI3K/AKT signaling pathway facilitates gluconeogenesis in the liver [44]. In the meantime, abnormally elevated insulin increases the synthesis of lipids in hepatocytes and decreases the oxidation of fatty acids, thus leading to the disorder of glucose and lipid metabolisms [45, 46]. Our *in vivo* data indicated that SZ significantly reduced FBG level and HOMA-IR, increased glucose tolerance, and dissipated liver fat accumulation in NAFLD mice. The AKT signaling pathway, once inactivated, was then upregulated by SZ treatment. These results demonstrated that SZ could ameliorate insulin resistance, which is consistent with that in our

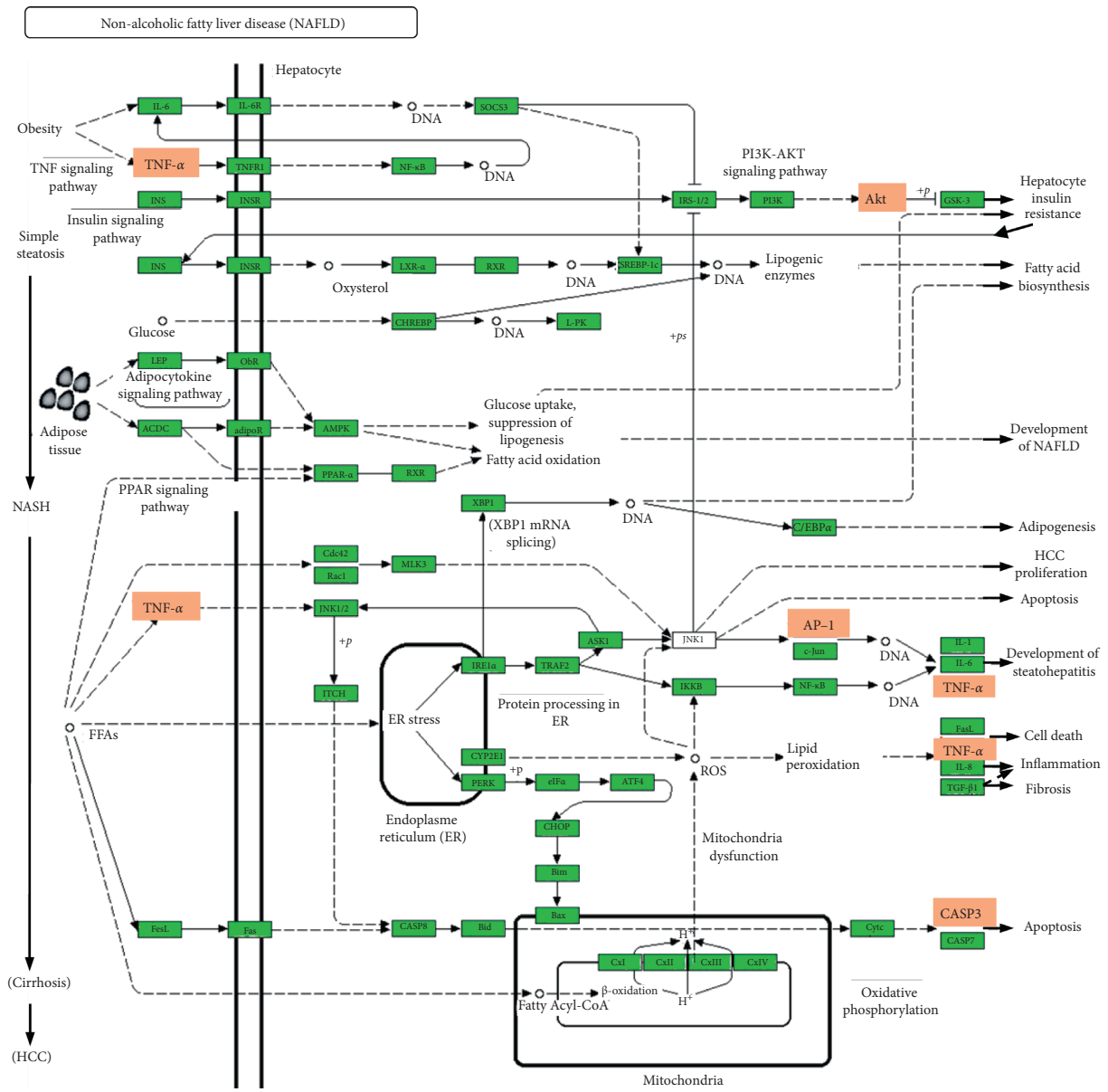

Figure 5: The NAFLD pathway enriched according to both SZ and NAFLD targets. The orange box marks the potential targets of SZ.

network pharmacological analysis. As one downstream molecule of IRS-1, AKT can be activated by phosphorylated IRS-1. Similarly, modified SZ can increase tyrosine-phosphorylated insulin receptor substrate-1 (IRS-1) in the skeletal muscle of T2DM rats to relieve insulin resistance [15].

TNF-α is critical for the development of NAFLD. It is reported that hepatocyte steatosis can activate NF-κB to trigger the production of TNF-α in NAFLD. On the one hand, TNF-α induces hepatocyte apoptosis by activating caspase and releasing cytochrome C to form apoptotic bodies [47, 48]. On the other hand, TNF-α can lead to hepatocyte necrosis through inducing mitochondrial dysfunction, production of reactive oxygen species (ROS), and lipid peroxidation [49, 50]. All these processes aggravate simple steatosis of the liver into irreversible NASH with inflammatory responses [51]. TNF-α is also involved in lipid metabolism. It stimulates the release of free fatty acid (FFA), which in turn promotes the release of TNF-α from macrophages, eventually enhancing lipid accumulation in the liver [52, 53]. By directly targeting the intracellular insulin signal transduction system, TNF-α can enhance insulin resistance through upregulating suppressor of cytokine signaling 3 (SOCS-3) [54] and inhibiting adiponectin activity [55]. Our results showed that TNF-α level in serum and liver tissues was higher in NAFLD mice than in controls but remarkably reduced by SZ intervention. The *in vivo* results were consistent with those of our network pharmacological analysis in that SZ may rely on the TNF-α signaling pathway to reverse NAFLD. It has been reported that SZ could treat bronchial asthma by blocking cysteinyl leukotrienes- (CysLTs-) mediated inflammatory pathways

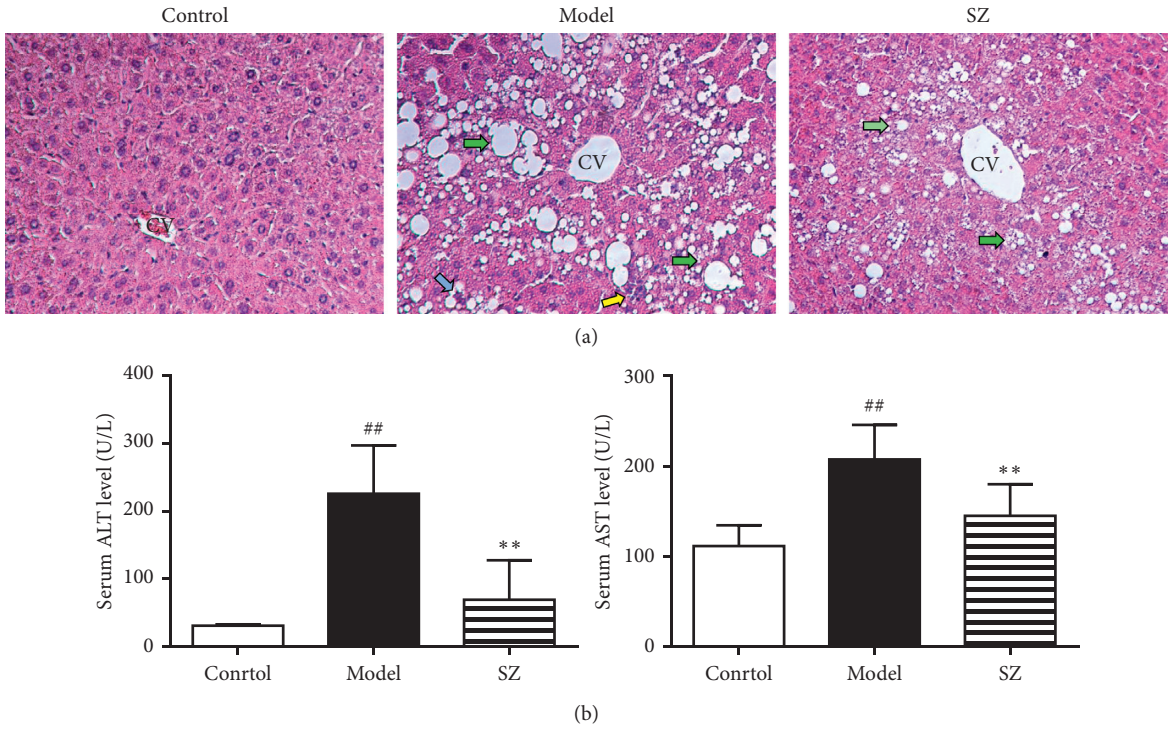

Figure 6: SZ alleviated liver tissue damage and improved liver function in NAFLD mice. (a) Representative photomicrographs of liver sections stained with hematoxylin and eosin (magnification: 200×). CV means centrilobular vein. The green arrow shows macrovesicular steatosis, the blue arrow shows ballooning degeneration of hepatocytes, and the yellow arrow shows infiltration of inflammatory cells. (b) Serum transaminase level. $n = 6$. $^{\#\#}p < 0.01$ vs control; $^{**}p < 0.01$ vs model.

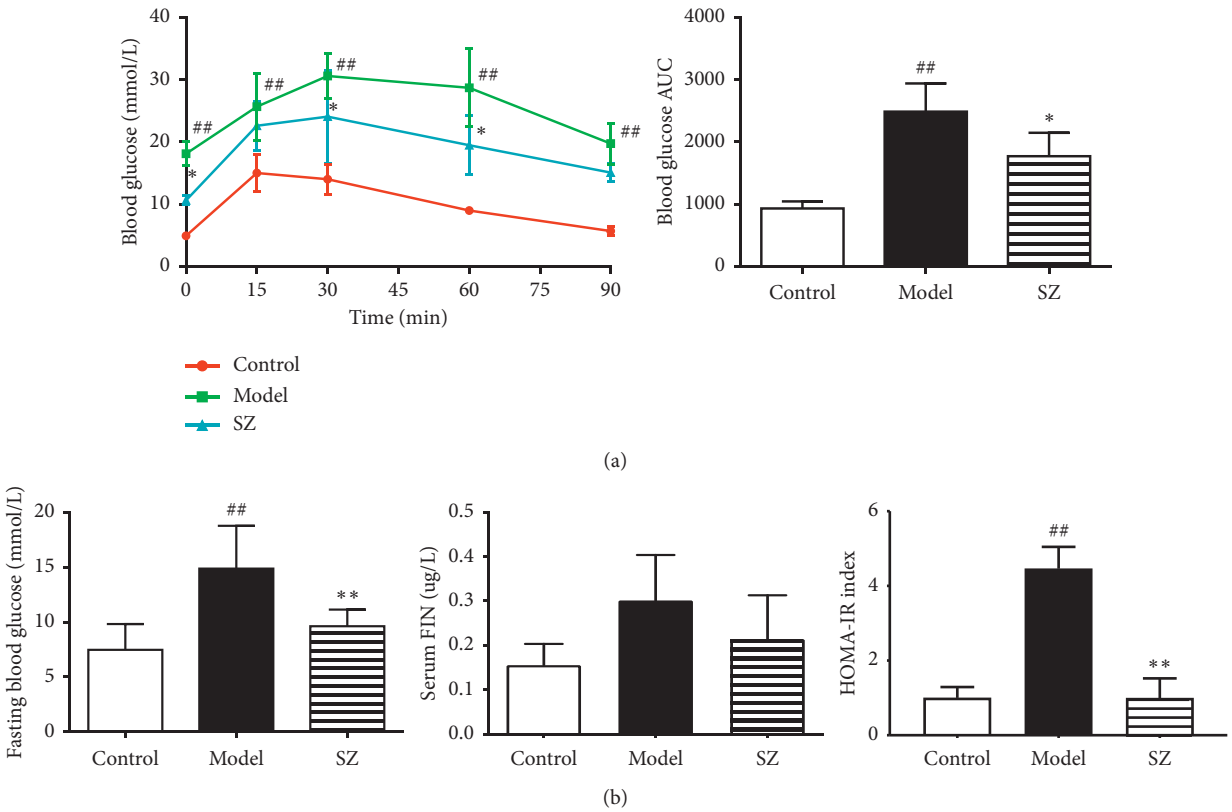

Figure 7: Continued.

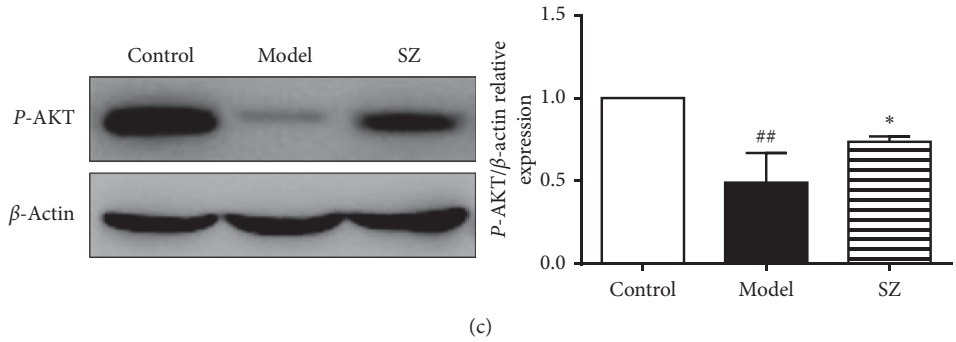

Figure 7: SZ increased glucose tolerance and decreased insulin resistance in NAFLD mice. (a) The IPGTT performed at the end of the 8-week treatment and the AUC calculated for the results of IPGTT. (b) Fasting blood glucose, insulin level, and the calculated HOMA-IR index. (c) The expression level of phospho-AKT in the liver tissues of mice. $n = 4$. $^{\#}p < 0.05$ vs contro1; $^{\#\#}p < 0.01$ vs control; $^{**}p < 0.01$ vs model; $^{*}p < 0.05$ vs model.

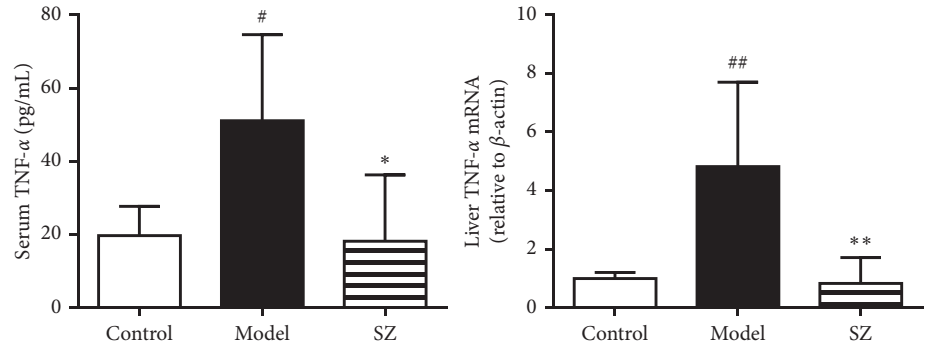

Figure 8: SZ downregulated TNF-α levels in serum and liver tissues of NAFLD mice. $n = 6$. $^{\#}p < 0.05$ vs contro1; $^{\#\#}p < 0.01$ vs control; $^{**}p < 0.01$ vs model; $^{*}p < 0.05$ vs model.

[56]. The combination of SZ with Erehen decoction has shown significant clinical efficacy in the treatment of acute exacerbation of COPD. It can significantly improve lung function and reduce inflammatory factors [57]. As one component of SZ, in silico, *in vitro*, *in vivo*, and clinical studies strongly suggest that luteolin exerts its function mainly depending on its anti-inflammatory activity. It can protect against non-alcoholic steatohepatitis in HFD induced NASH rats. TNF-α and other proinflammatory cytokines levels were decreased in the groups that received 50 and 100 mg/kg luteolin [38, 58].

During the development of NAFLD, oxidative stress, endoplasmic reticulum stress, mitochondrial dysfunction, and TNF-α signaling are all associated with the activation of c-Jun N-terminal kinase (JNK). They cooperate to trigger the damage of hepatocytes [59, 60]. AP-1 is a downstream molecule of JNK. The homodimer or heterodimer of AP-1, fabricated by C-Jun and C-Fos family members, copes with multiple stimuli by binding to DNA sequences of target genes. As our study revealed, AP-1 might be a target of SZ, indicating that SZ alleviates multi-hit liver injury via regulating the JNK pathway. The component of SZ luteolin can also inhibit LPS-induced IL-6 production by repressing the JNK signaling pathway and AP-1 activation in microglia, a process that mitigates neuroinflammation. Experiments have confirmed that, as the upstream regulator, luteolin can alter the transcriptional activation of NF-κB and AP-1 signaling pathways [58, 61]. During the development of NASH, multiple stimuli evoke hepatocyte apoptosis. Hepatocyte apoptosis is either a vital feature or a key factor leading to the aggravation of NASH. It is reported that the severity and extent of hepatocyte apoptosis in liver biopsy samples of NASH patients exceed those in non-NASH cases. The activity of caspase-3 is positively correlated with the symptom severity and pathologic stage of NASH [62]. Our results uncovered that caspase-3 may be targeted, and the apoptosis pathway is regulated by SZ. But, these findings still require further validation.

5. Conclusions

We have speculated that the TCM formula SZ might be applied to treat NAFLD according to the TCM principle of "homotherapy for heteropathy" and previously reported clinical cases. Based on network pharmacology-based analysis and *in vivo* experiments in SZ-intervened NAFLD mice, we for the first time verified the efficacy of SZ in alleviating NAFLD, providing evidence for its clinical application. This study also confirmed the TCM conception of "homotherapy for heteropathy" from the network molecular

level. Meanwhile, SZ may improve NAFLD through targeting AKT, TNF-α, AP-1, and caspase-3, and regulating pathways enriched in insulin resistance, TNF-α, apoptosis, T2DM, etc. These findings should be further clarified through *in vivo* and *in vitro* experiments in the future.

Data Availability

The datasets used to support the findings in the current study are included within the article and supplementary materials.

Conflicts of Interest

The authors declare no conflicts of interest.

Authors' Contributions

Haiyan Song and Peiyong Zheng contributed to study design; Yiping Li, Ming Yang, and Yang Liu carried out data collection; Jiaoya Xu conducted statistical analysis; Qianlei Wang, Yu Zheng, and Peiyong Zheng contributed to data interpretation; Yang Liu participated in literature search; Yiping Li and Haiyan Song performed manuscript preparation. All authors read and approved the final manuscript. Yiping Li and Yang Liu contributed equally to this work.

Acknowledgments

This study was supported by the National Natural Science Foundation of China (Nos. 81703867, 81873254, and 81704047) and Emerging Interdisciplinary Program of Traditional Chinese Medicine of Shanghai (Evidence-Based Traditional Chinese Medicine).

Supplementary Materials

Figure S1: GO enrichment analysis of molecular functions. Figure S2: GO enrichment analysis of cellular components. (*Supplementary Materials*)

References

[1] N. Katsiki, D. P. Mikhailidis, and C. S. Mantzoros, "Non-alcoholic fatty liver disease and dyslipidemia: an update," *Metabolism*, vol. 65, no. 8, pp. 1109–1123, 2016.

[2] Z. M. Younossi, A. B. Koenig, D. Abdelatif, Y. Fazel, L. Henry, and M. Wymer, "Global epidemiology of nonalcoholic fatty liver disease-meta-analytic assessment of prevalence, incidence, and outcomes," *Hepatology*, vol. 64, no. 1, pp. 73–84, 2016.

[3] G. Tarantino, V. Citro, and D. Capone, "Nonalcoholic fatty liver disease: a challenge from mechanisms to therapy," *Journal of Clinical Medicine*, vol. 9, no. 1, 2020.

[4] F. Bessone, M. V. Razori, and M. G. Roma, "Molecular pathways of nonalcoholic fatty liver disease development and progression," *Cellular and Molecular Life Sciences*, vol. 76, no. 1, pp. 99–128, 2019.

[5] Y. Hu, "Advantages and prospects of traditional Chinese medicine in treating nonalcoholic fatty liver disease," *World Chinese Medicine*, vol. 10, no. 02, pp. 149–152, 2015.

[6] J. Wang, "Experience of Lingtai Wang in treating fatty liver from phlegm," *Liaoning Journal of Traditional Chinese Medicine*, vol. 38, no. 05, pp. 832-833, 2020.

[7] X. Quan, X. Qi, and H. Liu, "Pharmacological action and clinical study development of perilla leaf," *Information on Traditional Chinese Medicine*, vol. 20, no. 02, pp. 21-22, 2004.

[8] L. Sui, S. Li, and W. Lv, "Summarization on the study progress of Sanzi Yangqing decoction in recent ten years," *Guiding Journal of Traditional Chinese Medicine and Pharmacy*, vol. 07, pp. 103-104, 2020.

[9] G. Yi, "Research progress on pharmacology and clinical application of San Zi Yang Qin decoction," *Contemporary Medicine*, vol. 16, no. 24, pp. 22-23, 2020.

[10] Q. Zhang and W. Liu, "New clinical examples of san Zi Yang Qin decoction," *Nei Mongol Journal of Traditional Chinese Medicine*, vol. 36, no. 19, p. 42, 2020.

[11] J. Peng and L. Yang, "Five prescriptions of Zhao Shaoqin," *Shandong Journal of Traditional Chinese Medicine*, vol. 10, pp. 458-459, 2020.

[12] H. Zhu, "47 cases of hyperlipidemia treated with San Zi Yang Qin decoction," *Henan Traditional Chinese Medicine*, vol. 22, no. 06, p. 28, 2020.

[13] R. Chen, "New clinical application of San Zi Yang Qin decoction," *Chinese Community Doctors*, vol. 28, no. 40, p. 9, 2019.

[14] X. Cheng and Q. Liu, "Clinical observation on 58 cases of cystic hyperplasia of mammary gland treated with Sanzi Yangqin decoction," *Journal of Traditional Chinese Medicine*, vol. 51, no. 01, pp. 41–43, 2016.

[15] Y. Wang, X. La, C. Tian et al., "Effects of modified sanzi yangqin decoction on tyrosine phosphorylation of IRS-1 in skeletal muscle of type 2 diabetic rats," *Evidence-Based Complementary and Alternative Medicine*, vol. 2018, Article ID 7092140, , 2018.

[16] R. Zuo, M. Wan, and J. Zou, "Evaluation of MA Wanqian Huatan Quyu decoction in treatment of non-alcoholic fatty liver with phlegm-stasis syndrome," *Journal of Liaoning University of Traditional Chinese Medicine*, vol. 22, no. 02, pp. 25–28, 2013.

[17] T. Yan, N. Yan, P. Wang et al., "Herbal drug discovery for the treatment of nonalcoholic fatty liver disease," *Acta Pharmaceutica Sinica B*, vol. 10, no. 1, pp. 3–18, 2020.

[18] S. Li and B. Zhang, "Traditional Chinese medicine network pharmacology: theory, methodology and application," *Chinese Journal of Natural Medicines*, vol. 11, no. 2, pp. 110–120, 2013.

[19] B. Boezio, K. Audouze, P. Ducrot, and O. Taboureau, "Network-based approaches in pharmacology," *Molecular Informatics*, vol. 36, no. 10, 2017.

[20] J. Huang, F. Cheung, H.-Y. Tan et al., "Identification of the active compounds and significant pathways of yinchenhao decoction based on network pharmacology," *Molecular Medicine Reports*, vol. 16, no. 4, pp. 4583–4592, 2017.

[21] Y.-f. Liu, N. Ai, A. Keys, X.-h. Fan, and M.-j. Chen, "Network pharmacology for traditional Chinese medicine research: methodologies and applications," *Chinese Herbal Medicines*, vol. 7, no. 1, pp. 18–26, 2015.

[22] S. Li, Y. Qian, R. Xie et al., "Exploring the protective effect of ShengMai-Yin and Ganmaidazao decoction combination against type 2 diabetes mellitus with nonalcoholic fatty liver disease by network pharmacology and validation in KKAy mice," *Journal of Ethnopharmacology*, vol. 242, Article ID 112029, 2019.

[23] M. Yang, J. Chen, L. Xu et al., "A network pharmacology approach to uncover the molecular mechanisms of herbal

formula Ban-Xia-Xie-Xin-Tang," *Evidence-Based Complementary and Alternative Medicine*, vol. 2018, Article ID 4050714, 22 pages, 2018.

[24] J. Ru, P. Li, J. Wang et al., "TCMSP: a database of systems pharmacology for drug discovery from herbal medicines," *Journal of Cheminformatics*, vol. 6, no. 1, p. 13, 2014.

[25] H. Ye, L. Ye, H. Kang et al., "HIT: linking herbal active ingredients to targets," *Nucleic Acids Research*, vol. 39, pp. D1055–D1059, 2011.

[26] L. Huang, D. Xie, Y. Yu et al., "TCMID 2.0: a comprehensive resource for TCM," *Nucleic Acids Research*, vol. 46, no. D1, pp. D1117–D1120, 2018.

[27] D. Szklarczyk, A. Santos, C. von Mering, L. J. Jensen, P. Bork, and M. Kuhn, "STITCH 5: augmenting protein-chemical interaction networks with tissue and affinity data," *Nucleic Acids Research*, vol. 44, no. D1, pp. D380–D384, 2016.

[28] X. Liang, H. Li, and S. Li, "A novel network pharmacology approach to analyse traditional herbal formulae: the Liu-Wei-Di-Huang pill as a case study," *Molecular BioSystems*, vol. 10, no. 5, pp. 1014–1022, 2014.

[29] M. Yang, J. Chen, L. Xu et al., "A novel adaptive ensemble classification framework for ADME prediction," *RSC Advances*, vol. 8, no. 21, pp. 11661–11683, 2018.

[30] G. R. Bickerton, G. V. Paolini, J. Besnard, S. Muresan, and A. L. Hopkins, "Quantifying the chemical beauty of drugs," *Nature Chemistry*, vol. 4, no. 2, pp. 90–98, 2012.

[31] D. S. Wishart, Y. D. Feunang, A. C. Guo et al., "DrugBank 5.0: a major update to the DrugBank database for 2018," *Nucleic Acids Research*, vol. 46, no. D1, pp. D1074–D1082, 2018.

[32] M. Safran, I. Dalah, J. Alexander et al., "GeneCards version 3: the human gene integrator," *Database*, vol. 2010, Article ID baq020, 2010.

[33] A. Gossmann, P. Zille, V. Calhoun, and Y. P. Wang, "FDR-corrected sparse canonical correlation analysis with applications to imaging genomics," *IEEE Transactions on Medical Imaging*, vol. 37, no. 8, pp. 1761–1774, 2018.

[34] L. Duan, B. Feng, B. Zhou, W. Wang, Y. Pei, and Y. Wang, "Study on chemical constituents for relieving couph and asthma in the extractives of Sanzhi Yangqin Tang," *Chinese Journal of Hospital Pharmacy*, vol. 28, no. 11, pp. 863-864, 2018.

[35] H. Zhao, Z. Zhang, Y. Li, S. Hu, W. Yao, and H. Kuang, "Chemical component study of Sanzi Yangqin Tang," *Acta Chinese MedicineE and Pharmacology*, vol. 31, no. 2, pp. 15-16, 2003.

[36] J. Zou, L. Pang, and X. Lu, "Network pharmacology analysis of Sanzi Yangqin Decoction in the treatment of asthma," *Liaoning Journal of Traditional Chinese Medicine*, vol. 47, no. 10, pp. 133–224, 2020.

[37] G. Kanuri and I. Bergheim, "In vitro and in vivo models of non-alcoholic fatty liver disease (NAFLD)," *International Journal of Molecular Sciences*, vol. 14, no. 6, pp. 11963–11980, 2013.

[38] N. Abu-Elsaad and A. El-Karef, "Protection against nonalcoholic steatohepatitis through targeting IL-18 and IL-1alpha by luteolin," *Pharmacological Reports*, vol. 71, no. 4, pp. 688–694, 2019.

[39] N. M. Gumede, B. W. Lembede, P. Nkomozepi, R. L. Brooksbank, K. H. Erlwanger, and E. Chivandi, "Beta-Sitosterol mitigates the development of high-fructose diet-induced nonalcoholic fatty liver disease in growing male Sprague-Dawley rats," *Canadian Journal of Physiology and Pharmacology*, vol. 98, no. 1, pp. 44–50, 2020.

[40] S. Feng, Z. Dai, A. B. Liu et al., "Intake of stigmasterol and β-sitosterol alters lipid metabolism and alleviates NAFLD in mice fed a high-fat western-style diet," *Biochimica et Biophysica Acta (BBA)-Molecular and Cell Biology of Lipids*, vol. 1863, no. 10, pp. 1274–1284, 2018.

[41] L. N. Bell, J. Wang, S. Muralidharan et al., "Relationship between adipose tissue insulin resistance and liver histology in nonalcoholic steatohepatitis: a pioglitazone versus vitamin E versus placebo for the treatment of nondiabetic patients with nonalcoholic steatohepatitis trial follow-up study," *Hepatology*, vol. 56, no. 4, pp. 1311–1318, 2012.

[42] D. M. Ferreira, R. E. Castro, M. V. Machado et al., "Apoptosis and insulin resistance in liver and peripheral tissues of morbidly obese patients is associated with different stages of non-alcoholic fatty liver disease," *Diabetologia*, vol. 54, no. 7, pp. 1788–1798, 2011.

[43] M. J. Watt, P. M. Miotto, W. De Nardo, and M. K. Montgomery, "The liver as an endocrine organ-linking NAFLD and insulin resistance," *Endocrine Reviews*, vol. 40, no. 5, pp. 1367–1393, 2019.

[44] S. Pisonero-Vaquero, A. Martinez-Ferreras, M. V. Garcia-Mediavilla et al., "Quercetin ameliorates dysregulation of lipid metabolism genes via the PI3K/AKT pathway in a diet-induced mouse model of nonalcoholic fatty liver disease," *Molecular Nutrition & Food Research*, vol. 59, no. 5, pp. 879–893, 2015.

[45] K. F. Leavens and M. J. Birnbaum, "Insulin signaling to hepatic lipid metabolism in health and disease," *Critical Reviews in Biochemistry and Molecular Biology*, vol. 46, no. 3, pp. 200–215, 2015.

[46] M. Asrih and F. R. Jornayvaz, "Metabolic syndrome and nonalcoholic fatty liver disease: is insulin resistance the link?" *Molecular and Cellular Endocrinology*, vol. 418, no. 1, pp. 55–65, 2015.

[47] Z. Xie, Z. Xiao, and F. Wang, "Hepatitis C virus nonstructural 5A protein (HCV-NS5A) inhibits hepatocyte apoptosis through the NF-kappab/miR-503/bcl-2 pathway," *Molecular Cell*, vol. 40, no. 3, pp. 202–210, 2017.

[48] H. A. Khan, M. Z. Ahmad, J. A. Khan, and M. I. Arshad, "Crosstalk of liver immune cells and cell death mechanisms in different murine models of liver injury and its clinical relevance," *Hepatobiliary & Pancreatic Diseases International*, vol. 16, no. 3, pp. 245–256, 2017.

[49] Z. Chen, R. Yu, Y. Xiong, F. Du, and S. Zhu, "A vicious circle between insulin resistance and inflammation in nonalcoholic fatty liver disease," *Lipids in Health and Disease*, vol. 16, no. 1, p. 203, 2017.

[50] I. Garcia-Ruiz, C. Rodriguez-Juan, T. Diaz-Sanjuan et al., "Uric acid and anti-TNF antibody improve mitochondrial dysfunction in ob/ob mice," *Hepatology*, vol. 44, no. 3, pp. 581–591, 2006.

[51] S. L. Friedman, B. A. Neuschwander-Tetri, M. Rinella, and A. J. Sanyal, "Mechanisms of NAFLD development and therapeutic strategies," *Nature Medicine*, vol. 24, no. 7, pp. 908–922, 2018.

[52] C. Monmai, S. H. Go, I. S. Shin et al., "Immune-enhancement and anti-inflammatory activities of fatty acids extracted from *Halocynthia aurantium* tunic in RAW264.7 cells," *Marine Drugs*, vol. 16, no. 9, 2018.

[53] X. Wang, M. Huang, and Y. Wang, "The effect of insulin, TNFalpha and DHA on the proliferation, differentiation and lipolysis of preadipocytes isolated from large yellow croaker (*Pseudosciaena Crocea* R.)," *PLoS One*, vol. 7, no. 10, Article ID e48069, 2012.

[54] E. Cobbina and F. Akhlaghi, "Non-alcoholic fatty liver disease (NAFLD)–pathogenesis, classification, and effect on drug metabolizing enzymes and transporters," *Drug Metabolism Reviews*, vol. 49, no. 2, pp. 197–211, 2017.

[55] Y. He, L. Lu, X. Wei et al., "The multimerization and secretion of adiponectin are regulated by TNF-alpha," *Endocrine*, vol. 51, no. 3, pp. 456–468, 2016.

[56] S. Xu, Y. Dong, K. Yang, X. Gong, and N. Li, "Effect of Sanzi Yangqin Tang on CysLTs mediated inflammatory pathways in bronchial epithelial cells," *Chinese Journal of Experimental Traditional Medical Formulae*, vol. 22, no. 11, pp. 137–141, 2019.

[57] H. Xu, J. Zhu, and Y. Wang, "Effect of erchen decoction and sanzi yangqin decoction on inflammatory cytokines in patients with acute exacerbation of COPD," *Journal of Emergency in Traditional Chinese Medicine*, vol. 28, no. 11, pp. 1889–1892, 2020.

[58] N. Aziz, M.-Y. Kim, and J. Y. Cho, "Anti-inflammatory effects of luteolin: a review of in vitro, in vivo, and in silico studies," *Journal of Ethnopharmacology*, vol. 225, pp. 342–358, 2018.

[59] S. Ezquerro, F. Mocha, G. Frühbeck et al., "Ghrelin reduces TNF-α-induced human hepatocyte apoptosis, autophagy and pyroptosis: role in obesity-associated NAFLD," *The Journal of Clinical Endocrinology & Metabolism*, vol. 104, no. 1, pp. 21–37, 2019.

[60] S. Aghazadeh and R. Yazdanparast, "Inhibition of JNK along with activation of ERK1/2 MAPK pathways improve steatohepatitis among the rats," *Clinical Nutrition*, vol. 29, no. 3, pp. 381–385, 2010.

[61] S. Jang, K. W. Kelley, and R. W. Johnson, "Luteolin reduces IL-6 production in microglia by inhibiting JNK phosphorylation and activation of AP-1," *Proceedings of the National Academy of Sciences-PNAS*, vol. 105, no. 21, pp. 7534–7539, 2008.

[62] A. E. Feldstein, A. Canbay, P. Angulo et al., "Hepatocyte apoptosis and fas expression are prominent features of human nonalcoholic steatohepatitis," *Gastroenterology*, vol. 125, no. 2, pp. 437–443, 2003.

Hindawi
Evidence-Based Complementary and Alternative Medicine
Volume 2020, Article ID 6697638, 15 pages
https://doi.org/10.1155/2020/6697638

Research Article

Effect of Sheng-Jiang Powder on Gut Microbiota in High-Fat Diet-Induced NAFLD

Juan Li,[1] **Qian Hu**,[1] **Dai Xiao-yu**,[1] **Lv Zhu**,[1] **Yi-fan Miao**,[1] **Hong-xin Kang**,[1] **Xian-lin Zhao**,[1] **Jia-qi Yao**,[1] **Dan Long**,[2] **Wen-fu Tang**,[1] **and Mei-hua Wan**[1]

[1]*Department of Integrated Traditional Chinese and Western Medicine, West China Hospital, Sichuan University, Chengdu 610041, Sichuan Province, China*
[2]*Key Laboratory of Transplant Engineering and Immunology, Sichuan University, Chengdu 610041, Sichuan Province, China*

Correspondence should be addressed to Mei-hua Wan; wanmh@scu.edu.cn

Received 12 October 2020; Revised 8 November 2020; Accepted 16 November 2020; Published 26 November 2020

Academic Editor: Hongwei Zhang

Background and Aims. Nonalcoholic fatty liver disease (NAFLD) is an alarming global health problem that is predicted to be the major cause of cirrhosis, hepatocellular carcinoma, and liver transplantation by next decade. Gut microbiota have been revealed playing an important role in the pathogenesis of NAFLD. Sheng-Jiang Powder (SJP), an empirical Chinese medicine formula to treat NAFLD, showed great hepatoprotective properties, but the impact on gut microbiota has never been identified. Therefore, we performed this study to investigate the effect of SJP on gut microbiota in NAFLD mice. *Methods*. NAFLD was induced by 12 weeks' high-fat diet (HFD) feeding. Mice were treated with SJP/normal saline daily for 6 weeks. Blood samples were obtained for serum biochemical indices and inflammatory cytokines measurement. Liver tissues were obtained for pathological evaluation and oil red O staining. The expression of lipid metabolism-related genes was quantified by RT-PCR and Western blotting. Changes in gut microbiota composition were analyzed by the 16s rDNA sequencing technique. *Results*. HFD feeding induced significant increase in bodyweight and serum levels of TG, TC, ALT, and AST. The pathological examination revealed obvious hepatic steatosis in HFD feeding mice. Coadministration of SJP effectively protected against bodyweight increase and lipid accumulation in blood and liver. Increased expression of PPARγ mRNA was observed in HFD feeding mice, but a steady elevation of PPARγ protein level was only found in SJP-treated mice. Meanwhile, the expression of FASN was much higher in HFD feeding mice. Microbiome analysis revealed obvious changes in gut microbiota composition among diverse groups. SJP treatment modulated the relative abundance of short-chain fatty acids (SCFAs) producing bacteria, including norank-f-*Erysipelotrichaceae* and *Roseburia*. *Conclusions*. SJP is efficient in attenuating HFD-induced NAFLD, and it might be partly attributed to the regulation of gut microbiota.

1. Introduction

Nonalcoholic fatty liver disease (NAFLD) is an alarming global health problem that is predicted to be the major cause of cirrhosis, hepatocellular carcinoma, and liver transplantation by 2030 [1, 2]. As the leading chronic liver disease, NAFLD is directly associated with the rising epidemic of obesity and causes huge social-economic burden impacting almost one quarter of the world's population [3, 4]. Characterized by excessive fat deposition in hepatocytes, NAFLD comprises a wide spectrum of liver conditions varying in severity of injury, ranging from simple steatosis to steatohepatitis, fibrosis, and finally cirrhosis [5]. However, the pathogenesis of NAFLD has not been fully addressed yet. A "two-hit" theory has been widely accepted for several years, and it suggests that a second hit from factors like inflammatory cytokines, lipid peroxidation, mitochondrial dysfunction, and especially oxidative stress leads to steatohepatitis in the setting of "first hit" involving simple hepatocyte steatosis [6, 7]. Actually, steatohepatitis is not always progressed from simple steatosis, and there are a variety of molecular pathways which bring about steatohepatitis [8, 9]. Therefore, this theory is currently considered outdated and gradually replaced by a "multiple hit" theory

[10] which reflects the interactions between multiple injuries, including insulin resistance, inflammatory cytokines, hereditary and epigenetic factors, oxidative stress, environmental and dietary factors, as well as gut microbiota [11]. Particularly, a growing body of evidence has revealed the important role of altered gut microbiota in the development of NAFLD.

There are trillions of the microbes colonized in the gastrointestinal tract, and the amounts and composition of gut microbiota are stable under normal conditions. Host environmental changes, including diet, alcohol intake, antibiotic abuse, and hereditary factors, may lead to dysbiosis of gut microbiota that intimately related to hepatic lipid accumulation and development of all stages of NAFLD [12]. Germ-free animals have been employed to define the impact of gut microbiota on the host physiological functions for decades. Accumulated evidences have shown that the absence or presence of these bacteria influences hepatic gene expression, calorie usage, lipid metabolism, insulin resistance, and cytokines production, which highlights the probable role of gut microbiota in NAFLD [13, 14]. Le Roy et al. [15] were the first to confirm that the gut microbiota are determinate to the development of NAFLD. They selected two donor mice showing different responses to high-fat diet and observed the consequent pathological response after their microbiota were transplanted into germ-free mice. Their results suggested a different gut microbiota composition in HFD-sensitive mice that finally developed NAFLD compared to HFD-resistant mice without any NAFLD features. And the propensity to develop NAFLD was transmissible as they occurred only in those who transplanted with the microbiota of NAFLD mice. However, the relationship of gut microbiota and NAFLD might be bidirectional as substantial evidences have disclosed obvious alterations in the composition of gut microbiota in NAFLD patients and mice compared to that of healthy individuals [16, 17]. All these discoveries highlighted the critical role of gut microbiota in the development of NAFLD and pointed out the potential of a gut microbiota-targeted therapeutic strategy.

Today, the fundamental treatment for NAFLD is lifestyle intervention as there is no licensed pharmacotherapy specific for NAFLD [18]. But actually, most people find it hard to adhere to lifestyle change whether it is physical activity implement or dietary restriction. So researchers are on the way of finding new agents to treat NAFLD. Numerous drugs have been tested for NAFLD treatment so far. These drugs are classified into several categories according to their pharmacological effect, including antioxidants, antidiabetic drugs, lipid lowering drugs, and prebiotics [19]. The above classes of drugs may have shown benefit for NAFLD controlling, but we are clearly aware of that it is difficult to find a pharmacological agent that targets wide ranging of the previous described complex physiopathology of NAFLD. Accordingly, the traditional Chinese herbal medicine shows great potential in treating NAFLD and preventing disease progression due to the multicomponent, multitarget, and multipathway properties. Emerging evidences have proved their role in regulating lipid metabolism, reducing oxidative stress, ameliorating insulin resistance, and modulating gut microbiota [20–22]. Given the pathogenesis of NAFLD, the theory of traditional Chinese medicine attributes NAFLD to a category of "liver turbidity" and the essential pathogenesis of NAFLD is disordered motion of qi, which further causes qi stagnation, phlegm retention, and blood stasis, and then induces the development of NAFLD. As a classic representative traditional Chinese medicine formula, Sheng-Jiang Powder (SJP) showed satisfying clinical effect in treating NAFLD with confirmed wide ranging of pharmacological effects, such as anti-inflammation, lowering body weight, mitigating insulin resistance, and regulating immune response [23]. Also, our previous study has demonstrated that SJP could effectively prevent HFD-induced weight gain and hepatic lipid accumulation and subsequent liver injury via regulating lipid metabolism-related pathways [24]. However, we have not had any knowledge about the impact of SJP on gut microbiota so far. Considering the critical role of gut microbiota on the development of NAFLD, the present study was designed to explore the effect of SJP on gut microbiota by using a mice model of NAFLD.

2. Materials and Methods

2.1. Design. A prospective, randomized controlled trial was conducted.

2.2. Settings. The study was conducted at Key Laboratory of Transplant Engineering and Immunology, West China School of Medicine, Sichuan University.

2.3. Ethics Statement. The protocol was approved by the Ethics Committee for Animal Experiments of Sichuan University. All mice were handled according to the University Guidelines and the Animal Care Committee Guidelines of West China Hospital. All efforts were made to minimize suffering of mice.

2.4. Preparation of Sheng-Jiang Powder. The preparation of SJP was described in our previous studies [25]. In brief, the spray-dried powder purchased from Chengdu New Green Herbal Pharmaceutical Co., Ltd. (Chengdu, China) was mixed together according to the original compatibility proportion of the crude drugs (the ratio of *Bombyx batryticatus* vs *Periostracum cicada* vs *Curcuma longa* vs raw rhubarb was 2 : 1 : 3 : 4) and reconstituted with distilled water at a concentration of 1 g/ml for the crude drug. The experimental mice were treated with SJP at a concentration of 5 g/kg.BW, which is 10-fold dose of an adult according to the equivalent dose ratio by surface area.

2.5. Animals and Treatment. Male C57BL/6 mice weighting 18–20 g were provided by Charles River (Beijing, China). All mice were kept under controlled temperature (22-23°C) and on a 12 h light/12 h dark cycle and followed by free access to a HFD to induce NAFLD or a control diet. All animal feed were provided by Trophic Animal Feed High-tech Co., Ltd

(Jiangsu, China). The specific information about the animal feed can be found at http://trophic.biomart.cn. In brief, the HFD we used was TP23300 with 60% of calories derived from fat, and the control diet was TP23302 with 16.7% of calories derived from fat. Animals were randomly allocated to the control group (AC, control diet, $n = 7$), NAFLD group (AT, high-fat diet, $n = 7$), and SJP treatment group (AS, high-fat diet plus SJP treatment, $n = 7$) by random number table. Special feeding lasted for 12 weeks, and the mice in the SJP group were gavaged with SJP once a day from the beginning of the seventh week, while mice in another two groups received equal volume of normal saline instead. We recorded the body weight every 3 weeks, and the fecal samples were collected under a sterile environment for gut microbiota analysis after 12-week feeding. All mice were sacrificed by breaking the neck. The blood and tissue samples were obtained for biochemical test, histopathological analysis, PCR, and Western blotting.

2.6. Serum Biochemical Test and Inflammatory Cytokine Analysis. All mice were fasted for 12 h before getting blood samples from the inner canthus vein. The blood samples were then centrifuged at 2500 rpm for 5 min, and the supernatants were collected for biochemical test and inflammatory cytokines analysis. Serum transaminase and lipid were tested by an automatic biochemical analyzer (HITACHI, 7170A, Japan), and serum IL-6 and IL-10 were analyzed by enzyme-linked immunosorbent assay (ELISA) with commercially available materials (eBio, Wuhan, China). According to the manufacturer's protocol, absorbance was measured at 450 nm with High-Throughput Universal Microplate Assay. The sample values were then read off the standard curve, and the relative concentrations were calculated.

2.7. Real-Time Quantitative Polymerase Chain Reaction (qRT-PCR). Expressions of sterol regulatory element-binding protein 1c (SREBP1c) and peroxisome proliferator-activated receptor γ (PPARγ) were quantified by qRT-PCR analysis. In brief, total RNA was extracted from fresh liver using TRIzol (15596018, Invitrogen) and reverse-transcribed into cDNA using an iScriptcDNA synthesis kit (Bio-Rad, USA). Real-time qPCR was performed using a Bio-Rad nucleic acid electrophoresis apparatus (Bio-Rad CFX96) and Bio-Rad gel imaging system (GelDoc XR). The primers for the target genes were synthesized by Bohao Biotechnology Co., Ltd. (Shanghai, China). The primer sequences used in this study were as follows: SREBP1c (forward: 5′-CTTTGGCCTCGCTTTTCGG-3′; reverse: 5′-TGGGTCCAATTAGAGCCATCTC-3′) and PPARγ (forward: 5′-CTCCAAGAATACCAAAGTGCGA-3′; reverse: 5′-GCCTGATGCTTTATCCCCACA-3′). GAPDH was used as the internal control. Relative fold changes in gene expression were determined by the $2^{-\Delta\Delta Ct}$ method.

2.8. Oil Red O Staining. Fresh liver samples were immediately embedded in tissue freezing medium (SAKURA Tissue-Tek O.C.T. Compound, Order Number 4583, USA) and absolutely frozen to a solid by a frozen slicer. Then, the frozen liver samples were sectioned into 5 μm slices and fixed by 4% paraformaldehyde for 10 minutes. Afterwards, the frozen liver slices were washed with phosphate buffer saline (PBS) twice and then stained with a freshly prepared working solution of Oil Red O (the stock solution was prepared with 0.5 g Oil red O dissolved in 100 ml isopropanol, and then, the working solution was prepared by adding distilled water to the stock solution at a proportion of 3 : 2) for 1 h at room temperature followed by being counterstained with hematoxylin before microscopic observation (Olympus BX63, Tokyo, Japan). And the images were captured using Cytation 5 cell Imaging Multimode reader (BioTek Instrument, USA).

2.9. 16s rDNA Bioinformatics Analysis. Genomic DNA was extracted from fecal samples using the MoBio Power Fecal DNA isolation kit (Qiagen, Germantown, MD) and then was detected by 1% agarose gel electrophoresis. Specific primers with barcode were synthesized according to the specified sequencing region of 16s rRNA gene for PCR amplification. PCR was performed using TransStart Fastpfu DNA Polymerase (TransGen AP221-02), and the PCR products were detected using QuantiFluor™-ST blue fluorescence quantitative system (Promega). All samples were sequenced in triplicate on the Illumina MiSeq platform (Illumina, San Diego, CA). Sequencing data were processed by using Quantitative Insights Into Microbial Ecology (QIIME, v.1.9.1, http://qiime.org/scripts/assign_taxonomy.html). PE reads obtained from MiSeq sequencing were first spliced according to the overlap relationship. At the same time, the sequence quality is controlled and filtered, and then, OTU clustering analysis and species taxonomy analysis were carried out after differentiating samples. We joined reads using a minimum overlap of 10 bp and a maximum percent difference within the overlap of 20%. Operational taxonomic units (OTUs) were assigned by clustering sequence reads at 97% similarity via Usearch platform (version 7.0, http://drive5.com/usearch/), and the chimeras were removed during the clustering process to obtain the OTU representative sequences. Then, OTUs were aligned against the Silva database (Release128, http://www.arb-silva.de). Taxonomic assignment was completed using the RDP classifier (version 2.2, http://sourceforge.net/projects/rdpclassifier/) with a confidence threshold of 0.7. Shannon rarefaction curve was made to make sure the sequencing depth was sufficient to capture biodiversity in the tested samples. Then, within-sample diversity (α-diversity) was evaluated by Shannon, Simpson, Chao, and Ace indexes. Between-sample diversity (β-diversity) was measured by hierarchical clustering of distance matrix. Ordination of β-diversity metrics was then visually displayed by principal coordinates analyses (PCoA) and partial least squares discriminant analysis (PLS-DA). Differences in microbial community abundance among three groups of samples at the OTUs and genus levels were examined by the Kruskal–Wallis H test, and $p < 0.05$ was considered statistically significant.

2.10. Immune Blotting of SREBP1c, LXR, FASN, and PPARγ. Expression of SREBP1c, liver X receptor (LXR), fatty acid synthase (FASN), and PPARγ were determined by Western blot analysis. In brief, fresh tissue samples pretreated with appropriate amount of RIPA buffer containing PMSF underwent a ultrasonication and then were centrifuged at 13000 rpm for 10 minutes. The supernatants were collected for total protein quantification. The protein concentrations were then determined using the Bio-Rad protein assay kit (Bio-Rad Laboratories) according to the manufacturer's instructions. The lysates were then separated on an 8% SDS/PAGE. Following electrophoretic transfer on to nitrocellulose membranes and blocking with 5% milk solution, blots were incubated overnight at 4°C with primary rabbit polyclonal/monoclonal antibodies against SREBP1c (1 : 1000, #9874, Cell Signaling Technology), LXR (1 : 1000, #ab176323, Abcam), FASN (1 : 1000, #3189, Cell Signaling Technology), and PPARγ (1 : 1000, #2430, Cell Signaling Technology) and with a secondary antibody conjugated with horseradish peroxidase (Bio-Rad Laboratories) for 3 h at room temperature. Membranes were processed for protein detection using SuperSignal substrate (Pierce), and anti-GAPDH (ABD Serotec) was used as the loading control.

2.11. Histopathological Analysis. Fresh tissue samples were fixed in 10% neutral formalin and embedded in paraffin and then sectioned into 5 μm slices and followed with hematoxylin and eosin (H and E) staining. All the histopathology specimens were reviewed and scored in a blinded fashion by two independent pathologists using a scoring system for the extent and severity of tissue injury (points 0–4, steatosis, inflammatory infiltration, necrosis, and fibrogenesis) as previously described [26]. The total histopathology score is the mean of the combined scores for each parameter from both investigators.

3. Statistical Analysis

All data were expressed as mean ± SD. Statistical analysis was performed with PEMS3.1 statistical program for Windows. One-way ANOVA was used to analyze group differences in the study. Differences with a $p < 0.05$ were considered to be statistically significant.

4. Results

4.1. SJP Protected against HFD-Induced Liver Injury. HFD feeding induced a significant weight gain at the end of the intervention period and treatment with SJP effectively prevented body weight increase. Histopathological injuries induced by HFD feeding were evaluated by steatosis, inflammatory infiltration, necrosis, and compensatory fibrogenesis. Although there was no difference in inflammatory cellular infiltration among the three experimental groups, steatosis and compensatory fibrogenesis were much severe in HFD feeding mice. Plus, oil red O staining showed that there were more lipid droplets accumulation in mice liver samples from the AT group, while SJP can dramatically reduce liver lipid droplets accumulation and mitigate steatosis and fibrogenesis (Figure 1). Also, we observed a significant increase in serum levels of triglyceride (TG), total cholesterol (TC), alanine aminotransferase (ALT), and aspartate aminotransferase (AST) in HFD feeding mice (Figure 2), but there was no difference observed in serum levels of IL-6 and IL-10 between AC and AT groups (data not shown). SJP treatment decreased serum levels of TG, AST, and ALT, but only the TG level was statistically different between AT and AS groups.

4.2. Effect of SJP on Expression of LXR, SREBP1-c, FASN, and PPARγ. SREBP1c and PPARγ are both important regulators of lipid metabolism and have significant effect on regulating lipogenetic gene expression. Compared with the control mice, we found a significant increase in PPARγ mRNA expression in HFD feeding mice with/without SJP treatment, but there was no statistical difference in SREBP1c mRNA expression among diverse groups. Likewise, there was no difference in the expression of LXR, an upstream regulator of SREBP1c, but we found a significant increase in expression of downstream FASN in liver tissues of HFD feeding mice. Interestingly, although there was a significant increase in PPARγ mRNA expression in HFD feeding mice, the protein level of PPARγ did not increase in those without SJP treatment (Figure 3).

4.3. SJP Changed the Altered Gut Microbiota Diversity Induced by NAFLD

4.3.1. Analysis of the Gut Microbiota Diversity. Gut microbiota diversity was evaluated in the setting of smooth Shannon rarefaction curves, demonstrating the sequencing depth was sufficient to capture biodiversity in the tested samples (data not shown here). The α-diversity was reflected by Shannon and/or Simpson index, indicating the community diversity and Chao and/or Ace index, indicating the community richness. The NAFLD mice had an obvious lower community richness than the control, while SJP can effectively alter this situation (Figures 4(b) and 4(c)). Although the Shannon index showed no difference among the three groups in community diversity in the OTU level (Figure 1(a)), there was a significant decrease in community diversity at genus level in NAFLD mice whether with or without SJP treatment (Figure 4(d)). PCoA and PLS-DA of the gut microbiota diversity revealed apparent clustering among the three experimental groups at both OTU and genus level, indicating that the gut micorobiota diversity changed in NAFLD mice and SJP was effective in modulating gut micorobiota diversity (Figure 5).

4.3.2. Analysis of the Gut Microbiota Composition. At the phylum level, the majority of the gut microbiota consisted of species from *Firmicutes*, *Bacteroidetes*, *Verrucomicrobia*, *Proteobacteria*, *Actinobacteria*, and *Tenericutes* (Figure 6(a)). The microbial composition altered in NAFLD mice with significant increased abundance of *Firmicutes* and *Proteobacteria* and simultaneously decreased abundance of

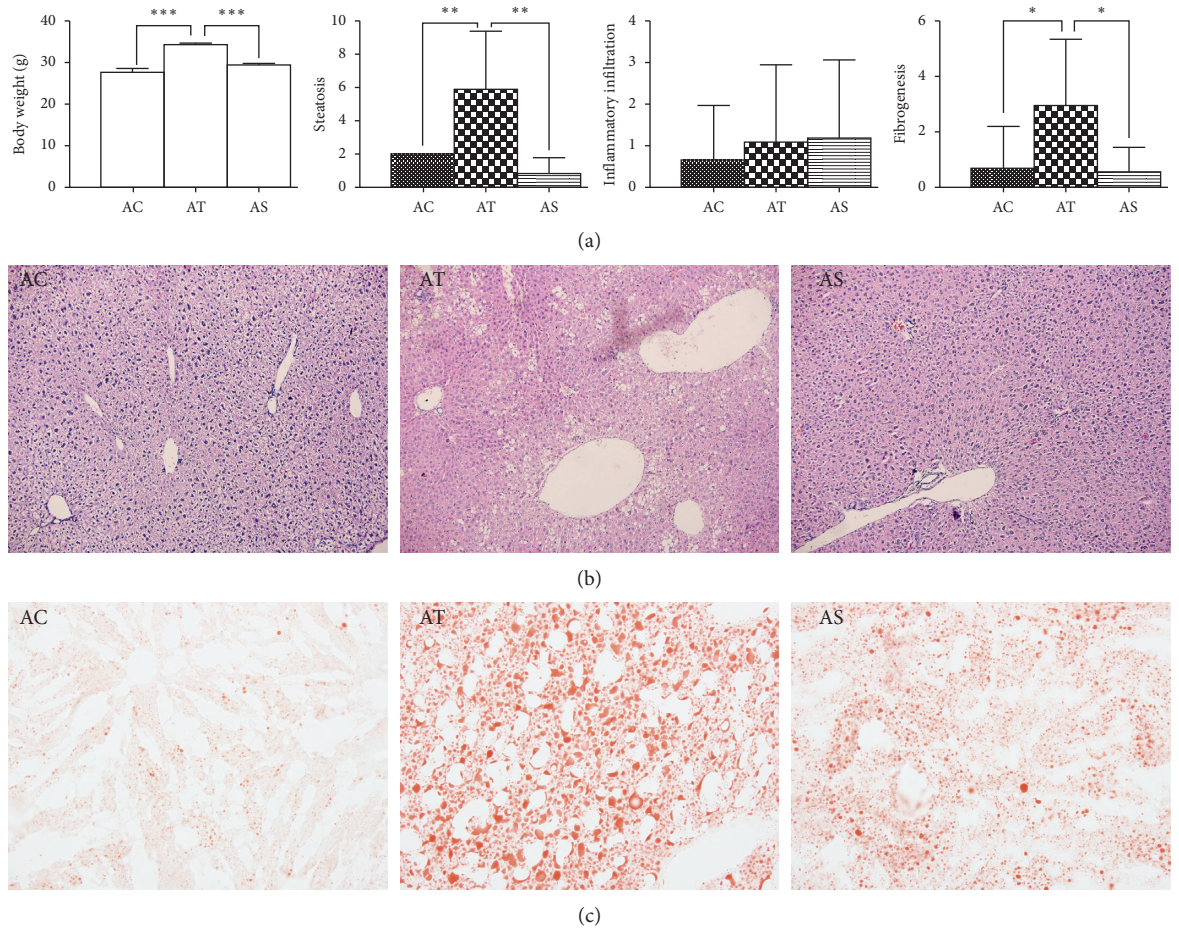

Figure 1: Comparation of body weight and histopathological injuries among groups. (a) Statistical analysis of body weight and pathological score. AC: control group; AT: NAFLD group; AS: SJP treatment group. $^{*}p < 0.05$, $^{**}p < 0.01$, and $^{***}p < 0.001$. (b) Pathological images of liver among diverse groups. Hematoxylin-eosin counterstain. Histological images are presented with original magnifcation 200x. Liver in HFG exhibited enlarged hepatocytes and extensive vacuolization which indicated liver steatosis in the AT group, and these changes were ameliorated in the AS group. (c) Oil red O staining of frozen liver sections. The frozen liver sections showed significant lipid droplets accumulation in the AT group, and the lipid droplets accumulation decreased dramatically in the AS group.

Bacteroidetes. The abundance of *Verrucomicrobia* and *Actinobacteria* decreased in NAFLD mice, and SJP showed potential to increase the abundance of *Verrucomicrobia*, but there was no statistical difference (Figure 6(b)). Additionally, we observed a decreased ratio of *Firmicutes*/*Bacteroidetes* in AT and AS groups, which were the top 2 major species in each group (the ratio was 0.28 in the AT group, 0.16 in the AS group, and 0.84 in the AC group). And the ratio might be related to obesity and related disease according to the emerging evidence.

The species community composition of the three experimental groups at the genus level appeared to be different too (Figure 7(a)). In our study, we selected the top 15 high abundant species to analyze their express in each group. We found species like *Faecalibaculum*, *Blautia*, norank-f-*Bacteroidales*-S24-7-group, *Desulfovibrio*, *achnospiraceae*-NK4A136-group, *Lactobacillus*, unclassified-f-*Lachnospiraceae*, *Ruminiclostridium*-9, norank-f-*Erysipelotrichaceae*, norank-f-*Lachnospiraceae*, and *Bifidobacterium* significantly contributed to the between group differences among the three groups (Figure 7(b)). To further identify the species that discriminate NALFD and the control or SJP-treated mice, differences in the microbial community abundance between groups (AC vs AT and AT vs AS) were analyzed by the Wilcoxon rank-sum test. Compared with the AC group, the abundance of *Desulfovibrio*, unclassified-f-*Lachnospiraceae*, and *Lachnospiraceae*-NK4A136-group was significantly increased in the AT group (10.69%, 5.99%, and 6.75% abundance in the AT group and 2.08%, 1.17%, and 1.81% abundance in the AC group, $p < 0.05$), while the abundance of *Lactobacillus* and *Bifidobacterium* was significant decreased (1.92% and 2.10% abundance in the AT group and 8.37% and 4.35% abundance in the AC group, $p < 0.05$). The abundance of *Desulfovibrio* decreased after being treated with SJP, but there was no significant statistic difference (the corresponding abundance of *Desulfovibrio* was 6.03%). Additionally, we found increased abundance of *faecalibaculum* and norank-f-*Erysipelotrichaceae* and decreased abundance of *Helicobacter* and *Akkermansia* in the AT group, while these species appeared to be changed in the

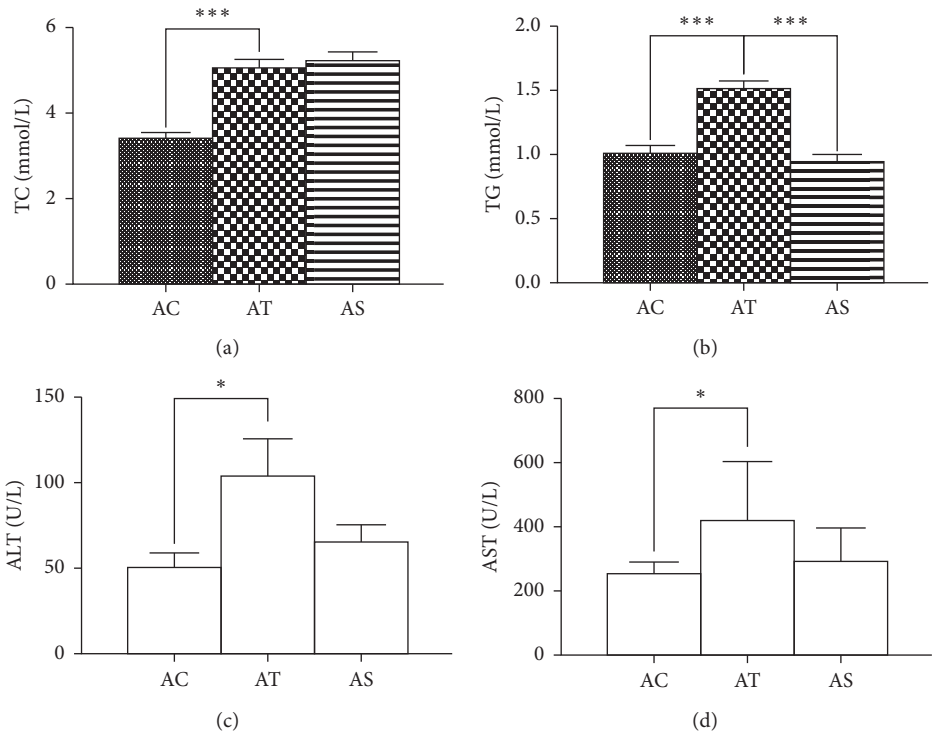

Figure 2: Serum levels of TG, TC, AST, and ALT. AC: control group; AT: NAFLD group; AS: SJP treatment group. $^{*}p < 0.05$ and $^{***}p < 0.001$.

opposite direction in the AS group. To our surprise, we found a significant increased abundance of *Roseburia* in the AS group which was not included in the top 15 species at the genus level (Figure 8).

4.3.3. Function Prediction of the Gut Microbiota. The OTU abundance was further analyzed by PICRUSt2 for function prediction. The top 30 high abundant species were involved in 6 metabolic pathways, and species with the highest abundance was enriched in metabolism pathway, including biosynthesis of amino acids, ABC transporters, carbon metabolism, ribosome, and purine metabolism. According to our results, the changed gut microbiota in the AT group were likely to affect a series of pathways, and SJP seemed to have a greater impact on these pathways, especially on biosynthesis of amino acid, cysteine and methionine metabolism, glycine, serine, and threonine metabolism, oxidative phosphorylation, and peptidoglycan biosynthesis (Figure 9).

5. Discussion

In the present study, HFD feeding induced a series of clinical features of NAFLD, including obesity, hyperlipidemia, liver function injury, and hepatic steatosis. SJP treatment protected against the increase in body weight and serum TG level, showed potential to improve liver function, and finally improved the pathological state of NAFLD mice. Additionally, increased expression of PPARγ mRNA was observed in HFD feeding mice, but a steady elevation of PPARγ protein level was only found in SJP-treated mice. Increased expression of FASN was also found in HFD feeding mice, while there seemed to be no difference in the expression of SREBP1-c and LXR.

Lipid synthesis in the liver is a strictly regulated process that is important for the formation of very low-density lipoproteins and the delivery of energy to other tissues. Excessive supply of fatty acid induces the formation of triglyceride, and then, lipid droplets accumulate in hepatocytes when triglyceride cannot be fully exported into the blood, which consequently leads to the development of NAFLD [27]. Transcription of lipid synthesis genes is regulated by a series of transcription factors such as steroid response element-binding proteins (SREBPs), liver X receptors (LXRs), and peroxisome proliferator-activated receptors (PPARs). SREBP1c is thought to be the most important regulator of lipogenic gene expression among the three subtypes of SREBPs [27]. Current studies reveal that the expression of SREBP1c is generally elevated in obese mice with insulin resistance and hepatic steatosis. LXR is another regulator of lipogeneic gene expression that activates lipogenic gene directly or indirectly inducing SREBP1c activation [28, 29]. Likewise, PPARγ also plays an important role in regulating lipid metabolism, especially in HFD feeding induced lipogeneic gene expression and hepatic lipid biosynthesis [30]. However, FANS is a multipeptide enzyme that is mainly responsible for the synthesis of palmitate, a

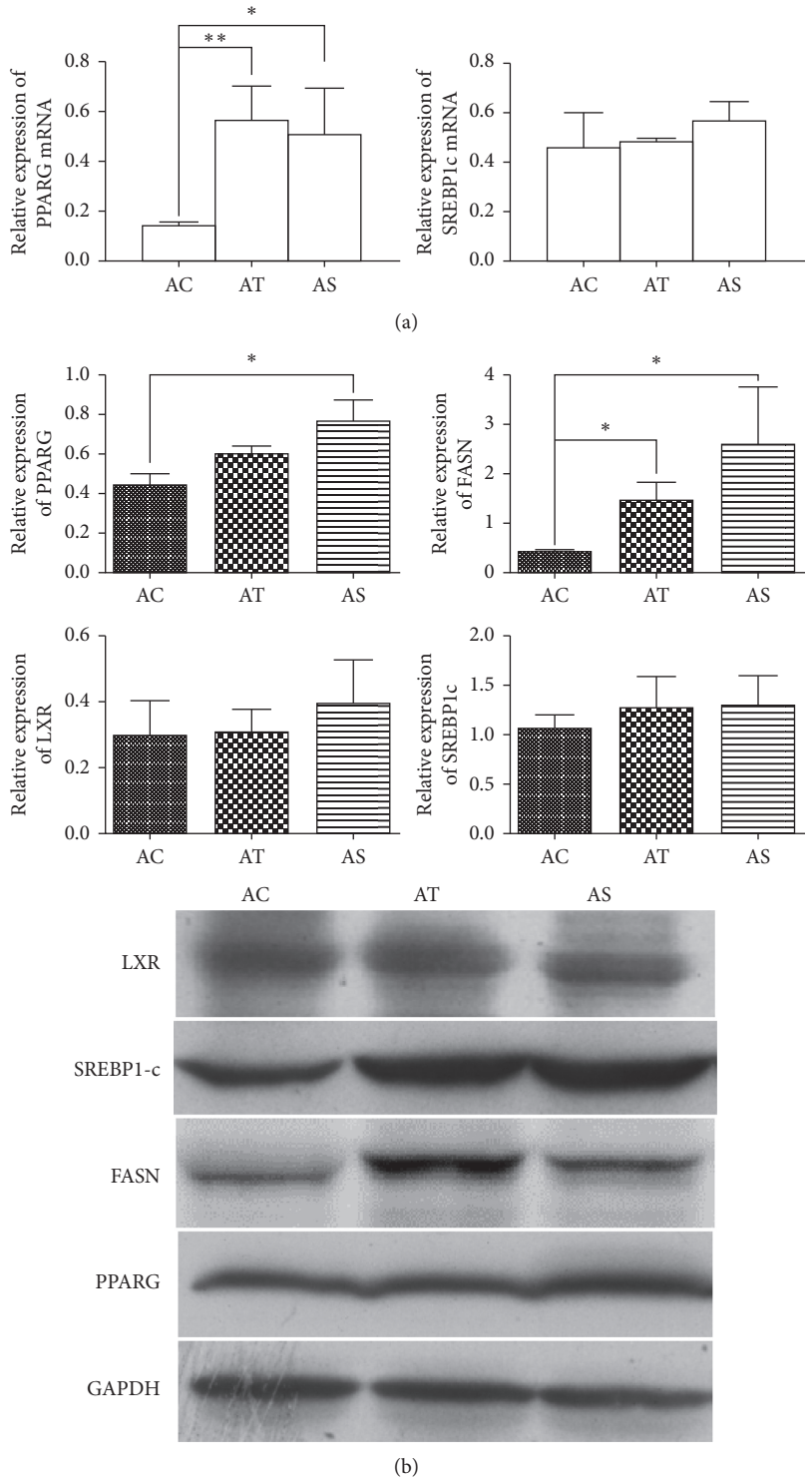

Figure 3: Expression of LXR, SREBP1-c, FASN, and PPARγ. (a) Expression of SREBP1-c mRNA and PPARγ mRNA quantified by PCR. (b) Western blot analysis of LXR, SREBP1-c, FASN, and PPARγ in liver samples among diverse groups. $^{*}p < 0.05$ and $^{**}p < 0.01$.

long-chain saturated fatty acid. In the present study, HFD feeding induced increased expression of FASN, serum lipid accumulation, and hepatic lipid deposition in mice, but the expression of upstream transcription factors LXR and SREBP1c was not changed. Except for obvious liver function injury, it is in accordance with our previous rat models of NAFLD with a higher expression of FASN and unchanged expression of SREBP1-c, and the difference might be due to different experimental species. SJP was demonstrated to be efficient in anti-inflammation, lowering body weight and blood lipid and mitigating insulin resistance. Herein, SJP showed great potential to protect against HFD-induced

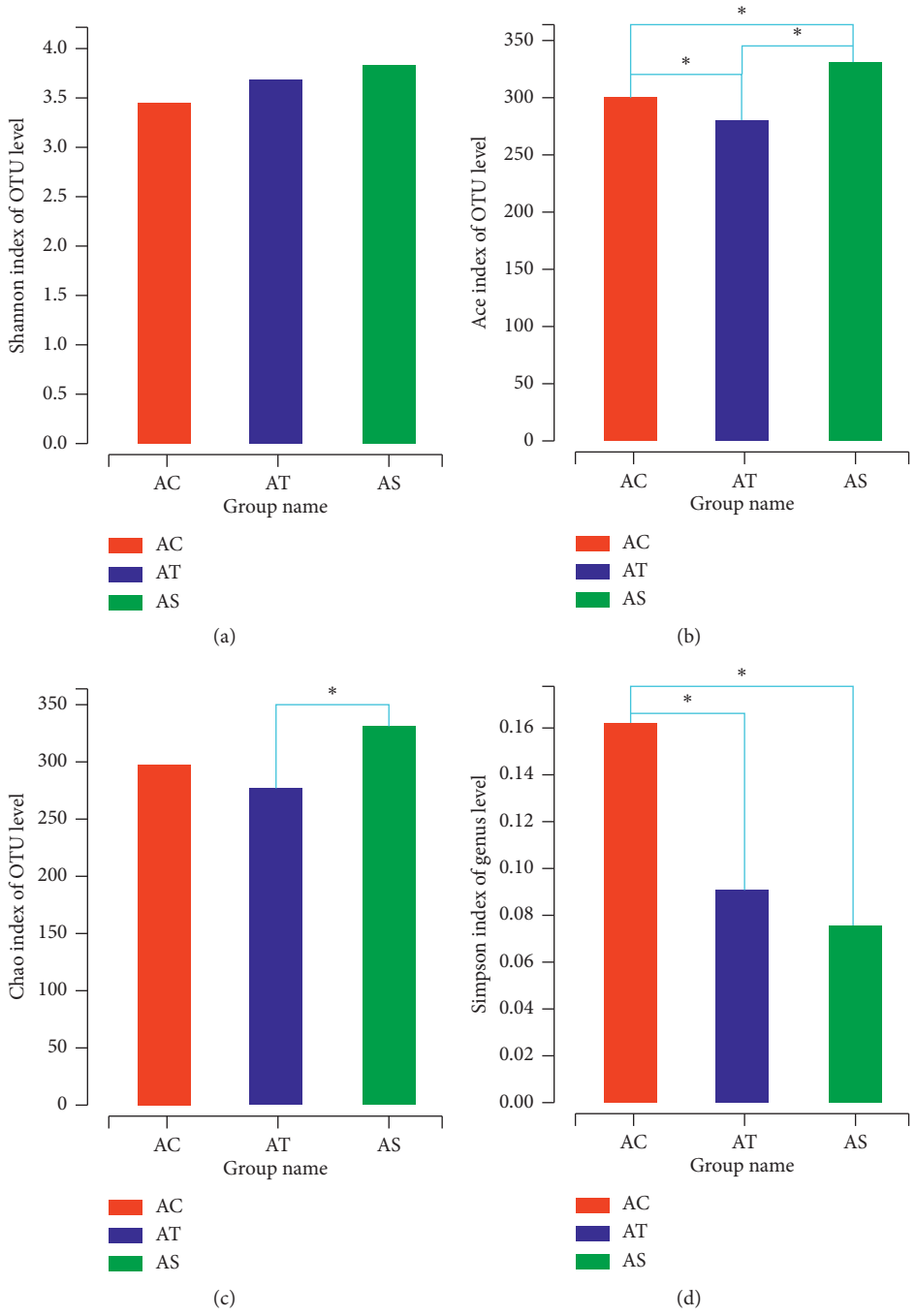

Figure 4: α-Diversity analysis of gut microbiota among the three experimental groups. Shannon and Simpson indexes indicate the community diversity (a, d), and Chao and Ace indexes indicate the community richness (b, c). $^{*}p < 0.05$.

metabolic changes as expected. Additionally, increased expression of PPARγ mRNA was observed in HFD feeding mice whether or not treated with SJP, but a steady elevation of PPARγ protein was only found in SJP-treated mice. This result will partly interpret the effect of SJP on improving insulin resistance as PPARγ is a transcription factor closely associated with insulin resistance.

The gut microbiota consist of trillions of microorganisms that affect body's physiological metabolism by interacting with different environmental conditions, such as diet, alcohol intake, antibiotic abuse, and hereditary factors [31] And these perturbations can result in a state of dysbiosis of the ecosystem [32]. Accumulated evidence has demonstrated that dietary fats intake might affect gut microbiota composition. HFD feeding was reported to induce changes in the intestinal microbiota composition in animal models, and the changed species was found to be closely related to obesity-associated metabolic parameters [33, 34]. According to the present studies, *Bacteroidetes* and *Firmicutes* were the most abundant species in the host microbiota and they

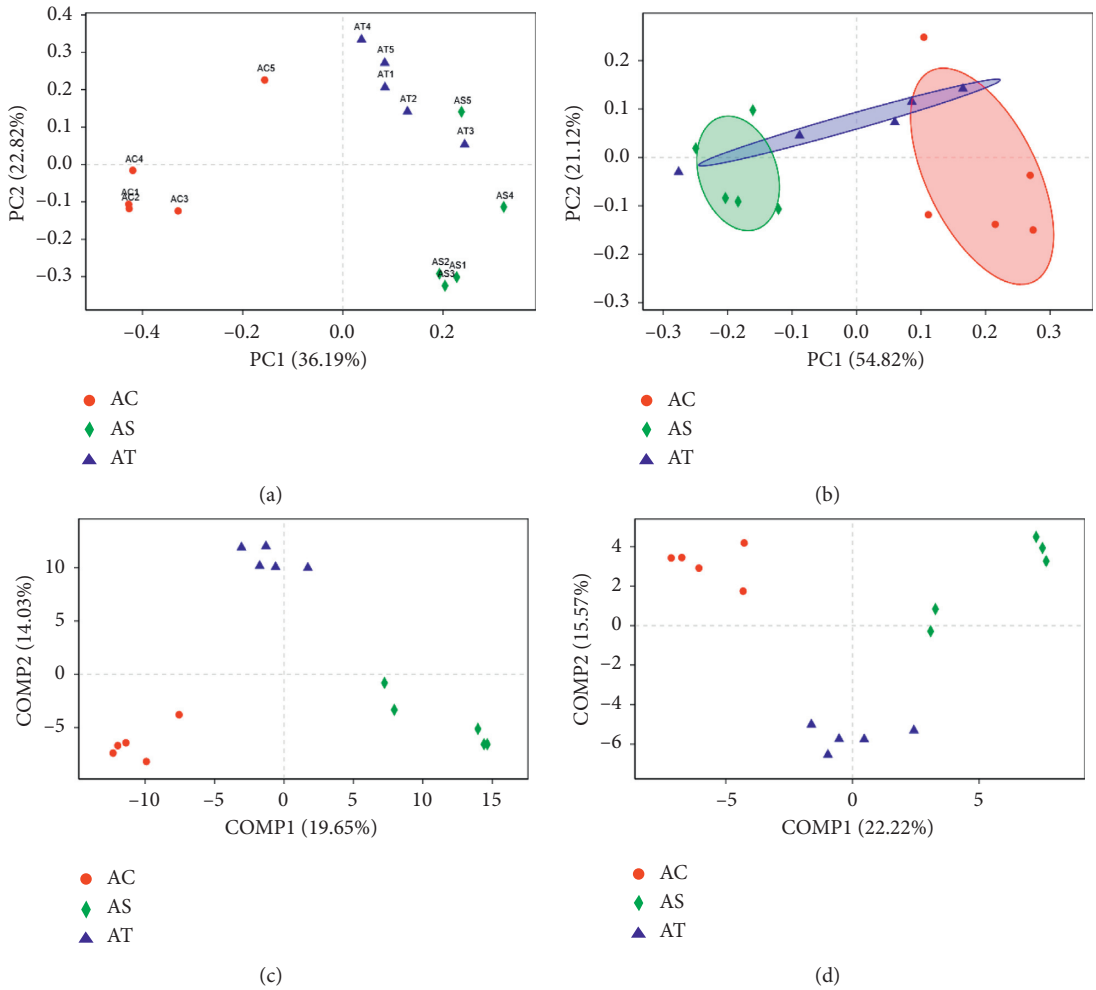

Figure 5: Principal coordinates analysis (PCoA) and partial least squares discriminant analysis (PLS-DA) for unweighted uniFrac distance metric in gut microbiota among diverse groups at both OTU and genus level. (a) PCoA on OTU level; (b) PCoA on genus level; (c) PLS-DA on OTU level; (d) PLS-DA on genus level.

played important roles in host metabolism. The increased ratio of *Firmicutes/Bacteroidetes* was related to obesity due to a higher capacity to harvest energy from the diet, thereby supplying more substrates for lipogenic pathways activation [33, 35]. In our study, we found that the proportion of *Firmicutes* and *Proteobacteria* was significantly increased in HFD feeding mice, while the proportion of *Bacteroidetes* was significantly decreased. We also observed a decrease in gut microbiota diversity in HFD feeding mice as the Ace index and Simpson index were much lower than the control mice. These changes in microbiota composition and diversity were in accordance with most of the current evidence [35, 36]. Of note, coadministration of SJP did not reverse the increased ratio of *Firmicutes/Bacteroidetes*, but it did protect against hepatic steatosis, hyperlipidemia, and obesity in HFD feeding mice. This might be partly attributed to the increased community richness.

At the genus level, we found that the majority of the species changed among the three experimental groups were involved in short-chain fatty acids (SCFAs) producing family, such as unclassified-f-*Lachnospiraceae*, *Lachnospiraceae*-NK4A136-group, *Faecalibacterium*, *Akkermansia*, *Bifidobacterium*, *Lactobacillus,* and *Roseburia*. As the end product of bacterial fermentation of soluble dietary fiber and indigestible carbohydrates, SCFAs might be able to regulate a series of process that alters energy harvest and metabolism, such as regulating appetite, promoting energy consumption, stimulating insulin sensitivity, and activating adenosine monophosphate-activated protein kinases (AMPK) in the liver and skeletal muscle, and thereby affecting the development of NAFLD [37]. In the present study, we found a HFD-induced decrease in the abundance of *Bifidobacterium* and *Lactobacillus* whose major function was participating in the metabolic process including anaerobic conversion of polymeric sugars into short-chain fatty acids (SCFAs) [38–40]. We also found an HFD-induced increase in the abundance of unclassified-f-*Lachnospiraceae*, *Lachnospiraceae*-NK4A136-group, and *Desulfovibrio*. Increased abundance of *Desulfovibrio* was considered to be associated with intestinal disorders [39]. And unclassified-f-*Lachnospiraceae* and *Lachnospiraceae*-NK4A136-group are both members of *Lachnospiraceae* family which are the main producers of SCFAs. Their changes in the present study aroused our attention as they were supposed to

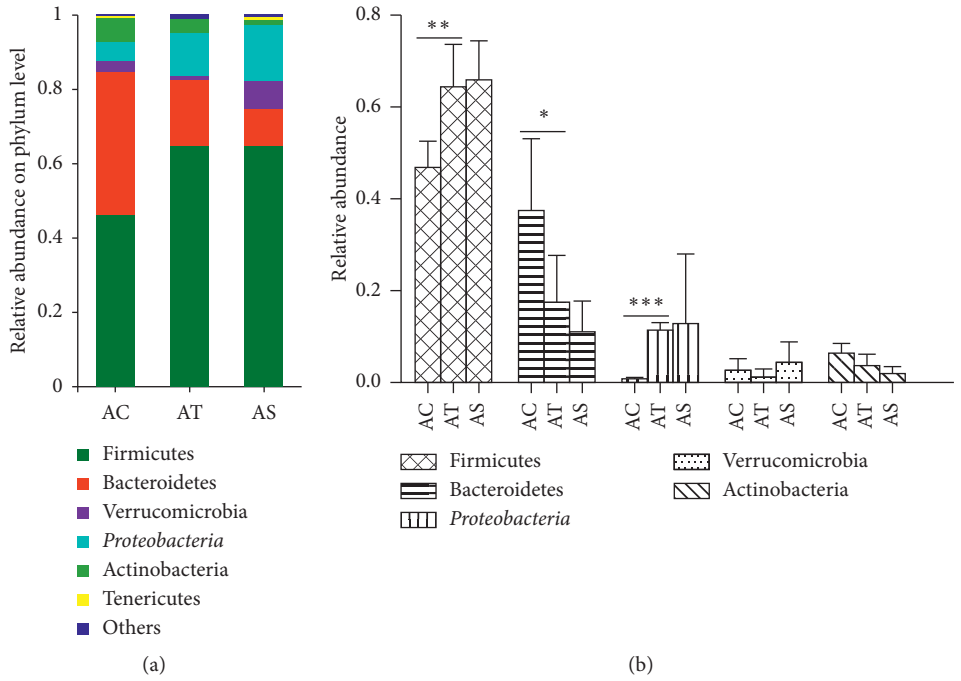

Figure 6: Relative abundance of intestinal microbiota at phylum level. Species with less than 1% abundance was classified into the "others" category. Differences in the microbial community abundance among the three groups were analyzed by one-way ANOVA. $^{*}p < 0.05$, $^{**}p < 0.01$, and $^{***}p < 0.001$.

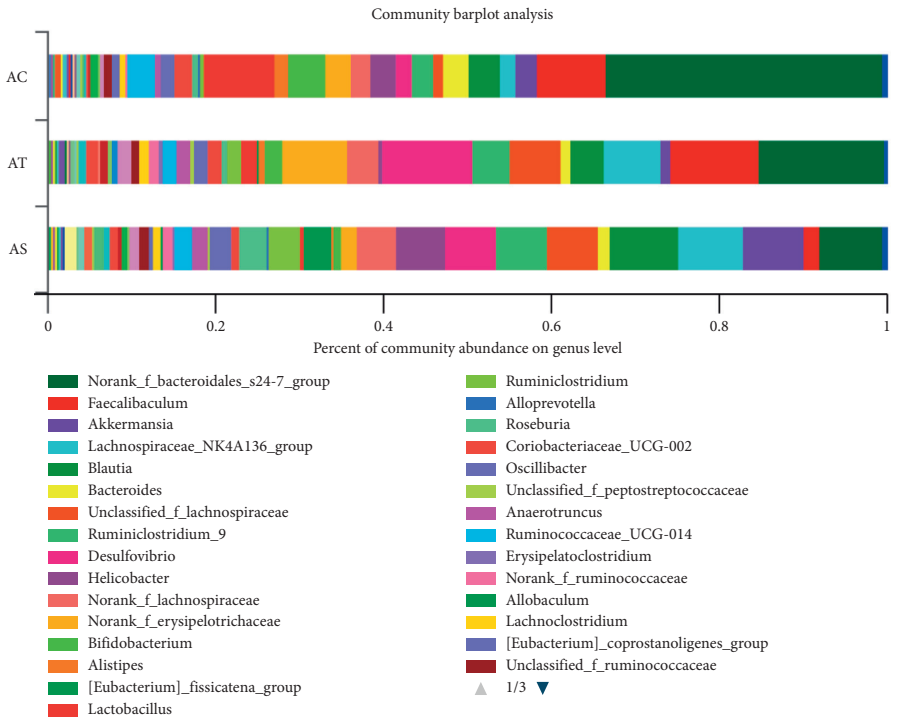

(a)

Figure 7: Continued.

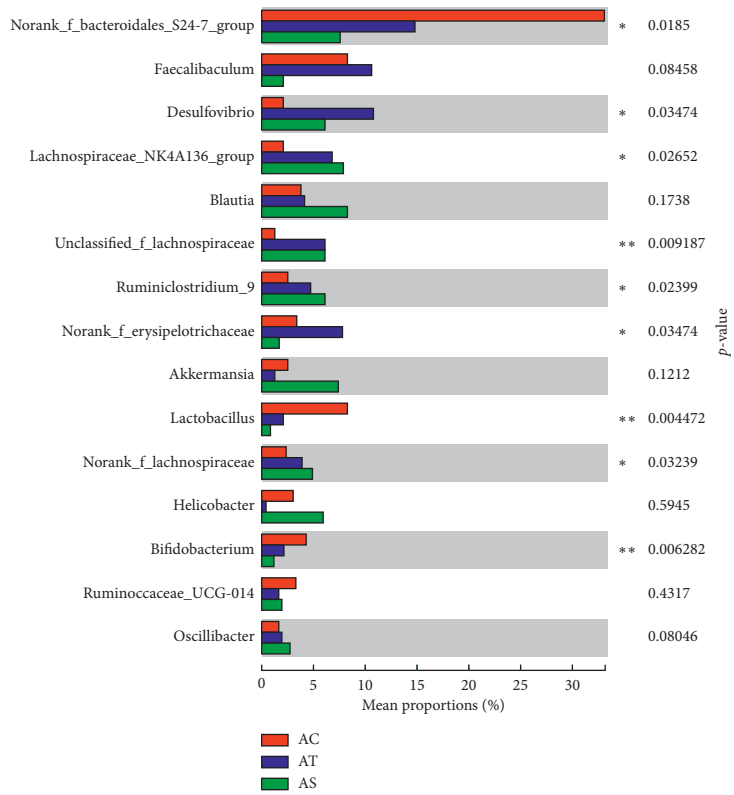

(b)

Figure 7: Relative abundance of intestinal microbiota at genus level. (a) Top 40 high abundant species at the genus level. (b) Top 15 high abundant species at the genus level. Differences in the microbial community abundance among the three groups were analyzed by the Kruskal–Wallis H test. $^{*}p < 0.05$; $^{**}p < 0.01$.

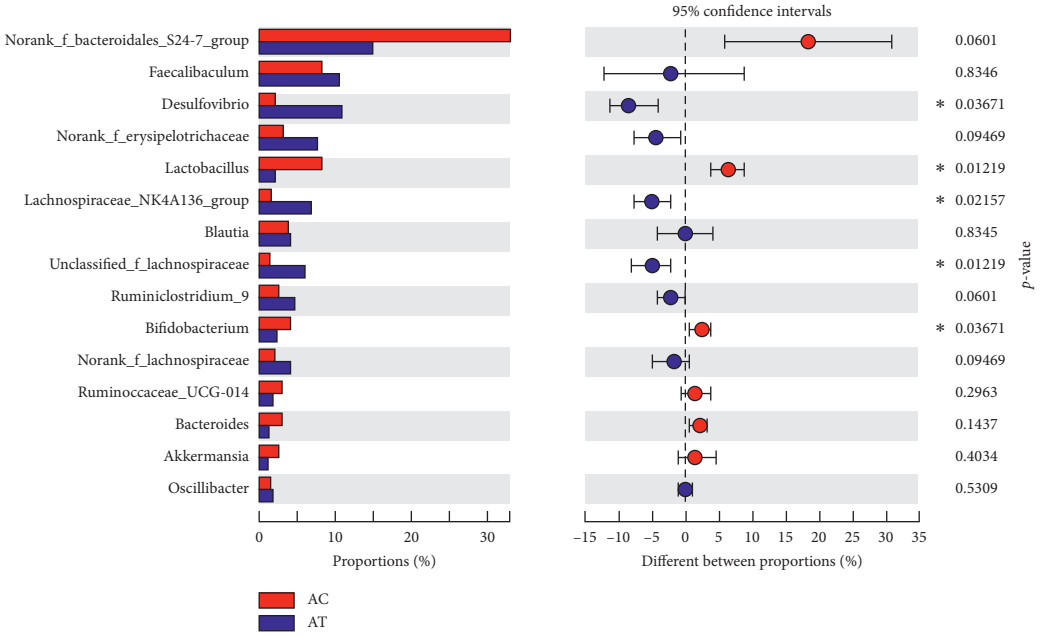

(a)

Figure 8: Continued.

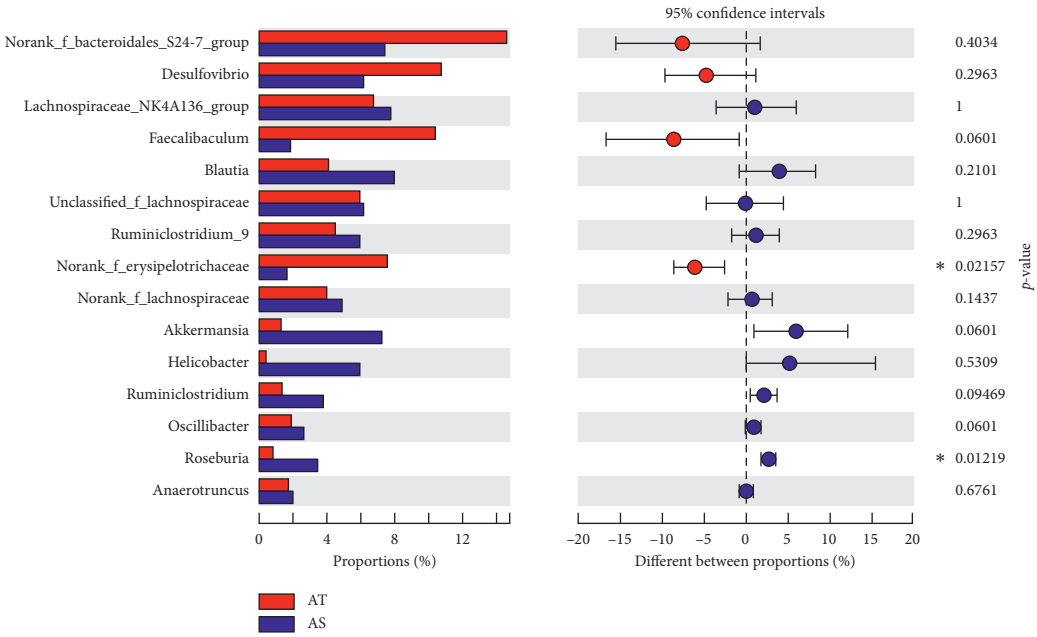

(b)

Figure 8: Top 15 high abundant species at the genus level. Differences in the microbial community abundance between groups (AC vs AT and AT vs AS) were analyzed by Wilcoxon rank-sum test. $^{*}p < 0.05$.

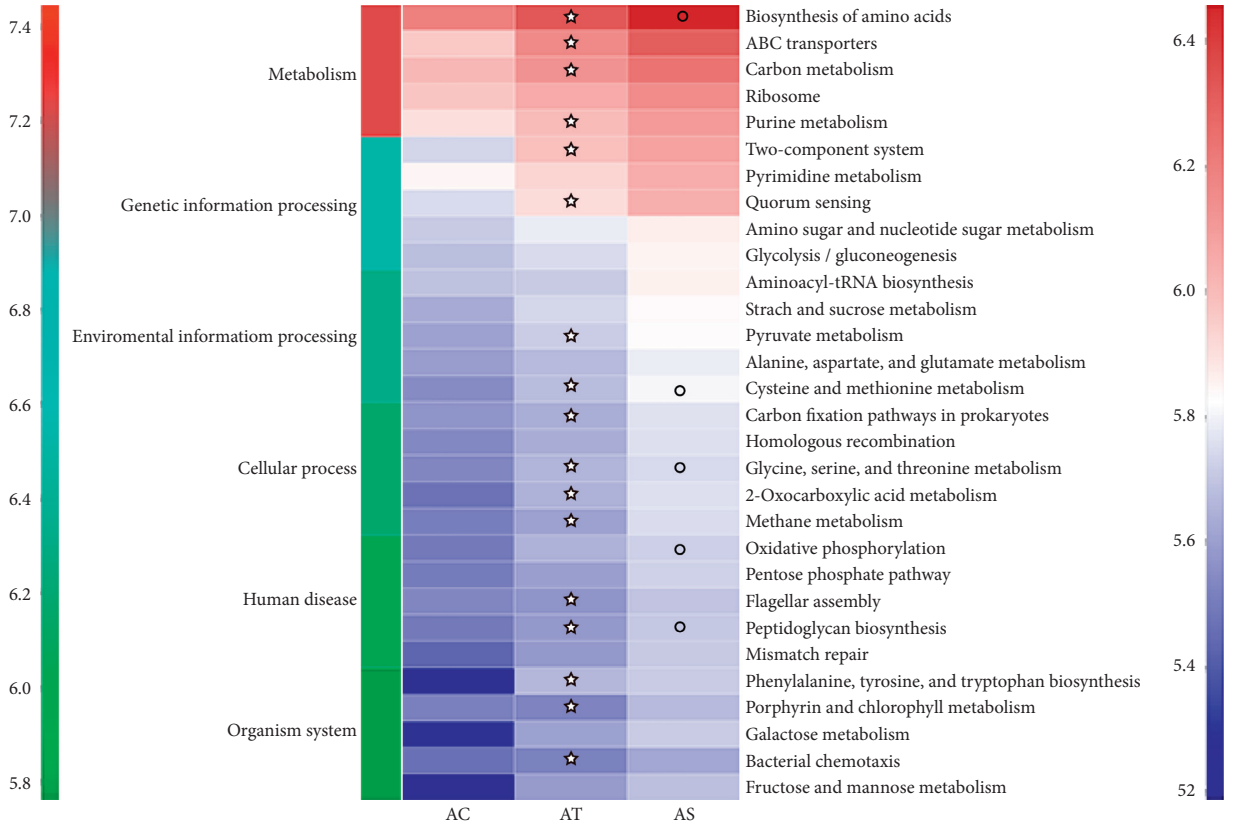

Figure 9: Function prediction of the gut microbiota. Top 30 high abundant species were included for function prediction using PICRUSt2. The x-axis indicates the sample groups, the y-axis indicates different pathways (left green-blue-red gradient bar represents pathway level 1, and right blue-white-red gradient bar represents pathway level 3). ✯, compared to the AC group, $p < 0.05$; ○, compared to the AT group, $p < 0.05$.

decrease according to the current evidence. Interestingly, their abundance was even higher in SJP-treated mice. Thus, their role in lipid metabolism may need further investigation.

The mechanism of SJP protecting against HFD-induced obesity and hepatic steatosis might be attributed to the regulation of SCFA-producing process as we found a remarkable decrease in the abundance of norank-f-*Erysipelotrichaceae* and increase in the abundance of *Roseburia* in SJP-treated mice. The above two species are both members of *Firmicutes* phylum and involved in the SCFA producing process. The former belongs to *Erysipelotrichaceae* family, while the latter belongs to *Lachnospiraceae* family. Current knowledge on the role of *Erysipelotrichaceae* and *Lachnospiraceae* in human disease mainly comes from studies focused on metabolic disorders and nutrition [41]. Generally, increased abundance of the members of *Erysipelotrichaceae* and *Lachnospiraceae* family was observed in obese individuals [42]. Also, high-fat diet induced increase in the abundance of *Erysipelotrichaceae* and *Lachnospiraceae* family [43]. Furthermore, a positive correlation with the abundance of *Erysipelotrichaceae* and liver fat was found in individuals on high-fat and choline deficiency diet [44]. An obvious decrease in the abundance of *Erysipelotrichaceae* was observed accompanied with lose in body weight, decline in blood lipids, and reduction in liver injury after treating with cholesterol lowing drugs, antibiotics, and some herbal extracts [45, 46]. Dietary intake also influences the abundance of *Roseburia* [47]. Current evidence found that the abundance of *Roseburia* was negatively correlated with high fat induced body weight increase, fat mass development, and hepatic lipid deposition [48]. However, Alejandra and colleagues found that *Roseburia* was significantly more abundant in obese Mexican women with or without metabolic disorder, while the abundance of *Erysipelotrichaceae* family was significantly decreased [49]. These different findings will promote further studies to explore the unknown effect of gut microbiota.

Function prediction of the top 30 species with highest abundance by PICRUSt2 suggested the enrichment of bacteria in the metabolism pathway. HFD feeding induced enhancement of the majority of the enriched biological pathways, while SJP appeared to have a greater impact on these pathways, especially on biosynthesis of amino acid, cysteine and methionine metabolism, glycine, serine, and threonine metabolism, oxidative phosphorylation, and peptidoglycan biosynthesis. Protein, lipid, and glucose metabolism were mainly involved in the above pathways [50]. In other words, SJP might have a deeper impact on the metabolic process of protein, lipid, and glucose. As the biological functions of the floras were complex, the mechanism of how the changed gut microbiota affect metabolism of nutrients and the development of NAFLD still need further investigation.

Herein, we established a mice model of NAFLD without obvious liver inflammation and fibrosis. The relevant parameters we detected and the effect of SJP we observed were limited to simple steatosis mice models. Further studies on more severe state of NAFLD will promote our understanding on the effect of SJP on gut microbiota.

In conclusion, SJP protected against HFD-induced NAFLD and this effect might be partly attributed to the regulation of gut microbiota.

Data Availability

The raw data can only be obtained by emailing the authors because some unpublished results are included in it.

Disclosure

The funder had no role in study design, data collection and analysis, decision to publish, and preparation of the manuscript.

Conflicts of Interest

The authors declare that there are no conflicts of interest.

Authors' Contributions

Juan Li, Mei-hua Wan, and Wen-fu Tang conceived and designed this experiment. Juan Li, Qian Hu, Xiao-yu Dai, Lv Zhu, and Jia-qi Yao performed the experiment. Yi-fan Miao, Hong-xin Kang, and Mei-hua Wan analyzed the data. Juan Li wrote the manuscript with the help of other authors. All authors reviewed the manuscript.

Acknowledgments

This study received financial support from the National Natural Science Foundation of China (Grant no. 81603519 and 81774160).

References

[1] C. Estes, Q. M. Anstee, M. T. Arias-Loste et al., "Modeling NAFLD disease burden in China, France, Germany, Italy, Japan, Spain, United Kingdom, and United States for the period 2016-2030," *Journal of Hepatology*, vol. 69, no. 4, pp. 896–904, 2018.

[2] Z. Younossi, Q. M. Anstee, M. Marietti et al., "Global burden of NAFLD and NASH: trends, predictions, risk factors and prevention," *Nature Reviews Gastroenterology & Hepatology*, vol. 15, no. 1, pp. 11–20, 2018.

[3] Z. M. Younossi, L. Henry, H. Bush, and A. Mishra, "Clinical and economic burden of nonalcoholic fatty liver disease and nonalcoholic steatohepatitis," *Clinics in Liver Disease*, vol. 22, no. 1, pp. 1–10, 2018.

[4] S. A. Polyzos, J. Kountouras, and C. S. Mantzoros, "Obesity and nonalcoholic fatty liver disease: from pathophysiology to therapeutics," *Metabolism*, vol. 92, pp. 82–97, 2019.

[5] L. Calzadilla Bertot and L. A. Adams, "The natural course of non-alcoholic fatty liver disease," *International Journal of Molecular Sciences*, vol. 17, no. 5, p. 744, 2016.

[6] B. A. Neuschwander-Tetri, "Non-alcoholic fatty liver disease," *BMC Medicine*, vol. 15, no. 1, p. 45, 2017.

[7] V. Manne, P. Handa, and K. V. Kowdley, "Pathophysiology of nonalcoholic fatty liver disease/nonalcoholic steatohepatitis," *Clinics in Liver Disease*, vol. 22, no. 1, pp. 23–37, 2018.

[8] C. Alonso, D. Fernández-Ramos, M. Varela-Rey et al., "Metabolomic identification of subtypes of nonalcoholic steatohepatitis," *Gastroenterology*, vol. 152, no. 6, pp. 1449–1461.e7, 2017.

[9] D. H. Ipsen, J. Lykkesfeldt, and P. Tveden-Nyborg, "Molecular mechanisms of hepatic lipid accumulation in non-alcoholic fatty liver disease," *Cellular and Molecular Life Sciences*, vol. 75, no. 18, pp. 3313–3327, 2018.

[10] E. Buzzetti, M. Pinzani, and E. A. Tsochatzis, "The multiple-hit pathogenesis of non-alcoholic fatty liver disease (NAFLD)," *Metabolism*, vol. 65, no. 8, pp. 1038–1048, 2016.

[11] S. L. Friedman, B. A. Neuschwander-Tetri, M. Rinella, and A. J. Sanyal, "Mechanisms of NAFLD development and therapeutic strategies," *Nature Medicine*, vol. 24, no. 7, pp. 908–922, 2018.

[12] A. Pascale, N. Marchesi, C. Marelli et al., "Microbiota and metabolic diseases," *Endocrine*, vol. 61, no. 3, pp. 357–371, 2018.

[13] S. Rabot, M. Membrez, A. Bruneau et al., "Germ-free C57BL/6J mice are resistant to high-fat-diet-induced insulin resistance and have altered cholesterol metabolism," *The FASEB Journal*, vol. 24, no. 12, pp. 4948–4959, 2010.

[14] B. Björkholm, C. M. Bok, A. Lundin, J. Rafter, M. L. Hibberd, and S. Pettersson, "Intestinal microbiota regulate xenobiotic metabolism in the liver," *PLoS One*, vol. 4, no. 9, p. e6958, 2009.

[15] T. Le Roy, M. Llopis, P. Lepage et al., "Intestinal microbiota determines development of non-alcoholic fatty liver disease in mice," *Gut*, vol. 62, no. 12, pp. 1787–1794, 2013.

[16] S. De Minicis, C. Rychlicki, L. Agostinelli et al., "Dysbiosis contributes to fibrogenesis in the course of chronic liver injury in mice," *Hepatology*, vol. 59, no. 5, pp. 1738–1749, 2014.

[17] J. Henao-Mejia, E. Elinav, C. Jin et al., "Inflammasome-mediated dysbiosis regulates progression of NAFLD and obesity," *Nature*, vol. 482, no. 7384, pp. 179–185, 2012.

[18] S. Marchisello, A. Di Pino, R. Scicali et al., "Pathophysiological, molecular and therapeutic issues of nonalcoholic fatty liver disease: an overview," *International Journal of Molecular Sciences*, vol. 20, no. 8, 2019.

[19] M. A. Konerman, J. C. Jones, and S. A. Harrison, "Pharmacotherapy for NASH: current and emerging," *Journal of Hepatology*, vol. 68, no. 2, pp. 362–375, 2018.

[20] Q. Chen, T. Wang, J. Li et al., "Effects of natural products on fructose-induced nonalcoholic fatty liver disease (NAFLD)," *Nutrients*, vol. 9, no. 2, p. 96, 2017.

[21] J.-M. Yang, Y. Sun, M. Wang et al., "Regulatory effect of a Chinese herbal medicine formula on non-alcoholic fatty liver disease," *World Journal of Gastroenterology*, vol. 25, no. 34, pp. 5105–5119, 2019.

[22] H. Zhou, W. Du, Y. Li et al., "Effects of melatonin on fatty liver disease: the role of NR4A1/DNA-PKcs/p53 pathway, mitochondrial fission, and mitophagy," *Journal of Pineal Research*, vol. 64, no. 1, 2018.

[23] J. Li, Y. M. Zhang, J. Y. Li et al., "Effect of Sheng-Jiang powder on obesity-induced multiple organ injuries in rats," *Evidence-Based Complementary and Alternative Medicine*, vol. 2017, Article ID 6575276, 8 pages, 2017.

[24] J. Li, L. Zhu, Y. M. Zhang et al., "Sheng-Jiang powder ameliorates high fat diet induced nonalcoholic fatty liver disease via inhibiting activation of akt/mTOR/S6 pathway in rats," *Evidence-Based Complementary and Alternative Medicine*, vol. 2018, Article ID 6190254, 9 pages, 2018.

[25] Y.-F. Miao, H.-X. Kang, J. Li et al., "Effect of Sheng-Jiang powder on multiple-organ inflammatory injury in acute pancreatitis in rats fed a high-fat diet," *World Journal of Gastroenterology*, vol. 25, no. 6, pp. 683–695, 2019.

[26] S. Wirtz, C. Neufert, B. Weigmann, and M. F. Neurath, "Chemically induced mouse models of intestinal inflammation," *Nature Protocols*, vol. 2, no. 3, pp. 541–546, 2007.

[27] F. Bril, D. Barb, P. Portillo-Sanchez et al., "Metabolic and histological implications of intrahepatic triglyceride content in nonalcoholic fatty liver disease," *Hepatology*, vol. 65, no. 4, pp. 1132–1144, 2017.

[28] M. C. Cave, H. B. Clair, J. E. Hardesty et al., "Nuclear receptors and nonalcoholic fatty liver disease," *Biochimica et Biophysica Acta (BBA)-Gene Regulatory Mechanisms*, vol. 1859, no. 9, pp. 1083–1099, 2016.

[29] C. Yan, Y. Zhang, X. Zhang, J. Aa, G. Wang, and Y. Xie, "Curcumin regulates endogenous and exogenous metabolism via Nrf2-FXR-LXR pathway in NAFLD mice," *Biomedicine & Pharmacotherapy*, vol. 105, pp. 274–281, 2018.

[30] P. Xu, Y. Zhai, and J. Wang, "The role of PPAR and its cross-talk with CAR and LXR in obesity and atherosclerosis," *International Journal of Molecular Sciences*, vol. 19, no. 4, p. 1260, 2018.

[31] M. Kussmann and P. J. Van Bladeren, "The extended nutrigenomics-understanding the interplay between the genomes of food, gut microbes, and human host," *Frontiers in Genetics*, vol. 2, p. 21, 2011.

[32] B. Stecher, L. Maier, and W.-D. Hardt, ""Blooming" in the gut: how dysbiosis might contribute to pathogen evolution," *Nature Reviews Microbiology*, vol. 11, no. 4, pp. 277–284, 2013.

[33] V. Lecomte, N. O. Kaakoush, C. A. Maloney et al., "Changes in gut microbiota in rats fed a high fat diet correlate with obesity-associated metabolic parameters," *PLoS One*, vol. 10, no. 5, Article ID e0126931, 2015.

[34] M. Zhang and X.-J. Yang, "Effects of a high fat diet on intestinal microbiota and gastrointestinal diseases," *World Journal of Gastroenterology*, vol. 22, no. 40, pp. 8905–8909, 2016.

[35] N. Harada, R. Hanaoka, H. Horiuchi et al., "Castration influences intestinal microflora and induces abdominal obesity in high-fat diet-fed mice," *Scientific Reports*, vol. 6, p. 23001, 2016.

[36] N. de Wit, M. Derrien, H. Bosch-Vermeulen et al., "Saturated fat stimulates obesity and hepatic steatosis and affects gut microbiota composition by an enhanced overflow of dietary fat to the distal intestine," *American Journal of Physiology-Gastrointestinal and Liver Physiology*, vol. 303, no. 5, pp. G589–G599, 2012.

[37] C. T. Pekmez, L. O. Dragsted, and L. K. Brahe, "Gut microbiota alterations and dietary modulation in childhood malnutrition-the role of short chain fatty acids," *Clinical Nutrition*, vol. 38, no. 2, pp. 615–630, 2019.

[38] E. Patterson, J. F. Cryan, G. F. Fitzgerald, R. P. Ross, T. G. Dinan, and C. Stanton, "Gut microbiota, the pharmabiotics they produce and host health," *Proceedings of the Nutrition Society*, vol. 73, no. 4, pp. 477–489, 2014.

[39] J. Zhang, L. Song, Y. Wang et al., "Beneficial effect of butyrate-producing *Lachnospiraceae* on stress-induced visceral hypersensitivity in rats," *Journal of Gastroenterology and Hepatology*, vol. 34, no. 8, pp. 1368–1376, 2019.

[40] D. J. Morrison and T. Preston, "Formation of short chain fatty acids by the gut microbiota and their impact on human metabolism," *Gut Microbes*, vol. 7, no. 3, pp. 189–200, 2016.

[41] N. O. Kaakoush, "Insights into the role of *Erysipelotrichaceae* in the human host," *Frontiers in Cellular and Infection Microbiology*, vol. 5, p. 84, 2015.

[42] K. Lippert, L. Kedenko, L. Antonielli et al., "Gut microbiota dysbiosis associated with glucose metabolism disorders and the metabolic syndrome in older adults," *Beneficial Microbes*, vol. 8, no. 4, pp. 545–556, 2017.

[43] C. K. Fleissner, N. Huebel, M. M. Abd El-Bary, G. Loh, S. Klaus, and M. Blaut, "Absence of intestinal microbiota does not protect mice from diet-induced obesity," *British Journal of Nutrition*, vol. 104, no. 6, pp. 919–929, 2010.

[44] M. D. Spencer, T. J. Hamp, R. W. Reid, L. M. Fischer, S. H. Zeisel, and A. A. Fodor, "Association between composition of the human gastrointestinal microbiome and development of fatty liver with choline deficiency," *Gastroenterology*, vol. 140, no. 3, pp. 976–986, 2011.

[45] J. K. Harris, K. C. El Kasmi, A. L. Anderson et al., "Specific microbiome changes in a mouse model of parenteral nutrition associated liver injury and intestinal inflammation," *PLoS One*, vol. 9, no. 10, Article ID e110396, 2014.

[46] U. Etxeberria, N. Arias, N. Boqué et al., "Reshaping faecal gut microbiota composition by the intake of trans-resveratrol and quercetin in high-fat sucrose diet-fed rats," *The Journal of Nutritional Biochemistry*, vol. 26, no. 6, pp. 651–660, 2015.

[47] T. Wu, M. Sun, R. Liu et al., "*Bifidobacterium longum* subsp. *longum* remodeled *Roseburia* and *Phosphatidylserine* levels and ameliorated intestinal disorders and liver metabolic abnormalities induced by high-fat diet," *Journal of Agricultural and Food Chemistry*, vol. 68, no. 16, pp. 4632–4640, 2020.

[48] A. M. Neyrinck, S. Possemiers, W. Verstraete, F. De Backer, P. D. Cani, and N. M. Delzenne, "Dietary modulation of clostridial cluster XIVa gut bacteria (*Roseburia* spp.) by chitin-glucan fiber improves host metabolic alterations induced by high-fat diet in mice," *The Journal of Nutritional Biochemistry*, vol. 23, no. 1, pp. 51–59, 2012.

[49] A. Chávez-Carbajal, K. Nirmalkar, A. Pérez-Lizaur et al., "Gut microbiota and predicted metabolic pathways in a sample of Mexican women affected by obesity and obesity plus metabolic syndrome," *International Journal of Molecular Sciences*, vol. 20, no. 2, p. 438, 2019.

[50] M. Machado and H. Cortez-Pinto, "Diet, microbiota, obesity, and NAFLD: a dangerous quartet," *International Journal of Molecular Sciences*, vol. 17, no. 4, p. 481, 2016.

Hindawi
Evidence-Based Complementary and Alternative Medicine
Volume 2020, Article ID 8591892, 12 pages
https://doi.org/10.1155/2020/8591892

Research Article

Fuzheng Huayu Recipe Prevented and Treated CCl4-Induced Mice Liver Fibrosis through Regulating Polarization and Chemotaxis of Intrahepatic Macrophages via CCL2 and CX3CL1

Man Zhang,[1] Hong-liang Liu,[1] Kai Huang,[1] Yuan Peng,[1] Yan-yan Tao,[1] Chang-qing Zhao,[1] Xu-dong Hu ,[2] and Cheng-hai Liu [1,3]

[1]*Institute of Liver Diseases, Shuguang Hospital Affiliated to Shanghai University of Traditional Chinese Medicine, 528 Zhangheng Road, Pudong New Area, Shanghai 201203, China*
[2]*Department of Biology, School of Basic Medical Sciences, Shanghai University of Traditional Chinese Medicine, 1200 Cailun Road, Pudong New Area, Shanghai 201203, China*
[3]*Shanghai Key Laboratory of Traditional Chinese Clinical Medicine, 528 Zhangheng Road, Pudong New Area, Shanghai 201203, China*

Correspondence should be addressed to Xu-dong Hu; huxudongsh@126.com and Cheng-hai Liu; chenghai.liu@outlook.com

Received 1 August 2020; Revised 22 October 2020; Accepted 2 November 2020; Published 26 November 2020

Academic Editor: Yunxia Li

Background. Fuzheng Huayu recipe (FZHY) is an original Chinese patent medicine which was developed and marketed by our institute. It could markedly improve liver tissue inflammation and ameliorate hepatic fibrosis in the clinical study. The intrahepatic macrophages recruitment and polarization play an important role in the progress of liver inflammation and fibrosis. Whether FZHY exerted its antiliver fibrosis effects through regulating intrahepatic macrophages phenotypic ratios is still unknown. This study aims to explore the antifibrosis mechanism of FZHY on regulating the recruitment and polarization of intrahepatic macrophages. *Methods*. C57/B6 mice were used for the establishment of the CCl4-induced mice liver fibrosis model. Liver inflammation and fibrosis were evaluated by HE and Sirius red staining, hydroxyproline assays, and biochemical tests. The levels of chemokines and inflammatory cytokines in liver tissue were measured by RNA-Seq transcriptome analysis, western blot assay, RT-qPCR, and immunofluorescence assay. The macrophages recruitment and phenotypic polarization were observed by flow cytometry. *Results*. FZHY significantly improved liver inflammation and reduced liver fibrosis degree. TNF signaling pathway, involved in macrophages recruitment and phenotypic polarization, was discovered by RNA-Seq transcriptome analysis. In TNF signaling pathway, CCL2 expression was significantly decreased and CX3CL1 expression was significantly upregulated by FZHY in liver tissue and primary intrahepatic macrophages. The ratio of proinflammatory hepatic resident macrophage-Kupffer cells ($F4/80^+CD11b^-CD86^+$) was downregulated by FZHY, while the proportion of anti-inflammatory Kupffer cells ($F4/80^+CD11b^-CD206^+$) was upregulated. Meanwhile, the ratio of proinflammatory $Ly6C^{high}$ macrophages ($F4/80^+CD11b^+Ly6C^{high}$) which were recruited from blood circulation by CCL2 was reduced by FZHY, while the ratio of restorative $Ly6C^{low}$ macrophages ($F4/80^+CD11b^+Ly6C^{low}$) which were recruited from blood circulation or induced from $Ly6C^{high}$ macrophages polarization by CX3CL1 was significantly increased. *Conclusions*. FZHY could regulate the recruitment and polarization of intrahepatic macrophages via CCL2 and CX3CL1, so as to play its anti-inflammation and antifibrosis pharmacological effects in the liver.

1. Introduction

Liver fibrosis is the common pathological basis of the development of many chronic severe liver diseases and is also the early and inevitable stage of liver cirrhosis. It is a pathological process caused by continuous injury-repair response. Hepatocytes are induced to apoptosis and necrosis by a variety of chronic liver diseases, such as viral hepatitis, metabolic liver disease, fatty liver disease, and autoimmune liver disease, and then intrahepatic macrophages are

activated and recruited. The activated and recruited intrahepatic macrophages produce a great number of inflammatory cytokines, such as tumor necrosis factor (TNF)-α and interleukin (IL)-6, to aggravate the damage of hepatocytes and stimulate the activation of hepatic stellate cells (HSCs). Activated HSCs are transformed into proliferative myofibroblasts which will lead to excessive deposition of extracellular matrix and the formation of liver fibrosis by secreting large amounts of collagen [1–4].

In the process of chronic liver diseases, the IFC axis (inflammation ⟶ fibrosis ⟶ cancer) has attracted more and more attention [5]. Chronic liver inflammation is the prerequisite for inducing liver fibrosis [6]. Intrahepatic macrophages are the most important immune- and inflammation-related cells in the liver inflammation. They are the main source cells of inflammatory cytokines and chemokines and play an important role in the process of liver fibrogenesis [7]. According to their origins, intrahepatic macrophages are divided into two groups: hepatic resident macrophages, Kupffer cells (KCs), which reside in the liver, and peripheral mononuclear-derived macrophages which are recruited from peripheral blood. Several studies with experimental mouse models have showed that the recruited monocytes have the crucial role on the progression of liver inflammation and fibrosis [8, 9]. Peripheral blood monocytes can constantly replenish to generate Kupffer cells, especially in acute or chronic liver injury [10]. Chemokines play an important role on monocytes recruitment. Chemokine monocyte chemotactic protein 1 (CCL2), which is mainly released by proinflammatory macrophages in the liver, recruits bone marrow-derived proinflammatory $Ly6C^{high}$ monocytes from the blood to the liver through recognizing receptor CCR2 on proinflammatory $Ly6C^{high}$ monocytes cell membrane. Proinflammatory $Ly6C^{high}$ monocytes will develop into proinflammatory $Ly6C^{high}$ macrophages. Then, proinflammatory $Ly6C^{high}$ macrophages together with proinflammatory Kupffer macrophages further aggravate the inflammatory injury of the liver by secreting proinflammatory factors. Fractalkine (CX3CL1), which is released by several cells such as hepatic endothelial cells and monocytes [11] in the liver, recruits bone marrow-derived restorative $Ly6C^{low}$ monocytes from the blood to the liver through recognizing receptor CX3CR1 on restorative $Ly6C^{low}$ monocyte cell membrane. Restorative $Ly6C^{low}$ monocytes will develop into restorative $Ly6C^{low}$ macrophages. CX3CL1 also can switch proinflammatory $Ly6C^{high}$ macrophages to restorative $Ly6C^{low}$ macrophages. Restorative $Ly6C^{low}$ macrophages show anti-inflammatory and tissue-protective features and exert their role on anti-inflammation and the promotion of liver tissue injury repair and finally inhibit the progress of liver fibrosis [12, 13].

Fuzheng Huayu recipe (FZHY), developed by our institute (Institute of Liver Diseases), is an effective original Chinese patent medicine for liver fibrosis. It is composed of Radix Salvia Miltiorrhizae, Semen Persicae, Cordyceps Sinensis Mycelia, Pollen Pini, Fructus Schisandrae, and *Gynostemma Pentaphyllum*. The clinical research results of FZHY against chronic hepatitis B-related liver fibrosis have showed that FZHY could significantly improve the inflammation of liver tissue while ameliorating hepatic fibrosis without adverse reactions [14]. Experiment results also showed that FZHY could inhibit the production of TGF-β and PDGF in primary Kupffer cells (KCs) from CCl4-injured rats [15]. Furthermore, FZHY could inhibit the activation of hepatic stellate cells by regulating the paracrine of KCs [16]. The above results suggest that the antiliver fibrosis effect of FZHY is related to its function of regulating macrophages polarization. But, the mechanism underlying is still unclear. This study was trying to elucidate whether FZHY exerted its anti-inflammation and antifibrosis effects through regulating intrahepatic macrophage polarization and recruitment.

2. Materials and Methods

2.1. Reagents. Carbon tetrachloride (CCl4, Cat No: 10006418) and olive oil (cat no: 69018028) were purchased from Sinopharm Co., Ltd, China. Hydroxyproline (Hyp), alanine transaminase (ALT) (cat no: C009), and aspartate transaminase (AST) (cat no: C010) kits were purchased from Nanjing-Jiancheng biological engineering research institute, China. An RNA simple Total RNA Kit was purchased from Tiangen Biotech, China. A ReverTra Ace qPCR RT Kit was purchased from Toyobo, Osaka, and Japan. RIPA buffer and BCA protein quantification kits were purchased from Beyotime Biotechnology, China. Nitrocellulose (NC) membrane (cat no: RPN303C) was purchased from Hybond, USA. Pronase E, collagenase IV, DNase I, and Histodenz were purchased from Sigma, USA. Anti-F4/80 immunohistochemical antibody (cat no: ab16911) was purchased from Abcam, UK. Anti-CCL2 immunohistochemical and western blot antibody (cat no: 25542-1-AP) was purchased from Proteintech, USA. Anti-CX3CL1 western blot antibody (cat no: 14-7986-81) was purchased from eBioscience, USA. Anti-GAPDH western blot antibody (cat no: 60004-I-Ig) was purchased from Proteintech, USA. Fluorescent second antibodies, goat anti-rabbit IgG H&L (FITC) (cat no: ab6717), and donkey anti-rat IgG H&L (Alexa Fluor 647) (cat no: ab150155) were purchased from Abcam, UK. DAPI (cat no: ab228549) was purchased from Abcam, UK. Flow cytometric antibodies including anti-CD45 (cat no: 557659), anti-CD11b (cat no: 564454), anti-F4/80 (cat no: 565613), anti-Ly6C (cat no: 560525), and anti-CD86 (cat no: 558703) were purchased from BD Pharmingen, USA. Anti-CD206 (cat no: 141720) was purchased from BioLegend, USA.

One dose of Fuzheng Huayu recipe (FZHY) is composed of Radix Salvia Miltiorrhizae (root of Salvia miltiorrhiza Bunge) (4 g), Semen Persicae (Prunus persica (L.) Batsch) (2 g), Cordyceps Sinensis mycelia (8 g), Pollen Pini (pollen of Pinus thunbergii Parl) (2 g), Fructus Schisandrae Chinensis (fruit of Schisandra chinensis (Turcz.) Baill.) (2 g), *Gynostemma pentaphyllum* (Thunb.) Makino (6 g) (SFDA approval number: Z2005050546 and batch number: 180206). The preparation of FZHY extracts was prepared and provided by Shanghai Huanghai Pharmaceutical Co. Ltd. (Shanghai, China) with a quality inspection report, including the chromatographic profile and the contents of adenosine, danshensu, and salvianolic acid B (2.26 mg/g, 8.3 mg/g, and 13.24 mg/g, respectively).

2.2. Animal Experiment. Six-week-old C57/B6 male mice (22–25 g) were purchased from Shanghai Lingchang Biotechnology co. Ltd (Shanghai, China). The mice were housed in a specific pathogen-free (SPF) grade and temperature-controlled room ($22 \pm 2^{\circ}$C) subjected to a 12 h light/dark cycle, with free access to water and food.

All mice were randomly separated into three groups: control group (normal group, $n = 16$), CCl4-induced liver fibrosis group (CCl4 group, $n = 16$), and FZHY-administered group (FZHY group, $n = 16$). Mice in the CCl4 group and FZHY group were administrated with 15% CCl4-injection intraperitoneally (dissolve CCl4 in olive oil, 2 ml/kg) thrice weekly for 6 weeks. At the same time, mice in the FZHY group were orally given FZHY (5.6 g/kg) daily for 6 weeks. Mice in the normal group were administrated with olive oil intraperitoneally and physiological saline orally. At the end of experimental period, mice were anesthetized by inhaling 3% isoflurane. Some of mice were drawn blood quickly through the inferior vena cava, and then their livers were taken and preserved for further testing, followed by cervical dislocation for confirmation of euthanasia. The others were punctured by the portal vein and their livers were perfused, then their intrahepatic macrophages were isolated, and the phenotypic typing of intrahepatic macrophages was observed by flow cytometry.

2.3. Measurement of Serum ALT and AST Levels. Serum was obtained by centrifugation after blood collection from the inferior vena cava of mice. According to the operation instructions of ALT and AST test kits, the serum was mixed with the reaction solution containing alanine and α-ketoglutarate (for ALT test) and the reaction solution containing α-ketoglutarate and aspartic acid (for AST test) for 30 min, respectively. Then, 2,4-dinitrophenylhydrazine (DNPH) hydrochloric acid solution was added to terminate the reaction and produce pyruvate phenylhydrazone. Finally, sodium hydroxide was added to develop the color. The OD value at 505 nm wavelength was read. The contents of ALT and AST in serum were calculated according to the ALT and AST standard curve.

2.4. Measurement of Liver Hydroxyproline (Hyp) Level. The liver tissue was homogenized and hydrolyzed in 50% hydrochloric acid at 110°C for 24 h. Then, the sample homogenate was filtered and roasted at 40°C for 48 h to obtain precipitation. Next, the sample precipitation was dissolved in 50% isopropanol. After that, chloramine-T working solution was added and mixed well. Then, the mixture was placed at room temperature for 10 min, and ER working solution was added and bathed in 50°C water for 90 min. Finally, the OD value at 558 nm was read. The content of hydroxyproline (Hyp) in the liver was calculated according to the Hyp standard curve.

2.5. Histopathological Examination. Liver tissues were fixed in 4% paraformaldehyde, followed by dehydration and embedding in paraffin, and finally 4 μm thick slices were stained with H&E and Sirius red for histopathological assessing [17].

2.6. RNA-Seq. Liver tissue was collected from the control group, CCl4-induced group, and FZHY-treated group. Total RNA was extracted using RNeasy Mini Kit (Cat#74106, Qiagen) following the manufacturer's instructions and checked for a RIN number to inspect RNA integrity by an Agilent Bioanalyzer 2100 (Agilent technologies, Santa Clara, CA, US). Qualified total RNA was further purified by RNA Clean XP Kit (Cat A63987, Beckman Coulter, Inc. Kraemer Boulevard Brea, CA, USA) and RNase-Free DNase Set (Cat#79254, QIAGEN, Gm BH, Germany). Following purification, the mRNA was isolated and fragmented. The cleaved RNA fragments were copied into first-strand complementary DNA (cDNA) using reverse transcriptase and random primers. This was followed by second-strand cDNA synthesis using DNA polymerase I and RNase H. Then, these cDNA fragments were run through an end-repair process, the addition of a single "A" base, and then ligation of the adapters. The products are then purified and enriched with PCR to create the final cDNA library. Purified libraries were quantified by a Qubit 2.0 Fluorometer (Life Technologies) and validated by an Agilent 2100 bioanalyzer (Agilent Technologies) to confirm the insert size and calculate the mole concentration. The cluster was generated by cBot with the library diluted to 10 pM and then sequenced on the Illumina HiSeq X ten (Illumina). The library construction and sequencing were performed at Shanghai Biotechnology Corporation, Shanghai, China.

2.7. Data Processing of Transcription Group Sequencing. The raw reads contain unqualified reads such as reads of the low-quality end, the reads including primers. To obtain clean reads for data analysis, these unqualified reads could be filtered by Seqtk screening.

2.8. Screening of Differential Expression Genes. The reads are not only proportional to the gene expression level but also related to the length of the gene itself and the amount of data sequenced. In order to obtain comparable data on the gene expression levels of different genes and different samples, the reads were converted into FPKM (fragments per kilobase of exon model per million mapped reads), to standardize the gene expression by three steps which were Stringtie count, TMM (trimmed mean of M values) normalization, and PERL script calculation. Using edgeR to perform differential gene analysis between samples, the p value was obtained and the multihypothesis test was performed. The threshold of p value was determined by controlling the FDR (false discovery rate). The corrected p value was the q value. At the same time, the differential expression multiple was calculated based on the FPKM value, which was fold change (FC). The screening conditions were $p \leq 0.05$ and $FC \geq 1.5$ or $FC \leq 0.67$.

2.9. Reverse Transcription-Quantitative Polymerase Chain Reaction (RT-qPCR). Total RNA was extracted from liver tissue using an RNA simple total RNA kit and reversed to cDNA using the ReverTra Ace qPCR RT kit. RT-qPCR was

performed on the ABI 7500 RT-PCR system (Applied Biosystems, Foster City, CA) under the following conditions: 95°C for 5 s, 60°C for 34 s (40 cycles), 95°C for 15 s, 60°C for 60 s, and 95°C for 15 s. The primer sequences are shown in Table 1. Each sample was performed 3 times. The relative expression level of genes was calculated using glyceraldehyde 3-phosphate dehydrogenase (GAPDH) as the internal control.

2.10. Western Blot. The liver tissues were homogenized with RIPA buffer. After centrifugation for 30 minutes at 12000 rpm, the homogenates were quantified using a BCA protein quantification kit. 30–50 micrograms of protein sample were separated by sodium dodecyl sulfate-polyacrylamide gel electrophoresis (SDS-PAGE) and transferred to a nitrocellulose (NC) membrane. The membrane was blocked with 5% bovine serum albumin in PBS and probed overnight at 4°C with the antibodies against CX3CL1 and GAPDH. After incubating with fluorescence anti-rabbit or anti-mouse antibody for 1 h at room temperature, the protein bands were scanned by the Odyssey infrared imaging system (LI-COR Biosciences, USA), and the densitometry analysis was calculated relative to GAPDH band using an Image J software.

2.11. Immunofluorescent Staining. The liver tissues were put into a Tissue-Tek OCT embedding medium and snap-frozen in liquid nitrogen, and then, 10 μm thick slices were stained with anti-CCL2 and anti-F4/80 immunohistochemical antibodies, following that fluorescent second antibodies like goat anti-rabbit IgG H&L (FITC) and donkey anti-rat IgG H&L (Alexa Fluor 647) were incubated. Next, the cell nuclei were stained with DAPI. Finally, the images were taken by a laser confocal microscope [18].

2.12. Flow Cytometry. To isolate liver macrophages from different groups, mice were anesthetized and perfused with SC-1 solution from the hepatic portal vein, then perfused with SC-2 solution containing pronase E (1 mg/30 ml) and SC-2 solution containing collagenase IV (1 mg/15 ml) successively. The liver was taken out, the liver capsule was torn gently, and then, the liver was kept in a culture dish on ice with 50 ml SC-2 solution containing 12.5 mg pronase E, collagenase IV, and 1 ml DNase I solution (adjust 2 mg/ml DNase I solution using GBSS/B); finally, the liver was stirred gently at 37°C for 20 min. Disaggregated cells were removed and pressed through 70 μm cell strainers to obtain single cell suspensions, and hepatocytes were eliminated by centrifugation three times at 500 rpm for 3 min. Macrophages was purified by using successive gradient centrifugations on 34.5% and 14.5% Histodenz solution. Purified macrophage suspension was counted by an automatic cell counter and incubated immediately with CD45, CD11b, F4/80, Ly6C, CD86, and CD206 monoclonal antibodies for 30 min in the dark at 4°C. Also, gating strategies for leukocyte of different subclasses were proinflammatory Ly6C^{high} macrophages ($CD45^+F4/80^-CD11b^+Ly6C^{high}$ cells), restorative Ly6C^{low} macrophages ($CD45^+F4/80^-CD11b^+Ly6C^{low}$ cells), proinflammatory KC cells ($CD45^+F4/80^+CD11b^-CD86^+$ cells), and anti-inflammatory KC cells ($CD45^+F4/80^+CD11b^-CD206^+$ cells). At last, the stained cells were detected on the DxFLEX flow cytometer, and data were analyzed by Flowjo software.

2.13. Statistical Analyses. All experimental data processing was carried out using SPSS18.0 and the GraphPad Prism 8.01 software. The results were shown as the mean ± standard deviation (SD). The significance of differences between two groups was determined by the t test and one-way ANOVA. Significance was accepted at a p value of ≤ 0.05.

3. Results

3.1. FZHY Inhibited Liver Inflammation and Fibrosis in CCl4-Induced Liver Fibrosis Mice. After mice were treated with carbon tetrachloride (CCl4) for 6 weeks, it was discovered that a large number of inflammatory cells were recruited in the portal area, numerous hepatocytes were degenerated and necrotized, and the liver lobule structure was destroyed in the liver tissues. Compared with the CCl4-induced liver fibrosis mice (CCl4 group), the infiltration of inflammatory cells and the necrosis of hepatocytes in the liver of Fuzheng Huayu recipe- (FZHY-) administered mice (FZHY group) were significantly reduced (Figure 1(a)). Collagen in the portal area was deposited extensively and extended to form fibrous septum in the liver tissues of CCl4 group mice, but the collagen deposition was significantly reduced and the fibrous septum became thinner or even disappeared in FZHY group mice (Figure 1(b)). Hydroxyproline (Hyp), which is a level major component of collagen proteins, was detected to assess liver fibrosis degree. Serum ALT and AST levels were measured to assess liver injury. The results showed that the liver Hyp levels (Figure 1(c)), serum ALT, and AST levels (Figure 1(d)) were significantly increased by CCl4 and significantly reduced by FZHY. These results showed that FZHY could markedly alleviate liver injury, inflammation, and fibrosis.

3.2. FZHY Exerted Its Anti-Inflammation Effect through TNF Signaling Pathway. In order to explore the cell signaling pathway and gene target which plays a key role in regulating macrophage phenotype, depending on which Fuzheng Huayu recipe (FZHY) exerted its anti-inflammation and antifibrosis effect, we carried out RNA-sequencing and transcriptome analysis.

Sifting with p value ≤ 0.05, FC ≥ 1.5, or FC ≤ 0.67, 4,417 differential expression genes were obtained from 18,652 genes in CCl4-treated mice compared with control mice, in which 3,382 genes were upregulated significantly and 1,035 genes were downregulated significantly. 3,880 differential expression genes were obtained from 18,853 genes in FZHY-administered mice compared with CCl4-treated mice, in which 1,603 genes were upregulated significantly and 2,277 genes were downregulated significantly (Figure 2(a)). To elucidate the improvement mechanism of FZHY on CCl4-induced liver inflammation and fibrosis,

Table 1: PCR primer sequence.

Gene	Forward primer	Reverse primer
β-actin	TGACGAGGCCCAGAGCAAGA	ATGGGCACAGTGTGGGTGAC
CCL2	ATTGGGATCATCTTGCTGGT	CCTGCTGTTCACAGTTGCC
CX3CL1	CTGCCCTCACTAAAAATGGTGG	AATGTGGCGGATTCAGGCTT
IL-1β	GCAACTGTTCCTGAACTCAACT	ATCTTTTGGGGTCCGTCAACT
TNF-α	CAGGCGGTGCCTATGTCTC	CGATCACCCCGAAGTTCAGTAG

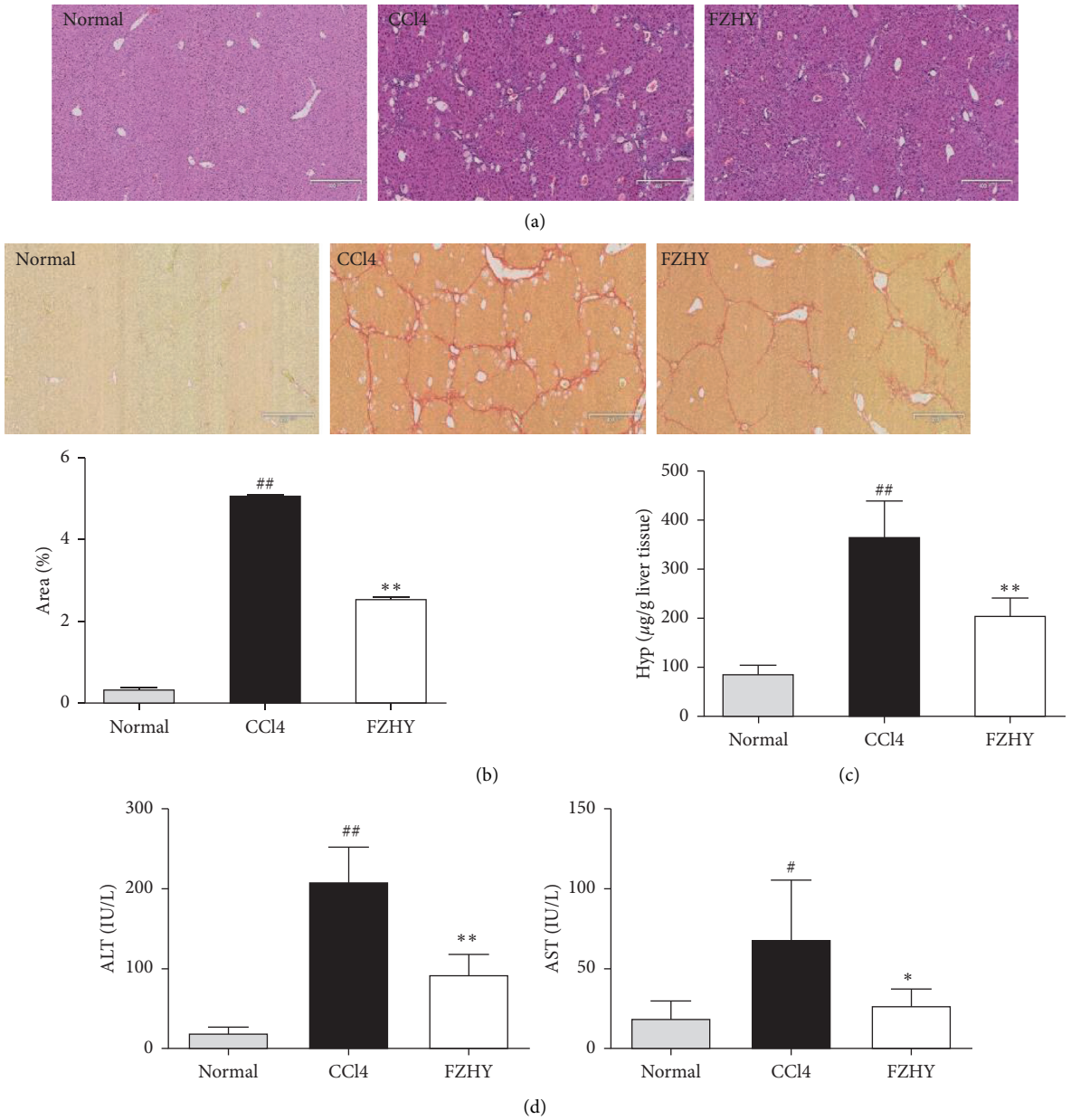

Figure 1: The prevention and curing effects of FZHY on CCl4-induced liver inflammation and fibrosis. (a) HE staining. (b) Sirius red staining. (c) Liver Hyp levels. (d) Serum ALT and AST levels. Results are expressed as means ± SD ($n = 8$). $^{\#}p < 0.05$ and $^{\#\#}p < 0.01$ vs. normal group, $^{*}p < 0.05$ and $^{**}p < 0.01$ vs. CCl4 group.

further differential genes screening had been carried out. The differential expression gene set from the CCl4 group vs. normal group was intersected with differential expression genes set from the FZHY group vs. CCl4 group. We got an

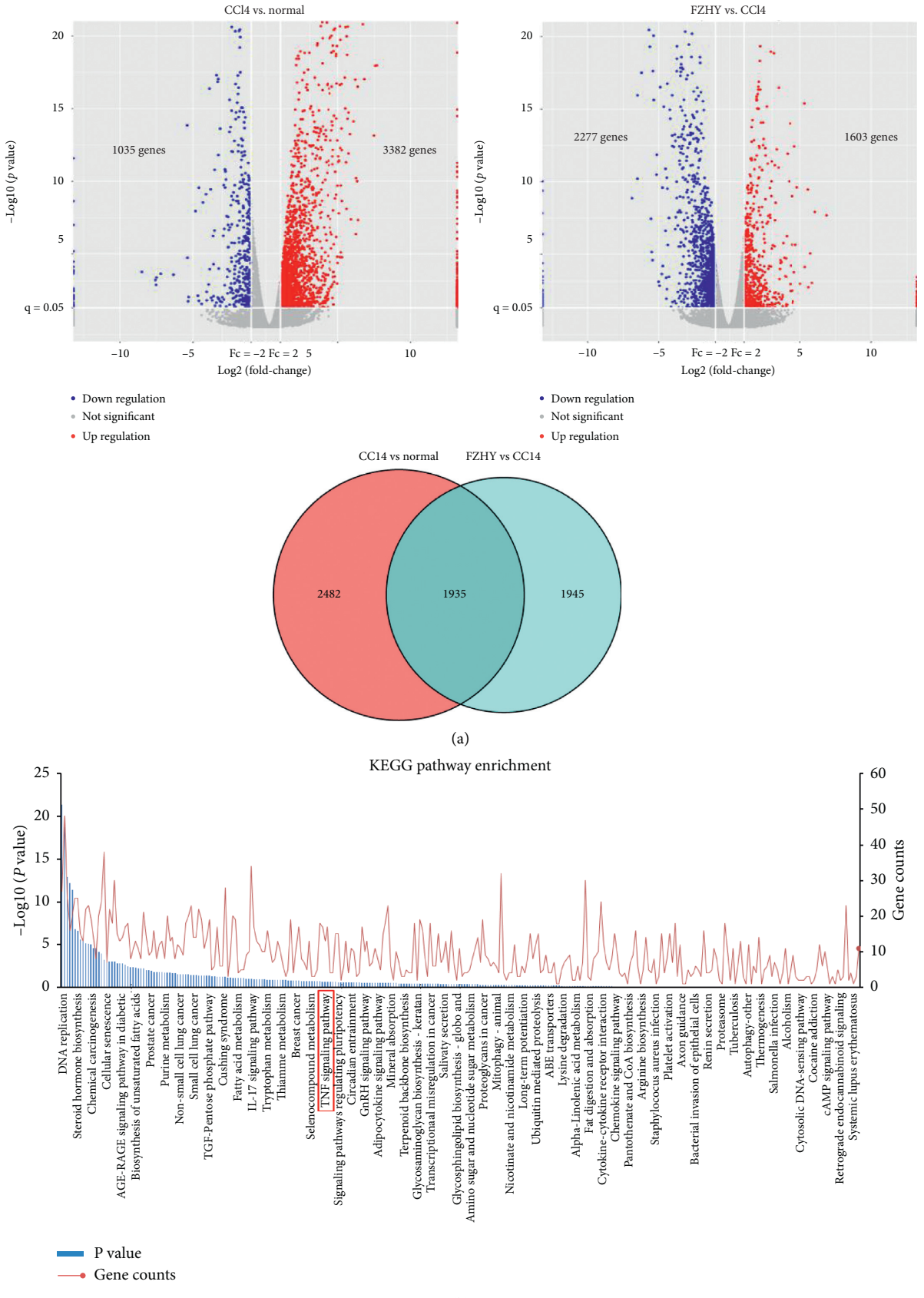

Figure 2: The analysis results of RNA-sequencing data ($n = 3$). (a) Volcano plot and Venn diagram of differently expressed genes. Red plots in volcano plot represent upregulated genes; blue plots in volcano plot represent downregulated genes. (b) KEGG pathway enrichment.

intersection set with 1,935 genes (Figure 2(a)). These genes should be involved in the effect of FZHY on alleviating liver damage and fibrosis.

To explore the key signaling pathways used by FZHY to inhibit liver inflammation and fibrosis in CCl4-induced hepatic fibrosis mice, we further input those 1,935 differentially expressed genes into the Kyoto Encyclopedia of Gene and Genomic (KEGG) database for pathway enrichment (http://bioconductor.org/biocLite.R). Enrichment results indicated that 310 signaling pathways were related to the inhibitory effects of FZHY on CCl4-induced mice hepatic fibrosis. Among them, TNF signaling pathway ($p = 0.213$) was the most relevant pharmacological pathway for the regulation of macrophage recruitment and phenotype polarization. 13 differently expressed genes, such as CCL2, CXCL1, SELE, SOCS3, MLKL, LIF, RPS6KA5, TRAF3, TNFAIP3, ICAM1, MAP3K14, CSF1, and RPS6KA4, were distributed in the TNF signaling pathway (Figure 2(b)). These results showed that FZHY may suppress liver injury and inflammation through the TNF signaling pathway.

3.3. FZHY Affected the Expression of CCL2 and CX3CL1 in the Liver Tissues of CCl4-Induced Hepatic Fibrosis Mice. Chemokine factors, CCL2 and CX3CL1, play a key role on the recruitment and polarization regulation of intrahepatic macrophages [13]. Therefore, we further evaluated the expression of CCL2 and CX3CL1 genes which were members of the TNF signaling pathway in liver tissues. Immunofluorescence and western blot results showed that the expression of CCL2 was significantly increased in the liver tissues of CCl4-induced liver fibrosis mice and the distribution of CCL2 was mainly along the fibrous interval. The positive staining of CCL2 was obviously decreased in FZHY-administered mice (Figures 3(a) and 3(b)). Western blot results revealed that the expression of CX3CL1 was significantly increased by FZHY (Figure 3(d)). Meanwhile, the qRT-PCR results showed that the gene expressions of inflammatory factors IL-1β and TNF-α were increased by CCl4 and decreased by FZHY (Figures 3(c) and 3(e)). These results showed that FZHY could alleviate liver inflammation by decreasing CCL2 production and increasing CX3CL1 production in liver tissues.

3.4. FZHY Promoted CX3CL1 Expression and Suppressed CCL2 Expression in Primary Intrahepatic Macrophages of CCL4-Induced Liver Fibrosis Mice. The data showed above were from the detection of liver tissues; in order to elucidate whether Fuzheng Huayu recipe (FZHY) reduces liver inflammation and fibrosis through regulating macrophage phenotype polarization, we isolated primary intrahepatic macrophages and examined the gene expression of chemokines CCL2 and CX3CL1. As shown in Figure 4, the gene expressions of CCL2 and CX3CL1 in primary intrahepatic macrophages from CCl4-induced liver fibrosis mice were all significantly increased, while the gene expression of CCL2 in primary intrahepatic macrophages from FZHY-administered mice was markedly decreased, but the gene expression of CX3CL1 was further obviously increased. These results showed that FZHY could regulate macrophage polarization and chemotaxis through affecting chemokine secretion.

3.5. FZHY Significantly Reduced the Recruitment of Ly6C^{high} Macrophages and Upregulated the Ratio of Ly6C^{low} Macrophages by Suppressing the Proinflammatory Polarization of Kupffer Macrophages. In order to further study whether FZHY could inhibit the recruitment of bone marrow-derived proinflammatory macrophages through reducing CCL2 expression and promote the polarization of restorative macrophages through increasing CX3CL1 expression, we isolated primary intrahepatic macrophages for flow cytometry detection.

The results showed that the ratio of peripheral mononuclear-derived macrophages ($CD45^+F4/80^+CD11B^+$) was significantly increased by CCl4 and significantly decreased by FZHY. The ratio of liver resident macrophages-Kupffer cells ($CD45^+F4/80^+CD11B^-$) was significantly increased by CCl4, and there was no significant change after FZHY was administered (Figure 5(a)). Further analysis on the phenotype of peripheral mononuclear-derived macrophages showed that the ratio of proinflammatory $Ly6C^{high}$ macrophages ($CD45^+F4/80^+CD11B^+Ly6C^{high}$) in peripheral mononuclear-derived macrophages was significantly increased by CCl4 and significantly decreased by FZHY, and the ratio of restorative $Ly6C^{low}$ macrophages ($CD45^+F4/80^+CD11B^+Ly6C^{low}$) was significantly increased by CCl4 and further significantly increased by FZHY (Figure 5(c)). Further analysis on the phenotype of Kupffer cells showed that the ratio of proinflammatory macrophages ($CD45^+F4/80^+CD11b^-CD86^+$) was significantly increased by CCl4 and significantly decreased by FZHY, and the ratio of anti-inflammatory macrophages ($CD45^+F4/80^+CD11b^-CD206^+$) was significantly increased by FZHY (Figure 5(b)). These results showed that FZHY could markedly inhibit the recruitment of bone marrow-derived proinflammatory $Ly6C^{high}$ macrophages and increase the recruitment of bone marrow-derived restorative $Ly6C^{low}$ macrophages through reducing the proinflammatory polarization of Kupffer macrophages.

4. Discussion

A large number of intrahepatic macrophages are located in the hepatic sinuses. It is estimated that there are 20–40 macrophages in every 100 hepatocytes in the liver of healthy animals [19]. Macrophages play a crucial role in the occurrence and progression of liver fibrosis [2]. Intrahepatic macrophages can be divided into two groups: Kupffer cells (KCs), which are residing in the liver, and peripheral mononuclear-derived macrophages, which are recruited from peripheral blood. Kupffer cells (KCs) are originated from yolk sac-derived specific progenitor cells and settled in the hepatic sinusoids. Normally, KCs are stationary and do not migrate [20]. They maintain the stability of the intrahepatic environment by identifying, phagocytizing, and degrading cell fragments, foreign bodies, and pathogens

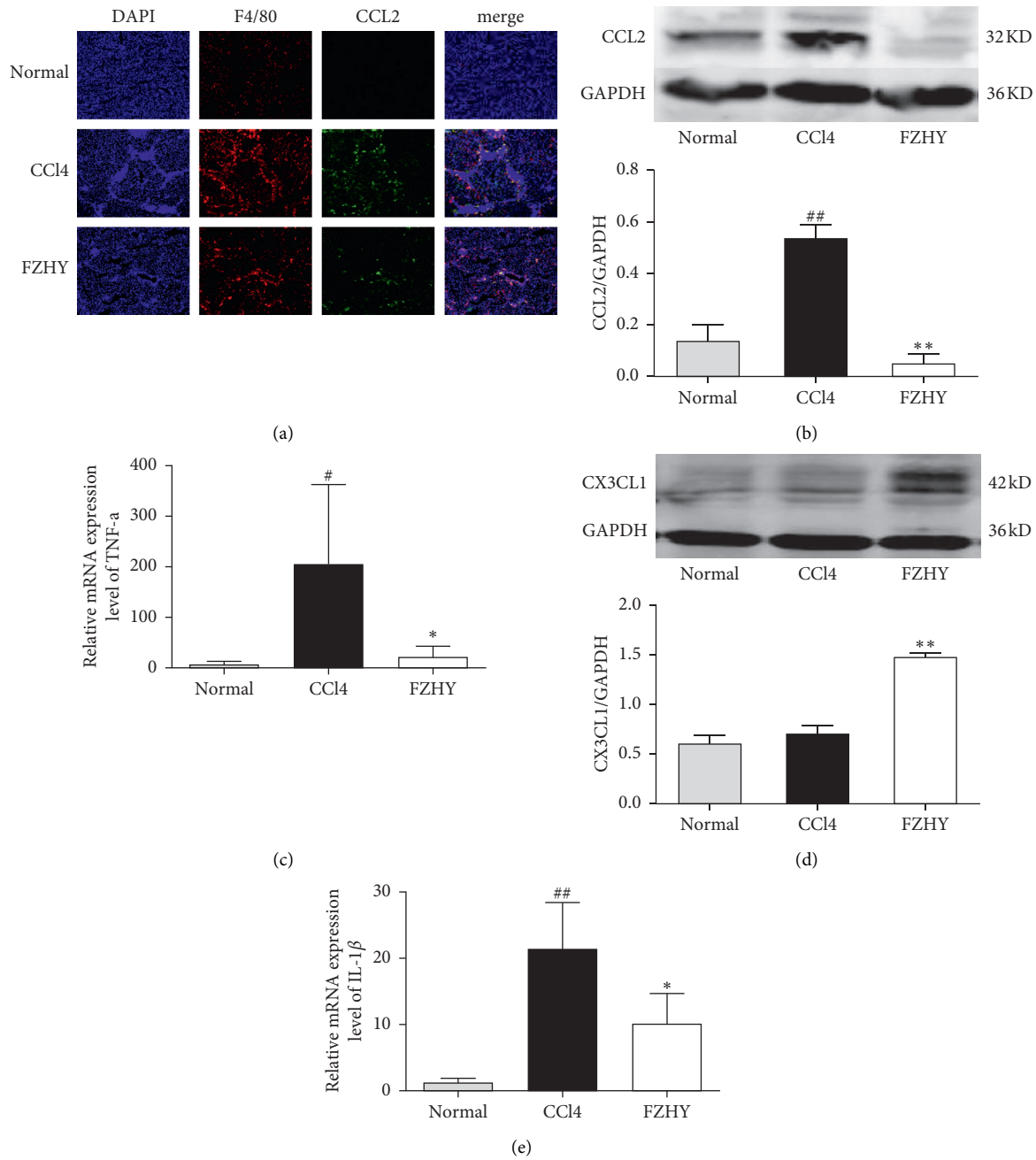

FIGURE 3: FZHY could regulate liver inflammatory cytokines and chemokines in liver tissue during liver fibrosis. (a) Immunofluorescence, (b, d) Western blot, and (c, e) qRT-PCR. Results are expressed as mean ± SD ($n = 3$). $^{\#}p < 0.05$ and $^{\#\#}p < 0.01$ vs. normal group, $^{*}p < 0.05$ and $^{**}p < 0.01$ vs. CCl4 group.

[21]. Stimulated by various extrahepatic pathogen associated molecular patterns (PAMPs) such as LPS and intrahepatic damage associated molecular patterns (DAMPs) from damaged hepatocytes and bile duct cells, KCs are polarized to proinflammatory $CD86^+$-KCs. $CD86^+$-KCs secrete enormous inflammatory cytokines, such as TNF-α, IL-1β, IL-6, and so on, which damage liver tissue and lead to liver inflammation and fibrosis. Meanwhile, the activated KCs recruited a large number of proinflammatory $Ly6C^{high}$ macrophages from peripheral blood by releasing monocyte chemotactic protein 1 (CCL2). Proinflammatory $Ly6C^{high}$ macrophages highly expressed CCR2, which combined with CCL2 expressed by KCs and infiltrated the liver [22]. Proinflammatory $Ly6C^{high}$ macrophages secrete a large number of inflammatory factors, which further promote the damage of liver tissue [13]. Therefore, inhibiting the inflammatory polarization of KCs to reduce the recruitment of proinflammatory $Ly6C^{high}$ macrophages is of great significance for the prevention and treatment of liver fibrosis (Figure 6).

Our results showed that Fuzheng Huayu recipe (FZHY) could significantly reduce the degree of CCl4-induced liver

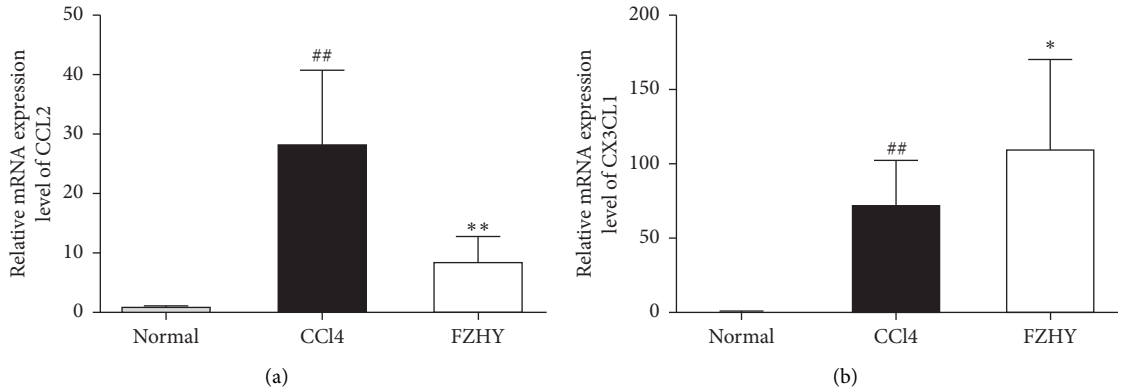

Figure 4: FZHY regulated the gene expression of chemokines CCL2 and CX3CL1 in primary intrahepatocyte macrophages. Results are expressed as mean ± SD ($n = 3$). $^{\#\#}p < 0.01$ vs. normal group, $^{*}p < 0.05$ and $^{**}p < 0.01$ vs. CCl4 group.

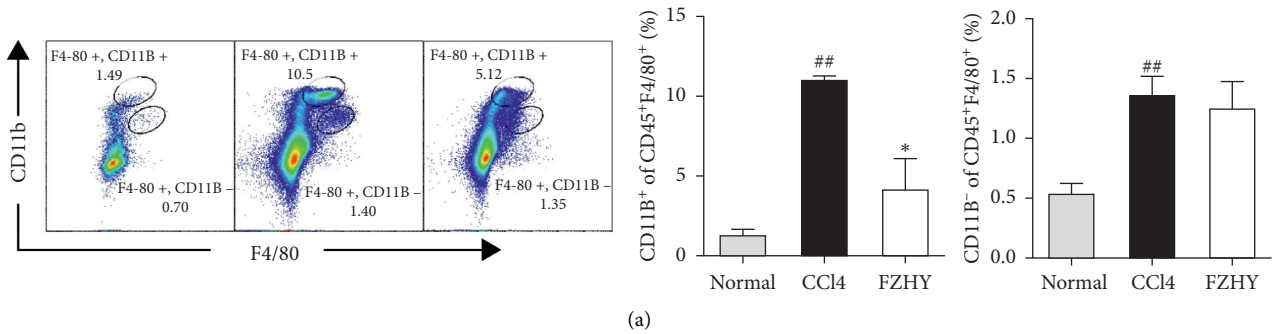

(a)

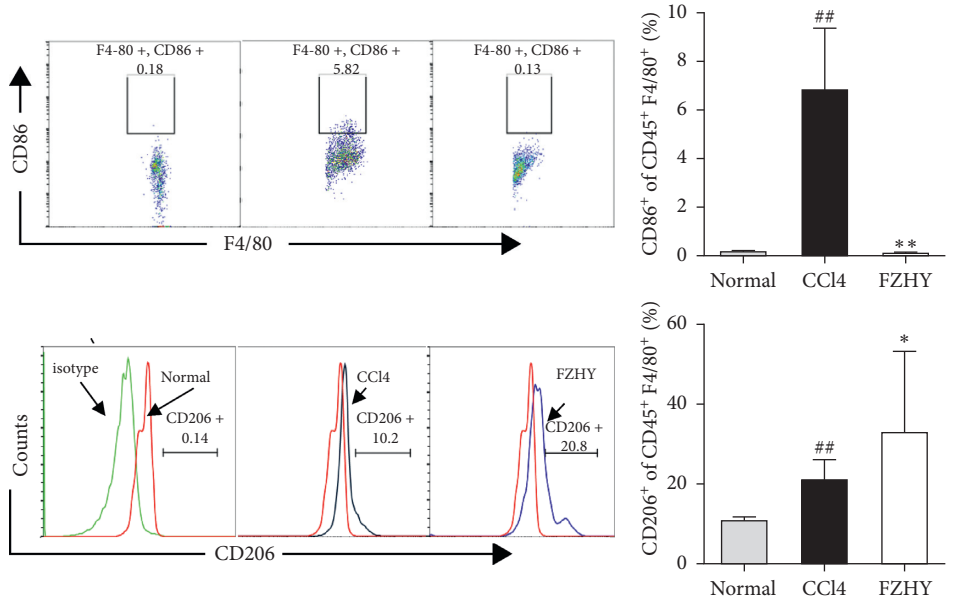

(b)

Figure 5: Continued.

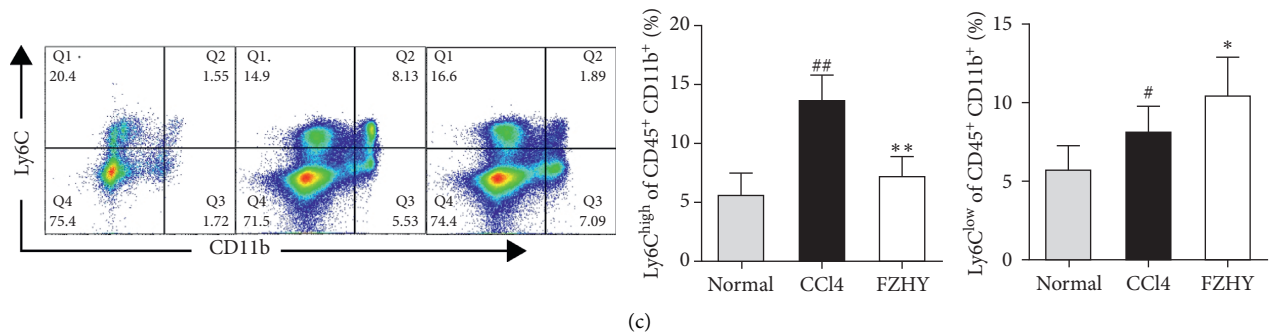

FIGURE 5: FZHY changed the macrophage phenotypes in the liver of CCl4-induced hepatic fibrosis mice and FZHY-administered mice. (a) Effect of FZHY on the ratio change of Kupffer and bone marrow-derived macrophages. (b) Effect of FZHY on the phenotype change of Kupffer macrophages. (c) Effect of FZHY on the phenotype change of bone marrow-derived macrophages. Results are expressed as mean ± SD ($n = 4$). $^{\#}p < 0.05$ and $^{\#\#}p < 0.01$ vs. normal group, $^{*}p < 0.05$ and $^{**}p < 0.01$ vs. CCl4 group.

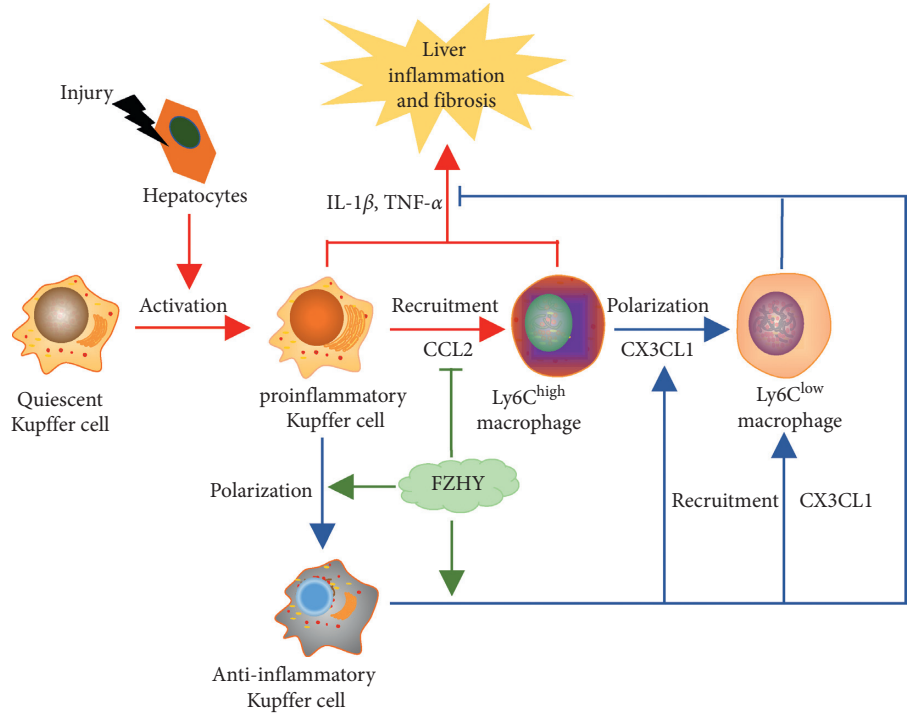

FIGURE 6: The prevention and treatment mechanism of FZHY on CCl4-induced hepatic fibrosis through regulating the recruitment and polarization of intrahepatic macrophages. FZHY reduced CCL2 gene expression of proinflammatory Kupffer cells which were activated in CCl4-damaged liver tissue, thereby reducing the recruitment of proinflammatory Ly6C^{high} macrophages. Meanwhile, FZHY promoted the phenotype polarization of proinflammatory Kupffer cells to anti-inflammatory Kupffer cells and increased CX3CL1 gene expression in intrahepatic macrophages, thereby it promoted the polarization and recruitment of restorative Ly6C^{low} macrophages. Anti-inflammatory Kupffer cells and restorative Ly6C^{low} macrophages exerts their anti-inflammation and antiliver fibrosis effects.

inflammation and improve the degree of CCl4-induced liver fibrosis in mice. At the same time, the data from RNA-seq of liver tissues showed that there were 1,935 differential expression genes among normal group mice, CCl4 group mice, and FZHY group mice. Enrichment analysis was carried out on these genes with KEGG database, and 310 pathways related to antiliver fibrosis effects of FZHY were discovered. TNF signaling pathway, which is the key pathway related to macrophage chemotaxis and inflammatory factor secretion, is one of them. These results indicated that FZHY might achieve its antifibrosis effects by regulating the recruitment and polarization of liver macrophages through the TNF signaling pathway. Among TNF signaling pathway-related genes, the expressions of CCL2, CXCL1, SELE, SOCS3, MLKL, LIF, RPS6KA5, TRAF3, TNFAIP3, ICAM1, MAP3K14, CSF1, and RPS6KA4 genes were significantly increased in CCl4 group mice and decreased in FZHY group mice and the expression of CX3CL1 gene was increased in

CCl4 group mice and further increased in FZHY group mice.

CCL2, one of the differentially expressed genes in TNF signaling pathway, is a key chemokine for recruitment of peripheral inflammatory monocytes [23]. Proinflammatory $Ly6C^{high}$ monocytes are recruited by CCL2, leading to further expansion of liver inflammation by releasing inflammatory factors and promoting the progression of liver fibrosis [24]. CCL2 is usually secreted by proinflammatory Kupffer macrophages in the liver. Our results discovered that the ratio of Kupffer macrophages ($CD45^+F4/80^+CD11b^-$) in the liver of FZHY group mice was not obviously different from those of CCl4 group mice, but the ratio of proinflammatory Kupffer macrophages marked by $CD86^+$ was significantly decreased and the ratio of anti-inflammatory Kupffer macrophages characterized by $CD206^+$ was significantly increased. The data further showed that CCL2 protein production in liver tissues and CCL2 gene expression in primary intrahepatic macrophages were notably decreased by FZHY. Correspondingly, the proinflammatory $Ly6C^{high}$ macrophages ($F4/80^+CD11b^+Ly6C^{high}$) which were developed from $Ly6C^{high}$ monocytes were also significantly reduced by FZHY. These results demonstrated that FZHY could inhibit the recruitment of proinflammatory $Ly6C^{high}$ macrophages through repressing the secretion of CCL2 in proinflammatory Kupffer macrophages.

CX3CL1, which is also one of the differentially expressed genes in TNF signaling pathway, is in charge of the recruitment of restorative $Ly6C^{low}$ monocytes which will develop to restorative $Ly6C^{low}$ macrophages in the liver. And, CX3CL1 will also promote the polarization of proinflammatory $Ly6C^{high}$ macrophages to restorative $Ly6C^{low}$ macrophages. Restorative $Ly6C^{low}$ macrophages are beneficial to the conversion of inflammation and liver fibrosis [13]. The results showed that CX3CL1 protein production in liver tissues and CX3CL1 gene expression in primary intrahepatic macrophages were significantly increased by FZHY. Correspondingly, the restorative $Ly6C^{low}$ macrophages ($F4/80^+CD11b^+Ly6C^{low}$) were also increased by FZHY. These results suggested that FZHY might promote the recruitment and polarization of restorative $Ly6C^{low}$ macrophages by increasing the CX3CL1 gene expression in intrahepatic macrophages.

5. Conclusions

In conclusion, it is clear that Fuzheng Huayu recipe (FZHY) could regulate the polarization and recruitment of intrahepatic macrophage through decreasing CCL2 gene expression and increasing CX3CL1 gene expression, thereby showing its prevention and treatment effects on liver inflammation and fibrosis (Figure 6).

Data Availability

The dataset supporting the conclusions of this study is publicly available.

Ethical Approval

All experimental protocols were approved by the Laboratory Animal Center of Shanghai University of Traditional Chinese Medicine (certificate of conformity: SCXK2018-0003; approval number: PZSHUTCM190315004).

Disclosure

The manuscript was submitted to the conference of the Asian Pacific Association for the Study of the Liver 2020, in Hepatol Int (2020) 14 (supply 1): S1–S470, Abstract #1718, https://doi.org/10.1007/s12072-020-10030-4

Conflicts of Interest

All authors declare that they have no conflicts of interest.

Authors' Contributions

CHL and XDH conceived and designed the study. MZ, LHL, KH, YP, YYT, and CQZ performed the experiments. MZ wrote the initial manuscript, XDH helped to revise it critically, and CHL gave final approval of the version to be published. MZ and XDH analyzed the data. MZ and XDH searched and reviewed the literature. All the authors read and approved the final manuscript.

Acknowledgments

The authors are grateful to Dr. Zhexiong Lian of Institutes for Life Sciences and School of Medicine, South China University of Technology, for technical support and assistance. At the same time, the authors would like to thank Hepatology International for publishing the manuscript's abstract This work was supported by the Key Program of the National Natural Science Foundation of China (grant number 81730109); the National Science and Technology Major Project (grant numbes 2018ZX10302204); and the National Natural Science Foundation of China (grant number 81673780).

References

[1] M. W. Robinson, C. Harmon, and C. O'Farrelly, "Liver immunology and its role in inflammation and homeostasis," *Cellular & Molecular Immunology*, vol. 13, no. 3, pp. 267–276, 2016.

[2] A. Pellicoro, P. Ramachandran, J. P. Iredale, and J. A. Fallowfield, "Liver fibrosis and repair: immune regulation of wound healing in a solid organ," *Nature Reviews Immunology*, vol. 14, no. 3, pp. 181–194, 2014.

[3] D. Schuppan, R. Surabattula, and X. Y. Wang, "Determinants of fibrosis progression and regression in NASH," *Journal of Hepatology*, vol. 68, no. 2, pp. 238–250, 2018.

[4] C. Trautwein, S. L. Friedman, D. Schuppan, and M. Pinzani, "Hepatic fibrosis: concept to treatment," *Journal of Hepatology*, vol. 62, no. 1, pp. S15–S24, 2015.

[5] A. M. Elsharkawy and D. A. Mann, "Nuclear factor-κB and the hepatic inflammation-fibrosis-cancer axis," *Hepatology*, vol. 46, no. 2, pp. 590–597, 2007.

[6] N. C. Henderson and J. P. Iredale, "Liver fibrosis: cellular mechanisms of progression and resolution," *Clinical Science*, vol. 112, no. 5, pp. 265–280, 2007.
[7] S. L. Friedman, "Hepatic fibrosis-overview," *Toxicology*, vol. 254, no. 3, pp. 120–129, 2008.
[8] E. Seki, S. de Minicis, S. Inokuchi et al., "CCR2 promotes hepatic fibrosis in mice," *Hepatology*, vol. 50, no. 1, pp. 185–197, 2009.
[9] M. Imamura, T. Ogawa, Y. Sasaguri, K. Chayama, and H. Ueno, "Suppression of macrophage infiltration inhibits activation of hepatic stellate cells and liver fibrogenesis in rats," *Gastroenterology*, vol. 128, no. 1, pp. 138–146, 2005.
[10] K. R. Karlmark, R. Weiskirchen, H. W. Zimmermann et al., "Hepatic recruitment of the inflammatory Gr1+ monocyte subset upon liver injury promotes hepatic fibrosis," *Hepatology*, vol. 50, no. 1, pp. 261–274, 2009.
[11] E. Efsen, C. Grappone, R. M. S. DeFranco et al., "Up-regulated expression of fractalkine and its receptor CX3CR1 during liver injury in humans," *Journal of Hepatology*, vol. 37, no. 1, pp. 39–47, 2002.
[12] F. Tacke, "Targeting hepatic macrophages to treat liver diseases," *Journal of Hepatology*, vol. 66, no. 6, pp. 1300–1312, 2017.
[13] O. Krenkel and F. Tacke, "Liver macrophages in tissue homeostasis and disease," *Nature Reviews Immunology*, vol. 17, no. 5, pp. 306–321, 2017.
[14] P. Liu, Y. Y. Hu, C. Liu et al., "Multicenter clinical study on Fuzhenghuayu capsule against liver fibrosis due to chronic hepatitis B," *World Journal of Gastroenterology*, vol. 11, no. 19, pp. 2892–2899, 2005.
[15] C. M. Jiang, C. Liu, C. H. Liu, and Y. Y. Hu, "Effect of Fuzheng Huayu decotion (FZHYF) on the function of Kupffer cells from acute injury liver induced by CCl4," *Chinese Journal of Integrated Traditional and Western Medicine on Liver Diseases*, vol. 5, pp. 26–28, 2000.
[16] C. Liu, C. M. Jiang, and P. Liu, "Inhibition of Fuzheng Huayu formulaon paracrine activation pathway in rat hepatic stellate cells," *Chinese Journal of Digestion*, vol. 6, pp. 43–45, 2001.
[17] G. Garcia-Tsao, S. Friedman, J. Iredale, and M. Pinzani, "Now there are many (stages) where before there was one: in search of a pathophysiological classification of cirrhosis," *Hepatology*, vol. 51, no. 4, pp. 1445–1449, 2010.
[18] H. L. Liu, J. Lv, Z. M. Zhao et al., "Fuzhenghuayu decoction ameliorates hepatic fibrosis by attenuating experimental sinusoidal capillarization and liver angiogenesis," *Scientific Reports*, vol. 9, p. 18719, 2019.
[19] B. G. Lopez, M. S. Tsai, J. L. Baratta, K. J. Longmuir, and R. T. Robertson, "Characterization of Kupffer cells in livers of developing mice," *Comparative Hepatology*, vol. 10, no. 1, p. 2, 2011.
[20] D. Dal-Secco, J. Wang, Z. Zeng et al., "A dynamic spectrum of monocytes arising from the in situ reprogramming of CCR2+ monocytes at a site of sterile injury," *Journal of Experimental Medicine*, vol. 212, no. 4, pp. 447–456, 2015.
[21] C. Varol, A. Mildner, and S. Jung, "Macrophages: development and tissue specialization," *Annual Review of Immunology*, vol. 33, no. 1, pp. 643–675, 2015.
[22] C. L. Elsegood, C. W. Chan, M. A. Degli-Esposti et al., "Kupffer cell-monocyte communication is essential for initiating murine liver progenitor cell-mediated liver regeneration," *Hepatology*, vol. 62, no. 4, pp. 1272–1284, 2015.
[23] J. Ehling, M. Bartneck, X. Wei et al., "CCL2-dependent infiltrating macrophages promote angiogenesis in progressive liver fibrosis," *Gut*, vol. 63, no. 12, pp. 1960–1971, 2014.
[24] F. Tacke, "Functional role of intrahepatic monocyte subsets for the progression of liver inflammation and liver fibrosis in vivo," *Fibrogenesis & Tissue Repair*, vol. 5, no. S1, p. S27, 2012.

Hindawi
Evidence-Based Complementary and Alternative Medicine
Volume 2020, Article ID 8872945, 9 pages
https://doi.org/10.1155/2020/8872945

Research Article

Rosanortriterpenes A–B, Two Promising Agents from *Rosa laevigata* var. *leiocapus*, Alleviate Inflammatory Responses and Liver Fibrosis in In Vitro Cell Models

Bai-Lin Li, Juan-Juan Hu, Jin-Dan Xie, Chen Ni, Hui-Jun Liang, Qian-Ran Li, Jie Yuan, and Jie-Wei Wu

Guangdong Provincial Key Laboratory of New Drug Development and Research of Chinese Medicine, Mathematical Engineering Academy of Chinese Medicine, Guangzhou University of Chinese Medicine, Guangzhou 510006, China

Correspondence should be addressed to Jie-Wei Wu; wujiewei@gzucm.edu.cn

Received 11 August 2020; Revised 18 October 2020; Accepted 24 October 2020; Published 11 November 2020

Academic Editor: Jianbo Wan

Rosanortriterpenes A–B (RTA and RTB), two nortriterpenoids, are characteristic constituents in the fruits of *Rosa laevigata* var. *leiocapus*. However, pharmacological studies on these compounds are still scarce. In the present study, we aim to investigate the anti-inflammatory mechanisms associated with the effects of RTA–B in RAW264.7 macrophages and LO_2 cells by detecting cell viabilities, nitric oxide (NO) production, tumour necrosis factor-alpha (TNF-α), and interleukin-6 (IL-6) production. Simultaneously, the anti-inflammatory action mechanisms of these two compounds were illustrated through western blot assay. Besides, the antihepatic fibrosis activities of these compounds have also been explored. The results demonstrated that RTA and RTB inhibited the production of NO, TNF-α, and IL-6 and suppressed liver fibrosis. RTA and RTB treatment also greatly inhibited the activation of NF-kappaB (NF-κB) pathway. Our study confirmed the promising anti-inflammatory and anti-liver fibrosis actions of RTA–B, suggesting that they might be developed as alternative and promising drugs for the treatment of hepatic inflammatory and fibrotic diseases.

1. Introduction

Inflammation is an immune response caused by tissue damages or pathogen infections [1]. Excessive and uncontrolled inflammations are harmful to the body, especially liver, the largest metabolic organ in the human body, as they may cause chronic diseases and further lead to fatty liver diseases, hepatitis, liver fibrosis, and even cirrhosis and liver cancer [2–6]. Currently, the commercial drugs utilized to treat inflammation are mainly steroidal anti-inflammatory drugs (SAIDs) and nonsteroidal anti-inflammatory drugs (NSAIDs). However, with the increasing number of medical side effects discovered in clinical applications such as low potassium and hypertension [7–11], novel inflammatory drugs are urgently needed [12]. Traditional diets, in particular, edible plants, with pharmacological functions such as pigeon pea, orange peel, and grapefruit [13–15] have been always regarded as an essential source for treatment of inflammation. Therefore, it may be a potential way to seek new anti-inflammatory agents from traditional medicinal food [16].

Rosa laevigata belonging to the Rosaceae family is widely distributed throughout southern China. Its fruits are recorded in Chinese Pharmacopoeia as a treatment for spermatorrhea, uroclepsia, frequent micturition, and uterine abscission and hence considered as a kind of traditional

medicinal food in East Asia [17]. *Rosa laevigata* var. *leiocapus*, a variety of *R. laevigata*, was firstly found and reported in Boluo county, Guangdong province, China, by Wang et al. in 1995 [18]. The specific morphological characteristics of this species attributed to its smooth fruits without any thorns. As a result of this distinction, *Rosa laevigata* var. *leiocapus* can be developed as an alternative to *R. laevigata*, which can improve production efficiency and save labor costs, since there is no need to remove thorns from the fruit during harvesting and processing.

However, as characteristic constituents isolated from *Rosa laevigata* var. *leiocapus* fruits [19], the bioactivity evaluations of rosanortriterpenes A–B (RTA and RTB) (Figure 1) have rarely been reported. Therefore, studies on anti-inflammatory and antiliver fibrosis activities of RTA and RTB are presented in this paper.

2. Materials and Methods

2.1. Reagents. RTA and RTB were isolated from *R. laevigata* var. *leiocapus* and stored in several small aliquots at −80°C. Materials used for cell culture such as FBS (made in Australia), DMEM (made in China), PBS (pH 7.4), and penicillin/streptomycin were obtained from Gibco Company. The LPS (*Escherichia coli* 0127:B8), MTT powder, indomethacin (Indo), silibinin (SLB), and DMSO solvent were obtained from Sigma-Aldrich (St. Louis, MO, USA). TNF-α and TGF-β were obtained from PeproTech (Rocky Hill, NJ, USA). Griess reagent, DAF-FM DA, RIPA buffer, and BCA protein assay kits were purchased from Biotine (Shanghai, China). Nuclear protein extraction kits and Hoechst 33342 were purchased from Solarbio (Beijing, China). PVDF membranes were obtained from Millipore (Bedford, MA, USA). The NF-κB pathway sampler kit and β-actin rabbit antibodies were brought from Cell Signaling Technology Company (Danvers, MA, USA). The collagen I antibody, alpha-SMA antibody, and the enhanced chemiluminescence kit were obtained from Affinity Biosciences (Cincinnati, OH, USA). TNF-α and IL-6 enzyme immunoassay kits were purchased from Dakewe Biotech (Shenzhen, China).

2.2. Cell Line Culture. The RAW264.7 and HSC-T6 cells were gained from the CAS Cell Bank in Kunming. The LO_2 cells were purchased from the Chinese Academy of Sciences. The abovementioned cells were, respectively, cultured at 37°C in the DMEM medium system containing 10% FBS as well as 1% penicillin/streptomycin.

2.3. MTT Assays. Cytotoxicity assays were carried out utilizing a typical MTT method based on the standard protocol. To be brief, RAW264.7, LO_2, and HSC-T6 cells were cultured in 96-well cell culture microplates with a density of 10^4 cells per well for LO_2 and HSC-T6 cells and 5×10^4 cells per well for RAW264.7. After cell adhesion, 100 μL of culture medium with established concentrations of RTA, RTB, or equal volume of DMSO replaced the original medium, and then, the cells were further incubated for 24 h. 20 μL of MTT (5 mg/mL) was added to all wells and coincubated for 3 h. After removing the medium, DMSO (150 μL) was subjected to the wells to dissolve the formazan crystals. The solution was monitored using a microplate reader (Thermo, Massachusetts, USA) at 490 nm.

2.4. NO Production Assay. RAW264.7 macrophages were dispensed in 96-well plates with a density of 5×10^4 cells per well. After cell adhesion, different concentrations of RTA and RTB were added to the cell culture medium 2 hours before LPS (100 ng/mL) stimulation. After 24 h, 100 μL of Griess reagents A and B were added to the removed cell culture medium, respectively. The absorbance of the mixture was detected at 540 nm using the aforementioned microplate reader.

2.5. Intracellular NO Assays. The fluorescence data of intracellular NO were also detected using a NO-sensitive fluorescence probe DAF-FM DA. Briefly, RAW264.7 cells were dispensed in 96-well microplates with a density of 5×10^4 cells per well, and RTA and RTB were added to the cell culture medium 2 hours before LPS stimulation after adhesion. After 24 h incubation, cells were loaded with 10 μM of DAF-FM DA for 40 min at 37°C, then cells were carefully rinsed with PBS three times, and the data were recorded with 495 nm as excitation wavelength and 515 nm as emission wavelength using a microplate reader (Thermo, Massachusetts, USA).

The fluorescence microscopy imaging of intracellular NO was recorded utilizing DAF-FM DA. Similarly, RAW264.7 murine macrophages were dispensed in 96-well microplates with a density of 5×10^4 cells per well. After cell adhesion, RTA and RTB were added to the cell culture medium 2 hours before LPS stimulation. After 24 h incubation, cells were loaded with 10 μM of DAF-FM DA for 40 min at 37°C [20]. Then, cells were carefully rinsed by PBS for three times and then incubated for 30 min with Hoechst 33342. Fluorescence was detected with a fluorescence microscope (BX-53, Olympus, Japan).

2.6. Western Blot Analysis. RAW264.7, LO_2, and HSC-T6 cells were seeded in 6-well plates, and then different concentrations of RTA–B were added to cells 2 h before LPS (100 ng/mL), TNF-α (20 ng/mL), or TGF-β (10 ng/mL) stimulation. After treatment for 24 h, cells were collected to extract protein for further western blot analysis.

2.7. ELISA. The experimental protocol is based on the previous report; briefly, RAW 264.7 cells and LO_2 were

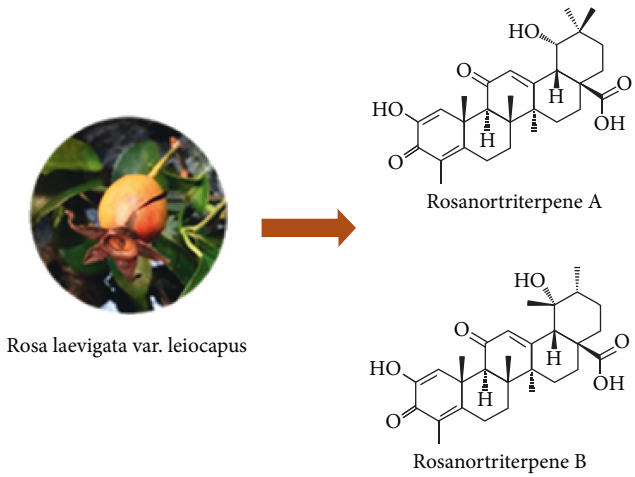

Figure 1: Structures of compounds RTA and RTB.

dispensed in 96-well plates, and RTA and RTB at prescribed concentrations were added to the culture medium 2 h prior to LPS or TNF-α stimulation [14]. After 24 h, productions of TNF-α or IL-6 in the cell culture medium were detected according to the instruction of manufacturers after dilution.

2.8. Statistical Analysis. The data in this work were expressed as mean ± standard deviation (SD). One-way analysis of variance (ANOVA) together with Tukey multiple comparison tests were performed with GraphPad Prism 5 software.

3. Results and Discussion

3.1. Anti-Inflammatory Activities of RTA and RTB

3.1.1. Cell Viability. Recruited myelo-derived free macrophages are important factors accounting for acute and chronic hepatitis [21]. Hence, two cell lines, RAW264.7 and LO_2, were selected for the study on RTA and RTB for inflammation treatment. As a preliminary step, we tested their cytotoxicity against the two cells in 24 h treatment duration. As a result, even at the concentration of 100 μM, viabilities of the two cells treated with both RTA–B were basically unchanged compared to the blank control group (Figures 2(a) and 2(b)), suggesting cytosafety of these compounds. In addition, we investigated the cell viability of LPS-stimulated RAW264.7 treated with RTA and RTB at the concentration of 3, 10, and 30 μM with 10 μM Indo acting as a positive control. The results are shown in Figure 2(c). 100 ng/mL LPS could stimulate the proliferation of RAW264.7; however, 24 h treatment by RTA and RTB could reduce the proliferation in a dose-dependent manner.

3.1.2. NO Production Assay. RAW264.7 once stimulated by LPS will generate a great amount of NO which is one of the active radical species [22]. Excessive NO in return may greatly facilitate cascade reactions of inflammation [6, 23]. It has been widely accepted that LPS stimulation can significantly increase NO release in macrophages. In order to study the anti-inflammatory activities of RTA–B, we applied them to RAW264.7 cells stimulated by LPS to measure their effects on NO production and Indo was still chosen as a positive control. Figure 3(a) displays a dosage-dependent NO production inhibition effects of the compounds. In terms of intracellular NO, consistent with the previous results, these compounds could inhibit the production of intracellular NO represented by the fluorescence intensity (Figure 3(b)). And as for intracellular NO microscopy imaging, for all groups, the blue fluorescence representing living cells stained by Hoechst 33342 remained almost stable. The control group showed weak green fluorescence representing intracellular NO. In contrast, cells treated by LPS exhibited strong green fluorescence. However, green fluorescence significantly weakened by RTA and RTB treatment implying their potential for anti-inflammatory activities (Figure 3(c)).

3.1.3. Inhibition of NF-kB Activation by RTA and RTB. NF-κB is one of the most significant signal pathways regulating proinflammatory genes whose productions in return give rise in the persistent activation of NF-κB pathway and further exacerbate inflammatory response [24]. In resting cells, NF-κB is normally present in the cytoplasm in formation as an inactive IκBα/p50/p65 heterotrimer. Stimulated by activators such as LPS or TNF-α, IKKα/β is phosphorylated and activated IKKα/β triggers phosphorylation of IκBα and release of p65 from the complex [25]. Dissociative p65 once translocated into the nucleus would initiate transcription of downstream genes inducing those coding proinflammatory cytokines [26]. To determine whether RTA and RTB achieve their anti-inflammatory effects via NF-κB pathway, western blot analysis was launched to identify expressions of related proteins. Figure 4(a) shows that compared with the blank control group, the productions of p-IKKα/β and p-p65 along with p-IκBα in total lysate and p65 in the nucleus were significantly increased in the LPS-model group, while RTA and RTB remarkably suppressed the levels of these proteins in RAW264.7 cells. Similarly, the increase of p-p65 induced by TNF-α was also inhibited by RTA and RTB in LO_2 cells. Consistent with our expectations, both RTA and RTB

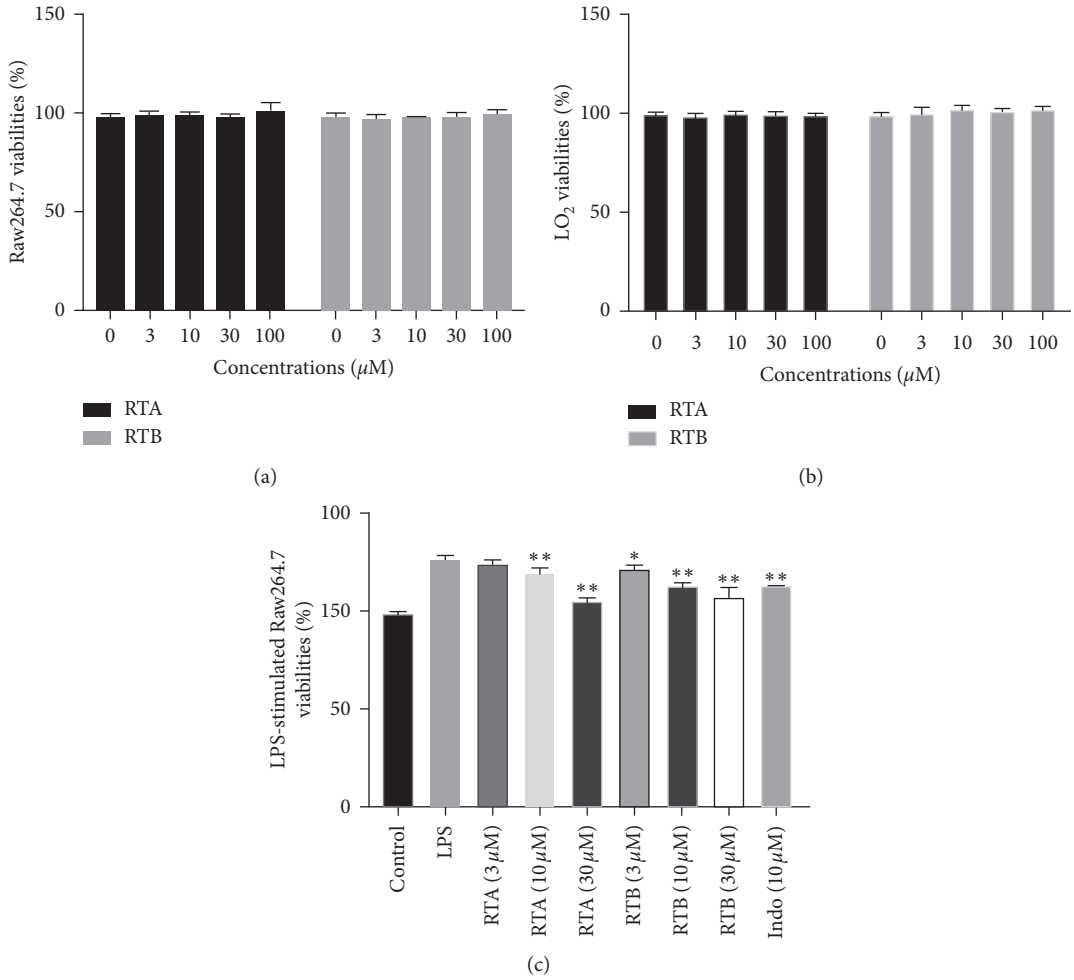

Figure 2: Effects of RTA and RTB on cell viabilities of (a) RAW264.7 and (b) LO_2. $^{*}p < 0.05$ and $^{**}p < 0.01$ compound treatment groups vs. DMSO group. (c) Effects of RTA and RTB on cell viabilities of RAW264.7 stimulated by LPS (100 ng/mL). $^{*}p < 0.05$ and $^{**}p < 0.01$ compound treatment groups vs. LPS group.

showed suppression of activated NF-κB pathway both in macrophages and hepatic cells.

3.1.4. Inhibition of TNF-α and IL-6 Production by RTA and RTB. TNF-α and IL-6 are two essential proinflammatory cytokines in inflammation, and their high expressions are commonly found in liver injuries [27–29]. In order to further clarify the anti-inflammatory effects of RTA and RTB, we detected the productions of these two proinflammatory cytokines in LPS-stimulated RAW264.7 and IL-6 in TNF-α-stimulated LO_2. The results are displayed in Figure 5. The productions of TNF-α and IL-6 in the medium supernatant after treatment with different concentrations of RTA or RTB were lower than those only treated with LPS in a dose-dependent manner proving that these two compounds could reduce the productions of critical proinflammatory cytokines.

3.2. Antifibrotic Activities of RTA and RTB

3.2.1. Cell Viability. In order to explore whether the compounds have antifibrotic activities in hepatic cells, we first tested their cytotoxicity against hepatic stellate cells, HSC-T6. Consistent with previous results, after 24 h treatment, viabilities of HSC-T6 treated by both compounds showed no significant differences compared to the blank control group even at the concentration of 100 μM (Figure 6(a)). Additionally, we further investigated the cell viability of TGF-β-stimulated HSC-T6 treated by RTA and RTB at the concentration of 3, 10, and 30 μM with 10 μM SLB acting as a positive control. The results are shown in Figure 6(b). Stimulated by TGF-β, proliferation of HSC-T6 increased significantly; however, 24 h treatment by RTA and RTB could reduce the proliferation in a dose-dependent manner.

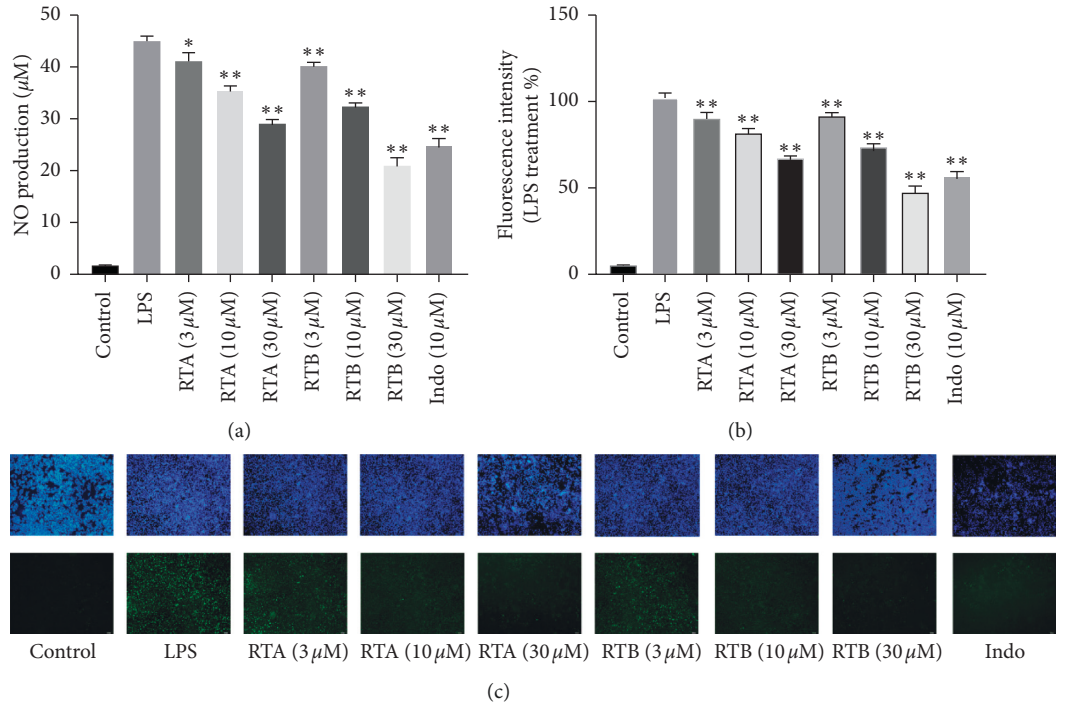

Figure 3: Effects of RTA–B on NO production. (a) Inhibitory effects of RTA and RTB on NO production of RAW264.7 murine macrophages stimulated with LPS (100 ng/mL). (b) Fluorescence data of intracellular NO of RAW264.7. $^{*}p < 0.05$ and $^{**}p < 0.01$ compound treatment groups vs. LPS group. (c) Intracellular NO microscopy imaging of RAW264.7, blue for the nucleus of living cells and green for intracellular NO with × 20 magnification.

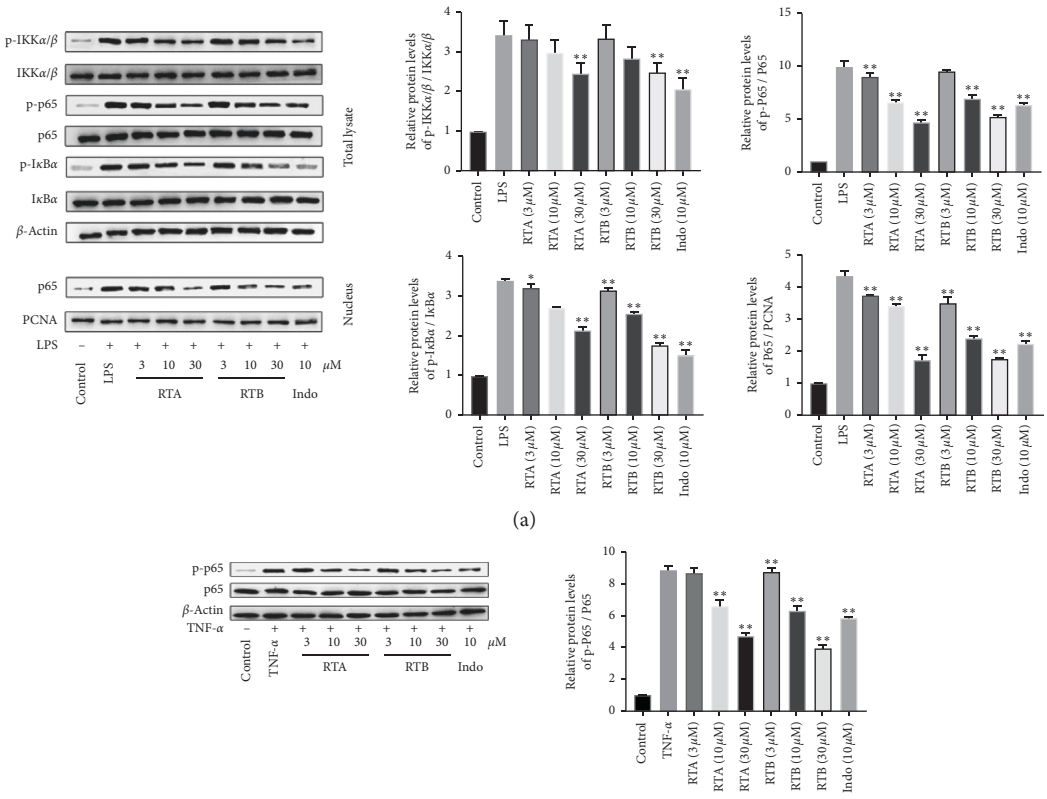

Figure 4: Detraction influences of RTA–B on protein expressions in NF-κB pathway in (a) RAW264.7 cells stimulated by LPS (100 ng/mL) and (b) LO2 cells stimulated by TNF-α (20 ng/mL). $^{*}p < 0.05$ and $^{**}p < 0.01$ compound treatment groups vs. model group.

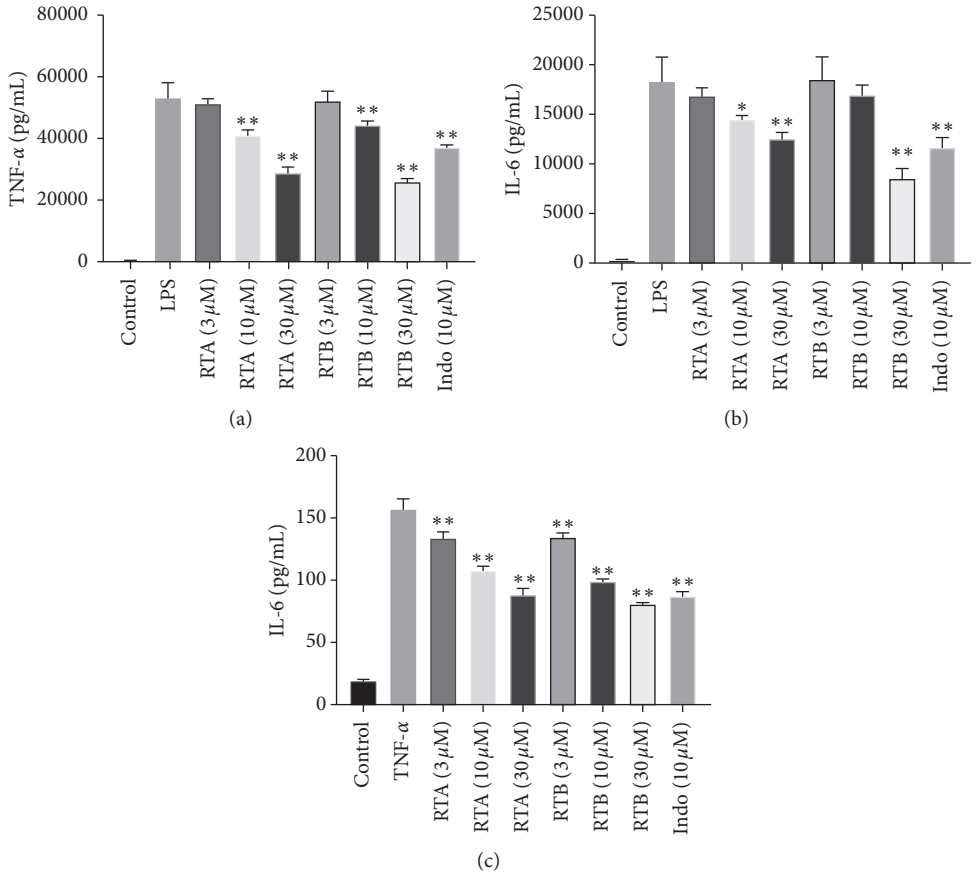

Figure 5: Detraction influences of RTA–B on (a) TNF-α in RAW264.7 stimulated by LPS (100 ng/mL), (b) IL-6 levels in RAW264.7 stimulated by LPS (100 ng/mL), and (c) IL-6 levels in LO_2 stimulated by TNF-α (20 ng/mL). $^{*}p < 0.05$ and $^{**}p < 0.01$ compound treatment groups vs. model group.

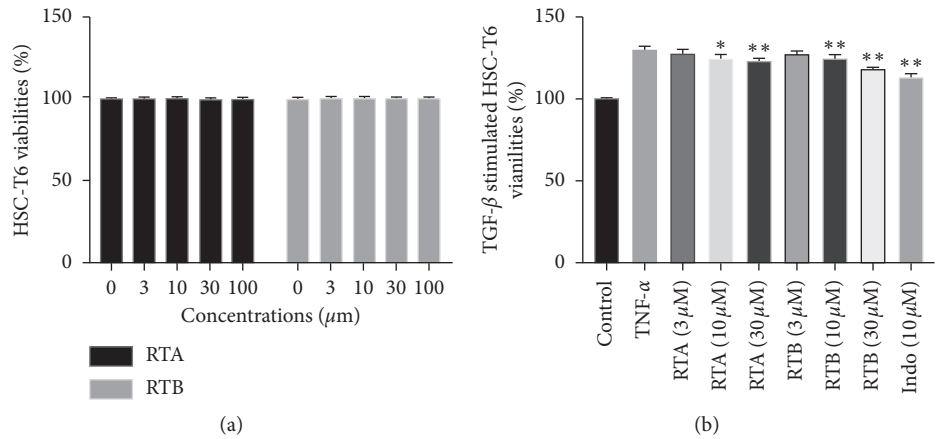

Figure 6: Effects of RTA and RTB on cell viabilities of (a) HSC-T6. $^{*}p < 0.05$ and $^{**}p < 0.01$ compound treatment groups vs. DMSO group. (b) Effects of RTA and RTB on cell viabilities of HSC-T6 stimulated by TGF-β (10 ng/mL). $^{*}p < 0.05$ and $^{**}p < 0.01$ compound treatment groups vs. TGF-β group.

3.2.2. Western Blot Analysis. Liver fibrosis is characterized by excess deposition of extracellular matrix (ECM) such as collagen type-I (Col1) and α-smooth muscle actin (α-SMA) [30]. So we detected the effect of the compounds on the expression of the above proteins, and results are shown in Figure 7. After 24 h treatment, both RTA and RTB could inhibit the increase of ECM-related proteins stimulated by TGF-β in a dose-dependent manner. Besides, NF-κB is also an important signaling pathway in the development of liver fibrosis that not only participates in the proliferation and

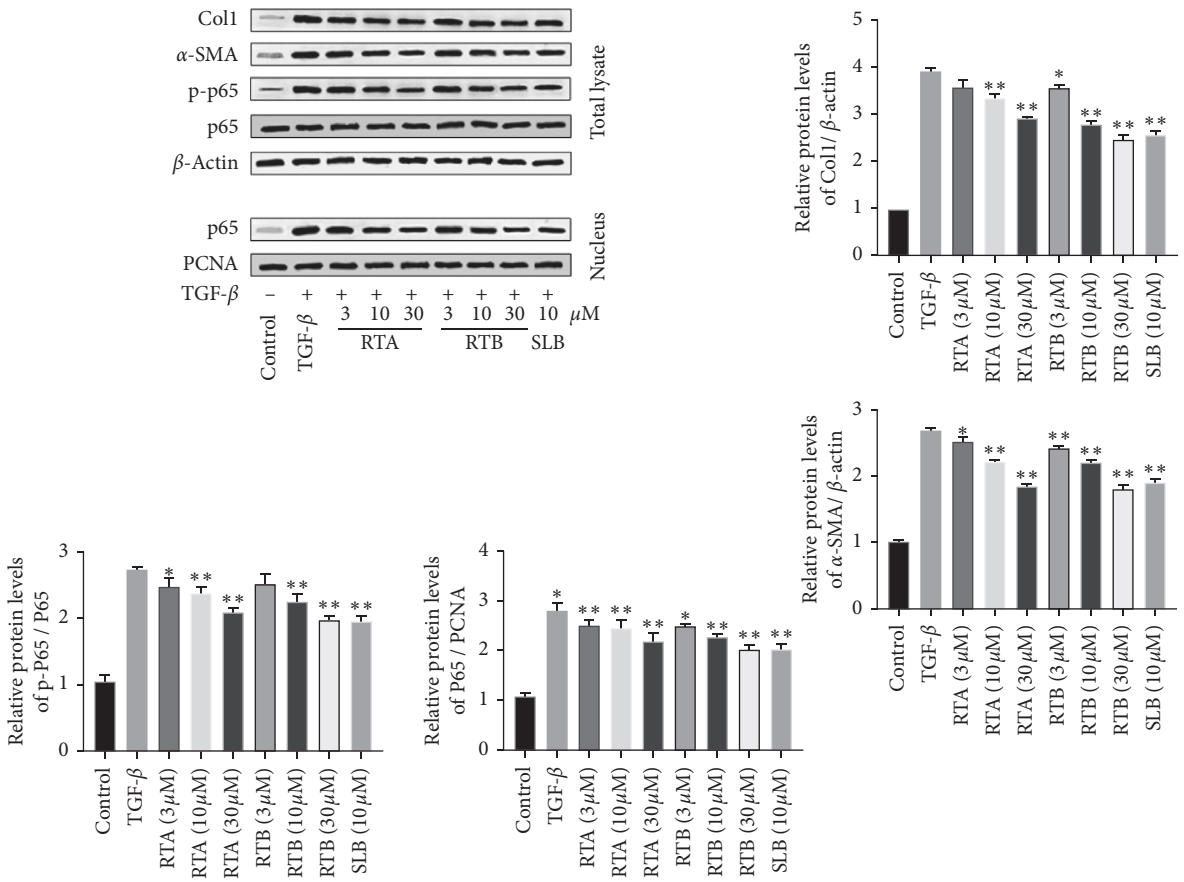

Figure 7: Influences of RTA–B on fibrosis-related protein expressions in HSC-T6 cells stimulated by TGF-β (10 ng/mL). $^{*}p < 0.05$ and $^{**}p < 0.01$ compound treatment groups vs. model group.

apoptosis of liver cells but also promotes activation of hepatic stellate cells [31]. In HSC-T6 cells stimulated by TGF-β, the p-p65 was significantly increased, as well as p65 in nucleus. While under the treatment of the compounds, the levels of these two proteins decreased indicating that RTA and RTB could suppress NF-kB activation and ECM deposition induced by TGF-β in hepatic stellate cells.

4. Conclusions

In various cultures around the world, inflammation and relative diseases have always been treated by plant and plant-derived agents [32]. Among them, fruits of *Rosaceae* were reported to possess potential anti-inflammatory activities [33–35]. As a potential substitute for *R. laevigata*, the convenience of *Rosa laevigata* var. *leiocapus* in the food processing makes it more favorable to serve as a medicinal food source. In addition, the COVID-19 epidemic has seriously affected the world's political and economic patterns leading to food insecurity [36, 37]; hence, seeking and making full use of food resources with pharmacological values seems more significant in the current crisis. Thus, the medicinal values of *Rosa laevigata* var. *leiocapus* need to be determined urgently. In this present study, the anti-inflammatory and anti-liver fibrosis effects of two characteristic compounds from *Rosa laevigata* var. *leiocapus*, RTA and RTB, were elaborated. Taking together, our work not only lays a foundation for the development and application of *Rosa laevigata* var. *leiocapus* but also provides dietary supplements targeting at liver inflammation and fibrosis.

Data Availability

The materials and data presented in the work are available from the authors upon reasonable request.

Conflicts of Interest

All authors declare that there are no conflicts of interest.

Authors' Contributions

Bai-Lin Li and Juan-Juan Hu contributed equally to this work.

Acknowledgments

This work was financially supported by the National Natural Science Foundation (No. 81903509).

References

[1] K. R. Chen and P. Ling, "Emerging roles of an innate immune regulator TAPE in toll-like receptors, RIG-I-like receptors, and beyond," *European Journal of Immunology*, vol. 46, p. 646, 2016.

[2] B. Sun and M. Karin, "Obesity, inflammation, and liver cancer," *Journal of Hepatology*, vol. 56, no. 3, pp. 704–713, 2012.

[3] H. Tilg and A. R. Moschen, "Evolution of inflammation in nonalcoholic fatty liver disease: the multiple parallel hits hypothesis," *Hepatology*, vol. 52, no. 5, pp. 1836–1846, 2010.

[4] H. Takeda, A. Takai, T. Inuzuka, and H. Marusawa, "Genetic basis of hepatitis virus-associated hepatocellular carcinoma: linkage between infection, inflammation, and tumorigenesis," *Journal of Gastroenterology*, vol. 52, no. 1, pp. 26–38, 2017.

[5] J. P. Iredale, "Models of liver fibrosis: exploring the dynamic nature of inflammation and repair in a solid organ," *Journal of Clinical Investigation*, vol. 117, no. 3, pp. 539–548, 2007.

[6] M. S. Baig, S. V. Zaichick, M. Mao et al., "NOS1-derived nitric oxide promotes NF-κB transcriptional activity through inhibition of suppressor of cytokine signaling-1," *Journal of Experimental Medicine*, vol. 212, no. 10, pp. 1725–1738, 2015.

[7] S. Harirforoosh, W. Asghar, and F. Jamali, "Adverse effects of nonsteroidal antiinflammatory drugs: an update of gastrointestinal, cardiovascular and renal complications," *Journal of pharmacy & pharmaceutical sciences :a publication of the Canadian Society for Pharmaceutical Sciences, Societe canadienne des sciences pharmaceutiques*, vol. 16, no. 5, pp. 821–847, 2013.

[8] M. Pirmohamed, S. James, S. Meakin et al., "Adverse drug reactions as cause of admission to hospital: prospective analysis of 18 820 patients," *British medical journal*, vol. 329, no. 7456, pp. 15–19, 2004.

[9] P. J. Rooney and R. H. Hunt, "The risk of upper gastrointestinal haemorrhage during steroidal and non-steroidal anti-inflammatory therapy," *Baillière's Clinical Rheumatology*, vol. 4, no. 2, pp. 207–217, 1990.

[10] T. D. Warner, F. Giuliano, I. Vojnovic, A. Bukasa, J. A. Mitchell, and J. R. Vane, "Nonsteroid drug selectivities for cyclo-oxygenase-1 rather than cyclo-oxygenase-2 are associated with human gastrointestinal toxicity: a full in vitro analysis," *Proceedings of the National Academy of Sciences*, vol. 96, no. 13, pp. 7563–7568, 1999.

[11] S. L. Wilson and N. R. Poulter, "The effect of non-steroidal anti-inflammatory drugs and other commonly used non-narcotic analgesics on blood pressure level in adults," *Journal of Hypertension*, vol. 24, no. 8, pp. 1457–1469, 2006.

[12] B. Botz, K. Bolcskei, and Z. Helyes, "Challenges to develop novel anti-inflammatory and analgesic drugs," *Wiley Interdisciplinary Reviews-Nanomedicine and Nanobiotechnology*, vol. 9, no. 3, 2017.

[13] I. Ignat, I. Volf, and V. I. Popa, "A critical review of methods for characterisation of polyphenolic compounds in fruits and vegetables," *Food Chemistry*, vol. 126, no. 4, pp. 1821–1835, 2011.

[14] M.-Y. Huang, J. Lin, K. Lu et al., "Anti-inflammatory effects of cajaninstilbene acid and its derivatives," *Journal of Agricultural and Food Chemistry*, vol. 64, no. 14, pp. 2893–2900, 2016.

[15] E. M. Galati, "Biological effects of hesperidin, a citrus flavonoid .1. antiinflammatory and analgesic activity," *Farmaco*, vol. 49, no. 11, pp. 709–712, 1994.

[16] F. Maione, R. Russo, H. Khan, and N. Mascolo, "Medicinal plants with anti-inflammatory activities," *Natural Product Research*, vol. 30, no. 12, pp. 1343–1352, 2016.

[17] J.-Q. Yuan, X.-Z. Yang, J.-H. Miao et al., "New triterpene glucosides from the roots of Rosa laevigata michx," *Molecules*, vol. 13, no. 9, pp. 2229–2237, 2008.

[18] W. Yingqiang and C. Pngyu, "New taxa of guangdong plants," *Journal of Tropical & Subtropical Botan*, vol. 3, pp. 27–33, 1995.

[19] Y. N. Tian and A.-B. Rosanortriterpenes, "Two new nortriterpenes from the fruits of rosa laevigata var. leiocapus," *Natural Product Research*, p. 8, 2019.

[20] C. G. Barp, C. Mendes, E. Lemos-Senna, and J. Assreuy, "7-nitroindazol-loaded nanoemulsions: preparation, characterization and its improved inhibitory effect on nitric oxide synthase-1," *Nitric Oxide*, vol. 76, pp. 129–135, 2018.

[21] C. Brenner, L. Galluzzi, O. Kepp, and G. Kroemer, "Decoding cell death signals in liver inflammation," *Journal of Hepatology*, vol. 59, no. 3, pp. 583–594, 2013.

[22] M. H. Zaki, T. Akuta, and T. Akaike, "Nitric oxide-induced nitrative stress involved in microbial pathogenesis," *Journal of Pharmacological Sciences*, vol. 98, no. 2, pp. 117–129, 2005.

[23] H. Ohshima and H. Bartsch, "Chronic infections and inflammatory processes as cancer risk factors: possible role of nitric oxide in carcinogenesis," *Mutation Research/Fundamental and Molecular Mechanisms of Mutagenesis*, vol. 305, no. 2, pp. 253–264, 1994.

[24] C. Sano, T. Shimizu, and H. Tomioka, "Effects of secretory leukocyte protease inhibitor on the tumor necrosis factor-alpha production and NF-κB activation of lipopolysaccharide-stimulated macrophages," *Cytokine*, vol. 21, no. 1, pp. 38–42, 2003.

[25] Y. Yamamoto and R. B. Gaynor, "IκB kinases: key regulators of the NF-κB pathway," *Trends in Biochemical Sciences*, vol. 29, no. 2, pp. 72–79, 2004.

[26] S. Ghosh and M. S. Hayden, "New regulators of NF-κB in inflammation," *Nature Reviews Immunology*, vol. 8, no. 11, pp. 837–848, 2008.

[27] B. Gao, "Hepatoprotective and anti-inflammatory cytokines in alcoholic liver disease," *Journal of Gastroenterology and Hepatology*, vol. 27, pp. 89–93, 2012.

[28] A.-R. El-Zayadi, "Heavy smoking and liver," *World Journal of Gastroenterology*, vol. 12, no. 38, pp. 6098–6101, 2006.

[29] Y. Sheng, Y. Ma, Z. Deng, Z. Wang, and L. Ji, "Cytokines as potential biomarkers of liver toxicity induced by dioscorea bulbifera L," *Bioscience Trends*, vol. 8, no. 1, pp. 32–37, 2014.

[30] S. L. Friedman, "Mechanisms of hepatic fibrogenesis," *Gastroenterology*, vol. 134, no. 6, pp. 1655–1669, 2008.

[31] A. M. Elsharkawy and D. A. Mann, "Nuclear factor-κB and the hepatic inflammation-fibrosis-cancer axis," *Hepatology*, vol. 46, no. 2, pp. 590–597, 2007.

[32] M. Mueller, S. Hobiger, and A. Jungbauer, "Anti-inflammatory activity of extracts from fruits, herbs and spices," *Food Chemistry*, vol. 122, no. 4, pp. 987–996, 2010.

[33] E.-M. Choi and J.-K. Hwang, "Investigations of anti-inflammatory and antinociceptive activities of piper cubeba, physalis angulata and rosa hybrida," *Journal of Ethnopharmacology*, vol. 89, no. 1, pp. 171–175, 2003.

[34] M. Liu, Y. Xu, X. Han et al., "Potent effects of flavonoid-rich extract from rosa laevigata michx fruit against hydrogen peroxide-induced damage in PC12 cells via attenuation of oxidative stress, inflammation and apoptosis," *Molecules*, vol. 19, no. 8, pp. 11816–11832, 2014.

[35] X. Tao, X. Sun, L. Xu et al., "Total flavonoids from rosa laevigata michx fruit ameliorates hepatic ischemia/reperfusion injury through inhibition of oxidative stress and inflammation in rats," *Nutrients*, vol. 8, no. 7, pp. 418–432, 2016.

[36] M. Haghani, C. J. B. Michiel, F. Goerlandt, and J. Li, "The scientific literature on corona viruses, COVID-19 and its associated safety-related research dimensions: a scientometric analysis and scoping review," *Safety Science*, vol. 129, Article ID 104806, 2020.

[37] A. M. Leddy, S. D. Weiser, K. Palar, and H. Seligman, "A conceptual model for understanding the rapid COVID-19-related increase in food insecurity and its impact on health and healthcare," *The American Journal of Clinical Nutrition*, 2020.

Hindawi
Evidence-Based Complementary and Alternative Medicine
Volume 2020, Article ID 3843752, 9 pages
https://doi.org/10.1155/2020/3843752

Research Article

Effects of Yinzhihuang Granules on Serum Liver Enzymes in Jaundice Patients: A Real-World Study Based on HIS Data

Cheng Zhang,[1] **Lidan Zhang**,[1] **Jian Lyu**,[1] **Yanming Xie**,[1] **and Yuting Xie**[2]

[1]*Institute of Basic Research in Clinical Medicine, China Academy of Chinese Medical Sciences, Beijing 100700, China*
[2]*School of Statistics, Renmin University of China, Beijing 100872, China*

Correspondence should be addressed to Yanming Xie; ktzu2018@163.com

Received 20 July 2020; Revised 10 September 2020; Accepted 30 September 2020; Published 5 November 2020

Academic Editor: Yunxia Li

Objective. Our aim was to analyze the influence of Yinzhihuang granules on serum liver enzymes in jaundice patients and to provide real-world evidence for the efficacy evaluation of Yinzhihuang granules in treating jaundice. *Methods*. We constructed a data warehouse which integrates real-world electronic medical records from the hospital information system of multiple 3A hospitals in China and used a descriptive statistical method to analyze the changes in the serum liver enzymes of the jaundice patients treated with Yinzhihuang granules and then used Wilcoxon signed-rank to test the changes in the indicators caused by the treatment. *Results*. After being treated with Yinzhihuang granules, the jaundice patients had a decrease in the average serum levels of total bilirubin, indirect bilirubin, aspartate aminotransferase, glutamyl transpeptidase, and alkaline phosphatase, and the differences were statistically significant ($P < 0.05$) but had no significant changes in the average serum levels of direct bilirubin and alanine aminotransferase ($P > 0.05$). *Conclusion*. The data analysis on the real-world electronic medical records demonstrate that Yinzhihuang granules help to reduce jaundice patients' serum levels of total bilirubin, indirect bilirubin, aspartate aminotransferase, glutamyl transpeptidase, and alkaline phosphatase, but there is no evidence that Yinzhihuang granules help to reduce the jaundice patients' serum levels of direct bilirubin and alanine aminotransferase.

1. Introduction

Jaundice, the yellow staining of the skin, sclera, and mucous membrane caused by the elevation of bilirubin, is a common indicator of hepatobiliary diseases [1]. Jaundice occurs when the plasma bilirubin is excessive or when the damaged liver fails to clear bodily bilirubin [2]. In addition to yellow skin, jaundice patients may suffer from stomachache, nausea, fever, weight loss, or itching [3]. The disease should be treated differently in accordance with the different disease etiology, but the general principle is "to remove jaundice, protect liver, reduce enzyme." With the verified effectiveness and very few adverse reactions reported, the traditional Chinese medicine (TCM) has certain advantages in treating jaundice. According to TCM, jaundice is a common clinical syndrome primarily indicated by yellow skin, yellow eye, and yellow urine [4] and has multiple different pathogenesis such as dampness, heat, cold, blood stasis, and spleen deficiency, with pathogenic dampness being the dominant one; thus, the treatment should be based on syndrome differentiation. For the patients with damp-heat brewing internally, Zhongjing Zhang wrote in "Treatise on Febrile Diseases" that Yinchenhao decoction can be used to treat them [5].

Yinzhihuang granule, derived from Yinchenhao decoction, is a proprietary Chinese medicine to treat jaundice. Its ingredients are extracted from *Artemisiae Scopariae Herba*, *Gardeniae Fructus*, *Scutellariae Radix*, and *Lonicerae Japonicae Flos*. According to the drug package insert records, it is effective in clearing heat and detoxifying and clearing dampness and removing jaundice. It can be used to treat jaundice caused by liver-gallbladder dampness-heat with the symptoms of yellow skin and eye, chest pain, nausea and vomiting, reddish yellow urine, and the acute or chronic hepatitis with the aforementioned syndromes.

At present, the evaluation of effectiveness of Yinzhihuang granules on jaundice is based primarily on

randomized controlled trials; for example, the latest systematic review included nine randomized controlled trials [6]. The evaluation demonstrated that the blue light treatment of neonatal pathologic jaundice, when combined with Yinzhihuang granules administration, was better than the sole blue light treatment, in terms of both clinical effective rate and jaundice fading time ($P < 0.05$). In terms of safety studies, no serious adverse reactions have been reported in the literature, but the instructions of Yinzhihuang granules indicate that there are reports of diarrhea, vomiting, and rash.

The elevation of serum liver enzyme levels is common in liver diseases; the abnormalities of liver enzyme indicators are associated with the possible etiology of liver disease. The enzymes that are commonly detected include alanine aminotransferase (ALT), aspartate aminotransferase (AST), alkaline phosphatase (ALP), γ-glutamyl transpeptidase (GGT), and serum bilirubin [7]. These liver enzymes are not only important diagnosis biomarkers but also important indicators of curative effects on, and prognosis of jaundice. The elevation of serum bilirubin levels is the direct cause of jaundice [8]. ALT, present in high concentrations in hepatocyte cytoplasm, is very sensitive to hepatocyte injury and is the most specific traditional biomarker. AST, also present in hepatocytes, can be used to determine whether or not jaundice is caused by liver injury [9], but its liver specificity is relatively low [10]. The elevation of ALP and GGT levels indicate cholestasis. In jaundice patients, the elevation of ALP levels can be used to diagnose obstructive jaundice because it may indicate diffuse hepatocyte dysfunction or severe bile duct obstruction, which obstructs the adequate bile flow [11].

Unlike the traditional randomized controlled trial performed under strict conditions, the real-world study, which can evaluate the actual drug efficacy, is based on the actual medical environment. We performed a retrospective study of hospital electronic medical records data, analyzed the changes in the serum liver enzyme indicators caused by Yinzhihuang granules intervention, and provided the real-world evidences to support Yinzhihuang granules in treating jaundice.

2. Materials and Methods

2.1. Data Source and Normalization. The data we used were taken from a large-scale data warehouse where electronic medical records are integrated and which was constructed, on the basis of the Chinese 3A hospital information system (HIS), by Institute of Basic Research in Clinical Medicine, China Academy of Chinese Medical Sciences [12]. From the warehouse, we extracted the data of 3610 jaundice patients who had been treated with Yinzhihuang granules and who met the jaundice diagnosis standard: serum total bilirubin (TBil) > 17.1 μmol/L (namely, 1.0 mg/dl) [13]. Their laboratory test information was extracted and analyzed, including seven serum liver enzyme indicators: TBil, direct bilirubin (DBil), indirect bilirubin (IBil), ALT, AST, GGT, and ALP.

Because the data used were from different hospitals in the country and they might adopt different standards for the same project, the investigators, to facilitate analysis [14], normalized the data by converting the units of TBil, DBil, and IBil from mg/dl to μmol/L, which entailed multiplying the value by 17.1 [13].

2.2. Inclusion and Exclusion Criteria. The jaundice patients from the HIS database who met the following criteria were included in our study: (1) they were treated with Yinzhihuang granules; (2) their TBil values were greater than 17.1 μmol/L (1.0 mg/dl) for at least one test; (3) there were at least one detection of serum liver enzymes seven days before and seven days after the use of Yinzhihuang granules. On the other hand, those jaundice patients were excluded from the study whose serum liver enzyme detections before and after the medication were both absent.

2.3. Data Definition and Outcome Determination. For every included patient, two sets of liver enzyme data were extracted: one set was obtained within seven days before Yinzhihuang granules treatment, and the other set was obtained within seven days after the medication withdrawal. If there were more than one set of data satisfying the condition, then the latest one within seven days before the treatment was defined to be the "pre-medication physicochemical indicator" and the earliest one within seven days after the medication withdrawal was defined to be the "post-medication physicochemical indicator" [15].

The criteria for liver enzyme abnormality were based on each hospital's respective physicochemical reference value. A liver enzyme indicator is abnormal if it is above the upper bound of the normal values. No matter whether the pre-medication indicators were normal or not, as long as the postmedication indicators were normal, the patient was recorded as "post-medication normal changes." If both the pre- and postmedication indicators were abnormal but the degree of abnormality decreased after the medication, then the patient was also recorded as "post-medication normal changes." If the patient was normal before medication but abnormal after the medication, or abnormal before the medication and more abnormal after the medication, then the patient was recorded as "post-medication abnormal changes" [16].

2.4. Statistical Analysis Methods and Software. All the data analyses were performed by the software SAS 9.4. We did the descriptive statistics and quantitative analysis on the general data of the jaundice patients' serum liver enzymes tested before and after the medication. For the normally distributed variables, the mean, standard deviation, median value, maximum value, and minimum value were obtained. For the nonnormally distributed variables, the median value, interquartile range, maximum value, and minimum value were obtained. Qualitative analysis was performed on the normal/abnormal changes of the jaundice patients' liver enzymes caused by the medication; namely, the

postmedication live enzyme values were compared to the premedication live enzyme values. When the difference between the two datasets followed the normal distribution, it was tested by the paired sample t-test. When the difference did not follow the normal distribution, it was tested by the nonparametric test (Wilcoxon signed-rank). $P < 0.05$ was considered statistically significant.

3. Results

3.1. The Characteristics of the Jaundice Patients. The demographic and clinical characteristics of the 3610 patients with jaundice are shown in Table 1. Among the patients, 68.67% were male and approximately 50% were older than 45. The patients had an average age of 39.33 (median: 45). For the treatment, the average single dose was 5.66 g (median: 6), and the average duration was 6.62 days (median: 4).

3.2. Description and Analysis of the Liver Enzyme Indicators before and after the Medication. We respectively described and analyzed the general data of the jaundice patients' liver enzymes tested before medication (Table 2) and after medication (Table 3). We compared the jaundice patients' postmedication liver enzyme data boxplot with the premedication boxplot (Figures 1–7) and found that, while the average levels of TBil, IBil, AST, GGT, and ALP decreased after the medication, the average levels of DBil and ALT did not change significantly. In the figures, the middle line represents the average level of the liver enzyme analyzed.

3.3. Qualitative Analysis of Liver Enzyme Changes after the Medication. The liver enzyme changes in jaundice patients are presented in Tables 4 and 5, which show that, for most patients, the serum liver enzyme levels decreased after Yinzhihuang granule treatment. The patients with decreased IBil and TBil levels comprised the largest percentages, 61.22% and 56.64%, respectively, of the total patients. After Yinzhihuang granule treatment, the serum liver enzyme levels of most jaundice patients returned to normal. The patients with ALT and ALP levels normalized comprised the largest percentages, 81.93% and 79.22%, respectively, of the total patients.

3.4. Test of the Difference in Liver Enzyme Indicators before and after the Medication. Because the difference in liver enzyme indicators before and after the medication did not follow the normal distribution, we performed a nonparametric test known as Wilcoxon signed-rank, with the results presented in Table 6, from which one sees that the average TBil, IBil, GGT, and ALP levels decreased after Yinzhihuang granule treatment. Because P values were all less than 0.05, the differences were statistically significant, and the null hypothesis was rejected, demonstrating that the test results had a difference before and after the medication. TBil was an important indicator for diagnosing and judging the severity of jaundice, which can be used to estimate the curative effect. If TBil increased with the IBil increased significantly, it might be diagnosed as hemolytic jaundice [13]. The decrease of TBil and IBil indicated that Yinzhihuang granules can improve the degree of jaundice. The increase of GGT and ALP was more common in cholestatic jaundice [17]. The decrease of their values proved that cholestasis has been alleviated in patients with jaundice. After the Yinzhihuang granule treatment, the patients' average DBil level raised slightly and the average ALT level decreased, but both P values were greater than 0.05 ($P = 0.3801$ and 0.0656, respectively), indicating that the differences were not statistically significant. After the Yinzhihuang granule treatment, the patients' average AST level

Table 1: The demographic and clinical characteristics of the jaundice patients.

Characteristic	Population
Gender	
Male	2479
Female	1087
Missing	44
Age	
≤12 yr	760
12–18 yr	54
18–45 yr	1029
45–65 yr	1242
65–85 yr	507
>85 yr	16
Hospitalization time	
≤3 d	242
3–7 d	491
7–14 d	831
14–28 d	1065
Missing	67
Western medicine diagnosis[a]	
Neonatal hyperbilirubinemia	238
Pulmonary tuberculosis	170
Chronic active hepatitis B	79
TCM syndrome[b]	
Damp-heat brewing internally	67
Deficiency of both qi and blood	32
Yang qi deficiency	32
Single dose	
≤6 g	3337
6–12 g	47
12–18 g	16
18–30 g	37
30–60 g	23
>60 g	20
Missing	6
Course of treatment	
≤3 d	1269
4–7 d	567
8–14 d	530
15–28 d	432
Missing	649
Combined use of drugs[c]	
TCM: Ganmao Qingre granules	416
TCM: Kuhuang injection	382
TCM: Bupleurum injection	360
Western medicine: glycyrrhizic acid	1831
Western medicine: thymosin	1028
Western medicine: dexamethasone	592

[a,b,c]The top three in population.

Table 2: Description of premedication serum liver enzyme indicators (nonnormal distribution)*.

Variable	Number of case (*n*)	Median	Lower quartile	Interquartile range	Upper quartile	Minimum	Maximum
TBil (μmol/L)	952	79.00	35.50	169.80	205.30	12.00	609.60
DBil (μmol/L)	1027	16.90	9.00	37.00	46.00	0.10	402.90
IBil (μmol/L)	241	66.10	27.20	134.40	161.60	8.50	379.30
ALT (U/L)	596	25.00	13.00	50.50	63.50	4.00	3160.0
AST (U/L)	586	62.00	38.00	83.00	121.00	6.00	2232.0
GGT (U/L)	706	105.00	43.00	181.00	224.00	4.00	2487.0
ALP (U/L)	732	143.50	100.00	107.50	207.50	43.60	2098.0

*The number of cases (*n*) counts the patients who had a premedication test.

Table 3: Description of the postmedication serum liver enzyme indicators (nonnormal distribution)*.

Variable	Number of case (*n*)	Median	Lower quartile	Interquartile range	Upper quartile	Minimum	Maximum
TBil (μmol/L)	549	69.10	28.20	146.20	174.40	5.70	766.60
DBil (μmol/L)	550	14.75	8.00	30.50	38.50	0.30	560.20
IBil (μmol/L)	62	43.55	19.80	72.90	92.70	10.10	289.90
ALT (U/L)	245	27.00	14.00	57.00	71.00	3.00	3160.0
AST (U/L)	225	29.00	35.00	82.00	117.00	15.00	13750.0
GGT (U/L) 357	94.00	43.00	173.00	216.00	9.00	3645.00	
ALP (U/L) 349	124.00	91.00	97.00	188.00	15.00	1683.00	

*The number of cases (*n*) counts the patients who had a postmedication test.

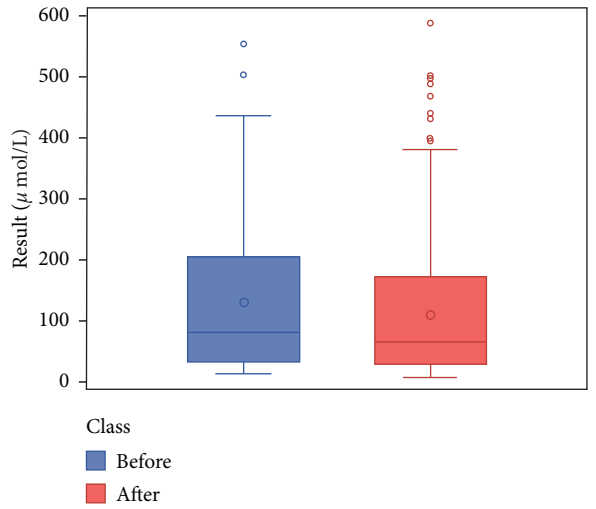

Figure 1: TBil boxplot ($n = 369$).

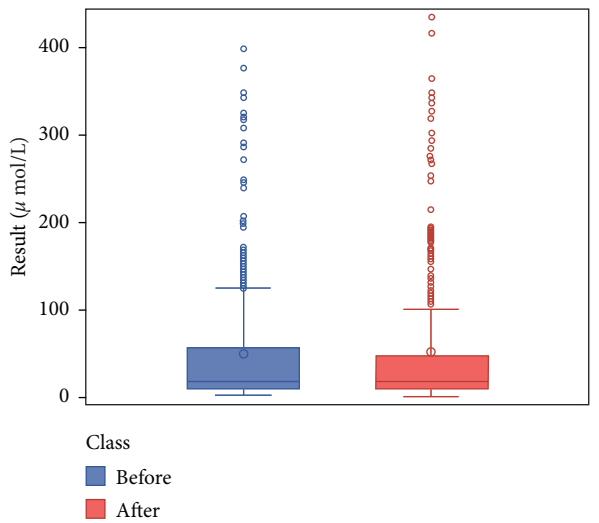

Figure 2: DBil boxplot ($n = 392$).

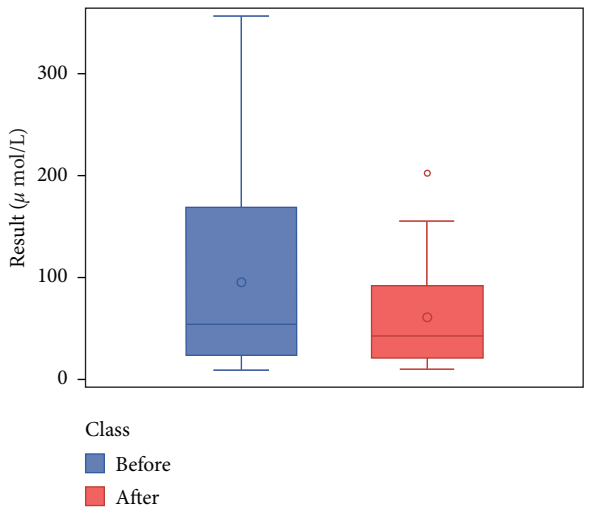

Figure 3: IBil boxplot ($n = 49$).

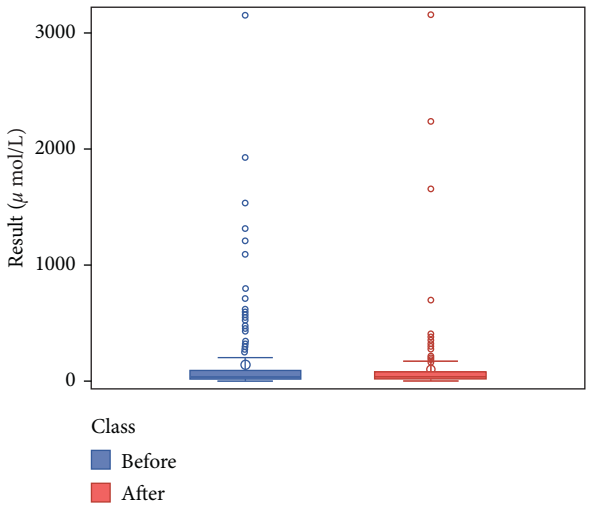

Figure 4: ALT boxplot ($n = 166$).

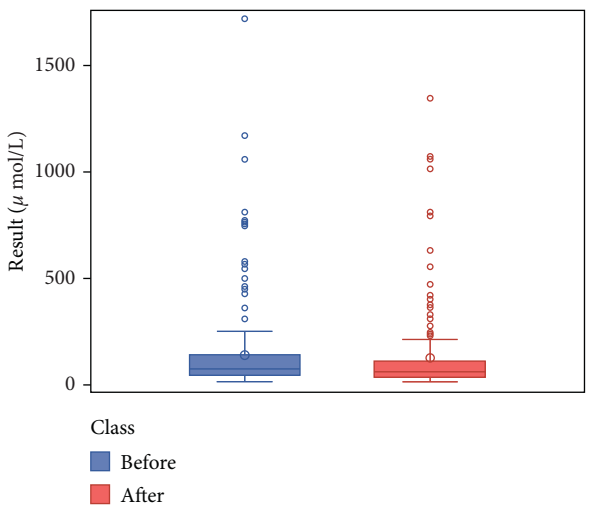

Figure 5: AST boxplot ($n = 158$).

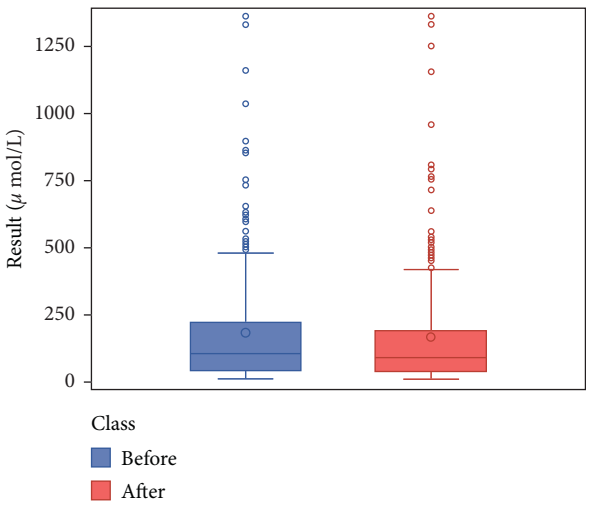

Figure 6: GGT boxplot ($n = 228$).

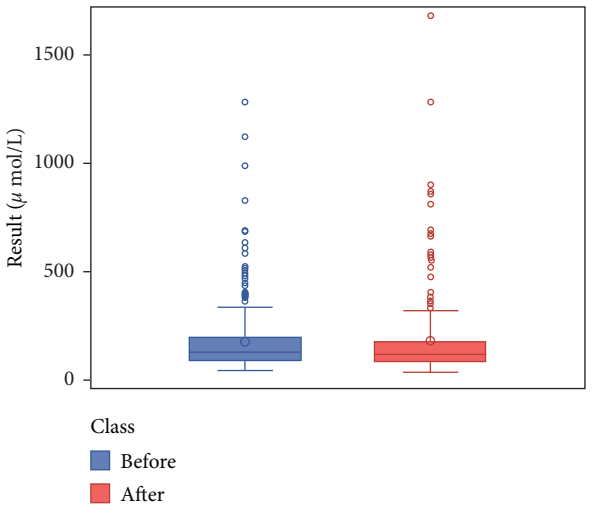

Figure 7: ALP boxplot ($n = 231$).

markedly elevated. Considering that both sets of data were not normally distributed, the mean value may be inappropriate to describe the central tendency, and the use of the median value may be more reasonable. The postmedication median AST level of the jaundice patients was 29.00 U/L, which was lower than that before the medication (62.00 U/L). Because $P = 0.0278$, the difference was statistically significant. The determination of ALT and AST showed that before the treatment of Yinzhihuang granules, the values of ALT and AST in patients with jaundice were 1.2 times higher than the normal upper limit, which reached the standard of diagnosis of liver injury [18]. After drug intervention, the values of ALT and AST decreased significantly, which showed that Yinzhihuang granules could reduce the degree of liver injury in patients with jaundice.

4. Discussion

4.1. Effects of Yinzhihuang Granules on Liver Enzyme Indicators in Jaundice Patients. TCM has a long history in

Table 4: Changes of serum liver enzyme indicators after the medication (decrease/increase).

Variable	Decrease/counts	Increase/counts	Invariance/counts	Total
TBil (μmol/L)	209 (56.64%)	88 (23.85%)	72 (19.51%)	369 (100%)
DBil (μmol/L)	177 (45.15%)	13 (35.20%)	77 (19.64%)	392 (100%)
IBil (μmol/L)	30 (61.22%)	16 (32.65%)	3 (6.12%)	49 (100%)
ALT (U/L)	78 (46.99%)	60 (36.14%)	28 (16.87%)	166 (100%)
AST (U/L)	84 (53.16%)	54 (34.18%)	20 (12.66%)	158 (100%)
GGT (U/L)	122 (53.51%)	73 (32.02%)	33 (14.47%)	228 (100%)
ALP (U/L)	119 (51.52%)	79 (34.20%)	33 (14.29)	231 (100%)

Table 5: Classification of serum liver enzyme indicators after the medication (normal/abnormal).

Variable	Normal/counts	Abnormal/counts	Total
TBil (μmol/L)	281 (76.15%)	88 (23.85%)	369 (100%)
DBil (μmol/L)	268 (68.37%)	124 (31.63%)	392 (100%)
IBil (μmol/L)	35 (71.43%)	14 (28.57%)	49 (100%)
ALT (U/L)	136 (81.93%)	30 (18.07%)	166 (100%)
AST (U/L)	114 (72.15%)	44 (27.85%)	158 (100%)
GGT (U/L)	177 (77.63%)	51 (22.37%)	228 (100%)
ALP (U/L)	183 (79.22%)	48 (20.78%)	231 (100%)

treating jaundice. Huang Di Nei Jing stated that "when heat and dampness intersect, the people become sick." According to Huang Di Nei Jing, the primary pathogenesis of jaundice is the accumulation of dampness and heat, which is caused by the pathogenic wind, which combines Yang with internal dampness, heat, and dampness accumulates in the spleen and spreads to the muscle surface. In treatment, it is necessary to remove dampness and yellow and dredge the viscera to relieve heat [19]. Zhongjing Zhang believes that the main cause of jaundice is spleen dampness and heat stasis, and the disease lies in Yangming Meridian, which is discussed in article 236: "Yangming disease, fever and sweating, this is heat, cannot yellowing. But the head is sweating, the body is not sweaty, the neck is close to the neck, and the urination is disadvantageous, and those who thirst for water are stagnant and hot, and the body will turn yellow. Yinchenhao decoction is the main one." It is considered that jaundice caused by damp-heat should be treated with Yinchenhao decoction [20]. Yinzhihuang granules are derived from Yinchenhao decoction. The prescription consisting of four Chinese medicines (*Artemisiae Scopariae Herba*, *Scutellariae Radix*, *Gardeniae Fructus*, and *Lonicerae Japonicae*) [21] is used to treat jaundice caused by liver-gallbladder dampness-heat. The prescription retains the two main medicines in Yinchenhao decoction (*Artemisiae Scopariae Herba* and *Gardeniae Fructus*) with the strong purgative effect changed in *Scutellariae Radix* and *Lonicerae Japonicae*, which can slow down its purging ability and enhance its effect of clearing heat and removing dampness. According to TCM, the monarch drug *Artemisiae Scopariae Herba* is bitter, acrid, and slightly cold and has the effects of clearing damp-heat, increasing choleresis, and relieving jaundice [22]; the minister drug *Gardeniae Fructus* is bitter and cold and has the effects of purging fire, relieving restlessness, and clearing damp-heat [23]; *Scutellariae Radix* is bitter and cold and has the effects of clearing away heat and dry dampness, purging fire to eliminate toxin [24], and the compatibility of the three medicines strengthens the effect of clearing away dampness and heat; *Lonicerae Japonicae Flos* is cold and tastes sweet and has the effects of clearing heat, detoxifying, and anti-inflammation [25]. The four Chinese medicines work together compatibly to play the role of clearing heat and detoxifying and clearing dampness and removing jaundice. The clinical application of Yinzhihuang granules is mostly to treat neonatal jaundice [26] whose effectiveness has been verified in clearing jaundice and reducing enzyme activity. For example, some scholars demonstrated that Yinzhihuang granules, when combined with intermittent blue light irradiation, can reduce the bilirubin levels in jaundice neonates [27], the GGT levels, and the ALP levels; the differences were statistically significant ($P < 0.05$); the effectiveness and safety were both better than the sole blue light irradiation treatment [28].

The present study demonstrated that the jaundice patients' average serum TBil, IBil, AST, GGT, and ALP levels decreased after the Yinzhihuang granule treatment ($P < 0.05$), but their ALT levels were not significantly affected. Although the ALT levels decreased by 17.11 U/L, the difference was not statistically significant because $P = 0.0656$. After the Yinzhihuang granule treatment, the average DBil level increased by 3.77 μmol/L ($P > 0.05$). This elevation might be associated with the change of the conditions of the patients who had not yet recovered. These results, which were obtained by analyzing the existing real-world HIS data, demonstrate that Yinzhihuang granules help to reduce the jaundice patients' TBil ($P < 0.0001$), IBil ($P = 0.0017 < 0.05$), AST ($P = 0.0278 < 0.05$), GGT ($P = 0.0002 < 0.05$), and ALP ($P = 0.0009 < 0.05$) levels, but do not imply that Yinzhihuang granules help to reduce the jaundice patients' DBil ($P = 0.3801 > 0.05$) and ALT ($P = 0.0656 > 0.05$) levels.

The pharmacological mechanisms of Yinzhihuang granules have not yet been completely understood due to its complex active ingredients and versatile action pathways. Modern pharmacological studies have found that the volatile oil component contained in the monarch drug *Artemisiae Scopariae Herba* can obviously antagonize the serum ALT and AST activities induced by carbon tetrachloride (CCl4) in mice with liver injury and can thus protect the liver from CCl4 injury [29]. By inducing the liver enzyme system, *Artemisiae Scopariae Herba* enhances the liver's absorption, binding, and excretion of bilirubin and promotes the removal of bilirubin [30]. The minister drug *Gardeniae Fructus* may play an anticholestasis role by participating in biological

Table 6: Difference in the serum liver enzyme levels before and after the medication.

Variable	Number of case (*n*)	Premedication (mean ± SD)	Postmedication (mean ± SD)	Statistics (*S*)	*P* value
TBil (μmol/L)	369	126.46 ± 109.82	112.42 ± 109.64	9106.50	≤0.001
DBil (μmol/L)	392	43.19 ± 62.70	46.96 ± 79.43	1422.50	0.3801
IBil (μmol/L)	49	96.22 ± 82.22	63.03 ± 53.66	277.00	0.0017
ALT (U/L)	166	108.87 ± 295.46	91.76 ± 282.56	865.50	0.0656
AST (U/L)	158	135.55 ± 241.51 Median = 62.00	200.28 ± 986.27 Median = 29.00	1031.50	0.0278
GGT (U/L)	228	190.13 ± 250.46	182.61 ± 288.87	2872.50	≤0.001
ALP (U/L)	231	187.77 ± 163.00	186.43 ± 197.09	2656.50	≤0.001

processes such as the acute inflammatory response, positive regulation of reactive oxygen metabolism, and nitric oxide anabolism [31], thereby promoting bilirubin excretion [32]. In one study, Yinzhihuang granules were used to intervene estrogen-induced cholestasis in rats. After 14 days, it was found that the bile flow rate and the total bile flux increased, and that the levels of ALT, AST, ALP, TBil, DBil, IBil, and total bile acid (TBA) were significantly reduced [33]. The mechanism of removing jaundice and increasing choleresis may be the upregulation of the expression of multidrug resistance transporters Mrp2 and Mrp3 in the hepatocyte membrane and the enhancing of the excretion capability of hepatocytes with cholestasis [34], thereby reducing the accumulation of bilirubin and cholate in the hepatocytes [35]. Through network pharmacology studies, some scholars found that the target of Yinzhihuang granule-aided liver disease treatment may be the epidermal growth factor receptor (EGFR). Studies have confirmed that the EGFR plays an indispensable role in hepatocytes repair and regeneration and is a key regulator of the hepatocytes proliferation in the early stage of liver regeneration [36]. By promoting the proliferation of hepatocytes, EGFR plays a role in resisting liver damage [37]. There was a synergistic effect among the four traditional Chinese medicines of Yinzhihuang granules. Studies have confirmed that these four herbs can act directly on target proteins such as the androgen receptor, retinoic acid receptor β, and hepatocyte growth factor receptor, mainly by interfering with the phosphatidylinositol 3-kinase (phosphatidylcholine3-kinase, PI3K) signal pathway [37]. Among them, the hepatocyte growth factor was been proved to regulate the initiation of $CD8^+$ T cells in the hepatitis virus model, thus inhibiting liver inflammation and injury [38]. It was also an important biomarker for the diagnosis of biliary obstruction and liver injury in patients with obstructive jaundice [39].

Taken the present information together, Yinzhihuang granules have the following four mechanisms to remove jaundice, protect liver, and reduce enzyme activities: (1) preventing liver injury by antagonizing the serum ALT and AST activities induced by CCl4; (2) anticholestasis, promoting bilirubin excretion and clearance; (3) upregulating the expression of Mrp2 and Mrp3, reducing the accumulation of bilirubin; and (4) promoting the proliferation, repair, and regeneration of hepatocytes, thereby protecting the liver.

Although the above studies have beneficially explored from different angles, the mechanisms of Yinzhihuang granules in removing jaundice and reducing enzyme activities, more bioinformatics studies and experimental verifications are further needed to learn the mechanisms of multiingredient, multitarget, and multipathway drug action to remove jaundice and reduce enzyme activities, in consideration that the active ingredients of Yinzhihuang granules are complex and unclear, as well as the ingredient targets.

4.2. Real-World Research Based on the HIS Database. As a new research field, real-world studies have received ever-increasing attentions from the broad masses of doctors, researchers, and policy makers and have thus exerted profound influences upon the formulation of health policies. In 2010, Yanming Xie's research group published an article entitled "real-world research: a new idea for evaluating the effect of traditional Chinese medicine intervention measures," which introduced the concept of real-world research to China for the first time [40]. After nearly a decade of development, China's real-world research has made progress in the fields of postmarketing evaluation of drugs, medical insurance decision-making, and medical equipment supervision. In the field of TCM, some scholars found that the primary applications of real-world research are the effectiveness and safety evaluation of the proprietary Chinese medicines after entering the market. Because 49.60% of the data were from HIS [41], HIS-based data analysis is the main mode of real-world research in the present field of TCM. The real-world evidences obtained by the HIS-based analysis make up to a certain degree the extrapolation limits of randomized controlled trial conclusions and can better evaluate the actual therapeutic effect and safety of a proprietary Chinese medicine in the practical medical environment [42]. Although the efficacy of Yinzhihuang granules in treating jaundice has been confirmed by a number of randomized controlled trials, the questions have not been answered by relevant research studies such as the actual effects of clinical application and the influence upon the liver enzyme indicators. By extracting a huge amount of data from many 3A hospitals in China, a large-scale electronic medical record integration data warehouse was established by the Institute of Basic Research in Clinical Medicine, China Academy of Chinese Medical Science [43]. Through processes such as data cleaning and standardization, the analyzable real-world data were finally formed, which laid the groundwork for the evaluation of the safety

and real-world effectiveness of Yinzhihuang granules after entering into the market. Through the analysis of HIS data by the descriptive statistical method and nonparametric test (Wilcoxon sign-ranked), we obtained the actual intervention effect of Yinzhihuang granules on the serum liver enzymes of jaundice patients in the real medical environment, and the results were consistent with the relevant literature. The real-world evidence obtained in this study can supplement to some degree the evidence chain of the effectiveness evaluation of Yinzhihuang granules after entering into the market and provide reference and basis for further clinical trials and research studies on pharmacological mechanisms.

However, HIS data-based real-world studies are limited by data missing and confounding factors, which reduce to some degree the accuracy of causal inference. This study only described the changes of serum liver enzyme indicators in jaundice patients, without considering the other factors that could affect the curative effect (e.g., the use of other drugs to treat jaundice may decrease the levels of serum liver enzymes); thus, the causal inference of therapeutic outcomes was not very convincing. Randomized controlled trials remained the primary means of efficacy evaluation. For the next step, the results should be verified by carrying out multicenter, randomized, double-blind, controlled trials that are of high-quality and prospective; the pharmacological mechanisms also need to be further studied. Moreover, this study was not able to evaluate the safety of treating jaundice patients with Yinzhihuang granules due to the lack of records of adverse reactions and the fact that the patients were not followed up for a certain period. Prospective, multicenter, safe hospital monitoring should also be the focus of the next step research.

5. Conclusions

Based on the existing real-world HIS data analysis, we found that Yinzhihuang granules help to decrease jaundice patients' TBil, IBil, AST, GGT, and ALP levels; there are no evidence of Yinzhihuang granules decreasing jaundice patients' DBil and ALT levels.

Data Availability

The datasets used and/or analyzed during the current study are available from the corresponding author upon request.

Conflicts of Interest

The authors declare that they have no conflicts of interest.

Acknowledgments

The authors would like to thank Yan Zhuang for the extraction of HIS data. This work was supported by the National Key R&D Program of China (2018YFC1707400).

References

[1] X. Li, W. L. Yu, S. Xu, S. Shi, and Y. J. Zhang, "The animal experimental study of the function of magnesium isoglycyrrhizinate for the liver protective effect during the liver injury induced by biliary obstruction," *Progress in Modern Biomedicine*, vol. 15, pp. 425–428, 2015.

[2] J. Winger and A. Michelfelder, "Diagnostic approach to the patient with jaundice," *Primary Care: Clinics in Office Practice*, vol. 38, no. 3, pp. 469–482, 2011.

[3] AAFP, "Jaundice in adults," *American Family Physician*, vol. 95, 2017.

[4] M. H. Wu and X. Y. Wang, "TCM internal medicine," in *Hepatobiliary Syndrome: The Jaundice*, P. X. Xiao, Ed., p. 250, 9nd edition, China Press of Traditional Chinese Medicine, Beijing, China, 2012.

[5] X. Li, X. Y. Wang, and S. Y. Wang, "Differentiation and treatment of jaundice with reference to treatise on cold pathogenic and miscellaneous diseases and internal medicine of traditional Chinese Medicine," *Shandong University of Traditional Chinese Medicine*, vol. 44, pp. 19–22, 2020.

[6] L. H. Cheng and W. C. Zhang, "System evaluation of Yinzhihuang granules combined with blue light irradiation treating to newborn pathological jaundice," *Jiangxi University of Traditional Chinese Medicine*, vol. 30, pp. 44–48, 2018.

[7] S. Agrawal, R. K. Dhiman, and J. K. Limdi, "Evaluation of abnormal liver function tests," *Postgraduate Medical Journal*, vol. 92, no. 1086, p. 223, 2016.

[8] S. Mitra and J. Rennie, "Neonatal jaundice: aetiology, diagnosis and treatment," *British Journal of Hospital Medicine*, vol. 78, no. 12, pp. 699–704, 2017.

[9] R. J. Church and P. B. Watkins, "In silico modeling to optimize interpretation of liver safety biomarkers in clinical trials," *Experimental Biology and Medicine*, vol. 243, no. 3, pp. 300–307, 2018.

[10] D. D. Houlihan, P. N. M. J. Armstrong, and P. N. Newsome, "Investigation of jaundice," *Medicine*, vol. 39, no. 9, pp. 518–522, 2011.

[11] B. Gondal and A. Aronsohn, "A systematic approach to patients with jaundice," *Seminars in Interventional Radiology*, vol. 33, no. 4, pp. 253–258, 2016.

[12] Y. Zhuang, B. T. Xie, S. X. Weng, and Y. M. Xie, "Construction and realization of real world integrated data warehouse from HIS on re-evaluation of post-maketing traditional Chinese medicine," *China Journal of Chinese Materia Medica*, vol. 36, no. 20, pp. 2883–2887, 2011.

[13] X. H. Wan, X. F. Liu, and C. Y. Liu, "Diagnostics," in *The Jaundice*, J. Wu and Y. Q. Zhang, Eds., People's Medical Publishing House, Beijing, China, 9nd edition, 2018.

[14] J. Yang, L. Li, Y. M. Xie, H. Shen, and Y. Zhuang, "Outcome study on parenterally administered Shenfu in treatment of coronary heart disease," *China Journal of Chinese Materia Medica*, vol. 38, pp. 3099–3103, 2013.

[15] Y. Zhang, W. Yang, J. J. Jiang, Z. F. Wang, and L. Li, "Impact analysis of the clinical use of shenfu injection on liver function by using propensity score methods," *Liaoning University of Traditional Chinese Medicine*, vol. 18, pp. 66–70, 2016.

[16] Q. H. Ai, Y. M. Xie, L. Li, and W. Yang, "Research on the effect of Shenqifuzheng injection on aspartate aminotransferase in real world:with propensity score analysis," *Journal of Traditional Chinese Medicine*, vol. 55, pp. 1596–1600, 2014.

[17] Y. Zhang, H.-Y. Jiang, Y. Wei, and B. Song, "Sinusoidal obstruction syndrome: a systematic review of etiologies, clinical symptoms, and magnetic resonance imaging features," *World Journal of Clinical Cases*, vol. 7, no. 18, pp. 2746–2759, 2019.

[18] X. H. Xiao, X. H. Li, Y. Zhu et al., "Guideline for diagnosis and treatment of herb-induced liver injury," *China Journal of Chinese Materia Medica*, vol. 41, pp. 1165–1172, 2016.

[19] L. L. Li, "Experience in the treatment of damp-heat jaundice with traditional Chinese medicine," *Yunnan Journal of Traditional Chinese Materia Medica*, vol. 26, 2005.

[20] X. L. Wang, G. Y. Huang, K. J. Zhao et al., "Clinical research progress of Jingfang in the treatment of jaundice," *Clinical Traditional Chinese Medicine*, vol. 31, pp. 792–795, 2019.

[21] Q. W. Kang and S. Yan, "Progress in pharmacological action and clinical application of Yinchenhao decoction," *Chinese Journal of Integrated Traditional and Western Medicine*, vol. 19, pp. 473–475, 2013.

[22] Y. P. Liu, X. Y. Qiu, Y. Liu, and G. Ma, "Research progress on pharmacological effect of Artemisiae Scopariae Herba," *Chinese Traditional and Herbal Drugs*, vol. 50, pp. 2235–2241, 2019.

[23] Y. P. Shi, H. T. Kong, H. N. Li et al., "Research progress on chemical composition and pharmacological effects of Gardenia jasminoides and predictive analysis on quality marker (Q-marker)," *Chinese Traditional and Herbal Drugs*, vol. 50, pp. 281–289, 2019.

[24] J. Y. Wang, "Research progress on pharmacological effects of scutellaria baicalensis Georgi," *Mongol Journal of Traditional Chinese Medicine*, vol. 39, pp. 167-168, 2020.

[25] Y. F. Liu, L. P. Li, H. Y. Ma et al., "Research progress on the chemical constituents and pharmacological effects of lonicera Japonica Thunb," *Journal of Liaoning Normal University(Natural Science)*, vol. 45, pp. 255–262, 2018.

[26] M. Cao, "The effect of Yinzhihuang combined blue light therapy on breast milk jaundice," *Journal of North Pharmacy*, vol. 13, pp. 36-37, 2016.

[27] J. Q. Luo and J. L. Rao, "Yinzhihuang granule combined with intermittent blue light irradiation in the treatment of 42 cases of neonatal jaundice," *Guangming Journal of Chinese Medicine*, vol. 34, pp. 3644-3645, 2019.

[28] Y. Ma, L. Gu, L. Gao, and Z. Y. Gu, "Clinical Observation and safety analysis of blue light irradiation combined with Yindanhuang granule on neonatal jaundice," *WJTCM*, vol. 14, pp. 3237–3240, 2019.

[29] Q. Gao, X. Zhao, L. Yin et al., "The essential oil of Artemisia capillaris protects against CCl4-induced liver injury in vivo," *Revista Brasileira De Farmacognosia*, vol. 26, no. 3, pp. 369–374, 2016.

[30] O. Ulicná, M. Greksák, O. Vancová et al., "Hepatoprotective effect of rooibos tea (Aspalathus linearis) on CCl4-induced liver damage in rats," *Physiological Research*, vol. 52, no. 4, pp. 461–466, 2003.

[31] H. Chen, X. Gao, W. Zhao et al., "Mechanism of gardenia jasminoides against cholestasis based on network pharmacology," *China Journal of Chinese Materia Medica*, vol. 44, pp. 2709–2718, 2019.

[32] Y. Li, X. X. Gao, and X. M. Qin, "Advances in research of traditional Chinese medicine for promoting bile secretion and excretion," *China Journal of Chinese Materia Medica*, vol. 45, pp. 1287–1296, 2020.

[33] G. Q. Zhang, *Preliminary Study on the Mechanism of Yinzhihuang Granule in the Treatment of Estrogen-Induced Cholestasis in Rats*, Lanzhou University, Lanzhou, China, 2012.

[34] O. Fardel, E. Jigorel, M. Le Vee, and L. Payen, "Physiological, pharmacological and clinical features of the multidrug resistance protein 2," *Biomedicine & Pharmacotherapy*, vol. 59, no. 3, 2005.

[35] G. Q. Zhang, "Study on the cholagogic mechanism of Yinzhihuang granule based on hepatocyte membrane multidrug resistance-related transporter," in *Proceedings of the China Pharmaceutical Congress and the 13th China Pharmacists Week*, Guangxi, China, 2013.

[36] K. Komposch and M. Sibilia, "EGFR signaling in liver diseases," *International Journal of Molecular Sciences*, vol. 17, no. 1, p. 30, 2015.

[37] H. Wang, J. Xie, H. F. He, Y. M. Pan, and Y. L. Zhao, "Network pharmacology study of liver disease adjuvant characteristics of Yinzhihuang granules based on correlation mechanism," *Evaluation Analysis Drug-use Hospitals China*, vol. 16, pp. 1585–1587, 2016.

[38] N. Molnarfi, M. Benkhoucha, H. Funakoshi, T. Nakamura, and P. H. Lalive, "Hepatocyte growth factor: a regulator of inflammation and autoimmunity," *Autoimmunity Reviews*, vol. 14, no. 4, pp. 293–303, 2015.

[39] N. Ozturk, G. Ozturk, S. Cerrah et al., "Evaluation of liver function by means of serum cytokeratin 18 and hepatocyte growth factor levels in patients with obstructive jaundice," *Acta Chirurgica Belgica*, vol. 118, no. 3, pp. 167–171, 2018.

[40] F. Tian and Y. M. Xie, "Real-world study: a potential new approach to effectiveness evaluation of traditional Chinese medicine interventions," *Journal of Chinese Integrative Medicine*, vol. 8, no. 4, pp. 301–306, 2010.

[41] J. Chen, Y. Sun, Y. X. Bu, and J. H. Tian, "Analysis of real world studies on traditional Chinese medicine in China," *Chinese Journal of Evidence-Based Medicine*, vol. 18, pp. 1216–1223, 2018.

[42] X. Sun, J. Tan, L. Tang, L. Li, and W. Wang, "Synergy between observational and experimental studies in the real-world research," *Chinese Journal of Evidence-Based Medicine*, vol. 18, pp. 277–283, 2018.

[43] M. Y. Gao, Y. M. Xie, Y. Zhang, C. Chen, and Y. Zhuang, "Research on clinical application of Fufangkushen injection in treating indication (therioma) in real world based on hospital information system database," *Chinese Traditional and Herbal Drugs*, vol. 49, pp. 3143–3147, 2018.

Hindawi
Evidence-Based Complementary and Alternative Medicine
Volume 2020, Article ID 5956940, 10 pages
https://doi.org/10.1155/2020/5956940

Research Article

Differences in MicroRNA Expression in Chronic Hepatitis B Patients with Early Liver Fibrosis Based on Traditional Chinese Medicine Syndromes

Mei-Jie Shi,[1,2] Huan-Ming Xiao,[1] Yu-Bao Xie,[1] Jun-Min Jiang,[1] Peng-Tao Zhao,[1] Gao-Shu Cai,[1] Ying-Xian Li,[1] Sheng Li,[1] Chao-Zhen Zhang,[1] Min-Ling Cao,[1] Qu-Bo Chen,[1] Zhi-Jian Tan,[1] Heng-Jun Gao,[3,4] and Xiao-Ling Chi [1]

[1]*The Second Affiliated Hospital of Guangzhou University of Chinese Medicine, Guangdong Provincial Hospital of Chinese Medicine, Guangzhou 510120, China*
[2]*Guangzhou University of Chinese Medicine, Guangzhou 510006, China*
[3]*National Engineering Center for Biochip at Shanghai, Shanghai 201203, China*
[4]*Institute of Digestive Diseases, School of Medicine, Tongji University, Tongji Hospital Affiliated to Tongji University, Shanghai 200065, China*

Correspondence should be addressed to Xiao-Ling Chi; chixiaolingqh@163.com

Received 28 May 2020; Revised 15 August 2020; Accepted 17 September 2020; Published 31 October 2020

Academic Editor: Yunxia Li

The aim of this study was to determine if microRNA (miRNA) expression is different among chronic hepatitis B (CHB) patients with early liver fibrosis classified according to traditional Chinese medicine (TCM) syndromes. Eighteen CHB-fibrosis patients and 12 CHB patients without fibrosis were enrolled. The CHB-fibrosis group included 9 patients with the TCM syndrome of Ganyu Pixu Xueyu (GYPXXY), characterized by liver stagnation, spleen deficiency, and blood stasis, and 9 patients with the TCM syndrome of Qixu Xueyu (QXXY), characterized by deficiency of qi, blood, and blood stasis. Agilent miRNA microarray was performed first in liver specimens to determine whether miRNA expression is different in patients with these two TCM syndromes of CHB-fibrosis. Gene Ontology (GO) analysis and KEGG analysis were applied to determine the roles of the differentially expressed miRNAs. QRT-PCR was performed to validate the Agilent miRNA microarray results. Compared with GYPXXY patients, 6 differentially expressed miRNAs were upregulated (miR-144-5p, miR-18a-5p, miR-148b-3p, miR-654-3p, miR-139-3p, and miR-24-1-5p) and 1 was downregulated (miR-6834-3p) in QXXY patients. According to qRT-PCR data, miR-144-5p and miR-654-3p were confirmed as upregulated in CHB-liver fibrosis patients compared to CHB patients without fibrosis, whereas the other 4 miRNAs were not significantly different. More importantly, miR-654-3p was confirmed to be significantly upregulated in QXXY patients compared with values in GYPXXY patients, whereas no significant difference was found in miR-144-5p. Moreover, the pathways of central carbon metabolism in cancer and cell cycle related to miR-654-3p and the target genes of PTEN and ATM were found to be different between QXXY patients and GYPXXY patients. These results indicate that there are different miRNAs, pathways, and target genes between QXXY patients and GYPXXY patients. However, due to the limited sample, whether miR-654-3p and the target genes PTEN and ATM could be molecular markers to differentiate TCM syndromes could not be established.

1. Introduction

Chronic hepatitis B (CHB) virus infection is a major global public health problem. Twenty-five percent of patients who have the disease die from cirrhotic complications, liver failure, and hepatocellular carcinoma (HCC) [1], which is a serious risk factor. In China, more than 300,000 CHB patients die of cirrhosis and HCC every year [2]. Liver fibrosis is a precursor of HCC in CHB [3, 4]; thus, blocking the development of fibrosis or reversing it

at an early stage is a worthy goal in the management of CHB.

However, antifibrotic drugs are still in the animal experimental stage, and no effective antifibrotic drug is available in Western medicine [5]. Most CHB patients with hepatic fibrosis are treated with antiviral drugs, which have the potential for promoting regression of fibrosis; however, fibrosis progresses in many CHB-fibrosis patients treated with these medications. Consequently, increasing numbers of CHB patients are using traditional Chinese medicines (TCM) for blocking liver fibrosis. Unique advantages of TCM in the treatment of fibrotic-stage liver disease without side effects have been reported [6–9]. Examples are relieving the patient symptoms, nourishing the liver, and reducing liver inflammation and fibrosis. This holistic but individualized TCM treatment can target the complex pathological mechanism of hepatic fibrosis in multiple ways.

TCM syndrome, the basis of prescription of Chinese herbs, is based on a patient's signs and symptoms, which are often subjective and not uniform. Various doctors may diagnose different TCM syndromes in the same patient [10]. Thus, it is urgent that an objective and useful method to differentiate TCM syndromes is established. Many microRNAs (miRNAs) have been correlated with liver fibrosis in CHB patients [11–13], and miRNAs have been suggested as biomarkers for liver fibrosis [14]. However, specific miRNAs have not been correlated with individual TCM syndromes. It is also unknown whether miRNAs can be used as markers for differentiation of TCM syndromes in CHB-fibrosis patients.

The TCM syndromes of Ganyu Pixu Xueyu (GYPXXY), which is characterized by liver stagnation, spleen deficiency, and blood stasis, and of Qixu Xueyu (QXXY), which is characterized by deficiency of qi, blood, and blood stasis, are the two major TCM syndromes of CHB-fibrosis at the early stage. Therefore, the current study aims to identify whether miRNAs are expressed differently between these two major TCM syndromes. Positive results will lay the foundation for the next study, which will aim to determine whether miRNAs can be a marker to differentiate TCM syndrome GYPXXY from QXXY patients among CHB-fibrosis patients.

2. Methods/Design

2.1. Patient Population and Setting. We recruited 18 CHB patients with early liver fibrosis (Scheuer fibrosis stage F1 or F2) [15] and 12 CHB patients without liver fibrosis, who were identified by screening or were enrolled in our previous study (2013ZX10005002-002). The 18 CHB patients with liver fibrosis included 9 patients with GYPXXY syndrome and 9 patients with QXXY syndrome. The current study conformed to the Declaration of Helsinki and was approved by the Ethics Committee of Guangdong Provincial Hospital of Chinese Medicine (B2013-087-01). All patients gave written informed consent before entering the study.

2.2. Diagnostic Criteria. Patients' diagnoses were based on the Guideline of Prevention and Treatment of Chronic Hepatitis B of Hepatology Branch of the Chinese Medical Association (2010 version) [16] and the Guidelines for Diagnostic and Treatment of Hepatic Fibrosis of the Chinese Association of Integrative Medicine [17]. The diagnoses of TCM syndromes were based on the Standards of Traditional Chinese Medicine Syndrome Differentiation for Viral Hepatitis [18] and confirmed by three senior TCM physicians, based on clinical symptoms, tongue manifestation, and pulse condition. The final result of TCM syndrome can be determined only when the results of these three experts are consistent. If the results of the three experts are inconsistent, discussion should be conducted to determine the final result.

2.3. Clinical and Laboratory Assessment. Demographic, clinical, and laboratory data were collected at the time of liver biopsy. Serum HBsAg was measured with electrochemical immunoassay (Elecsys 2010; Roche Diagnostics, Mannheim, Germany). Serum HBV DNA was measured with a lower limit of detection of 100 IU/mL (ABI 7300, Applied Biosystems Inc, USA).

2.4. Liver Specimens. All patients received liver biopsy. The liver specimens were frozen immediately in liquid nitrogen until used.

2.5. RNA Extraction. Total RNA was isolated by use of the TRI reagent (Merck, Darmstadt, Germany). The quantity and integrity of the extracted RNA were determined with UV spectrophotometry. Total RNA was quantified with formaldehyde denaturing gel electrophoresis.

2.6. Agilent miRNA Microarray. Thirty samples were analyzed with a Microarray Scanner G2505C (Agilent Technologies) using Agilent microarray slides. It contains all microRNAs from the Sanger miRBase release 22. Each glass slide is formatted with 8 high-definition 60K arrays (8×60K design/8 arrays with 60,000 features each). In addition to 20 replicates of each microRNA, each array carries control probes for grid alignment, as well as labeling and hybridization of control spike-ins. The Agilent microRNA Complete Labeling and Hybridization kit (Agilent Technologies) contains cyanine 3-cytidine biphosphate (pCp) for labeling; the hybridization time was 20 h at 55°C with 20 rpm. Results were analyzed with Agilent Feature Extraction software (10.7.3.1) (Agilent Technologies).

2.7. Data Analysis. Feature Extraction software (version10.7.1.1, Agilent Technologies) was used to analyze array images for raw data. Genespring software (version 14.8, Agilent Technologies) was used to finish the basic analysis with the raw data, which was normalized with the quantile algorithm. Probes that had at least 1 condition out of 2 conditions with flags "Detected" were chosen for further data analysis. Differentially expressed genes were identified through fold change, and a P value was calculated with a t-

test. The threshold set for up- and downregulated genes was a fold change >2.0 and a P value <0.05. Gene Ontology (GO) analysis and KEGG analysis were, then, applied to determine the roles of the differentially expressed miRNAs. Hierarchical clustering was performed to reveal the expression pattern of distinguishable genes among samples.

2.8. Quantitative Real-Time PCR (qRT-PCR). To validate the above microarray results, qRT-PCR was performed in 27 CHB patients (9 in the GYPXXY group, 6 in the QXXY group, and 12 in the nonfibrosis group). qRT-PCR was performed in a 20 μl reaction mixture consisting of 2X miRcute Plus miRNA Premix (miRcute miRNA, TIANGEN, FP411-02), 0.4 μm of each forward primer, and 20 ng of cDNA as the template. qPCR was performed in a Roche 480II PCR System (Roche, USA). PCR conditions were initial denaturation at 95°C for 15 min followed by 40 cycles of denaturation at 95°C for 20 s and annealing at 60°C for 34 s. After PCR amplification, melt-curve analysis of the amplicons was conducted at 60°C to 95°C, and data were collected at 0.3°C intervals.

2.9. Statistical Analysis. Continuous variables are expressed as the mean and standard deviation or median and interquartile range, as assessed by Student's t-test or a nonparametric test (Mann–Whitney), as appropriate. Categorical parameters among groups were compared with the Chi-squared test. All P values were two-sided, and statistical significance was set at $P < 0.05$. All statistical analyses were performed with SPSS software version 20.0 (SPSS Inc., Chicago, IL, USA).

3. Results

3.1. Clinical Characteristics of Enrolled Patients. Clinical characteristics of the three patient groups are listed in Table 1. The groups did not differ significantly in age, gender, alanine aminotransferase, and HBV DNA. There was no significant difference in the liver fibrosis stage between the GYPXXY group and the QXXY group ($P > 0.05$).

3.2. Agilent miRNA Microarray of Differentially Expressed miRNAs in CHB-Fibrosis Patients with Different TCM Syndromes. Compared with miRNAs in CHB patients without liver fibrosis, 145 miRNAs were upregulated and 124 were downregulated in CHB patients with liver fibrosis (fold change > 2.0; P value < 0.05). Compared with miRNA expression in the nonfibrosis group, 155 miRNAs were differentially expressed in the GYPXXY group and 132 were differentially expressed in the QXXY group. More importantly, 7 miRNAs were differentially expressed in the QXXY group compared with expression in the GYPXXY group. Furthermore, as shown in Table 2, 6 of the 7 differentially expressed miRNAs were upregulated (miR-144-5p, miR-18a-5p, miR-148b-3p, miR-654-3p, miR-139-3p, and miR-24-1-5p), and 1 was downregulated (miR-6834-3p) in the QXXY group. The heatmap plots and volcano plots of differentially expressed miRNAs are presented in Figure 1.

3.3. qRT-PCR Validation of Differentially Expressed miRNAs in CHB-Fibrosis Patients with Different TCM Syndromes. The 7 miRNAs that were upregulated in the QXXY group, as compared to the miRNAs in the GYPXXY group, were chosen for validation by qRT-PCR in liver samples from 12 patients in the nonfibrosis group, 6 patients in the QXXY group, and 9 patients in the GYPXXY group. Six of the 7 miRNAs (miR-6834-3p excluded) were validated by qRT-PCR, and miR-144-5p and miR-654-3p were confirmed to be upregulated in CHB-liver fibrosis patients compared with values in the nonfibrosis group (Figure 2). Moreover, miR-654-3p was confirmed to be upregulated in the QXXY group compared with that in the GYPXXY group, while no significant difference was found in miR-144-5p (Figure 3). However, miR-18a-5p, miR-148b-3p, miR-139-3p, and miR-24-1-5p were not significantly different between the CHB-fibrosis group and the nonfibrosis group (Figure 2), but all these miRNAs were significantly upregulated in the QXXY group compared with values in the GYPXXY group (Figure 3).

3.4. miRNA Target Gene Prediction and Enrichment Analysis in CHB-Fibrosis Patients with Different TCM Syndromes. Target scan, PITA, and miRNA org databases were used to predict the target genes of differentially expressed miRNAs. Overall, 271 common target genes from these three databases were selected for pathway analysis. The top 20 GO terms between the QXXY group and the GYPXXY group were classified by the biological process, cellular component, and molecular function (Figures 4(a)–4(c)). Positive regulation of transcription DNA-templated was the most significantly enriched biological process term. The most significantly enriched cellular component term and molecular function term were Golgi apparatus and protein binding, respectively. Further KEGG pathway analysis revealed 36 significant related pathways involved in target genes of miRNAs between the QXXY group and the GYPXXY group. Furthermore, Venn analysis was performed to identify the TCM syndrome-related pathways [19]. As a result, 31 overlapped pathways caused by disease were filtered out, and 5 differential pathways caused by different TCM syndromes were identified between the GYPXXY group and the QXXY group (Figure 5). The five pathways, as detailed in Figure 4(d), were central carbon metabolism in cancer, cell cycle, viral carcinogenesis, basal transcription factors, and Epstein–Barr virus infection. The GO terms and KEGG pathway analyses implied that molecular mechanisms are different between the two CHB-fibrosis syndromes. Moreover, three pathways, including central carbon metabolism in cancer, cell cycle, and basal transcription factors, were involved in the pathogenesis of fibrosis (Table 3). The pathways of central carbon metabolism in cancer and cell cycle related to miR-654-3p and the target genes of PTEN and ATM were different between the QXXY and GYPXXY patients.

Table 1: Clinical characteristics of enrolled patients.

Variables	GYPXXY group ($n = 9$)	QXXY group ($n = 9$)	Nonfibrosis group ($n = 12$)
Demographic characteristics			
Median age, years (range)	37 (25–53)	39 (26–65)	39 (24–47)
Males, *n* (%)	5 (55.6)	5 (55.6)	7 (58.3)
Laboratory data			
Median ALT, U/L (range)	24 (10–53)	23 (11–76)	18 (8–88)
Median HBV DNA (range), log10 IU/m	5.1 (2.4, 8.1)	4.8 (2.4, 8.5)	2.8 (2.4, 8.4)
Liver histology			
Inflammation activity, *n* (%)			
*G*0, *n* (%)	0	0	11 (91.7)
*G*1, *n* (%)	7 (77.8)	6 (66.7)	1 (8.3)
*G*2, *n* (%)	2 (22.2)	3 (33.3)	0
Fibrosis stage, *n* (%)			
*F*0, *n* (%)	0	0	12 (100)
*F*1, *n* (%)	5 (55.6)	4 (44.4)	0
*F*2, *n* (%)	4 (44.4)	5 (55.6)	0

*Abbreviations: ALT, alanine aminotransferase.

Table 2: Differentially expressed miRNAs in CHB-fibrosis patients with GYPXXY syndrome or QXXY syndrome.

miRNA	Regulation	Fold change (QXXY/GYPXXY)	*P* values
Hsa-miR-144-5p	Up	5.93	0.028
Hsa-miR-18a-5p	Up	4.23	0.013
Hsa-miR-148b-3p	Up	3.94	0.021
Hsa-miR-654-3p	Up	3.47	0.016
Hsa-miR-139-3p	Up	3.34	0.048
Hsa-miR-24-1-5p	Up	3.32	0.021
Hsa-miR-6834-3p	Down	−4.98	0.022

*Abbreviations: GYPXXY, TCM syndrome of Ganyu Pixu Xueyu (liver stagnation, spleen deficiency, and blood stasis); QXXY, TCM syndrome of Qixu Xueyu (deficiency of qi, blood and blood stasis).

4. Discussion

In the recent years, studies have demonstrated that miRNAs are potential markers for differentiation of TCM syndromes [20–23], and many miRNAs have been found upregulated or downregulated during liver fibrogenesis [13]. For example, miR-542-3p upregulation [24] and miR-454 [25] downregulation have been reported to promote liver fibrosis. However, no study has focused on miRNAs in differentiating TCM syndromes with CHB-fibrosis. This study is the first analysis of expression profiles of miRNAs in different TCM syndromes in CHB patients with fibrosis. Results of the study might provide new ideas for how to make differentiation of TCM syndromes more objective.

We used miRNA microarray to determine the expression of miRNAs in 30 samples of liver tissues of CHB patients. Six differentially expressed miRNAs were found upregulated (miR-144-5p, miR-18a-5p, miR-148b-3p, miR-654-3p, miR-139-3p, and miR-24-1-5p), whereas one was downregulated (miR-6834-3p) in the QXXY group compared with miRNA expression in the GYPXXY group. qRT-PCR analysis confirmed that miR-144-5p and miR-654-3p were upregulated in CHB patients with liver fibrosis compared with those without fibrosis. Moreover, miR-654-3p was confirmed as upregulated in the QXXY group compared with that in the GYPXXY group, while no significant difference was found in miR-144-5p. These results indicate that patients with the syndrome of QXXY might be more prone to develop liver fibrosis than patients with the syndrome of GYPXXY. Also, miR-654-3p might be a molecular marker for distinguishing TCM syndromes in CHB-fibrosis patients; we intend to explore this possibility in future studies. However, we found that miR-18a-5p, miR-148b-3p, miR-139-3p, and miR-24-1-5p did not distinguish CHB patients with fibrosis from those without fibrosis, as all these miRNAs were upregulated in the QXXY group compared with miRNAs in the GYPXXY group; this result may be due to the different miRNA levels between the QXXY group and GYPXXY group.

In this study, we also found that positive regulation of transcription DNA-templated, Golgi apparatus, and protein binding were the most significantly enriched biological process term, cellular component term, and molecular function term, respectively. Furthermore, KEGG revealed that three pathways—central carbon metabolism in cancer, cell cycle, and basal transcription factors—related to fibrosis pathogenesis were different between the QXXY group and the GYPXXY group. The GO terms and KEGG pathway analysis implied that molecular mechanisms are different between the two CHB-fibrosis syndromes. Moreover, the target genes of PTEN and ATM, as well as the differentially expressed miR-654-3p, were found related to the pathways of central carbon metabolism in cancer and cell cycle. The pathway of central carbon metabolism in cancer has been postulated to be involved in the pathogenesis of HCC [26] and liver fibrosis [27]. We found that PTEN, an important

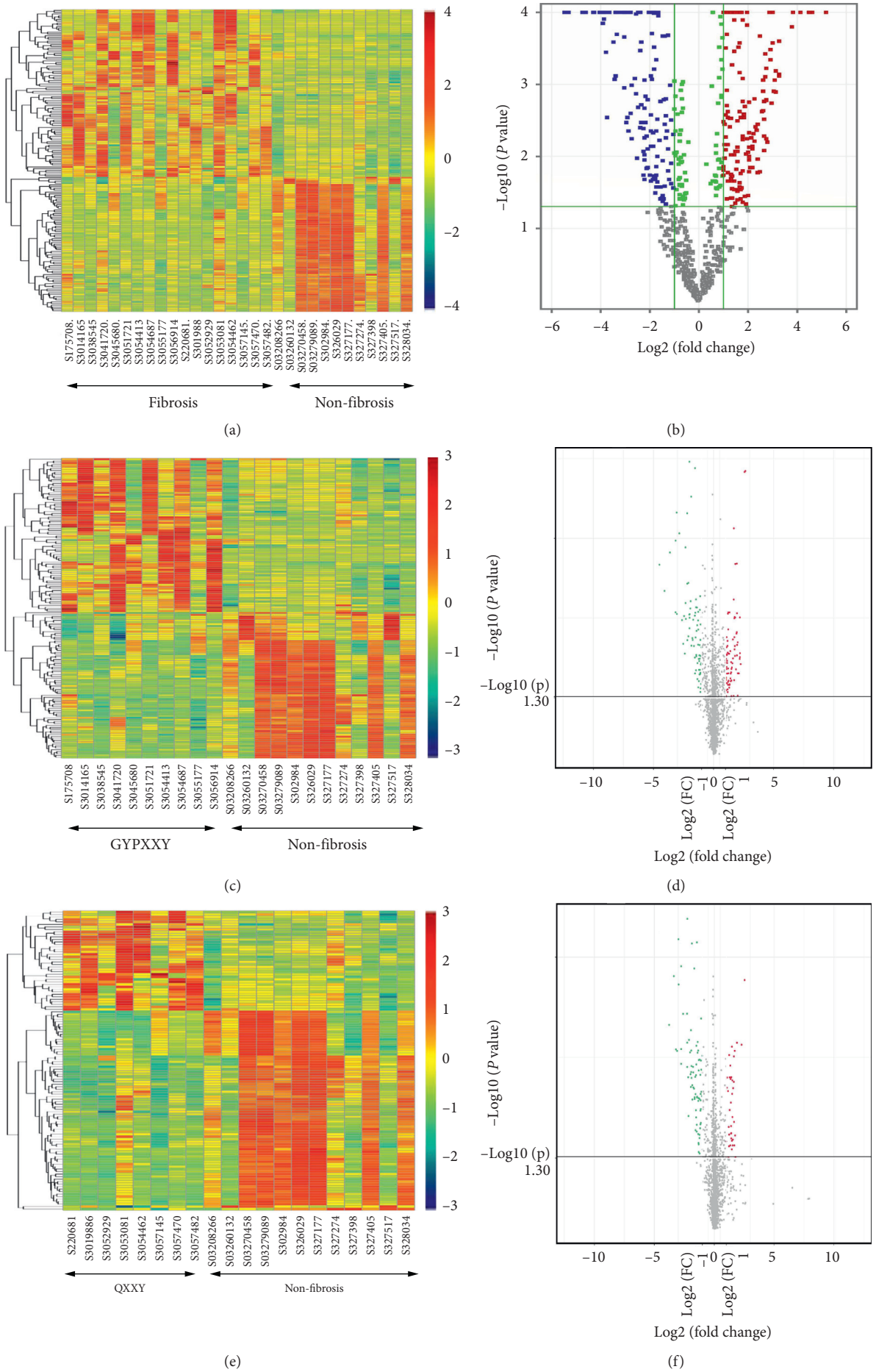

Figure 1: Continued.

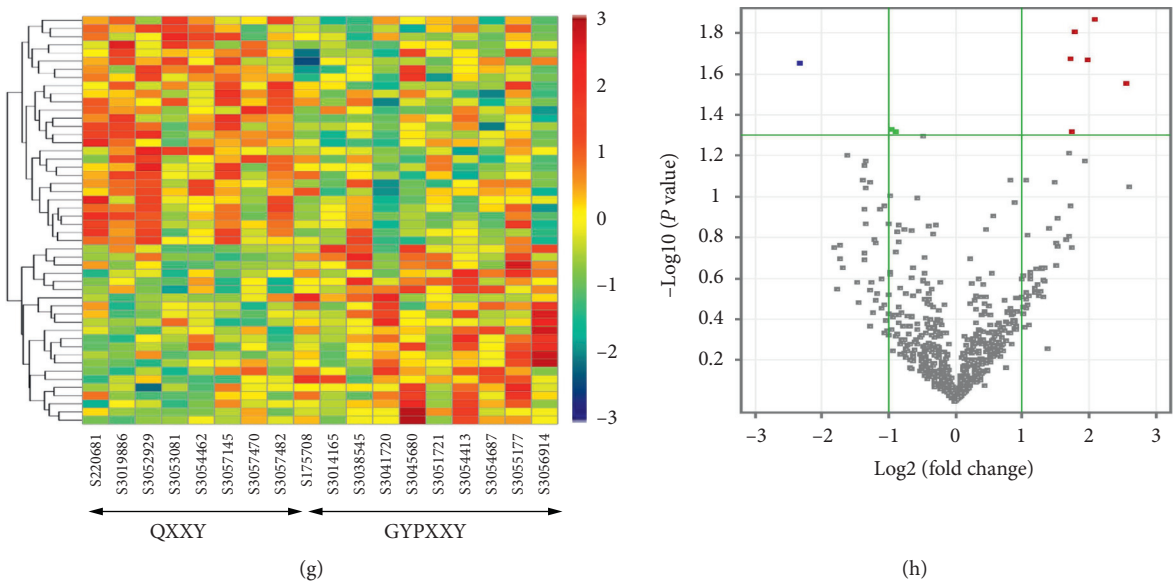

Figure 1: The heat maps and volcano plots of differentially expressed miRNAs among CHB-fibrosis patients with different TCM syndromes, (a) (b) differentially expressed miRNAs between the CHB patients with liver fibrosis and those without fibrosis, (c), (d) differentially expressed miRNAs between the CHB-fibrosis patients with TCM syndrome of GYPXXY and those without fibrosis, (e), (f) differentially expressed miRNAs between the CHB-fibrosis patients with TCM syndrome of QXXY and those without fibrosis, (g), (h) differentially expressed miRNAs between CHB-fibrosis patients with TCM syndrome of GYPXXY and those of QXXY.

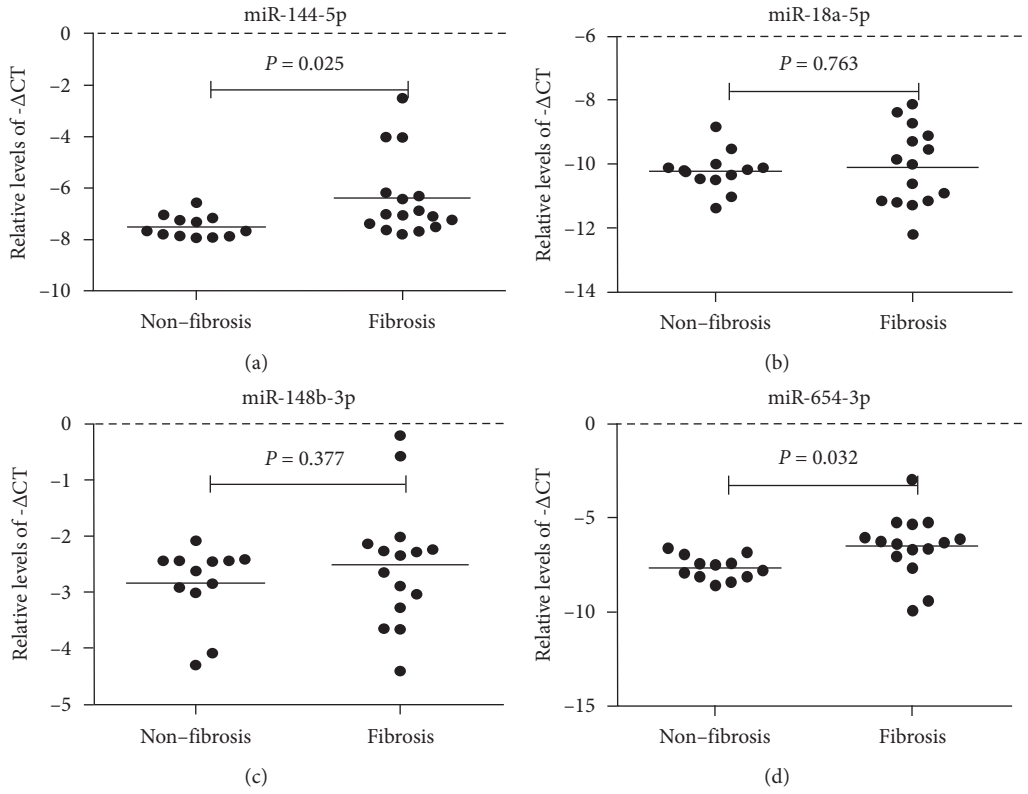

Figure 2: Continued.

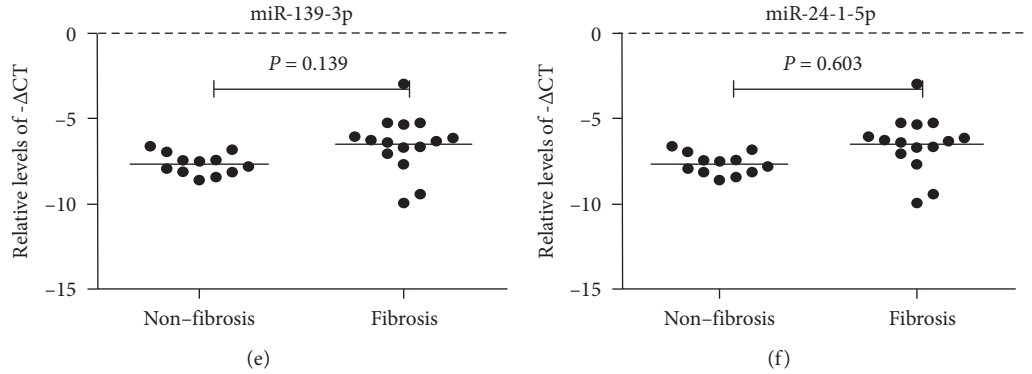

Figure 2: The miRNAs expressed levels from qRT-PCR data between the nonfibrosis group and fibrosis group. The levels of miR-144-5p (a), miR-18a-5p (b), miR-148b-3p (c), miR-654-3p (d), miR-139-3p (e), and miR-24-1-5p (f) in CHB patients with liver fibrosis ($n = 15$) and nonfibrosis ($n = 12$) were measured by qRT-PCR. The line at each group represents the median value of indicated miRNA.

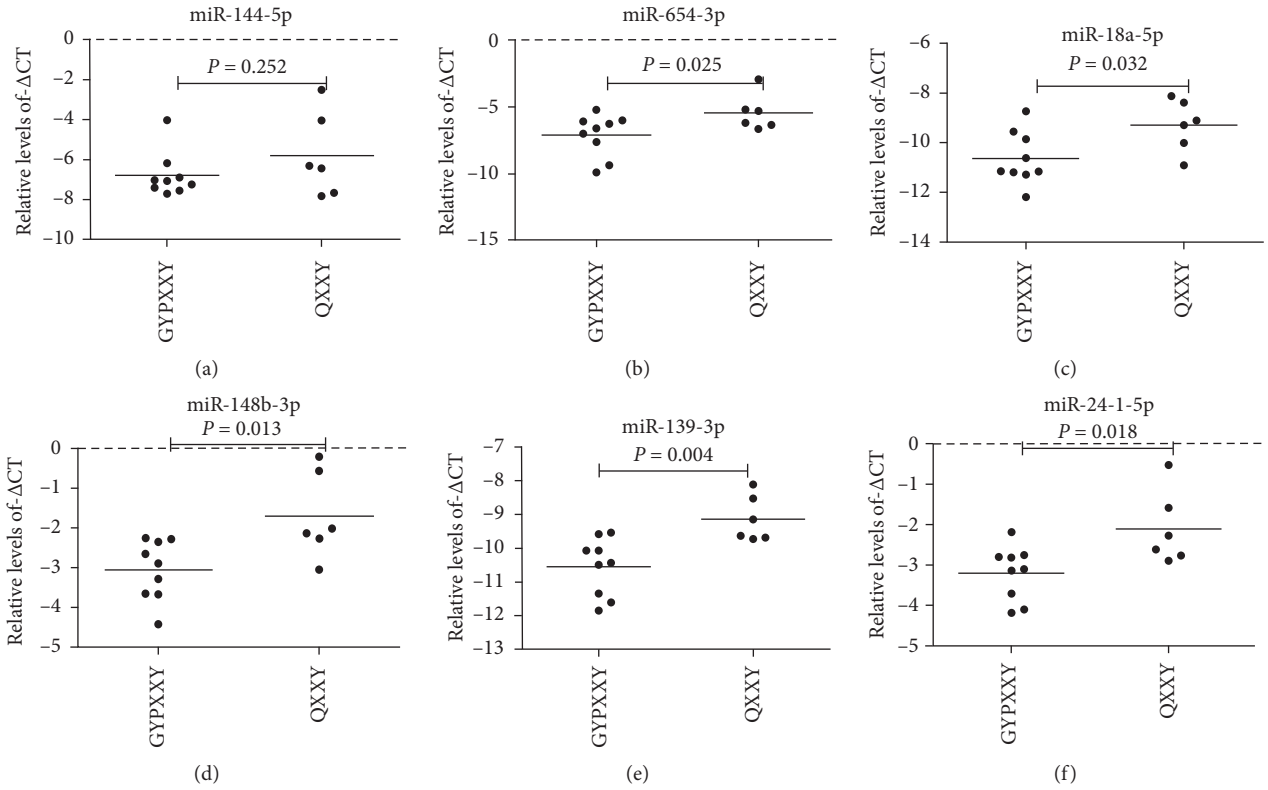

Figure 3: The miRNAs expressed levels from qRT-PCR data between the GYPXXY group and QXXY group. The levels of miR-144-5p (a), miR-654-3p (b), miR-18a-5p (c), miR-148b-3p (d), miR-139-3p (e), and miR-24-1-5p (f) in GYPXXY ($n = 9$) and QXXY ($n = 6$) were measured by qRT-PCR. The line at each group represents the median value of indicated miRNA.

gene in this pathway, may be the target gene of upregulated differential miR-654-3p. It has been reported that upregulation of PTEN expression can inhibit the progress of liver fibrosis [28]. Therefore, we speculate that the gene PTEN has low expression in CHB-liver fibrosis associated with the TCM syndrome of QXXY compared with that of GYPXXY.

It is well known that activated hepatic stellate cells contribute to the progression of liver fibrosis. Therefore, the pathway of cell cycle, which is closely associated with the proliferation of hepatic stellate cells, may be involved in the progression of liver fibrosis [29, 30]. Interestingly, we found that ATM, an important gene in this pathway, is predicted to be the target gene of miR-654-3p. qRT-PCR data revealed that the level of miR-654-3p was significantly higher in the QXXY group than in the GYPXXY group; thus, the target gene ATM might be expressed less in the QXXY group. These results indicate that the target genes of PTEN and ATM, as well as miR-654-3p, might be important molecular markers for

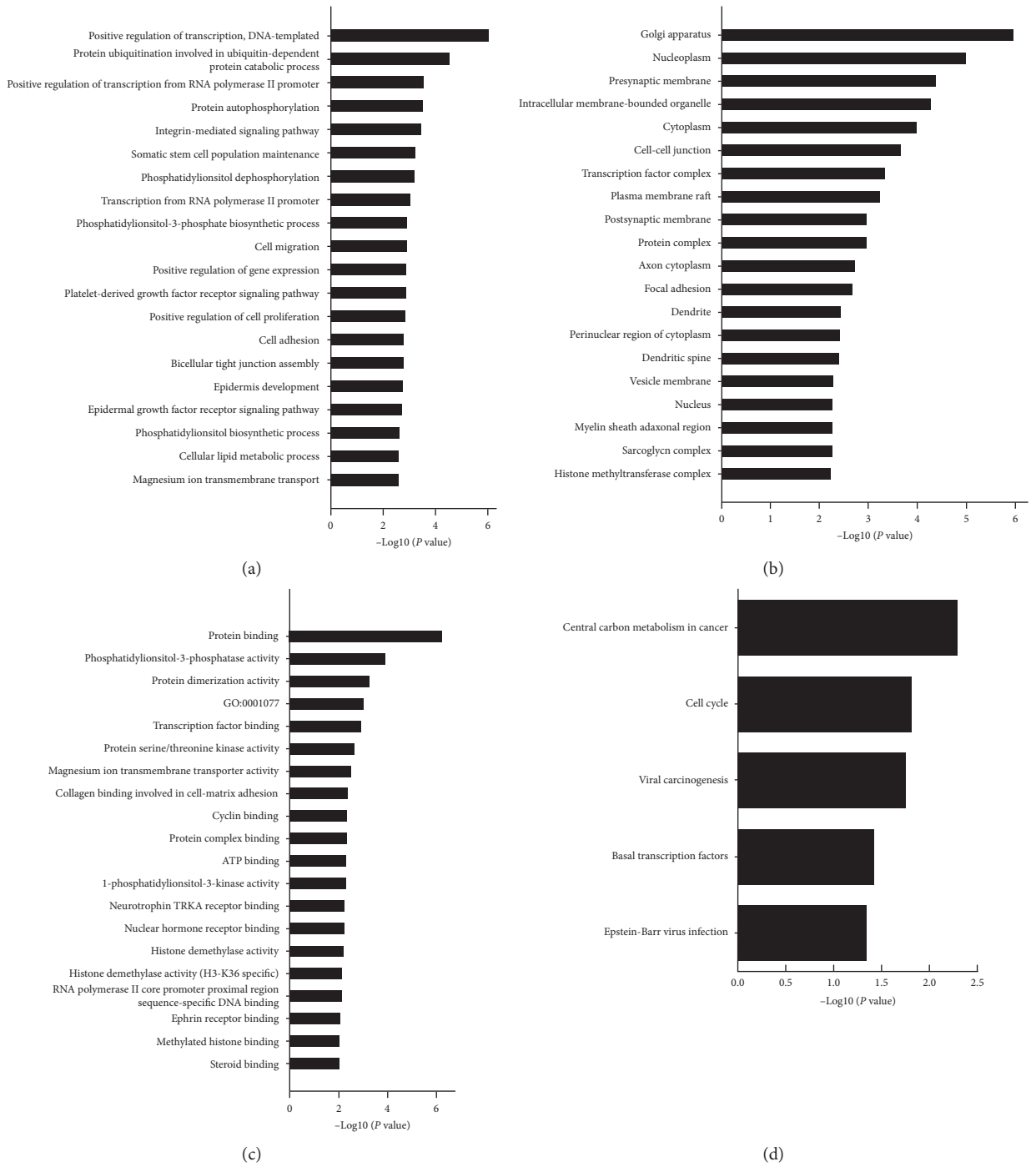

Figure 4: Gene Ontology and KEGG pathway analyses of differentially expressed miRNAs target genes between the GYPXXY group and QXXY group: (a) biological process, (b) cellular component, (c) molecular function, and (d) KEGG pathway analysis.

differentiation of the two TCM syndromes. However, this possibility requires verification in future studies.

Our study has limitations. First, due to the difficulty in obtaining liver tissues and the shortage of research funds, the number of liver samples studied for miRNAs and RT-qPCR validation was limited. Nevertheless, the number was adequate to provide proof of expression profiles of miRNAs in TCM syndromes in CHB-fibrosis patients. Second, the role of miR-654-3p in the diagnostic performances of TCM syndromes of GYPXXY and QXXY has not been assessed with the area under the receiver-operator curve, although it has been demonstrated as a potential marker for differentiating these two TCM syndromes. Third, TCM syndrome differentiation is always subjective. There is no objective method to ensure the accuracy of TCM syndrome differentiation in this study. However, we invited three senior TCM experts to determine the final result of TCM syndrome, which might partly obviate this problem.

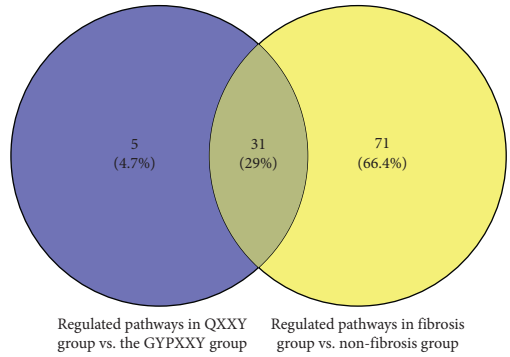

Figure 5: Venn analysis of differential pathways between two TCM syndromes of CHB-fibrosis patients and nonfibrosis patients.

Table 3: The significant pathways involved in fibrosis pathogenesis between the GYPXXY and QXXY groups after Venn analysis.

Pathways	Target genes	Differentially expressed miRNAs	*P* values
Central carbon metabolism in cancer	PTEN; KIT; HIF1A; NRAS; AKT3	Hsa-miR-18a-5p; hsa-miR-654-3p; Hsa-miR-148b-3p	0.028
Cell cycle	ATM; CDC14A; CDK2; E2F3; CCND2; CDC23	Hsa-miR-18a-5p; hsa-miR-148b-3p; Hsa-miR-654-3p	0.013
Basal transcription factors	GTF2H1; TBPL1; TAF4B	Hsa-miR-18a-5p; hsa-miR-148b-3p	0.021

*Abbreviations: GYPXXY, TCM syndrome of Ganyu Pixu Xueyu (liver stagnation, spleen deficiency and blood stasis); QXXY, TCM syndrome of Qixu Xueyu (deficiency of qi, blood and blood stasis).

5. Conclusions

Differential miRNAs were found in CHB-fibrosis patients with two common yet different TCM syndromes, GYPXXY and QXXY. miR-654-3p was more upregulated in QXXY patients than in GYPXXY patients. The pathways of central carbon metabolism in cancer, cell cycle related to miR-654-3p, and the target genes of PTEN and ATM were different between QXXY patients and GYPXXY patients. These results indicate that miR-654-3p and the target genes of PTEN and ATM might be molecular markers for differentiating the TCM of GYPXXY and QXXY syndromes, a possibility that requires additional study.

Data Availability

The datasets supporting the conclusions of the current study are available in the Guangdong Provincial Hospital of Chinese Medicine.

Ethical Approval

This study protocol was approved by the Ethics Review Committee of Guangdong Provincial Hospital of Chinese Medicine (B2013-087-01) and all other participating centers. This study conformed to the ethical guidelines of the Declaration of Helsinki and Good Clinical Practice.

Disclosure

This study has been presented as a conference abstract for the 2020 Asian Pacific Association for the Study of the Liver.

Conflicts of Interest

The authors declare that they have no conflicts of interest.

Acknowledgments

The authors thank all their colleagues of the Hepatology Department at the Guangdong Provincial Hospital of Chinese Medicine who assisted in this study. The present study was funded by the biological resources project collaborated by Guangdong Provincial Hospital of Chinese Medicine and Shanghai Chip National Engineering Center (YN2016XP03), the Twelfth Five-Year Plan for Major and Special Program of the National Science and Technology of China (2013ZX10005002-002), and the Thirteen Five-Year Plan for Major and Special Program of the National Science and Technology of China (2018ZX10725506-003).

References

[1] J. J. Ott, J. Horn, G. Krause, and R. T. Mikolajczyk, "Time trends of chronic HBV infection over prior decades—a global analysis," *Journal of Hepatology*, vol. 66, no. 1, pp. 48–54, 2017.

[2] J.-L. Hou and W. Lai, "The guideline of prevention and treatment for chronic hepatitis B: a 2015 update," *Chinese Journal of Hepatology*, vol. 23, no. 12, pp. 888–905, 2015.

[3] D. S. Manning and N. H. Afdhal, "Diagnosis and quantitation of fibrosis," *Gastroenterology*, vol. 134, no. 6, pp. 1670–1681, 2008.

[4] Q. Wang, M. I. Fiel, S. Blank et al., "Impact of liver fibrosis on prognosis following liver resection for hepatitis B-associated hepatocellular carcinoma," *British Journal of Cancer*, vol. 109, no. 3, pp. 573–581, 2013.

[5] P. Manka, A. Zeller, and W. K. Syn, "Fibrosis in chronic liver disease: an update on diagnostic and treatment modalities," *Drugs*, vol. 79, no. 9, pp. 903–927, 2019.

[6] J. Y. Chen, H.-L. Chen, J.-C. Cheng et al., "A Chinese herbal medicine, Gexia-Zhuyu Tang (GZT), prevents dimethylnitrosamine-induced liver fibrosis through inhibition of hepatic stellate cells proliferation," *Journal of Ethnopharmacology*, vol. 142, no. 3, pp. 811–818, 2012.

[7] Z. Gong, J. Lin, J. Zheng et al., "Dahuang Zhechong pill attenuates CCl4-induced rat liver fibrosis via the PI3K-Akt signaling pathway," *Journal of Cellular Biochemistry*, vol. 121, no. 2, pp. 1431–1440, 2019.

[8] R. Wu, S. Dong, F.-F. Cai et al., "Active compounds derived from fuzheng huayu formula protect hepatic parenchymal cells from apoptosis based on network pharmacology and transcriptomic analysis," *Molecules*, vol. 24, no. 2, p. 338, 2019.

[9] C. Huang, D. Shen, S. Sun et al., "Effect of Fufang Biejia Ruangan Tablet on lowering biochemical and virological parameters of hepatic fibrosis in patients with chronic hepatitis B: protocol for a systematic review and meta-analysis of randomized controlled trials and cohort studies," *Medicine*, vol. 98, no. 17, Article ID e15297, 2019.

[10] Z. Gu, X. Qi, X. Zhai et al., "Study on TCM syndrome differentiation of primary liver cancer based on the analysis of latent structural model," *Evidence-Based Complementary and Alternative Medicine*, vol. 2015, Article ID 761565, 9 pages, 2015.

[11] J. Lambrecht, S. Verhulst, H. Reynaert, and L. A. Van Grunsven, "The miRFIB-score: a serological miRNA-based scoring algorithm for the diagnosis of significant liver fibrosis," *Cells*, vol. 8, no. 9, p. 1003, 2019.

[12] P. Gupta, T. N. Sata, A. K. Yadav et al., "TGF-β induces liver fibrosis via miRNA-181a-mediated down regulation of augmenter of liver regeneration in hepatic stellate cells," *PLoS One*, vol. 14, no. 6, Article ID e0214534, 2019.

[13] Z. Zhao, C.-Y. Lin, and K. Cheng, "siRNA- and miRNA-based therapeutics for liver fibrosis," *Translational Research*, vol. 214, pp. 17–29, 2019.

[14] T. Z. Wang, D. D. Lin, B. X. Jin, X. Y Sun, and N. Li, "Plasma microRNA: a novel non-invasive biomarker for HBV-associated liver fibrosis staging," *Experimental and Therapeutic Medicine*, vol. 17, no. 3, pp. 1919–1929, 2019.

[15] P. J. Scheuer, "Classification of chronic viral hepatitis: a need for reassessment," *Journal of Hepatology*, vol. 13, no. 3, pp. 372–374, 1991.

[16] Chinese Society of Hepatology and Chinese Society of Infectious Diseases and Chinese Medical Association, "The guideline of prevention and treatment for chronic hepatitis B (2010 version)," *Zhonghua Liu Xing Bing Xue Za Zhi*, vol. 32, no. 4, pp. 405–415, 2011.

[17] Liver Disease Committee and Chinese Association of Integrative Medicine, "Guidelines for the diagnosis and treatment of liver fibrosis in integrative medicine practice," *Zhonghua Gan Zang Bing Za Zhi*, vol. 14, no. 11, pp. 866–870, 2006.

[18] Chinese Society of Traditional Chinese medicine, "Standards of traditional Chinese medicine syndrome differentiation for viral hepatitis (trial implementation)," *Journal of Traditional Chinese Medicine*, vol. 5, pp. 39-40, 1991.

[19] J. L. McKinney, D. J. Murdoch, J. Wang et al., "Venn analysis as part of a bioinformatic approach to prioritize expressed sequence tags from cardiac libraries," *Clinical Biochemistry*, vol. 37, no. 11, pp. 953–960, 2004.

[20] H. Zhang, Y. Guan, Y.-Y. Lu, Y.-Y. Hu, S. Huang, and S.-B. Su, "Circulating miR-583 and miR-663 refer to ZHENG differentiation in chronic hepatitis B," *Evidence-Based Complementary and Alternative Medicine*, vol. 2013, Article ID 751341, 8 pages, 2013.

[21] Q.-L. Chen, Y.-Y. Lu, G.-B. Zhang et al., "Progression from excessive to deficient syndromes in chronic hepatitis B: a dynamical network analysis of miRNA array data," *Evidence-Based Complementary and Alternative Medicine*, vol. 2013, Article ID 945245, 10 pages, 2019.

[22] J. Liao, Y. Liu, and J. Wang, "Identification of more objective biomarkers for blood-stasis syndrome diagnosis," *BMC Complementary and Alternative Medicine*, vol. 16, p. 371, 2016.

[23] Y. Liu, M. Wang, Y. Luo et al., "MiRNA-target network analysis identifies potential biomarkers for Traditional Chinese Medicine (TCM) syndrome development evaluation in hepatitis B caused liver cirrhosis," *Scientific Reports*, vol. 7, no. 1, Article ID 11054, 2017.

[24] Y.-Z. Wang, W. Zhang, Y.-H. Wang, X.-L. Fu, and C.-Q. Xue, "Repression of liver cirrhosis achieved by inhibitory effect of miR-454 on hepatic stellate cells activation and proliferation via Wnt10a," *The Journal of Biochemistry*, vol. 165, no. 4, pp. 361–367, 2019.

[25] F. Ji, K. Wang, Y. Zhang et al., "MiR-542-3p controls hepatic stellate cell activation and fibrosis via targeting BMP-7," *Journal of Cellular Biochemistry*, vol. 120, no. 3, pp. 4573–4581, 2019.

[26] M. I. Mora, M. Molina, L. Odriozola et al., "Prioritizing popular proteins in liver cancer: remodelling one-carbon metabolism," *Journal of Proteome Research*, vol. 16, no. 12, pp. 4506–4514, 2017.

[27] Y. Liu, X. Yang, Y. Jing et al., "Contribution and mobilization of mesenchymal stem cells in a mouse model of carbon tetrachloride-induced liver fibrosis," *Scientific Reports*, vol. 5, no. 1, Article ID 17762, 2015.

[28] N. S. Li, Z. M. Wang, and J. H. Lin, "Up-regulated expression of PTEN after splenetomy may prevent the progression of liver fibrosis in rats," *Journal of Hepato-Biliary-Pancreatic Sciences*, vol. 23, no. 1, pp. 50–56, 2015.

[29] G. Lou, Y. Yong, F. Liu et al., "MiR-122 modification enhances the therapeutic efficacy of adipose tissue-derived mesenchymal stem cells against liver fibrosis—MALAT1 functions as a competing endogenous RNA to mediate Rac1 expression by sequestering miR-101b in liver fibrosis," *Journal of Cellular and Molecular Medicine*, vol. 21, no. 11, pp. 2963–2973, 2015.

[30] F. Yu, Z. Lu, J. Cai et al., "MALAT1 functions as a competing endogenous RNA to mediate Rac1 expression by sequestering miR-101b in liver fibrosis," *Cell Cycle*, vol. 14, no. 24, pp. 3885–3896, 2015.

Hindawi
Evidence-Based Complementary and Alternative Medicine
Volume 2020, Article ID 2305784, 10 pages
https://doi.org/10.1155/2020/2305784

Research Article

Resina Draconis Reduces Acute Liver Injury and Promotes Liver Regeneration after 2/3 Partial Hepatectomy in Mice

Zhi-yong He,[1,2] Kai-han Lou,[1] Jia-hui Zhao,[1] Ming Zhang,[1] Lan-chun Zhang,[3] Ju Li,[4] Hao-fei Yu,[3] Rong-ping Zhang,[3,4] and Hu Wei-yan[1,2,3]

[1]*The Key Laboratory of Stem Cell and Regenerative Medicine, Institute of Molecular and Clinical Medicine, Kunming Medical University, Kunming 650500, China*
[2]*Monash Immune Regeneration and Neuroscience Laboratories, Department of Anatomy and Developmental Biology, Monash University, Clayton, Melbourne 3800, Australia*
[3]*School of Pharmaceutical Science & Yunnan Key Laboratory of Pharmacology for Natural Products, Kunming Medical University, Kunming 650500, China*
[4]*Yunnan University of Chinese Medicine, Kunming 650500, China*

Correspondence should be addressed to Rong-ping Zhang; zhrpkm@163.com and Hu Wei-yan; huweiyan2004@163.com

Received 25 June 2020; Revised 17 August 2020; Accepted 7 September 2020; Published 7 October 2020

Academic Editor: Hongwei Zhang

Aim. To investigate the protective effects and possible mechanisms of action of resina draconis (RD) on acute liver injury and liver regeneration after 2/3 partial hepatectomy (PH) in mice. *Methods*. 2/3 PH was used to induce acute liver injury. Mice were divided into three groups: sham, vehicle + 2/3 PH, and RD + 2/3 PH. Resina draconis was administered intragastrically after 2/3 PH into the RD + 2/3 PH group, and the same volume of vehicle (1% sodium carboxymethyl cellulose) was injected into the vehicle + 2/3 PH group and sham group mice. The index of liver to body weight (ILBW) and proliferating cell nuclear antigen (PCNA) were assayed to evaluate liver regeneration. Blood and liver tissues were collected for serological and western blotting analysis. *Results*. Resina draconis protected against 2/3 PH-induced acute severe liver injury and promoted liver regeneration as shown by significantly increased ILBW compared with that of controls. 2/3 PH increased serum AST and ALT levels, which were significantly decreased by RD treatment, while 2/3 PH decreased serum TP and ALB, which were increased by RD treatment. In the RD + 2/3 PH group, PCNA expression was significantly increased compared with the 2/3 PH group. Further, hepatocyte growth factor (HGF), TNF*α*, and EGFR levels were increased in the RD group at postoperative days 2 and 4 compared with the those in the 2/3 PH group. *Conclusion*. Our results suggest that RD ameliorates acute hepatic injury and promotes liver cell proliferation, liver weight restoration, and liver function after 2/3 PH, probably via HGF, TNF*α*, and EGFR signaling.

1. Introduction

The liver plays a central role in detoxification and protein synthesis and produces digestive biochemicals. It also possesses the unique ability to regenerate after surgical resection or injury to maintain these essential functions [1–4]. The clinical application of partial hepatectomy (PH) or living donor liver transplantation (LDLT) for the treatment of primary or metastatic liver tumors and end-stage liver disease depends on effective liver regeneration [5–7]. Optimizing liver regeneration would have great clinical potential in improving outcomes from liver disease. Two-thirds (2/3) PH is a well-validated experimental model of liver regeneration that has been extensively used to study the underlying molecular and cellular mechanisms [8–12].

Growth factors such as TGF*α*, EGF, and HGF are highly expressed after PH and are thought to be important in regulating hepatocyte activation, proliferation, migration, and survival during liver regeneration [13–15]. Hepatocyte growth factor (HGF) is the major hepatocyte mitogen [16], and HGF is upregulated after PH. HGF initiates hepatocyte DNA synthesis and stimulates hepatocyte growth [16, 17].

Overexpression of HGF also increases hepatocyte proliferation and accelerates liver regeneration after PH [18]. Mice lacking c-MET, the HGF receptor, show delayed liver regeneration after PH, with hepatocytes showing S-phase entry defects [19].

TNFα is an important regulator of the "priming phase" of liver regeneration, and blocking TNFα signaling in rats prior to PH significantly reduces the proliferation of hepatocytes and nonparenchymal liver cells [20, 21]. TNFα, together with its downstream effector IL-6, initiates hepatocyte transition from G0 to G1 phase of the cell cycle [21–23]. TNFα also activates transcription factors like STAT3 and NF-κB, which in turn promote the expression of cell cycle regulator genes such as cyclin D [24, 25].

The EGF receptor (EGFR) also plays a vital role in liver regeneration, since liver regeneration is not impaired in mice lacking TGFα because other EGFR ligands compensate for the absence of TGFα [14, 26]. EGFR is expressed at high levels in the adult liver and regulates liver development, function, and regeneration [13]. Transgenic mice lacking EGFR have a higher mortality rate after PH, with surviving mice showing increased hepatocyte proliferation due to low cyclin D1 expression. The EGFR pathway regulates hepatocyte proliferation and efficient liver regeneration after PH [27, 28].

Resina draconis (RD), a bright resin extracted from *Dracaena cochinchinensis* (Lour.) S. C. Chen, is a Chinese Herbal medicine with a well-established safety and bioactivity record [29, 30]. RD contributes to skin repair and can promote the development of transplanted epidermis, enhance the capillary proliferation [31], and promote the growth of fetal rat skin fibroblasts [32]. It can also improve wound healing [33] and has been used for the treatment of skin diseases [34, 35]. Further, RD can facilitate blood circulation and improve platelet function [36, 37]. RD has anti-inflammatory effects [38] and antitumor activities [39, 40]. Of these multiple activities, RD strongly promotes tissue recovery after injury. However, the effects of RD on liver regeneration after extended hepatectomy have not been investigated. Here, we explored the effect and possible mechanisms of RD treatment on liver regeneration in 2/3 PH mice. The involvement of HGF, TNFα, and EGFR signaling in RD-stimulated liver regeneration was also investigated.

2. Materials and Methods

2.1. Preparation of Drugs. Resina draconis powder (Xishuangbanna Rainforest Pharmaceutical Co., Ltd., Jinghong, China) was dispersed in 1% sodium carboxymethyl cellulose (Na-CMC) at 10 mg/mL, 20 mg/mL, and 40 mg/mL before intragastric injection into mice.

2.2. Animals. One-hundred forty-four 6-8 week-old male C57BL/6 mice weighing between 20 and 25 g were used. Animals were divided into three groups ($n = 8$ in each group): sham, vehicle + 2/3 PH, and RD + 2/3 PH. The RD + 2/3 PH group received intragastric injections of 0.2 mL RD solution at doses of 0.1 g/kg, 0.2 g/kg, or 0.4 g/kg body weight once daily for 10 days after 2/3 PH surgery. All experiments were conducted under the institutional guidelines of the Animal Ethics Committee, Kunming Medical University.

2.3. Surgical Procedure and Anesthesia. 2/3 PH was performed in the vehicle + 2/3 PH and RD + 2/3 PH groups using a slight modification of the methods developed by Harkness [41, 42]. Briefly, after general anesthesia, the left lateral, left median, and right median lobes were resected. Laparotomy was performed in the sham group without ligation and 2/3 PH.

2.4. Liver Tissue Collection. On days 0, 2, 4, 6, 8, and 10 after 2/3 PH, animals in each group were weighed and sacrificed humanly, liver tissues were collected and weighed, and the index of liver to body weight (ILBW) recorded.

2.5. Serum Parameters. Peripheral blood was collected and centrifuged. Serum alanine transaminase (ALT), aspartate transaminase (AST), alkaline phosphatase (ALP), albumin (ALB), and total protein (TP) were measured in U/L with a serum multiple biochemical analyzer (Diamond Diagnostics Inc., Holliston, USA).

2.6. Western Blotting. Liver tissue proteins were prepared as previously described [43]. Western blotting was performed using antibodies targeting PCNA (Invitrogen, Thermo Fisher Scientific, Waltham, MA, USA), β-actin (Sigma Aldrich, St. Louis, MO, USA), HGF (Abcam, Cambridge, UK), EGFR (Abcam), and TNF-α (Abcam). Super Signal West Dura Extended Duration Substrate (Pierce, Thermo Fisher Scientific, Waltham, MA, USA) was used to visualize antibody-antigen complexes.

2.7. Data Analysis. Three-way ANOVA was applied to analyze BW, ILBW, TP, ALB, ALT, ALP, and AST using the factors 2/3 PH operation, RD treatment, and time after injury. Tukey's post hoc tests were applied as appropriate. Student's t test was used to analyze data between two groups. All values were expressed as mean ± SEM, and a p value <0.05 was considered statistically significant.

3. Results

3.1. Resina Draconis Treatment Promotes Liver Weight Recovery after 2/3 PH. To address the effect of RD on general mouse health after PH, mouse body weights were monitored after 2/3 PH. The body weights of mice reduced on days 2 and 4 after 2/3 PH followed by weight gain on day 6. RD treatment at different doses induced faster and longer-lasting weight gain than vehicle group over 10 days (Figure 1(a)).

The ILBW from days 2 to 10 was measured after 2/3 PH to address the effect of RD on liver recovery. The ILBW was significantly higher on days 2, 4, 6, 8, and 10 in RD-treated

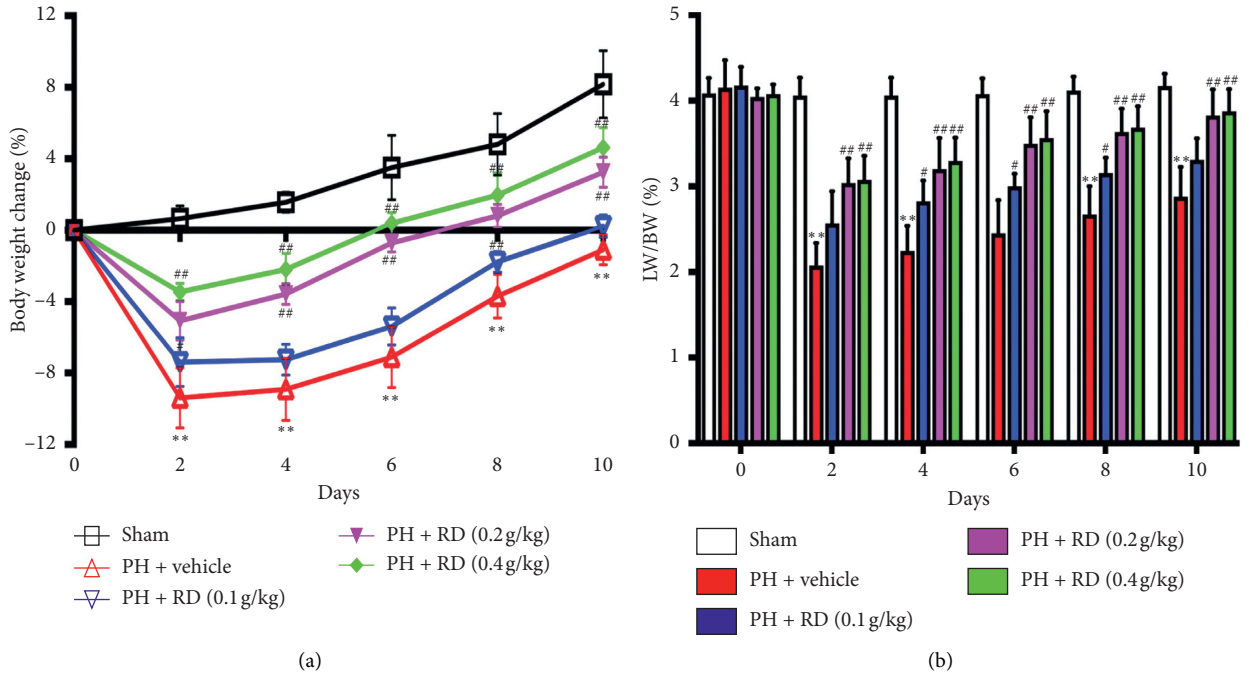

FIGURE 1: Resina draconis increases body weight and index of liver to body weight (ILBW) after 2/3 PH. (a) RD treatment at different doses increases body weight gain over time in mice receiving 2/3 PH. Results are represented as mean ± SEM of percentage change in body weight versus original body weight before 2/3 PH. $n = 8$ mice/time point. $^{**}p < 0.01$, vehicle + 2/3 PH group *vs* sham group; $^{\#\#}p < 0.01$, RD + 2/3 PH group *vs* vehicle + 2/3 PH group; $^{\#}p < 0.05$, RD vehicle + group *vs* vehicle + 2/3 PH group. (b) RD treatment increases ILBW over time in mice receiving 2/3 PH. Data are expressed as mean ± SEM. $n = 8$ mice/time point. $^{**}p < 0.01$, vehicle + 2/3 PH group *vs* sham group; $^{\#\#}p < 0.01$, RD + 2/3 PH group *vs* vehicle + 2/3 PH group; $^{\#}p < 0.05$, RD + 2/3 PH group *vs* vehicle + 2/3 PH group.

mice versus vehicle controls (Figure 1(b)). Of the different RD concentrations tested, the 0.2 g/kg and 0.4 g/kg doses were most effective, with no significant difference between the 0.4 g/kg treatment and 0.2 g/kg treatment. Therefore, 0.2 g/kg was used in subsequent experiments. These data indicate that RD treatment promotes liver recovery.

Resina draconis treatment prevents decreases in serum total protein (TP) and albumin (ALB) after 2/3 PH.

Given that RD treatment promoted liver regeneration, we further measured changes in serum total protein (TP) and albumin (ALB). TP and ALB levels were attenuated in both the 2/3 PH group and the RD-treated 2/3 PH group on days 2, 4, 6, 8, and 10 after PH. However, TP and ALB levels were significantly higher in the RD-treated 2/3 PH group compared with the vehicle + 2/3 PH group ($p < 0.01$) (Figures 2(a) and 2(b)). Furthermore, there was no unequivocal changes in the RD-treated 2/3 PH group and the sham group on days 4, 6, 8, and 10 after PH.

3.2. Resina Draconis Treatment Restores Liver Function after 2/3 PH. Serum AST, ALT, and ALP levels are biomarkers of liver function. Serum AST and ALT levels significantly increased in both the 2/3 PH and RD groups on days 2, 4, 6, 8, and 10 after PH. However, the levels were significantly different in the 2/3 PH group and the RD group ($p < 0.01$) (Figures 3(a) and 3(b)). ALP levels also significantly increased in the 2/3 PH and RD groups on days 2, 4, 6, and 8 after PH. However, the levels were significantly different in the 2/3 PH group and the RD group on days 2 and 4 ($p < 0.01$) (Figure 3(c)). Interestingly, the ALP and ALT levels in the RD group and vehicle group showed no significant difference on days 6, 8, and 10 after PH. These results indicate that RD treatment not only enhances liver regeneration after 2/3 PH but also restores 2/3 PH-induced loss of liver function as measured by liver function biomarkers.

3.3. Resina Draconis Treatment Enhances Hepatocyte Proliferation after 2/3 PH. Liver regeneration is closely related to hepatocyte proliferation. As RD promoted liver recovery, we hypothesized that RD enhanced hepatocyte proliferation. To address this hypothesis, we compared proliferating cell nuclear antigen (PCNA) levels in liver tissues between the different groups. PCNA expression was significantly higher on days 2, 4, and 6 in the RD-treated group compared with the 2/3 PH group (Figures 4(a) and 4(b)), with no observable change in PCNA expressed observed in the sham group.

3.4. Resina Draconis Treatment Induces HGF and Increases EGFR and TNFα after 2/3 PH. HGF, EGFR, and TNFα are important growth factors that stimulate hepatocyte mitogenesis in liver regeneration [44, 45]. To explore the possible mechanism by which RD promotes liver regeneration after 2/3 PH, HGF, EGFR, and TNFα expressions were measured in liver tissue by western blotting. In the vehicle + 2/3 PH group and RD + 2/3 vehicle group, HGF, EGFR, and TNFα increased significantly on day 2 after 2/3

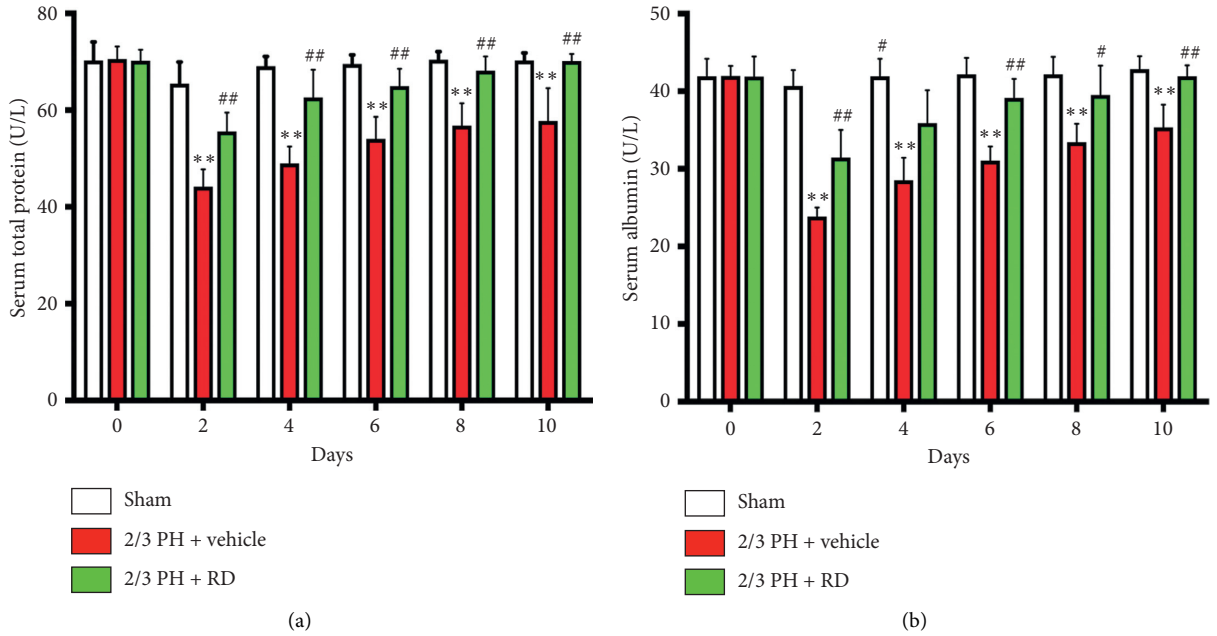

Figure 2: Resina draconis treatment prevents loss of serum TP and ALB after 2/3 PH. (a) RD treatment increases serum TP over time in mice receiving 2/3 PH. Results are represented as mean ± SEM. $n = 8$ mice/time point. $^{**}p < 0.01$, vehicle + 2/3 PH group *vs* sham group; $^{\#\#}p < 0.01$, RD + 2/3 PH group *vs* vehicle + 2/3 PH group. (b) RD treatment increases serum ALB over time in mice receiving 2/3 PH. Data are expressed as mean ± SEM. $n = 8$ mice/time point. $^{**}p < 0.01$, vehicle + 2/3 PH group *vs* sham group; $^{\#\#}p < 0.01$, RD + 2/3 PH group *vs* vehicle + 2/3 PH group; $^{\#}p < 0.05$, RD group *vs* 2/3 PH group.

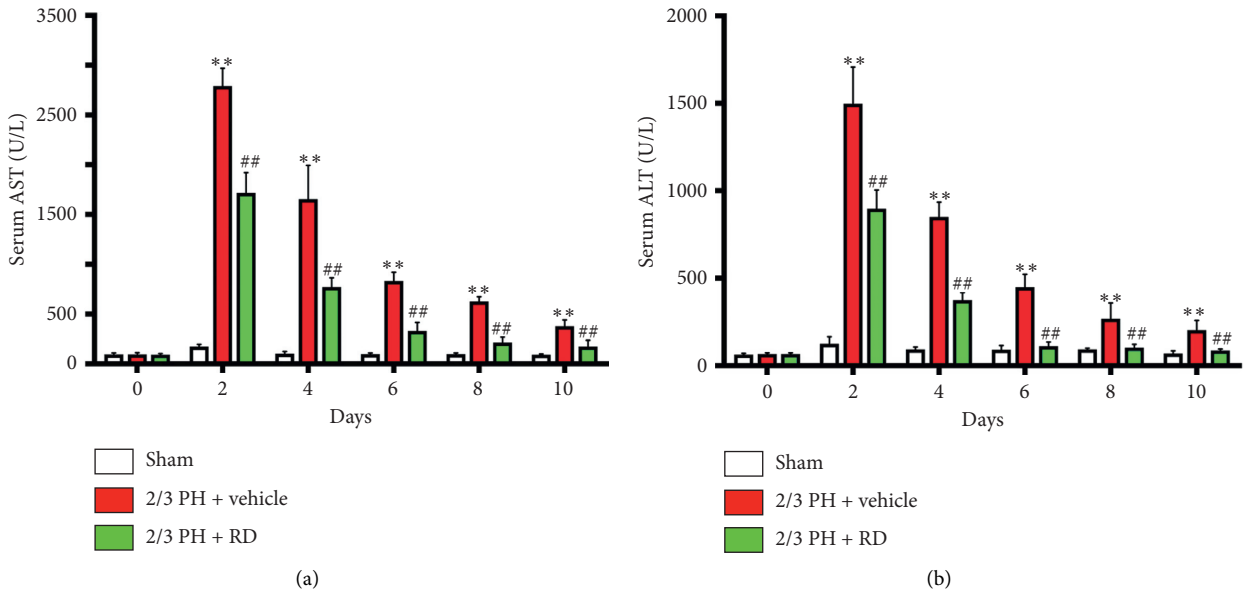

Figure 3: Continued.

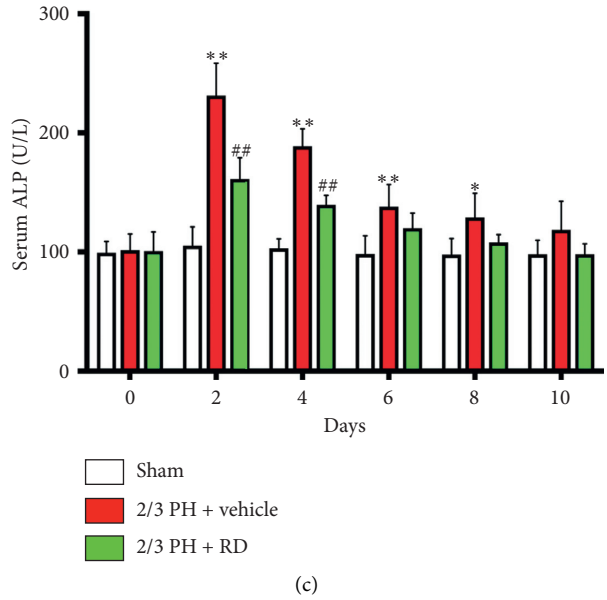

(c)

Figure 3: Resina draconis treatment prevents loss of liver function after 2/3 PH. (a) Serum AST levels were significantly increased in both the 2/3 PH group and the RD group on days 2, 4, 6, 8, and 10 following 2/3 PH. Results are represented as mean ± SEM. $n = 8$ mice/time point. $^{**}p < 0.01$, vehicle + 2/3 PH group *vs* sham group; $^{\#\#}p < 0.01$, RD + 2/3 PH group *vs* vehicle + 2/3 PH group. (b) Serum ALT levels were significantly increased in both the 2/3 PH group and the RD group on days 2, 4, 6, 8, and 10 following 2/3 PH. Results are represented as mean ± SEM. $n = 8$ mice/time point. $^{**}p < 0.01$, vehicle + 2/3 PH group *vs* sham group; $^{\#\#}p < 0.01$, RD + PH group *vs* vehicle + 2/3 PH group. (c) Serum ALP levels were significantly increased in both the 2/3 PH group and the RD group on day 2, 4, 6, and 8 following 2/3 PH. Results are represented as mean ± SEM. $n = 8$ mice/time point. $^{**}p < 0.01$, vehicle + 2/3 PH group *vs* sham group; $^{*}p < 0.05$, vehicle + 2/3 PH group *vs* sham group; $^{\#\#}p < 0.01$, RD + 2/3 PH group *vs* vehicle + 2/3 PH group.

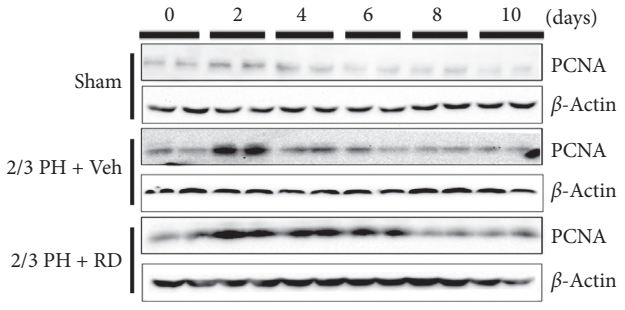

(a)

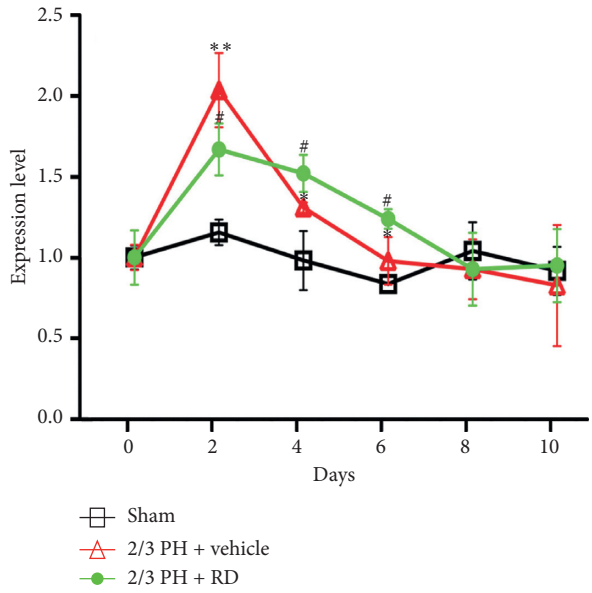

(b)

Figure 4: Resina draconis treatment enhances hepatocyte proliferation after 2/3 PH. (a). Representative western blotting analysis of PCNA protein in mouse livers after 2/3 PH and sham operation. RD treatment increases PCNA expression after 2/3 PH. (b). Quantification of PCNA normalized to β-actin. Data are expressed as mean ± SEM. $n = 5$. $^{**}p < 0.01$, 2/3 PH group *vs* sham group; $^{*}p < 0.05$, 2/3 PH group *vs* sham group; $^{\#\#}p < 0.01$, RD + 2/3 PH group *vs* vehicle + 2/3 PH group; $^{\#}p < 0.05$, RD + 2/3 PH group *vs* vehicle + 2/3 PH group.

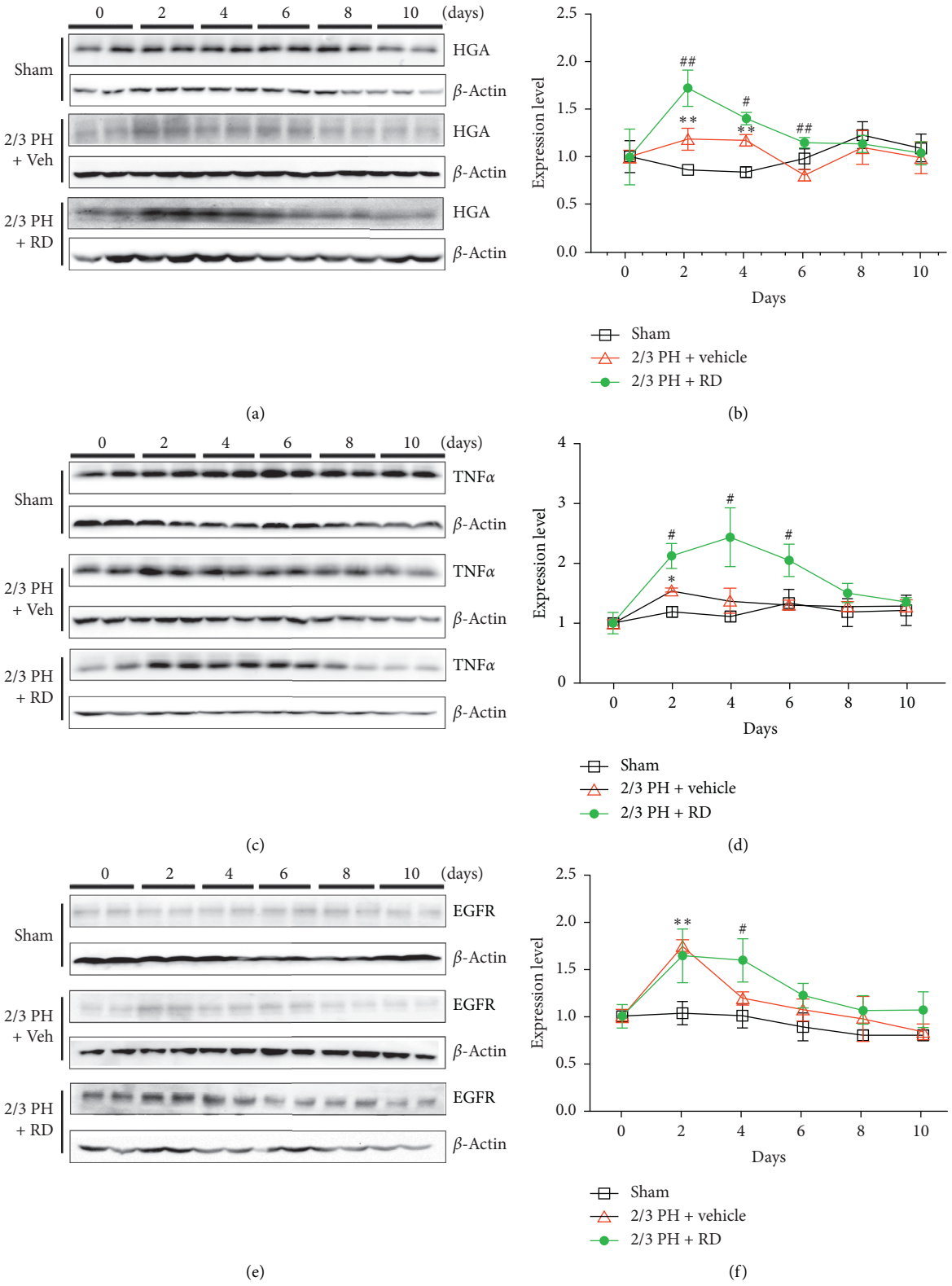

Figure 5: Resina draconis treatment affects HGF, EGFR, and TNFα levels after 2/3 PH. (a) and (b). Representative western blotting analysis of HGF protein in mouse livers after 2/3 PH and sham operations. RD treatment increases the HGF expression after 2/3 PH. Quantifications were normalized to β-actin. (c) and (d). Representative western blotting analysis of HGF protein in mouse livers after 2/3 PH and sham operations. RD treatment increases TNFα expression after 2/3 PH. Quantifications were normalized to β-actin. (e) and (f). Representative western blotting analysis of EGFR protein in mouse livers after 2/3 PH and sham operations. RD treatment increases the TNFα expression after 2/3 PH. Quantifications were normalized to β-actin. All the data are expressed as mean ± SEM. $n = 5$. $^{**}p < 0.01$, vehicle + 2/3 PH group *vs* sham group; $^{*}p < 0.05$, vehicle + 2/3 PH group *vs* sham group; $^{\#}p < 0.05$, RD + 2/3 PH group vs 2/3 PH group.

PH and decreased progressively to preoperative levels by the end of the observation period. However, the levels of HGF (Figures 5(a) and 5(b)), EGFR (Figures 5(c) and 5(d)), and TNFα (Figures 5(e) and 5(f)) were significantly higher on day 2 and day 4 after 2/3 PH ($p < 0.05$) in the RD + 2/3 PH group than in vehicle + 2/3 PH group and sham group. Further, trends in these increases continued to day 6 and day 8.

4. Discussion

Despite clinical advances, liver diseases remain a severe health problem worldwide. Liver resection is the primary treatment modality for liver cancer and other serious liver diseases [46–52]. Liver regeneration plays a vital role in recovery after resection. Acute liver failure after hepatectomy is a main cause of postoperative mortality and morbidity [53–57]. How to protect against postoperative liver injury and promote liver regeneration remains an urgent unmet clinical need. RD has been used for many years to promote wound healing [32, 58] and as an anticoagulant [59–61]. Several studies have shown that RD has hemostatic and anti-inflammatory properties and promotes blood circulation and skin repair [62–65]. Here, for the first time, we provide evidence that RD treatment is beneficial to liver regeneration and protects against liver injury after 2/3 PH. Furthermore, RD-stimulated HGF, EGFR, and TNFα signaling during liver regeneration after 2/3 PH. These findings offer a new avenue for protecting against postoperative liver failure and controlling liver regeneration after liver resection.

The exact mechanisms of liver regeneration after 2/3 PH are complicated and have not been fully defined, although a number of growth factors are implicated in the process. HGF, EGFR, and TNFα are potential initiators of liver regeneration and increase immediately and are maintained after 2/3 PH. Here, we found that the expressions of HGF, EGFR, and TNFα increased significantly after 2/3 PH compared with those of controls on days 2 and 4 after 2/3 PH and were significantly higher in the RD-treated 2/3 PH group than in the vehicle-treated 2/3 PH group. Expression of these growth factors is a key step to initial hepatocyte proliferation and improving liver regeneration and functional recovery. The promitogenic effect of RD-induced expression of these factors was further supported by the observation of higher expression of proliferating cell nuclear antigen (PCNA) in RD-treated mice.

Serum AST and ALT liver function biomarkers are inversely related to the severity of liver damage [66–68]. We found that both ALT and AST levels were significantly higher in the 2/3 PH group mice than in the sham group mice on day 2 and day 4 after 2/3 PH and that RD treatment reversed these changes. TB and ALB are markers of liver synthetic function [69–72]. Our study revealed that TB and ALB levels were higher in the RD-treated 2/3 PH group on day 2 and day 4 after the operation than in vehicle-treated 2/3 PH. Interestingly, RD-treated not only reduced the liver function biomarker levels compared with the vehicle-treated PH group but also it recovered levels to sham over the study period. These results strongly indicate that RD treatment protects against acute liver damage and stimulates liver regeneration after 2/3 PH.

Taken together, our results confirm that intragastric injection of RD after 2/3 PH prevents acute liver failure and promotes liver regeneration. HGF, EGFR, and TNFα are involved in this process. These results indicate that RD may be useful in the treatment of acute liver injury.

Abbreviations

RD: Resina draconis
PH: Partial hepatectomy
ILBW: Index of liver to body weight
PCNA: Proliferating cell nuclear antigen
AST: Aspartate transaminase
ALT: Alanine transaminase
TP: Total protein
ALB: Albumin
HGF: Hepatocyte growth factor
TNFα: Tumor necrosis factor
EGF: Epidermal growth factor
LDLT: Living donor liver transplantation
NF-κB: Nuclear factor kappa B.

Data Availability

The data used to support the study findings are available within the article.

Conflicts of Interest

The authors declare that there are no conflicts of interest.

Authors' Contributions

Zhi-yong He, Kai-han Lou, and Jia-hui Zhao performed the research; Wei-yan Hu and Rong-ping Zhang designed the research; Wei-yan Hu and Zhi-yong He analyzed the data and wrote the paper; Ming Zhang revised the manuscript; Lang-chun Zhang, Ju Li and Hao-fei Yu prepared the figures.

Acknowledgments

This work was supported by grants from the National Natural Science Foundation of China (81960666 and 81860254, W.Y.H.), the National Natural Science Foundation of Yunnan (2019FA033, R.P.Z.), the Program for Innovative Research Team in Science and Technology in Yunnan Province (2019HC008), and Yunnan Provincial Science and Technology Department (202005AF150043). The support provided by Yunnan Key Laboratory of Stem Cell and Regenerative Medicine (M. Z. and W.Y.H.) is also appreciated.

Supplementary Materials

This section includes graphical abstract. (*Supplementary Materials*)

References

[1] J. A. Cienfuegos, F. Rotellar, J. Baixauli et al., "Liver regeneration—the best kept secret: a model of tissue injury response," *Revista Española de Enfermedades Digestivas*, vol. 106, no. 3, pp. 171–194, 2014.

[2] N. Fausto, J. S. Campbell, and K. J. Riehle, "Liver regeneration," *Hepatology*, vol. 43, no. 2, pp. S45–S53, 2000.

[3] J. M. Gentile, L. Avila, and J. T. Grace, "Liver regeneration. old and new concepts," *The American Journal of Surgery*, vol. 120, no. 1, pp. 2–6, 1970.

[4] K. J. Riehle, Y. Y. Dan, J. S. Campbell, and N. Fausto, "New concepts in liver regeneration," *Journal of Gastroenterology and Hepatology*, vol. 26, no. 1, pp. 203–212, 2011.

[5] A. Cieslar-Pobuda and E. Wiechec, "Research on liver regeneration as an answer to the shortage of donors for liver transplantation," *Hepatology Research*, vol. 44, no. 9, pp. 944–946, 2014.

[6] K. M. Olthoff, J. C. Emond, T. H. Shearon et al., "Liver regeneration after living donor transplantation: adult-to-adult living donor liver transplantation cohort study," *Liver Transplantation*, vol. 21, no. 1, pp. 79–88, 2015.

[7] D. Pagano, M. Spada, V. Parikh et al., "Liver regeneration after liver resection: clinical aspects and correlation with infective complications," *World Journal of Gastroenterology*, vol. 20, no. 22, pp. 6953–6960, 2014.

[8] N. L. Bucher and G. C. Weir, "Insulin, glucagon, liver regeneration, and dna synthesis," *Metabolism*, vol. 25, no. 11, pp. 1423–1425, 1976.

[9] A. N. Kandilis, J. Koskinas, I. Vlachos et al., "Liver regeneration: immunohistochemichal study of intrinsic hepatic innervation after partial hepatectomy in rats," *BMC Gastroenterology*, vol. 14, no. 1, p. 202, 2014.

[10] K. N. Tzirogiannis, K. T. Kourentzi, S. Zyga et al., "Effect of 5-HT 7 receptor blockade on liver regeneration after 60–70% partial hepatectomy," *BMC Gastroenterology*, vol. 14, no. 1, p. 201, 2014.

[11] J. H. Wolf, T. R. Bhatti, S. Fouraschen et al., "Heat shock protein 70 is required for optimal liver regeneration after partial hepatectomy in mice," *Liver Transplantation*, vol. 20, no. 3, pp. 376–385, 2014.

[12] T. Wu, J. Huang, S. Wu et al., "Deficiency of periostin impairs liver regeneration in mice after partial hepatectomy," *Matrix Biology*, vol. 66, pp. 81–92, 2018.

[13] U. Marti, S. J. Burwen, and A. L. Jones, "Biological effects of epidermal growth factor, with emphasis on the gastrointestinal tract and liver: an update," *Hepatology*, vol. 9, no. 1, pp. 126–138, 1989.

[14] G. K. Michalopoulos, "Advances in liver regeneration," *Expert Review of Gastroenterology & Hepatology*, vol. 8, no. 8, pp. 897–907, 2014.

[15] G. K. Michalopoulos and Z. Khan, "Liver regeneration, growth factors, and amphiregulin," *Gastroenterology*, vol. 128, no. 2, pp. 503–506, 2005.

[16] R. Imamura and K. Matsumoto, "Hepatocyte growth factor in physiology and infectious diseases," *Cytokine*, vol. 98, pp. 97–106, 2017.

[17] C. G. Huh, V. M. Factor, A. Sanchez et al., "Hepatocyte growth factor/c-met signaling pathway is required for efficient liver regeneration and repair," *Proceedings of the National Academy of Sciences*, vol. 101, no. 13, pp. 4477–4482, 2004.

[18] X. F. Cao, S. Z. Jin, L. Sun et al., "Therapeutic effects of hepatocyte growth factor-overexpressing dental pulp stem cells on liver cirrhosis in a rat model," *Scientific Reports*, vol. 7, no. 1, Article ID 15812, 2017.

[19] S. Paranjpe, W. C. Bowen, A. W. Bell et al., "Cell cycle effects resulting from inhibition of hepatocyte growth factor and its receptor c-Met in regenerating rat livers by RNA interference," *Hepatology*, vol. 45, no. 6, pp. 1471–1477, 2017.

[20] G. M. Argast, J. S. Campbell, J. T. Brooling, and N. Fausto, "Epidermal growth factor receptor transactivation mediates tumor necrosis factor-induced hepatocyte replication," *Journal of Biological Chemistry*, vol. 279, no. 33, pp. 34530–34536, 2004.

[21] J. Sun, Z. Yang, X. C. Shi et al., "G0S2a1 (G0/G1 switch gene 2a1) is downregulated by TNF-alpha in grass carp (*Ctenopharyngodon idellus*) hepatocytes through PPARalpha inhibition," *Gene*, vol. 641, pp. 1–7, 2018.

[22] D. E. Cressman, L. E. Greenbaum, R. A. DeAngelis et al., "Liver failure and defective hepatocyte regeneration in interleukin-6-deficient mice," *Science*, vol. 274, no. 5291, pp. 1379–1383, 1996.

[23] G. M. Ledda-Columbano, M. Curto, R. Piga et al., "In vivo hepatocyte proliferation is inducible through a TNF and IL-6-independent pathway," *Oncogene*, vol. 17, no. 8, pp. 1039–1044, 1998.

[24] W. Li, X. Liang, C. Kellendonk, V. Poli, and R. Taub, "STAT3 contributes to the mitogenic response of hepatocytes during liver regeneration," *Journal of Biological Chemistry*, vol. 277, no. 32, pp. 28411–28417, 2002.

[25] Y. Yamada, I. Kirillova, J. J. Peschon, and N. Fausto, "Initiation of liver growth by tumor necrosis factor: deficient liver regeneration in mice lacking type I tumor necrosis factor receptor," *Proceedings of the National Academy of Sciences*, vol. 94, no. 4, pp. 1441–1446, 1997.

[26] G. K. Michalopoulos, "Principles of liver regeneration and growth homeostasis," *Comprehensive Physiology*, vol. 3, no. 1, pp. 485–513, 2013.

[27] B. Bhushan, H. Chavan, P. Borude et al., "Dual role of epidermal growth factor receptor in liver injury and regeneration after acetaminophen overdose in mice," *Toxicological Sciences*, vol. 155, no. 2, pp. 363–378, 2017.

[28] H. Zhang, J. H. Shi, H. Jiang et al., "ZBTB20 regulates EGFR expression and hepatocyte proliferation in mouse liver regeneration," *Cell Death & Disease*, vol. 9, no. 5, p. 462, 2018.

[29] M. Bruck, "Dragon's blood. A glance into the history of pharmacognosy," «*Bulletin de la Société des Sciences Médicales du Grand Duché de Luxembourg*, vol. 1, pp. 96–101, 1999.

[30] L. L. Fan, P. F. Tu, J. X. He, H. B. Chen, and S. Q. Cai, "Microscopical study of original plant of Chinese drug "dragon's blood" dracaena cochinchinensis and distribution and constituents detection of its resin," *Zhongguo Zhong Yao Za Zhi*, vol. 33, no. 10, pp. 1112–1117, 2008.

[31] A. J. Liu, Y. H. Zhu, and Z. X. Zhao, "Effect of resina draconis is in the repair of skin defect treated with tissue engineering skin," *Guangzhou University of Chinese Medicine*, vol. 26, pp. 260–262, 2009.

[32] A. J. Liu, J. T. Huang, and L. Q. Zhang, "Growth of fetal mouse skin filbrobasts stimulated by effect locus of resina draconis," *Journal of Sichuan Traditional Chinese Medicine*, vol. 28, pp. 46–48, 2014.

[33] F. Namjoyan, F. Kiashi, Z. B. Moosavi, F. Saffari, and B. S. Makhmalzadeh, "Efficacy of dragon's blood cream on wound healing: a randomized, double-blind, placebo-controlled clinical trial," *Journal of Traditional and Complementary Medicine*, vol. 6, pp. 37–40, 2016.

[34] J. S. Li, "Application of dragon's blood in treating surface wounds and burns," *Journal of Harbin Medical University*, vol. 21, p. 70, 2001.

[35] X. P. Lu, "20 cases of alopecia areata treatment efficacy blood capsules," *Jilin Medical Journal*, vol. 30, p. 1391, 2009.

[36] X. Nian, J. L. Yu, and L. Yan, "Dragon's blood extract has antithrombotic properties, affecting platelet aggregation functions and anticoagulation activities," *Journal of Ethnopharmacology*, vol. 135, pp. 510–514, 2011.

[37] J. Sun, J.-N. Liu, and B. Fan, "Phenolic constituents, pharmacological activities, quality control, and metabolism of dracaena species: a review," *Journal of Ethnopharmacology*, vol. 244, 2019.

[38] Y. D. Zhu, P. Zhang, and H. P. Yu, "Anti-helicobacter pylori and thrombin inhibitory components from Chinese dragon's blood *Dracaena cochinchinensis*," *Journal of Natural Products*, vol. 70, pp. 1570–1577, 2007.

[39] F. Wen, X. Zhao, Y. Zhao, Z. Lu, and Q. Guo, "The anticancer effects of resina draconis extract on cholangiocarcinoma," *Tumour Biology*, vol. 37, no. 11, pp. 15203–15210, 2016.

[40] Y.-N. Zhao, A.-L. Yang, D.-R. Pang et al., "Anti-tumor activity of HIS-4,a biflavonoid from resina draconis,on human hepatoma HepG2 and SK-HEP-1 cells," *Zhongguo Zhong Yao Za Zhi*, vol. 44, no. 7, pp. 1442–1449, 2019.

[41] R. D. Harkness, "Changes in the liver of the rat after partial hepatectomy," *The Journal of Physiology*, vol. 117, no. 3, pp. 267–277, 1952.

[42] R. D. Harkness, "Collagen in regenerating liver of the rat," *The Journal of Physiology*, vol. 117, no. 3, pp. 257–266, 1952.

[43] K. Lou, M. Yang, E. Duan et al., "Rosmarinic acid stimulates liver regeneration through the mTOR pathway," *Phytomedicine*, vol. 23, no. 13, pp. 1574–1582, 2016.

[44] A. Blindenbacher, X. Wang, I. Langer et al., "Interleukin 6 is important for survival after partial hepatectomy in mice," *Hepatology*, vol. 38, no. 3, pp. 674–682, 2003.

[45] I. Quetier, N. Brezillon, M. Duriez et al., "Hepatitis B virus HBx protein impairs liver regeneration through enhanced expression of IL-6 in transgenic mice," *The Journal of Physiology*, vol. 59, no. 2, pp. 285–291, 2013.

[46] B. Aussilhou, G. Doufle, C. Hubert et al., "Extended liver resection for polycystic liver disease can challenge liver transplantation," *Annals of Surgery*, vol. 252, no. 5, pp. 735–743, 2010.

[47] T. Belda, E. M. Montalva, R. Lopez-Andujar et al., "Role of resection surgery in breast cancer liver metastases: experience over the last 10 years in a reference hospital," *Cirugía Española*, vol. 88, no. 3, pp. 167–173, 2010.

[48] A. Bueno, F. Rotellar, A. Benito et al., "Laparoscopic limited liver resection decreases morbidity irrespective of the hepatic segment resected," *HPB*, vol. 16, no. 4, pp. 320–326, 2014.

[49] D. Ehrl, K. Rothaug, D. Hempel, and H. G. Rau, "Importance of liver resection in case of hepatic breast cancer metastases," *Hepato-Gastroenterology*, vol. 60, no. 128, pp. 2026–2033, 2013.

[50] C. Marin, R. Robles, M. Fuster, and P. Parrilla, "Laparoscopic liver resection of a desmoplastic nested spindle cell tumor of the liver," *The American Surgeon*, vol. 76, no. 9, pp. E184–E185, 2010.

[51] J. P. McAteer, A. B. Goldin, P. J. Healey, and K. W. Gow, "Surgical treatment of primary liver tumors in children: outcomes analysis of resection and transplantation in the SEER database," *Pediatric Transplantation*, vol. 17, no. 8, pp. 744–750, 2013.

[52] L. Vigano, L. Capussotti, G. De Rosa et al., "Liver resection for colorectal metastases after chemotherapy: impact of chemotherapy-related liver injuries, pathological tumor response, and micrometastases on long-term survival," *Ann Surg*, vol. 258, no. 5, pp. 731–740, 2013.

[53] I. Colle, X. Verhelst, A. Vanlander et al., "Pathophysiology and management of post resection liver failure," *Acta Chirurgica Belgica*, vol. 113, no. 3, pp. 155–161, 2013.

[54] T. Hirashita, M. Ohta, Y. Iwashita et al., "Risk factors of liver failure after right-sided hepatectomy," *The American Journal of Surgery*, vol. 206, no. 3, pp. 374–379, 2013.

[55] K. J. Roberts, K. G. Bharathy, and J. P. Lodge, "Kinetics of liver function tests after a hepatectomy for colorectal liver metastases predict post-operative liver failure as defined by the international study group for liver surgery," *HPB*, vol. 15, no. 5, pp. 345–351, 2013.

[56] E. Vibert, G. Pittau, M. Gelli et al., "Actual incidence and long-term consequences of posthepatectomy liver failure after hepatectomy for colorectal liver metastases," *Surgery*, vol. 155, no. 1, pp. 94–105, 2014.

[57] D. C. Yu, W. B. Chen, C. P. Jiang, and Y. T. Ding, "Risk assessment in patients undergoing liver resection," *Hepatobiliary & Pancreatic Diseases International*, vol. 12, no. 5, pp. 473–479, 2013.

[58] L. Pieters, T. De Bruyne, B. Van Poel et al., "In vivo wound healing activity of dragon's blood (croton spp.), a traditional south American drug, and its constituents," *Phytomedicine*, vol. 2, no. 1, pp. 17–22, 1995.

[59] D. Gupta, B. Bleakley, and R. K. Gupta, "Dragon's blood: botany, chemistry and therapeutic uses," *Journal of Ethnopharmacology*, vol. 115, no. 3, pp. 361–380, 2008.

[60] L. Pieters, T. De Bruyne, M. Claeys et al., "Isolation of a dihydrobenzofuran lignan from south American dragon's blood (croton spp.) as an inhibitor of cell proliferation," *Journal of Natural Products*, vol. 56, no. 6, pp. 899–906, 1993.

[61] N. Xin, Y. J. Li, X. Li et al., "Dragon's blood may have radioprotective effects in radiation-induced rat brain injury," *Radiation Research*, vol. 178, no. 1, pp. 75–85, 2012.

[62] J. Y. Fan, T. Yi, C. M. Sze-To et al., "A systematic review of the botanical, phytochemical and pharmacological profile of *Dracaena cochinchinensis*, a plant source of the ethnomedicine "dragon's blood"," *Molecules*, vol. 19, no. 7, pp. 10650–10669, 2014.

[63] N. Li, Z. Ma, M. Li, Y. Xing, and Y. Hou, "Natural potential therapeutic agents of neurodegenerative diseases from the traditional herbal medicine Chinese dragon's blood," *Journal of Ethnopharmacology*, vol. 152, no. 3, pp. 508–521, 2014.

[64] Y. S. Li, J. X. Wang, M. M. Jia et al., "Dragon's blood inhibits chronic inflammatory and neuropathic pain responses by blocking the synthesis and release of substance P in rats," *Journal of Pharmacological Sciences*, vol. 118, no. 1, pp. 43–54, 2012.

[65] V. S. Rao, L. A. Gurgel, R. C. Lima-Junior et al., "Dragon's blood from *Croton urucurana* (baill.) attenuates visceral nociception in mice," *Journal of Ethnopharmacology*, vol. 113, no. 2, pp. 357–360, 2007.

[66] B. Avci, A. Bahadir, O. K. Tuncel, and B. Bilgici, "Influence of alpha-tocopherol and alpha-lipoic acid on bisphenol-A-

induced oxidative damage in liver and ovarian tissue of rats," *Toxicology and Industrial Health*, vol. 32, 2016.

[67] S. Gurgen, A. Yucel, A. Karakus et al., "Usage of whey protein may cause liver damage via inflammatory and apoptotic responses," *Human & Experimental Toxicology*, vol. 34, 2015.

[68] G. Henrique Da Silva, P. P. Barros, G. M. Silva Goncalves, and M. A. Landi, "Hepatoprotective effect of *Lycopodium clavatum* 30CH on experimental model of paracetamol-induced liver damage in rats," *Homeopathy*, vol. 104, no. 1, pp. 29–35, 2015.

[69] S. A. Akuyam, O. K. Uchenna, A. Adamu et al., "Liver function tests profile in cancer patients on cytotoxic chemotherapy: a preliminary report," *Nigerian Postgraduate Medical Journal*, vol. 18, no. 1, pp. 34–33, 2011.

[70] J. X. Li, H. Wu, J. W. Huang, and Y. Zeng, "The influence on liver function after transcatheter arterial chemoembolization combined with percutaneous radiofrequency ablation in patients with hepatocellular carcinoma," *Journal of the Formosan Medical Association*, vol. 111, no. 9, pp. 510–515, 2012.

[71] Z. Wang, X. P. Chen, Z. Q. Liang et al., "Therapeutic effect of autologous bone marrow stem cell transplantation in the treatment of severe liver damage," *Nan Fang Yi Ke Da Xue Xue Bao*, vol. 30, no. 12, pp. 2762–2764, 2010.

[72] L. Zhu, Z. C. Yang, A. Li, and D. C. Cheng, "Protective effect of early enteral feeding on postburn impairment of liver function and its mechanism in rats," *World Journal of Gastroenterology*, vol. 6, no. 1, pp. 79–83, 2000.

Hindawi
Evidence-Based Complementary and Alternative Medicine
Volume 2020, Article ID 7171498, 19 pages
https://doi.org/10.1155/2020/7171498

Review Article

A Comprehensive Review of Natural Products against Liver Fibrosis: Flavonoids, Quinones, Lignans, Phenols, and Acids

Xiaoqi Pan,[1,2,3] **Xiao Ma**,[1] **Yinxiao Jiang**,[1] **Jianxia Wen**,[1] **Lian Yang**,[2] **Dayi Chen**,[2] **Xiaoyu Cao**,[1,3] **and Cheng Peng**[1,3]

[1]*School of Pharmacy, Chengdu University of Traditional Chinese Medicine, Chengdu 611137, China*
[2]*School of Public Health, Chengdu University of Traditional Chinese Medicine, Chengdu 611137, China*
[3]*State Key Laboratory of Southwestern Chinese Medicine Resources, Chengdu University of Traditional Chinese Medicine, Chengdu 611137, China*

Correspondence should be addressed to Cheng Peng; pengchengchengdu@126.com

Received 24 June 2020; Revised 23 July 2020; Accepted 25 July 2020; Published 5 October 2020

Guest Editor: Hongwei Zhang

Liver fibrosis resulting from continuous long-term hepatic damage represents a heavy burden worldwide. Liver fibrosis is recognized as a complicated pathogenic mechanism with extracellular matrix (ECM) accumulation and hepatic stellate cell (HSC) activation. A series of drugs demonstrate significant antifibrotic activity in vitro and in vivo. No specific agents with ideally clinical efficacy for liver fibrosis treatment have been developed. In this review, we summarized the antifibrotic effects and molecular mechanisms of 29 kinds of common natural products. The mechanism of these compounds is correlated with anti-inflammatory, antiapoptotic, and antifibrotic activities. Moreover, parenchymal hepatic cell survival, HSC deactivation, and ECM degradation by interfering with multiple targets and signaling pathways are also involved in the antifibrotic effects of these compounds. However, there remain two bottlenecks for clinical breakthroughs. The low bioavailability of natural products should be improved, and the combined application of two or more compounds should be investigated for more prominent pharmacological effects. In summary, exploration on natural products against liver fibrosis is becoming increasingly extensive. Therefore, natural products are potential resources for the development of agents to treat liver fibrosis.

1. Introduction

Liver fibrosis is a progressive liver disease that results from a chronic wound healing response to various pathogenic factors, such as chronic infection with hepatitis B virus (HBV)/hepatitis C virus (HCV), alcohol abuse, nonalcoholic fatty liver disease (NAFLD)/nonalcoholic steatohepatitis (NASH), autoimmune hepatitis, hemochromatosis, or primary/secondary biliary cholangitis [1, 2]. Liver fibrosis gradually develops into cirrhosis and causes liver dysfunction with liver failure. This progression is estimated to influence approximately 1% to 2% of the population worldwide. Moreover, over 1 million people will suffer death annually worldwide [3]. It is believed that liver fibrosis is characterized by redundant deposition and intrahepatic accumulation of extracellular matrix (ECM). In the fibrotic liver, quiescent hepatic stellate cells (HSCs) differentiate into proliferative and contractile myofibroblasts. This activation of HSCs plays a primary role in ECM accumulation [4]. The hepatic sinusoid is a well-organized structural and biochemical microenvironment for liver cell survival and communication. This microenvironment is a multidirectional interaction complex with multiple signals or targets [5]. Besides injured hepatocytes, hepatic macrophages, endothelial cells, and lymphocytes are also included due to the abundant blood supply in this microenvironment. Thus, the death of hepatocytes is progressively to release cellular contents and reactive oxygen species (ROS) that activate hepatic immune response containing resident macrophages (Kupffer cells) with excessive proinflammatory factors like TNF-α, IL-1β, and IL-6 [6]. On the other hand, after sustained liver injury from this progress, liver sinusoidal

endothelial cells (LSECs) lose their phenotype and protective properties, promoting angiogenesis and vasoconstriction. It further contributes to repeating inflammation and triggers fibrosis [7]. All these actions will contribute to HSCs activation. HSCs are one of the vital constituents in liver sinusoidal cells and are located between LSECs and hepatocytes. Thus, HSC activation and fibrogenesis are associated with a series of mechanisms, such as transforming growth factor-β (TGF-β) secretion, autophagy, endoplasmic reticulum stress, oxidative stress, and cholesterol stimulation [4]. Apart from HSC activation, liver fibrosis is widely associated with hepatocyte apoptosis and dysregulation of inflammation. To date, no satisfactory agents for liver fibrosis treatment have been developed due to the complicated progression of liver fibrosis.

In recent years, a number of natural products derived from formulae or composites have drawn much attention as resources for drug discovery [8]. The prevailing natural products involving plants, animals, fungi, and microorganisms are widely used in traditional Chinese medicine (TCM), Ayurveda, Kampo, and Unani. Some natural products have exhibited therapeutic effects on liver diseases for thousands of years. In particular, several kinds of representative natural products, such as flavonoids, quinones, lignans, phenols, and acids, demonstrate potent function in liver protection, cholestasis prevention, NASH inhibition, and hepatocellular carcinoma (HCC) suppression [9, 10]. In addition, natural products that have promising efficacy in preventing fibrosis have been under rapid development [11–13]. Hence, this review provides a comprehensive overview of the potential effects and possible mechanisms of several natural products against liver fibrosis.

2. Flavonoids

Flavonoids, a type of compounds with a 2-phenyl flavone structure, are widely distributed in nature, which are characterized by a variety of biological activities, including cardiovascular activity, antibacteria, antivirus, antitumor, antioxidant, anti-inflammatory, and liver protection. Chemical structure of some common flavonoids that have antifibrotic effects is shown in Figure 1.

2.1. Silibinin. Silibinin is one kind of flavonolignans isolated from the plant *Silybum marianum* (L.) (milk thistle). It is the major bioactive component and accounts for approximately 60% of silymarin. In recent years, silibinin has been widely applied as a hepatoprotective compound for the treatment of a variety of liver diseases [14]. A team of Italian researchers first confirmed that silibinin at a dose of 100 mg/kg alleviated iron-induced liver fibrosis with mitochondrial dysfunction [15, 16]. Then, another chronic CCl_4-induced liver fibrosis model was assessed. However, the results indicated that silibinin at 50 mg/kg did not significantly reverse fibrogenic progression [17]. In addition, Wang's team reported that silibinin at 200 mg/kg inhibited thioacetamide- (TAA-) induced liver injury and fibrosis by decreasing α-SMA and inflammatory cytokines IL-1β, IL-6, and TNF-α levels, which was associated with the upregulation of CYP3A via pregnane *X* receptor (PXR) [18]. Silibinin at a dose of 105 mg/kg was effective for preventing hepatic steatosis and fibrosis in a NASH mouse model through regulating lipid metabolism-related gene expression, activating Nrf2, and inhibiting the NF-κB signaling pathway [19]. In an in vitro study, 25–50 μmol/L silybin dose-dependently inhibited the activation of HSC proliferation, cell motility, and ECM deposition through anti-inflammatory activities [20]. Moreover, another recent study indicated that silibinin inhibited LX-2 cell proliferation in a dose- and time-dependent manner and arrested HSC cell cycle by enhancing p53/p27 ratio and inhibiting Akt downstream signaling [21].

2.2. Silymarin. Silymarin is a mixture of flavonolignans that mainly contains silybin, silydianin, and silychristin, which are extracted from *Silybum marianum* (L.) [22]. Silymarin is a well-known complex with antioxidant, anti-inflammatory, and immunomodulatory effects on various liver disorders [23]. Silymarin showed antifibrotic effects in a variety of liver fibrosis models, such as alcohol, CCl_4, TAA, and schistosomiasis-induced models [24–27]. The antihepatic fibrosis mechanism of silymarin seems to be varied. El-Lakkany reported that silymarin at 750 mg/kg alleviated *Schistosoma mansoni*-induced liver fibrosis by downregulating MMP-2 and TGF-β1 and upregulating glutathione (GSH) [28]. In a series of CCl_4-induced liver fibrosis studies, silymarin significantly decreased connective tissue growth factor (CTGF), regulated Kupffer cells, inhibited inflammation via NF-κB signaling, and suppressed the activation of HSCs [29–31]. Moreover, silymarin relieved diet-induced NASH with liver fibrosis by suppressing HSC activation and TNF-α release [32]. The combined application of silymarin with other agents, such as caffeine, lisinopril, and taurine, also displayed remarkable antifibrotic effects through the downregulation of LPAR1 and NF-κB expression [33–35].

2.3. Puerarin. Puerarin is an isoflavone that is extracted from the plant *Pueraria lobata* (Willd.) Ohwi. Puerarin has abundant pharmacological effects, including cardiovascular protection, neuroprotection, and liver injury prevention [36]. In recent years, puerarin was confirmed to be effective for the treatment of liver fibrosis with multiple target hits. A study suggested that puerarin at doses of 40–80 mg/kg significantly increased the activated HSCs apoptosis and downregulated Bcl-2 expression in a CCl_4-induced liver fibrosis model [37]. Apart from apoptosis signaling, it is believed that puerarin also alleviates liver fibrosis via inhibition of excessive collagen deposition through peroxisomal proliferator-activated receptor γ (PPAR-γ) expression and the PI3K/Akt pathway, attenuation of inflammatory response through the TNF-α/NF-κB pathway, and suppression of PARP-1 and mitochondrial dysfunction [38–40]. Moreover, puerarin also blocked the TGF-β1/Smad signaling pathway in dimethylnitrosamine- (DMN-) induced liver fibrosis and HSC-T6 in a dose-dependent manner [41]. Similarly, puerarin was showed to alleviate TAA-induced liver fibrosis by reducing HSC activation and alleviating

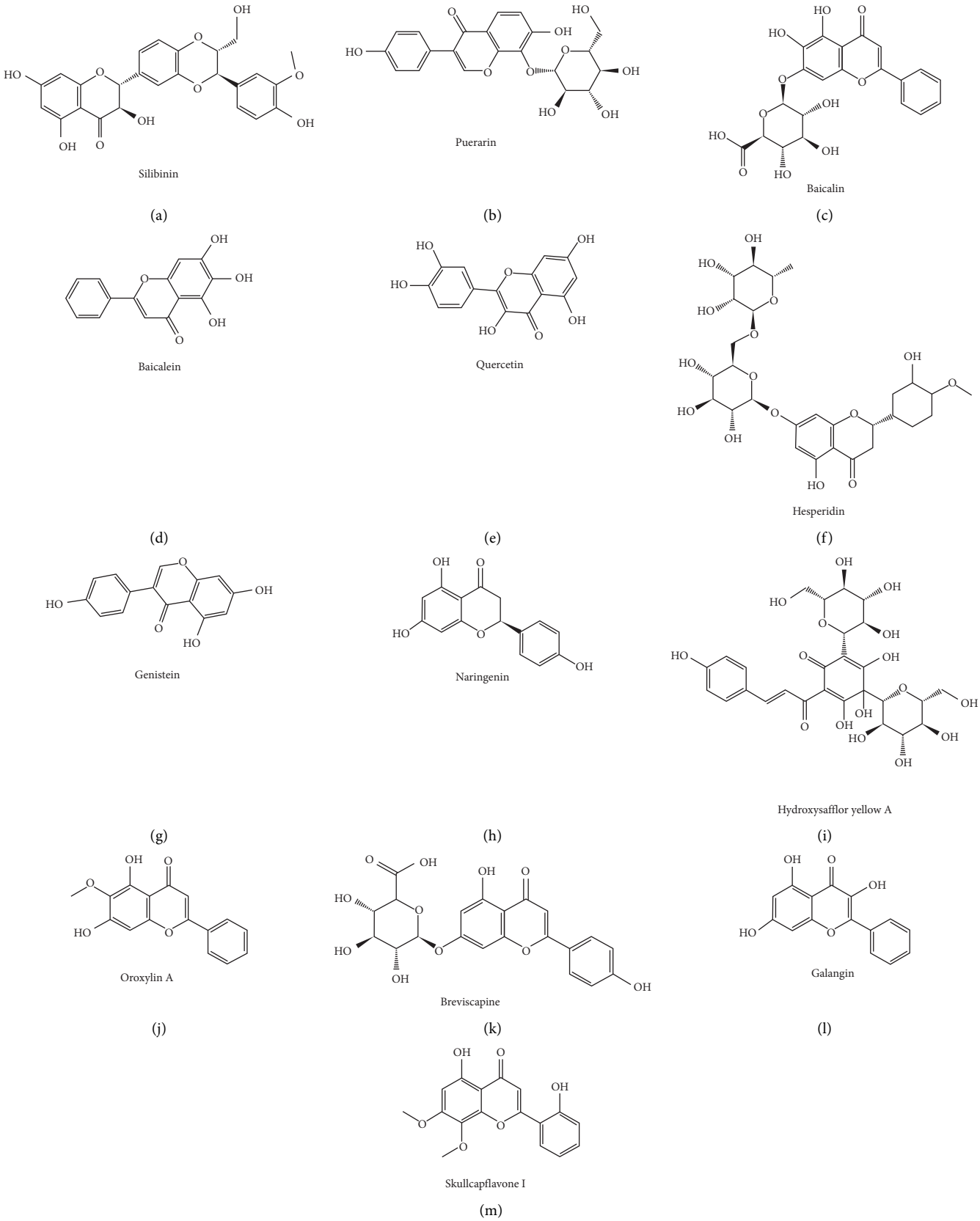

Figure 1: Chemical structures of flavonoid compounds against liver fibrosis.

ECM expression through the downregulation of the TGF-β/ERK1/2 pathway [42]. In addition, the combined application of puerarin and vitamin D showed a significant effect against liver fibrosis through the Wnt/β-catenin signaling pathway [43].

2.4. Baicalin. Baicalin primarily derived from *Scutellaria baicalensis* Georgi is an active flavonoid compound and is believed to be a specific TCM for treating liver diseases [44]. In the past 15 years, this compound has been widely suggested to have a therapeutic effect on liver fibrosis. Peng's research demonstrated that 70 mg/kg baicalin had a significant effect on CCl_4-induced liver fibrosis, which was correlated with immunoregulation of the imbalance between profibrotic and anti-fibrotic cytokines, including TGF-β1, TNF-α, IL-6, and IL-10 expression [45]. Another study also confirmed that baicalin could enhance PPAR-γ levels contributing to the downregulation of the TGF-β1 signaling pathway and the suppression of HSC activation to play antifibrotic effect [46]. Baicalin also decreased liver fibrosis progression with marked inhibition of α-SMA, TGF-β1, and Col1A1 expression in a NASH model [47]. Furthermore, baicalin at doses of 50–150 μmol/L inhibited platelet-derived growth factor-B subunit homodimer- (PDGF-BB-) induced HSC-T6 activation via the miR-3595/ACSL4 axis in vitro [48]. Other systematic studies indicated that baicalin combined with rosmarinic acid suppressed fibrotic effects via PPAR-γ in HSCs [49].

2.5. Baicalein. Baicalein is another active flavonoid from *Scutellaria baicalensis* Georgi. Baicalein possesses hepatoprotective activities via a variety of biological properties [50]. Treatment with 20–80 mg/kg baicalein dose-dependently decreased hydroxyproline and MMPs in CCl_4-induced liver fibrosis, which was related to reduction of inflammation, liver structural repair, and protein synthesis inhibition of the PDGF-β receptor [51]. Moreover, 3–30 μmol/L baicalein presented potent antiproliferative effect in HSCs stimulated with PDGF-BB-, indicating that baicalein could be regarded as a potential antifibrotic drug [52].

2.6. Hesperidin. Hesperidin is a flavanone glycoside that is widely found in citrus fruits and has various biological activities, such as neuroprotection, liver protection, anticancer effects, and inflammatory regulation [53, 54]. Hesperidin was found to be effective for liver fibrosis treatment based on a series of liver fibrosis models. Hesperidin at doses of 100 and 200 mg/kg demonstrated antifibrotic effects by reducing HSC activation in DMN-induced fibrosis [55]. In a CCl_4-induced liver fibrosis model, hesperidin at 200 mg/kg decreased lipid peroxidation, NF-κB, TGF-β, CTGF, and IL-1β and increased IL-10 expression [56]. Moreover, hesperidin prevented from the progression of BDL-induced liver fibrosis through inhibition of TGF-β1/Smad signaling pathway-mediated ECM deposition and apoptosis [57]. A similar study in vitro indicated that hesperidin inhibited HSC-T6 proliferation and activation by modulating the TGF-β1/Smad signaling pathway [58].

2.7. Quercetin. Quercetin, a well-known flavonoid, is widely found in various vegetables and fruits, including onion, mulberry, tomato, apples, and tea [59]. Quercetin is thought to effectively suppress liver fibrosis involving multiple mechanisms. A study from Lee first reported that administration of quercetin at 10 mg/kg markedly prevented from DMN-induced liver fibrosis by reducing TGF-β1 expression [60]. Quercetin at doses of 5–200 mg/kg significantly alleviated liver fibrosis induced by CCl_4 through regulating inflammation involving NF-κB and MAPK signals and protecting from apoptosis via inhibiting proapoptotic gene Bax and improving antiapoptotic gene Bcl-2 expression [61]. Quercetin also reduced autophagy via the TGF-β1/Smad and PI3K/Akt pathways, improving HSC apoptosis and activating MMPs, as well as inhibiting macrophage infiltration and modulating M1 macrophage polarization by regulating the Notch1 signaling pathway [62–64]. In addition, quercetin modulated the HMGB1-TLR2/4-NF-κB signaling pathways to inhibit HSC activation in CCl_4-induced liver fibrosis [65]. In BDL-induced liver fibrosis rats, quercetin markedly inhibited ROS-associated inflammation and ameliorated insulin resistance via the STAT3/SOCS3/IRS1 signaling pathway [66]. In vitro research also showed that liver steatosis, inflammatory cell accumulation, oxidative stress, and liver fibrosis were totally or partially prevented by treatment with quercetin [67].

2.8. Genistein. Genistein is an isoflavone that is found in several soy products and has potential therapeutic effects on a multitude of diseases [68]. Increasing evidence has shown that genistein is specifically hepatoprotective [69–71]. Ganai reported that genistein at a dose of 5 mg/kg ameliorated D-GalN-induced liver fibrosis by inhibiting the TGF-β/Smad2/3 signaling pathway [72]. Genistein also significantly attenuated CCl_4-induced and BDL-induced liver fibrosis [73, 74]. Schistosomiasis-induced liver fibrosis was also markedly reversed by genistein through the NF-κB signaling pathway [75, 76]. Furthermore, genistein significantly decreased hepatic injury and fibrosis induced by chronic alcohol after treatment with 0.5–2 mg/kg [77]. Genistein inhibited proliferation and activation of HSCs as a tyrosine protein kinase inhibitor in vitro [78]. In addition, several studies conducted by Liao indicated that genistein combined with taurine and epigallocatechin gallate had a significantly preventive effect on liver fibrosis via protein metabolism, as well as glycolysis, gluconeogenesis, and ribosomal regulation [79–84].

2.9. Naringenin. Naringenin is a specific flavanone that is distributed in several plants, such as cherries, cocoa, grapes, tangelos, and lemons [85]. Naringenin displays wide preventative properties in liver damage induced by alcohol, CCl_4, lipopolysaccharide, and heavy metals [86]. For instance, naringenin at doses of 20 and 50 mg/kg prevented

from liver fibrosis induced by DMN [87]. Naringenin at a dose of 100 mg/kg significantly reversed CCl_4-induced liver fibrosis by blocking the TGF-β-Smad3 and JNK-Smad3 signaling pathways [88]. In addition, in vitro research revealed that naringenin exerted antifibrotic effects by downregulating Smad3 and TGF-β phosphorylation in activated HSCs [89].

2.10. Hydroxysafflor Yellow A. Hydroxysafflor yellow A, a flavonoid compound extracted from *Carthamus tinctorius* L., has received extensive attention and possesses broad pharmacological activities [90]. Zhang's research revealed that 5 mg/kg hydroxysafflor yellow A attenuated liver fibrosis by downregulating TGF-β1, inhibiting phosphorylation of Smad4, and suppressing the ERK5 signaling pathways [91, 92]. The antifibrotic effect of hydroxysafflor yellow A was also correlated with the regulation of the PPAR-γ/p38 MAPK signaling pathway and a reduction in oxidative stress [93, 94]. Hydroxysafflor yellow A was further proven effective in stimulating PPAR activity, reducing cell proliferation, and suppressing ECM synthesis in vivo and in vitro [95]. Apart from these signaling pathways, hydroxysafflor yellow A also induced apoptosis by blocking ERK1/2 kinase in primary HSCs [96].

2.11. Oroxylin A. Oroxylin A is the main bioactive flavonoid extracted from *Scutellaria baicalensis* Georgi. Many studies have shown that oroxylin A demonstrates a variety of pharmacological properties against oxidative stress, inflammation, metastasis, and hepatosteatosis [97–100]. A series of studies showed that oroxylin A ameliorated hepatic fibrosis by inhibiting HSC activation. Zheng revealed that continuous treatment with oroxylin A at 20 mg/kg reduced CCl_4-induced liver fibrosis. Oroxylin A significantly inhibited the reversion of lipid droplets by reducing ROS-dependent adipose triglyceride lipase in activated HSCs [101]. Angiogenesis of liver sinusoidal endothelial cells is closely related to liver fibrosis. Oroxylin A prevented from angiogenesis of LSECs in liver fibrosis via inhibition of the YAP/HIF-1α signaling pathway [102]. Moreover, inhibition of glycolysis-dependent contraction via suppression of lactate dehydrogenase-A (LDH-A) and induction of apoptosis via endoplasmic reticulum (ER) stress in HSCs were involved in antihepatic fibrosis effects of oroxylin A [103, 104]. Apart from these signaling pathways, oroxylin A also alleviated CCl_4-induced liver fibrosis by activating autophagy signaling [105].

2.12. Anthocyanins. Anthocyanins are compounds that are widely isolated from fruits and dietary supplements, such as grapes, blueberries, purple-fleshed sweet potatoes, and peanuts. Anthocyanins are believed to have many health-promoting benefits with prominent anti-inflammatory, antioxidant, and immunomodulatory effects [106]. Choi reported that treatment with 50–200 mg/kg anthocyanins significantly decreased DMN-induced enhancement of α-SMA and collagen types I and III levels in a liver fibrosis model, as well as TNF-α and TGF-β [107]. Another study further indicated that anthocyanins were efficient in attenuating HSC-T6 proliferation, which was associated with blocking the PDGFRβ signaling pathway and suppressing Akt and ERK1/2 activation and α-SMA expression [108]. Anthocyanins alleviated HSC activation and liver fibrosis in both HSCs-T6 cells and CCl_4-treated rats. Anthocyanins from blueberries improved liver function and liver fibrosis by regulating histone acetylation in rats with hepatic fibrosis [109]. In addition, a study revealed that anthocyanins ameliorated liver fibrosis in a network manner by manipulating oxidative stress, inflammation, and HSC activation to remodel ECM deposition [110]. Cyanidin-3-O-β-glucoside is a classical anthocyanin with potent antifibrotic activity. A series of studies from Ling's team suggested that 800 mg/kg dietary cyanidin-3-O-β-glucoside alleviated liver fibrosis by suppressing inflammatory factors, such as TNF-α, IL-6, and IL-10. The progression of HSC activation was also blocked by cyanidin-3-O-β-glucoside through significant inhibition of HSC proliferation and migration [111, 112].

2.13. Other Flavonoids. There are other flavonoid compounds that improve liver fibrosis, such as breviscapine, galangin, and skullcapflavone I. A study from Liu indicated that 15–30 mg/kg breviscapine dose-dependently reduced collagen deposition and narrowed fibrotic area induced by CCl_4, which was partially related to inhibition of inflammatory apoptotic response and ROS generation [113]. Treatment with 20–80 mg/kg galangin also significantly reversed CCl_4-induced rat liver fibrosis by inhibiting HSC activation and proliferation [114]. In early research, skullcapflavone I could induce apoptosis of HSCs to exert antifibrotic effects by activating caspase-3 and caspase-9 [115].

3. Quinones

Quinones belong to aromatic organic compounds with cyclic diketone structure of six-carbon atom containing two double bonds, including emodin and rhein, tanshinone IIA, and thymoquinone (Figures 2(a)–2(d)). Anthraquinone and its derivatives are particularly important in TCM. These quinones have various physiological activities, such as excretion promotion, diuretic effect, antibacteria and antivirus, hemostasis, and spasmolysis.

3.1. Emodin and Rhein. Emodin and rhein are the main bioactive anthraquinones derived from the rhizome of *Rheum palmatum* L. . Treatment with 20–80 mg/kg emodin significantly alleviated hepatic fibrosis [116]. Zhao's research indicated that the mechanism of emodin against liver fibrosis was partially related to a reduction in the infiltration of Gr1hi monocytes [117]. Moreover, emodin also protected against liver fibrosis and HSC activation by reducing TGF-β1 and Smad4 expression and inhibiting tissue inhibitor of metalloproteinases-1 (TIMP-1) expression, and epithelial-mesenchymal transition [118–120]. In addition, 25 and 100 mg/kg rhein inhibited liver fibrosis induced by CCl_4/

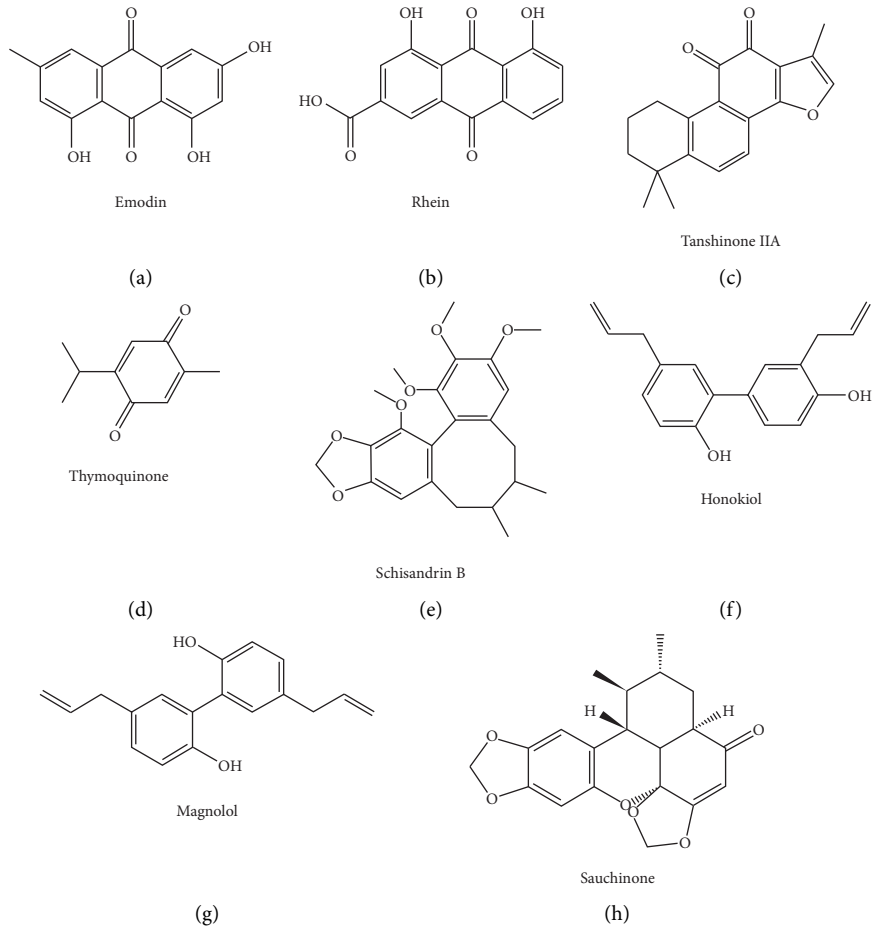

Figure 2: Chemical structures of quinone and lignan compounds against liver fibrosis.

ethanol in rats, which possibly benefited from antioxidant and anti-inflammatory activities of rhein. The antifibrotic effect of rhein was also related to inhibition of TGF-β1 [121].

3.2. Tanshinone IIA. Tanshinone IIA is the main active diterpene quinone phytochemical extracted from *Salvia miltiorrhiza* Bunge (Labiatae). Tanshinone IIA has been commonly used for the treatment of liver diseases, such as hepatic injury, NASH, hepatic fibrosis, and HCC in recent years [122]. A systematic review summarized that tanshinone IIA at doses of 2–200 mg/kg significantly improved liver function in CCl_4, DMN, TAA, and pig serum-induced liver fibrosis. Various mechanisms, such as reduction of inflammation, inhibition of immunity and antiapoptotic processes, and induction of apoptosis to inhibit HSC activation, are involved in antifibrosis effects of tanshinone IIA [123]. For example, tanshinone IIA enhanced apoptosis of HSCs by promoting the ERK-Bax-caspase signaling pathway via the C-Raf/prohibition complex [124]. Tanshinone IIA also inhibited cell proliferation by arresting the cell cycle in S phase in activated rat HSCs [125]. Moreover, the antifibrotic effect of tanshinone IIA was proved by the team's further research. Su and Zhang found that tanshinone IIA was able to significantly alleviate ECM accumulation HSC proliferation as well as activation. The molecular mechanism involved MAPK, Wnt, and PI3K/Akt signaling pathways via inhibiting c-Jun, p-c-Jun, c-Myc, CCND1, MMP9, P65, p-P65, PI3K, and P38 [126]. In addition, tanshinone IIA could also work effectively in combination application such as Fuzheng Huayu formula, a well-known Chinese patent medicine used for liver fibrosis, according to a series of high-quality studies [127–129].

3.3. Thymoquinone. Thymoquinone is the active ingredient from *Nigella sativa* plants. This compound has a protective effect against various types of liver diseases primarily due to its anti-inflammatory and antioxidant properties [130]. A study from Bai demonstrated that 20 and 40 mg/kg thymoquinone significantly enhanced the phosphorylation of AMPK and LKB-1. Thus, regulation of the AMPK signaling pathway might be involved in the inhibitory effect of thymoquinone on ECM accumulation and TAA-induced liver fibrosis [131]. Another study indicated that thymoquinone at 25 mg/kg alleviated CCl_4-induced liver fibrosis through markedly suppressing activated rat HSCs and LX2 cells by inhibiting the proinflammatory response [132]. Furthermore, the antifibrosis mechanism of thymoquinone was correlated with blocking TLR4 expression and inhibiting the

phosphorylation of PI3K in activated HSCs [133]. The combination of thymoquinone and vitamin D exhibited marked antifibrotic effects by downregulating TGF-β1, IL-6, and IL-22 and upregulating MMP-9 and IL-10 [134].

4. Lignans

Lignans are a kind of natural compounds synthesized by the polymerization of two phenylpropanol derivatives (C6–C3 monomer), such as schisandrin B, honokiol and magnolol, and sauchinone (Figures 2(e)–2(h)). Most of them are free, while a few glycosides are combined with sugar and exist in the wood and resin of plants. Lignans have the functions of antitumor, liver protection, antioxidation, antivirus, and neuromodulation.

4.1. Schisandrin B. Schisandrin B is an important bioactive lignan derived from a well-known herbal medicine named *Schisandra chinensis* that has been used for liver protection in recent years. Schisandrin B at 25 and 50 mg/kg significantly attenuated liver damage and liver fibrosis progression in CCl_4-treated rats. Schisandrin B also markedly suppressed HSC-T6 activation. Schisandrin B could exert antifibrotic effects by increasing the Nrf2-ARE signaling pathway and decreasing the TGF-β/Smad signaling pathway [135]. Schisandrin B at 2.5 and 5 μmol/L also attenuated lipopolysaccharide- (LPS-) induced HSCs activation by upregulating Nrf-2 expression [136]. Moreover, transcriptomic analyses were also applied for mechanistic investigation. The results indicated that metabolic pathways, CYP450 enzymes, and the PPAR signaling pathway were the major target pathways of schisandrin B [137].

4.2. Honokiol and Magnolol. Honokiol and magnolol are the main bioactive lignans isolated from *Magnolia officinalis* Rehd. et Wils [138]. In recent years, a number of studies have focused extensive attention on the hepatoprotective effect of honokiol and magnolol. Treatment with honokiol at 10 mg/kg alleviated ConA-induced liver fibrosis by downregulating hydroxyproline, α-SMA, and collagen fiber deposition, which was associated with restoring antioxidant defense, regulating inflammatory cascades, and inhibiting the TGF-β/Smad/MAPK signaling pathway [139]. In vitro research showed that 12.5–50 μmol/L honokiol induced apoptotic death in activated rat HSCs through the release of mitochondrial cytochrome C [140]. Magnolol also attenuated ConA-induced liver fibrosis and suppressed human LX2 HSC activation, which was closely related to inhibiting Th17 cell differentiation by suppressing IL-17A generation [141]. In addition, other honokiol derivatives, such as 4′-O-methylhonokiol, also prevented from HSC activation and induced apoptosis via regulation of Bak1 and Bcl-2 expression [142].

4.3. Sauchinone. Sauchinone is a bioactive lignan that is mainly extracted from *Saururus chinensis* and has been widely used for treating fever, edema, jaundice, and several inflammatory diseases [143]. A team from Korea investigated the effect of sauchinone on liver fibrosis. The results showed that sauchinone at 10 and 20 mg/kg alleviated CCl_4-induced liver fibrosis and inhibited TGF-β1-induced HSC activation, which might be associated with suppressing autophagy and oxidative stress in HSCs [144]. Sauchinone also has liver protection effect to resist liver fibrosis. For instance, sauchinone protected the liver from toxicity induced by iron accumulation by regulating LKB1-dependent AMPK activation [145].

5. Phenols and Acids

One or more hydroxyl groups are directly connected to the benzene ring in the chemical structure of phenolic compounds with weak acid, which is easy to be oxidized in the environment. Chemical structure of several representative phenols and acids is shown in Figure 3. Phenols always have the functions of antioxidation, anti-inflammatory, antiviral, and antitumor.

5.1. Salvianolic Acid B. Salvianolic acid B (SA-B) is a water-soluble phenolic acid isolated from *Salvia miltiorrhiza* Bunge. SA-B is a promising compound for the treatment of liver fibrosis according to reports in vivo and in vitro. Previous studies showed that SA-B significantly inhibited HSC activation by modulating the MAPK and Smad3 signaling pathways and ROS accumulation to reduce matrix collagen deposition and TGF-β1 expression [146–148]. Inhibition of ERK, MEF2, and p38 MAPK-MKK3/6 signaling was also involved in the antifibrotic effect of SA-B both in vivo and in vitro [149, 150]. SA-B prevented from liver fibrosis in CCl_4- and DMN-treated models, which were probably related to downregulating the Ang II signaling pathway by AT1R, ERK, and c-Jun phosphorylation and by regulating the NF-κB/IkBα signaling pathway [151, 152]. Yu reported that SA-B also inhibited the microRNA-17-5p-activated Wnt/β-catenin pathway and modulated lincRNA-p21 expression in HSC activation [153, 154]. In addition, a series of studies testified that the regulation of TGF-β/Smad, MAPK, TbR-I kinase, and microRNA-152 targets contributed to the antifibrotic effect of SA-B [155–157].

5.2. Resveratrol. Resveratrol is a natural polyphenol that is widely found in grapes, peanuts, berries, and nuts. A variety of studies have focused on the antifibrotic effect of resveratrol in recent years. Treatment with 10–50 mg/kg resveratrol prevented from liver fibrosis induced by CCl_4. The reduction in NF-κB activation and Akt/NF-κB signaling pathways might contribute to the antagonistic effect of resveratrol on liver fibrosis [158–160]. Another study indicated that resveratrol alleviated fibrosis by producing IL-10 through polarization of macrophages in a CCl_4-induced model [161]. Resveratrol also significantly inhibited DMN-induced liver fibrosis at doses of 10–20 mg/kg through improving antioxidant defense and alleviating oxidative stress [162, 163]. In addition, resveratrol was proven to be effective in N'-nitrosodimethylamine-

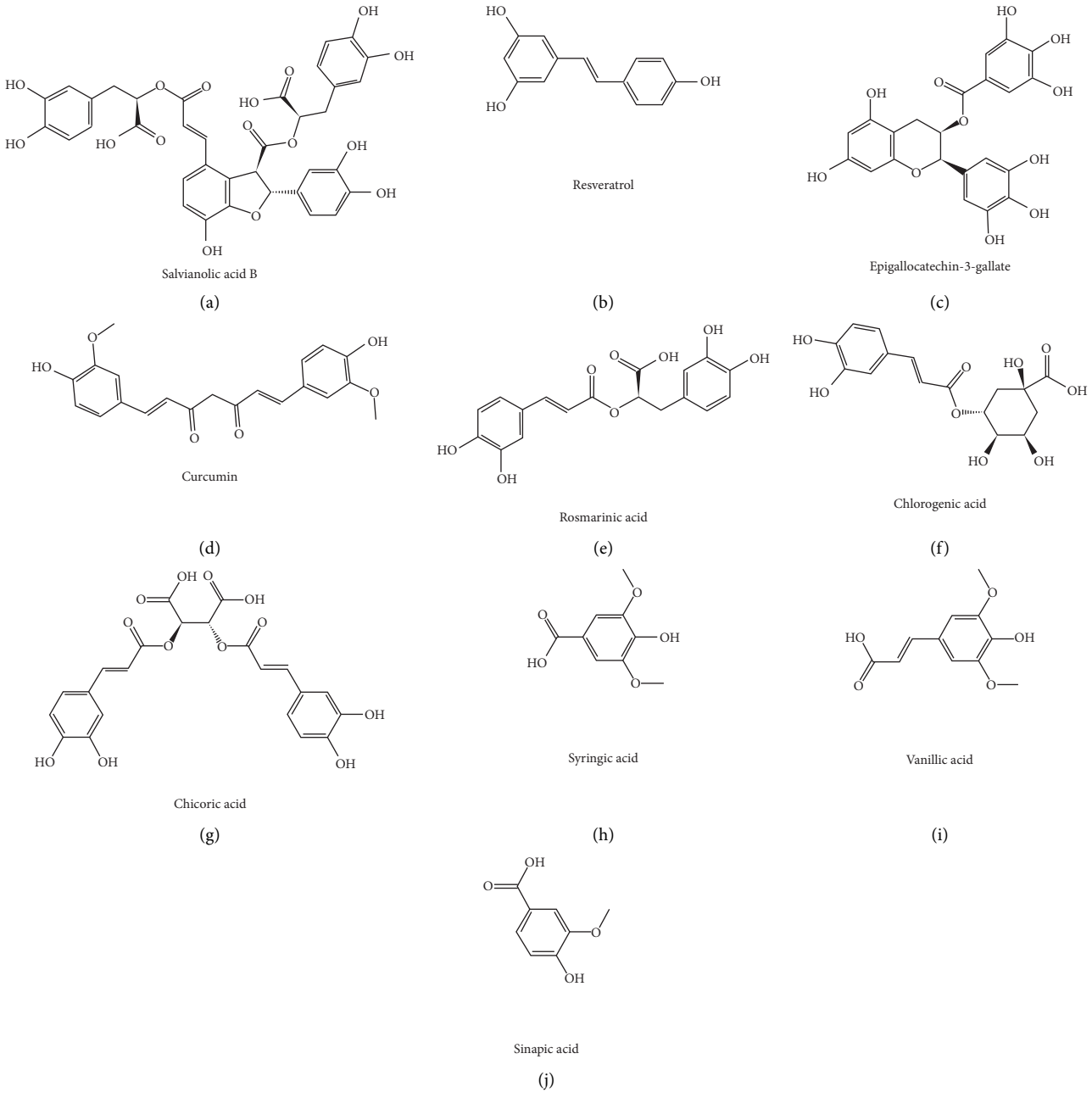

Figure 3: Chemical structures of phenol and acid compounds against liver fibrosis.

(NDMA-) induced fibrosis via reducing oxidative damage and resisting HSC activation [164]. Resveratrol demonstrated an antifibrotic effect by modulating alpha fetoprotein transcriptional levels and normalization of protein kinase C (PKC) responses in a TAA-treated model [165]. Resveratrol also had a potent effect on fibrosis induced by NASH and *Schistosoma japonicum* infection [166, 167]. Similar studies in vitro verified that resveratrol inhibited the activation of HSCs by modulating PPAR-γ/SIRT1 signals and blocking NF-κB activation, as well as PI3K/Akt phosphorylation [168, 169]. Resveratrol also induced HSC apoptosis by modulating autophagy/mitophagy and mitochondrial biogenesis [170].

5.3. Epigallocatechin-3-Gallate. Epigallocatechin-3-gallate (EGCG) is a major polyphenol that accounts for 10%–15% of the components in green tea [166]. EGCG is also a well-known antioxidant with potent activity in various diseases [171]. Several studies revealed that 25–300 mg/kg EGCG attenuated CCl_4-induced liver fibrosis partially through inhibiting HSC activation and targeting MMP-2 via the modulation of membrane type 1-MMP activity [172]. The reduction in oxidative stress and proinflammatory response may also contribute to the effect of EGCG against liver fibrosis [173]. EGCG effectively altered fibrogenesis by blocking ERK and Smad1/2 phosphorylation, as well as targeting PDGFRβ and IGF-1R [174, 175]. Moreover, EGCG

markedly inhibited BDL-induced liver fibrosis and TGF-β1-stimulated LX-2 cells and downregulated profibrotic markers. The antifibrotic effect of EGCG was related to inhibiting the PI3K/Akt/Smad signaling pathway and modulating mitochondrial oxidative stress and inflammation [176, 177]. Arffa reported that EGCG reduced TAA-induced fibrosis and inhibited osteopontin by upregulating miR-221 [178]. Furthermore, EGCG treatment counteracted the activated effects of the TGF/Smad, PI3K/Akt/FoxO1, and NF-κB signaling pathways to alter hepatic fibrosis in NAFLD models [179]. Studies have revealed that EGCG inhibits HSC activation in primary rat HSCs, TWNT-4 cells, and LI90 cells. A study by Sakata revealed that EGCG inhibited PDGF-BB-induced cell proliferation of LI90 cells by blocking PDGF-BB binding to its receptor in a noncompetitive manner [180]. Moreover, Nakamuta found a similar antifibrotic effect of EGCG in TWNT-4 human HSCs by regulating ERK1/2, c-Jun kinase, and p38 via the suppression of Rho signaling pathways [181, 182]. Further studies also suggested that EGCG suppressed MMP-2 activation and HSC invasiveness and induced *de novo* synthesis of GSH [183, 184]. In addition, the combination therapy of EGCG with taurine, genistein, or atorvastatin also demonstrated a significant antifibrotic effect [78, 185].

5.4. Curcumin. Curcumin is a well-known polyphenolic compound that is mainly isolated from *Curcuma longa* [186]. In the past 20 years, accumulating evidence in vivo and in vitro has shown that curcumin is a promising agent for liver fibrosis treatment. Studies indicated that curcumin exerted antifibrotic effect via networks and multiple signals. For example, curcumin suppressed HSCs by targeting PPAR-γ signaling in vitro [187, 188]. The increase in PPAR-γ might inhibit the gene expression of receptor for advanced glycation end-products (RAGE) and attenuate oxidative stress in HSCs [189]. Moreover, inhibition of srebp-2 by modulating specificity protein-1 and suppressing inflammatory cytokines, including IL-6, TNF-α, and INF-γ, also contributed to antihepatic fibrosis effect of curcumin [190, 191]. Other studies revealed that curcumin could promote apoptosis of activated HSCs by upregulating caspase-3, Bax, and p53 and downregulating Bcl-2 to alleviate liver fibrosis [192–195]. Wu's team suggested that curcumin primarily attenuated liver fibrosis by modulating immune system by blocking Gr1hi monocytes via MCP-1 and reducing Ly6Chi monocyte infiltration via Kupffer cell activation [196, 197]. In addition, curcumin also reversed aberrant methylation in liver fibrosis in vivo and in vitro [198]. Several studies from Zhou's group indicated that curcumin inhibited HSCs by affecting the β-catenin signaling pathway and regulating the Shh-associated delta-like homolog 1 (DLK1) signaling pathway [199, 200]. Furthermore, curcumin could exert antifibrotic activity through regulating the AMPK/PGC-1α axis to inhibit HSC activation [200]. Another team found that the core mechanism by which curcumin affected liver fibrosis was inhibiting the TGF-β1/Smad signaling pathway and CTGF expression [201]. The inhibition of the TGF-β/Smad signaling pathway was also observed in alcohol-induced hepatic fibrosis [202]. In addition to the above signals, curcumin also reduced HMGB1, TLR4, and TLR2 expression in fibrogenesis, while ameliorating intrahepatic angiogenesis and capillarization of the sinusoids during liver fibrosis [203, 204]. A series of studies revealed that curcumin alleviated ECM deposition and regulated HSC senescence by suppressing cannabinoid receptor type-1 (CBR1) signaling, activating the PPAR-γ/p53 signaling pathway, inhibiting sinusoidal angiogenesis, and activating Nrf2 to induce the lipocyte phenotype in HSCs [205, 206]. Furthermore, NK cells and Hedgehog signaling are also regulated by curcumin to inhibit fibrotic progression [207, 208]. A study initially verified that curcumin protected against CCl_4-induced hepatic fibrosis by suppressing HIF-1α via the ERK-dependent signaling pathway [209]. Another study further showed that curcumin prevented from the activation of HSCs by blocking the succinate/HIF-1α signaling pathway [210]. Several other signals, including the modulation of CB1 receptors, IRS1, SOCS3, and STAT3 targets, MyD88 pathway, CXCL12/CXCR4 biological axis, Plin5 gene expression, and LD formation, were also involved in various mechanisms underlying antihepatic fibrosis effect of curcumin [211–215].

5.5. Rosmarinic Acid. Rosmarinic acid is a natural polyphenolic antioxidant derived from a variety of common herbal plants [216]. Studies indicated that rosmarinic acid might have a therapeutic effect on liver fibrosis. For instance, a study from Li revealed that 2.5–10 mg/kg rosmarinic acid significantly suppressed TGF-β1 and CTGF expression in CCl_4-induced liver fibrosis. Rosmarinic acid markedly inhibited HSC proliferation and activation by decreasing α-SMA, TGF-β1, and CTGF levels in HSC-T6 cell line [217]. Similarly, El-Lakkany reported that rosmarinic acid inhibited liver fibrosis progression by inhibiting HSC activation and proliferation by initiating apoptosis-related signals in a TAA-induced model and HSC-T6 cells [218]. Furthermore, rosmarinic acid stimulated the activity of ARE promoter through enhancing GSH level and removing ROS by stimulating Nrf2 translocation into the nucleus, GSH enhancement, and subsequent GCLC upregulation. Thus, ROS elimination by rosmarinic acid directly inhibited NF-κB-dependent MMP-2 expression and suppressed HSC activation [219]. In addition, rosmarinic acid is also the active ingredient in a potent antifibrotic herbal medicine named Yang-Gan-Wan. Rosmarinic acid and Yang-Gan-Wan are effective against liver fibrosis by suppressing the canonical Wnt signaling pathway and reducing PPAR-γ in HSCs [47].

5.6. Chlorogenic Acid. Chlorogenic acid is one of most plentiful phenolic acids and is widely distributed in various fruits, plants, and vegetables [220]. Many studies have confirmed that chlorogenic acid is specifically potent in liver protection. A series of studies indicated that 30 and 60 mg/kg chlorogenic acid significantly repressed liver fibrosis induced by CCl_4 by inhibiting HSC activation and downregulating fibrogenetic factors [221]. Moreover, chlorogenic

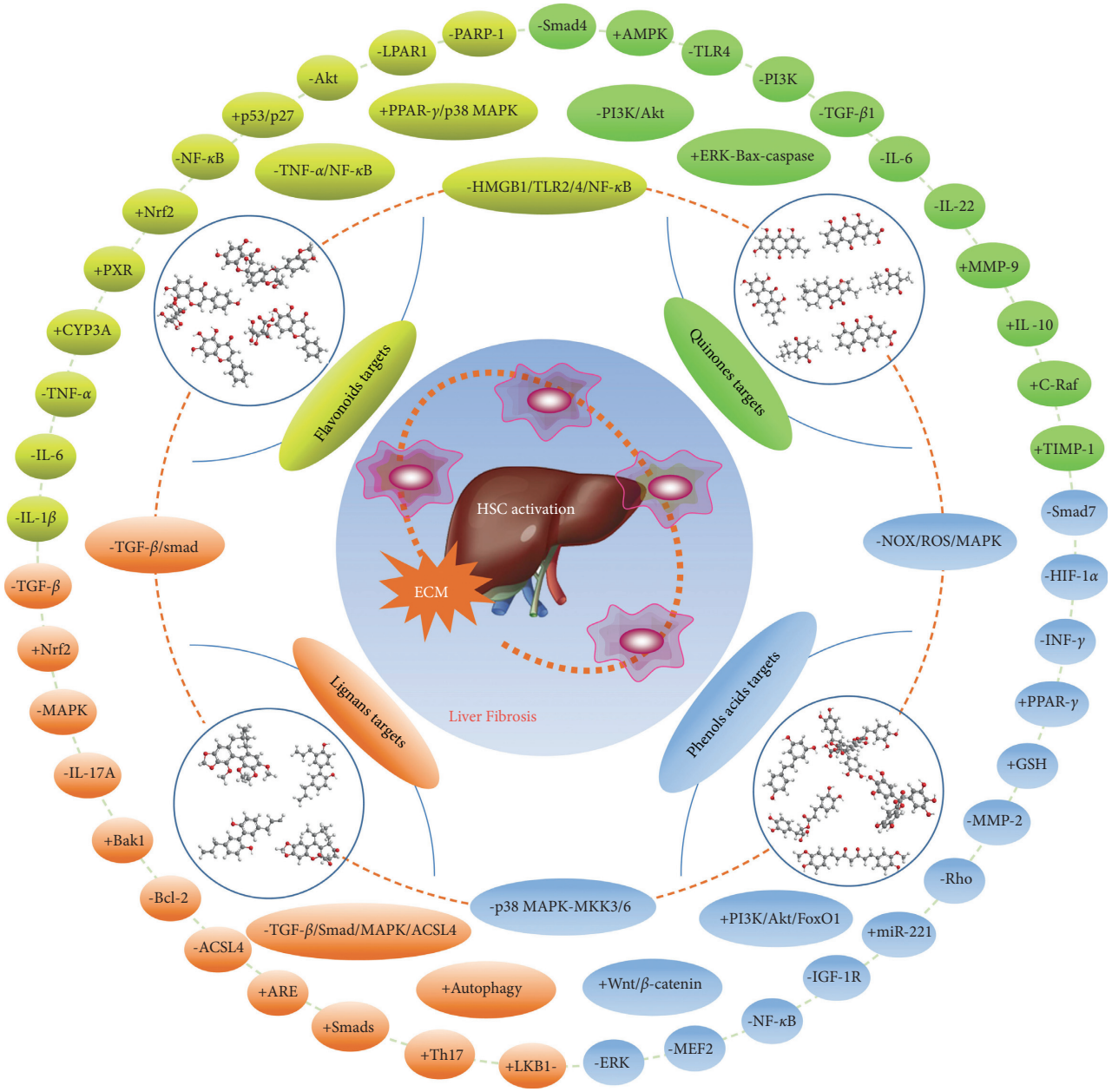

Figure 4: The interaction network mechanism of natural products against liver fibrosis.

acid could present the hepatoprotective effect through inhibiting the TLR4/MyD88/NF-κB signaling pathway by downregulating several cytokines, such as IL-1β, IL-6, TNF-α, iNOS, and COX-2 [222]. In addition, a study reported that NOX subunits expression, ROS generation, and the phosphorylated levels of p38 and ERK1/2 decreased in HSCs, while Nrf2 and Nrf2-regulated antioxidant genes (HO-1, GCLC, and NQO-1) increased in liver tissues after chlorogenic acid intervention. Therefore, chlorogenic acid could prevent from liver fibrosis by activation of Nrf2 pathway and inhibition of NOX/ROS/MAPK pathway [223]. Another research group revealed that chlorogenic acid displayed significant antifibrotic effects on the hepatic stellate LX2 cell line and *Schistosome*-infected mice mainly through IL-13/miR-21/Smad7 signaling interaction [224]. Chlorogenic acid also blocked the miR-21-regulated TGF-β1/Smad7 signaling pathway by decreasing the expression of α-SMA, TGF-β1, and collagen I in CCl_4-induced liver fibrosis and LX2 cells [225].

5.7. Other Phenols and Acids. Apart from the above compounds, there are several other phenols and acids used for liver fibrosis treatment, such as chicoric acid, syringic acid, vanillic acid, and sinapic acid. Chicoric acid is a natural phenolic acid that is mainly isolated from chicory and *Echinacea* plants [226]. A study from Kim suggested that 10–30 mg/kg chicoric acid significantly reduced liver fibrosis through downregulating α-SMA, TGF-β1, and collagen expression in NASH mice. Inhibition of NF-κB-regulated

inflammatory response, suppression of AMPK-mediated lipid/triglyceride accumulation, and enhancement of Nrf2 antioxidant defense system might contribute to the effect of chicoric acid against NASH and fibrosis [227]. Syringic acid and vanillic acid are two phenolic compounds found in fruits and vegetables, which markedly suppressed collagen accumulation and decreased the hepatic hydroxyproline content in CCl_4-induced liver fibrosis [228, 229]. Moreover, these compounds inhibited the activation of cultured HSCs but did not influence hepatocyte viability [230]. Thus, treatment with syringic acid and vanillic acid could suppress the progression of fibrosis during chronic liver injury. Sinapic acid is an orally bioavailable phenolic acid from spices, citrus and berry fruits, and vegetables with wide pharmacological effects [231]. Shin revealed that 10 and 20 mg/kg sinapic acid significantly ameliorated of α-SMA, TGF-β1, and col I expression in DMN-induced liver fibrosis, which might be relevant to antioxidant effect and suppression of NF-κB and TGF-β1 signals [232].

6. Outlook and Conclusions

6.1. Limitations and Outlook. Growing evidence suggests that liver fibrosis is a complicated process involving multiple dysfunctions of sinusoidal cells [5]. HSC activation and ECM deposition are thought to be the key markers of fibrogenesis. Recently, many attempts have been made to explore the antifibrotic effects of some natural products to promote drug discovery. Previous study by us reviewed the risk components of TCM-induced liver injury, including alkaloids, glycosides, toxic proteins, terpenoids and lactones, anthraquinones, and heavy metals [233]. In this review, we summarized only four kinds of natural compounds that exert potential antifibrotic function, especially their biological activities and potential mechanisms against liver fibrosis. However, three aspects should be noted. First, the transition from bench to bedside is limited for most natural products. Silymarin and silybin are currently used in the clinic for liver protection during fibrosis in China [234, 235]. However, other promising compounds, such as genistein, quercetin, resveratrol, and curcumin, are still waiting for further clinical confirmation or more evidence of efficacy. Secondly, most of these compounds show antifibrotic effects via multiple targets or signaling pathways (Figure 4). For instance, curcumin inhibits HSC proliferation and activation and modulates the immune microenvironment. The protection of hepatocytes by reducing oxidative stress and inflammatory responses is also involved in the antifibrotic effects of some natural products, such as silibinin, silymarin, anthocyanins, and emodin and rhein. Finally, the strength of evidence for the antifibrotic effect of several natural products is different based on various liver fibrosis models. Most natural products, including flavonoids, quinones, lignans, and phenols and acids, present excellent antifibrotic function in CCl_4, DMN, TAA, *Schistosome*, and ethanol-treated models. However, a few compounds, such as skullcapflavone I and magnolol, have only been confirmed to have effects on HSCs in vitro. Stronger evidence is needed for the effects of these compounds in liver fibrosis. Despite the rapid growth of studies on antifibrotic natural products, there are still future breakthroughs in two aspects. The potent effects of natural compounds have been presented, but the low bioavailability of several compounds vastly limits their clinical application. Enhancement of pharmacokinetic parameters for these compounds should be investigated. Moreover, the combined application of several natural products seems to be a promising method for liver fibrosis treatment. The combination of silymarin with caffeine, puerarin with vitamin D, baicalin with rosmarinic acid, and genistein with taurine and EGCG has been explored in previous studies. The results also show the potent synergistic effect of these combinations.

7. Conclusions

In summary, exploration on natural products against liver fibrosis is increasingly thorough. Natural products are a potential resource for the development of agents to treat liver fibrosis. Thus, natural products are very valuable when seeking novel therapeutic agents for liver fibrosis.

Abbreviations

ECM: Extracellular matrix
HSCs: Hepatic stellate cells
HBV: Hepatitis B virus
NAFLD: Nonalcoholic fatty liver disease
NASH: Nonalcoholic steatohepatitis
ROS: Reactive oxygen species
LSECs: Liver sinusoidal endothelial cells
TGF-β: Transforming growth factor-β
TCM: Traditional Chinese medicine
HCC: Hepatocellular carcinoma
TAA: Thioacetamide
GSH: Glutathione
CTGF: Connective tissue growth factor
PPAR-γ: Peroxisomal proliferator-activated receptor γ
DMN: Dimethylnitrosamine
PDGF-BB: Platelet-derived growth factor-B subunit homodimer
LDH-A: Lactate dehydrogenase-A
ER: Endoplasmic reticulum
TIMP-1: Tissue inhibitor of metalloproteinases-1
LPS: Lipopolysaccharide
NDMA: N′-Nitrosodimethylamine
PKC: Protein kinase C
EGCG: Epigallocatechin-3-gallate
RAGE: Receptor for advanced glycation end-products
DLK1: Delta-like homolog 1
CBR1: Cannabinoid receptor type-1.

Conflicts of Interest

The authors declare that there are no conflicts of interest.

Authors' Contributions

The authors Xiaoqi Pan and Xiao Ma contributed equally to this work.

Acknowledgments

This work was supported by the National Natural Science Foundation of China (81891010, 81891012, 81630101, and 81874365), China Postdoctoral Science Foundation (2018M631070), Sichuan Science and Technology Program (2019YJ0492 and 2018JZ0081), Chengdu University of TCM Found Grant (QNXZ2018025), and Xinlin Scholar Research Promotion Project of Chengdu University of Traditional Chinese Medicine.

References

[1] T. Higashi, S. L. Friedman, and Y. Hoshida, "Hepatic stellate cells as key target in liver fibrosis," *Advanced Drug Delivery Reviews*, vol. 121, pp. 27–42, 2017.

[2] K. Böttcher and M. Pinzani, "Pathophysiology of liver fibrosis and the methodological barriers to the development of anti-fibrogenic agents," *Advanced Drug Delivery Review*, vol. 121, pp. 3–8, 2017.

[3] M. H. Forouzanfar and L. Alexander, "Global, regional, and national comparative risk assessment of 79 behavioural, environmental and occupational, and metabolic risks or clusters of risks in 188 countries, 1990–2013: a systematic analysis for the Global Burden of Disease Study 2013," *The Lancet*, vol. 386, pp. 2287–2323, 2015.

[4] T. Tsuchida and S. L. Friedman, "Mechanisms of hepatic stellate cell activation," *Nature Reviews Gastroenterology & Hepatology*, vol. 14, pp. 397–411, 2017.

[5] G. Marrone, V. H. Shah, and J. Gracia-Sancho, "Sinusoidal communication in liver fibrosis and regeneration," *Journal of Hepatology*, vol. 65, pp. 608–617, 2016.

[6] C. Trautwein, S. L. Friedman, and D. Schuppan, "Hepatic fibrosis: concept to treatment," *Journal of Hepatology*, vol. 62, pp. S15–S24, 2015.

[7] E. Lafoz, M. Ruart, and A. Anton, "The endothelium as a driver of liver fibrosis and regeneration," *Cells*, vol. 9, 2020.

[8] J. M. Luk, X. Wang, and P. Liu, "Traditional Chinese herbal medicines for treatment of liver fibrosis and cancer: from laboratory discovery to clinical evaluation," *Liver International*, vol. 27, pp. 879–890, 2007.

[9] A. Zhang, H. Sun, and X. Wang, "Recent advances in natural products from plants for treatment of liver diseases," *European Journal of Medicinal Chemistry*, vol. 63, pp. 570–577, 2013.

[10] X. Ma, Y. Jiang, and W. Zhang, "Natural products for the prevention and treatment of cholestasis : a review," *Phytotherapy Research*, vol. 34, no. 6, pp. 1291–1309, 2020.

[11] Y. Zhao, X. Ma, and J. Wang, "A system review of anti-fibrogenesis effects of compounds derived from Chinese herbal medicine," *Mini Reviews in Medicinal Chemistry*, vol. 16, no. 2, pp. 163–175, 2016.

[12] X. Lv, S. Liu, and Z. W. Hu, "Autophagy-inducing natural compounds: a treasure resource for developing therapeutics against tissue fibrosis," *Journal of Asian Natural Products Research*, vol. 19, pp. 101–108, 2017.

[13] D. Q. Chen, Y. L. Feng, and G. Cao, "Natural products as a source for antifibrosis therapy," *Trends in Pharmacological Sciences*, vol. 39, pp. 937–952, 2018.

[14] A. Federico, M. Dallio, and C. Loguercio, "Silymarin/silybin and chronic liver disease: a marriage of many years," *Molecules*, vol. 22, p. 191, 2017.

[15] A. Pietrangelo, G. Montosi, and C. Garuti, "Iron-induced oxidant stress in nonparenchymal liver cells: mitochondrial derangement and fibrosis in acutely iron-dosed gerbils and its prevention by silybin," *Journal of Bioenergetics and Biomembranes*, vol. 34, pp. 67–79, 2002.

[16] A. Masini, D. Ceccarelli, and F. Giovannini, "Iron-induced oxidant stress leads to irreversible mitochondrial dysfunctions and fibrosis in the liver of chronic iron-dosed gerbils. the effect of silybin," *Journal of Bioenergetics and Biomembranes*, vol. 32, pp. 175–182, 2000.

[17] P. Muriel, M. G. Moreno, and M. D. C. Hernández, "Resolution of liver fibrosis in chronic CCl4 administration in the rat after discontinuation of treatment: effect of silymarin, silibinin, colchicine and trimethylcolchicinic acid," *Basic & Clinical Pharmacology & Toxicology*, vol. 96, pp. 375–380, 2005.

[18] Y. Xie, H. P. Hao, and H. Wang, "Reversing effects of silybin on TAA-induced hepatic CYP3A dysfunction through PXR regulation," *Chinese Journal of Natural Medicines*, vol. 11, pp. 645–652, 2013.

[19] Q. Ou, Y. Weng, and S. Wang, "Silybin alleviates hepatic steatosis and fibrosis in NASH mice by inhibiting oxidative stress and involvement with the nf-κb pathway," *Digestive Diseases and Sciences*, vol. 63, pp. 3398–3408, 2018.

[20] M. Trappoliere, A. Caligiuri, and M. Schmi, "Silybin, a component of sylimarin, exerts anti-inflammatory and anti-fibrogenic effects on human hepatic stellate cells," *Journal of Hepatology*, vol. 50, pp. 1102–1111, 2009.

[21] D. Ezhilarasan, J. Evraerts, and B. Sid, "Silibinin induces hepatic stellate cell cycle arrest via enhancing p53/p27 and inhibiting Akt downstream signaling protein expression," *Hepatobiliary & Pancreatic Diseases International*, vol. 16, pp. 80–87, 2017.

[22] P. Ferenci, "Silymarin in the treatment of liver diseases: what is the clinical evidence?" *Clinical Liver Disease*, vol. 7, pp. 8–10, 2016.

[23] E. Shaker, H. Mahmoud, and S. Mnaa, "Silymarin, the antioxidant component and Silybum marianum extracts prevent liver damage," *Food and Chemical Toxicology*, vol. 48, pp. 803–806, 2010.

[24] I. S. Chen, Y. C. Chen, and C. H. Chou, "Hepatoprotection of silymarin against thioacetamide-induced chronic liver fibrosis," *Journal of the Science of Food and Agriculture*, vol. 92, pp. 1441–1447, 2012.

[25] H. A. Mata-Santos, F. G. Lino, and C. C. Rocha, "Silymarin treatment reduces granuloma and hepatic fibrosis in experimental schistosomiasis," *Parasitology Research*, vol. 107, pp. 1429–1434, 2010.

[26] J. H. Tsai, J. Y. Liu, and T. T. Wu, "Effects of silymarin on the resolution of liver fibrosis induced by carbon tetrachloride in rats," *Journal of Viral Hepatitis*, vol. 15, pp. 508–514, 2008.

[27] C. S. Lieber, M. A. Leo, and Q. Cao, "Silymarin retards the progression of alcohol-induced hepatic fibrosis in baboons," *Journal of Clinical Gastroenterology*, vol. 37, pp. 336–339, 2003.

[28] N. M. El-Lakkany, O. A. Hammam, and W. H. El-Maadawy, "Anti-inflammatory/anti-fibrotic effects of the hepatoprotective silymarin and the schistosomicide praziquantel against Schistosoma mansoni-induced liver fibrosis," *Parasites & Vectors*, vol. 5, p. 9, 2012.

[29] J. I. Tzeng, M. F. Chen, and H. H. Chung, "Silymarin decreases connective tissue growth factor to improve liver fibrosis in rats treated with carbon tetrachloride," *Phytotherapy Research*, vol. 27, pp. 1023–1028, 2013.

[30] S. Clichici, D. Olteanu, and A. L. Nagy, "Silymarin inhibits the progression of fibrosis in the early stages of liver injury in CCl_4-treated rats," *Journal of Medicinal Food*, vol. 18, pp. 290–298, 2015.

[31] S. Clichici, D. Olteanu, and A. Filip, "Beneficial effects of silymarin after the discontinuation of CCl_4-induced liver fibrosis," *Journal of Medicinal Food*, vol. 19, pp. 789–797, 2016.

[32] M. Kim, S. G. Yang, and J. M. Kim, "Silymarin suppresses hepatic stellate cell activation in a dietary rat model of non-alcoholic steatohepatitis: analysis of isolated hepatic stellate cells," *International Journal of Molecular Medicine*, vol. 30, pp. 473–479, 2012.

[33] S. Saber, R. Goda, and G. S. El-Tanbouly, "Lisinopril inhibits nuclear transcription factor kappa B and augments sensitivity to silymarin in experimental liver fibrosis," *International Immunopharmacology*, vol. 64, pp. 340–349, 2018.

[34] S. M. Eraky, M. El-Mesery, and A. El-Karef, "Silymarin and caffeine combination ameliorates experimentally-induced hepatic fibrosis through down-regulation of LPAR1 expression," *Biomedicine & Pharmacotherapy*, vol. 101, pp. 49–57, 2018.

[35] A. M. Abdel-Moneim, M. A. Al-Kahtani, and M. A. El-Kersh, "Free radical-scavenging, anti-inflammatory/anti-fibrotic and hepatoprotective actions of taurine and silymarin against CCl4 induced rat liver damage," *PLoS One*, vol. 10, Article ID e0144509, 2015.

[36] Y. X. Zhou, H. Zhang, and C. Peng, "Puerarin: a review of pharmacological effects," *Phytotherapy Research*, vol. 28, pp. 961–975, 2014.

[37] S. Zhang, G. Ji, and J. Liu, "Reversal of chemical-induced liver fibrosis in Wistar rats by puerarin," *Journal of Nutritional Biochemistry*, vol. 17, pp. 485–491, 2006.

[38] C. Guo, L. Xu, and Q. He, "Anti-fibrotic effects of puerarin on CCl4-induced hepatic fibrosis in rats possibly through the regulation of PPAR-γ expression and inhibition of PI3K/Akt pathway," *Food and Chemical Toxicology*, vol. 56, pp. 436–442, 2013.

[39] R. Li, L. Xu, and T. Liang, "Puerarin mediates hepatoprotection against CCl4-induced hepatic fibrosis rats through attenuation of inflammation response and amelioration of metabolic function," *Food and Chemical Toxicology*, vol. 52, pp. 69–75, 2013.

[40] S. Wang, X. L. Shi, and M. Feng, "Puerarin protects against CCl4-induced liver fibrosis in mice: possible role of PARP-1 inhibition," *International Immunopharmacology*, vol. 38, pp. 238–245, 2016.

[41] L. Xu, N. Zheng, and Q. He, "Puerarin, isolated from Pueraria lobata (Willd.), protects against hepatotoxicity via specific inhibition of the TGF-β1/Smad signaling pathway, thereby leading to anti-fibrotic effect," *Phytomedicine*, vol. 20, pp. 1172–1179, 2013.

[42] X. Li, H. Zhang, and L. Pan, "Puerarin alleviates liver fibrosis via inhibition of the ERK1/2 signaling pathway in thioacetamide-induced hepatic fibrosis in rats," *Experimental and Therapeutic Medicine*, vol. 18, pp. 133–138, 2019.

[43] G. R. Huang, S. J. Wei, and Y. Q. Huang, "Mechanism of combined use of vitamin D and puerarin in anti-hepatic fibrosis by regulating the Wnt/β-catenin signalling pathway," *World Journal of Gastroenterology*, vol. 24, pp. 4178–4185, 2018.

[44] B. Dinda, S. Dinda, and S. DasSharma, "Therapeutic potentials of baicalin and its aglycone, baicalein against inflammatory disorders," *European Journal of Medicinal Chemistry*, vol. 131, pp. 68–80, 2017.

[45] X. D. Peng, L. L. Dai, and C. Q. Huang, "Correlation between anti-fibrotic effect of baicalin and serum cytokines in rat hepatic fibrosis," *World Journal of Gastroenterology*, vol. 15, pp. 4720–4725, 2009.

[46] H. Qiao, H. Han, and D. Hong, "Protective effects of baicalin on carbon tetrachloride induced liver injury by activating PPARγ and inhibiting TGFβ1," *Pharmaceutical Biology*, vol. 49, pp. 38–45, 2011.

[47] J. Zhang, H. Zhang, and X. Deng, "Baicalin attenuates non-alcoholic steatohepatitis by suppressing key regulators of lipid metabolism, inflammation and fibrosis in mice," *Life Sciences*, vol. 192, pp. 46–54, 2018.

[48] X. Wu, F. Zhi, and W. Lun, "Baicalin inhibits PDGF-BB-induced hepatic stellate cell proliferation, apoptosis, invasion, migration and activation via the miR-3595/ACSL4 axis," *International Journal of Molecular Medicine*, vol. 41, pp. 1992–2002, 2018.

[49] M. D. Yang, Y. M. Chiang, and R. Higashiyama, "Rosmarinic acid and baicalin epigenetically derepress peroxisomal proliferator-activated receptor γ in hepatic stellate cells for their antifibrotic effect," *Hepatology*, vol. 55, pp. 1271–1281, 2012.

[50] W. Sun, P. Liu, and T. Wang, "Baicalein reduces hepatic fat accumulation by activating AMPK in oleic acid-induced HepG2 cells and high-fat diet-induced non-insulin-resistant mice," *Food & Function*, vol. 11, pp. 711–721, 2020.

[51] H. Sun, Q. M. Che, and X. Zhao, "Antifibrotic effects of chronic baicalein administration in a CCl_4 liver fibrosis model in rats," *European Journal of Pharmacology*, vol. 631, pp. 53–60, 2010.

[52] T. Inoue and E. K. Jackson, "Strong antiproliferative effects of baicalein in cultured rat hepatic stellate cells," *European Journal of Pharmacology*, vol. 378, pp. 129–135, 1999.

[53] M. Hajialyani, M. Hosein Farzaei, and J. Echeverría, "Hesperidin as a neuroprotective agent: a review of animal and clinical evidence," *Molecules*, vol. 24, p. 648, 2019.

[54] Y. S. Wang, C. Y. Shen, and J. G. Jiang, "Antidepressant active ingredients from herbs and nutraceuticals used in TCM: pharmacological mechanisms and prospects for drug discovery," *Pharmacological Research*, vol. 150, Article ID 104520, 2019.

[55] S. M. Elshazly and A. A. A. Mahmoud, "Antifibrotic activity of hesperidin against dimethylnitrosamine-induced liver fibrosis in rats," *Naunyn-Schmiedeberg's Archives of Pharmacology*, vol. 387, pp. 559–567, 2014.

[56] R. Kong, N. Wang, and H. Luo, "Hesperetin mitigates bile duct ligation-induced liver fibrosis by inhibiting extracellular matrix and cell apoptosis via the TGF-β1/smad pathway," *Current Molecular Medicine*, vol. 18, pp. 15–24, 2018.

[57] J. E. Pérez-Vargas, N. Zarco, and M. Shibayama, "Hesperidin prevents liver fibrosis in rats by decreasing the expression of nuclear factor-κB, transforming growth factor-β and connective tissue growth factor," *Pharmacology*, vol. 94, pp. 80–89, 2014.

[58] F. Wu, L. Jiang, and X. He, "Effect of hesperidin on TGF-beta1/Smad signaling pathway in HSC," *Zhongguo Zhong Yao Za Zhi*, vol. 40, pp. 2639–2643, 2015.

[59] Y. J. Kim and W. Park, "Anti-inflammatory effect of quercetin on RAW 264.7 mouse macrophages induced with polyinosinic-polycytidylic acid," *Molecules*, vol. 21, p. 450, 2016.

[60] E. S. Lee, H. E. Lee, and J. Y. Shin, "The flavonoid quercetin inhibits dimethylnitrosamine-induced liver damage in rats," *Journal of Pharmacy and Pharmacology*, vol. 55, pp. 1169–1174, 2003.

[61] R. Wang, H. Zhang, and Y. Wang, "Inhibitory effects of quercetin on the progression of liver fibrosis through the regulation of NF-κB/IκBα, p38 MAPK, and Bcl-2/Bax signaling," *International Immunopharmacology*, vol. 47, pp. 126–133, 2017.

[62] L. Wu, Q. Zhang, and W. Mo, "Quercetin prevents hepatic fibrosis by inhibiting hepatic stellate cell activation and reducing autophagy via the TGF-β1/Smads and PI3K/Akt pathways," *Science Reports*, vol. 7, p. 9289, 2017.

[63] L. D. Hernández-Ortega, B. E. Alcántar-Díaz, and L. A. Ruiz-Corro, "Quercetin improves hepatic fibrosis reducing hepatic stellate cells and regulating pro-fibrogenic/anti-fibrogenic molecules balance," *Journal of Gastroenterology & Hepatology*, vol. 27, pp. 1865–1872, 2012.

[64] X. Li, Q. Jin, and Q. Yao, "The flavonoid quercetin ameliorates liver inflammation and fibrosis by regulating hepatic macrophages activation and polarization in mice," *Frontiers in Pharmacology*, vol. 9, pp. 1–14, 2018.

[65] X. Li, Q. Jin, and Q. Yao, "Quercetin attenuates the activation of hepatic stellate cells and liver fibrosis in mice through modulation of HMGB1-TLR2/4-NF-κB signaling pathways," *Toxicology Letters*, vol. 261, pp. 1–12, 2016.

[66] A. Khodarahmi, A. Eshaghian, and F. Safari, "Quercetin mitigates hepatic insulin resistance in rats with bile duct ligation through modulation of the STAT3/SOCS3/IRS1 signaling pathway," *Journal of Food Science*, vol. 84, pp. 3045–3053, 2019.

[67] E. Marcolin, B. San-Miguel, and D. Vallejo, "Quercetin treatment ameliorates inflammation and fibrosis in mice with nonalcoholic steatohepatitis1–3," *Journal of Nutrition*, vol. 142, pp. 1821–1828, 2012.

[68] P. Thangavel, A. Puga-Olguín, and J. F. Rodríguez-Landa, "Genistein as potential therapeutic candidate for menopausal symptoms and other related diseases," *Molecules*, vol. 24, p. 3892, 2019.

[69] M. Gan, L. Shen, and Y. Fan, "MicroRNA-451 and genistein ameliorate nonalcoholic steatohepatitis in mice," *International Journal of Molecular Sciences*, vol. 20, p. 6084, 2019.

[70] O. Akinci, V. Durgun, and N. Kepil, "The role of genistein in experimental hepatic ischemia–reperfusion model in rats," *Bratislavske lekarske listy*, vol. 120, pp. 558–562, 2019.

[71] Q. Zhang, J. Bao, and J. Yang, "Genistein-triggered anticancer activity against liver cancer cell line HepG2 involves ROS generation, mitochondrial apoptosis, G2/M cell cycle arrest and inhibition of cell migration," *Archives of Medical Science*, vol. 15, pp. 1001–1009, 2019.

[72] A. A. Ganai and M. Husain, "Genistein attenuates D-GalN induced liver fibrosis/chronic liver damage in rats by blocking the TGF-β/Smad signaling pathways," *Chemico-Biological Interactions*, vol. 261, pp. 80–85, 2017.

[73] A. Leija Salas, T. Díaz Montezuma, and G. Garrido Fariña, "Genistein modifies liver fibrosis and improves liver function by inducing uPA expression and proteolytic activity in CCl4-treated rats," *Pharmacology*, vol. 81, pp. 41–49, 2007.

[74] A. L. Salas, G. Ocampo, and G. G. Fariña, "Genistein decreases liver fibrosis and cholestasis induced by prolonged biliary obstruction in the rat," *Annals of Hepatology*, vol. 6, pp. 41–47, 2007.

[75] M. M. K. Sobhy, S. S. Mahmoud, and S. H. El-Sayed, "Impact of treatment with a protein tyrosine kinase inhibitor (genistein) on acute and chronic experimental schistosoma mansoni infection," *Experimental Parasitology*, vol. 185, pp. 115–123, 2018.

[76] C. Wan, F. Jin, and Y. Du, "Genistein improves schistosomiasis liver granuloma and fibrosis via dampening NF-kB signaling in mice," *Parasitology Research*, vol. 116, pp. 1165–1174, 2017.

[77] X. J. Liu, L. Yang, and Y. Q. Mao, "Effects of the tyrosine protein kinase inhibitor genistein on the proliferation, activation of cultured rat hepatic stellate cells," *World Journal of Gastroenterology*, vol. 8, pp. 739–745, 2002.

[78] Q. Huang, R. Huang, and S. Zhang, "Protective effect of genistein isolated from Hydrocotyle sibthorpioides on hepatic injury and fibrosis induced by chronic alcohol in rats," *Toxicology Letters*, vol. 217, pp. 102–110, 2013.

[79] Y. Luo, Y. Huo, and P. Song, "Validation and functional analysis of the critical proteins in combination with taurine, epigallocatechin gallate and genistein against liver fibrosis in rats," *Biomedicine & Pharmacotherapy*, vol. 115, Article ID 108975, 2019.

[80] Y. Li, M. Zhu, and Y. Huo, "Anti-fibrosis activity of combination therapy with epigallocatechin gallate, taurine and genistein by regulating glycolysis, gluconeogenesis, and ribosomal and lysosomal signaling pathways in HSC-T6 cells," *Experimental and Therapeutic Medicine*, vol. 16, pp. 4329–4338, 2018.

[81] L. Zhuo, M. Liao, and L. Zheng, "Combination therapy with taurine, epigallocatechin gallate and genistein for protection against hepatic fibrosis induced by alcohol in rats," *Biological and Pharmaceutical Bulletin*, vol. 35, pp. 1802–1810, 2012.

[82] Y. Li, Y. Luo, and X. Zhang, "Combined taurine, epigallocatechin gallate and genistein therapy reduces HSC-T6 cell proliferation and modulates the expression of fibrogenic factors," *International Journal of Molecular Sciences*, vol. 14, pp. 20543–20554, 2013.

[83] W. Cao, Y. Li, and M. Li, "Txn1, Ctsd and Cdk4 are key proteins of combination therapy with taurine, epigallocatechin gallate and genistein against liver fibrosis in rats," *Biomedicine & Pharmacotherapy*, vol. 85, pp. 611–619, 2017.

[84] W. Cao, Y. Zhou, and Y. Li, "ITRAQ-based proteomic analysis of combination therapy with taurine, epigallocatechin gallate, and genistein on carbon tetrachloride-induced liver fibrosis in rats," *Toxicology Letters*, vol. 232, pp. 233–245, 2015.

[85] F. L. Yen, T. H. Wu, and L. T. Lin, "Naringenin-loaded nanoparticles improve the physicochemical properties and the hepatoprotective effects of naringenin in orally-administered rats with CCl(4)-induced acute liver failure," *Pharmaceutical Research*, vol. 26, pp. 893–902, 2009.

[86] E. Hernández-Aquino and P. Muriel, "Beneficial effects of naringenin in liver diseases: molecular mechanisms," *World Journal of Gastroenterology*, vol. 24, pp. 1679–1707, 2018.

[87] E. Hernández-Aquino, M. A. Quezada-Ramírez, and A. Silva-Olivares, "Naringenin attenuates the progression of liver fibrosis via inactivation of hepatic stellate cells and profibrogenic pathways," *European Journal of Pharmacology*, vol. 865, Article ID 172730, 2019.

[88] R. Tovar, R. E. Flores-Beltrán, and L. Favari, "Naringenin prevents experimental liver fibrosis by blocking TGFβ-Smad3 and JNK-Smad3 pathways," *World Journal of Gastroenterology*, vol. 23, pp. 4354–4368, 2017.

[89] X. Liu, W. Wang, and H. Hu, "Smad3 specific inhibitor, naringenin, decreases the expression of extracellular matrix

induced by TGF-beta1 in cultured rat hepatic stellate cells," *Pharmaceutical Research*, vol. 23, pp. 82–89, 2006.

[90] H. Ao, W. Feng, and C. Peng, "Hydroxysafflor yellow A: a promising therapeutic agent for a broad spectrum of diseases," *Evidence-Based Complementary and Alternative Medicine*, vol. 2018, Article ID 8259280, 2018.

[91] Y. Zhang, J. Guo, and H. Dong, "Hydroxysafflor yellow A protects against chronic carbon tetrachloride-induced liver fibrosis," *European Journal of Pharmacology*, vol. 660, pp. 438–444, 2011.

[92] Y. B. Zhang, H. Y. Dong, and X. M. Zhao, "Hydroxysafflor yellow A attenuates carbon tetrachloride-induced hepatic fibrosis in rats by inhibiting Erk5 signaling," *American Journal of Chinese Medicine*, vol. 40, pp. 481–494, 2012.

[93] Y. Li, Y. Shi, and Y. Sun, "Restorative effects of hydroxysafflor yellow A on hepatic function in an experimental regression model of hepatic fibrosis induced by carbon tetrachloride," *Molecular Medicine Reports*, vol. 15, pp. 47–56, 2017.

[94] Q. Liu, C. Y. Wang, and Z. Liu, "Hydroxysafflor yellow A suppresses liver fibrosis induced by carbon tetrachloride with high-fat diet by regulating PPAR-γ/p38 MAPK signaling," *Pharmaceutical Biology*, vol. 52, pp. 1085–1093, 2014.

[95] C. Y. Wang, Q. Liu, and Q. X. Huang, "Activation of PPARγ is required for hydroxysafflor yellow A of Carthamus tinctorius to attenuate hepatic fibrosis induced by oxidative stress," *Phytomedicine*, vol. 20, pp. 592–599, 2013.

[96] C. C. Li, C. Z. Yang, and X. M. Li, "Hydroxysafflor yellow A induces apoptosis in activated hepatic stellate cells through ERK1/2 pathway in vitro," *European Journal of Pharmaceutical Sciences*, vol. 46, pp. 397–404, 2012.

[97] Q. Han, H. Wang, and C. Xiao, "Oroxylin A inhibits H(2)O(2)-induced oxidative stress in PC12 cells," *Natural Product Research*, vol. 31, pp. 1339–1342, 2017.

[98] W. T. Ku, J. J. Tung, and T. J. F. Lee, "Long-term exposure to oroxylin A inhibits metastasis by suppressing CCL2 in oral squamous cell carcinoma cells," *Cancers (Basel)*, vol. 11, p. 353, 2019.

[99] H. Jin, N. Lian, and M. Bian, "Oroxylin A prevents alcohol-induced hepatic steatosis through inhibition of hypoxia inducible factor 1alpha," *Chemico-Biological Interactions*, vol. 285, pp. 14–20, 2018.

[100] W. Zhou, X. Liu, and X. Zhang, "Oroxylin A inhibits colitis by inactivating NLRP3 inflammasome," *Oncotarget*, vol. 8, pp. 58903–58917, 2017.

[101] Z. Zhang, M. Guo, and M. Shen, "Oroxylin A regulates the turnover of lipid droplet via downregulating adipose triglyceride lipase (ATGL) in hepatic stellate cells," *Life Sciences*, vol. 238, Article ID 116934, 2019.

[102] C. Zhang, M. Bian, and X. Chen, "Oroxylin A prevents angiogenesis of LSECs in liver fibrosis via inhibition of YAP/HIF-1α signaling," *Journal of Cellular Biochemistry*, vol. 119, pp. 2258–2268, 2018.

[103] F. Wang, Y. Jia, and M. Li, "Blockade of glycolysis-dependent contraction by oroxylin a via inhibition of lactate dehydrogenase-a in hepatic stellate cells," *Cell Communication and Signaling*, vol. 17, pp. 1–13, 2019.

[104] M. Bian, J. He, and H. Jin, "Oroxylin A induces apoptosis of activated hepatic stellate cells through endoplasmic reticulum stress," *Apoptosis*, vol. 24, pp. 905–920, 2019.

[105] W. Chen, Z. Zhang, and Z. Yao, "Activation of autophagy is required for Oroxylin A to alleviate carbon tetrachloride-induced liver fibrosis and hepatic stellate cell activation," *International Immunopharmacology*, vol. 56, pp. 148–155, 2018.

[106] J. He and M. M. Giusti, "Anthocyanins: natural colorants with health-promoting properties," *Annual Review of Food Science and Technology*, vol. 1, pp. 163–187, 2010.

[107] J. H. Choi, Y. P. Hwang, and C. Y. Choi, "Anti-fibrotic effects of the anthocyanins isolated from the purple-fleshed sweet potato on hepatic fibrosis induced by dimethylnitrosamine administration in rats," *Food and Chemical Toxicology*, vol. 48, pp. 3137–3143, 2010.

[108] J. H. Choi, Y. P. Hwang, and B. H. Park, "Anthocyanins isolated from the purple-fleshed sweet potato attenuate the proliferation of hepatic stellate cells by blocking the PDGF receptor," *Environmental Toxicology and Pharmacology*, vol. 31, pp. 212–219, 2011.

[109] W. Zhan, X. Liao, and R. J. Xie, "The effects of blueberry anthocyanins on histone acetylation in rat liver fibrosis," *Oncotarget*, vol. 8, pp. 96761–96773, 2017.

[110] J. Sun, Y. Wu, and C. Long, "Anthocyanins isolated from blueberry ameliorates CCl4 induced liver fibrosis by modulation of oxidative stress, inflammation and stellate cell activation in mice," *Food and Chemical Toxicology*, vol. 120, pp. 491–499, 2018.

[111] X. Jiang, T. Shen, and X. Tang, "Cyanidin-3-O-β-glucoside combined with its metabolite protocatechuic acid attenuated the activation of mice hepatic stellate cells," *Food & Function*, vol. 8, pp. 2945–2957, 2017.

[112] X. Jiang, H. Guo, and T. Shen, "Cyanidin-3-O-β-glucoside purified from black rice protects mice against hepatic fibrosis induced by carbon tetrachloride via inhibiting hepatic stellate cell activation," *Journal of Agricultural and Food Chemistry*, vol. 63, pp. 6221–6230, 2015.

[113] Y. Liu, P. H. Wen, and X. X. Zhang, "Breviscapine ameliorates CCl4-induced liver injury in mice through inhibiting inflammatory apoptotic response and ROS generation," *International Journal of Molecular Medicine*, vol. 42, pp. 755–768, 2018.

[114] X. Wang, G. Gong, and W. Yang, "Antifibrotic activity of galangin, a novel function evaluated in animal liver fibrosis model," *Environmental Toxicology and Pharmacology*, vol. 36, pp. 288–295, 2013.

[115] E. J. Park, Y. Z. Zhao, and L. Lian, "Skullcapflavone I from Scutellaria baicalensis induces apoptosis in activated rat hepatic stellate cells," *Planta Medica*, vol. 71, pp. 885–887, 2005.

[116] Y. Zhan, D. Li, and H. Wei, "Emodin on hepatic fibrosis in rats," *Chinese Medical Journal (England)*, vol. 113, pp. 599–601, 2000.

[117] X. A. Zhao, G. Chen, and Y. Liu, "Emodin alleviates liver fibrosis of mice by reducing infiltration of Gr1 hi monocytes," *Evidence-Based Complementary and Alternative Medicine*, vol. 2018, Article ID 5738101, 2018.

[118] M. X. Dong, Y. Jia, and Y. B. Zhang, "Emodin protects rat liver from CCl(4)-induced fibrogenesis via inhibition of hepatic stellate cells activation," *World Journal of Gastroenterology*, vol. 15, pp. 4753–4762, 2009.

[119] M. Gui, Y. F. Zhang, and Z. Y. Xiao, "Inhibitory effect of emodin on tissue inhibitor of metalloproteinases-1 (TIMP-1) expression in rat hepatic stellate cells," *Digestive Diseases and Sciences*, vol. 52, pp. 200–207, 2007.

[120] F. Liu, J. Zhang, and J. Qian, "Emodin alleviates CCl4-induced liver fibrosis by suppressing epithelial-mesenchymal transition and transforming growth factor-β1 in rats," *Molecular Medicine Reports*, vol. 18, pp. 3262–3270, 2018.

[121] M. Z. Guo, X. S. Li, and H. R. Xu, "Rhein inhibits liver fibrosis induced by carbon tetrachloride in rats," *Acta Pharmaceutica Sinica B*, vol. 23, pp. 739–744, 2002.

[122] M. J. Shi, B. S. Dong, and W. N. Yang, "Preventive and therapeutic role of Tanshinone IIA in hepatology," *Biomedicine & Pharmacotherapy*, vol. 112, Article ID 108676, 2019.

[123] Q. Ying, Y. Teng, and J. Zhang, "Therapeutic effect of tanshinone IIA on liver fibrosis and the possible mechanism: a preclinical meta-analysis," *Evidence-Based Complementary and Alternative Medicine*, vol. 2019, Article ID 7514046, 2019.

[124] T. L. Pan and P. W. Wang, "Explore the molecular mechanism of apoptosis induced by tanshinone IIA on activated rat hepatic stellate cells," *Evidence-Based Complementary and Alternative Medicine*, vol. 2012, Article ID 734987, 2012.

[125] X. H. Che, E. J. Park, and Y. Z. Zhao, "Tanshinone II A induces apoptosis and s phase cell cycle arrest in activated rat hepatic stellate cells," *Basic & Clinical Pharmacology & Toxicology*, vol. 106, pp. 30–37, 2010.

[126] M. J. Shi, X. L. Yan, and B. S. Dong, "A network pharmacology approach to investigating the mechanism of Tanshinone IIA for the treatment of liver fibrosis," *Journal of Ethnopharmacology*, vol. 253, Article ID 112689, 2020.

[127] R. Wu, S. Dong, and F. F. Cai, "Active compounds derived from Fuzheng Huayu formula protect hepatic parenchymal cells from apoptosis based on network pharmacology and transcriptomic analysis," *Molecules*, vol. 24, 2019.

[128] X. Q. Hu, Y. N. Song, and R. Wu, "Metabolic mechanisms of Fuzheng-Huayu formula against liver fibrosis in rats," *Journal of Ethnopharmacology*, vol. 238, Article ID 111888, 2019.

[129] S. Dong, F. F. Cai, and Q. L. Chen, "Chinese herbal formula Fuzheng Huayu alleviates CCl4-induced liver fibrosis in rats: a transcriptomic and proteomic analysis," *Acta Pharmaceutica Sinica B*, vol. 39, pp. 930–941, 2018.

[130] S. Bimonte, V. Albino, and A. Barbieri, "Dissecting the roles of thymoquinone on the prevention and the treatment of hepatocellular carcinoma: an overview on the current state of knowledge," *Infectious Agents and Cancer*, vol. 14, p. 10, 2019.

[131] T. Bai, Y. Yang, and Y. L. Wu, "Thymoquinone alleviates thioacetamide-induced hepatic fibrosis and inflammation by activating LKB1-AMPK signaling pathway in mice," *International Immunopharmacology*, vol. 19, pp. 351–357, 2014.

[132] M. Ghazwani, Y. Zhang, and X. Gao, "Anti-fibrotic effect of thymoquinone on hepatic stellate cells," *Phytomedicine*, vol. 21, pp. 254–260, 2014.

[133] T. Bai, L. H. Lian, and Y. L. Wu, "Thymoquinone attenuates liver fibrosis via PI3K and TLR4 signaling pathways in activated hepatic stellate cells," *International Immunopharmacology*, vol. 15, pp. 275–281, 2013.

[134] A. H. Abdelghany, M. A. BaSalamah, and S. Idris, "The fibrolytic potentials of vitamin D and thymoquinone remedial therapies: insights from liver fibrosis established by CCl_4 in rats," *Journal of Translational Medicine*, vol. 14, pp. 1–15, 2016.

[135] Q. Chen, H. Zhang, and Y. Cao, "Schisandrin B attenuates CCl(4)-induced liver fibrosis in rats by regulation of Nrf2-ARE and TGF-β/Smad signaling pathways," *Drug Design, Development and Therapy*, vol. 11, pp. 2179–2191, 2017.

[136] Z. Yao, J. Han, and S. Lou, "Schisandrin B attenuates lipopolysaccharide-induced activation of hepatic stellate cells through Nrf-2-activating anti-oxidative activity," *International Journal of Clinical and Experimental Pathology*, vol. 11, pp. 4917–4925, 2018.

[137] H. Zhang, Q. Chen, and A. Dahan, "Transcriptomic analyses reveal the molecular mechanisms of schisandrin B alleviates CCl4-induced liver fibrosis in rats by RNA-sequencing," *Chemico-Biological Interactions*, vol. 309, Article ID 108675, 2019.

[138] Y. Huang, C. Liu, and S. Liu, "In vitro metabolism of magnolol and honokiol in rat liver microsomes and their interactions with seven cytochrome P substrates," *Rapid Communication and Mass Spectrom*, vol. 33, pp. 229–238, 2019.

[139] M. G. Elfeky, E. M. Mantawy, and A. M. Gad, *Mechanistic Aspects of Antifibrotic Effects of Honokiol in Con A-Induced Liver Fibrosis in Rats: Emphasis on TGF-β/SMAD/MAPK Signaling Pathways*, Elsevier, Amsterdam, Netherlands, 2020.

[140] E. J. Park, Y. Z. Zhao, and Y. H. Kim, "Honokiol induces apoptosis via cytochrome c release and caspase activation in activated rat hepatic stellate cells in vitro," *Planta Medica*, vol. 71, pp. 82–84, 2005.

[141] H. Zhang, B. Ju, and X. Zhang, "Magnolol attenuates concanavalin A-induced hepatic fibrosis, inhibits CD4+ T helper 17 (Th17) cell differentiation and suppresses hepatic stellate cell activation: blockade of smad3/smad4 signalling," *Basic & Clinical Pharmacology & Toxicology*, vol. 120, pp. 560–570, 2017.

[142] E. Patsenker, A. Chicca, and V. Petrucci, "4-O'-methylhonokiol protects from alcohol/carbon tetrachloride-induced liver injury in mice," *ournal of Molecular Medicine (Berlin)*, vol. 95, pp. 1077–1089, 2017.

[143] S. H. Sung and Y. C. Kim, "Hepatoprotective diastereomeric lignans from Saururus chinensis herbs," *Journal of Natural Products*, vol. 63, pp. 1019–1021, 2000.

[144] J. H. Lee, E. J. Jang, and H. L. Seo, "Sauchinone attenuates liver fibrosis and hepatic stellate cell activation through TGF-β/Smad signaling pathway," *Chemico-Biological Interactions*, vol. 224, pp. 58–67, 2014.

[145] Y. W. Kim, S. M. Lee, and S. M. Shin, "Efficacy of sauchinone as a novel AMPK-activating lignan for preventing iron-induced oxidative stress and liver injury," *Free Radical Biology and Medicine*, vol. 47, pp. 1082–1092, 2009.

[146] Y. L. Lin, C. H. Wu, and M. H. Luo, "In vitro protective effects of salvianolic acid B on primary hepatocytes and hepatic stellate cells," *Journal of Ethnopharmacology*, vol. 105, pp. 215–222, 2006.

[147] J. F. Zhao, C. H. Liu, and Y. Y. Hu, "Effect of salvianolic acid B on Smad3 expression in hepatic stellate cells," *Hepatobiliary & Pancreatic Diseases International*, vol. 3, pp. 102–105, 2004.

[148] P. Liu, C. H. Liu, and H. N. Wang, "Effect of salvianolic acid B on collagen production and mitogen-activated protein kinase activity in rat hepatic stellate cells," *Acta Pharmaceutica Sinica B*, vol. 23, pp. 733–738, 2002.

[149] Z. Lv, Y. Song, and D. Xue, "Effect of Salvianolic-acid B on inhibiting MAPK signaling induced by transforming growth factor-β1 in activated rat hepatic stellate cells," *Journal of Ethnopharmacology*, vol. 132, pp. 384–392, 2010.

[150] W. Zhang, J. Ping, and Y. Zhou, "Salvianolic acid B inhibits activation of human primary hepatic stellate cells through downregulation of the myocyte enhancer factor 2 signaling pathway," *Frontiers in Pharmacology*, vol. 10, 2019.

[151] S. Li, L. Wang, and X. Yan, "Salvianolic acid B attenuates rat hepatic fibrosis via downregulating angiotensin II signaling,"

Evidence-Based Complementary and Alternative Medicine, vol. 2012, Article ID 160726, 2012.

[152] R. Wang, X. Y. Yu, and Z. Y. Guo, "Inhibitory effects of salvianolic acid B on CCl4-induced hepatic fibrosis through regulating NF-κB/IκBα signaling," *Journal of Ethnopharmacology*, vol. 144, pp. 592–598, 2012.

[153] F. Yu, Y. Guo, and B. Chen, "LincRNA-p21 inhibits the Wnt/β-catenin pathway in activated hepatic stellate cells via sponging MicroRNA-17-5p," *Cellular Physiology & Biochemistry*, vol. 41, pp. 1970–1980, 2017.

[154] F. Yu, Z. Lu, and K. Huang, "MicroRNA-17-5p-activated Wnt/β-catenin pathway contributes to the progression of liver fibrosis," *Oncotarget*, vol. 7, pp. 81–93, 2016.

[155] C. Wu, W. Chen, and H. Ding, "Salvianolic acid B exerts anti-liver fibrosis effects via inhibition of MAPK-mediated phospho-Smad2/3 at linker regions in vivo and in vitro," *Life Science*, vol. 239, Article ID 116881, 2019.

[156] F. Yu, Z. Lu, and B. Chen, "Salvianolic acid B-induced microRNA-152 inhibits liver fibrosis by attenuating DNMT1-mediated Patched1 methylation," *Journal of Cellular and Molecular Medicine*, vol. 19, pp. 2617–2632, 2015.

[157] Y. Y. Tao, Q. L. Wang, and L. Shen, "Salvianolic acid B inhibits hepatic stellate cell activation through transforming growth factor beta-1 signal transduction pathway in vivo and in vitro," *Experimental biology and medicine (Maywood)*, vol. 238, pp. 1284–1296, 2013.

[158] E. Chávez, K. Reyes-Gordillo, and J. Segovia, "Resveratrol prevents fibrosis, NF-kappaB activation and TGF-beta increases induced by chronic CCl4 treatment in rats," *Journal of Applied Toxicology*, vol. 28, pp. 35–43, 2008.

[159] M. Di Pascoli, M. Diví, and A. Rodríguez-Vilarrupla, "Resveratrol improves intrahepatic endothelial dysfunction and reduces hepatic fibrosis and portal pressure in cirrhotic rats," *Journal of Hepatology*, vol. 58, pp. 904–910, 2013.

[160] H. Zhang, Q. Sun, and T. Xu, "Resveratrol attenuates the progress of liver fibrosis via the Akt/nuclear factor-κB pathways," *Molecular Medicine Reports*, vol. 13, pp. 224–230, 2016.

[161] B. Yu, S. yu Qin, and B. li Hu, "Resveratrol improves CCL4-induced liver fibrosis in mouse by upregulating endogenous IL-10 to reprogramme macrophages phenotype from M(LPS) to M(IL-4)," *Biomedicine & Pharmacotherapy*, vol. 117, 2019.

[162] E. S. Lee, M. O. Shin, and S. Yoon, "Resveratrol inhibits dimethylnitrosamine-induced hepatic fibrosis in rats," *Archives of Pharmacal Research*, vol. 33, pp. 925–932, 2010.

[163] S. W. Hong, K. H. Jung, and H. M. Zheng, "The protective effect of resveratrol on dimethylnitrosamine-induced liver fibrosis in rats," *Archives of Pharmacal Research*, vol. 33, pp. 601–609, 2010.

[164] A. Ahmad and R. Ahmad, "Resveratrol mitigate structural changes and hepatic stellate cell activation in N′-nitrosodimethylamine-induced liver fibrosis via restraining oxidative damage," *Chemico-Biological Interactions*, vol. 221, pp. 1–12, 2014.

[165] A. F. Hessin, R. R. Hegazy, and A. A. Hassan, "Resveratrol prevents liver fibrosis via two possible pathways: modulation of alpha fetoprotein transcriptional levels and normalization of protein kinase C responses," *Indian Journal of Pharmacology*, vol. 49, pp. 282–289, 2017.

[166] T. T. Chen, S. Peng, and Y. Wang, "Improvement of mitochondrial activity and fibrosis by resveratrol treatment in mice with Schistosoma japonicum infection," *Biomolecules*, vol. 9, 2019.

[167] T. Kessoku, K. Imajo, and Y. Honda, "Resveratrol ameliorates fibrosis and inflammation in a mouse model of non-alcoholic steatohepatitis," *Science Reports*, vol. 6, pp. 3–9, 2016.

[168] I. C. C. de Souza, L. A. M. Martins, and M. de Vasconcelos, "Resveratrol regulates the quiescence-like induction of activated stellate cells by modulating the pparγ/SIRT1 ratio," *Journal of Cellular Biochemistry*, vol. 116, pp. 2304–2312, 2015.

[169] D. Q. Zhang, P. Sun, and Q. Jin, "Resveratrol regulates activated hepatic stellate cells by modulating NF-κB and the PI3K/Akt signaling pathway," *Journal of Food Sciences*, vol. 81, pp. H240–H245, 2016.

[170] L. A. Meira Martins, M. Q. Vieira, and M. Ilha, "The interplay between apoptosis, mitophagy and mitochondrial biogenesis induced by resveratrol can determine activated hepatic stellate cells death or survival," *Cell Biochemistry and Biophysics*, vol. 71, pp. 657–672, 2014.

[171] B. N. Singh, S. Shankar, and R. K. Srivastava, "Green tea catechin, epigallocatechin-3-gallate (EGCG): mechanisms, perspectives and clinical applications," *Biochemical Pharmacology*, vol. 82, pp. 1807–1821, 2011.

[172] M. chuan Zhen, Q. Wang, and X. hui Huang, "Green tea polyphenol epigallocatechin-3-gallate inhibits oxidative damage and preventive effects on carbon tetrachloride-induced hepatic fibrosis," *Journal of Nutritional Biochemistry*, vol. 18, pp. 795–805, 2007.

[173] G. L. Tipoe, T. M. Leung, and E. C. Liong, "Epigallocatechin-3-gallate (EGCG) reduces liver inflammation, oxidative stress and fibrosis in carbon tetrachloride (CCl4)-induced liver injury in mice," *Toxicology*, vol. 273, pp. 45–52, 2010.

[174] L. Wang, G. Yang, and L. Yuan, "Green tea catechins effectively altered hepatic fibrogenesis in rats by inhibiting ERK and smad1/2 phosphorylation," *Journal of Agricultural and Food Chemistry*, vol. 67, pp. 5437–5445, 2019.

[175] Y. Yasuda, M. Shimizu, and H. Sakai, "(−)-Epigallocatechin gallate prevents carbon tetrachloride-induced rat hepatic fibrosis by inhibiting the expression of the PDGFRbeta and IGF-1R," *Chemico-Biological Interactions*, vol. 182, pp. 159–164, 2009.

[176] K. Shen, X. Feng, and R. Su, "Epigallocatechin 3-gallate ameliorates bile duct ligation induced liver injury in mice by modulation of mitochondrial oxidative stress and inflammation," *PLoS One*, vol. 10, Article ID e0126278, 2015.

[177] D. K. Yu, C. X. Zhang, and S. S. Zhao, "The anti-fibrotic effects of epigallocatechin-3-gallate in bile duct-ligated cholestatic rats and human hepatic stellate LX-2 cells are mediated by the PI3K/Akt/Smad pathway," *Acta Pharmaceutica Sinica B*, vol. 36, pp. 473–482, 2015.

[178] M. L. Arffa, M. A. Zapf, and A. N. Kothari, "Epigallocatechin-3-Gallate upregulates miR-221 to inhibit osteopontin-dependent hepatic fibrosis," *PLoS One*, vol. 11, Article ID e0167435, 2016.

[179] J. Xiao, C. T. Ho, and E. C. Liong, "Epigallocatechin gallate attenuates fibrosis, oxidative stress, and inflammation in non-alcoholic fatty liver disease rat model through TGF/SMAD, PI3 K/Akt/FoxO1, and NF-kappa B pathways," *European Journal of Nutrition*, vol. 53, pp. 187–199, 2014.

[180] R. Sakata, T. Ueno, and T. Nakamura, "Green tea polyphenol epigallocatechin-3-gallate inhibits platelet-derived growth factor-induced proliferation of human hepatic stellate cell line LI90," *Journal of Hepatology*, vol. 40, pp. 52–59, 2004.

[181] M. Nakamuta, N. Higashi, and M. Kohjima, "Epigallocatechin-3-gallate, a polyphenol component of green

tea, suppresses both collagen production and collagenase activity in hepatic stellate cells," *International Journal of Molecular Medicine*, vol. 16, pp. 677–681, 2005.

[182] N. Higashi, M. Kohjima, and M. Fukushima, "Epigallocatechin-3-gallate, a green-tea polyphenol, suppresses Rho signaling in TWNT-4 human hepatic stellate cells," *Journal of Laboratory and Clinical Medicine*, vol. 145, pp. 316–322, 2005.

[183] M. Zhen, X. Huang, and Q. Wang, "Green tea polyphenol epigallocatechin-3-gallate suppresses rat hepatic stellate cell invasion by inhibition of MMP-2 expression and its activation," *Acta Pharmaceutica Sinica B*, vol. 27, pp. 1600–1607, 2006.

[184] F. Yumei, Y. Zhou, and S. Zheng, "The antifibrogenic effect of (−)-epigallocatechin gallate results from the induction of de novo synthesis of glutathione in passaged rat hepatic stellate cells," *Laboratory Investigation*, vol. 86, pp. 697–709, 2006.

[185] L. Ying, F. Yan, and Y. Zhao, "(−)-Epigallocatechin-3-gallate and atorvastatin treatment down-regulates liver fibrosis-related genes in non-alcoholic fatty liver disease," *Clinical and Experimental Pharmacology*, vol. 44, pp. 1180–1191, 2017.

[186] H. Khan, H. Ullah, and S. M. Nabavi, "Mechanistic insights of hepatoprotective effects of curcumin: therapeutic updates and future prospects," *Food and Chemical Toxicology*, vol. 124, pp. 182–191, 2019.

[187] S. Zheng and A. Chen, "Activation of PPARγ is required for curcumin to induce apoptosis and to inhibit the expression of extracellular matrix genes in hepatic stellate cells in vitro," *Biochemical Journal*, vol. 384, pp. 149–157, 2004.

[188] J. Xu, Y. Fu, and A. Chen, "Activation of peroxisome proliferator-activated receptor-gamma contributes to the inhibitory effects of curcumin on rat hepatic stellate cell growth," *American Journal of Physiology-Gastrointestinal and Liver Physiology*, vol. 285, pp. G20–G30, 2003.

[189] J. Lin, Y. Tang, and Q. Kang, "Curcumin inhibits gene expression of receptor for advanced glycation end-products (RAGE) in hepatic stellate cells in vitro by elevating PPARγ activity and attenuating oxidative stress," *British Journal of Pharmacology*, vol. 166, pp. 2212–2227, 2012.

[190] Y. Fu, S. Zheng, and J. Lin, "Curcumin protects the rat liver from CCl4-caused injury and fibrogenesis by attenuating oxidative stress and suppressing inflammation," *Molecular Pharmacology*, vol. 73, pp. 399–409, 2008.

[191] Q. Kang and A. Chen, "Curcumin inhibits srebp-2 expression in activated hepatic stellate cells in vitro by reducing the activity of specificity protein-1," *Endocrinology*, vol. 150, pp. 5384–5394, 2009.

[192] M. E. Wang, Y. C. Chen, and I. S. Chen, "Curcumin protects against thioacetamide-induced hepatic fibrosis by attenuating the inflammatory response and inducing apoptosis of damaged hepatocytes," *Journal of Nutritional Biochemistry*, vol. 23, pp. 1352–1366, 2012.

[193] S. Priya and P. R. Sudhakaran, "Curcumin-induced recovery from hepatic injury involves induction of apoptosis of activated hepatic stellate cells," *Indian Journal of Biochemistry and Biophysics*, vol. 45, pp. 317–325, 2008.

[194] J. C. Shu, Y. J. He, and X. Lv, "Curcumin prevents liver fibrosis by inducing apoptosis and suppressing activation of hepatic stellate cells," *Journal of Natural Medicines*, vol. 63, pp. 415–420, 2009.

[195] Y. J. He, K. Kuchta, and X. Lv, "Curcumin, the main active constituent of turmeric (Curcuma longa L.), induces apoptosis in hepatic stellate cells by modulating the abundance of apoptosis-related growth factors," *Zeitschrift Fur Naturforsch.-Section C Journal of Biosciences*, vol. 70, pp. 281–285, 2015.

[196] R. Huang, Y. Liu, and Y. Xiong, "Curcumin protects against liver fibrosis by attenuating infiltration of gr1hi monocytes through inhibition of monocyte chemoattractant protein-1," *Discovery medicine*, vol. 21, 2016.

[197] X. A. Zhao, G. Chen, and Y. Liu, "Curcumin reduces Ly6Chi monocyte infiltration to protect against liver fibrosis by inhibiting Kupffer cells activation to reduce chemokines secretion," *Biomedicine & Pharmacotherapy*, vol. 106, pp. 868–878, 2018.

[198] P. Wu, R. Huang, and Y. L. Xiong, "Protective effects of curcumin against liver fibrosis through modulating DNA methylation," *Chinese Journal of Natural Medicines*, vol. 14, pp. 255–264, 2016.

[199] L. Cui, X. Jia, and Q. Zhou, "Curcumin affects β-catenin pathway in hepatic stellate cell in vitro and in vivo," *Journal of Pharmacy and Pharmacology*, vol. 66, pp. 1615–1622, 2014.

[200] J. Qiu, Q. Zhou, and X. Zhai, "Curcumin regulates delta-like homolog 1 expression in activated hepatic stellate cell," *European Journal of Pharmacology*, vol. 728, pp. 9–15, 2014.

[201] Q. yan Yao, B. li Xu, and J. yao Wang, "Inhibition by curcumin of multiple sites of the transforming growth factor-beta1 signalling pathway ameliorates the progression of liver fibrosis induced by carbon tetrachloride in rats," *BMC Complementary and Alternative Medicine*, vol. 12, 2012.

[202] N. Chen, Q. Geng, and J. Zheng, "Suppression of the TGF-β/Smad signaling pathway and inhibition of hepatic stellate cell proliferation play a role in the hepatoprotective effects of curcumin against alcohol-induced hepatic fibrosis," *Internatioanl Journal of Molecular Medicine*, vol. 34, pp. 1110–1116, 2014.

[203] C. tao Tu, Q. yan Yao, and B. li Xu, "Protective effects of curcumin against hepatic fibrosis induced by carbon tetrachloride: modulation of high-mobility group box 1, Toll-like receptor 4 and 2 expression," *Food and Chemical Toxicology*, vol. 50, pp. 3343–3351, 2012.

[204] Q. Yao, Y. Lin, and X. Li, "Curcumin ameliorates intrahepatic angiogenesis and capillarization of the sinusoids in carbon tetrachloride-induced rat liver fibrosis," *Toxicology Letters*, vol. 222, pp. 72–82, 2013.

[205] Z. Zhang, Y. Guo, and S. Zhang, "Curcumin modulates cannabinoid receptors in liver fibrosis in vivo and inhibits extracellular matrix expression in hepatic stellate cells by suppressing cannabinoid receptor type-1 in vitro," *European Journal of Pharmacology*, vol. 721, pp. 133–140, 2013.

[206] H. Jin, N. Lian, and F. Zhang, "Activation of PPARγ/p53 signaling is required for curcumin to induce hepatic stellate cell senescence," *Cell Death Disease*, vol. 7, pp. 1–11, 2016.

[207] H. Jin, Y. Jia, and Z. Yao, "Hepatic stellate cell interferes with NK cell regulation of fibrogenesis via curcumin induced senescence of hepatic stellate cell," *Cell Signaling*, vol. 33, pp. 79–85, 2017.

[208] N. Lian, Y. Jiang, and F. Zhang, "Curcumin regulates cell fate and metabolism by inhibiting hedgehog signaling in hepatic stellate cells," *Laboratory Investigation*, vol. 95, pp. 790–803, 2015.

[209] Y. Zhao, X. Ma, and J. Wang, "Curcumin protects against ccl4-induced liver fibrosis in rats by inhibiting HIF-1α through an erk-dependent pathway," *Molecules*, vol. 19, pp. 18767–18780, 2014.

[210] L. She, D. Xu, and Z. Wang, "Curcumin inhibits hepatic stellate cell activation via suppression of succinate-associated HIF-1α induction," *Molecular and Cellular Endocrinology*, vol. 476, pp. 129–138, 2018.

[211] S. El Swefy, R. A. Hasan, and A. Ibrahim, "Curcumin and hemopressin treatment attenuates cholestasis-induced liver fibrosis in rats: role of CB1 receptors," *Naunyn-Schmiedeberg's Archives of Pharmacology*, vol. 389, pp. 103–116, 2016.

[212] A. Eshaghian, A. Khodarahmi, and F. Safari, "Curcumin attenuates hepatic fibrosis and insulin resistance induced by bile duct ligation in rats," *British Journal of Nutrition*, vol. 120, pp. 393–403, 2018.

[213] Y. J. He, K. Kuchta, and Y. M. Deng, "Curcumin promotes apoptosis of activated hepatic stellate cells by inhibiting protein expression of the MyD88 pathway," *Planta Medica*, vol. 83, pp. 1392–1396, 2017.

[214] L. Qin, J. Qin, and X. Zhen, "Curcumin protects against hepatic stellate cells activation and migration by inhibiting the CXCL12/CXCR4 biological axis in liver fibrosis: A study in vitro and in vivo," *Biomedicine & Pharmacotherapy*, vol. 101, pp. 599–607, 2018.

[215] X. Qun Han, S. Qing Xu, and J. Guo Lin, "Curcumin recovers intracellular lipid droplet formation through increasing perilipin 5 gene expression in activated hepatic stellate cells in vitro," *Current Medical Science*, vol. 39, pp. 766–777, 2019.

[216] S. Nunes, A. R. Madureira, and D. Campos, "Therapeutic and nutraceutical potential of rosmarinic acid-Cytoprotective properties and pharmacokinetic profile," *Critical Reviews in Food Science and Nutrition*, vol. 57, pp. 1799–1806, 2017.

[217] G. S. Li, W. L. Jiang, and J. W. Tian, "In vitro and in vivo antifibrotic effects of rosmarinic acid on experimental liver fibrosis," *Phytomedicine*, vol. 17, pp. 282–288, 2010.

[218] N. M. El-Lakkany, W. H. El-Maadawy, and S. H. Seif el-Din, "Rosmarinic acid attenuates hepatic fibrogenesis via suppression of hepatic stellate cell activation/proliferation and induction of apoptosis," *Asian Pacific Journal of Tropical Medicine*, vol. 10, pp. 444–453, 2017.

[219] C. Lu, Y. Zou, and Y. Liu, "Rosmarinic acid counteracts activation of hepatic stellate cells via inhibiting the ROS-dependent MMP-2 activity: involvement of Nrf2 antioxidant system," *Toxicology and Applied Pharmacology*, vol. 318, pp. 69–78, 2017.

[220] M. N. Clifford, "Chlorogenic acids and other cinnamates–nature, occurrence and dietary burden," *Journal of the Science of Food and Agriculture*, vol. 79, pp. 362–372, 1999.

[221] H. Shi, L. Dong, and Y. Bai, "Chlorogenic acid against carbon tetrachloride-induced liver fibrosis in rats," *European Journal of Pharmacology*, vol. 623, pp. 119–124, 2009.

[222] H. Shi, L. Dong, and J. Jiang, "Chlorogenic acid reduces liver inflammation and fibrosis through inhibition of toll-like receptor 4 signaling pathway," *Toxicology*, vol. 303, pp. 107–114, 2013.

[223] H. Shi, A. Shi, and L. Dong, "Chlorogenic acid protects against liver fibrosis in vivo and in vitro through inhibition of oxidative stress," *Clinical Nutrition*, vol. 35, pp. 1366–1373, 2016.

[224] Y. Wang, F. Yang, and J. Xue, "Antischistosomiasis liver fibrosis effects of chlorogenic acid through IL-13/miR-21/Smad7 signaling interactions in vivo and in vitro," *Antimicrobial Agents and Chemotherapy*, vol. 61, Article ID e01347, 2017.

[225] F. Yang, L. Luo, and Z. De Zhu, "Chlorogenic acid inhibits liver fibrosis by blocking the miR-21-regulated TGF-β1/Smad7 signaling pathway in vitro and in vivo," *Frontiers in Pharmacology*, vol. 8, 2017.

[226] Q. Liu, Y. Chen, and C. Shen, "Chicoric acid supplementation prevents systemic inflammation-induced memory impairment and amyloidogenesis via inhibition of NF-κB," *FASEB Journal*, vol. 31, pp. 1494–1507, 2017.

[227] M. Kim, G. Yoo, and A. Randy, "Chicoric acid attenuate a nonalcoholic steatohepatitis by inhibiting key regulators of lipid metabolism, fibrosis, oxidation, and inflammation in mice with methionine and choline deficiency," *Molecular Nutrition & Food Research*, vol. 61, 2017.

[228] C. Srinivasulu, M. Ramgopal, and G. Ramanjaneyulu, "Syringic acid (SA)–a review of its occurrence, biosynthesis, pharmacological and industrial importance," *Biomedicine & Pharmacotherapy*, vol. 108, pp. 547–557, 2018.

[229] M. D. Vithana, Z. Singh, and S. K. Johnson, "Regulation of the levels of health promoting compounds: lupeol, mangiferin and phenolic acids in the pulp and peel of mango fruit: a review," *Journal of the Science of Food and Agriculture*, vol. 99, pp. 3740–3751, 2019.

[230] A. Itoh, K. Isoda, and M. Kondoh, "Hepatoprotective effect of syringic acid and vanillic acid on CCl4-induced liver injury," *Biological and Pharmaceutical Bulletin*, vol. 33, pp. 983–987, 2010.

[231] C. Chen, "Sinapic acid and its derivatives as medicine in oxidative stress-induced diseases and aging," *Oxidative Medicine and Cellular Longevity*, vol. 2016, Article ID 3571614, 2016.

[232] D. S. Shin, K. W. Kim, and H. Y. Chung, "Effect of sinapic acid against dimethylnitrosamine-induced hepatic fibrosis in rats," *Archives of Pharmacal Research*, vol. 36, pp. 608–618, 2013.

[233] X. Q. Pan, J. Zhou, and Y. Chen, "Classification, hepatotoxic mechanisms, and targets of the risk ingredients in traditional Chinese medicine-induced liver injury," *oxicology Letters*, vol. 323, pp. 48–56, 2020.

[234] C. Loguercio and D. Festi, "Silybin and the liver: from basic research to clinical practice," *World Journal of Gastroenterology*, vol. 17, pp. 2288–2301, 2011.

[235] M. Zhenzeng and L. Lunge, "New advances in drug therapies for liver fibrosis," *Journal of Clinical Hepatology*, vol. 32, pp. 1183–1187, 2016.

Hindawi
Evidence-Based Complementary and Alternative Medicine
Volume 2020, Article ID 7603410, 15 pages
https://doi.org/10.1155/2020/7603410

Review Article

Clinical Efficacy and Safety of Eight Traditional Chinese Medicine Combined with Entecavir in the Treatment of Chronic Hepatitis B Liver Fibrosis in Adults: A Network Meta-Analysis

Tao Wang,[1,2] Wei Jin,[3] Qianqian Huang,[1] Haotian Li,[2] Yun Zhu,[4] Honghong Liu,[4] Huadan Cai,[2] Jiabo Wang,[5] Ruilin Wang,[4] Xiaohe Xiao,[5] Yanling Zhao,[2] and Wenjun Zou[1]

[1]*College of Pharmacy, Chengdu University of Traditional Chinese Medicine, Chengdu 611137, China*
[2]*Department of Pharmacy, 302 Military Hospital of China, Beijing 100039, China*
[3]*Hospital of Chengdu University of Traditional Chinese Medicine, Chengdu 610075, China*
[4]*Integrative Medical Center, 302 Military Hospital of China, Beijing 100039, China*
[5]*China Military Institute of Chinese Medicine, 302 Military Hospital of China, Beijing 100039, China*

Correspondence should be addressed to Yanling Zhao; 2964842070@qq.com and Wenjun Zou; zouwenjun@163.com

Received 10 June 2020; Accepted 5 August 2020; Published 30 September 2020

Guest Editor: Hongwei Zhang

Background. Traditional Chinese medicine (TCM) is used as an adjuvant drug for the treatment of chronic hepatitis B liver fibrosis and is used frequently. We still do not know which TCM has the best curative effect as an adjuvant drug. Therefore, we decided to use network meta-analysis to solve this problem. *Methods*. We used the RevMan software (5.3) and Stata software (13.0) to achieve this network meta-analysis (NMA). The primary outcomes of this study were HA, LN, PCIII, and IV-C; the secondary outcomes of this study were AST, ALT, and HBV-DNA negative conversion rate, and the Cochrane risk-of-bias tool was used to assess the quality of the included studies. For all outcomes, the scissors funnel plot, Egger test, and Begg test were used to detect publication bias, and sensitivity analysis was used to investigate the stability of the results. And the meta-regression was used to explore the source of heterogeneity. *Results*. A total of 34 articles were included in this study. The study involved a total of 3199 patients, of which 1578 were assigned to the control group and 1621 patients were assigned to the experimental group. The number of men and women is roughly equal, and the average age is about 43 years old. In addition, nine treatment strategies were involved in this study. The combination of TCM and entecavir can significantly improve the patients' HA, LN, PCIII, IV-C, AST, ALT, and HBV-DNA negative conversion rates. The comprehensive evaluation results showed that FHC combined with entecavir has more advantages than other treatment strategies. *Conclusion*. For improving the HBV-DNA negative conversion rates, adding TCM to the therapeutic strategies does not seem to show absolute superiority. Finally, FHC combined with entecavir is the best therapeutic strategy.

1. Introduction

Chronic hepatitis B (CHB) is one of the most serious infectious diseases in the world today. It has extremely high morbidity and mortality, and it is a serious threat to human health [1, 2]. Every year, more than 600,000 people die from hepatitis B virus (HBV)-related diseases in the world [3]. Liver fibrosis, which as a process of hepatic repair and healing, can eventually develop into cirrhosis or even liver cancer if the liver damage factors cannot be removed over a long period of time. In addition, hepatitis B virus is one of the most common causes of liver cirrhosis in China. Statistical studies have shown that 3% of patients with chronic hepatitis B (CHB) have decompensated liver cirrhosis every year, 2% to 8% of patients have primary liver cancer, and once they progress to decompensation liver cirrhosis, its 5-

year cumulative survival rate was only 14% to 35% [4]. Therefore, for liver fibrosis, which as the starting point for serious liver disease, if this process can be well inhibited, it will be able to prevent liver disease from worsening in time.

At present, nucleoside (acid) analogues are mainly used clinically to treat hepatitis B liver fibrosis, such as adefovir dipivoxil, entecavir, and tenofovir disoproxil, which mainly through the continuous suppression of HBV-DNA replication to alleviate B hepatitis liver fibrosis. In particular, entecavir has become one of the main first-line drugs for the treatment of liver fibrosis in chronic hepatitis B in China. However, the use of Western medicine (such as entecavir) for the treatment of chronic hepatitis B liver fibrosis has a long cycle of treatment and even requires the patient to take medicine for life, causing a certain burden on the patient's family and greatly affecting the patient's own quality of life. And entecavir is a kind of guanine nuclear analog, although it has good safety, but there are still some studies reported that it caused lactic acidosis [5]. However, the cost of TCM treatment is relatively low, and TCM can act on multiple targets in the body at the same time. Many studies have shown that the use of Chinese and Western medicine in the treatment of chronic hepatitis B liver fibrosis can achieve better effect [6].

In China, there are many types of TCM used by clinicians in the treatment of chronic hepatitis B liver fibrosis. Among them, there are 8 kinds of TCM used as first-line drugs and included in the Chinese Pharmacopoeia: Anluo Huaxian Pill (AHP), Dahuang Zhechong Capsule (DZC), and Tanshinone Capsule (TSC), Danshen Injection (DI), Fuzheng Huayu Capsule (FHC), Biejia Ruangan Tablet (BRT), Danshendi Tablet (DDT), and Liuwei Wuling Tablet (LWT). The efficacy of these commonly used TCM is definite, and combined with the current first-line drug entecavir can significantly improve the clinical efficacy. This conclusion is not only due to long-term clinical experience. In recent years, many scholars have used meta-analysis and systematic review of evidence-based medical research methods to analyze the efficacy of the joint use of Chinese and Western medicine. Wang et al. showed that FHC combined with entecavir can significantly improve liver function and liver fibrosis in chronic hepatitis B patients [7]. Duan et al. also reached a similar conclusion when studying the effect of BRT combined with entecavir on the improvement of chronic hepatitis B cirrhosis [8]. In addition, LWT and AHP are also good auxiliary drugs [9, 10]. Although some researchers use meta-analysis methods to compare different treatment strategies, each comparison can only solve the problem of which of the two treatment strategies is better. When doctors choose treatment strategies, there are many kinds of TCM that can be selected, and which kind of TCM can achieve the best effect when used as an auxiliary medicine. This is still a problem that cannot be ignored. Therefore, we use the NMA to compare and rank the safety and effectiveness of the 8 TCMs which often used for adjuvant treatment of chronic hepatitis B liver fibrosis.

2. Materials and Methods

2.1. Search Strategy and Selection Criteria. We searched China National Knowledge Infrastructure, Wanfang Database, VIP medicine information system, PubMed, Embase, and Cochrane Library. The search time ranges from database establishment to May 2018. The initial search items were used as follows: "Fuzheng Huayu capsule," "Biejia Ruangan Tablets," "Liuwei Wuling Tablets," "Anluo Huaxian Pills," "Dahuang Zhechong Pills," "Tanshinone capsules," "Danshen Injection," "Entecavir," and "Chinese Medicine" [Title/Abstract] AND "Chronic hepatitis B liver fibrosis" [Title/Abstract] OR "Chronic hepatitis B" [Title/Abstract] OR "Liver Fibrosis" [Title/Abstract] OR "Hepatitis B" [Title/Abstract]. And the full text of the search results is downloaded. The inclusion criteria were as follows: (1) all randomized controlled trials (RCTs) and semirandomized controlled trials of Chinese Medicine combine with entecavir were included. (2) Chronic hepatitis B liver fibrosis was diagnosed according to definite diagnostic criteria. (3) The studies with an experimental group using entecavir combined with Chinese medicine and the control using entecavir were included. (4) The gender and age of patients were not limited. (5) The language of the literature is not limited. The exclusion criteria were as follows: (1) the repeated published literature, (2) studies with incomplete or incorrect data, (3) control group combined with other medicine during treatment, and (4) animal experiments and the review literature. And all patients were not treated with drugs such as interferon or nucleoside (acid) for six months before treatment.

2.2. Data Extraction and Quality Assessment. Three researchers (Tao Wang, Yanling Zhao, and Haotian Li) independently performed data extraction and quality assessment. Two researchers (Qianqian Huang and Huadan Cai) formed a review team to independently verify the accuracy of data extraction, quality assessment, and all materials for this study. Basic information was extracted from the included studies (name of the study included, average age of patients, number of patients, therapeutic strategies, mode of administration, dose administered, course of treatment, outcome, etc.) (Supplementary Table 1). The primary outcomes of this study were HA, LN, PCIII, and IV-C; the secondary outcomes of this study were AST, ALT, and HBV-DNA negative conversion rate, and the Cochrane Risk of Bias tool was used to assess the quality of the included studies. All the differences that occurred in the study were discussed by three researchers, and they were then agreed by the review team.

2.3. Statistical Analysis. We performed this study using RevMan software (5.3) and Stata software (13.0) and constructed a treatment strategy network. For the continuous variables, we calculated the normalized mean difference (MD), and for the dichotomous variable, we calculated the odds ratios (ORs). All of them were expressed with 95% CI. We compared each therapeutic strategy in pairs.

Subsequently, I^2 and chi-square tests were used to assess the heterogeneity between therapeutic strategies, and we use meta-regression to explore the source of heterogeneity. For all outcomes, the shear funnel plot, Egger test, and Begg test were used to detect publication bias, and sensitivity analysis was used to investigate the stability of the results. For all outcomes, the scissors funnel plot, Egger test, and Begg test were used to detect publication bias, and sensitivity analysis was used to investigate the stability of the results. Finally, we used the surface under the cumulative ranking curve (SUCRA) to rank the efficacy of the therapeutic strategy in each outcome. In addition, we did this NMA within a frequentist framework.

2.4. Statement. This study is registered with PROSPERO, number CRD42018095445. Finally, we need to state that the research funders did not interfere with any aspect of research design, data collection, data analysis, data interpretation, and article writing.

3. Results and Discussion

3.1. Results

3.1.1. Quality and Characteristics of the Included Studies. Through the key words in the search strategy, a total of 4969 articles were obtained, of which 3455 were excluded from repetitive reports, 68 articles were excluded from the review, and 1288 articles that did not use TCM + entecavir as a treatment strategy were excluded. In addition, we also excluded 124 articles which the control group did not use entecavir alone or experiment group combination with a variety of TCM, and eventually included 34 articles [11–44] (Figure 1(a)). In the literature included in this study, a total of 7 studies reported the randomization method, 7 studies did not adopt a completely random grouping method, and the rest of the studies only mentioned randomized grouping but did not explicitly report the randomization method. In terms of data integrity, 28 studies have good data integrity, 5 studies cannot clearly determine whether the data are complete, and 1 study has missing data. In addition, unfortunately, all the included studies did not explicitly mention the blinding method, so they could not judge whether they had adopted the blinding method in the trial. However, there are no selective reports in all the included studies. We assessed the quality of included studies in accordance with the Cochrane risk-of-bias tool. Each evaluation principle was divided into "high risk," "low risk," and "unclear" (Figure 1(b)). All the studies included in this study were designed in parallel, and the test sites were all in China. All patients were diagnosed with chronic hepatitis B liver fibrosis according to definite diagnostic criteria and confirmed in regular hospitals. The control group was given entecavir, and the experimental group was combined with a traditional Chinese medicine based on the treatment strategy of the control group. The study involved a total of 3199 patients, of which 1578 were assigned to the control group and 1621 patients were assigned to the experimental group. The number of men and women is roughly equal, and the average age is about 43 years old. In addition, nine treatment strategies were involved in this study (Figure 1(c)).

3.1.2. Primary Outcomes. The primary outcomes of our study were liver fibrosis (HA, LN, PCIII, and IV-C). All the included studies have reported on these four indicators. Compared with entecavir alone, we found that TCM combined with entecavir can significantly improve liver fibrosis in patients (HA: MD = −57.15, 95% CI: −69.06–45.25, $P < 0.00001$; LN: MD = −35.04, 95% CI: −43.32–26.76, $P < 0.00001$; PCIII: MD = −29.32, 95% CI: −31.68–26.96, $P < 0.00001$; IV-C: MD = −38.98, 95% CI: −48.32–29.64, $P < 0.00001$) (Figure 2). We considered the internal heterogeneity of the studies, so we decided to use the random-effects model for data analysis. Moreover, in order to further verify the reliability of the results of this study, we use sensitivity analysis (Table 1) to explore the stability of the results and use funnel charts and statistical tests (Egger test and Begg test) to explore whether there is publication bias (Table 1 and Supplementary Figures 1–4). As a result, it was found that some of the results of this study were unstable, but most of the studies were stable and there was no significant publication bias. In addition, our meta-regression showed that the difference in sample size between the studies did not cause significant heterogeneity. The difference in therapeutic strategies is the main source of heterogeneity in this study (Table 1).

Based on the above results, we use Stata software to make a mixed comparison of all therapeutic strategies and calculate the OR value (Supplementary Tables 2–5), which also helps to eliminate the heterogeneity caused by the variety of therapeutic strategies between studies. Subsequently, based on the effect of various therapeutic strategies on liver fibrosis improvement, we use SUCAR charts to rank treatment decisions and calculate the average ranking of each therapeutic strategies to further explore which TCM as an adjuvant drug is the best therapeutic strategies (Figure 3). The results showed that FHC (2.25), TSC (3.25), and LWT (3.75) were the top three, followed by BRT (4.00), DI (4.50), DDT (4.75), DZC (6.00), and entecavir (7.50). The combination of AHP (9) and entecavir was the most unfavorable treatment strategy. Since direct and indirect comparisons between treatment strategies all contribute to the final results, we finally calculated the contribution of the direct and indirect comparisons to the final results in order to make the results of this study clearer, and the detailed results of this section are listed in the annex (Supplementary Figure 5).

3.1.3. Secondary Outcomes. There are 3 secondary outcomes in our study: liver function index (AST and ALT) and HBV-DNA negative conversion rate. A total of 13 studies reported the improvement of HBV-DNA negative conversion rate by TCM; 21 studies reported the improvement of ALT and AST by TCM. Our research found that (Figure 4) entecavir combined with TCM compared to entecavir alone and HBV-DNA negative conversion rate did not show a significant difference (OR = 1.27, 95% CI: 0.92–1.76, $P = 0.14$) but significantly improved ALT and AST (MD = −13.33, 95% CI:

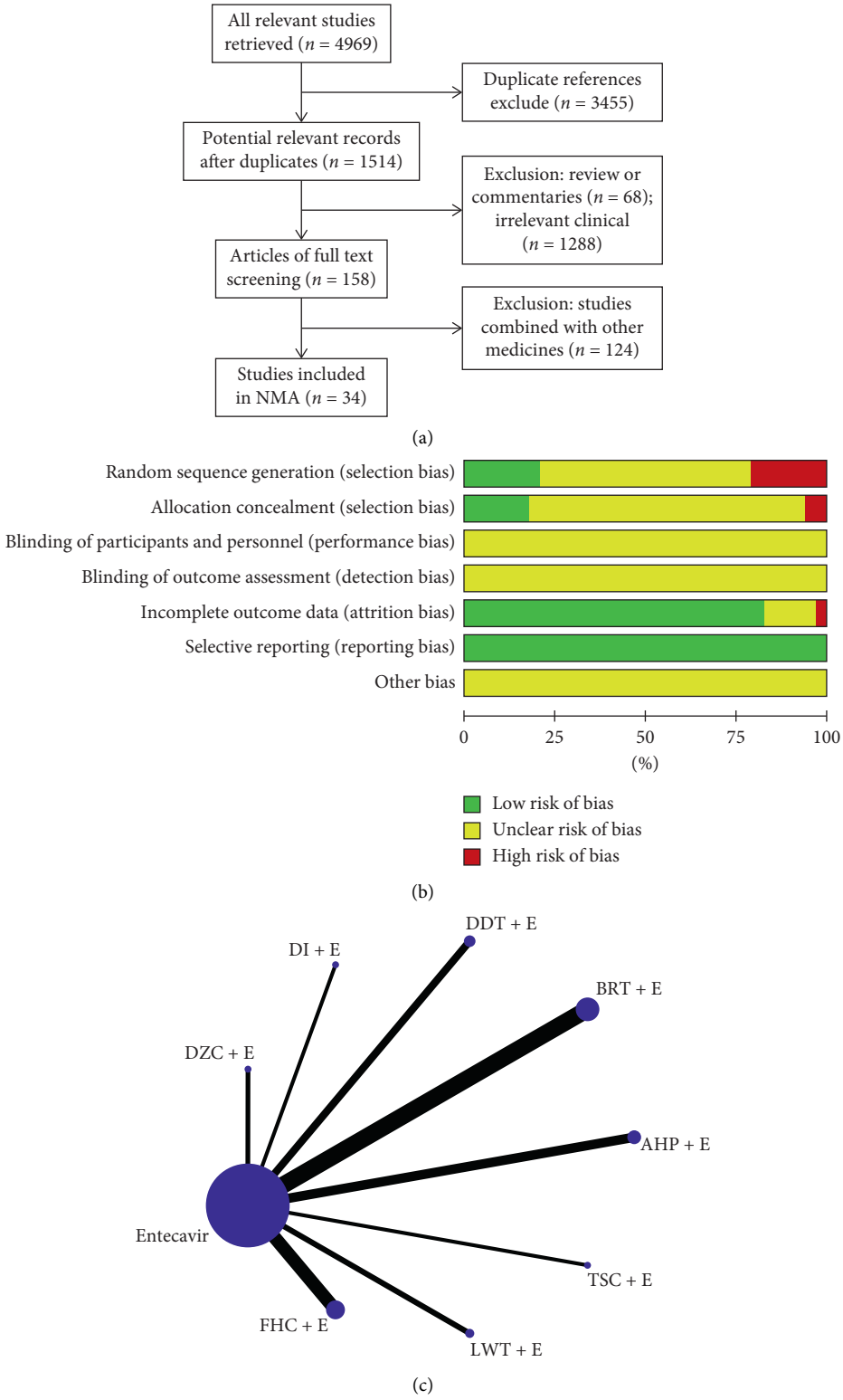

Figure 1: (a) Flowchart of study selection; (b) methodological quality assessment of the risk of bias for each included study; (c) network of eligible comparisons of efficacy of treatment.

−16.99–9.68, $P < 0.00001$; MD = −9.92, 95% CI: −13.40–6.44, $P < 0.00001$). In order to further explore the stability of the results and whether the results were affected by potential biases, we performed sensitivity analyses (Table 1), scissors funnel plot (Supplementary Figures 6–8), Egger test, and Begg test (Table 1). We found that the results of this study were stable, there was a slight publication bias in HBV-DNA negative conversion rate, and there was no significant

Study or subgroup	Experimental			Control			Weight	Mean difference	Mean difference
	Mean	SD	Total	Mean	SD	Total	(%)	IV, random, 95% CI	IV, random, 95% CI
C Xie 2016	88	24	50	100.42	34.52	50	3.1	−12.42 [−24.07, −0.77]	
CR Shen 2010	98.64	30.78	46	151.05	43.12	50	3.1	−52.41 [−67.31, −37.51]	
DJ Chen 2017	110.5	33.4	36	153.4	44.6	36	3.0	−42.90 [−61.10, −24.70]	
F Zhang 2017	121	28.3	35	170.8	36.8	35	3.1	−49.80 [−65.18, −34.42]	
FL Long 2011	82.4	32.2	57	189.6	24.1	59	3.2	−107.20 [−117.58, −96.82]	
GQ Chen 2016	66.27	19.18	45	103.3	37.21	45	3.1	−37.03 [−49.26, −24.80]	
HD Qi 2008	110.7	84.5	30	194.7	95.3	28	2.2	−84.00 [−130.48, −37.52]	
HS Xie 2016	124.7	65.8	65	156.3	82.7	63	2.8	−31.60 [−57.54, −5.66]	
HT Zhang 2015	106.8	81.8	100	142.5	91.2	100	2.9	−35.70 [−59.71, −11.69]	
J Shi 2013	149.3	92.5	20	204.5	69.8	20	2.0	−55.20 [−105.99, −4.41]	
JH Zhang 2014	105.4	23.5	23	136.2	26.3	23	3.1	−30.80 [−45.21, −16.39]	
L Xiao 2013	110.4	33.5	54	153.3	44.7	54	3.1	−42.90 [−57.80, −28.00]	
LL Wu 2013	86.2	23.3	55	141.6	23.8	55	3.2	−55.40 [−64.20, −46.60]	
Q Yang 2015	85.3	20.1	50	100.3	52.4	50	3.1	−15.00 [−30.56, 0.56]	
RF Zhang 2014	98.97	50.42	57	130.12	49.89	55	3.0	−31.15 [−49.73, −12.57]	
RQ Fan 2013	95.6	47.6	38	203.7	73.4	35	2.7	−108.10 [−136.74, −79.46]	
SQ Pang 2013	88.5	28.7	50	128	22.9	50	3.2	−39.50 [−49.68, −29.32]	
W Guo 2010	137.4	68.4	43	174.8	72.6	42	2.7	−37.40 [−67.40, −7.40]	
XL Zhang 2016	101.7	30.1	63	182.2	87.7	71	2.9	−80.50 [−102.21, −58.79]	
XP Pan 2016	95.6	28.5	50	187.5	37	50	3.1	−91.90 [−104.85, −78.95]	
XQ Chen 2016	116.54	36.77	68	133.57	26.6	68	3.2	−17.03 [−27.82, −6.24]	
Y Zuo 2015	181.4	51.8	43	285	17.6	43	3.1	−103.60 [−119.95, −87.25]	
YH Gong 2010	106	30.2	28	196.6	38.2	24	3.0	−90.60 [−109.54, −71.66]	
YH Zeng 2013	145.4	86.5	30	249.3	116.5	30	2.0	−103.90 [−155.82, −51.98]	
YJ Qiu 2017	77.5	52.1	64	221.9	50.15	64	3.0	−144.40 [−162.12, −126.68]	
YL Fan 2009	107.4	39.79	28	133	46.4	26	2.9	−25.60 [−48.74, −2.46]	
YQ Zhao 2015	95.3	25.1	57	133.5	30.3	55	3.2	−38.20 [−48.52, −27.88]	
YY Sun 2017	190.25	13.12	38	198.13	14.15	38	3.2	−7.88 [−14.02, −1.74]	
YZ Song 2012	126.2	47.7	36	172.7	65.4	32	2.8	−46.50 [−74.00, −19.00]	
ZF Shangguan 2013	98.7	28.8	41	160.9	60.8	40	2.9	−62.20 [−83.00, −41.40]	
ZG Wu 2017	67.8	42.7	45	99.4	46.7	47	3.0	−31.60 [−49.87, −13.33]	
ZG Zhang 2012	91.3	43.5	43	187.5	56.3	43	2.9	−96.20 [−117.47, −74.93]	
ZH Hu 2016	94.2	30.28	43	185.38	40.05	43	3.1	−91.18 [−106.19, −76.17]	
ZJ Huang 2016	75.3	9.1	68	146.5	34.3	66	3.2	−71.20 [−79.75, −62.65]	
Total (95% CI)			*1599*			*1590*	*100.0*	*−57.15 [−69.06, −45.25]*	

Heterogeneity: tau^2 = 1138.98; chi^2 = 740.96, df = 33 (P < 0.00001); I^2 = 96%

Test for overall effect: Z = 9.41 (P < 0.00001)

−100 −50 0 50 100

Favours (control) Favours (experimental)

(a)

Study or subgroup	Experimental			Control			Weight	Mean difference	Mean difference
	Mean	SD	Total	Mean	SD	Total	(%)	IV, random, 95% CI	IV, random, 95% CI
C Xie 2016	27.86	10	43	32.58	4.88	43	3.4	−4.72 [−8.05, −1.39]	
CR Shen 2010	68.35	18.32	46	114.16	40.18	50	3.2	−45.81 [−58.14, −33.48]	
DJ Chen 2017	165.8	58.7	36	113.6	30.1	36	2.8	52.20 [30.65, 73.75]	
F Zhang 2017	130.7	36.4	35	160.3	41.3	35	2.9	−29.60 [−47.84, −11.36]	
FL Long 2011	102.5	26.6	57	122.9	23.6	59	3.3	−20.40 [−29.56, −11.24]	
GQ Chen 2016	95.53	27.65	45	149.17	39.23	45	3.1	−53.64 [−67.66, −39.62]	
HD Qi 2008	107.1	21.7	30	126.8	24.8	28	3.2	−19.70 [−31.73, −7.67]	
HS Xie 2016	79.8	62.5	65	95.3	78.4	63	2.6	−15.50 [−40.11, 9.11]	
HT Zhang 2015	125.4	72.2	100	155.2	77.6	100	2.8	−29.80 [−50.57, −9.03]	
J Shi 2013	131.8	64.37	20	119.21	55.62	20	2.0	12.59 [−24.69, 49.87]	
JH Zhang 2014	126.3	24.8	23	167.3	27.3	23	3.1	−41.00 [−56.07, −25.93]	
L Xiao 2013	90.7	28.3	54	113.5	30.2	54	3.2	−22.80 [−33.84, −11.76]	
LL Wu 2013	76.5	18.4	55	127.2	36.4	55	3.2	−50.70 [−61.48, −39.92]	
Q Yang 2015	100.5	25	50	256.3	55.6	50	3.0	−155.80 [−172.70, −138.90]	
RF Zhang 2014	132.48	101.83	57	178.8	99.5	55	2.0	−46.32 [−83.61, −9.03]	
RQ Fan 2013	87.5	33.2	38	151.4	68.3	35	2.6	−63.90 [−88.87, −38.93]	
SQ Pang 2013	92.1	35.3	50	100.2	25.1	50	3.2	−8.10 [−20.11, 3.91]	
W Guo 2010	139.1	85.4	43	164.3	93.8	42	2.0	−25.20 [−63.36, 12.96]	
XL Zhang 2016	147.4	41.1	63	183.5	56.4	71	3.0	−36.10 [−52.69, −19.51]	
XP Pan 2016	85.3	21.5	50	135.6	29.6	50	3.2	−50.30 [−60.44, −40.16]	
XQ Chen 2016	64.23	11.63	68	82.61	14.37	68	3.4	−18.38 [−22.77, −13.99]	
Y Zuo 2015	125	34.9	43	185	45.2	43	3.0	−60.00 [−77.07, −42.93]	
YH Gong 2010	123.3	61.5	28	228.3	51.3	24	2.3	−105.00 [−135.66, −74.34]	
YH Zeng 2013	135.6	78.6	30	182.3	72.5	30	2.0	−46.70 [−84.96, −8.44]	
YJ Qiu 2017	66.2	18.5	64	109.9	23.4	64	3.3	−43.70 [−51.01, −36.39]	
YL Fan 2009	130.93	51.08	28	169.03	58.72	26	2.4	−38.10 [−67.55, −8.65]	
YQ Zhao 2015	56.4	9.5	57	82.6	15.6	55	3.4	−26.20 [−31.00, −21.40]	
YY Sun 2017	73.34	5.67	38	70.15	5.12	38	3.4	3.19 [0.76, 5.62]	
YZ Song 2012	96.4	33.1	36	122.5	35.2	32	3.0	−26.10 [−42.40, −9.80]	
ZF Shangguan 2013	78.4	26.3	41	126.6	46.3	40	3.0	−48.20 [−64.65, −31.75]	
ZG Wu 2017	103.1	20.2	45	132.7	23.8	47	3.3	−29.60 [−38.61, −20.59]	
ZG Zhang 2012	102.3	30.9	43	142.8	41.6	43	3.1	−40.50 [−55.99, −25.01]	
ZH Hu 2016	84.79	20.82	43	132.47	28.26	43	3.2	−47.68 [−58.17, −37.19]	
ZJ Huang 2016	80.4	9.5	68	103.6	15.6	66	3.4	−23.20 [−27.59, −18.81]	
Total (95% CI)			*1592*			*1583*	*100.0*	*−35.04 [−43.32, −26.76]*	

Heterogeneity: tau^2 = 522.45; chi^2 = 978.92, df = 33 (P < 0.00001); I^2 = 97%

Test for overall effect: Z = 8.30 (P < 0.00001)

−100 −50 0 50 100

Favours (control) Favours (experimental)

(b)

Study or subgroup	Experimental Mean	SD	Total	Control Mean	SD	Total	Weight (%)	Mean difference IV, random, 95% CI
C Xie 2016	20.76	7	50	28.69	5.7	50	8.8	−7.93 [−10.43, −5.43]
CR Shen 2010	188.08	58.55	46	250.12	55.23	50	1.0	−62.04 [−84.86, −39.22]
DJ Chen 2017	122.8	31.3	36	145.7	33.8	36	2.0	−22.90 [−37.95, −7.85]
F Zhang 2017	96.8	27.8	35	160.1	39.7	35	1.8	−63.30 [−79.36, −47.24]
FL Long 2011	92.8	10	57	126.5	53.3	59	2.2	−33.70 [−47.55, −19.85]
GQ Chen 2016	186.1	47.53	45	159.12	49.14	45	1.2	26.98 [7.01, 46.95]
HD Qi 2008	111.2	33.3	30	149.5	50.1	28	1.0	−38.30 [−60.35, −16.25]
HS Xie 2016	86.4	78.7	65	115.3	90.6	63	0.6	−28.90 [−58.34, 0.54]
HT Zhang 2015	0.6	0.3	100	1	0.6	100	9.8	−0.40 [−0.53, −0.27]
J Shi 2013	44.41	11.56	20	58.7	15.36	20	4.4	−14.29 [−22.72, −5.86]
JH Zhang 2014	102.1	24.2	23	139.1	28.3	23	1.9	−37.00 [−52.22, −21.78]
L Xiao 2013	122.7	31.4	54	145.6	33.9	54	2.7	−22.90 [−35.22, −10.58]
LL Wu 2013	72.3	41.2	55	241.2	69.2	55	1.1	−168.90 [−190.18, −147.62]
Q Yang 2015	103.4	20.1	50	200.8	35.6	50	3.0	−97.40 [−108.73, −86.07]
RF Zhang 2014	117.96	26.02	57	131.98	28.03	55	3.5	−13.97 [−24.00, −3.94]
RQ Fan 2013	83.2	41.8	38	167.6	81.4	35	0.6	−84.40 [−114.46, −54.34]
SQ Pang 2013	88.7	26.9	50	108.3	22.9	50	3.7	−19.60 [−29.39, −9.81]
W Guo 2010	78.3	56.8	43	92.4	52.96	42	0.9	−14.10 [−37.44, 9.24]
XL Zhang 2016	32.3	12.7	63	89.1	19.2	71	6.4	−56.80 [−62.26, −51.34]
XP Pan 2016	80.5	18.7	50	130.5	35.3	50	3.1	−50.00 [−61.07, −38.93]
XQ Chen 2016	101.45	18.66	68	122.57	26.39	68	4.8	−21.12 [−28.80, −13.44]
Y Zuo 2015	94.3	42	43	178	51.8	43	1.2	−83.70 [−103.63, −63.77]
YH Gong 2010	103.2	40.5	28	151.8	52.6	24	0.8	−48.60 [−74.44, −22.76]
YH Zeng 2013	91.6	50.1	30	156.7	52.8	30	0.8	−65.10 [−91.15, −39.05]
YJ Qiu 2017	99.8	31.9	64	158.9	50.1	64	2.1	−59.10 [−73.65, −44.55]
YL Fan 2009	104.37	22.17	28	140.17	23.21	26	2.7	−35.80 [−47.93, −23.67]
YQ Zhao 2015	99.5	17.4	57	117.2	3.1	55	7.2	−17.70 [−22.29, −13.11]
YY Sun 2017	8.2	0.61	38	8.9	0.27	38	9.8	−0.70 [−0.91, −0.49]
YZ Song 2012	99.5	28.8	36	115.7	30.8	32	2.2	−16.20 [−30.43, −1.97]
ZF Shangguan 2013	70.3	50.8	41	240.6	77.6	40	0.6	−170.30 [−198.94, −141.66]
ZG Wu 2017	73.6	62.3	45	102.5	65.9	47	0.8	−28.90 [−55.10, −2.70]
ZG Zhang 2012	122.4	61.3	43	242.5	70.8	43	0.7	−120.10 [−148.09, −92.11]
ZH Hu 2016	79.15	19.35	43	125.4	38.14	43	2.5	−46.25 [−59.03, −33.47]
ZJ Huang 2016	89.5	18.4	68	127.2	31.4	66	4.2	−37.70 [−46.45, −28.95]
Total (95% CI)			*1599*			*1590*	*100.0*	*−29.32 [−31.68, −26.96]*

Heterogeneity: tau^2 = 14.80; chi^2 = 1894.00, df = 33 (P < 0.00001); I^2 = 98%
Test for overall effect: Z = 24.34 (P < 0.00001)

Mean difference IV, random, 95% CI
−100 −50 0 50 100
Favours (control) Favours (experimental)

(c)

Study or subgroup	Experimental Mean	SD	Total	Control Mean	SD	Total	Weight (%)	Mean difference IV, random, 95% CI
C Xie 2016	21.33	7	50	24.96	8.76	50	3.1	−3.63 [−6.74, −0.52]
CR Shen 2010	94.55	21.25	46	155.45	40.18	50	3.0	−60.90 [−73.62, −48.18]
DJ Chen 2017	97.3	35.7	36	123.7	40.5	36	2.8	−26.40 [−44.04, −8.76]
F Zhang 2017	72.6	20.6	35	98.8	25.7	35	3.0	−26.20 [−37.11, −15.29]
FL Long 2011	72.5	10.7	57	80.2	11.3	59	3.1	−7.70 [−11.70, −3.70]
GQ Chen 2016	95.43	23.32	45	160.5	38.22	45	3.0	−65.07 [−78.15, −51.99]
HD Qi 2008	78.1	17.2	30	89.3	16.9	28	3.1	−11.20 [−19.98, −2.42]
HS Xie 2016	85.4	40.7	65	103.4	52.7	63	2.9	−18.00 [−34.35, −1.65]
HT Zhang 2015	90.6	79.1	100	134.2	67.7	100	2.7	−43.60 [−64.01, −23.19]
J Shi 2013	74.28	21.69	20	86.54	19.58	20	3.0	−12.26 [−25.07, 0.55]
JH Zhang 2014	46.9	12.9	23	78.8	18.3	23	3.0	−31.90 [−41.05, −22.75]
L Xiao 2013	97.2	35.8	54	123.6	40.6	54	2.9	−26.40 [−40.84, −11.96]
LL Wu 2013	62.3	15.6	55	140.5	46.8	55	3.0	−78.20 [−91.24, −65.16]
Q Yang 2015	85.6	36.4	50	258.7	22.6	50	3.0	−173.10 [−184.98, −161.22]
RF Zhang 2014	172.4	58.16	57	218.13	75.32	55	2.6	−45.73 [−70.71, −20.75]
RQ Fan 2013	76.5	21.4	38	104.6	37.8	35	2.9	−28.10 [−42.35, −13.85]
SQ Pang 2013	66.3	21.2	50	116.8	34.49	50	3.0	−50.50 [−61.72, −39.28]
W Guo 2010	72.8	33.2	43	91.7	38.7	42	2.9	−18.90 [−34.24, −3.56]
XL Zhang 2016	38.9	9.4	63	74.9	31.3	71	3.1	−36.00 [−43.64, −28.36]
XP Pan 2016	72.7	22.6	50	88.5	20.4	50	3.1	−15.80 [−24.24, −7.36]
XQ Chen 2016	73.65	10.02	68	106.22	17.39	68	3.1	−32.57 [−37.34, −27.80]
Y Zuo 2015	89	31.2	43	156	44.9	43	2.9	−67.00 [−83.34, −50.66]
YH Gong 2010	86.1	23.2	28	145.5	26.3	24	2.9	−59.40 [−72.99, −45.81]
YH Zeng 2013	69.4	12.5	30	105.2	81.2	30	2.4	−35.80 [−65.20, −6.40]
YJ Qiu 2017	70.1	22.1	64	89.9	23.1	64	3.1	−19.80 [−27.63, −11.97]
YL Fan 2009	47.97	33.3	28	73.53	32.03	26	2.8	−25.56 [−42.99, −8.13]
YQ Zhao 2015	90.1	16.5	57	132.6	25.7	55	3.1	−42.50 [−50.53, −34.47]
YY Sun 2017	115.32	10.11	38	122.15	11.56	38	3.1	−6.83 [−11.71, −1.95]
YZ Song 2012	92.3	30.9	36	128.1	39.7	32	2.8	−35.80 [−52.86, −18.74]
ZF Shangguan 2013	60.8	30.6	41	140.2	50.3	40	2.8	−79.40 [−97.59, −61.21]
ZG Wu 2017	78.2	26.2	45	108.7	35.9	47	3.0	−30.50 [−43.30, −17.70]
ZG Zhang 2012	104.9	31.9	43	170.4	51.7	43	2.8	−65.50 [−83.66, −47.34]
ZH Hu 2016	74.1	20.28	43	97.39	22.46	43	3.0	−23.29 [−32.33, −14.25]
ZJ Huang 2016	90.4	23.5	68	122.6	18.7	66	3.1	−32.20 [−39.38, −25.02]
Total (95% CI)			*1599*			*1590*	*100.0*	*−38.98 [−48.32, −29.64]*

Heterogeneity: tau^2 = 723.28; chi^2 = 1225.36, df = 33 (P < 0.00001); I^2 = 97%
Test for overall effect: Z = 8.18 (P < 0.00001)

Mean difference IV, random, 95% CI
−100 −50 0 50 100
Favours (control) Favours (experimental)

(d)

Figure 2: (a) The HA of TCM plus entecavir versus entecavir. (b) The LN of TCM plus entecavir versus entecavir. (c) The PCIII of TCM plus entecavir versus entecavir. (d) The IV-C of TCM plus entecavir versus entecavir. I^2 and P are the criterion for the heterogeneity test, ◆ pooled odds ratio, —■— odds ratio, and 95% CI.

Table 1: The table of sensitivity analysis, bias test, and meta-regression.

Outcome	Fixed model	Random model	Begg test (P)	Egger test (P)	Meta-regression (P)
HA	MD = −48.59, 95% CI: −51.00–46.18	MD = 57.15, 95% CI: −69.06–45.25	0.882	0.878	0.610; 0.007
LN	MD = −18.37, 95% CI: −19.69–17.00	MD = −35.04, 95% CI: −43.32–26.78	0.534	0.565	0.341; 0.033
PCIII	MD = −31.17, 95% CI: −33.68–28.68	MD = −29.32, 95% CI: −31.68–26.96	0.767	0.902	0.902; 0.071
IV-C	MD = −23.46, 95% CI: −24.91–22.00	MD = −38.98, 95% CI: −48.32–29.64	0.813	0.665	0.627; 0.303
AST	MD = −10.82, 95% CI: −12.10–9.55	MD = −9.92, 95% CI: −13.40–6.44	0.415	0.877	0.987; 0.866
ALT	MD = −15.69, 95% CI: −16.94–14.45	MD = −13.33, 95% CI: −16.99–9.68	0.608	0.153	0.496; 0.570
HBV-DNA	OR = 1.27, 95% CI: 0.92–1.76	OR = 1.33, 95% CI: 0.86–2.07	0.012	0.017	0.010; 0.722

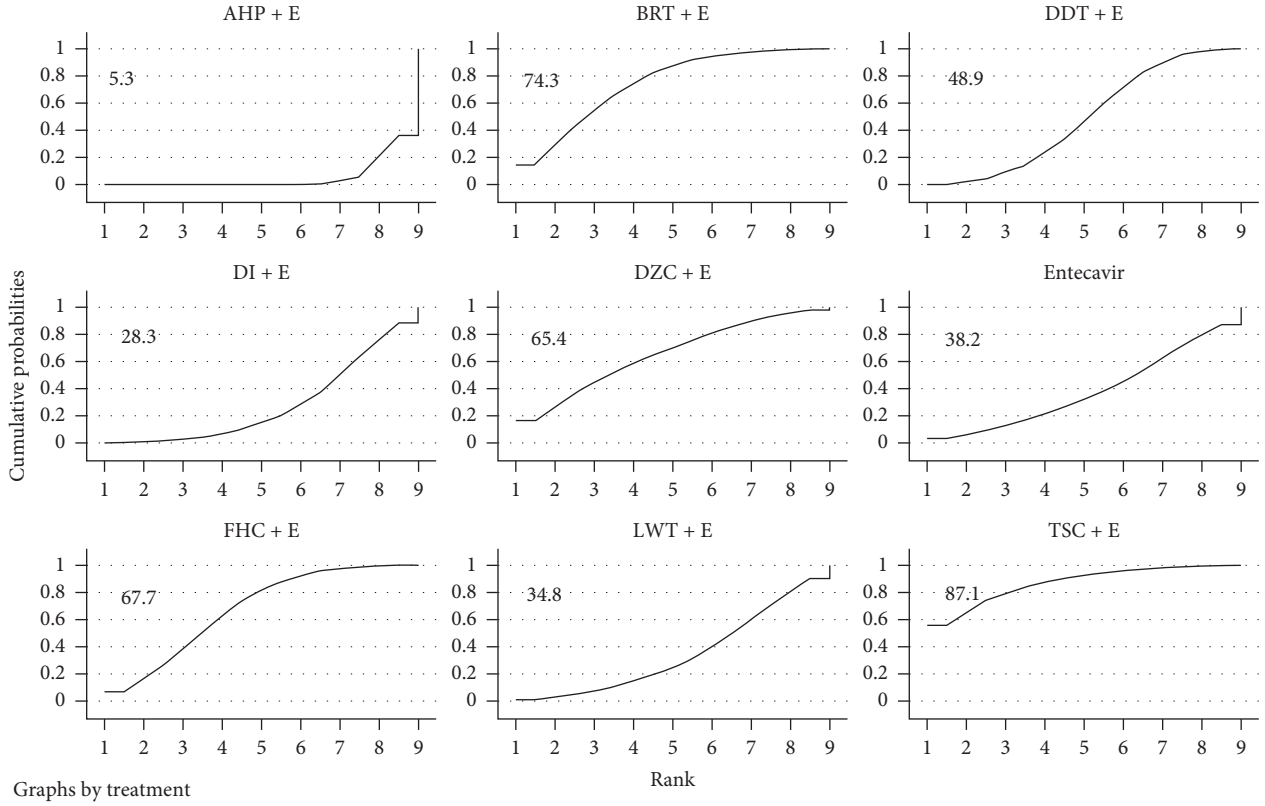

(a)

Figure 3: Continued.

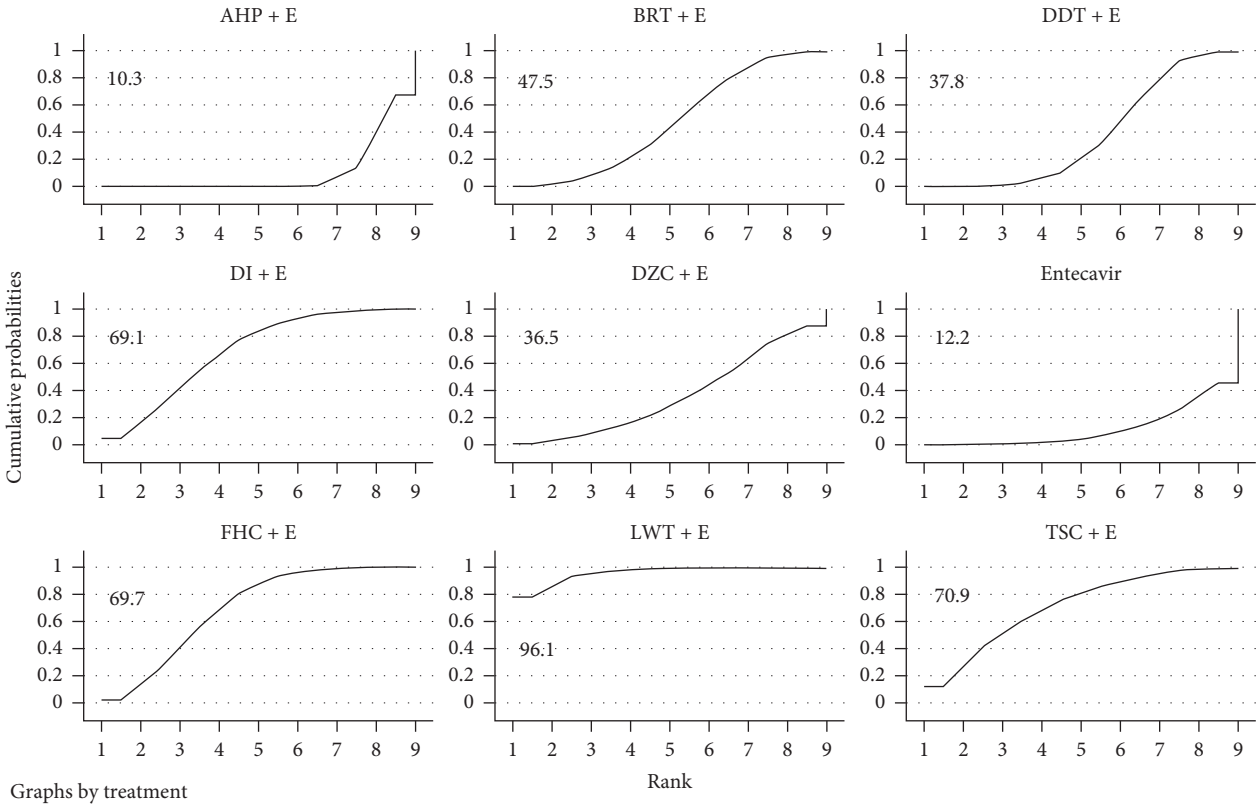

(b)

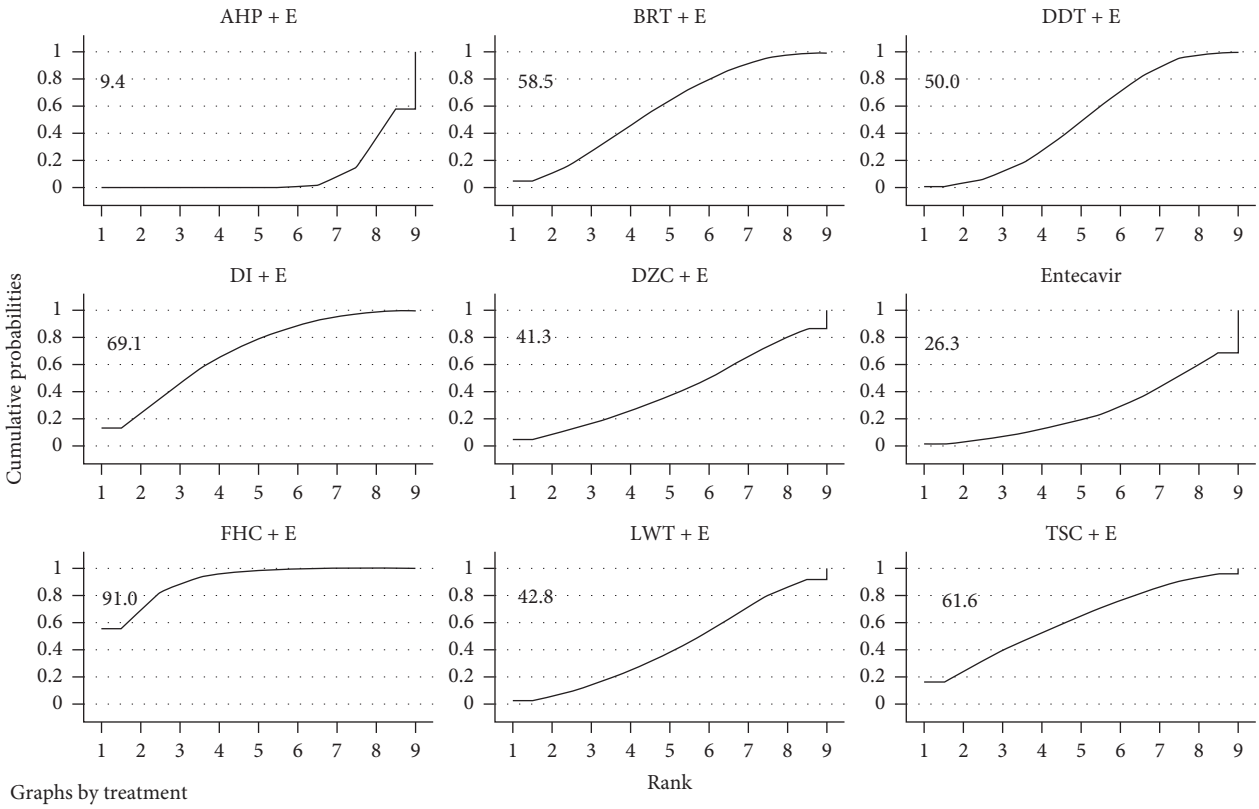

(c)

Figure 3: Continued.

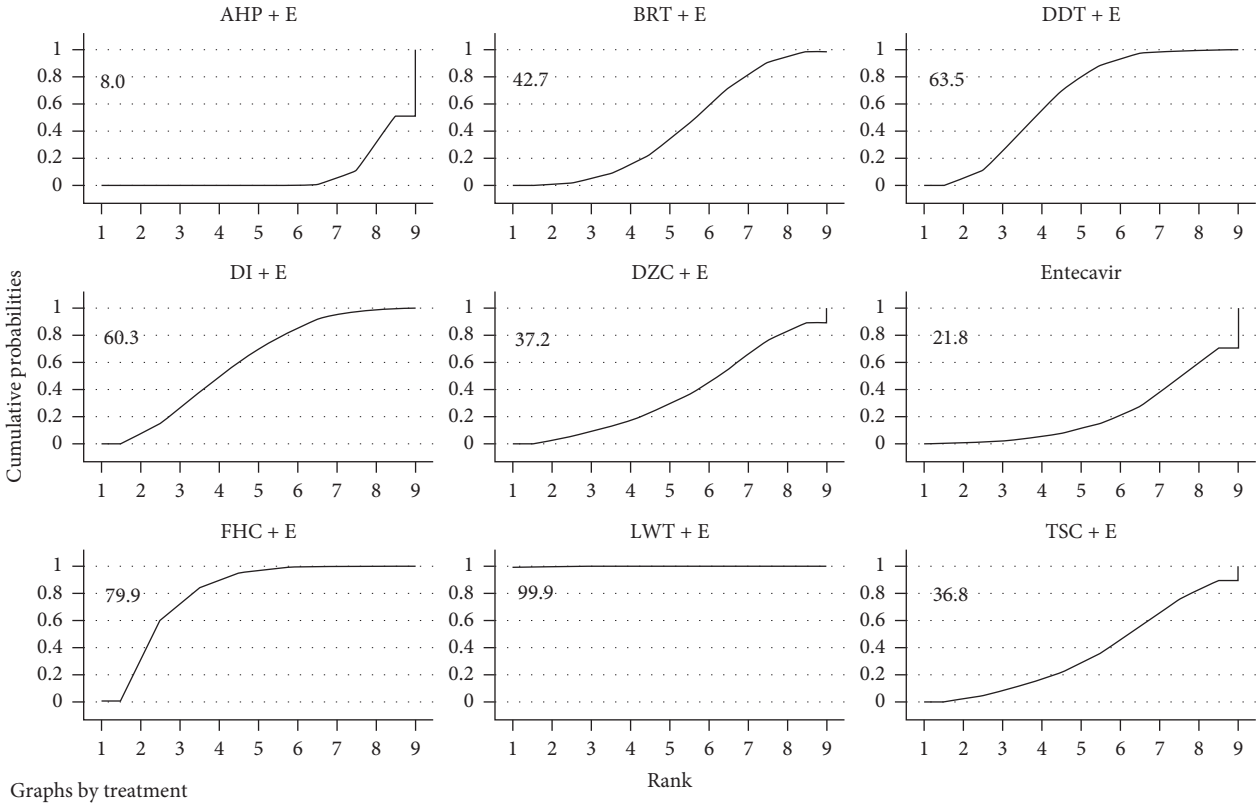

(d)

Figure 3: (a) Ranking for efficacy of HA; (b) ranking for efficacy of LN; (c) ranking for efficacy of PCIII; (d) ranking for efficacy of IV-C.

Study or subgroup	Experimental Events	Experimental Total	Control Events	Control Total	Weight (%)	Odds ratio M-H, fixed, 95% CI
F Zhang 2017	33	35	31	35	2.7	2.13 [0.36, 12.46]
GQ Chen 2016	29	45	26	45	14.1	1.32 [0.57, 3.10]
HD Qi 2008	28	30	25	28	2.6	1.68 [0.26, 10.89]
JH Zhang 2014	22	23	15	23	1.0	11.73 [1.33, 103.80]
RF Zhang 2014	50	57	47	55	9.0	1.22 [0.41, 3.62]
RQ Fan 2013	35	38	32	35	4.0	1.09 [0.21, 5.81]
XP Pan 2016	45	50	44	50	6.7	1.23 [0.35, 4.32]
YC Xie 2016	37	50	34	50	13.5	1.34 [0.56, 3.19]
YL Fan 2009	28	30	26	30	2.6	2.15 [0.36, 12.76]
YY Sun 2017	8	38	1	38	1.2	9.87 [1.17, 83.35]
ZG Wu 2017	37	45	38	47	10.1	1.10 [0.38, 3.14]
ZH Hu 2016	40	43	38	43	4.1	1.75 [0.39, 7.85]
ZJ Huang 2016	45	66	59	68	28.3	0.33 [0.14, 0.78]
Total (95% CI)		*550*		*547*	*100.0*	*1.27 [0.92, 1.76]*
Total events	437		416			

Heterogeneity: chi^2 = 17.93, df = 12 (P = 0.12); I^2 = 33%
Test for overall effect: Z = 1.46 (P = 0.14)

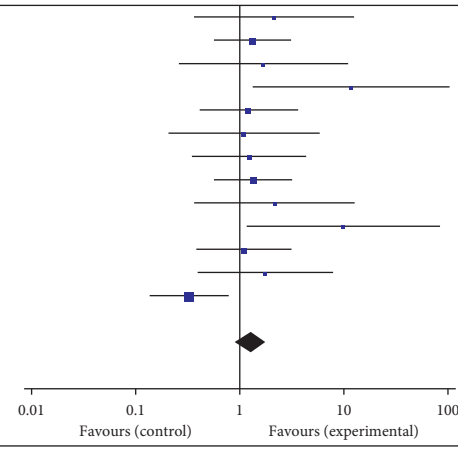

(a)

Figure 4: Continued.

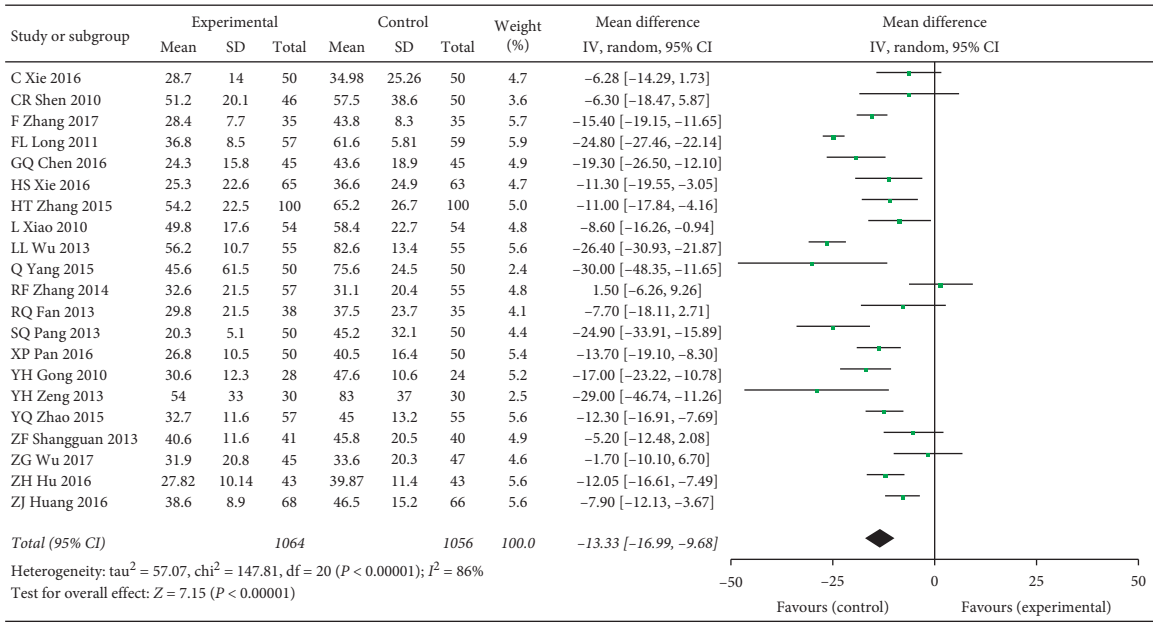

(b)

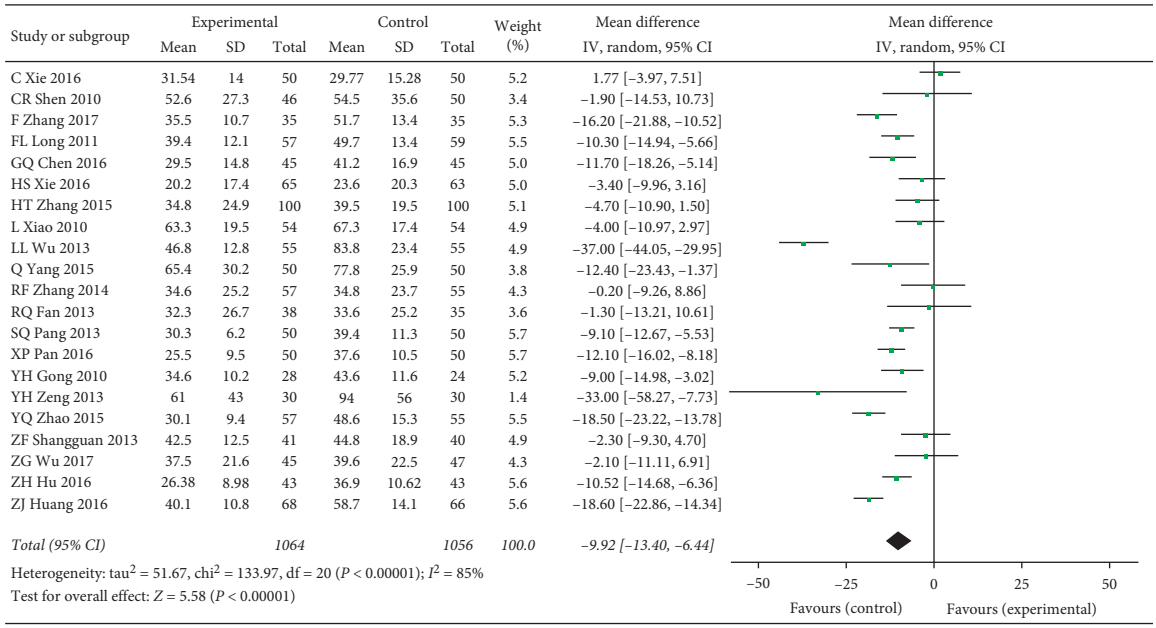

(c)

Figure 4: (a) The HBV-DNA negative conversion rate of TCM plus entecavir versus entecavir. (b) The ALT of TCM plus entecavir versus entecavir. (c) The AST of TCM plus entecavir versus entecavir. I^2 and P are the criterion for the heterogeneity test, ◆ pooled odds ratio, —■— odds ratio, and 95% CI.

publication bias in liver function indicators. We then compared and ranked all of the treatment strategies (Supplementary Tables 6 and 7, Figure 5) and obtained the average ranking of the various treatment strategies. We found that BRT (1), LWT (2.5), DZC (3.5), and FHC (4) were more effective as adjuvant drugs in improving liver function, but AHP (8) achieved the worst results.

3.1.4. Safety Assessment. A total of nine studies reported adverse events. These adverse reactions are mainly gastrointestinal discomfort such as nausea, vomiting, mild diarrhea, and loss of appetite; occasional allergies; and dizziness. However, none of the above symptoms were serious and disappeared after drug withdrawal. No related treatment was performed. Compared with the control group, the use of

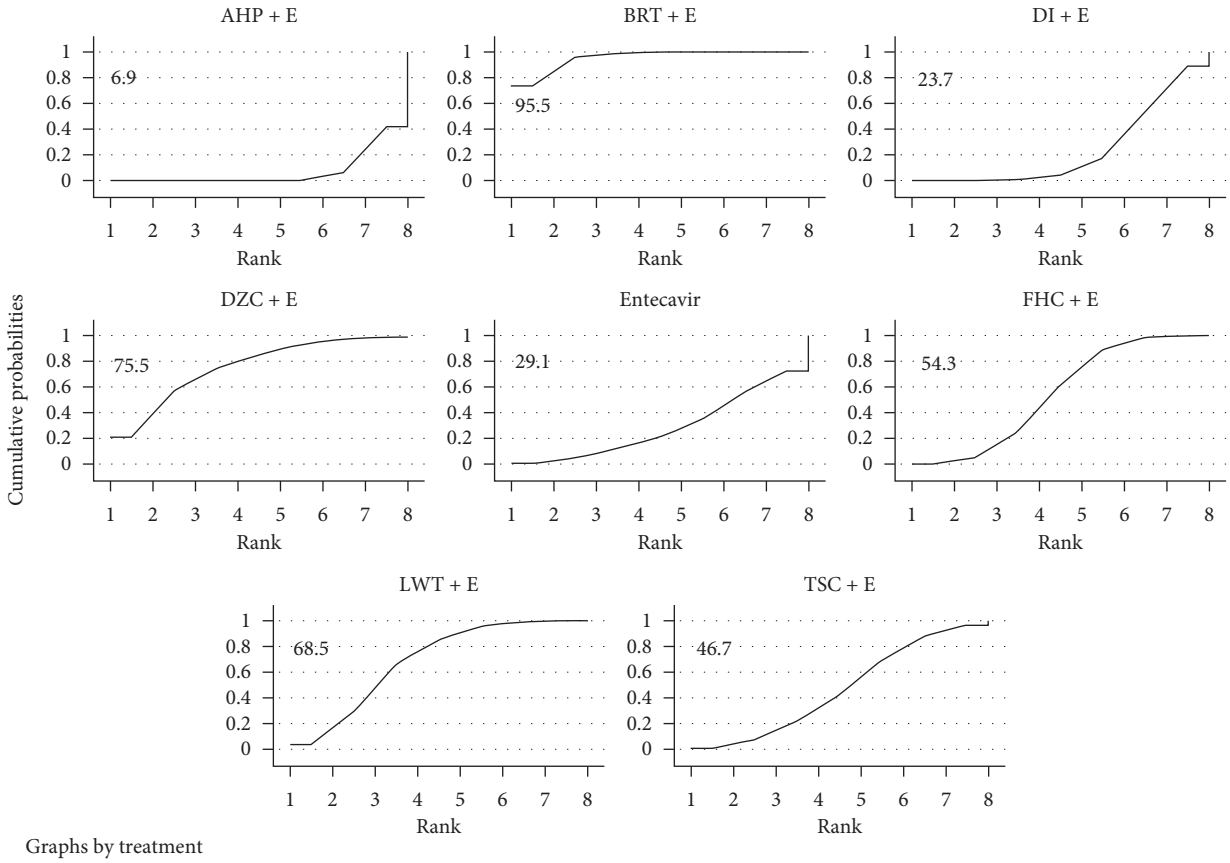

(a)

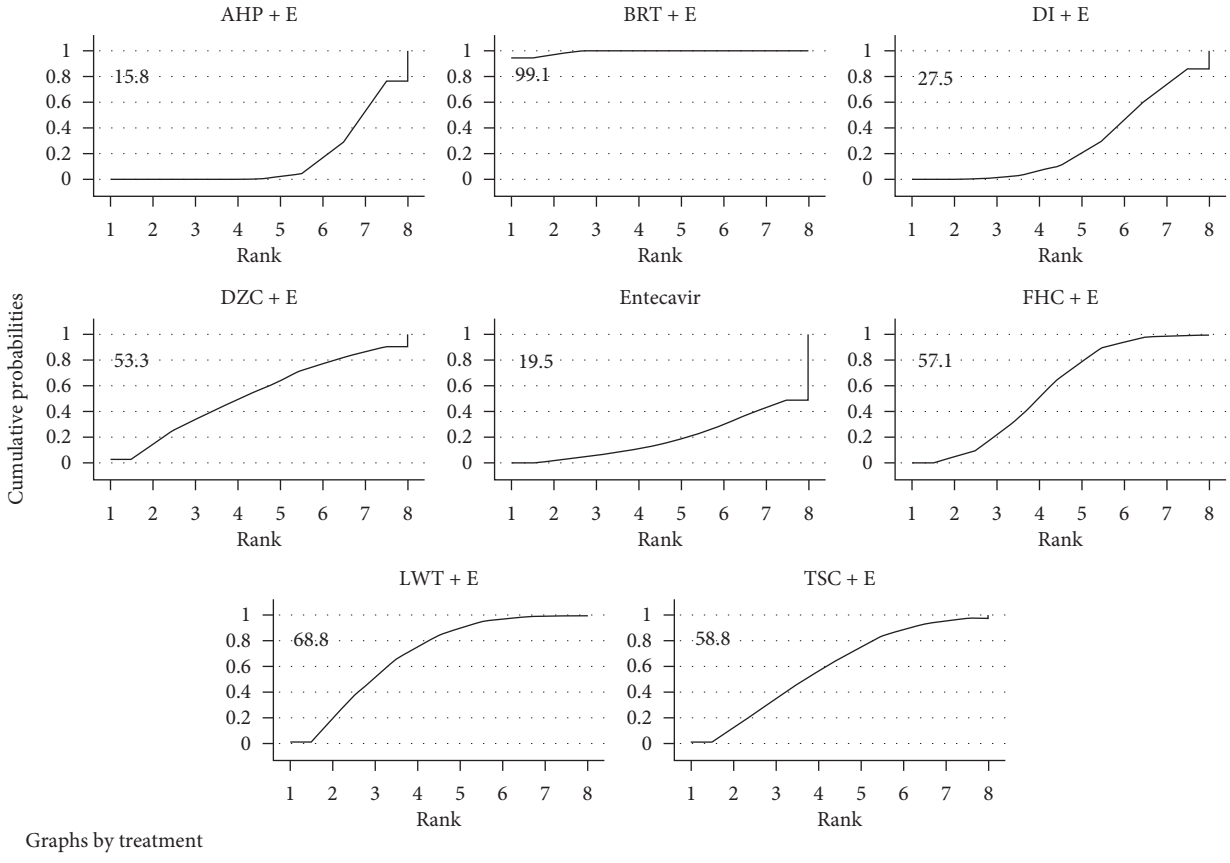

(b)

Figure 5: (a) Ranking for efficacy of ALT; (b) ranking for efficacy of AST.

TCM did not have a significant impact on the incidence of adverse events. This shows that entecavir combined with TCM is safe in clinical use. In addition, details of the adverse events reported by the nine institutes are listed in the annex (Supplementary Table 8).

3.2. Discussion. Liver fibrosis caused by hepatitis B hepatitis is a reversible wound repair response characterized by the accumulation of extracellular matrix, which is the formation of scar tissue, which occurs after chronic or non-self-limiting liver disease, and it will eventually lead to cirrhosis. [45] In the world, the first-line drugs currently used are nucleoside (acid) analogues and interferon drugs, and their treatment cycles are generally long. In recent years, more and more research studies have found that TCM contains multiple active ingredients that can relieve or even reverse hepatitis B liver fibrosis. For example, *Salvia miltiorrhiza* and *Cordyceps sinensis*, they all have a variety of antifibrotic components, and in clinical use, there are many examples of using them to treat chronic hepatitis B liver fibrosis [46–48]. Rui's research further pointed out the pharmacological mechanisms of *Salvia miltiorrhiza* against liver fibrosis. The results of the study showed that *Salvia miltiorrhiza* water extract can inhibit the expression of GST-P and α-SMA during the process of hepatic fibrosis, and the alanine transaminase, aspartate aminotransferase, γ-glutamyltransferase, alkaline phosphatase, hyaluronic acid, direct bilirubin, and total bilirubin were significantly inhibited [49]. In addition, Peng et al. found that the main active components of *Cordyceps sinensis* against liver fibrosis are cordyceps polysaccharide, cordycepic acid, cordycepin, and ergosterol [50]. All these indicate that TCM is likely to play its unique role in the treatment of chronic hepatitis B liver fibrosis. Moreover, in long-term clinical practice, Chinese physicians have used and summarized many effective TCMs which are often combined with the current first-line drugs for the treatment of chronic hepatitis B liver fibrosis, and they were included in the Chinese Pharmacopoeia.

In this NMA, we found that 8 kinds of TCM as adjuvant medicines can improve liver fibrosis in patients with chronic hepatitis B liver fibrosis. The combination of FHC and entecavir is the best therapeutic strategy. It not only has a significant effect in improving the state of liver fibrosis in patients but also has a good effect in the improvement of liver function in patients. FZHY capsule is a commonly used TCM formula against liver fibrosis in clinic. It has been verified in research to exert antifibrosis effect through several mechanisms such as antilipid peroxidation and endothelial injury, inhibiting hepatic stellate cell activation, promoting matrix metalloproteinase activity, and degradation of pathological deposition of collagen. [51] In addition, there is an article using transcriptional profiling and miRNA-target network analysis to identify potential biomarkers for efficacy evaluation of FZHY formula-treated hepatitis B caused liver cirrhosis. [52] The use of AHP as an adjuvant drug in this study has shown a weaker effect and is lower than the single use of entecavir in the ranking, which is a very surprising result. In addition, the comprehensive evaluation results showed that the addition of TCM did not appear to have a significant impact on the improvement of HBV-DNA negative conversion rates, but when the therapeutic strategies were compared individually, some of the therapeutic strategies showed a significant improvement in the negative conversion rates, which is worth in-depth explore the phenomenon. First, we considered whether the results of this study were affected by publication bias. For this purpose, we conducted relevant statistical tests and scissors funnel plot to determine whether there was publication bias. However, the results showed that there were no significant publication biases other than HBV-DNA negative conversion rates in the seven outcomes of this study. The inconsistency in our study of HBV-DNA negative conversion rates is likely due to publication bias in this outcome measure. Therefore, this has also weakened the strength of the evidence in this NMA, which in judging whether the combined use of Chinese and Western medicine can enhance the improvement of HBV-DNA negative conversion rates. Subsequently, in order to evaluate the stability of the results of this network meta-analysis, we performed a dual modeling analysis of the fixed-effects model and the random-effects model for all indicators in turn. As a result, it was found that only the LN and IV-C outcomes were slightly unstable in all indicators, and there was no contradictory research result, and the remaining outcomes all had good stability. This NMA includes many documents, there are differences in the size of the sample and there are many types of treatment strategies, so in the process of research, we also pay attention to the heterogeneity between the studies. We not only used literature analysis methods to explore the sources of heterogeneity but also used meta-regression analysis to conduct relevant research. As mentioned earlier, in evidence-based medicine research, there are often small sample sizes of studies, and these small sample studies often show relatively unstable results. Therefore, we first examine whether it caused the heterogeneity between studies by using the sample size as a variable. It was found that when we used the sample size as a variable for regression analysis, the Tau2 of HBV-DNA negative conversion rates was 0, so the difference in sample size was the source of the heterogeneity of the outcome. Therefore, this also reduces our ability to demonstrate whether TCM as an auxiliary drug can increase the HBV-DNA negative conversion rates in another aspect. However, it is worth noting that the heterogeneity of the remaining indicators does not originate from the sample size. Subsequently, we considered whether the heterogeneity between studies was caused by the large number of treatment decisions, and the results were as we suspected. Meta-regression analysis showed that this factor actually contributed 71.64% and 80.32% of the heterogeneity of HA and LN. In addition, the gender ratio of patients in this study is balanced, but the age difference among patients in some studies is likely to be one of the reasons for heterogeneity. However, because some studies did not provide detailed reports on the age of patients, we did not consider this factor as a variable for meta-regression analysis. In terms of drug safety, there was no serious adverse reaction after the use of TCM combined with entecavir, and the combined use of drugs did

not increase the risk of adverse events. Therefore, the use of 8 kinds of TCM combined with entecavir is safe.

Although there are slight instability and bias in the results of this study and there are limitations in the quality of RCTs, these have reduced the strength of the NMA. However, overall, this NMA still provides clinicians with detailed comparisons of common therapeutic strategies and provides reference for clinical use. In addition, in the future, large-scale, high-quality RCTs should be conducted to further provide evidence that FHC has efficacy and safety as adjuvant drugs for the treatment of hepatitis B and liver fibrosis in clinical applications.

4. Conclusions

The NMA showed that compared with entecavir, combined TCM did not increase the risk of adverse reactions and could significantly improve the effect of chronic hepatitis B liver fibrosis. In addition, in a variety of therapeutic strategies, the combination of FHC and entecavir is the best therapeutic strategy. However, TCM as a complementary drug has not shown significant advantages in improving the HBV-DNA negative conversion rates. Finally, due to the low quality of the included studies, the strength of the research results is limited. Therefore, strict RCTs are still needed in the future to further validate the effectiveness and safety of FHC as an adjuvant drug for the treatment of chronic hepatitis B liver fibrosis.

Data Availability

All the data in this study have been uploaded.

Conflicts of Interest

The authors declare that there are no conflicts of interest regarding the publication of this paper.

Authors' Contributions

Tao Wang and Wei Jin contributed equally to this work. Tao Wang, Yanling Zhao, and Haotian Li independently performed data extraction and quality assessment. Qianqian Huang and Huadan Cai formed a review team to independently verify the accuracy of data extraction, quality assessment, and all materials for this study. Tao Wang, Wei Jin, Yun Zhu, Honghong Liu, and Jiabo Wang are responsible for writing articles. Wenjun Zou, Yanling Zhao, Wei Jin, Ruilin Wang, and Xiaohe Xiao are responsible for the supervision and design of the entire study.

Acknowledgments

The current study was financially supported by the Project of Chinese Medicine Education Association (no. 2016SKT-Z003).

Supplementary Materials

See Figures S1–S8 in the Supplementary Material for comprehensive image analysis, and see Tables S1–S8 for the raw data of the index in this study. (*Supplementary Materials*)

References

[1] X. He, Y. Hong, X. Wang et al., "Identification and clinical significance of an elevated level of serum aminoacylase-1 autoantibody in patients with hepatitis B virus-related liver cirrhosis," *Molecular Medicine Reports*, vol. 14, no. 5, pp. 4255–4262, 2016.

[2] X. Luo, Y. Huang, Y. Chen et al., "Association of hepatitis B virus covalently closed circular DNA and human APOBEC3B in hepatitis B virus-related hepatocellular carcinoma," *PLoS One*, vol. 11, no. 6, Article ID e0157708, 2016.

[3] R. Lozano, M. Naghavi, K. Foreman et al., "Global and regional mortality from 235 causes of death for 20 age groups in 1990 and 2010: a systematic analysis for the global burden of disease study 2010," *Lancet (London, England)*, vol. 380, no. 9859, pp. 2095–2128, 2012.

[4] V. Calvaruso and A. Craxì, "Fibrosis in chronic viral hepatitis," *Best Practice & Research Clinical Gastroenterology*, vol. 25, no. 2, pp. 219–230, 2011.

[5] C. M. Lange, J. Bojunga, W. P. Hofmann et al., "Severe lactic acidosis during treatment of chronic hepatitis B with entecavir in patients with impaired liver function," *Hepatology*, vol. 50, no. 6, pp. 2001–2006, 2009.

[6] Z. L. Yang and P. L. Yuan, "Clinical efficacy of combined use of traditional Chinese and western medicine in patients with Hepatitis B cirrhosis," *Journal of Guangxi Medical University*, vol. 2, pp. 330–332, 2016.

[7] T. Wang, X. Zhou, H. Liu et al., "Fuzheng Huayu capsule as an adjuvant treatment for HBV-related cirrhosis: a systematic review and meta-analysis," *Phytotherapy Research*, vol. 32, no. 5, pp. 757–768, 2017.

[8] X. L. Duan, G. Y. Li, S. M. Li et al., "Meta-analysis of influences of Fufang Biejia Ruangan Pian combined with entecavir on serum liver fibrosis markers of chronic hepatitis B," *Chinese Journal of Hospital Pharmacy*, vol. 35, no. 19, pp. 1762–1765, 2015.

[9] Y. Zhou, H. Liu, J. Fang et al., "Meta-analysis of Liuwei wuling tablets combined with entecavir in the treatment of chronic hepatitis B," *China Pharmacy*, vol. 28, no. 36, 2017.

[10] Z. Wen, Z. Wang, J. Zheng et al., "Meta-analysis on entecavir combined with anluohuaxian pills in the treatment of hepatitis B-related cirrhosis," *Guangming Journal of Chinese Medicine*, vol. 31, no. 12, 2016.

[11] J. H. Zhang and X. F. Guo, "Clinical study of entecavir combined with Danshendi tablets for chronic hepatitis B liver fibrosis," *China Modern Medicine*, vol. 52, no. 20, pp. 49–51, 2014.

[12] Y. J. Qiu, "Analysis of efficacy of entecavir combined with Danshendi tablets in treatment of chronic hepatitis B liver fibrosis," *Chinese Journal of Histochemistry & Cytochemistry*, vol. 32, no. 16, p. 1, 2017.

[13] Y. Zou, "Clinical observation of entecavir combined with Danshendi tablets for chronic hepatitis B liver fibrosis," *Jilin Medical Journal*, vol. 36, no. 9, pp. 1748-1749, 2015.

[14] Y. L. Fan, Y. Yuan, and Z. C. Feng, "Clinical study of entecavir combined with Danshendi tablets for chronic hepatitis B liver

fibrosis," *China Modern Medicine*, vol. 16, no. 13, pp. 5-6, 2009.

[15] G. O. Chen, "Therapeutic effect of Liuwei wuling tablets combined with entecavir on chronic hepatitis B liver fibrosis," *The Journal of Medical Theory and Practice*, vol. 29, no. 5, pp. 629-630, 2016.

[16] Q. Yang, "Therapeutic effect of Liuwei Wuling tablet combined with entecavir on chronic hepatitis B liver fibrosis," *Contemporary Medicine Forum*, vol. 13, no. 20, pp. 173-174, 2015.

[17] Y. Q. Zhao, "Clinical efficacy of entecavir combined with Liuwei Wuling Tablets in treating chronic hepatitis B liver fibrosis," *Chinese Journal of Integrated Traditional and Western Medicine on Liver Diseases*, vol. 25, no. 6, pp. 364-365, 2015.

[18] C. R. Shen, J. C. Guo, X. L. Yu et al., "Observation of the curative effect of entecavir combined with compound Biejia ruangan tablet on chronic hepatitis B liver fibrosis," *Journal of Zhejiang Chinese Medical University*, vol. 34, no. 3, pp. 370-371, 2010.

[19] D. J. Chen, "Effect of entecavir combined with compound Biejia ruangan tablets on chronic hepatitis B liver fibrosis," *Chinese Healing Standard Management*, vol. 8, no. 28, pp. 111–113, 2017.

[20] H. T. Zhang, X. Y. Zhang, Z. Y. Me et al., "Clinical observation on chronic hepatitis B liver fibrosis treated by compound Biejia ruangan tablets combined with entecavir," *Chinese Journal of Coal Industry Medicine*, vol. 18, no. 7, pp. 1120–1122, 2015.

[21] L. Xiao, Y. Y. Yang, L. Xu et al., "Clinical efficacy of entecavir combined with compound Biejia Ruangan tablets in treating chronic hepatitis B liver fibrosis," *China Medicine and Pharmacy*, vol. 3, no. 14, pp. 59-60, 2013.

[22] R. F. Zhang, Y. J. Yao, Z. L. You et al., "Clinical observation on treatment of chronic hepatitis B liver fibrosis with fufang Biejia ruangan tablets combined with entecavir," *Journal of Third Military Medical University*, vol. 36, no. 18, pp. 1961–1963, 2014.

[23] X. L. Zhang, "Clinical effect of compound Biejia ruangan tablets combined with entecavir on chronic hepatitis B liver fibrosis," *China Metallurgical Industry Medical Journal*, vol. 33, no. 6, pp. 680-681, 2016.

[24] Y. Y. Sun and Z. X. Zhu, "Clinical efficacy of entecavir combined with compound Biejia Ruangan tablets in treating chronic hepatitis B liver fibrosis," *Journal of Clinical Rational Drug Use*, vol. 10, no. 33, pp. 67-68, 2017.

[25] Z. G. Wu, G. D. Zhou, Y. Y. Chen et al., "Clinical study on treatment of chronic hepatitis B liver fibrosis with compound Biejia ruangan tablets and entecavir," *Drug Evaluation Research*, vol. 40, no. 3, pp. 351–355, 2017.

[26] Z. G. Zhang, "Effect of entecavir combined with compound Biejia ruangan tablets on chronic hepatitis B liver fibrosis," *Guide of China Medicine*, vol. 10, no. 36, pp. 456–458, 2012.

[27] H. S. Xie, L. M. Cai, H. M. Yan et al., "Effect of entecavir combined with Fuzheng Huayu capsule on chronic hepatitis B liver fibrosis," *Zhejiang Medical Journal*, vol. 38, no. 8, pp. 555–557, 2016.

[28] L. L. Wu, "Effect of entecavir and Fuzheng Huayu capsules on hepatic fibrosis in patients with chronic hepatitis B," *Modern Journal of Integrated Traditional Chinese and Western Medicine*, vol. 22, no. 35, pp. 3952-3953, 2013.

[29] R. Q. Fan, C. Z. Su, G. J. Zhu et al., "Effect of entecavir combined with Fuzheng Huayu capsule on chronic hepatitis B liver fibrosis: a clinical observation of 73 cases," *Chinese Journal of Gastroenterology and Hepatology*, vol. 22, no. 1, pp. 31–33, 2013.

[30] S. Q. Pang, S. Wu, G. Q. Wang et al., "Entecavir combined with Fuzheng Huayu Capsule for treating 50 cases of chronic hepatitis B liver fibrosis," *China Pharmacy*, vol. 22, no. 8, pp. 120-121, 2013.

[31] Y. H. Gong, J. J. Chen, J. H. Xue et al., "Combination of entecavir and Fuzheng Huayu capsule for 28 cases of chronic hepatitis B liver fibrosis," *Chinese Journal of Integrated Traditional and Western Medicine on Liver Diseases*, vol. 20, no. 2, pp. 119-120, 2010.

[32] Y. Z. Song and T. T. Zhuang, "Therapeutic effect of Fuzheng Huayu capsule combined with entecavir on chronic hepatitis B liver fibrosis," *Fujian Medical Journal*, vol. 34, no. 6, pp. 89-90, 2012.

[33] Z. F. Shuangguan, "Effect of entecavir and Fuzheng Huayu capsules on hepatic fibrosis in patients with chronic hepatitis B," *Chinese Journal of Rural Medicine and Pharmacy*, vol. 20, no. 1, pp. 39-40, 2013.

[34] Y. C. Xie, G. X. Hu, Y. Z. Peng et al., "Therapeutic effect of Dahuang Zhechong capsule combined with entecavir on hepatic fibrosis in chronic hepatitis B," *Journal of Clinical Hepatology*, vol. 32, no. 8, pp. 1502–1507, 2016.

[35] J. Shi, H. L. Tang, and C. Chen, "Dahuang Zhechong capsule combined with entecavir for chronic hepatitis B liver fibrosis in 20 cases," *Hunan Journal of Traditional Chinese Medicine*, vol. 29, no. 5, pp. 19-20, 2013.

[36] X. P. Pan and Q. Dong, "Effect of entecavir combined with tanshinone capsule on liver fibrosis in patients with chronic hepatitis B," *Chinese Journal of Rural Medicine and Pharmacy*, vol. 23, no. 19, pp. 32-33, 2016.

[37] Z. H. Hu and Y. H. Wu, "Entecavir and tanshinone capsules for the treatment of chronic hepatitis B liver fibrosis," *Zhejiang Journal of Integrated Traditional Chinese and Western Medicine*, vol. 26, no. 3, pp. 243–246, 2016.

[38] X. Q. Chen, "Danshen injection combined with entecavir for chronic hepatitis B liver fibrosis," *Drugs & Clinic*, vol. 31, no. 6, pp. 878–881, 2016.

[39] F. L. Long, H. Qiu, Y. Q. Chen et al., "Clinical observation on the treatment of chronic hepatitis B liver fibrosis with danshen injection combined with entecavir," *Guiding Journal of Traditional Chinese Medicine and Pharmacy*, vol. 17, no. 8, pp. 16-17, 2011.

[40] F. Zhang and S. R. Li, "Clinical observation of entecavir combined with Anluo huaxian Pill in treating chronic hepatitis B liver fibrosis," *Military Medical Journal of South China*, vol. 31, no. 5, pp. 344-345, 2017.

[41] H. D. Qi, Y. Yang, and S. J. Gong, "Therapeutic effect of Anluo huaxian Pill combined with entecavir on hepatic fibrosis in patients with chronic hepatitis B," *Modern Chinese Doctor*, vol. 11, pp. 88-89, 2008.

[42] W. Guo, Y. Zhou, Y. S. Lu et al., "Treatment of chronic hepatitis B liver fibrosis with entecavir combined with anluohuaxian Pill," *Herald of Medicine*, vol. 29, no. 9, pp. 1157–1159, 2010.

[43] Y. H. Zeng, "Clinical study on entecavir combined with anluohuaxian Pill in treating hepatitis B liver fibrosis," *Hubei Journal of Traditional Chinese Medicine*, vol. 35, no. 6, pp. 11-12, 2013.

[44] Z. J. Huang and C. P. Zeng, "Treatment of liver fibrosis with HBeAg positive chronic hepatitis B in 134 patients with entecavir combined with Anluo Huaxian pills," *Chinese Journal of Integrated Traditional and Western Medicine on Liver Diseases*, vol. 26, no. 2, pp. 74-75, 2016.

[45] Y. J. Cai, J. J. Dong, X. D. Wang et al., "A diagnostic algorithm for assessment of liver fibrosis by liver stiffness measurement in patients with chronic hepatitis B," *Journal of Viral Hepatitis*, vol. 24, no. 11, pp. 1005–1015, 2017.

[46] L. L. Xiong, "Therapeutic effect of combined therapy of salvia miltiorrhiza and polyporus umbellatus polysaccharide in treating chronic hepatitis B," *Zhong Guo Zhong Xi Yi Jie He Za Zhi*, vol. 13, pp. 533–535, 1993.

[47] F. Ye, Y. Liu, G. Qiu et al., "Clinical study on treatment of cirrhosis by different dosages of salvia injection," *Zhong Yao Cai*, vol. 28, pp. 850–854, 2005.

[48] J. Peng, X. Li, Q. Feng, L. Chen, L. Xu, and Y. Hu, "Anti-fibrotic effect of Cordyceps sinensis polysaccharide: inhibiting HSC activation, TGF-β1/smad signalling, MMPs and TIMPs," *Experimental Biology and Medicine*, vol. 238, no. 6, p. 668, 2013.

[49] W. Rui, L. Xie, X. Liu et al., "Compound Astragalus and Salvia miltiorrhiza extract suppresses hepatocellular carcinoma progression by inhibiting fibrosis and PAI-1 mRNA transcription," *Journal of Ethnopharmacology*, vol. 151, no. 1, pp. 198–209, 2014.

[50] Y. Peng, Y. Y. Tao, Q. L. Wang et al., "Ergosterol is the active compound of cultured mycelium cordyceps sinensis on antiliver fibrosis," *Evidence-Based Complementary and Alternative Medicine*, vol. 2014, Article ID 537234, 12 pages, 2014.

[51] T. Zhou, X. C. Yan, Q. Chen et al., "Effects of Chinese herbal medicine Fuzheng Huayu recipe and its components against hepatocyte apoptosis in mice with hepatic injury," *Journal of Chinese Integrative Medicine*, vol. 9, no. 1, pp. 57–63, 2011.

[52] Q. Chen, F. Wu, M. Wang et al., "Transcriptional profiling and miRNA-target network analysis identify potential biomarkers for efficacy evaluation of fuzheng-huayu formula-treated hepatitis B caused liver cirrhosis," *International Journal of Molecular Sciences*, vol. 17, no. 6, p. 883, 2016.

Hindawi
Evidence-Based Complementary and Alternative Medicine
Volume 2020, Article ID 4875764, 13 pages
https://doi.org/10.1155/2020/4875764

Research Article

An Overview of the Mechanism of *Penthorum chinense* Pursh on Alcoholic Fatty Liver

Xingtao Zhao,[1,2,3] **Liao Li**,[1,2,3] **Mengting Zhou**,[1,2,3] **Meichen Liu**,[1,2,3] **Ying Deng**,[1,2,3] **Linfeng He**,[1,2,3] **Chaocheng Guo**,[1,2,3] **and Yunxia Li**[1,2,3]

[1]*School of Pharmacy, Chengdu University of Traditional Chinese Medicine, Chengdu 611137, China*
[2]*Key Laboratory of Standardization for Chinese Herbal Medicine, Ministry of Education, Chengdu 611137, China*
[3]*National Key Laboratory Breeding Base of Systematic Research, Development and Utilization of Chinese Medicine Resources, Chengdu 611137, China*

Correspondence should be addressed to Yunxia Li; lyxtgyxcdutcm@163.com

Received 12 July 2020; Revised 13 August 2020; Accepted 28 August 2020; Published 17 September 2020

Academic Editor: Hongwei Zhang

Alcohol liver disease (ALD) caused by excessive alcohol consumption is a progressive disease, and alcohol fatty liver disease is the primary stage. Currently, there is no approved drug for its treatment. Abstinence is the best way to heal, but patients' compliance is poor. Unlike other chronic diseases, alcohol fatty liver disease is not caused by nutritional deficiencies; it is caused by the molecular action of ingested alcohol and its metabolites. More and more studies have shown the potential of *Penthorum chinense* Pursh (PCP) in the clinical use of alcohol fatty liver treatment. The purpose of this paper is to reveal from the essence of PCP treatment of alcohol liver mechanism mainly by the ethanol dehydrogenase (ADH) and microsomal ethanol oxidation system-dependent cytochrome P4502E1 (CYP2E1) to exert antilipogenesis, antioxidant, anti-inflammatory, antiapoptotic, and autophagy effects, with special emphasis on its mechanisms related to SIRT1/AMPK, KEAP-1/Nrf2, and TLR4/NF-κB. Overall, data from the literature shows that PCP appears to be a promising hepatoprotective traditional Chinese medicine (TCM).

1. Introduction

According to the World Health Organization (WHO), excessive alcohol consumption causes 3 million deaths worldwide each year and is a major cause of death in western and industrialized countries. Alcohol and nonalcohol fatty liver disease have replaced viral hepatitis as the leading cause of disease [1], and among people less than 20 years of age, alcohol is the leading global risk factor for death, with the latest data showing [2] consistently high rates of alcohol-related harm in England. In 2016-2017, one million hospital admissions had a primary or secondary diagnosis related to alcohol consumption [2], causing significant national economic burden. Alcohol abstinence is the best way to fundamentally treat alcohol fatty liver disease [3], but this is poorly complied with patients; regarding ALD medication, it is currently clinically limited to severe alcohol hepatitis with steroids, hexaketocyclohexane (TNF-α inhibition), and vitamin E and silymarin (antioxidants), but the clinical effect is not significant and may be related to the complexity of the pathogenesis of alcohol liver disease [4, 5].

Alcohol liver disease (ALD) [1] is a progressive disease that includes a series of dynamic pathologies such as alcohol fatty liver disease (a type of liver damage that is reversible upon abstinence from alcohol), alcohol steatohepatitis, and cirrhosis to liver cancer. Unlike other chronic diseases, alcohol fatty liver disease is not caused by nutritional deficiencies [6], but it is caused by the molecular action of ingested alcohol and its metabolites, etc. After drinking alcohol [7], only about 5–10% passes in nonmetabolic forms through urine (2–4%), exhaled air (2–4%), and skin evaporation (1-2%) and is excreted from the body. The remaining 90–95% is biotransformed in hepatic parenchymal cells (85% of the absorbed dose) and ethanol is excreted in the liver via the ethanol-derived fraction. Dehydrogenase (ADH) (70–80%) and microsomal ethanol oxidation system

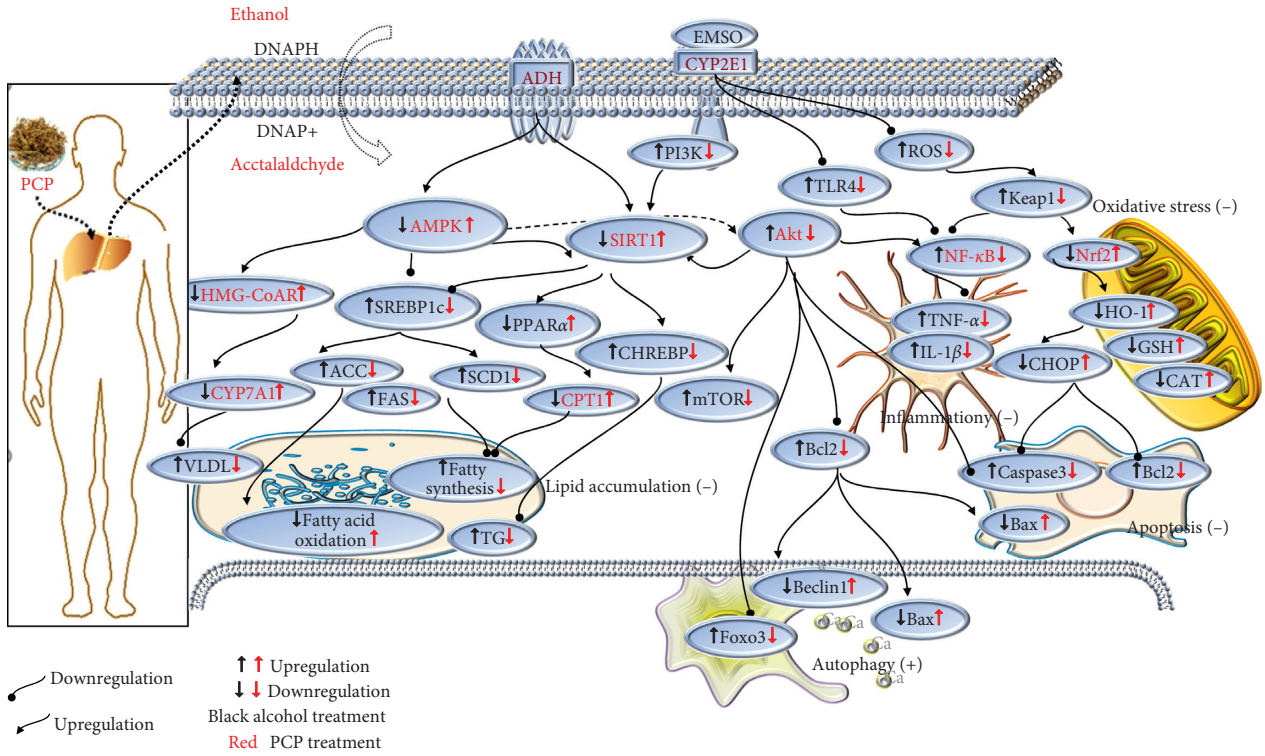

Figure 1: Diagram of the mechanism of PCP on alcohol liver disease.

(MEOS) (20–25%) Cytochrome P4502E1 (CYP2E1) metabolism [8], which induced reduction of NAD^+ to NADH, inhibits the tricarboxylic acid cycle and β-oxidation of fatty acids, in addition to the production of acetaldehyde and lipid peroxidation products which leads to the formation of protein adducts, additionally producing acetaldehyde and lipid peroxidation products form protein adducts that lead to impaired secretion of VLDL-TG. This leads to a barrier to the transport of synthetic lipids, inhibition of fatty acid oxidation, and enhanced lipogenesis, resulting in steatosis, a series of hepatotoxins such as ethanol and the metabolite acetaldehyde further interfering with hepatic parenchymal cells, nonparenchymal cells such as Kupffer cells (KCs), hepatic stellate cells (HSCs), and hepatic sinusoidal endothelial cells (LSECs), as well as the intestinal tract to promote ROS and endotoxin production, which then exacerbate the multiple blows of hepatic lipid accumulation, redox imbalance, inflammatory response, and apoptosis and aggravate the development of the disease [9–11].

According to the therapeutic principle of traditional Chinese medicine (TCM), the treatment of alcohol fatty liver belongs to liver depression and spleen deficiency type, and TCM treatment is multicomponent and multitarget, with low toxicity and side effects, and mostly adopts liver and spleen evacuation, combined with blood activating and stasis resolving drugs, which shows significant therapeutic effect.

In China, *Penthorum chinense* Pursh (PCP) has been used for hundreds of years traditionally with the functions of "promote diuresis and reduce swelling," "circulation of blood," "circulation of blood stasis," and "soothing liver and invigorating spleen," for alleviating symptoms by excessive intake of alcohol as well as in the treatment of traumatic injury, edema, and liver diseases. Recently, it has a wide range of pharmacological effects, such as antiaging [12], antioxidant [13], anti-inflammatory [14], hypoglycemic [15], antibacterial [12], and promoting immune regulation. Modern studies have shown that PCP protects the liver and treats acute viral hepatitis and chronic liver diseases, such as viral hepatitis, alcoholic hepatitis, and other alcohol liver diseases [13]. 12 Chinese patent pharmaceutical preparations have been approved by the China Food and Drug Administration (CFDA) [16]; PCP and its extract have been developed into tea, drinks or tablets, granules, capsules, and pills in the market under the trade name of "Gansu" in China for treatment of liver diseases [17, 18], which is considered as a potential candidate and can be further developed and used. It is worthy of further study and discussion, so this article provides an overview of its possible active ingredients and related mechanisms, aiming to elucidate its underlying molecular mechanisms.

2. The Therapeutic Effects of PCP on Alcohol Fatty Liver Disease

In recent years, more and more researches have been reported for alcohol liver treatment, which are summarized in Table 1. Expression of activity-regulation-related factors, mainly through SIRT1/AMPK, SREBP-1C, C/EBP, and PPAR-α, affects ADH and ALDH activity, further reduces cholesterol synthesis, promotes fatty acid oxidation, and

Table 1: Therapeutic effects of PCP and its active ingredients on alcohol fatty liver disease and related mechanisms.

Animal model	Medicine	Dose/treatment	Effect	Mechanism	Reference
Mice fed with high fat diet and alcohol at the dose of 3 g/kg	PCP (95% ethanol)	20, 40, 80 mg/kg 21 d	TG, TC, ALT, AST↓ ↑MDA	Antilipogenesis	[19]
L02 feed with 1.5% $FeSO_4$ with 50% ethanol	PCP (50% ethanol)	40 μg/mL 12 d	TG, ALT, AST↓	Antilipogenesis	[20]
Feed with 1.5% $FeSO_4$ and 50% ethanol for rats	PCP (95% ethanol) quercetin	4000, 2000 mg/kg 50 mg/kg 6 w	TG, TC, ALT, AST↓ *P. chinense* Pursh played a more significant role than quercetin	Antilipogenesis	[21]
Feed with high fat iron with 52% ethanol, 15% sugar for rats	PCP (35, 75, 95% ethanol)	3 g/kg 4 w	TC, TG, LDL-C, AST↓ 75%, 95% ethanol extract *P. chinense* Pursh played a more significant role	Antilipogenesis	[22]
Rats fed with 1.5% $FeSO_4$ and 45% ethanol	PCP (aqueous)	1.67, 8.4, 4.2 g/kg 6 w	TG, CHO, LDL-C, NEAF↓ ALT, AST, TBIL↓ ↑HDL-C	Antilipogenesis	[23]
1.5% ferrous sulfate feed, 50% 8 g/kg alcohol	PCP (aqueous) total flavonoids	2000 mg/kg 800 mg/kg 14 d	TG, TC, ALT, AST↓ total flavonoids played a more significant role than *P. chinense* Pursh	Antilipogenesis	[24]
Fatty acids, cholesterol, neutral lipids, phospholipids, and very-low-density lipoproteins (VLDL) were investigated in rat hepatocyte	Quercetin	50–25 μM	TG, VLDL↓ HMG-CoA-R, ACC↓	Antilipogenesis	[25]
Lipid accumulation in human hepatoma (HepG2 cells)	Quercetin	10 μM 24 h, 48 h	TC, TG, ABCA1↓ HMGCR, SREBP-1c↓ ↑CYP7A1, AMPKα2, PPARγ, C/EBPα↓	Antilipogenesis	[26]
Adipogenesis in 3T3-L1cell	Quercetin	100 Mm 24 h, 48 h	↑AMPK ACC↓ ↑MAPK/ERK1/2 Cytochrome c↓	Antilipogenesis Autophagy	[27]
Adipogenesis and apoptosis in 3T3-L1 cells	Quercetin	10, 20, 40, 80 μM 5, 15, 45, 135 μM 4 w	PPARγ, C/EBPα↓ SREBP-1c↓	Antilipogenesis	[28]
Rats ingesting 65% ethanol solution	Resveratrol	250 mg/kg 4 w	TG, ALT, AST↓	Antilipogenesis	[29]
HepG2 cells with 100 μM oleic acid and 87 mM alcohol	Resveratrol	5, 15, 45, 135 μM 24 h	TG↓ ↑AMPK ACC, SREBP-1c, PGC-1α↓ ↑PPAR-α, Lipin1	Antilipogenesis Antiadipogenic	[30]
Rats ingesting 10% ethanol solution	Quercetin	10 mg/kg 2 w	↑Insulin, adiponectin ↑AMPK ACC↓	Antiadipogenic	[31]
Vitro model of a normal rat's liver cell (BRL-3A).	PCP (ethanol) (70% ethanol)	6.25–100 mg/kg	70% ethanol extract *P. chinense* Pursh played a more significant role than aqueous extract	Antioxidant	[20]
HepG2 cells were induced by free fatty acid (FFA)	Effective flavonone	PCB, MPG (1, 10, 100 μM) PCBG (0.1, 1, 10 μM)	ALT, AST↓ ↑AMPK/SRIT1 ↑PPAR-α FAS, ACC, SCD1↓ ↑MDA, GSH-Px	Antioxidant Antilipogenesis	[32]
ABTS, hydroxyl radical scavenging, DPPH tests	PCP (75% ethanol)	0.5–50 mg/kg	DPPH, ABTS, and hydroxyl radicals scavenging↓ lipid peroxidation↓	Antioxidant Antilipogenesis	[12]
t-BHP-induced liver damage in LO2 cells	PCP (aqueous)	100, 200, 400 mg/kg 12 h	Caspase-9, caspase-3↓ ↑PARP, Bcl-xl, Bcl-2 ↑Nrf2, HO-1, SOD-2	Antioxidant Antiapoptotic	[33]
t-BHP-induced liver damage in LO2 cells	PCP (aqueous)	50 mg/kg 12 h	KEAP-1↓ ↑Bcl-2 E50M60 subfraction was more significant than *P. chinense* at 200 μg/mL	Antioxidant Antiapoptotic	[34]
Ethanol gavage (4.7 g/kg) every 12 h for a total of three doses	PCP (aqueous)	5.2, 10.3 g/kg 7 d	TG, ATGL, ALT, AST↓ CYP2E1↓ ↑MDA, GSH, SOD, CAT TNF-α, IL-6↓	Antilipogenesis Antioxidant Anti-inflammatory	[35]
Mice were fed a Lieber-De Carli liquid diet containing alcohol	PCP (aqueous)	5, 10, 30 g/kg 4 w	ALT, AST↓ TNF-α, IL-6↓ ↑MDA, GSH, SOD, GPx CYP2E1↓ ↑Nrf2/HO-1	Antioxidant Anti-inflammatory	[36]
RAW264.7 cell with LPS (1 ng/mL)	PCP (80% ethanol) PCPP, PCPP1a	15, 30, 60, 120 μg/mL 24 h	NO, TNF-α, IL-1β↓	Anti-inflammatory	[14]
Human LX-2 cells and rat HSC-T6 cells	PCP (aqueous)	25, 50, 100 mg/kg 24 h	Collagen I, α-SMA, TGF-β1↓ ↑SIRT3, SOD2, GSK3β PI3K-Akt↓	Antioxidant	[35]
Male C57BL/6J mice fed Lieber-De Carli diets containing ethanol (30% of total calories) hepatocytes with ethanol (100 mM)	Quercetin	100 μM 24 h	TC, TG, ALT, AST↓ ↑GSH, MDA, TfR1 ↑BMP6/SMAD4, ↑hepcidin	Antioxidant Autophagy	[37]
Chronic alcohol (30% of total calories) or iron (0.2%)-fed adult male C57BL/J mice	Quercetin	100 μM	↑Metal transporter 1, zinc transporter member 14, mucolipin 1, transferrin receptor 1	Hepatoprotective Antioxidant	[38]

Table 1: Continued.

Animal model	Medicine	Dose/treatment	Effect	Mechanism	Reference
Mouse primary hepatocytes were incubated with ethanol (100 mM)	Quercetin	100 μM	ALT↓ ↑HDL ↑ROS, SOD, MDA, GSH	Hepatoprotective Antioxidant	[39]
Male C57BL/6J mice fed Lieber-De Carli diets containing ethanol	Quercetin	100 μM	AST, ALT, LDH↓ ↑MDA, GSH, GSSH caspase-3↓	Antiapoptosis	[40]
MS rats with 30% sucrose in drinking water	Quercetin	0.95 mg/kg	TG, HOMA↓ ↑GSH, Nrf2	Antioxidant	[41]
Ethanol (4.0 g/kg) to rats	Quercetin	100 mg/kg 9 d	AST, LDH↓ CYP2E1↓ ↑MDA, GST, GPx, CAT, ↑HO-1	Antioxidant	[42]
Ethanol-incubated primary rat hepatocytes (100 mM)	Quercetin	50 μM 2 h	AST, LDH↓ ↑MDA, GSH, SOD, CAT ↑Nrf-2/HO-1	Antioxidant	[43]
HepG2 cell model induced by ethanol in vitro	Quercetin	25 μM	CYP2E1↓ ↑MDA, 4-HNE, GPx ↑Nrf2/HO-1	Antioxidant	[44]
RAW 264.7 cells with LPS (100 ng/ml)	Quercetin	20 μM 24 h	TNF-α, IL-1β, IL-6, MyD88, PGE2, iNOS, COX-2↓ ↑HO−1 PI3K/Akt/NF-κB, TRAF6 JNK, p38MAPK↓	Anti- inflammatory Antioxidant	[45]
Mice fed with 35%, 40%, 52% v/v ethanol (3 g/kg)	Quercetin	60 mg/kg 3 w	ALT, AST, TG↓ ↑TBIL TNF-α, IL-1β, IL-2, IL-6↓ ↑IL-10 ↑SOD, GSH-Px, MDA ↑Bcl-xl, Bcl-2 Caspase-3↓ PI3K/Akt/NF-κB↓ ↑STAT3, PARP	Antioxidant Anti- inflammatory Antilipophagy Antiapoptosis	[46]
Ethanol-dosed adult male Balb/c mice (5.0 g/kg) or primary rat hepatocytes (100 mM)	Quercetin	2.5 mg/kg	AST, ALT, LDH↓ ↑GSH, SOD, MDA TNF-α, IL-6↓ p38 MAPK↓ ↑HO-1	Antioxidant Anti- inflammatory	[43]
Treated with 5% alcohol for 24 h HepG2 cells	Quercetin	10, 20 μM 1 h	ALT, AST↓ ↑ROS, MDA, GSH NO, TNF-α↓ ↑Nrf2/HO-1	Antioxidant Anti- inflammatory	[44]
25 patients with AH/rats with 50% (v/v) ethanol 5 g/kg body weight every 12 h three times	Quercetin	100 mg/kg 14 d	ALT, AST↓ ↑MDA, GSH-Px TNF-α, IL-1β, IL-18, NLRP3↓ ↑IL-10 ↑Nrf2/HO-1 ASC, caspase-1↓	Antioxidant Anti- inflammatory	[47]
Pregnant rats received 1 ml/day of 40% v/v ethanol (4 g/kg)	Quercetin	50 mg/kg 21 d	↑MDA, PC, GSH, SOD, CAT TNF-α, IL-1β, IL-6, NF-κB↓	Antioxidant Anti- inflammatory	[48]
BALB/c mice had induced liver fibrosis by carbon tetrachloride (CCl4)	Quercetin	50 mg/kg 8 w	TNF-α, IL-1β, IL-6, MCP-1↓	Anti- inflammatory	[45]
Peripheral blood of 15 healthy male and female nonsmoking and nondrinking donors	Resveratrol	5, 25, 50 μM	↑ADH1B, ALDH2	Antioxidant	[49]
Mice fed with 3 gavages of calories of dextrin-maltose (MP biomedicals) or ethanol at 3.5 g/kg	Resveratrol	50 μM	AST, ALT, TG↓ ↑ADH, NADH/NAD$^+$ ↑SIRT1, AMPK, ChREBP, FAS, SCD1↓	Antioxidant	[50]
Rats were fed either control or ethanol liquid diets containing 0.8, 1.6, and 2.4 g/kg ethanol	Resveratrol	100 mg/kg 22 w	↑ALDH2, ADH, SIRT1 CYP2E1↓	Antioxidant	[51]
Ethanol-induced oxidative DNA damage in human peripheral lymphocytes	Resveratrol	5, 25, 50 μM	↑ADH1B, ALDH2	Antioxidant	[52]
t-BHP-induced liver damage in LO2 cells	Resveratrol	25, 50, 75 μM	↑SOD, GPx, GR, NQO1, GST, ↑Nrf2	Antioxidant	[53]
Mice administered alcohol in drinking 10% up to 40% v/v	Resveratrol	10 mg/ml 4 w	TG↓ TNF-α, IL-1↓ ALT, AST, ALP, CHO↓	Anti- inflammatory	[30]
Lipopolysaccharides-induced rats' model	Resveratrol	3.125, 6.25, 12, 5 μM 25 h	NF-κB/p65, TLR4, MyD88, TRAF6↓ TNF-α, IL-1, IL-1β, IL-6↓ NO, iNOS, COX-2↓ ↑MAPKs ↑IL-10 PI3K/Akt↓	Anti- inflammatory	[54]
Mice with carbon tetrachloride (CCl4) induced liver fibrosis	Resveratrol	10, 20, 30 mg/kg	ALT, AST↓ NLRP3, IL-1β, IL-18↓ ↑Caspase1	Anti- inflammatory	[55]

Table 1: Continued.

Animal model	Medicine	Dose/treatment	Effect	Mechanism	Reference
Mice with carbon tetrachloride (CCl4) induced liver fibrosis	Resveratrol	50 mg/kg	ALT, AST↓ TNF-α, Akt/NF-κB (IκB)↓	Anti-inflammatory	[56]
Male Foxo3a/mice administered 33% (v/v) ethanol at a total dose of 4.5 g/kg	Resveratrol	6, 12 mg/kg 16 h	↑Ulk1, Atg5, 7, 14 ↑Vps34, LC3II, beclin 1 ↑FoxO3a	Autophagy	[57]
AFL mice fed with an ethanol Lieber-De Carli liquid diet, and HepG2 cells in the presence of oleic acid and alcohol	Resveratrol	10, 30, 100 mg/kg	ALT, AST, TG, LDL-C↓ ↑HDL-C ↑LC3-II, P62	Autophagy	[58]
Mice were fed 30% Lieber-De Carli liquid diet containing alcohol	Quercetin	100 mg/kg 15 w	↑LC3II, parkin, p62 ↑VDAC1, FoxO3a ↑AMPK, ERK2	Autophagy	[59]
Pair fed with liquid diets containing ethanol (28% of total calories) and treated mice	Quercetin	100 mg/kg 12 w	ALT, AST, TC, TG↓ ↑AMPK, ERK, PLIN2 ↑LC3II, p62	Autophagy	[60]
t-BHP-induced liver damage in LO2 cells	Quercetin	50 μM 12 h	↑Nrf2, HO-1, SOD-2 KEAP-1↓ ↑BcL-2	Autophagy	[61]
Mice administered alcohol in drinking 6% up to 20% v/v	Resveratrol	250 mg/kg 16 w	ALT, AST↓ ↑MDA, SOD, CAT, GPX CYP2E1↓ caspase 3↓ ↑SIRT1	Antioxidant Antiapoptotic	[62]
Human hepatocyte Chang cell line induced by ethanol	Resveratrol	10 μM 6 h	Caspase-12↓ ↑ADH-2, ALDH-2, ↑GRP78, p-IRE1α, p-eIF2α p-PERK, ATF4↓ caspase-3/12↓ ↑CHOP, Bcl-xl	Antiapoptotic	[51, 63]

Note: TG, triglyceride; TC, serum total cholesterol; TBil, total bilirubin; LDL-C, low-density lipoprotein cholesterol; HDL-C, high-density lipoprotein cholesterol; VLDL, very low-density lipoprotein cholesterol; VDACT1, voltage-dependent anion channel; DBIL, direct bilirubin; HMGCR, 3-hydroxy-3-methylglutaryl-coenzyme A reductase; ALT, alanine aminotransferase; AST, aspartate transaminase; ADH, alcohol dehydrogenase; ALDH, aldehyde dehydrogenase; CYP2E1, cytochrome P450 2E1; ABCA1, ATP-binding cassette transporter; CYP7A1, cholesterol 7-hydroxylase; MDA, malondialdehyde; FAS, fatty acid synthase; ACC, acetyl coenzyme A carboxylase; SCD1, stearoyl coenzyme A desaturase 1; GSH, glutathione; SOD, superoxide dismutase; CAT, catalase; GPx, glutathione peroxidation chemotaxis; HO-1, heme oxygenase; NQO1, NADPH quinone oxidoreductase 1; COX-2, cyclooxygenase-2; IL-1, interleukin-1; IL-6, interleukin-6; IL-10, interleukin-10; TNF-α, tumor necrosis factor alpha; TLR4, toll-like receptor 4; TRAF6, tumor necrosis factor receptor-associated factor; AMPK, AMP-activated protein kinase; SIRT1, sirtuin1; ERK, extracellular signal-regulated kinase; PPAR-α, proliferator-activated receptor alpha; C/EBP, CCAAT/enhancer-binding protein; HA, hyaluronic acid; LN, laminin; PC III, procollagen III; PCIII, type III pre-collagen; LC3-II, light chain 3-II; Bcl2, B-cell lymphoma.

inhibits the oxidation of fatty acids. Increased CYP2E1 activates the KEAP-1/Nrf2-HO-1 signaling pathway to affect relevant oxidative stress factors expression and exert antioxidant effects, which in turn inhibits the MyD88/TLR4/NF-κB signaling pathway and exerts anti-inflammatory effects and finally exerts antiapoptotic effects through PI3K/Akt promotion of B-cell lymphoma (Bcl2), Bcl-2 Associated X Protein (Bax) apoptosis regulator, and inhibition of Caspase 3 protein expression levels, in addition to mediated activation of autophagy which may be related to AMP-activated protein kinase (AMPK) and Sirtuin1 (SIRT1); the specific mechanisms are shown in Figure 1.

2.1. Antilipogenesis. The accumulation of fat in the liver is the earliest response to alcohol abuse and is also the first crucial step in the pathogenesis of alcohol liver disease, the early diagnosis of alcohol fatty liver disease is clinically based on the amount of alcohol equivalent to ethanol consumption >40 g/d in men, >20 g/d in women, or >80 g/d in two weeks. Liver fat droplets or total fat cells greater than 5% of liver weight are the criteria for initial diagnosis of steatosis [4]. Importantly, ethanol-induced hepatic lipid accumulation is known to be reversed, and recent studies have shown that PCP had shown great efficacy in the treatment of alcohol fatty liver disease.

Gamma-glutamyl transferase (GGT) is one of the traditional hallmarks of alcoholism [64]. With increased alcohol intake, the blood activity of GGT increases. Aspartate aminotransferase (AST) and alanine aminotransferase (ALT) are involved in the metabolism of amino acids and are ethanol-induced hepatocyte A sensitive indicator of injury. Alkaline phosphatase (ALP) [65] catalyzes the dephosphorylation of different compounds and is a less specific marker of liver injury. Pathological examination of the liver of rats in PCP experimental group detected a significant decrease in the serum content of AST and ALT and a reduction in hepatic fatty infiltration.

The main manifestation of hepatic fat accumulation is the accumulation of triglycerides (TG) [66]. The aqueous extract of PCP played an important role in fat accumulation from chronic alcohol exposure. In adipose tissue, key enzymes were involved in intracellular lipids through upregulation of triacylglycerols, such as adipose triglyceride lipase (ATGL) [67]. Equal amounts of total flavonoids lowered lower-density lipoprotein (LDL), cholesterol (TC), and triglycerides (TG) more significantly than the aqueous extract of chased grass [13], and 95% of the ethanol extracts increased serum high-density lipoprotein (HDL) compared to other volume fractions of ethanol extract group [22]. The fractional ethanol rush extract group was significant, in the

dose range of 25–200 g/mL, polyphenols in the 70% ethanol extract. The substances and flavonoids were enriched to a high degree and had significantly stronger hepatoprotective activity than the aqueous extracts [68].

In recent years, there has been great progress in the study of the chemical composition of PCP, the main types of components of polyphenols (flavonoids, coumarins, and lignans), organic acids, sterols, etc. [13]. Among them, polyphenols have shown good efficacy in the treatment of alcohol liver [69].

Quercetin significantly reduced acetyl coenzyme A carboxylase (ACC) activity in rat hepatic suspension cells and decreased fatty acid de novo and TAG synthesis, resulting in VLDL-TAG formation being reduced for lipid-lowering purposes in chronic ethanol-induced alcohol fatty liver disease in rats. Quercetin exerted hepatoprotective effects by lowering LDL, TC, TG, and increased serum HDL [25]; the combination of resveratrol and quercetin reduced peroxidase expression of the proliferator-activated receptor (PPAR) [70] and CCAAT/enhancer-binding protein (C/EBP) [28], via inhibiting the preadipocyte differentiation and exerting potential antiobesity effects, which is primarily associated with upregulation of phosphorylated adenosine monophosphate-activated protein kinase (AMPK) and its substrate ACC levels, and in HepG2 cells [26], quercetin-composed complex increased ATP-binding cassette transporter (ABCA1), cholesterol 7-hydroxylase (CYP7A1), and AMP-activated protein kinase (AMPK) mRNA expression while decreasing sterol regulatory element-binding protein 1c (SREBP-1c) and liver X receptor (LXR) mRNA expression.

Resveratrol was able to inhibit ethanol metabolism and adipogenesis from the head by regulating ethanol dehydrogenase 1B (ADH1B) and acetaldehyde dehydrogenase 2 (ALDH2) mRNA [51, 71] and improving the ratio of NAD^+/NADH to regulate SIRT1. 3T3-L1 [27] preadipocytes indicated that SIRT1 mediated gene and protein expression of the transcription factors PPARγ, C/EBP, and SREBP-1c, which were involved in the regulation of adipogenesis by resveratrol [71], with PPARγ, PGC-1α, and PPAR-α being considered as the major adipogenic regulators [72]. In an in vivo animal study, resveratrol treatment increased SIRT1 expression levels and stimulated AMPK activity in the liver of ethanol-fed mice. Resveratrol-mediated increase in SIRT1 and AMPK activity with SREBP-1 inhibition and activation of the peroxisome proliferation-activated receptor coactivator (PGC-1) were associated [73]. Meanwhile, in ethanol-fed mice, resveratrol significantly increased circulating lipofuscin levels and enhanced hepatic lipofuscin receptor mRNA expression (AdipoR1/R2) to prevent the development of alcohol liver steatosis [71].

It has also been shown that the three flavonoids of PCP were induced by free fatty acids (FFA) in a model of hepatic steatosis in HepG2 cells [32]. Pinocembrin-7-O-β-d-glucoside (PCBG), Pinocembrin (PCB), and 5-methoxy-pinocembrin-7-O-β-d-glucoside (MPG) enhanced phosphorylation of AMPK and silenced mating-type information regulated the expression of SIRT1 and PPAR-α and reduced the expression of sterol regulatory SREBP-1c and the downstream targets were fatty acid synthase (FAS). Acetyl coenzyme A carboxylase (ACC) and stearoyl coenzyme A desaturase 1 (SCD1) played a preventive role in hepatic steatosis.

In conclusion, the effect of PCP and its active ingredients on the fat accumulation in alcohol liver was mainly due to the effect of SIRT1/AMPK, SREBP-1C, C/EBP, and PPAR-α on the activity of ADH and ALDH to reduce the synthesis of cholesterol and promote the oxidation of fatty acids.

2.2. Antioxidant. Excess hepatic acetaldehyde and alcohol oxidation metabolites induce hepatocyte microsomal enzyme cytochrome P450 system activity which promoted high ROS production by a variety of cells including hepatocytes, Kupffer cells, endothelial cells, and infiltrating inflammatory leukocytes, leading to oxidation reduction of imbalance. Antioxidant therapy may be an effective way to correct the imbalance of oxidants and antioxidants in the development of alcohol liver disease and can prevent alcohol liver damage.

Aqueous extracts of PCP [35] had a protective effect against ethanol-induced acute and chronic liver injury and in an ethanol-induced chronic liver injury model. Aqueous extract of PCP downregulated MDA levels in alcohol fatty liver rats by inhibiting CYP2E1-mediated oxidative stress. The potential hepatoprotective effects of SOD were exerted by increasing the activity of SOD, enhancing the scavenging ability of oxygen free radicals and resisting lipid peroxidation. The 95% ethanol extract of PCP increased the liver MDA content and liver SOD content, which had a protective effect on the liver of alcohol rats. The stems of PCP had strong antioxidant activity and low cytotoxicity, making it a better bioactive site. The polyphenols enriched in the ethyl acetate part of PCP directly scavenged ROS and reduced liver enzymes and indirectly increased antioxidant levels. They promoted the production of nuclear factor-like 2 (NRF2), superoxide dismutase-2 (SOD-2), and heme oxygenase-2 (H2O2); HO-1 expression inhibits the Kelch-like ECH associated protein 1 (KEAP-1) expression [36] and thus is resistant to ROS-induced mitochondrial oxidative stress, and quercetin pre-intervention on the hepatocyte alcohol oxidative damage [34] was protective and mediated through Nrf2/HO-1 signaling pathway.

Pinocembrin mitigated ROS accumulation through SIRT3 activation of SOD2 and inhibited KEAP-1 by activating the Nrf2/HO-1 pathway, restored endogenous non-enzymatic (e.g., glutathione (GSH)) depletion, and increased related antioxidant genes (e.g., superoxide dismutase (SOD) and catalase (CAT)) and glutathione peroxidation chemotaxis (GPx) and heme oxygenase (HO-1) activities.

Quercetin inhibited oxidative stress and MDA [39, 40] in HepG2 cells overexpressing CYP2E1 treated with 100 mM ethanol attenuated alcohol-induced increment of hepatic 4-hydroxynonenal (4-HNE) formation with the elevation of hepatic GPX and SOD. Quercetin attenuated CYP2E1-mediated ethanol hepatotoxicity via HO-1 induction, and HO-1-released CO via the activation of the p38 MAPK pathway inhibits ethanol-induced hepatic oxidative damage [47].

The liver is a major site of iron storage and a target organ for iron-induced injury. Hepatic iron content is increased in alcohol fatty liver disease, and hepatic iron can further synergistically amplify ethanol-induced oxidative stress and enhance hepatic tissue and hepatocytes of lipid peroxidative damage, thereby exacerbating fatty liver. In an animal model of alcohol liver, quercetin reduced oxidatively active iron-mediated ROS overproduction in lysosomes and transferrin receptor (TfR) 1 expression and attenuated ethanol-induced hepatic oxidative damage.

Resveratrol significantly reduced alcohol-induced increase in CYP2E1 [41], promoted antioxidant CAT, SOD, GSH, MDA, NADPH quinone oxidoreductase e (NQO1), and glutathione-s-transferase activity (GST), and regulated antioxidation via Nrf2 transcription factor.

In summary, the treatment of alcohol fatty liver disease with PCP exerted antioxidant effects by inhibiting the increase of CYP2E1 and influencing the expression of relevant oxidative stress factors through the KEAP-1/Nrf2-HO-1 signaling pathway.

2.3. Anti-Inflammatory. CYP2E1 produces a large number of inflammatory factors through chemotaxis of inflammatory factors, not only ethanol; particularly acetaldehyde in the intestinal tract will destroy tight junction proteins and increase intestinal permeability in vivo and in vitro, via hepatic and intestinal circulation leading to an increase in endotoxin causing induced liver injury.

The water extract of PCP significantly reduced the hepatic lipid accumulation and inflammatory cytokines (e.g., TNF-α, IL-6) induced by chronic ethanol exposure. Compared with LPS treatment, the polysaccharide components of PCP protected alcohol fatty liver in rats and exhibited strong anti-inflammatory properties in RAW264.7 cells by inhibiting the release of NO, TNF-α, and IL-1β activity [14]. The further development of inflammation may lead to liver fibrosis, and total flavonoids of PCP significantly inhibited the decrease of body mass and mitigated further development of liver fibrosis in alcohol rats, then elevated liver coefficient, decreased serum hyaluronic acid (HA), laminin (LN), type III pre-collagen (PCIII) levels, and the content of Hyp in liver tissue, and reduced serum TNF-α, IL-6 levels. Moreover, pinocembrin reduced production of the transforming growth factor TGF-β, as well as the activation of glycogen synthase kinase 3 via SIRT3/GSK3 to enhance smad protein degradation to treat liver fibrosis [35].

Quercetin inhibited lipopolysaccharide-induced inflammation via the p38MAPK and JNK signaling pathways [45] to inhibit inflammatory mediators (release of PGE2, iNOS, COX-2, TNF-α, IL-1β, IL-6, and NO) [74]; STAT3 proinflammatory factors play an important role in alcohol liver, and quercetin phosphorylates transcripts by inhibiting signal transducers and activating STAT3, a known PI3K inhibitor, which is also mediated by the TLR4 signaling pathway, thereby disrupting the linkage of the p85 subunit to the adapter protein MyD88 and the TLR4 complex, inhibiting downstream nuclear phosphorylation levels of transcription factor (NF-κB) [48] and protein kinase B (a protein kinase) to treat alcohol-induced liver injury in rats [75]. Quercetin also upregulated the expression of the anti-inflammatory factor IL-10 [43], then inhibiting NLRP3 inflammasome activation and inflammatory factor secretion to maintain liver function in acute alcohol [46].

Resveratrol was able to inhibit TLR4 protein expression [55] by downregulating the mRNA levels of MyD88 and TRAF6, thereby inhibiting TLR4 signaling pathway. It also inhibited the NF-κB/p65 signaling cascade and MAPKs in the liver (p38MAPK, ERK1, ERK2, and ERK5) signaling pathways [54], reducing mRNA levels of proinflammatory mediators and cytokines (IL-1, IL -6, NO, iNOS, and COX-2) [30] to reduce the LPS-induced inflammatory response.

In conclusion, the treatment of alcohol fatty liver disease with PCP mainly exerted anti-inflammatory effects by inhibiting CYP2E1 to attenuate the release of endotoxin and inhibiting MyD88/TLR4/NF-κB signaling pathway.

2.4. Autophagy. Autophagy is the phagocytosis of LDs by autophagosomes and their subsequent fusion with lysosomes to form autophagic lysosomes, which is an important pathway for lipid catabolism in lipid droplets, and the promotion of autophagy helps to reduce lipid accumulation in cells.

Four novel autophagy compounds were identified from PCP [76] that activate the AMPK and mTOR-mediated autophagy pathway to restore mitochondrial membrane potential (MMP) and thereby reduce reactive oxygen species (ROS) production in human umbilical cord blood.

Quercetin was able to mediate apoptosis in mature adipocytes by regulating the ERK and JNK pathways [37], and recent studies have shown that quercetin-mediated chronic ethanol-induced mitochondrial autophagy activates AMPK by reducing lipoprotein 2 (PLIN2) levels [60] and extracellular signal-regulated kinase 2 (ERK2), increasing hepatic LC3II, parkin, p62, and the voltage-dependent anion channel 1 (VDAC1) [59], FoxO3a, regulates ethanol-induced autophagy and cell survival. The key factor, quercetin-mediated enhancement of FoxO3a transcriptional activity, was involved in protection against ethanol-induced inhibition of mitochondrial autophagy effects.

Resveratrol increased the levels of microtubule-associated protein LC3-II and Beclin1 [58] and decreased the levels of expression of p62 protein induced autophagy to exert protective effects against alcohol fatty liver disease [57]. Moreover, resveratrol, a well-known SIRT1 agonist, was targeted by FoxO3a genes and increased in primary hepatocytes and mouse liver after treated with ethanol; however, the exact mechanism of action remains to be further studied, which may be related to the increased deacetylation of FoxO3a.

All in all, PCP-mediated activation of autophagy was related to AMPK, SIRT1, and ERK pathways.

2.5. Antiapoptosis. Hepatocyte apoptosis induced by ethanol involves oxidative stress and inflammation through induction of associated enzymes (e.g., CYP2E1) and cytokine (e.g., TNF-α) production or involvement of death receptors.

The potent hepatoprotective effects of PCP on t-BHP-induced injury in human hepatic L02 cells were mainly mediated by mediating ROS clearance and upregulating the expression of B-cell lymphoma 2 protein (Bcl-2) and Bcl 2-associated X (Bax) [33] and downregulating the caspase cleavage products caspase-7, caspase-9, and PARP to attenuate t-BHP-induced hepatocyte apoptosis [77].

Iron-mediated production of lysosomal ROS leads to lysosomal membrane permeability (LMP) and subsequent release of histone proteases into the cytoplasm, and quercetin induces apoptosis by activating MMP, activating the osteogenic protein/BMP6/SMAD4 pathway, and upregulating iron-regulator expression [37].

Quercetin, a known PI3K inhibitor, prevented alcohol-induced liver injury through the phosphatidylinositol 3-kinase PI3K/Akt/NF-κB and STAT3 signaling pathways and also promoted B-cell lymphoma (Bcl2) and Bcl 2-associated X (Bax) apoptosis regulator, inhibited protein expression levels of caspase 3 and poly ADP ribose polymerase, and decreased apoptosis [46].

Apoptosis is the result of further development of oxidative stress and is mainly executed by caspase 3, and studies have shown that resveratrol attenuated alcohol-induced oxidative stress in rats and then inhibited caspase 3 activity to suppress apoptosis.

In conclusion, the treatment of alcohol liver with PCP mainly inhibited the activity of CYP2E1 enzyme, PI3K/Akt promoted Bcl2, and Bax-related apoptosis regulator, and inhibited the expression of caspase 3 protein to play an antiapoptotic role.

3. Discussions

The pathogenesis of alcohol fatty liver is complex, but the essence is mainly through the influence of alcohol dehydrogenase (ADH) (70–80%) and cytochrome P4502E1 (CYP2E1) enzyme activity [78] of microsomal ethanol oxidation system (MEOS) (10–25%), influence of ethanol metabolism; ADH enzyme activity [79] regulates lipid metabolism by affecting SIRT1 [80], AMPK [79], SREBP-1C, ChREBP, and PPAR-α. Moreover, CYP2E1 can induce oxidative stress, autophagy, and apoptosis via producing a series of ROS and endotoxin after alcohol [4]; the study shows PCP in the treatment of alcohol fatty liver from the essence of the ADH, CYP2E1 enzyme activity, and then it regulates ethanol metabolism, which is unified with the theory of Chinese medicine "both the symptoms and the treatment."

Among the relevant regulators that affect lipid metabolism by affecting ADH enzyme activity are SIRT1, AMPK, SREBP-1C, ChREBP, and PPAR-α.

SIRT1 [81] is an NAD^+ dependent histone deacetylase involved in the regulation of many processes, such as mitochondrial biology occurrence, inflammation, intracellular metabolism, resistance, and apoptosis; SIRT1 [82] can be regulated by directly modifying histones or indirectly modulating several transcriptional regulator activity to act as a major metabolic regulator, and increased SIRT1 activity [83] may be caused by blocking ethanol metabolism $[NAD^+]$: changes in the [NADH] ratio mediated by Sirt1 activation may involve activation of AMPK [84], and in addition, SIRT1 may enable SREBP-1 [85], the ChREBP deacetylates, thereby inhibiting SREBP-1 [86] and ChREBP activity [87].

AMPK [88] is an intracellular energy sensor and activation of this enzyme inhibits anabolic pathways while promoting lipid decomposition of metabolic processes [89], ADH and/or acute ethanol-induced cardiac contraction, and intracellular Ca^{2+} responses with hyperactivation AMPK signaling cascade [90], phosphorylating downstream targets, including ACC which ultimately promotes long-chain fatty acids of β oxidation and leads to decreased accumulation of lipids in tissues, and the increased lipofuscin signaling allows the liver to stimulate AMPK [79] in the liver by lipofuscin resulting in the development of new lipid metabolism [91]. Hepatic fatty acid oxidation is increased [92], thereby preventing hepatic lipid accumulation in ethanol-fed mice after resveratrol, instead of PCP [93].

SREBP-1 [94] is a negative regulator of the ADH gene; sterol regulatory element-binding protein 1 (SREBP-1) and its target transcriptional acetyl coenzyme A carboxylase (ACC), fatty acid synthase (FAS), and stearoyl coenzyme A desaturase levels can be chronically administered by ethanol administration1 (SCD1), and ATP citrate lyase and mitochondrial glyceryl 3-phosphate acyltransferase (GPAT1) can lead to increased fatty acid synthesis and triglyceride accumulation in animal livers.

In addition to SREBP-1c, ChREBP is another factor that regulates sugar and lipid metabolism [95], the ChREBP/SIRT1/ADH axis [96] controls alcohol metabolism, silencing ChREBP can inhibit intrahepatic triglyceride accumulation by activating SIRT1 to reduce ADH acetylation and its enzymatic activity, and in addition, acetaldehyde is a precursor of acetic acid and acetyl coenzyme A (coenzyme A), a source of acetyl groups merged on ChREBP [97], which can effectively alleviate lipid accumulation [98].

The CYP2E1-induced oxidative stress may be related to ethanol-induced inhibition of Akt phosphorylation [99] by reducing its activity affecting the Nrf2/HO-1 signaling pathway, in which NF-κB is an important transcription factor in the development of the inflammatory response, and its activation plays a crucial role in the production of various proinflammatory mediators [100].

Autophagy plays an important role in the pathogenesis of alcohol hepatitis, although it has not been reported in the treatment of alcohol hepatitis with PCP [101].

However, PCP-EE has antiapoptotic, antiaging, and anti-inflammatory properties that protect HaCaT cells from UVB radiation or H_2O_2 lethal-induced oxidative stress and increases the promoter activity of the type 1 collagen gene Col1A1 and decreases the UVB radiation or H_2O_2 induced oxidative stress induced MMPs, COX-2, IL-6, and hyaluronan [12], suggesting that the treatment of alcohol liver-induced oxidative stress by autophagy is a novel mechanism [102], combined with quercetin, and the therapeutic results of resveratrol in alcohol liver suggest that it may regulate autophagy through the core regulator of autophagy; the transcription factor forkhead box protein O3 (FOXO3a)

[103] plays an important role in the pathogenesis of alcohol liver [104], and there is crosstalk between autophagy and apoptosis; PCP and its active ingredients inhibit the PI3K/AKT pathway through SIRT1 activation [105] by promoting Bcl-xl, the expression of Bcl2, and caspases proteins to regulate apoptosis, and it has been shown that Bcl-2 protein not only counteracts the activity of proapoptotic proteins to downregulate apoptosis but also interacts with Beclin-1 to prevent autophagy. The results suggest that there is some crosstalk between autophagy and apoptosis, providing a new thought on the mechanism of action of PCP in the treatment of alcohol liver [106].

Quercetin and resveratrol have been shown to promote autophagy in the treatment of alcoholic liver but recent reports showed that it is reasonable to think that, under mTOR inhibition or caloric restriction, resveratrol could act as an autophagy suppressor instead of behaving as an autophagy inducer. Additionally, because autophagy induced by quercetin or resveratrol is negatively regulated by mTOR, which acts as an autophagy inhibitor or blocker by at least modulating AMPK phosphorylation levels and downregulating HO-1 expression, in this sense, it has been previously shown by other authors that resveratrol induced lysosome leakage. Furthermore, resveratrol-mediated autophagy and apoptosis in cervical cancer cells were related to resveratrol-mediated cathepsin-L release from the lysosomes So, it is feasible to think that, in our experimental model, at least, some part of the proapoptotic signaling could be also mediated by cathepsin release. In this sense, in the quercetin + resveratrol condition, it would be likely that resveratrol is "loading" HepG2 cells with AV (autophagolysosomes) that are permeated by resveratrol. It is harmful to the cytosol (inducing a potent proapoptotic effect). This would also explain why the maximal mTOR inhibition occurs in the quercetin + resveratrol condition; we observed a significant decrease or blockade on the autophagy process [107]; in acute alcoholic fatty liver, the protective effect is played by promoting autophagy to reduce damaged mitochondria and lipid droplets and reduce hepatocyte apoptosis and steatosis. However, in chronic alcoholic fatty liver, autophagy is reduced, leading to lysosome depletion and inhibiting hepatocyte lipid overload, and preventing neutrophil recruitment to the liver; there is a great similarity between them, suggesting that autophagy is an important mechanism of alcoholic liver therapy.

Quercetin, resveratrol, and other flavonoids in PCP have shown good results in the treatment of alcohol liver disease, and the mechanism is similar to that of PCP, and quercetin is also used as an index of quality evaluation for heparin preparations at present, but some studies have proposed that the therapeutic effect of a single ingredient is not as good as that of PCP, which corresponds to the multicomponent, multitarget feature of Chinese medicine, prompting us to look for more quality standards [69].

Recent researches showed that the flavonoids content in the stems of PCP was higher and the antioxidant capacity was stronger [108], which suggested that the pharmacological effects of different medicinal parts were not the same, which can be carried out in the following researches.

With respective clinical applications, quercetin and resveratrol had relatively poor bioavailability due to their low aqueous solubility, short metabolic period, and toxicity. Therefore, extensive efforts have been made to increase the bioavailability and decrease the toxicity of quercetin by encapsulating it in drug delivery systems including silica nanoparticles and so on [109].

4. Conclusion

To summarize, this review critically demonstrates that PCP exhibits strong defensive effects against the treatment of alcohol liver, which is mainly concerned with regulating the expression of enzyme activity related ethanol metabolism factors, including SIRT1/AMPK, SREBP-1C, C/EBP, and PPAR-α influencing ADH and ALDH activity to reduce cholesterol synthesis and promote the oxidation of fatty acids, the inhibition of CYP2E1 enzyme activity, and the activation of KEAP-1/Nrf2-HO-1 oxidative stress-related signaling pathway to exert antioxidant effects, then inhibiting MyD88/TLR4/NF-κB signaling pathway to exert anti-inflammatory effects and finally promote B-cell lymphoma via PI3K/Akt (Bcl2), Bcl 2-associated X (Bax) apoptosis regulator, and inhibition of caspase 3 protein expression levels to exert antiapoptosis, and additionally mediating activation of autophagy may be related to AMPK and SIRT1. Thus its potential in the mechanism of alcohol fatty liver deserves consideration and further validation.

Data Availability

All the references can be found on PubMed, the citations are marked in the articles, and the corresponding references are listed in the references list.

Disclosure

The authors declare that the work described was an original research that has not been published previously and not under consideration for publication elsewhere, in whole or in part.

Conflicts of Interest

The authors declare that they have no conflicts of interest.

Acknowledgments

The research was supported by the National Science Foundation of China (Grant nos. 81373943, 81573583, and U19A2010), Sichuan Provincial Science Technology Department of Youth Science and Technology Innovation Research Team Program (Grant no. 2017TD0001), and Xinglin Scholar Research Promotion Project of Chengdu University of TCM (Grant no. CXTD20180019).

References

[1] J. D. Browning and J. D. Horton, "Molecular mediators of hepatic steatosis and liver injury," *Journal of Clinical Investigation*, vol. 114, no. 2, pp. 147–152, 2004.

[2] R. Williams, G. Alexander, R. Aspinall et al., "Gathering momentum for the way ahead: fifth report of the lancet standing commission on liver disease in the UK," *The Lancet*, vol. 392, no. 10162, pp. 2398–2412, 2018.

[3] A. K. Singal, R. Bataller, J. Ahn, P. S. Kamath, and V. H. Shah, "ACG clinical guideline: alcoholic liver disease," *American Journal of Gastroenterology*, vol. 113, no. 2, pp. 175–194, 2018.

[4] F. Stickel, C. Datz, J. Hampe, and R. Bataller, "Pathophysiology and management of alcoholic liver disease: update 2016," *Gut and Liver*, vol. 11, no. 2, pp. 173–188, 2017.

[5] K. S. Gala and V. Vatsalya, "Emerging noninvasive biomarkers, and medical management strategies for alcoholic hepatitis: present understanding and scope," *Cells*, vol. 9, no. 3, p. 524, 2020.

[6] K. G. Ishak, H. J. Zimmerman, and M. B. Ray, "Alcoholic liver disease: pathologic, pathogenetic and clinical aspects," *Alcoholism: Clinical and Experimental Research*, vol. 15, no. 1, pp. 45–66, 1991.

[7] A. Rocco, D. Compare, and D. Angrisani, "Alcoholic disease: liver and beyond," *World Journal of Gastroenterology*, vol. 20, no. 40, pp. 14652–14659, 2014.

[8] R. Teschke, "Alcoholic liver disease: alcohol metabolism, cascade of molecular mechanisms, cellular targets, and clinical aspects," *Biomedicines*, vol. 6, no. 4, p. 106, 2018.

[9] D. Seth, P. S. Haber, W.-K. Syn, A. M. Diehl, and C. P. Day, "Pathogenesis of alcohol-induced liver disease: classical concepts and recent advances," *Journal of Gastroenterology and Hepatology*, vol. 26, no. 7, pp. 1089–1105, 2011.

[10] L. Z. Kong, N. Chandimali, Y. H. Han et al., "Pathogenesis, early diagnosis, and therapeutic management of alcoholic liver disease," *International Journal of Molecular Sciences*, vol. 20, no. 11, p. 2712, 2019.

[11] C. García-Ruiz, N. Kaplowitz, and J. C. Fernandez-Checa, "Role of mitochondria in alcoholic liver disease," *Current Pathobiology Reports*, vol. 1, no. 3, pp. 159–168, 2013.

[12] D. Jeong, J. Lee, and S. H. Park, "Antiphotoaging and antimelanogenic effects of *Penthorum chinense* Pursh ethanol extract due to antioxidant and autophagy-inducing properties," *Oxidative Medicine and Cellular Longevity*, vol. 2019, Article ID 9679731, 14 pages, 2019.

[13] A. Wang, M. Li, H. Huang et al., "A review of *Penthorum chinense* Pursh for hepatoprotection: traditional use, phytochemistry, pharmacology, toxicology and clinical trials," *Journal of Ethnopharmacology*, vol. 251, Article ID 112569, 2020.

[14] L. M. Lin, L. J. Zhao, and J. Deng, "Enzymatic extraction, purification, and characterization of polysaccharides from *Penthorum chinense* Pursh: natural antioxidant and anti-inflammatory," *BioMed Research International*, vol. 2018, Article ID 3486864, 13 pages, 2018.

[15] D. Huang, Y. Jiang, W. Chen, F. Yao, G. Huang, and L. Sun, "Evaluation of hypoglycemic effects of polyphenols and extracts from *Penthorum chinense*," *Journal of Ethnopharmacology*, vol. 163, pp. 256–263, 2015.

[16] A. Wang, L. Lin, and Y. Wang, "Traditional Chinese herbal medicine *Penthorum chinense* Pursh: a phytochemical and pharmacological review," *The American Journal of Chinese Medicine*, vol. 43, no. 4, pp. 601–620, 2015.

[17] Y. Qu, L. Zong, L. Shen et al., "Effects of Gansu on oxidative stress and expressions of collagens in rats with CCl4-induced liver fibrosis," *Chinese Journal of Gastroenterology*, vol. 16, no. 4, pp. 196–201, 2011.

[18] Z. Yang, J.-h. Wang, and T.-j. Zhao, "Meta analysis of the curative effect of Gansu Granule on chronic hepatitis B," *Chinese Journal of Modern Medicine*, vol. 28, pp. 47–52, 2018.

[19] X.-y. Hu, M. Wei, Y.-F. Yuan, and W.-x. Yang, "Experimental study on alcoholic fatty liver of mice treated with the southwest military medical," *Chinese Medicine*, vol. 17, pp. 288–290, 2015.

[20] T.-T. Zhang, X.-L. Xu, M.-H. Jiang, and J.-G. Jiang, "Hepatoprotective function of *Penthorum chinense* Pursh," *Food & Function*, vol. 4, no. 11, pp. 1581–1585, 2013.

[21] T. Yong, C. Zhang, G.-c. li, and Y. Chonglin, "Effect of ethanol extract of *Herba edulis* on alcoholic fatty liver in rats," *Chinese Traditional Patent Medicine*, vol. 38, pp. 1601–1605, 2016.

[22] Q. Lu, M.-H. Jiang, J.-G. Jiang, R.-F. Zhang, and M.-W. Zhang, "Isolation and identification of compounds from *Penthorum chinense* Pursh with antioxidant and antihepatocarcinoma properties," *Journal of Agricultural and Food Chemistry*, vol. 60, no. 44, pp. 11097–11103, 2012.

[23] L.-p. Xiao, *Master*, Chengdu University of TCM, Chengdu, China, 2015.

[24] Y. Yuan and X. Ou, "Research on acute toxicity of *Penthorum chinense* Pursh. Total flavonoids and therapeutic effect on AFL rats," *Medicinal Plant*, vol. 9, pp. 56–59, 2018.

[25] G. V. Gnoni, G. Paglialonga, and L. Siculella, "Quercetin inhibits fatty acid and triacylglycerol synthesis in rat-liver cells," *European Journal of Clinical Investigation*, vol. 39, no. 9, pp. 761–768, 2009.

[26] E. Leng, Y. Xiao, and Z. Mo, "Synergistic effect of phytochemicals on cholesterol metabolism and lipid accumulation in HepG2 cells," *BMC Complementary and Alternative Medicine*, vol. 18, no. 1, p. 122, 2018.

[27] J. Ahn, H. Lee, S. Kim, J. Park, and T. Ha, "The anti-obesity effect of quercetin is mediated by the AMPK and MAPK signaling pathways," *Biochemical and Biophysical Research Communications*, vol. 373, no. 4, pp. 545–549, 2008.

[28] J.-Y. Yang, M. A. Della-Fera, S. Rayalam et al., "Enhanced inhibition of adipogenesis and induction of apoptosis in 3T3-L1 adipocytes with combinations of resveratrol and quercetin," *Life Sciences*, vol. 82, no. 19-20, pp. 1032–1039, 2008.

[29] Z. Ma, Y. Zhang, and Q. Li, "Resveratrol improves alcoholic fatty liver disease by downregulating HIF-1alpha expression and mitochondrial ROS production," *PLoS One*, vol. 12, no. 8, Article ID e0183426, 2017.

[30] L. Y. Tang, Y. Chen, B. B. Rui, and C. M. Hu, "Resveratrol ameliorates lipid accumulation in HepG2 cells, associated with down-regulation of lipin1 expression," *Canadian Journal of Physiology and Pharmacology*, vol. 94, no. 2, pp. 185–189, 2016.

[31] M.-J. Seo, Y.-J. Lee, J.-H. Hwang, K.-J. Kim, and B.-Y. Lee, "The inhibitory effects of quercetin on obesity and obesity-induced inflammation by regulation of MAPK signaling," *The Journal of Nutritional Biochemistry*, vol. 26, no. 11, pp. 1308–1316, 2015.

[32] W. W. Guo, X. Wang, and X. Q. Chen, "Flavonones from *Penthorum chinense* ameliorate hepatic steatosis by activating the SIRT1/AMPK pathway in HepG2 cells," *International Journal of Molecular Sciences*, vol. 19, no. 9, p. 2555, 2018.

[33] M. Wang, X. J. Zhang, and R. Feng, "Hepatoprotective properties of *Penthorum chinense* Pursh against carbon tetrachloride-induced acute liver injury in mice," *Chinese Medicine*, vol. 12, no. 1, p. 32, 2017.

[34] A. Wang, S. Wang, Y. Jiang, M. Chen, Y. Wang, and L. Lin, "Bio-assay guided identification of hepatoprotective polyphenols from *Penthorum chinense* Pursh on *t*-BHP induced oxidative stress injured L02 cells," *Food & Function*, vol. 7, no. 4, pp. 2074–2083, 2016.

[35] F. Zhou, A. Wang, D. Li, Y. Wang, and L. Lin, "Pinocembrin from *Penthorum chinense* Pursh suppresses hepatic stellate cells activation through a unified SIRT3-TGF-β-Smad signaling pathway," *Toxicology and Applied Pharmacology*, vol. 341, pp. 38–50, 2018.

[36] Y.-W. Cao, Y. Jiang, D.-Y. Zhang et al., "Protective effects of *Penthorum chinense* Pursh against chronic ethanol-induced liver injury in mice," *Journal of Ethnopharmacology*, vol. 161, pp. 92–98, 2015.

[37] Y. Tang, Y. Li, H. Yu et al., "Quercetin prevents ethanol-induced iron overload by regulating hepcidin through the BMP6/SMAD4 signaling pathway," *The Journal of Nutritional Biochemistry*, vol. 25, no. 6, pp. 675–682, 2014.

[38] Y. Tang, Y. Li, H. Yu et al., "Quercetin attenuates chronic ethanol hepatotoxicity: implication of "free" iron uptake and release," *Food and Chemical Toxicology*, vol. 67, pp. 131–138, 2014.

[39] Y. Li, Y. Deng, Y. Tang et al., "Quercetin protects rat hepatocytes from oxidative damage induced by ethanol and iron by maintaining intercellular liable iron pool," *Human & Experimental Toxicology*, vol. 33, no. 5, pp. 534–541, 2014.

[40] Y. Li, M. Chen, Y. Xu et al., "Iron-mediated lysosomal membrane permeabilization in ethanol-induced hepatic oxidative damage and apoptosis: protective effects of quercetin," *Oxidative Medicine and Cellular Longevity*, vol. 2016, Article ID 4147610, 15 pages, 2016.

[41] M. E. Rubio-Ruiz, V. Guarner-Lans, and A. Cano-Martinez, "Resveratrol and quercetin administration improves antioxidant DEFENSES and reduces fatty liver in metabolic syndrome rats," *Molecules*, vol. 24, no. 7, p. 1297, 2019.

[42] Y. Tang, H. Tian, Y. Shi et al., "Quercetin suppressed CYP2E1-dependent ethanol hepatotoxicity via depleting heme pool and releasing CO," *Phytomedicine*, vol. 20, no. 8-9, pp. 699–704, 2013.

[43] Y. Li, C. Gao, Y. Shi et al., "Carbon monoxide alleviates ethanol-induced oxidative damage and inflammatory stress through activating p38 MAPK pathway," *Toxicology and Applied Pharmacology*, vol. 273, no. 1, pp. 53–58, 2013.

[44] J. Oliva, F. Bardag-Gorce, B. Tillman, and S. W. French, "Protective effect of quercetin, EGCG, catechin and betaine against oxidative stress induced by ethanol in vitro," *Experimental and Molecular Pathology*, vol. 90, no. 3, pp. 295–299, 2011.

[45] X. Li, Q. Jin, Q. Yao et al., "The flavonoid quercetin ameliorates liver inflammation and fibrosis by regulating hepatic macrophages activation and polarization in mice," *Frontiers in Pharmacology*, vol. 9, p. 72, 2018.

[46] M. Zhu, X. Zhou, and J. Zhao, "Quercetin prevents alcohol-induced liver injury through targeting of PI3K/Akt/nuclear factor-κB and STAT3 signaling pathway," *Experimental and Therapeutic Medicine*, vol. 14, pp. 6169–6175, 2017.

[47] S. Liu, L. Tian, G. Chai, B. Wen, and B. Wang, "Targeting heme oxygenase-1 by quercetin ameliorates alcohol-induced acute liver injury via inhibiting NLRP3 inflammasome activation," *Food & Function*, vol. 9, no. 8, pp. 4184–4193, 2018.

[48] E. Ince, "The protective effect of quercetin in the alcohol-induced liver and lymphoid tissue injuries in newborns," *Molecular Biology Reports*, vol. 47, no. 1, pp. 451–459, 2020.

[49] Y. Yan, J.-Y. Yang, Y.-H. Mou, L.-H. Wang, Y.-N. Zhou, and C.-F. Wu, "Differences in the activities of resveratrol and ascorbic acid in protection of ethanol-induced oxidative DNA damage in human peripheral lymphocytes," *Food and Chemical Toxicology*, vol. 50, no. 2, pp. 168–174, 2012.

[50] G. Luo, B. Huang, and X. Qiu, "Resveratrol attenuates excessive ethanol exposure induced insulin resistance in rats via improving NAD^+/NADH ratio," *Molecular Nutrition & Food Research*, vol. 61, no. 11, Article ID 1700087, 2017.

[51] L. Liu, Z. Fan, Y. Tang, and Z. Ke, "The resveratrol attenuates ethanol-induced hepatocyte apoptosis via inhibiting ER-related caspase-12 activation and PDE activity in vitro," *Alcoholism: Clinical and Experimental Research*, vol. 38, no. 3, pp. 683–693, 2014.

[52] L. Xue, W. Zhu, F. Yang et al., "Appropriate dose of ethanol exerts anti-senescence and anti-atherosclerosis protective effects by activating ALDH2," *Biochemical and Biophysical Research Communications*, vol. 512, no. 2, pp. 319–325, 2019.

[53] J. A. Rubiolo, G. Mithieux, and F. V. Vega, "Resveratrol protects primary rat hepatocytes against oxidative stress damage: activation of the Nrf2 transcription factor and augmented activities of antioxidant enzymes," *European Journal of Pharmacology*, vol. 591, no. 1–3, pp. 66–72, 2008.

[54] G. Wang, Z. Hu, and Q. Fu, "Resveratrol mitigates lipopolysaccharide-mediated acute inflammation in rats by inhibiting the TLR4/NF-κBp65/MAPKs signaling cascade," *Scientific Reports*, vol. 7, no. 1, Article ID 45006, 2017.

[55] F. Li, Y. Yang, L. Yang et al., "Resveratrol alleviates FFA and CCl4 induced apoptosis in HepG2 cells via restoring endoplasmic reticulum stress," *Oncotarget*, vol. 8, no. 27, pp. 43799–43809, 2017.

[56] D.-Q. Zhang, P. Sun, Q. Jin et al., "Resveratrol regulates activated hepatic stellate cells by modulating NF-κB and the PI3K/Akt signaling pathway," *Journal of Food Science*, vol. 81, no. 1, pp. H240–H245, 2016.

[57] H.-M. Ni, K. Du, M. You, and W.-X. Ding, "Critical role of FoxO3a in alcohol-induced autophagy and hepatotoxicity," *The American Journal of Pathology*, vol. 183, no. 6, pp. 1815–1825, 2013.

[58] L. Tang, F. Yang, Z. Fang, and C. Hu, "Resveratrol ameliorates alcoholic fatty liver by inducing autophagy," *The American Journal of Chinese Medicine*, vol. 44, no. 6, pp. 1207–1220, 2016.

[59] X. Yu, Y. Xu, and S. Zhang, "Quercetin attenuates chronic ethanol-induced hepatic mitochondrial damage through enhanced mitophagy," *Nutrients*, vol. 8, no. 1, p. 27, 2016.

[60] H. Zeng, X. Guo, F. Zhou et al., "Quercetin alleviates ethanol-induced liver steatosis associated with improvement of lipophagy," *Food and Chemical Toxicology*, vol. 125, pp. 21–28, 2019.

[61] C.-J. Weng, M.-J. Chen, C.-T. Yeh, and G.-C. Yen, "Hepatoprotection of quercetin against oxidative stress by induction of metallothionein expression through activating MAPK and PI3K pathways and enhancing Nrf2 DNA-binding activity," *New Biotechnology*, vol. 28, no. 6, pp. 767–777, 2011.

[62] H. Peiyuan, H. Zhiping, and S. Chengjun, "Resveratrol ameliorates experimental alcoholic liver disease by modulating oxidative stress," *Evidence-Based Complementary and Alternative Medicine*, vol. 2017, no. 10, Article ID 4287890, 2017.

[63] L. Bujanda, M. Garcia-Barcina, and V. Gutierrez-de Juan, "Effect of resveratrol on alcohol-induced mortality and liver

lesions in mice," *BMC Gastroenterology*, vol. 6, no. 1, p. 35, 2006.

[64] O. Niemelä, "Biomarker-based approaches for assessing alcohol use disorders," *International Journal of Environmental Research and Public Health*, vol. 13, no. 2, p. 166, 2016.

[65] M. Wang, L.-J. Ma, Y. Yang, Z. Xiao, and J.-B. Wan, "*n*-3 polyunsaturated fatty acids for the management of alcoholic liver disease: a critical review," *Critical Reviews in Food Science and Nutrition*, vol. 59, no. 1, pp. S116–S129, 2019.

[66] S. Venkatesan, R. J. Ward, and T. J. Peters, "Effect of chronic ethanol feeding on the hepatic secretion of very-low-density lipoproteins," *Biochimica et Biophysica Acta (BBA)–Lipids and Lipid Metabolism*, vol. 960, no. 1, pp. 61–66, 1988.

[67] X. Hu, M. Wei, Y. Yuan, and W. Yang, "Experimental study of *Penthorum chinense* Pursh on mouse with alcoholic fatty liver disease," *Medicinal Plant*, vol. 6, no. 1/2, pp. 44–46, 2015.

[68] L. He, S. Zhang, C. Luo et al., "Functional teas from the stems of *Penthorum chinense* Pursh.: phenolic constituents, antioxidant and hepatoprotective activity," *Plant Foods for Human Nutrition*, vol. 74, no. 1, pp. 83–90, 2019.

[69] W. Guo, Y. Jiang, X. Chen et al., "Identification and quantitation of major phenolic compounds from *Penthorum chinense* Pursh. by HPLC with tandem mass spectrometry and HPLC with diode array detection," *Journal of Separation Science*, vol. 38, no. 16, pp. 2789–2796, 2015.

[70] G. Ye, H. Gao, and Z. Wang, "PPARα and PPARγ activation attenuates total free fatty acid and triglyceride accumulation in macrophages via the inhibition of Fatp1 expression," *Cell Death & Disease*, vol. 10, no. 2, p. 39, 2019.

[71] J. M. Ajmo, X. Liang, C. Q. Rogers, B. Pennock, and M. You, "Resveratrol alleviates alcoholic fatty liver in mice," *American Journal of Physiology-Gastrointestinal and Liver Physiology*, vol. 295, no. 4, pp. G833–G842, 2008.

[72] G. Ye, G. Chen, H. Gao et al., "Resveratrol inhibits lipid accumulation in the intestine of atherosclerotic mice and macrophages," *Journal of Cellular and Molecular Medicine*, vol. 23, no. 6, pp. 4313–4325, 2019.

[73] X. Yang, S. Xu, Y. Qian, and Q. Xiao, "Resveratrol regulates microglia M1/M2 polarization via PGC-1α in conditions of neuroinflammatory injury," *Brain, Behavior, and Immunity*, vol. 64, pp. 162–172, 2017.

[74] M. J. Houghton, A. Kerimi, S. Tumova, J. P. Boyle, and G. Williamson, "Quercetin preserves redox status and stimulates mitochondrial function in metabolically-stressed HepG2 cells," *Free Radical Biology and Medicine*, vol. 129, pp. 296–309, 2018.

[75] M. Endale, S.-C. Park, S. Kim et al., "Quercetin disrupts tyrosine-phosphorylated phosphatidylinositol 3-kinase and myeloid differentiation factor-88 association, and inhibits MAPK/AP-1 and IKK/NF-κB-induced inflammatory mediators production in RAW 264.7 cells," *Immunobiology*, vol. 218, no. 12, pp. 1452–1467, 2013.

[76] X. Sun, A. Wu, B. Y. Kwan Law et al., "The active components derived from *Penthorum chinense* Pursh protect against oxidative-stress-induced vascular injury via autophagy induction," *Free Radical Biology and Medicine*, vol. 146, pp. 160–180, 2020.

[77] Y. Hu, S. Wang, A. Wang, L. Lin, M. Chen, and Y. Wang, "Antioxidant and hepatoprotective effect of *Penthorum chinense* Pursh extract against t-BHP-induced liver damage in L02 cells," *Molecules*, vol. 20, no. 4, pp. 6443–6453, 2015.

[78] B.-J. Song, M. A. Abdelmegeed, Y.-E. Cho et al., "Contributing roles of CYP2E1 and other cytochrome P450 isoforms in alcohol-related tissue injury and carcinogenesis," *Advances in Experimental Medicine and Biology*, vol. 1164, pp. 73–87, 2019.

[79] M. P. Srinivasan, K. K. Bhopale, S. M. Amer et al., "Linking dysregulated AMPK signaling and ER stress in ethanol-induced liver injury in hepatic alcohol dehydrogenase deficient deer mice," *Biomolecules*, vol. 9, no. 10, p. 560, 2019.

[80] K. Yaku, K. Okabe, M. Gulshan, K. Takatsu, H. Okamoto, and T. Nakagawa, "Metabolism and biochemical properties of nicotinamide adenine dinucleotide (NAD) analogs, nicotinamide guanine dinucleotide (NGD) and nicotinamide hypoxanthine dinucleotide (NHD)," *Scientific Reports*, vol. 9, no. 1, Article ID 13102, 2019.

[81] R.-B. Ding, J. Bao, and C.-X. Deng, "Emerging roles of SIRT1 in fatty liver diseases," *International Journal of Biological Sciences*, vol. 13, no. 7, pp. 852–867, 2017.

[82] T. W. Jung, K.-T. Lee, M. W. Lee, and K.-H. Ka, "SIRT1 attenuates palmitate-induced endoplasmic reticulum stress and insulin resistance in HepG2 cells via induction of oxygen-regulated protein 150," *Biochemical and Biophysical Research Communications*, vol. 422, no. 2, pp. 229–232, 2012.

[83] M. You, Q. Cao, X. Liang, J. M. Ajmo, and G. C. Ness, "Mammalian sirtuin 1 is involved in the protective action of dietary saturated fat against alcoholic fatty liver in mice," *The Journal of Nutrition*, vol. 138, no. 3, pp. 497–501, 2008.

[84] C. Chang, H. Su, D. Zhang et al., "AMPK-dependent phosphorylation of GAPDH triggers Sirt1 activation and is necessary for autophagy upon glucose starvation," *Molecular Cell*, vol. 60, no. 6, pp. 930–940, 2015.

[85] N. Zhang, Y. Hu, C. Ding et al., "Salvianolic acid B protects against chronic alcoholic liver injury via SIRT1-mediated inhibition of CRP and ChREBP in rats," *Toxicology Letters*, vol. 267, pp. 1–10, 2017.

[86] A. Defour, K. Dessalle, and A. Castro Perez, "Sirtuin 1 regulates SREBP-1c expression in a LXR-dependent manner in skeletal muscle," *PLoS One*, vol. 7, no. 9, Article ID e43490, 2012.

[87] M. You, X. Liang, J. M. Ajmo, and G. C. Ness, "Involvement of mammalian sirtuin 1 in the action of ethanol in the liver," *American Journal of Physiology-Gastrointestinal and Liver Physiology*, vol. 294, no. 4, pp. G892–G898, 2008.

[88] D. G. Hardie, "Minireview: the AMP-activated protein kinase cascade: the key sensor of cellular energy status," *Endocrinology*, vol. 144, no. 12, pp. 5179–5183, 2003.

[89] D. Carling, "The AMP-activated protein kinase cascade—a unifying system for energy control," *Trends in Biochemical Sciences*, vol. 29, no. 1, pp. 18–24, 2004.

[90] K. K. Hintz, D. P. Relling, J. T. Saari et al., "Cardiac overexpression of alcohol dehydrogenase exacerbates cardiac contractile dysfunction, lipid peroxidation, and protein damage after chronic ethanol ingestion," *Alcoholism: Clinical & Experimental Research*, vol. 27, no. 7, pp. 1090–1098, 2003.

[91] M. Hu, F. Wang, X. Li et al., "Regulation of hepatic lipin-1 by ethanol: role of AMP-activated protein kinase/sterol regulatory element-binding protein 1 signaling in mice," *Hepatology*, vol. 55, no. 2, pp. 437–446, 2012.

[92] R. Guo, J. Ren, and J. Ren, "Alcohol dehydrogenase accentuates ethanol-induced myocardial dysfunction and mitochondrial damage in mice: role of mitochondrial death pathway," *PLoS One*, vol. 5, no. 1, Article ID e8757, 2010.

[93] Z. Jiang, J. Zhou, D. Zhou, Z. Zhu, L. Sun, and A. A. Nanji, "The adiponectin-SIRT1-AMPK pathway in alcoholic fatty liver disease in the rat," *Alcoholism: Clinical and Experimental Research*, vol. 39, no. 3, pp. 424–433, 2015.

[94] L. He, F. A. Simmen, M. J. J. Ronis, and T. M. Badger, "Post-transcriptional regulation of sterol regulatory element-binding protein-1 by ethanol induces class I alcohol dehydrogenase in rat liver," *Journal of Biological Chemistry*, vol. 279, no. 27, pp. 28113–28121, 2004.

[95] S. Sato, H. Jung, T. Nakagawa et al., "Metabolite regulation of nuclear localization of carbohydrate-response element-binding protein (ChREBP): role of amp as an allosteric inhibitor," *Journal of Biological Chemistry*, vol. 291, no. 20, pp. 10515–10527, 2016.

[96] S. Liangpunsakul, "Carbohydrate-responsive element-binding protein, sirtuin 1, and ethanol metabolism: a complicated network in alcohol-induced hepatic steatosis," *Hepatology*, vol. 62, no. 4, pp. 994–996, 2015.

[97] L. Gao, W. Shan, W. Zeng et al., "Carnosic acid alleviates chronic alcoholic liver injury by regulating the SIRT1/ChREBP and SIRT1/p66shc pathways in rats," *Molecular Nutrition & Food Research*, vol. 60, no. 9, pp. 1902–1911, 2016.

[98] S. Marmier, R. Dentin, M. Daujat-Chavanieu et al., "Novel role for carbohydrate responsive element binding protein in the control of ethanol metabolism and susceptibility to binge drinking," *Hepatology*, vol. 62, no. 4, pp. 1086–1100, 2015.

[99] T. Zeng, C.-L. Zhang, N. Zhao et al., "Impairment of Akt activity by CYP2E1 mediated oxidative stress is involved in chronic ethanol-induced fatty liver," *Redox Biology*, vol. 14, pp. 295–304, 2018.

[100] B. Yu, S.-y. Qin, B.-l. Hu, Q.-y. Qin, H.-x. Jiang, and W. Luo, "Resveratrol improves CCL4-induced liver fibrosis in mouse by upregulating endogenous IL-10 to reprogramme macrophages phenotype from M(LPS) to M(IL-4)," *Biomedicine & Pharmacotherapy*, vol. 117, Article ID 109110, 2019.

[101] Z.-L. Sun, Y.-Z. Zhang, F. Zhang et al., "Quality assessment of *Penthorum chinense* Pursh through multicomponent qualification and fingerprint, chemometric, and anti-hepatocarcinoma analyses," *Food & Function*, vol. 9, no. 7, pp. 3807–3814, 2018.

[102] E. Ceni, T. Mello, and A. Galli, "Pathogenesis of alcoholic liver disease: role of oxidative metabolism," *World Journal of Gastroenterology*, vol. 20, no. 47, pp. 17756–17772, 2014.

[103] L. Qin, Z. Wang, L. Tao, and Y. Wang, "ER stress negatively regulates AKT/TSC/mTOR pathway to enhance autophagy," *Autophagy*, vol. 6, no. 2, pp. 239–247, 2010.

[104] Y. Zhang, Y. Cao, J. Chen, H. Qin, and L. Yang, "A new possible mechanism by which punicalagin protects against liver injury induced by type 2 diabetes mellitus: upregulation of autophagy via the akt/FoxO3a signaling pathway," *Journal of Agricultural and Food Chemistry*, vol. 67, no. 50, pp. 13948–13959, 2019.

[105] T. Koga, M. A. Suico, S. Shimasaki et al., "Endoplasmic reticulum (ER) stress induces sirtuin 1 (SIRT1) expression via the PI3K-Akt-GSK3β signaling pathway and promotes hepatocellular injury," *Journal of Biological Chemistry*, vol. 290, no. 51, pp. 30366–30374, 2015.

[106] K. Wang, "Autophagy and apoptosis in liver injury," *Cell Cycle*, vol. 14, no. 11, pp. 1631–1642, 2015.

[107] S. Tomas-Hernandez, J. Blanco, and C. Rojas, "Resveratrol potently counteracts quercetin starvation-induced autophagy and sensitizes HepG2 cancer cells to apoptosis," *Molecular Nutrition & Food Research*, vol. 62, no. 5, Article ID 1700610, 2018.

[108] A. Shaito, A. M. Posadino, and N. Younes, "Potential adverse effects of resveratrol: a literature review," *International Journal of Molecular Sciences*, vol. 21, no. 6, p. 2084, 2020.

[109] Y. Wang, B. Tao, Y. Wan et al., "Drug delivery based pharmacological enhancement and current insights of quercetin with therapeutic potential against oral diseases," *Biomedicine & Pharmacotherapy*, vol. 128, Article ID 110372, 2020.